N 121868

AD 654783

LRC66-509

LOCKHEED-GEORGIA COMPANY

A DIVISION OF LOCKHEED AIRCRAFT CORPORATION

REPORT NO. ER-7634

DATED 12 January 1965

LOCKHEED-GEORGIA COMPANY

A DIVISION OF LOCKHEED AIRCRAFT CORPORATION

MARIETTA GEORGIA

TITLE

FULL SCALE TESTS OF THE XV-4A HUMMINGBIRD
IN THE AMES 40 X 80 FOOT WIND TUNNEL

SUBMITTED UNDER

Contract No. DA 44-177-TC-773

MODEL XV-4A

REFERENCE Contract No. DA 44-177-TC-773

PREPARED BY O. G. Barnes, Jr.
O. G. Barnes, Jr.

GROUP Department 72-10

CHECKED BY

APPROVED BY

APPROVED BY J. G. McReynolds, Jr.
J. G. McReynolds, Jr.

APPROVED BY A. W. Mooney
A. W. Mooney

DATE	REV. BY	PAGES AFFECTED	REMARKS

FORM 402-2

CONTENTS

FIGURE INDEX

FIGURE INDEX (Continued)

FIGURE INDEX (Continued)

FIGURE INDEX (Continued)

FIGURE INDEX (Continued)

FIGURE INDEX (Continued)

FIGURE INDEX (Continued)

FIGURE INDEX (Continued)

FIGURE INDEX (Continued)

FIGURE INDEX (Continued)

FIGURE INDEX (Continued)

FIGURE INDEX (Continued)

FIGURE INDEX (Continued)

FIGURE INDEX (Continued)

I. INTRODUCTION

The U. S. Army XV-4A Hummingbird Aircraft Serial Number 24504 was tested in the 40 x 80 Foot Wind Tunnel of the Ames Research Center from August 28, 1964, through September 11, 1964. As a part of the original Hummingbird contract (DA 44-177-TC-773), these tests were to have been accomplished prior to the first transition attempts. A number of postponements resulted in the wind tunnel tests being conducted nearly a year after successful transitions were performed.

The tests consisted of 41 runs and a total of 944 test points. Tests were conducted over a range of speeds in all phases of flight from hover through transition to conventional flight. Pitch and yaw runs, as well as control effectiveness runs in all three modes were made. Many of the pitch runs were made well into the so-called deep stall angle of attack range.

II. SUMMARY

The results of the XV-4A Hummingbird tests in the Ames 40 x 80 Foot Wind Tunnel are presented and analyzed. The 41 runs made included pitch, yaw, and control effectiveness tests in hover, transition, and conventional flight.

As tested in the wind tunnel, the Hummingbird configuration was the same as that flight tested. To accomplish the test, the main landing gear was removed for attachment of the wind tunnel main supports, some wiring was run externally, and the rear wind tunnel support was attached to the aft fuselage. Electric actuators were provided for the remote control of all aircraft control systems. Control surface position potentiometers provided signals for the indication of control deflections on a remote readout panel adjacent to the remote control panel located in the wind tunnel control room.

The minimum printout unit values of 12 pounds in lift for pitching moment, 6 pounds in lift difference for rolling moment, and 2.4 pounds for the other components are larger than those desirable for the magnitude of forces and moments generated by the Hummingbird. Only a small percentage of the balance system capability was used for these tests. The IBM data reduction system used reduced data promptly.

The final wind tunnel data are plotted in two forms. A standard aerodynamic coefficient form is used for presentation of all of the data. In addition, the hover and transition data are also presented in the form of forces and moments. Only the conventional flight configuration test data are analyzed in the coefficient form, and the hover and transition data are analyzed in the dimensional form.

The tests of the conventional flight configuration with the engines thrusting indicate good agreement with other data in all parameters except the pitching

moment coefficient at zero lift with neutral elevator and the directional stability level. The pitching moment and yawing moment coefficients generated by the drag of the unshielded rear support can account for the majority of the discrepancy.

Good agreement is obtained between forces from the data based on the equations derived from the small scale wind tunnel tests of Reference 1, the limited flight test data, and the full scale wind tunnel test data in hover and transition except a partially unexplained 750 pound reduction in the ejector net force value from the full scale wind tunnel tests. The agreement between the moment data is not quite as good with the full scale wind tunnel data indicating increased stability in all modes, limited control effectiveness in some cases and a nose down shift in the pitching moment data. Although a crude shield for the rear support was installed and indicated little change in the data, the shift in the pitching moment data and the directional stability level change can be generated by the drag of the unshielded rear support which was used throughout the major portion of the tests.

If these tests had been conducted previous to successful transition flights of the Hummingbird, none of the results would have prevented these flights, but some of the data indicate the need for additional analyses to explain some of the differences observed between the full scale wind tunnel tests and the equations derived from the small scale wind tunnel tests with additional full scale tests probably being indicated in some areas.

III. DESCRIPTION OF AIRCRAFT AND TEST SETUP

The external configuration of the aircraft was unchanged from that which was flight tested, except that some wiring and plumbing had to be attached to the skin externally. The external wiring and plumbing were held to a minimum and were located mostly in the nacelle and under fuselage areas. Two external longitudinal tunnels were used under the fuselage between the ejectors, but these tunnels were also present during flight tests. The leads from the tail angle of attack indicator were attached to the lower surface of the horizontal stabilizer between the boom and the point where they entered the vertical stabilizer.

Figure 1 shows the Hummingbird mounted in the Ames 40 x 80 Foot Wind Tunnel, and Figure 2 gives the general arrangement with the basic dimensions of the aircraft noted on this figure. The theoretical aerodynamic data for the Hummingbird are given in Figure 3.

The aircraft was equipped for complete remote operation from the control panel located in the wind tunnel control room. This remote control panel supplied all functions necessary for operation of the aircraft in all flight regimes and included the controls for the fire extinguishing system. The engine fuel controls were positioned from the remote control panel by means of electrical actuators located in each nacelle. Fuel was supplied from an external tank to each wheel well with all internal tankage having been removed from the aircraft.

Electrical actuators, operated from the remote control panel, were located in the cockpit and supplied the forces and motions to the aircraft control system similar to normal pilot inputs. From this point, the normal aircraft control systems were used to position the aerodynamic control surfaces and the respective reaction controls. The ejection seat and much of the pilot's instrumentation

were removed from the cockpit to provide space for mounting the electrical control actuators. The existing aircraft systems were used through remote controls to position the flaps, the ejector inlet and exit doors, the nose gear, the boundary layer control air valve for the horizontal tail, the engine diverter valves, and the bleed air valves for the lateral reaction controls.

The positions of the various controls were shown by indicators mounted in the remote readout panel. These indicators were positioned by potentiometers installed at the respective control surfaces. Figure 4 is a typical picture of the remote readout panel as photographed for data recording. In addition to the control positions, operating pressures for the reaction control systems, the horizontal tail boundary layer control pressures, angle of attack, angle of sideslip, tail angle of attack, boom airspeed pressures, and engine tail pipe pressures (P_{t_5}'s) were presented on the remote readout panel.

The Hummingbird was mounted on the conventional wind tunnel three-strut support system, which is connected to the external balance. Special mounting pads were manufactured and installed in place of the main landing gear to which the ball and socket attachments of the two main wind tunnel struts were fastened. These mounting pads were designed to provide a distance between the main strut attachment points, or tread, of 88 inches, which permitted a yaw angle of 20 degrees before interference was encountered on the mounting system in the tunnel. A special fitting designed to distribute the load equally to three of the aft fuselage frames provided a mounting pad for the ball and socket of the rear wind tunnel strut. Since these frames are not normally subjected to high concentrated loads, local beefup of the three frames was required to transmit the loads into the aft fuselage basic structure. The tail length, or distance from the main strut center line to the center line of the tail strut socket, was 133.6 inches.

The remote control leads, instrumentation leads, fuel lines, CO_2 lines, and electrical start power lines were run from the wheel wells down the main struts. These leads were taped solid to the exposed potion of the struts and were run down through the windshields which protected the remainder of the forward struts from airloads which otherwise would be measured by the balance system. The regular fairing or windshield for the rear strut was damaged in the test preceding the Hummingbird test and was not used. However, a crude stationary windshield was fabricated and installed previous to Run 37. Runs 37 through 41 include the effect of this crude rear strut windshield.

Basically, the rear strut of the support system is designed to carry axial loads only, having a ball and socket mount at the aircraft and a gimbel attachment to the balance system underneath the tunnel floor. As the aircraft is yawed, the rear strut attachment under the tunnel floor follows a path perpendicular to the center line of the tunnel by means of a separate drive system controlled by limit switches. The main support struts remain vertical at all times, and move fore and aft, as well as crosswise, in the tunnel as the aircraft is yawed.

The external balance system of the tunnel is composed of four lift posts, two side force links, and one drag link. The details of the support and balance system are described more fully in Reference 2.

IV. DATA REDUCTION

All wind tunnel data were read on the external balance system and reduced to coefficient form based on the wing chord plane dimensions. The moment data were transferred to the stability axes with an origin at the 10 percent mean aerodynamic chord point which is located in the aircraft at fuselage station 285.5 and water line 100.0. Wing dimensions used for data reduction to coefficient form are:

Wing Area (S) = 104.17 square feet

Mean Aerodynamic Chord ($\bar{c}$) = 4.43 feet

Wing Span (b) = 25.0 feet

The wing span dimension used by Ames for their data reduction was 25.9 feet. However, for the data presented in this report, a correction was made to reflect a wing span of 25.0 feet as noted above. This correction was made to facilitate correlation with other data which were based on this theoretical value.

The control surface sign conventions used in all plotted data are included in the definition of symbols presented in Figure 5. These are used throughout the entire report.

In addition to the normal wind tunnel weight and data tares, a special correction was included in the data reduction for the drag of the rear strut which was not protected by a fairing or windshield. This drag value was based upon tunnel free-stream q; however, in most instances at least a portion of the rear strut was exposed to flow from the ejector which in general was at a much higher q than the free stream tunnel value, thus having a higher drag value than indicated by the correction. The drag on the rear strut also introduces a pitching moment into the data. No attempt was made to correct the data for this induced pitching moment, which is in a nose down or negative direction. The magnitude of this correction is discussed in Section VII. For Runs 37 through 41, a crude stationary

fairing was installed in the wind tunnel to protect the rear strut from most of the drag load induced by the air flow.

Normal wind tunnel wall effects corrections were applied to the data for the conventional flight configuration of the aircraft. Wall corrections were not applied to the transitional flight configurations data since the major portion of the lift forces are generated by engine thrust rather than by aerodynamic means and thus the wind tunnel wall effects are not well defined. In addition, Ames personnel expressed the opinion that the wall effects for the 40 x 80 Foot Wind Tunnel are negligible for transition tests. These tests were to serve as a check of wall effects by comparison with flight test data and the small scale wind tunnel tests. The amount of flight test data is too limited for a reasonable evaluation.

Two methods were used for recording the forces as indicated on the readout scales. One was a card punch system which recorded 10 samples for each data point. The IBM data reduction system averaged these 10 samples to give a single value for each of the components reduced for each test point. Prompt data reduction was supplied by this system throughout the test.

The smallest unit recorded on the data punch cards had the following values: 12 pounds in lift summation for pitching moment; 6 pounds in lift difference for rolling moment; and 2.4 pounds for drag or side force. When these values are reflected into moments, the printout accuracies are as follows: approximately 400 foot-pounds in pitching moment; approximately 200 foot-pounds in rolling moment, and approximately 60 foot-pounds in yawing moment. The overall accuracy of the balance system is not quoted; however, it was used to a small percentage of its capacity.

The second, or backup method of recording data consisted of a tape printout system at each of the individual scales. Five data samples were printed for each test

point. These tapes had to be read manually and were used only in case of a failure of the primary card punch system or in case there was any question of the final reduced values as obtained from the card punch system. The tapes were read to the nearest 5 pounds on all four lift values and to the nearest one pound on the other components. For the Hummingbird test, the card punched data was used entirely except for 3 or 4 runs in which cases significant discrepancies were found in the values used to determine the pitching moment. For these cases, the tape values were read and later used in the IBM reduction programs.

V. SCOPE OF THE TESTS

The full scale tests of the Hummingbird included some runs within all regimes of flight for VTOL aircraft consisting of hover, transition and conventional flight. The amount of hover testing was quite limited, primarily due to the restrictions imposed by the wind tunnel. Although the overhead doors of the test section were open for all hover testing, the tunnel walls still introduced certain restrictions on the test conditions, and continued hover testing induced tunnel q. The major portions of the tests were performed in the transition regime, which is the more difficult operational region for all VTOL aircraft. A few runs were made in the conventional flight regime at two velocities, in an attempt to determine some Reynolds number effects. In addition, an engine calibration run was made at zero tunnel q.

Figure 6 is a summary of the runs that were made during the test. The definitions of the various phases of transition which have been used throughout the entire Hummingbird program were adopted for the full scale test and are used in this figure. These phases are defined as follows:

Phase I - Both engines are diverted through the ejector lift system.

Phase II - Engine #1 is exhausting through the conventional tailpipe and engine #2 is diverted through the ejector lift system.

Phase III - Both engines are exhausting through the conventional tailpipes but with the ejector doors still opened.

The test speed is noted for each run with all runs being made between 0 and 100 knots. The engine thrust level for each of the runs is indicated by a P_{t_5} value which is the engine tailpipe pressure expressed in inches of mercury with a value of 30 noted for the engine inoperative condition.

Ejector exit rake surveys were made during the first two runs in an attempt to determine the gross thrust level of the ejector. These rakes were installed in the left ejector bays. Since the amount of pressure instrumentation provided by the limited number of rakes was considered to be inadequate, no data are presented; however, an examination of data by Ames showed fairly close agreement between the gross thrust values derived from these data and the net thrust values obtained from the balance system. After Runs 1 and 2 were completed these rakes were removed and no pressure instrumentation of any sort was used within the ejectors for the remainder of the test.

The maximum range of angles of attack for the polars was from -12 degrees to +28 degrees; however, many of the polars did not span this complete range of angles but were shortened somewhat on either end. The yaw angles tested ranged from -4 degrees to +10 degrees with many of the yaw runs only going to +8 degrees. For the powered runs, the P_{t_5}'s tested ranged between 35 and 66 inches of mercury. Nominal values of P_{t_5} of 46 inches of mercury and 60 inches of mercury were used for the constant thrust runs.

The control effectiveness runs were made over the complete range of deflections for each control surface. In the VTOL configurations, the elevator deflections tested were between 0 and 52 degrees. In the conventional flight configuration, these limits were plus and minus 30 degrees. The range of rudder deflections tested was between -20 and +17 degrees. For aileron effectiveness, the deflections varied from -17 to +17 degrees per aileron. In general, these control surface deflection limits were somewhat less than the design values for the airplane. One reason for this was the fact that the remote control actuators did not permit full deflection of most surfaces. However, in some cases, the actual design values were not realized partially because of control system deflections and stretch under load.

Since the Hummingbird was rigged for complete remote operation, the same number of test points could have been accumulated in a shorter period of time if it had not been for certain limitations on the tunnel operation, or conversely, more test points could have been accumulated during the span of the test. These limitations were temperature and contamination caused by the operation of the engines. Since the wind tunnel does not have facilities for exchanging the air while running, much time was consumed in airing out the tunnel between runs by opening the overhead test section doors while maintaining low tunnel q. An arbitrary limit on the maximum allowable temperature of the tunnel was originally set at 115 degrees F; however, on many runs this value was exceeded with the temperature during one run actually reaching 135 degrees F.

VI. PLOTTED COEFFICIENT DATA

All of the data accumulated during the tests are plotted in Figures 7 through 156 in the form of aerodynamic coefficients with the exception of the data for the effects of power and control in hover presented in actual forces and moments. These data are plotted in the standard form for wind tunnel test results, except that drag coefficients and pitching moment coefficients are plotted as a function of angle of attack rather than lift coefficient. Angle of attack is used for convenience since the lift coefficients have such high values for the transitional tests where test speeds are low and the forces due to ejector thrust are large.

The tunnel q values varied substantially during a constant q run. In the normal IBM data reduction procedures each test point is reduced at the individual q of the test point rather than at a nominal value for the complete run. For the tests in Phase I and Phase II of transition, the amount of scatter introduced by using individual q's is greater than that experienced in the conventional configuration since the forces and moments are primarily the result of the ejector thrust rather than normal aerodynamic forces and moments. The coefficient data as shown in this report have been reduced to a constant q value for each run thereby minimizing the amount of scatter due to the variation of q within a single run. The single value of q used is that based upon the specified test value of velocity for each run. Figure 157 gives a typical comparison of the coefficient data as presented by Ames using the individual q values for each test point and the coefficient data based upon a constant q throughout the entire run. To be consistent, all of the coefficient data are based upon the constant q value for each run.

VII. ANALYSIS OF THE CONVENTIONAL FLIGHT DATA

Since the Hummingbird has flight and handling characteristics similar to any other aircraft in the normal or conventional flight regime, the coefficient form of the wind tunnel data is used for this analysis. Figure 158 is a tabulation of the stability and control levels indicated by the full scale data in the conventional flight configuration and corresponding estimates based upon the results of the small scale wind tunnel tests of Reference 1. All of the normal aerodynamic parameters of interest are tabulated. A comparison of the two sets of data, point by point, indicates good agreement for the lift and side force coefficients. The agreement between the other components is somewhat poorer.

Although the agreement between the pitching moment coefficients is not very good for the power-off test, the agreement with power on is quite good except for the C_{M_o} value. The disagreement shown in the C_{M_o} values is probably due to the pitching moment caused by the drag of the unshielded rear strut. Using a C_{D_o} value of 1.18 for the drag coefficient of the circular rear strut as shown by Reference 3, an average diameter of 6 inches, a length of 20 feet, and the center of the strut drag 10 feet (d_1) below the Hummingbird center of gravity, an estimate of the generated pitching moment coefficient is as follows:

$$M = -D \times d_1 = -10D = -10\ C_D\ q\ S_{strut}$$

$$M = -10\ C_D\ q\ (20 \times 0.5) = -100\ C_D\ q$$

$$C_M = \frac{M}{q\ S_w\ \bar{c}_w} = \frac{M}{q\ (104.2)\ (4.43)} = \frac{-100\ C_D\ q}{q\ (104.2)\ (4.43)}$$

$$C_M = -0.217\ C_D = -0.217\ (1.18) = -0.256$$

$$C_M = -0.256$$

The data of Figure 158 show a difference in C_{M_o} of -0.358 between the full scale wind tunnel data and the estimates from the small scale wind tunnel data. A large

percentage of the discrepancy in C_{M_o} can be accounted for by considering the moment due to the rear strut drag in conventional flight. A forty percent increase in the rear strut drag over the above calculated value would give complete agreement.

A similar analysis of the effect of the rear strut drag on the directional stability (C_{N_β}) follows:

$$D = C_D \, q \, S_{strut} = 1.18 \, (10) \, q$$

$$N = D \, l_t \sin \beta = 11.8 \, q \left(\frac{133.6}{12}\right) \sin \beta$$

For small angles,

$$\sin \beta = \beta / 57.3$$

where β is in degrees, and

$$N = 11.8 \, q \left(\frac{133.6}{12}\right) \beta / 57.3 = 2.293 \, q \, \beta$$

$$C_N = 2.293 \, q \, \beta / q S_w b_w = \frac{2.293 \, \beta}{(104.7)\,(25.0)} = 0.00088 \, \beta$$

$$C_{N_\beta} = 0.00088/\text{Deg.}$$

This analysis indicates that the level (0.0045) shown for the full scale wind tunnel test data is too great by the 0.0009 value. A reduction by this amount gives a C_{N_β} level of 0.0036 as compared to 0.0030 for the small scale value. If the forty percent increase in the rear strut drag to give complete agreement for the C_{M_o} value is used, the C_{N_β} value becomes 0.0033 for the full scale wind tunnel tests which is good agreement.

The poor agreement, power off, may be partially explained by the change in the flow pattern about the aircraft due to the windmilling engines. The small scale model actually had open, free flow type nacelles, and the internal drag of the nacelle

system was removed from the wind tunnel data. Unfortunately, most of the full scale data were run with the engines windmilling rather than power on. All of the lateral directional tests were made with engines windmilling.

Little flight test data are available for comparison with the wind tunnel data of the conventional flight configuration. However, based upon pilot comments and observations, the flight characteristics of the Hummingbird tend to more nearly substantiate the estimates based upon the equation data derived from the small scale wind tunnel test data rather than the values obtained from the full scale wind tunnel data. The trim elevator settings required for the Hummingbird correspond more nearly with the small scale data, but good correlation with the full scale data can also be obtained if the above correction to C_{M_O} is made for the effect of the drag of the unprotected rear strut.

VIII. ANALYSIS OF THE HOVER AND TRANSITION DATA

All of the hover and transition data from the full scale tests of the Hummingbird are given in Figures 159 through 266 in terms of forces and moments rather than in coefficient form. This form of presentation is used for these data since the forces and moments are primarily a result of ejector thrust rather than the result of normal aerodynamic effects, and is considered more meaningful than the coefficient form. In addition, the equations of Reference 1, used to predict the Hummingbird characteristics in hover and transition, are written in terms of forces and moments rather than in the coefficient form. Values determined from these equations for the full scale wind tunnel test conditions are also plotted on Figures 159 through 266 for comparison with the actual full scale wind tunnel data. These calculated forces and moments are based on a net ejector hover thrust of 6650 pounds for sea level day take-off thrust on the two JT-12 engines installed in the aircraft.

The pitch reaction controls under these design conditions produce a thrust of 450 pounds which, when added to the net ejector thrust value, gives a net airplane thrust equal to 7100 pounds as shown in the data of Figure 267. This is the value obtained when the test data are extrapolated to the take-off thrust engine pressure ratio of 2.28. The lift and drag values of the four runs have been combined to give the resultant force curve shown in this figure. With everything considered, the data show a surprisingly small mount of scatter. However, the net ejector static thrust value of 6650 pounds at the design engine pressure ratio of 2.28 is 750 pounds less than the value of 7400 pounds which has been shown for the same ejector configuration on tests in the Lift Improvement Program conducted at the Lockheed-Georgia Company. The possibility of a small difference in the primary nozzle area of the manifolds of the two tests and some small secondary configuration differences exist which may account for some of the difference in these thrust values.

The 750 pound discrepancy in net ejector static thrust also may be partially explained by the vertical component of the ejector exit flow along the unshielded rear wind tunnel support. The moment generated by this negative lift force is positive or nose up which is opposite to the net moment generated as compared with the Lift Improvement Program data. However, the drag force on the rear strut generated by the horizontal component of the ejector exit flow acts at a larger arm near the wind tunnel floor giving a negative moment. With a drag force of the same order of magnitude as the negative lift on the rear strut, the pitching moment from drag is approximately twice that generated by negative lift. Although exact values cannot be placed on these effects, both the lift deficiency and the change in pitching moment can be generated by forces acting on the unshielded rear wind tunnel support even in the hover mode.

The value of net ejector thrust used in the small scale equations was the 6650 pound level indicated by the static test in the full scale wind tunnel. This value seems to match the lift data observed on the transition tests more nearly than would the 7400 pound thrust level. The use of this lower value also gives a more conservative comparison with the full scale wind tunnel results. A limited quantity of flight test data have been reduced. These values are shown on the corresponding plots of full scale wind tunnel data of Figures 217, 233, and 243.

The aerodynamic characteristics of the Hummingbird as predicted by the equations based on the small scale wind tunnel data of Reference 1 do not include the effects of the reaction controls. The reaction control effects are evaluated separately and added to the equation values. Figure 268 presents the reaction control pitching moments available as a function of elevator deflection for the two constant engine pressure ratios used throughout the test. The engine pressure ratio of 1.53 corresponds to a tailpipe pressure, P_{t_5}, of 46 inches of mercury and the pressure ratio value of 1.99 corresponds to a P_{t_5} value of 60 inches of mercury. These

engine pressure ratios are based on the average ambient pressure of 30.1 inches of mercury as observed during the test.

The yawing moments produced by reaction controls as a function of rudder deflection are shown in Figures 269 and 270 for fixed elevator deflections and for the two normally tested engine pressure ratios. The yawing moments are presented for the various elevator deflections which cover the test range to give the effect of the pitch reaction control on the yawing moment.

Figure 271 presents the rolling moment available from reaction control as a function of aileron deflection. The same two values of engine pressure ratio are used for these data.

All of the reaction control moments presented in these figures are based on the calibration curves for the aircraft as tested and on the respective gas flows for the particular reaction control corresponding to the test engine pressure ratio. The reaction control gas flows are based upon previously determined values for an engine design pressure ratio of 2.28. The estimated values of gas flow were used since the values which could be determined from the data presented on the readout panel during the test are open to question. The test values are questionable because time was not allowed for some test pressure gages to reach steady state values. The time required for some of the gages was quite large and was not expended in an attempt to obtain as many runs as possible during the limited span of the test.

The data of Figures 208 through 213 compare the actual reaction control effectiveness obtained in Run 39 for the Hummingbird as tested, with the values evaluated for addition to the small scale equations as described above. The pitching moment available from reaction control shows excellent agreement with the test data of Figure 208; however, at the high elevator deflections, some discrepancy does exist.

The agreement shown in Figure 211 for the reaction control in roll is acceptable, but the test data have been displaced through zero aileron deflection by approximately 2700 foot-pounds, and the test reaction control is not as effective for the negative aileron deflections. Figure 213 shows a slightly higher effectiveness from the yaw reaction control as determined for addition to the small scale equation data than the value obtained from the actual test points. However, the computed values are certainly within acceptable tolerances.

The pitch reaction control duct pressure data of points 12 through 17 of Run 26 indicate total pressure duct losses approximately equal to those originally estimated. These same points are used to evaluate the boom angle of attack and airspeed indicators. Of the six points, four show perfect correlation with wind tunnel angle of attack and the other two indicate 1/2 of a degree low. Half of the points indicate perfect agreement with the wind tunnel airspeed; the other half indicate 1/2 of a knot low.

An examination of the total duct pressures of the roll reaction control system of Run 18 indicates reasonable agreement with the expected values. No attempt to completely analyze the roll reaction control system is made because the duct q data are open to question. As mentioned above, these are the gages which were slow to indicate steady state values.

Each plot in this section of the report is not analyzed individually since comparative data are plotted on each figure. In general, the agreement obtained from the lift data is good between the full scale test and the data based on the small scale equations. For some test conditions, the equation data give slightly higher values of lift than do the full scale wind tunnel data; and for other test conditions, the reverse is true with the full scale wind tunnel data indicating higher values of lift. As mentioned previously, the equation data are based on a net ejector

thrust value of 6650 pounds rather than the 7400 pound level indicated in the Lift Improvement Program data. The possible reason for this 750 pound deficiency is discussed above.

The agreement obtained between the two sets of drag data is not as good as that obtained for the lift data. Except for a very few cases, the drag values obtained from the full scale wind tunnel data are greater than those obtained from the equation data. This higher drag value for the aircraft is easily explained when the condition of the airplane as tested is compared with the condition of the model on which the small scale equations are based. A general cleanup of the aircraft would certainly give an appreciable reduction in its drag level and produce a better agreement between the two sets of data. The influence of the ejector flow on the drag of the rear support strut is also reflected in this comparison.

A comparison of the side force data obtained from the test completes the picture so far as force data are concerned. Similar to the lift analysis, good agreement is obtained between the full scale wind tunnel data and the side force data based upon the equations derived from the small scale wind tunnel test data. Although the side force data are, in general, quite good, there are a few cases where the side forces do not pass through zero, but at zero sideslip, are offset by an appreciable amount parallel to the predicted levels. In other cases, a discontinuity in side force is shown for sideslip angles close to zero.

With generally good agreement of all of the force data, the same would be expected of the moment data, but this is not the case. A comparison between the two sets of pitching moment data indicates a somewhat higher stability level for the full scale wind tunnel test results and the total nose up pitching moment is shown to be less. Because of these two factors, although a reduction in the control effectiveness in pitch is indicated, the elevator angle required to trim under all test conditions

is less than that shown by the equations based on the small scale wind tunnel tests. A comparison of the elevator effectiveness (M_{δ_e}) through the mid deflection range indicates fairly good agreement between the two sets of data. However, the total effectiveness (total pitching moment produced in going from zero to maximum elevator deflection) shown by the full scale data is considerably less than that indicated by the equations. Some of this reduction in total elevator effectiveness is certainly due to the rigging of the control system so that the reaction controls tend to level off at a moderate deflection of the elevator.

Detailed analysis of the data by removing the reaction control effects indicates that the elevator alone is tending to reach its maximum effectiveness point at a relatively low deflection. For angles beyond 35 to 40 degrees, the additional pitching moment available with increasing elevator deflection appears to be quite small. This effect is hard to explain since observations of tufts on the horizontal tail indicated that the complete tail, including the elevator, was effective at large elevator deflections and large angles of attack of the aircraft. In spite of this reduced effectiveness, the pitch control system is shown capable of trimming the aircraft throughout the complete angle of attack range investigated. This included high angles of attack in the so-called deep stall regime.

In attempting to explain differences in the pitching moment data, discussions with Ames personnel indicated that the moment reference point used for data reduction was 2.6 inches ahead of the actual location of this point as tested. The original data from the test indicated an even higher longitudinal stability level than that shown by the data of this report since these data have been corrected for the 2.6 inch change in reference point. The effect of changing the data by this amount is the same as shifting the reference point 2.6 inches aft without changing the notation for the new location. The pitching moment data and all other moment data are still presented about the 10 percent mean aerodynamic chord point.

The difference of 2.0 inches consists of three small changes in the apparent dimensions. The attachment holes for the ball and socket attachments to the main mounting pads supplied with the Hummingbird were not located at the points originally intended. The use of the 10 degree wedge between the socket attachments and the mounting pads also changed the locations of the balls and sockets relative to the airplane. An error of an additional one inch was found in a basic dimension used in the data reduction equations. Lengthy examination revealed no other dimensional changes of the location of the airplane in the full scale wind tunnel. However, lost motion in the actuation system and connections of the support system could possibly account for some small differences in this area.

The conventional flight data, as presented in this report which includes the 2.0 inch change in the location of the Hummingbird within the tunnel, indicate excellent agreement in the longitudinal stability levels for the tests with power on. The only serious discrepancy in the comparison for this condition is the pitching moment coefficient for zero lift at zero elevator deflection. Most of this difference is explained by the drag of the unshielded rear strut. Everything else on this run tends to verify the revised location of the reference point of the airplane within the full scale tunnel.

Some of the remote readout panel data have been read for the tail angle of attack values indicated by the vane located on the boom ahead of the horizontal tail. Points from some of the transition tests were read and supplied by Ames personnel. In addition, some of the conventional flight values have been read in an attempt to explain some of the discrepancies in the pitching moment data. The reading accuracy of only ± 1.5 degrees when coupled with the general erratic nature of the downwash values obtained from the tail angle of attack indication makes the

data most questionable, and none of these data are presented in this report. A random single point downwash value, no matter how accurate, is not indicative of the average effective downwash field experienced by the horizontal tail.

In Phase I of transition the lateral and directional stability levels were tested only at the lower thrust level corresponding to a P_{t_5} of 46 inches of mercury. No lateral-directional tests were made in the Phase II configuration. The Phase I test results indicate increased stability levels in both the lateral and directional modes as compared to the levels predicted from the small scale tests. The indicated increase in directional stability can be accounted for by drag of the rear mounting strut as shown in Section VII. The indicated increase in lateral stability or dihedral effect is more difficult to explain. Although no direct effect of the unshielded rear strut on rolling moment has been isolated, an induced effect similar to those in pitching and yawing moments is not out of reason since the ejector exit flow induces angularity to the flow at the rear strut as the airplane is pitched and yawed.

In some of the tests, the data indicate that there is a discontinuity in both rolling moment and yawing moment through zero sideslip angle. In performing the yaw test, the aircraft was generally yawed from zero in one direction, returned to zero and yawed in the opposite direction, and finally returned to the zero yaw condition. By running the yaw test in this manner, the zero condition was approached from opposite directions during each run. Any lost motion in either the drive mechanism or the angle of yaw indication mechanism would result in a discontinuity of the data through zero, since the Hummingbird actually would be at a slightly different angle in the tunnel when a zero yawed condition is indicated.

Both lateral and directional control effectiveness data were run for all test conditions in Phase I of transition except at the extreme speed and thrust condition

of 70 knots for an EPR of 1.99. The only lateral directional control effectiveness tests performed in Phase II were at 100 knots and at an EPR of 1.99. In general, the lateral directional control effectiveness data obtained in the full scale wind tunnel tests are in agreement with those predicted by the equations based on the small scale wind tunnel tests. Some minor differences do exist in a few cases. However, the only significant difference indicated by the full scale wind tunnel data is the reduction in aileron effectiveness including the reaction control with negative deflection of the aileron. In most tests, this reduction in aileron effectiveness for negative deflections was quite pronounced, and in many cases the effectiveness actually went to zero. The only logical explanation of this effect was that some portion of the roll control system must have malfunctioned during the test.

Checks of the roll reaction control valves following the test indicated that the upward pointed valves under certain conditions could go into an overcenter control lever position. Under this condition, the affected roll control valve would remain at essentially a full open condition although the aileron was returned to its neutral position. Deflection of the aileron to a negative position would cause the valve to move toward its closed position. Evidence of such an overcenter condition was found for the upward pointing valve on the right wing tip. This evidence consisted of a bent place in the bullet fairing which houses the roll control valves. The size of the dent indicates that full down travel of the right aileron probably occurred with the roll control valve in the overcenter position.

The magnitude of the discrepancies observed in some cases cannot be explained entirely by this overcenter condition. Although the right upward pointed reaction control valve would be the one involved with a negative deflection of the ailerons, other minor malfunctions in the roll control system or in the wind tunnel force

readout system could have been associated with this condition also.

Although the control effectiveness level appeared good, in some cases the lateral directional data indicate a constant shift in the side force, rolling moment, or yawing moment levels occurred throughout the complete run. In other words, the full scale data show a control level parallel to that predicted from the small scale data but displaced by a constant increment. When this occurred in one component, one of the others usually indicated the same trend. The conclusion drawn is that one of the wind tunnel force readouts must have malfunctioned or shifted slightly during each of these tests. Normally, the magnitude of this shift is well within a reasonable change in force level.

The data of Run 41 plotted in Figures 261 through 266 indicate that such a shift or displacement occurred throughout the lateral directional control effectiveness portion of this run which was made with a constant foul indicated on the balance system. For the aileron effectiveness portion, a shift is observed in all three components: side force, yawing moment and rolling moment. Similar shifts occurred during the directional control effectiveness portion of this run. A comparison of these data indicate that the same shift, magnitude-wise, occurred in both sets of data for each component. The same thing occurred on a few other runs, but in general, only two out of the three components would be affected by this constant shift. The data so affected still appears to be valid so long as this shift is recognized. In many cases, the value of the shift which occurred is well within the accuracy expected of such a test.

With the exceptions noted, the agreement between the full scale wind tunnel test data and the data predicted by the equations based on the small scale test data are good. A slight change in the horizontal tail incidence of the aircraft or a minor change in the downwash field at the horizontal tail, coupled with the pitching

moment due to the drag of the unshielded rear support, accounts for the differences indicated in the pitching moments for zero lift at zero elevator deflection. The changes in stability level throughout Phases I and II of transition are not too alarming, nor are the orders of magnitude too great. The reduction in total effectiveness of the pitch control system going from zero elevator deflection to full elevator deflection is completely unexplained, but the level indicated by the full scale data still provides adequate control capability for the aircraft.

In general, nothing was indicated by the full scale wind tunnel test which would have prevented the aircraft having been flight tested throughout the transition regime, had the data been collected previous to the actual attempts. However, a more extensive or exhaustive examination of the data would certainly have been in order, since the differences between the full scale wind tunnel tests and the data derived from the small scale equations are partially unexplained in some areas. The largest discrepancy, of course, is in the net ejector lift value which was determined for the static test and used in the small scale equations data comparison for the other tests throughout transition. The shift in the zero lift value of pitching moment and the reduction in the overall value of reaction control in pitch are disturbing. The fact that the data indicate that successful transitions are completely feasible was verified by the number of transitions made in actual flight test.

IX. REFERENCES

1. Barnes, G. J., Jr., "The VZ-10 Hummingbird 0.19 Scale Model Wind Tunnel Test Results." Lockheed-Georgia Company ER-5623, April, 1962.

2. NACA, "Guide for Planning Investigations in the Ames 40- by 80- Foot Wind Tunnel," Ames Aeronautical Laboratory, January, 1957.

3. Hoerner, Sighard F., Fluid-Dynamic Drag. Published by the Author, 1958.

FIGURE 3

THEORETICAL AERODYNAMIC DATA

Wing	
Area	104.17 ft.
Aspect Ratio	6.0
Span	25.0 ft.
Flap Area	13.02 sq. ft.
Aileron Area	4.28 sq. ft.
Sweep at 50% Chord	0
Root Chord	72.0 in.
Root Airfoil	64_A012
Root Incidence	1.5°
Tip Chord	28.0 in.
Tip Airfoil	64_A212
Tip Incidence	1.5°
M.A.C. Length	53.23 in.
Vertical Tail	
Area	21.93 sq. ft.
Aspect Ratio	1.194
Span	61.414 in.
Rudder Area	4.59 sq. ft.
Root Chord	66.0 in.
Tip Chord	36.85 in.
Sweep at 25% Chord	32° 8'
Airfoil	64_A012
M.A.C. Length	52.491 in.
Volume Coefficient	0.1098

FIGURE 3 (Continued)

Horizontal Tail

Area	26.44 sq. ft.
Aspect Ratio	[illegible].303
Span	128.0 in.
Elevator Area	5.29 sq. ft.
Root Chord	42.5 in.
Tip Chord	17.0 in.
Incidence	0
Airfoil	0010-2.00 - 40/1.575
M.A.C. Length	31.5[illegible]1
Volume Coefficient	0.895

FIGURE 5

TABLE OF SYMBOLS

b	theoretical wingspan (25.0 ft.)
$\bar{c}$	mean aerodynamic chord (4.43 ft.)
C_D	drag coefficient (D/qS)
C_L	lift coefficient (L/qS)
C_l	rolling moment coefficient l/qSb)
C_m	pitching moment coefficient (M/q S)
C_n	yawing moment coefficient (N/qSb)
C_y	side force coefficient (Y/qS)
D	drag (lb, aft positive)
L	lift (lb, up positive)
l	rolling moment (ft-lb, right wing down positive)
M	pitching moment (ft-lb, nose up positive)
N	yawing moment (ft-lb, nose right positive)
Y	side force (lb, right positive)
EPR	engine pressure ratio (P_{t_5}/P_a)
P_a	ambient pressure (in. Hg)
P_{t_5}	engine tailpipe pressure (in. Hg)
q	dynamic pressure ($1/2\ \rho V^2$, lb/ft^2)
S	wing planform area (104.17 ft^2)
V	airspeed
α	angle of attack (deg, nose up positive)
β	angle of sideslip (deg, nose left positive)
δ_a	aileron deflection angle (deg, trailing edge down positive, total aileron is equal to right aileron deflection minus left aileron deflection)

FIGURE 5 (Continued)

δ_e	elevator deflection angle (deg, trailing edge down positive)
δ_r	rudder deflection angle (deg, trailing edge left positive)
ρ	atmospheric density (lb sec^2/ft^4)
ψ	angle of yaw (deg, nose right positive)

FIGURE 6

RUN SCHEDULE SUMMARY

Run	P_{t_5} (in. Hg)	V (knots)	Phase	Type of Run
1	Varied	Varied	I	Ejector Exit Rake Survey
			II	Ejector Exit Rake Survey
2	Varied	Varied	I	Ejector Exit Rake Survey
			II	Ejector Exit Rake Survey
3	Varied	0	I	Static Run $\alpha = 12$
	46	30	I	Polar
				Elevator Effectiveness $\alpha = 0$
4	46	50	I	Polar
5	46	40	I	Polar
6	46	67	II	Polar
				Elevator Effectiveness $\alpha = 0$
7	46	40	I	Polar
				Elevator Effectiveness $\alpha = -6$
8	46	85	II	Polar
				Elevator Effectiveness $\alpha = 0$
9	46	30	I	Polar
10	46	50	I	Elevator Effectiveness $\alpha = -10$
			II	Elevator Effectiveness $\alpha = 0$
11	46	40	I	Polar
12	46	50	II	Polar
13	46	20	I	Polar
14	46	20	I	Polar

FIGURE 6 (Continued)

Run	P_{t_5} (in. Hg)	V (knots)	Phase	Type of Run	
15	46	50	I	Polar	
				Elevator Effectiveness	$\alpha = 20$
	46	50		Yaw Run	
				Aileron Effectiveness	$\psi = 0$
16	46	20	I	Elevator Effectiveness	$\alpha = 0$
17	46	40	I	Yaw Run	
				Aileron Effectiveness	$\psi = 0$ & 8
				Rudder Effectiveness	$\psi = 0$ & 8
18	60	40	I	Aileron Effectiveness	$\psi = 0$
				Rudder Effectiveness	$\psi = 0$
19	46	30	I	Yaw Run	
20	46	40	I	Polar	
21	46	50	I	Polar	
22	60	30	I	Aileron Effectiveness	$\psi = 0$
				Rudder Effectiveness	$\psi = 0$
	46	30	I	Aileron Effectiveness	$\psi = 0$ & 10
				Rudder Effectiveness	$\psi = 0$ & 10
23	46	20	I	Aileron Effectiveness	$\psi = 0$ & 10
				Rudder Effectiveness	$\psi = 0$ & 10
				Yaw Run	
24	60	50	I	Polar	
				Elevator Effectiveness	$\alpha = 0$ & 20
25	60	[illegible]	I	Aileron Effectiveness	$\psi = 0$
				Rudder Effectiveness	$\psi = 0$

FIGURE 6 (Continued)

Run	P_{t_5} (in. Hg)	V (knots)	Phase	Type of Run
26	60	70	I	Polar
				Elevator Effectiveness $\alpha = 0$
27	60	30	I	Polar
				Elevator Effectiveness $\alpha = 0$
28	30	80	Conventional	Polar
				Elevator Effectiveness $\alpha = 0$
				Aileron Effectiveness $\psi = 0$
				Rudder Effectiveness $\psi = 0$
29	30	40	Conventional	Polar
30	30	80	Conventional	Yaw Run
				Aileron Effectiveness $\psi = 0$ & 8
				Rudder Effectiveness $\psi = 8$
31	30	80	Conventional	Polar
				Yaw Run
				Elevator Effectiveness $\alpha = 0$
				Aileron Effectiveness $\psi = 8$
				Rudder Effectiveness $\psi = 8$
32	Varied	0	Conventional	Power Effects $\alpha = 0$
33	Varied	80	Conventional	Power Effects $\alpha = 0$
	46	80	Conventional	Polar
				Elevator Effectiveness $\alpha = 0$
34	Varied	40	Conventional	Power Effects $\alpha = 0$
35	30	80	III	Polar
				Yaw Run $\alpha = 0$ & 8

FIGURE 6 (Continued)

Run	P_{t_5} (in. Hg)	V (knots)	Phase	Type of Run
36	60	100	II	Polar
37	Varied	0	I	Power Effects $\alpha = -12$
	46	30	I	Polar
				Elevator Effectiveness $\alpha = 0$
38	Varied	0	I	Power Effects $\alpha = 0$
	46	40	I	Polar
	46	40	I	Elevator Effectiveness $\alpha = 0$
				Aileron Effectiveness $\psi = 0$
				Rudder Effectiveness $\psi = 0$
39	Varied	0	I	Power Effects $\alpha = 12$
	60	0	I	Elevator Effectiveness $\alpha = 12$
				Aileron Effectiveness $\psi = 0$
				Rudder Effectiveness $\psi = 0$
40	60	50	I	Polar
				Elevator Effectiveness $\alpha = 0$
41	46	50	I	Polar
				Elevator Effectiveness $\alpha = 0$
	60	100	II	Elevator Effectiveness $\alpha = 0$ & 8
				Aileron Effectiveness $\psi = 0$
				Rudder Effectiveness $\psi = 0$

XV-4A
FULL SCALE WIND TUNNEL TEST 215

POWER EFFECTS ON LIFT IN HOVER

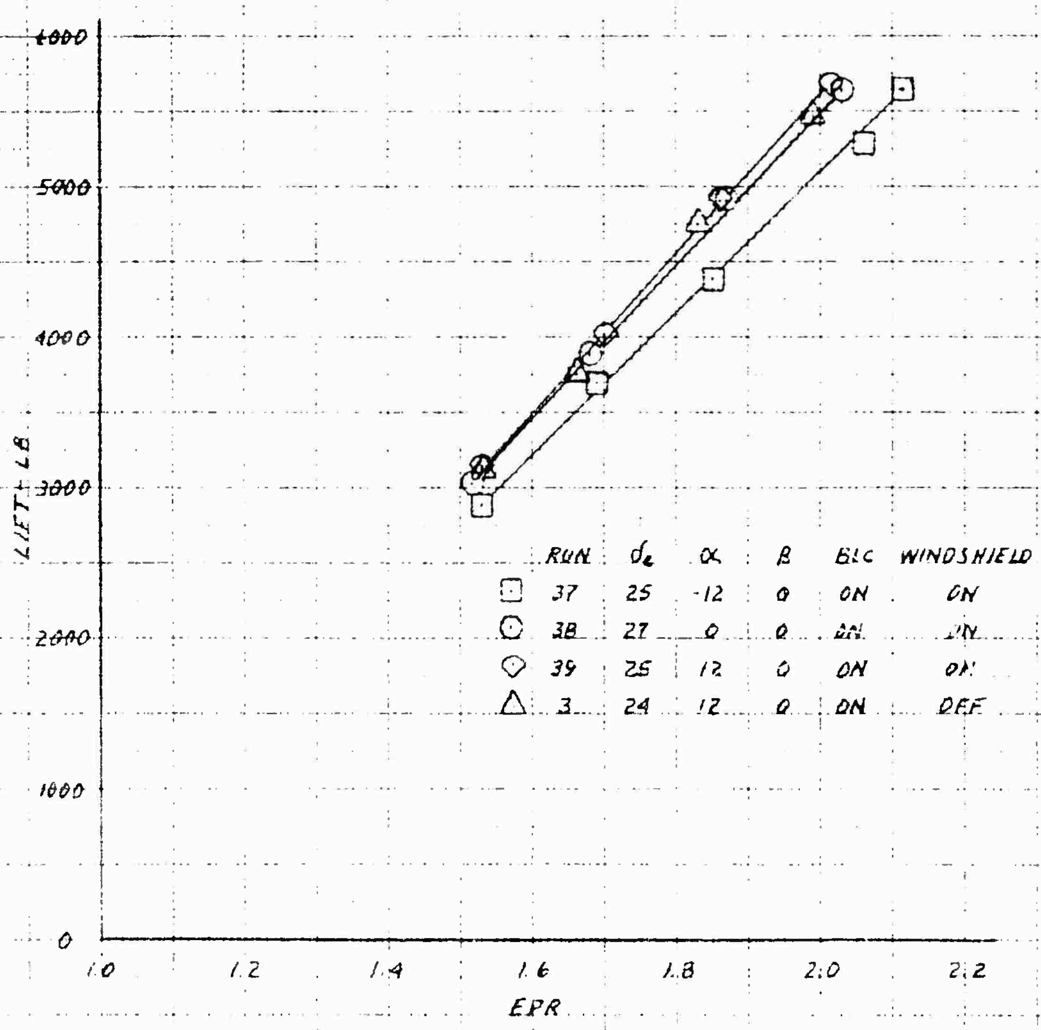

XV-4A

FULL SCALE WIND TUNNEL TEST 215

POWER EFFECTS ON DRAG IN HOVER

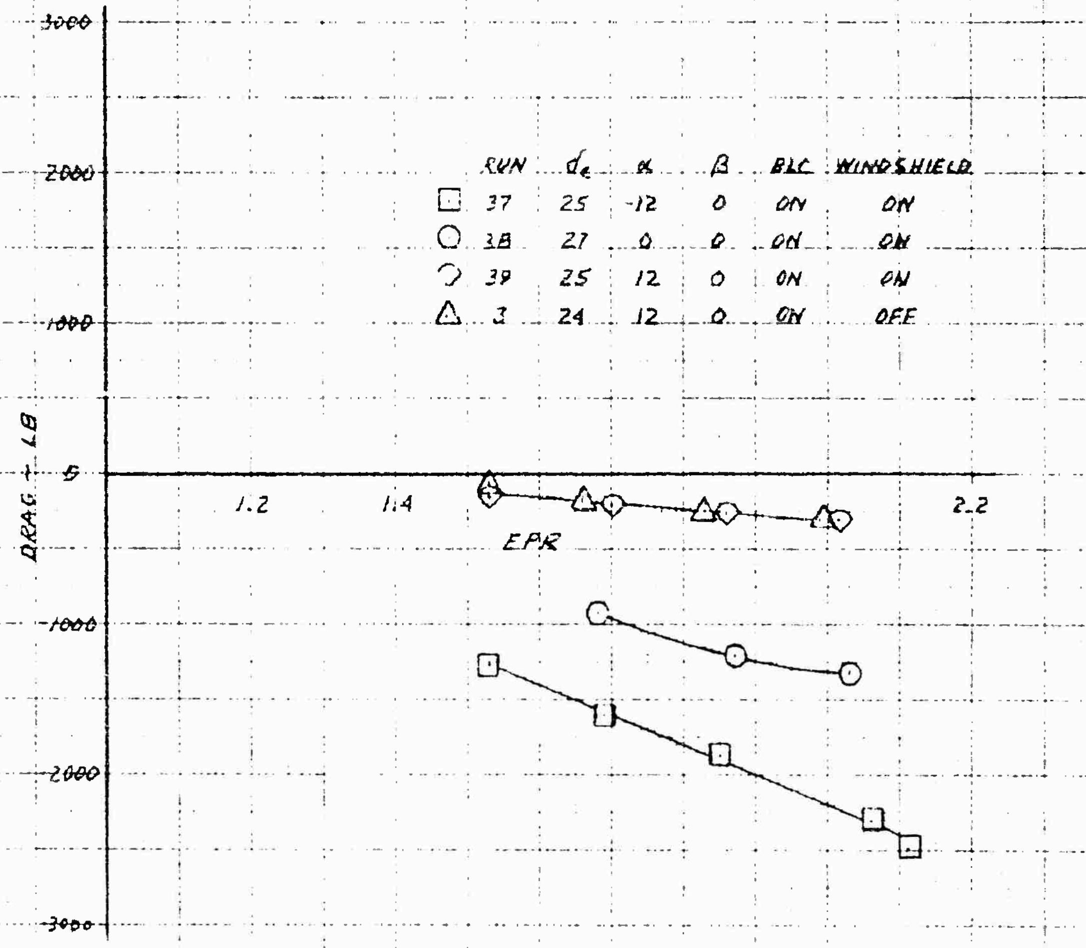

XV-4A
FULL SCALE WIND TUNNEL TEST 215
POWER EFFECTS ON PITCHING MOMENT IN HOVER

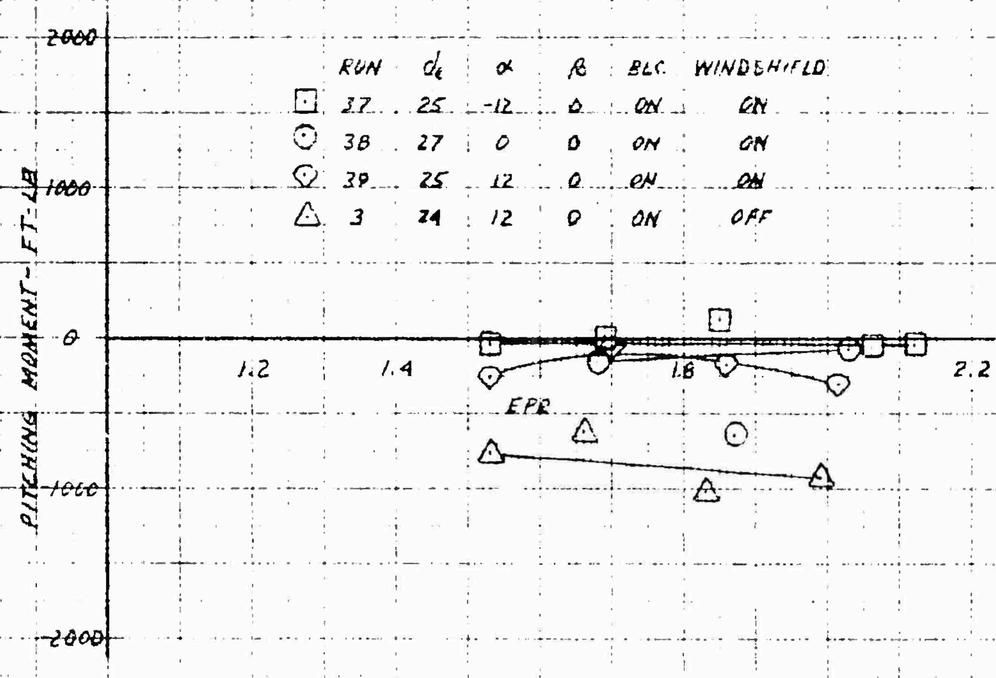

XV-4A

FULL SCALE WIND TUNNEL TEST 215

POWER EFFECT ON LIFT COEFFICIENT IN CONVENTIONAL FLIGHT AT 40 KNOTS

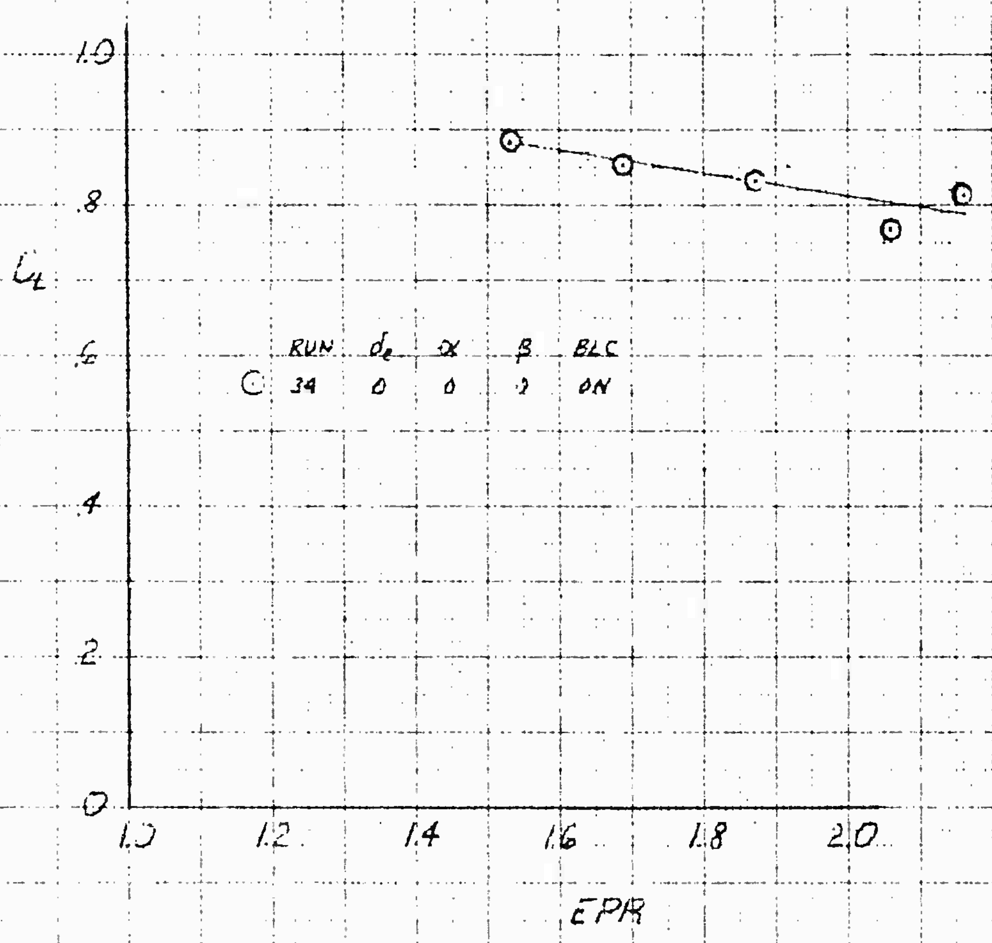

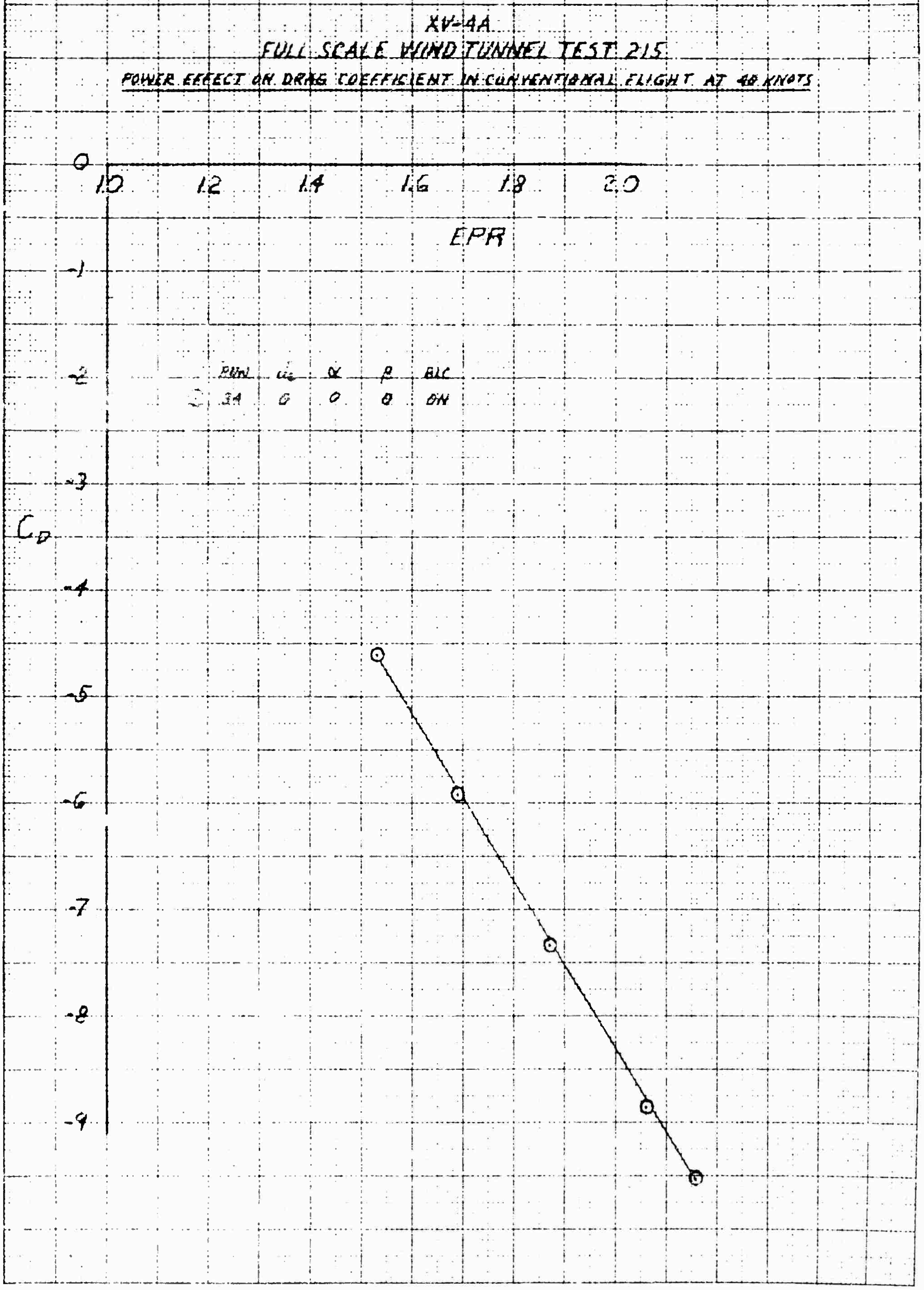
XV-4A
FULL SCALE WIND TUNNEL TEST 215
POWER EFFECT ON DRAG COEFFICIENT IN CONVENTIONAL FLIGHT AT 40 KNOTS
0
1.0
1.2
1.4
1.6
1.8
2.0
EPR
-1
-2
-3
-4
-5
-6
-7
-8
-9
C_D
RUN
i_w
α
β
BLC
34
0
0
0
ON

XV-4A

FULL SCALE WIND TUNNEL TEST 215

POWER EFFECT ON PITCHING MOMENT COEFFICIENT IN CONVENTIONAL FLIGHT AT 40 KNOTS

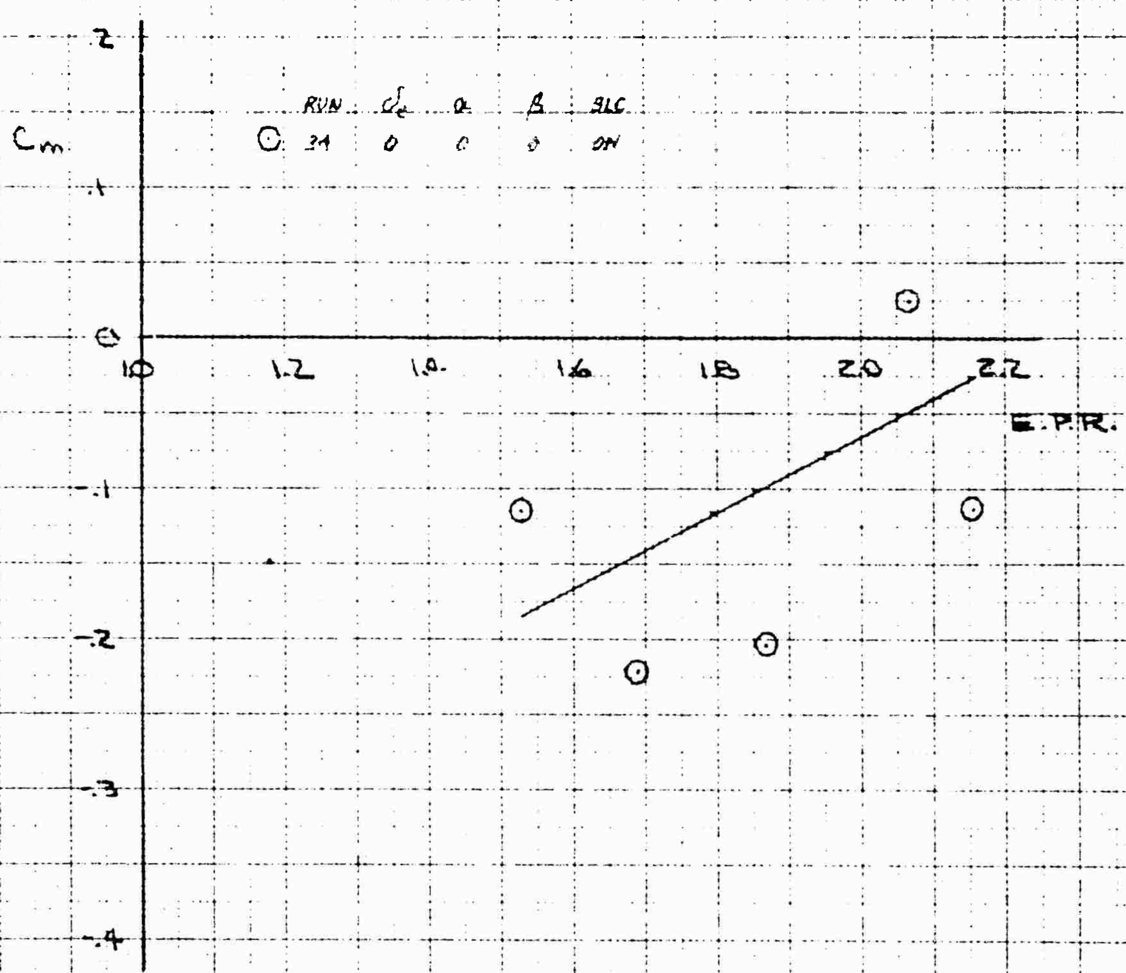

XV-4A

FULL SCALE WIND TUNNEL TEST 215

POWER EFFECT ON LIFT COEFFICIENT IN CONVENTIONAL FLIGHT AT 80 KNOTS

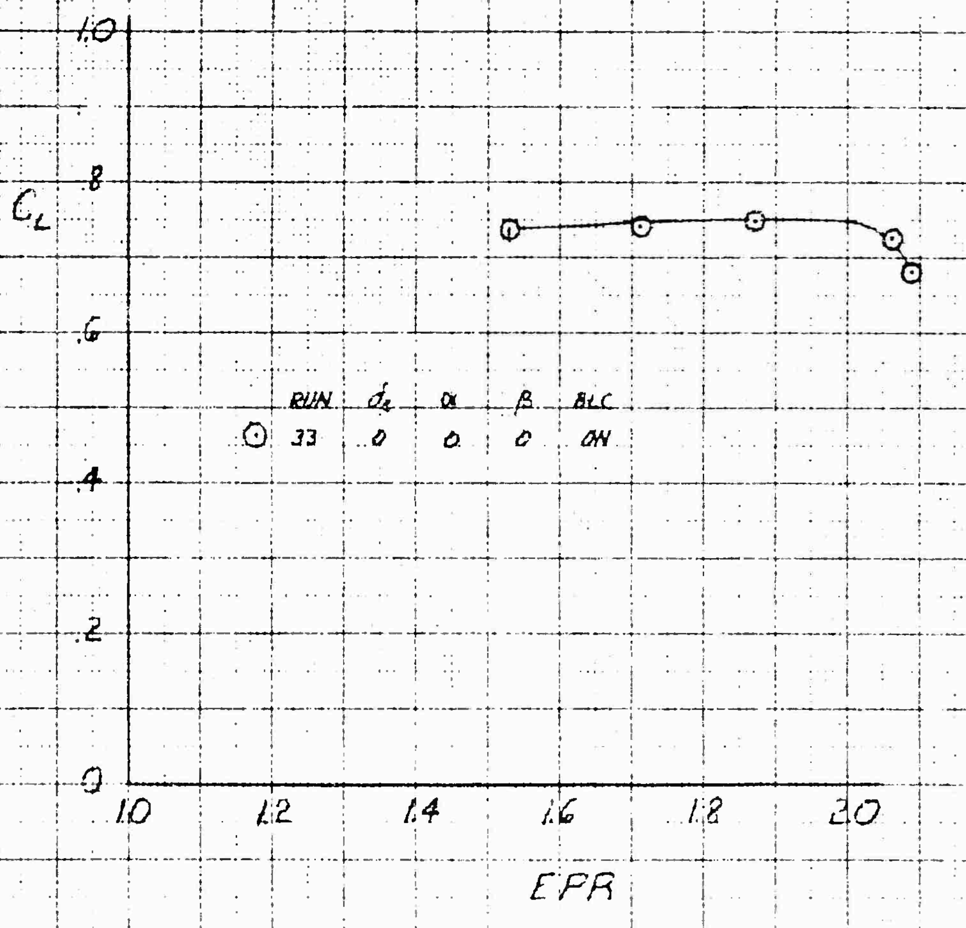

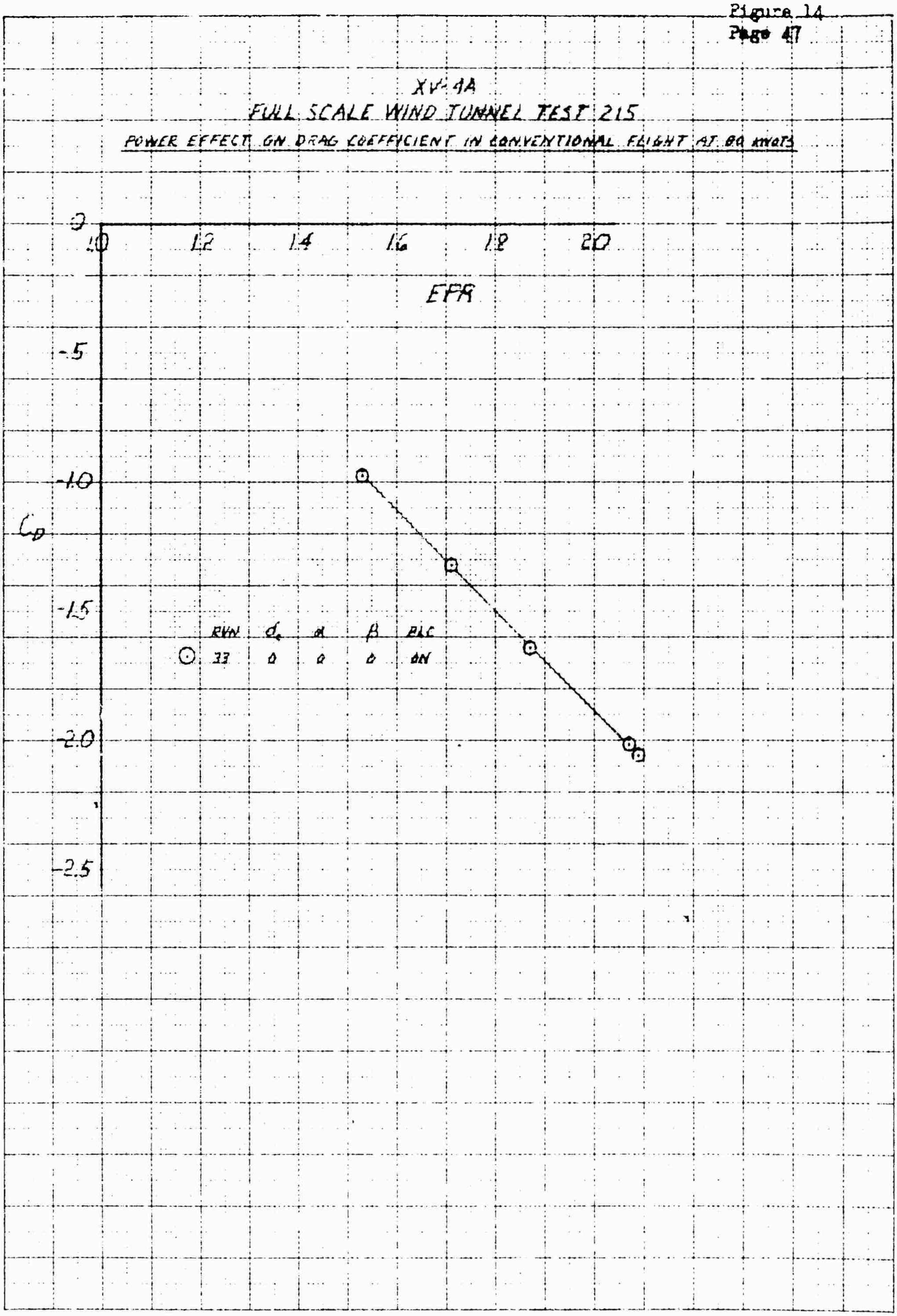
XV-4A
FULL SCALE WIND TUNNEL TEST 215
POWER EFFECT ON DRAG COEFFICIENT IN CONVENTIONAL FLIGHT AT 80 KNOTS
0
1.0
1.2
1.4
1.6
1.8
2.0
EPR
-.5
-1.0
C_D
-1.5
-2.0
-2.5
RUN
δ_e
α
β
BLC
33
0
0
0
ON

XV-4A
FULL SCALE WIND TUNNEL TEST 215
POWER EFFECT ON PITCHING MOMENT COEFFICIENT IN CONVENTIONAL FLIGHT AT 80 KNOTS

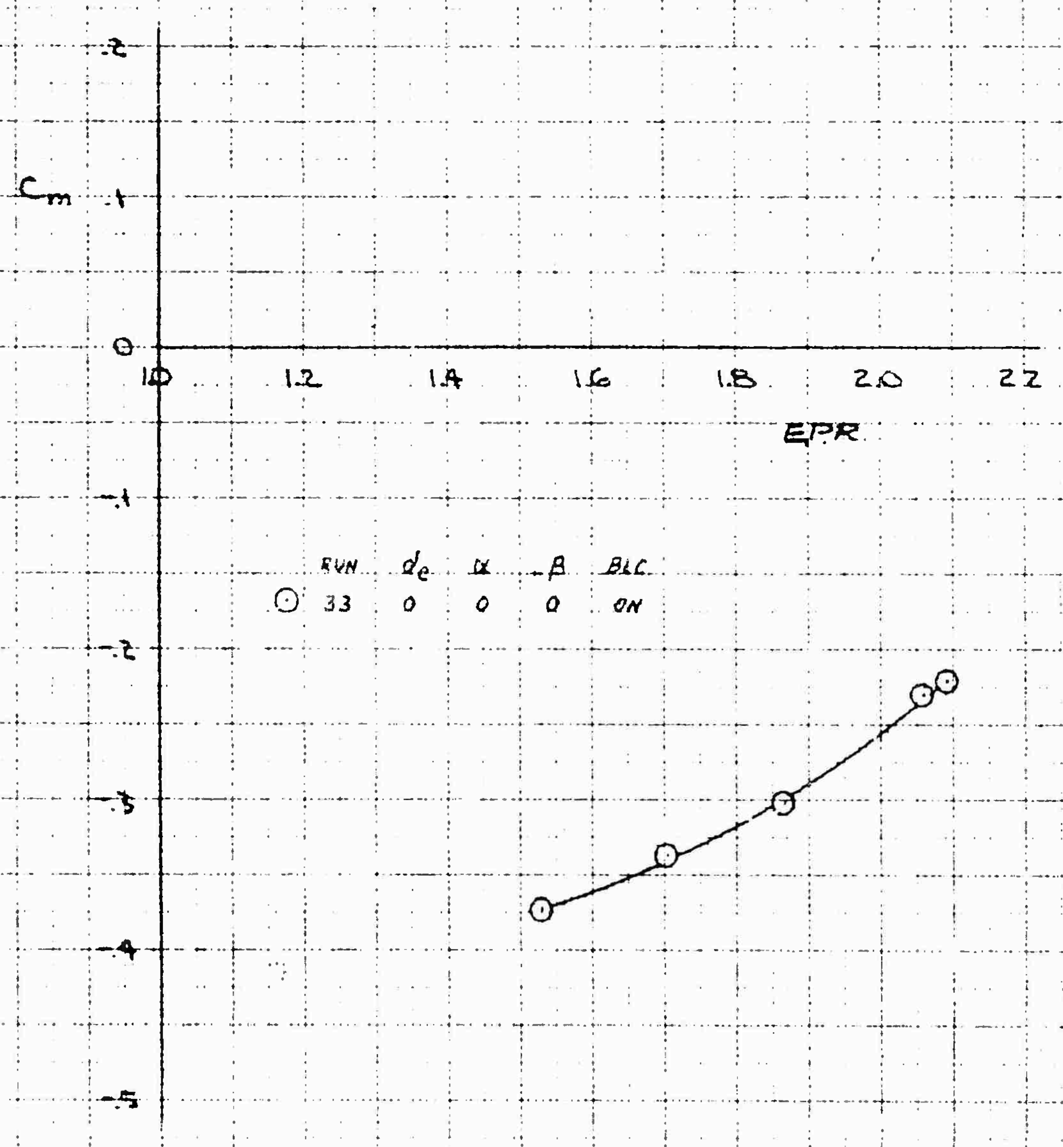

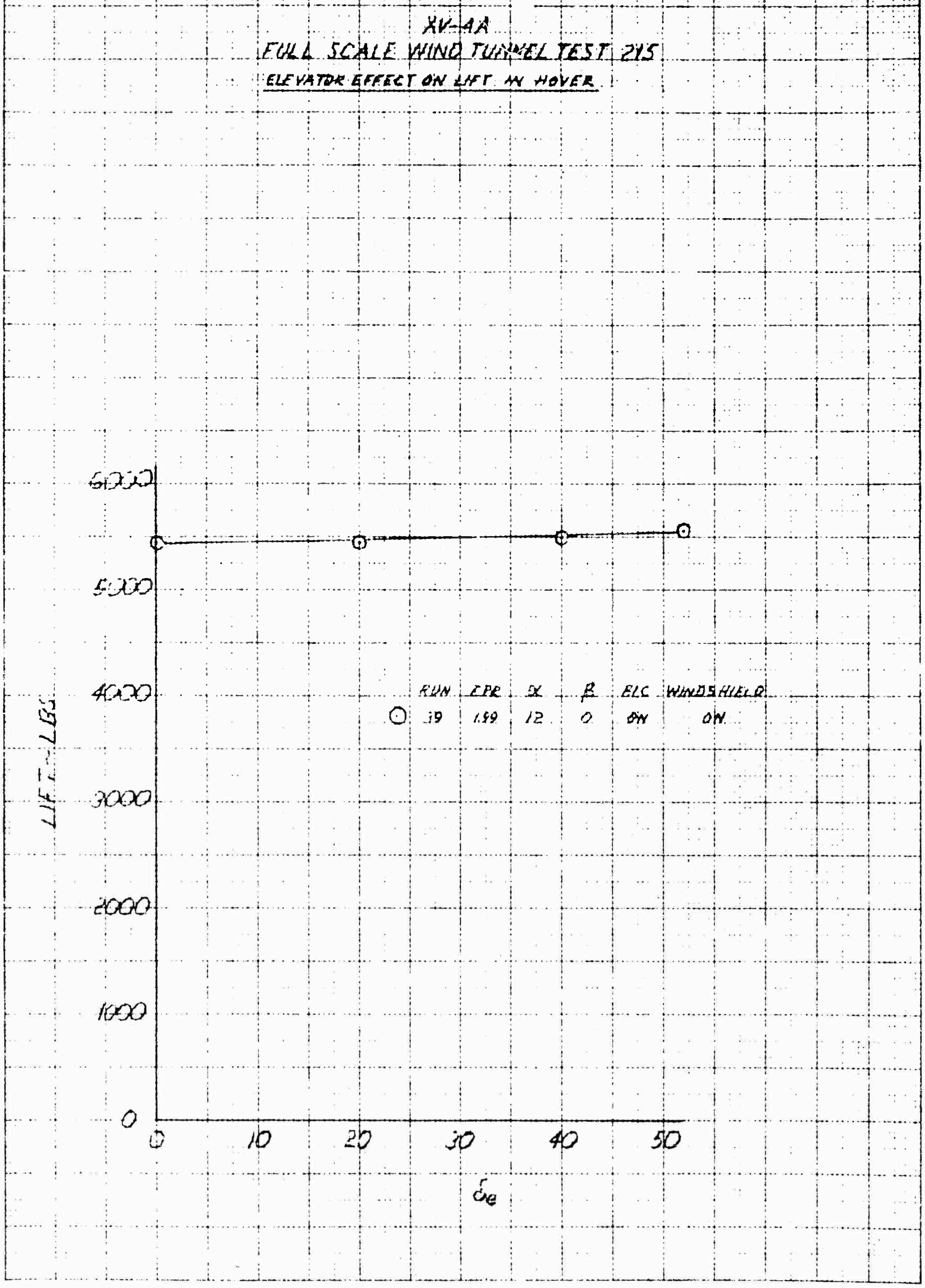
XV-4A
FULL SCALE WIND TUNNEL TEST 215
ELEVATOR EFFECT ON LIFT IN HOVER
LIFT ~ LBS
6000
5000
4000
3000
2000
1000
0
0
10
20
30
40
50
δe
RUN EPR ∑X β ELC WINDSHIELD
39 1.99 12 0 ON ON

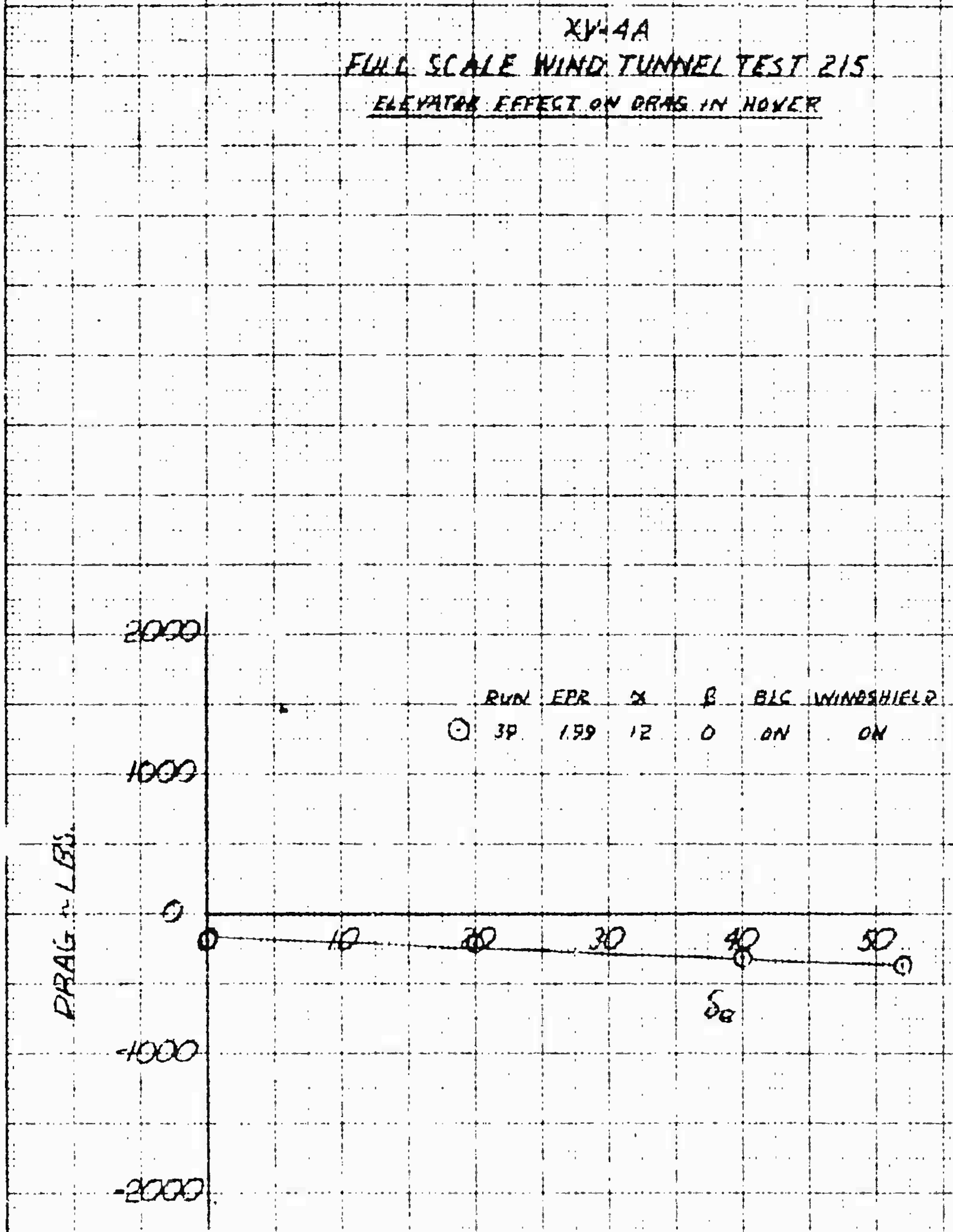
XV-4A
FULL SCALE WIND TUNNEL TEST 215
ELEVATOR EFFECT ON DRAG IN HOVER
RUN EPR α β BLC WINDSHIELD
39 1.99 12 0 ON ON
2000
1000
0
-1000
-2000
DRAG ~ LBS.
0
10
20
30
40
50
δ_e

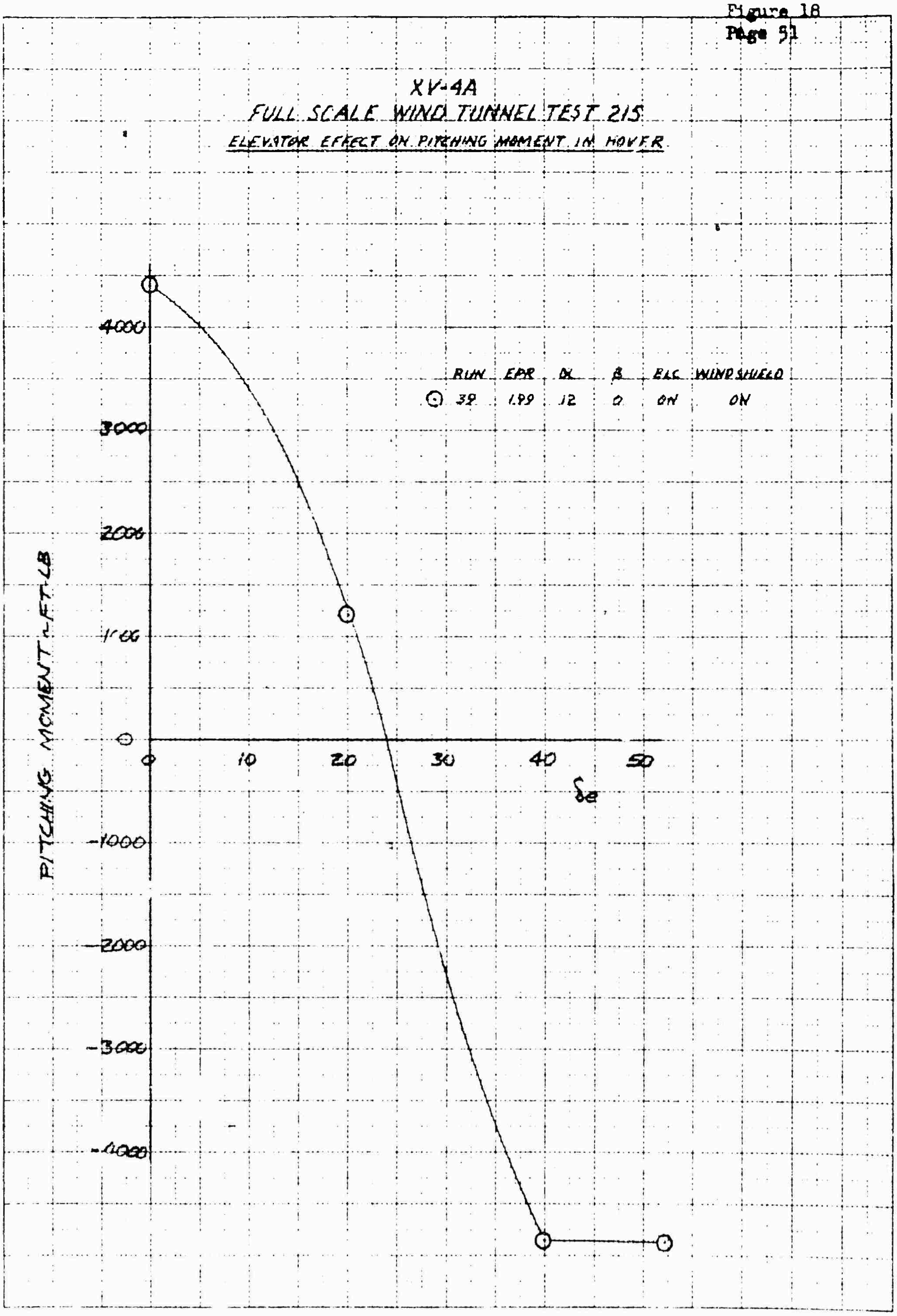
XV-4A
FULL SCALE WIND TUNNEL TEST 215
ELEVATOR EFFECT ON PITCHING MOMENT IN HOVER
RUN EPR α β ELC WINDSHIELD
39 1.99 12 0 ON ON
PITCHING MOMENT ~ FT-LB
4000
3000
2000
1000
0
-1000
-2000
-3000
-4000
0
10
20
30
40
50
δe

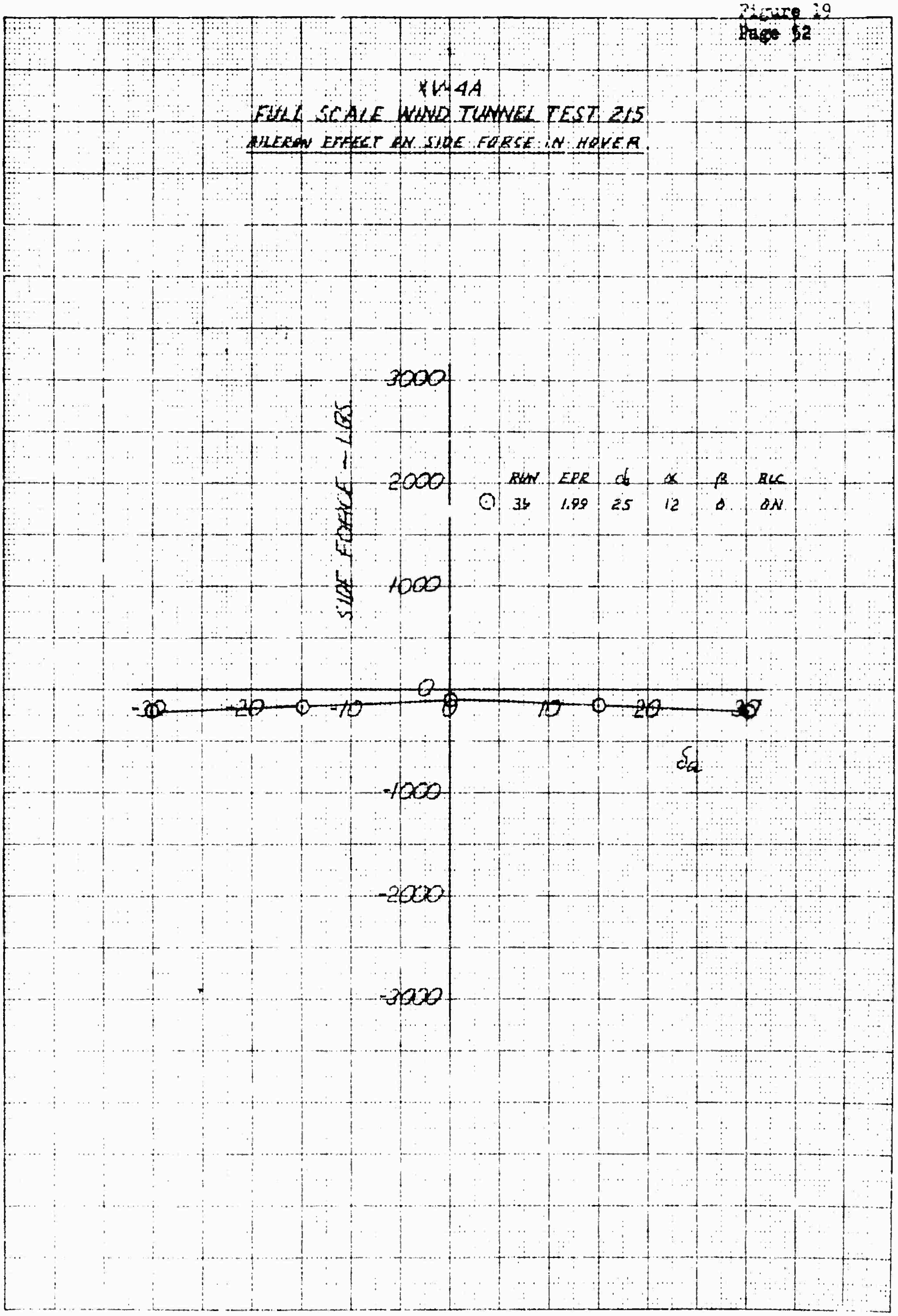
XV-4A
FULL SCALE WIND TUNNEL TEST 215
AILERON EFFECT ON SIDE FORCE IN HOVER
SIDE FORCE – LBS
3000
2000
1000
0
-1000
-2000
-3000
-30
-20
-10
10
20
30
δ_a
RUN EPR δ_f α β BLC
36 1.99 25 12 0 ON

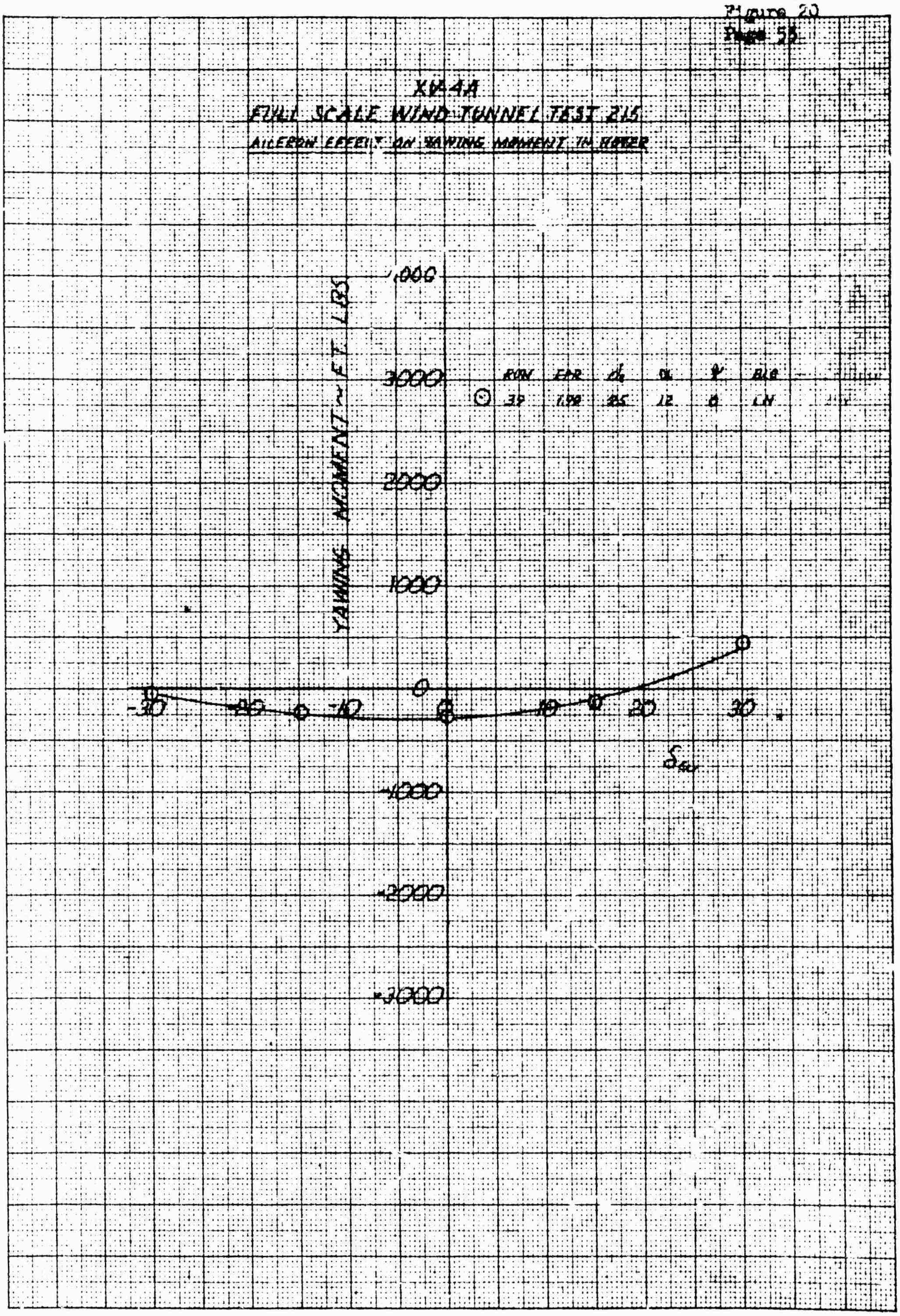
XV-4A
FULL SCALE WIND TUNNEL TEST 215
AILERON EFFECT ON YAWING MOMENT IN HOVER
YAWING MOMENT ~ FT LBS
4000
3000
2000
1000
0
-1000
-2000
-3000
-30
-20
-10
10
20
30
RPM
EPR
12
LH

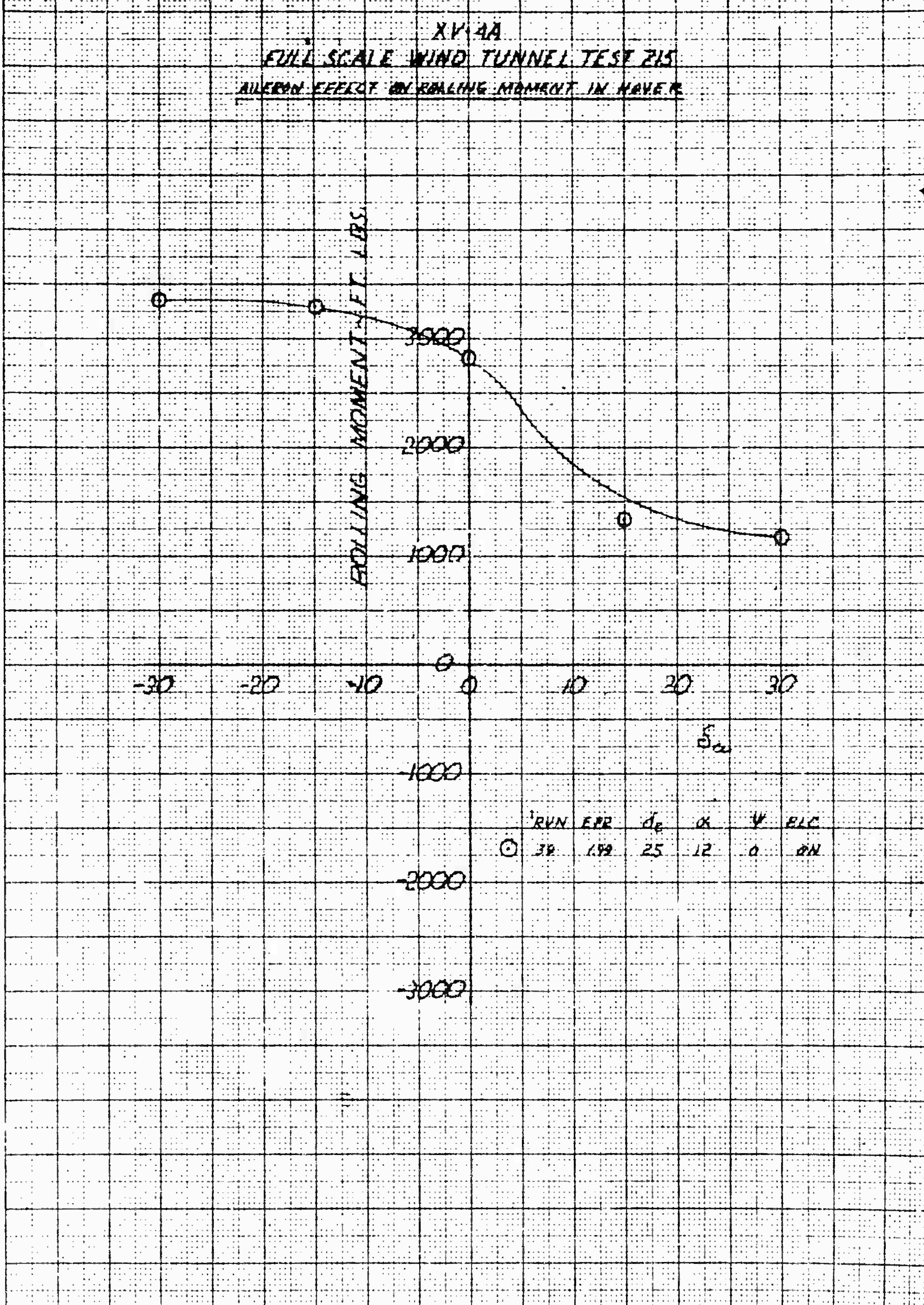
XV-4A
FULL SCALE WIND TUNNEL TEST 215
AILERON EFFECT ON ROLLING MOMENT IN HOVER
ROLLING MOMENT - FT. LBS.
3000
2000
1000
0
-1000
-2000
-3000
-30
-20
-10
0
10
20
30
δ_a
RUN EPR δ_e α ψ ELC
39 1.99 25 12 0 ON

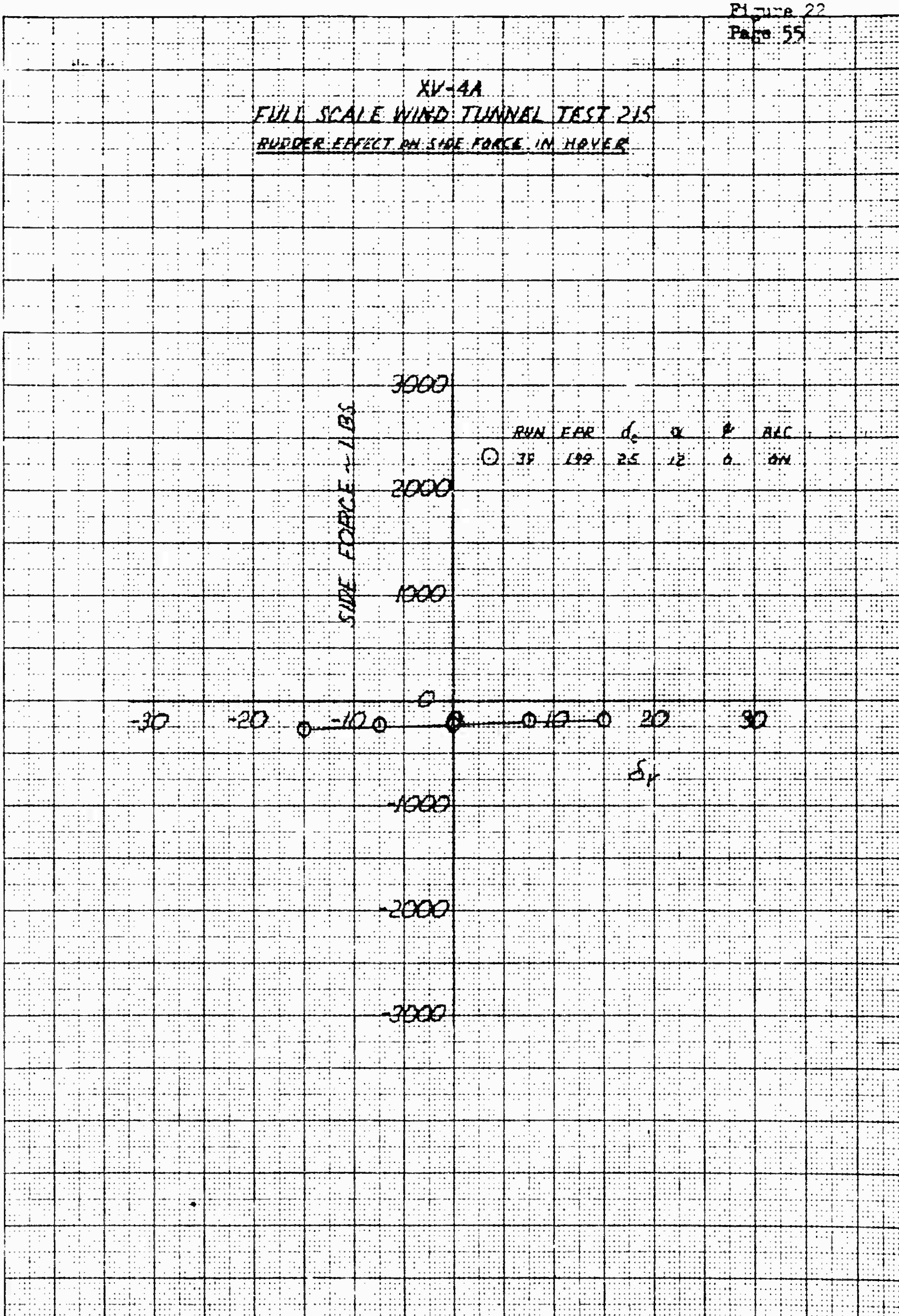
XV-4A
FULL SCALE WIND TUNNEL TEST 215
RUDDER EFFECT ON SIDE FORCE IN HOVER
SIDE FORCE ~ LBS
3000
2000
1000
0
-1000
-2000
-3000
RUN EPR d_c α β BLC
39 199 25 12 0 ON
-30 -20 -10 10 20 30
δ_r

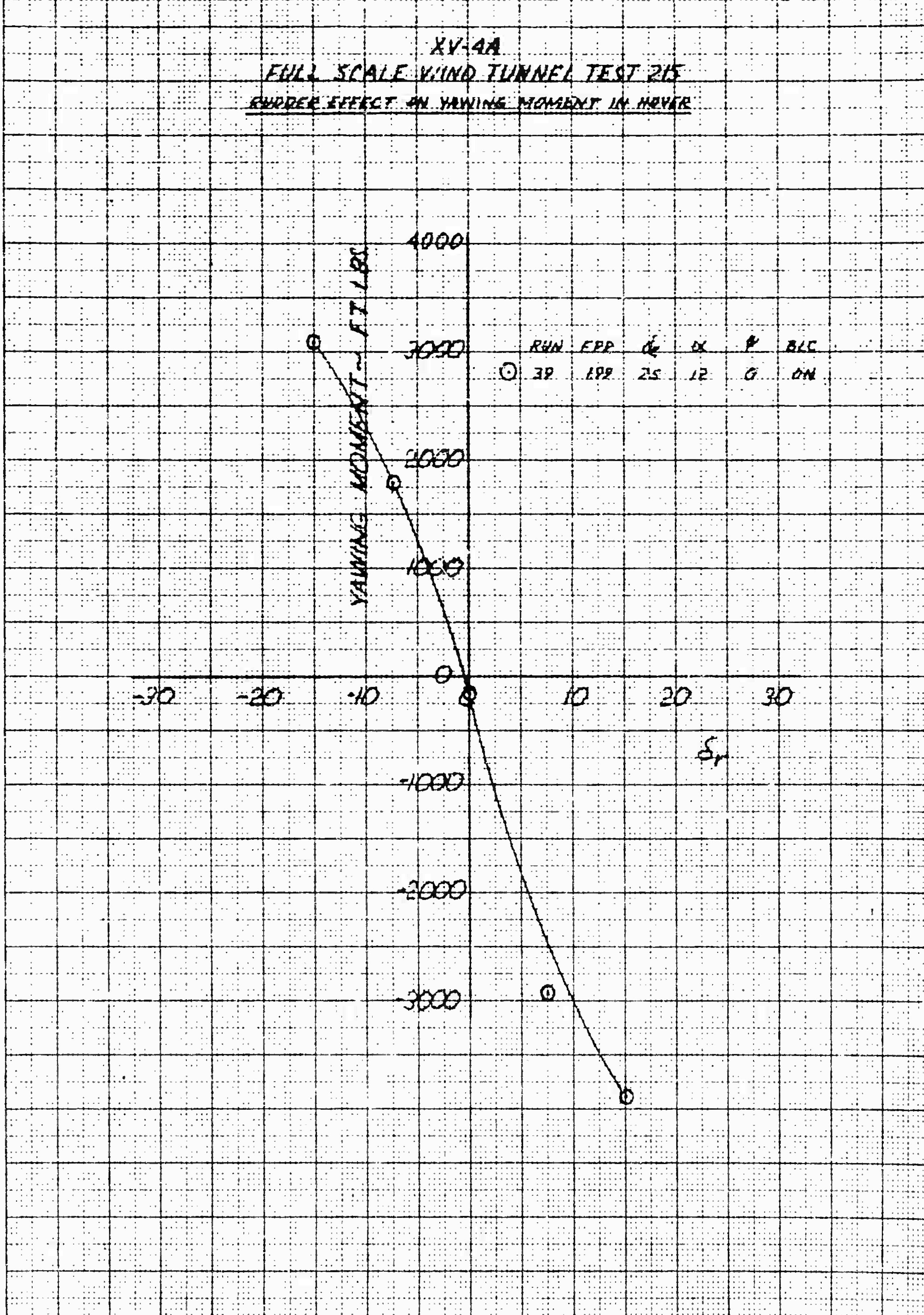
XV-4A
FULL SCALE WIND TUNNEL TEST 215
RUDDER EFFECT ON YAWING MOMENT IN HOVER
YAWING MOMENT ~ FT LBS
4000
3000
2000
1000
0
-1000
-2000
-3000
-30
-20
-10
10
20
30
δ_r
RUN FPP δ_f α ψ BLC
39 199 25 12 0 ON

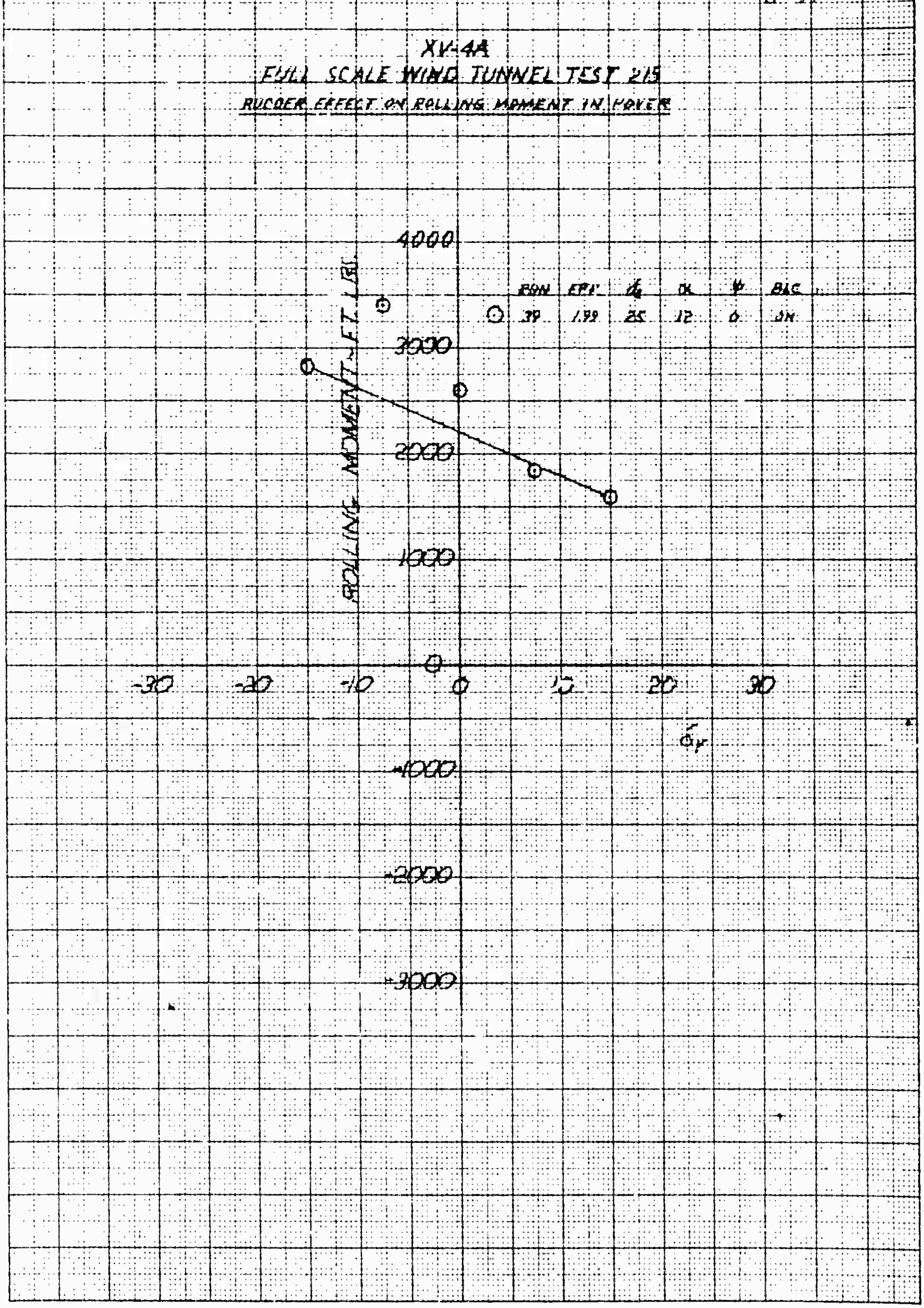
XV-4A
FULL SCALE WIND TUNNEL TEST 215
RUDDER EFFECT ON ROLLING MOMENT IN HOVER
ROLLING MOMENT ~ FT. LB.
4000
3000
2000
1000
-1000
-2000
-3000
-30
-20
-10
0
10
20
30
δ_r
RUN
EPI'
δ_f
α
ψ
B/C
.39
1.99
25
12
0
ON

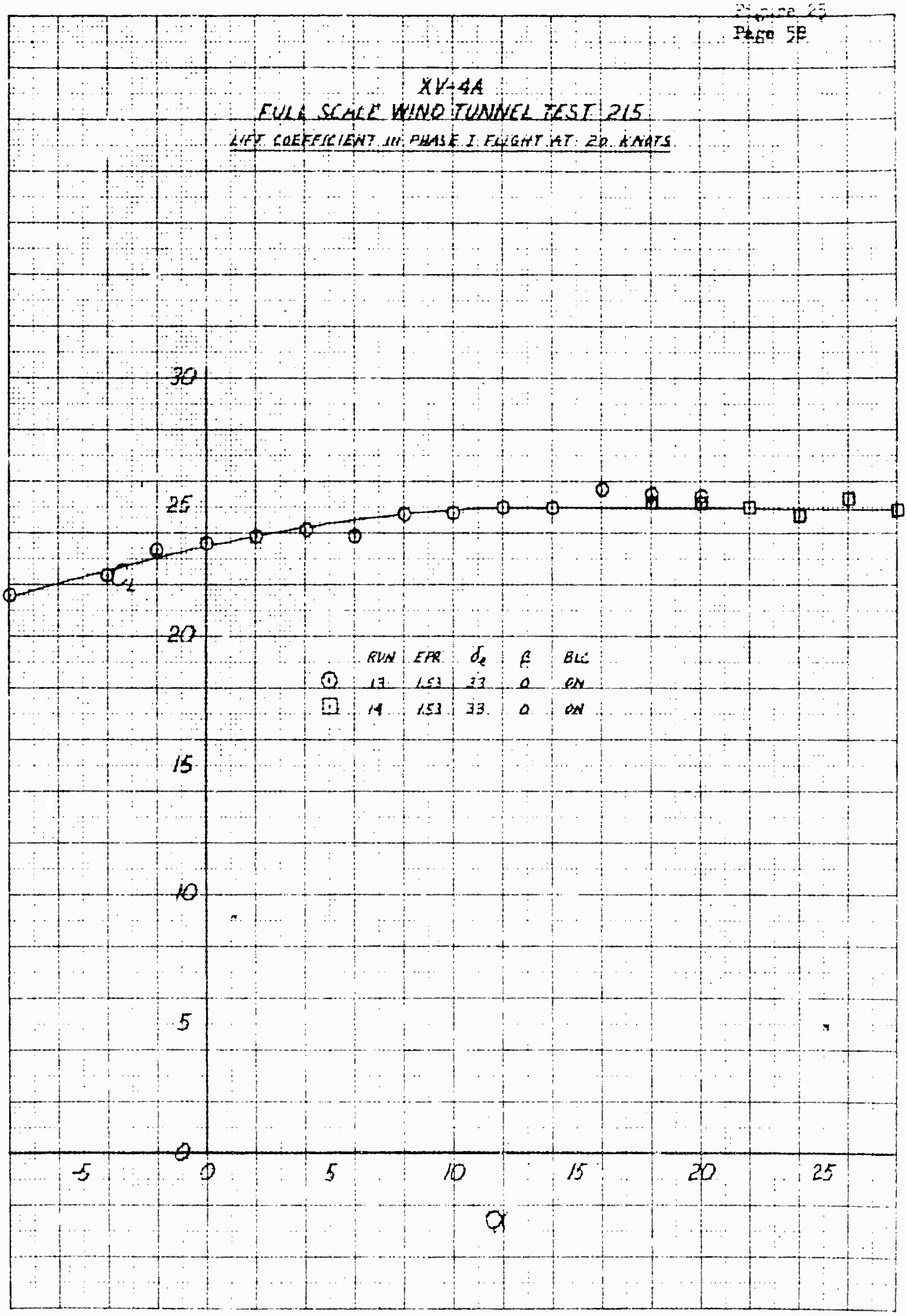
XV-4A
FULL SCALE WIND TUNNEL TEST 215
LIFT COEFFICIENT IN PHASE I FLIGHT AT 20 KNOTS
30
25
20
15
10
5
0
C_L
-5
0
5
10
15
20
25
α
RUN EPR δ_e β BLC
13 1.53 33 0 ON
14 1.53 33 0 ON

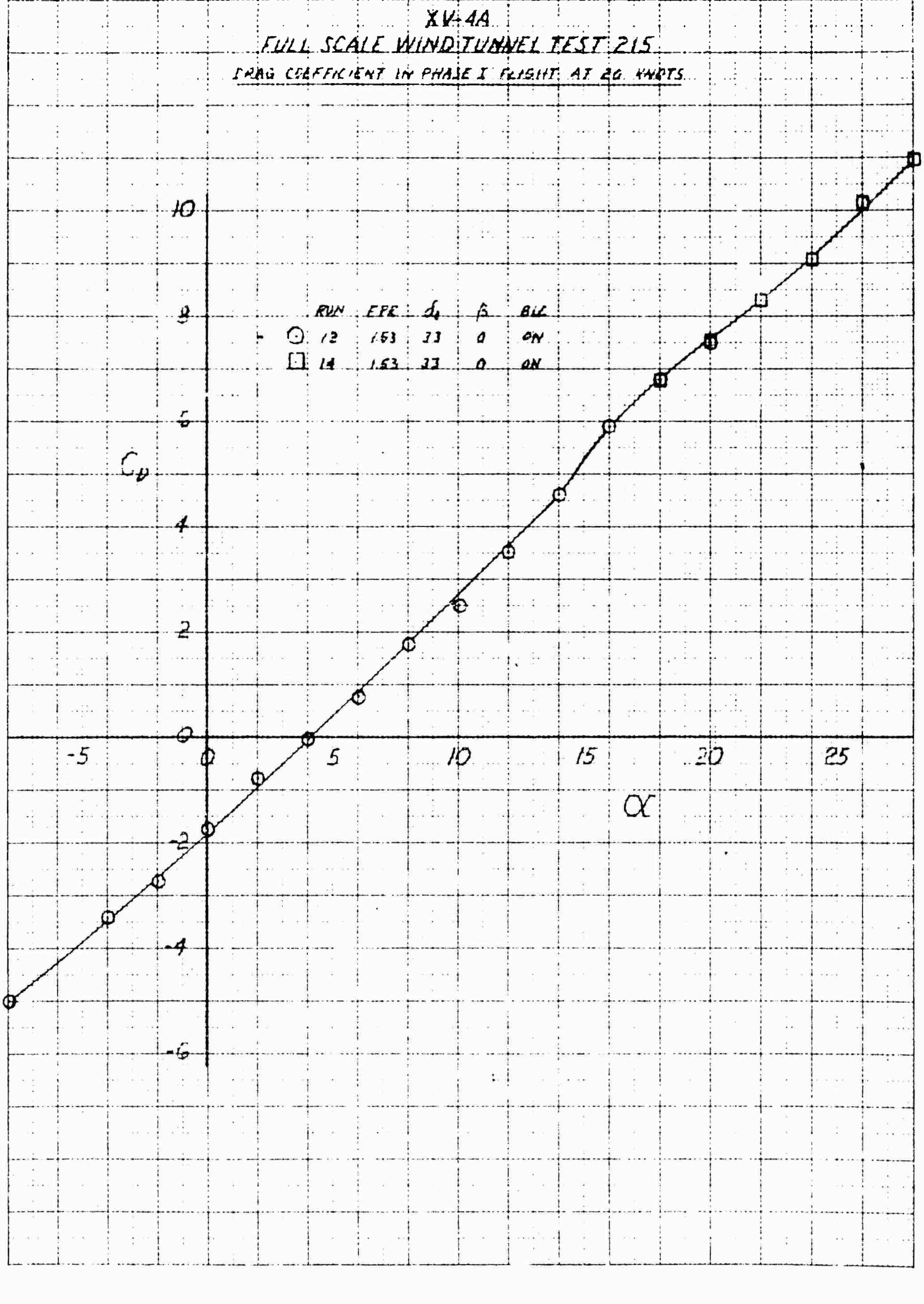
XV-4A
FULL SCALE WIND TUNNEL TEST 215
DRAG COEFFICIENT IN PHASE I FLIGHT AT 20 KNOTS
RUN EPE δ_f β BLC
12 1.53 33 0 ON
14 1.53 33 0 ON
C_D
10
8
6
4
2
0
-2
-4
-6
-5
0
5
10
15
20
25
α

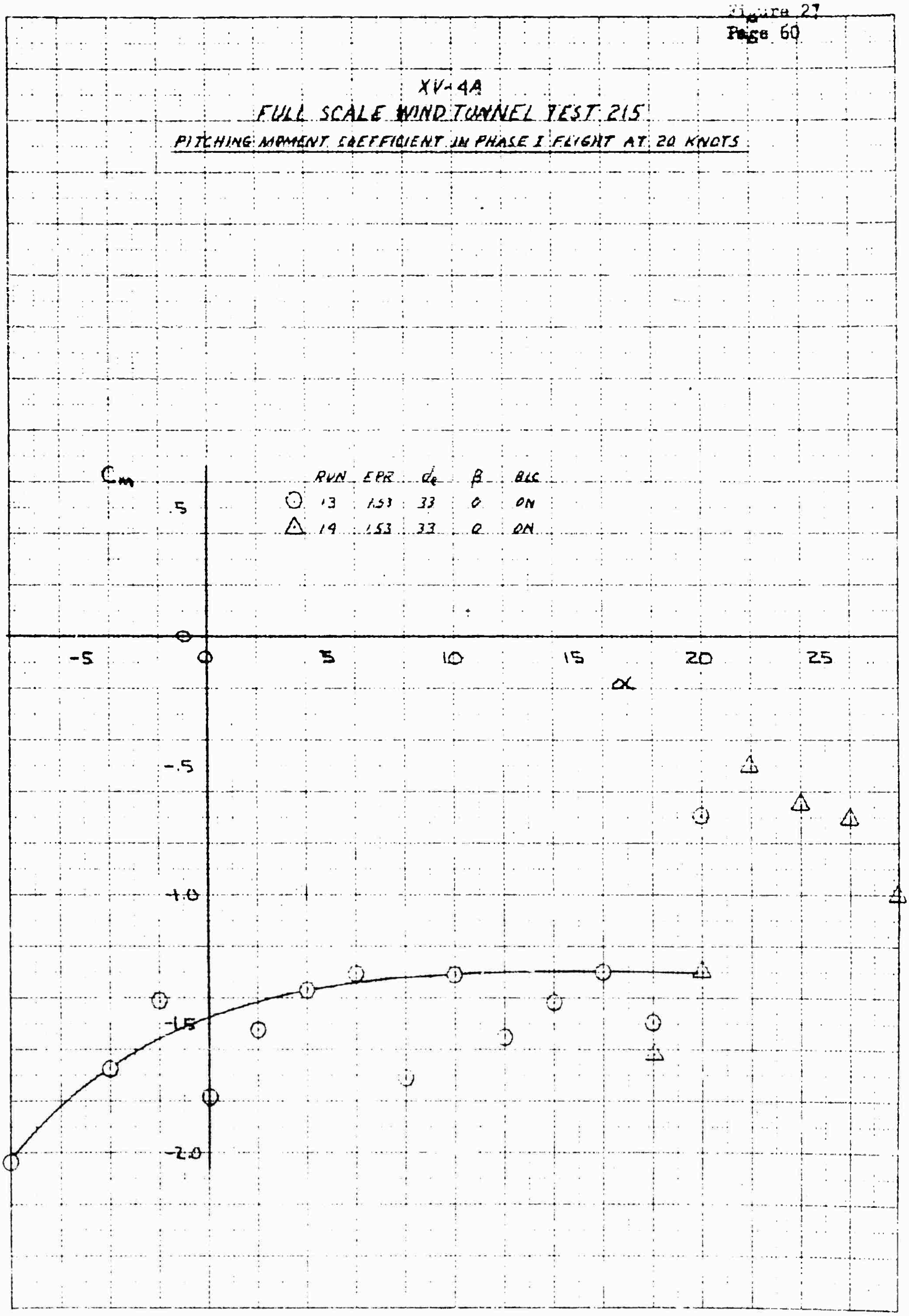
XV-4A
FULL SCALE WIND TUNNEL TEST 215
PITCHING MOMENT COEFFICIENT IN PHASE I FLIGHT AT 20 KNOTS
Cm
RUN EPR d_e β BLC
13 1.53 33 0 ON
19 1.53 33 0 ON
.5
-5
0
5
10
15
20
25
α
-.5
-1.0
-1.5
-2.0

XV-4A
FULL SCALE WIND TUNNEL TEST 215
SIDE FORCE COEFFICIENT IN PHASE I FLIGHT AT 20 KNOTS

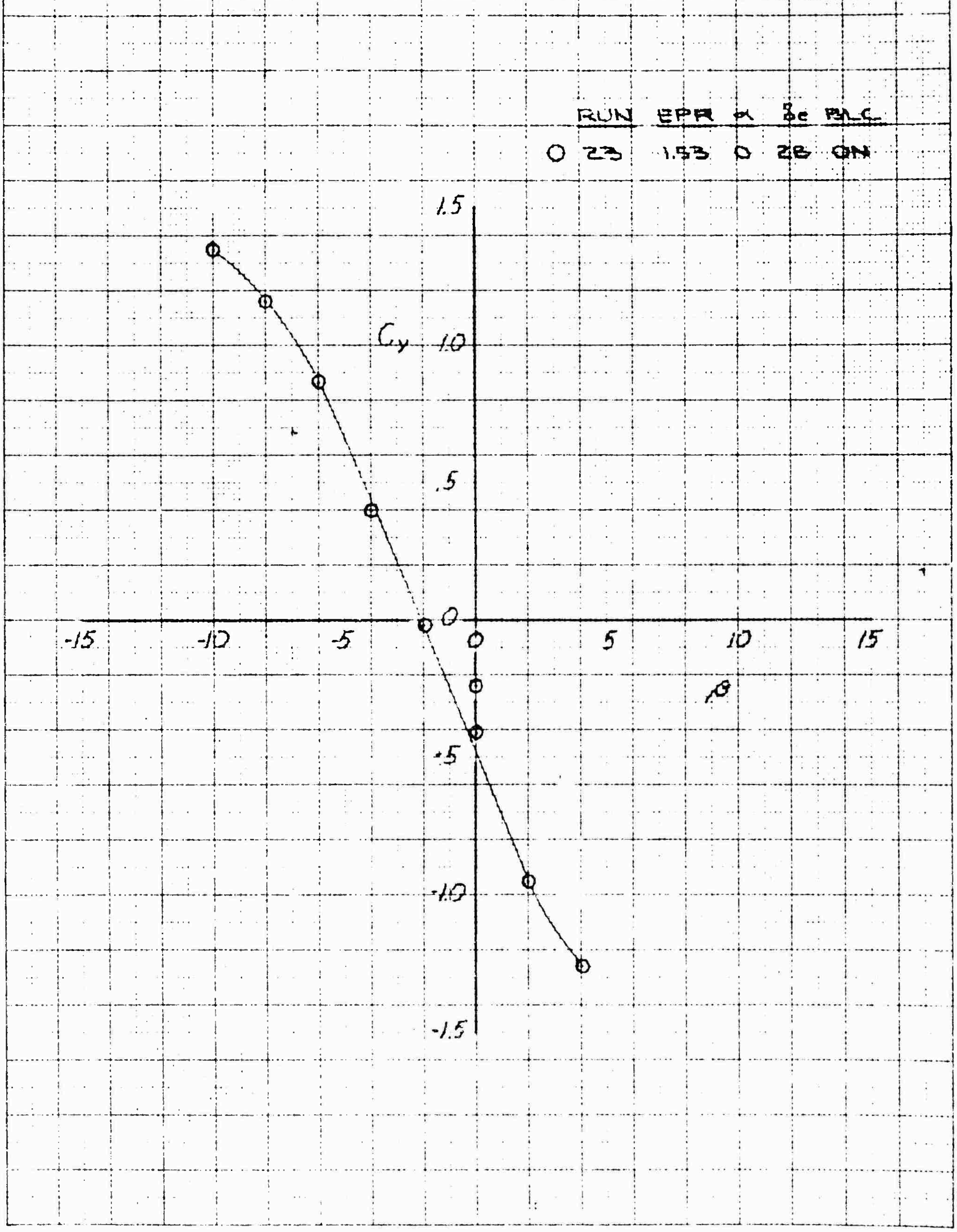

XV-4A
FULL SCALE WIND TUNNEL TEST 215
YAWING MOMENT COEFFICIENT IN PHASE I FLIGHT AT 20 KNOTS

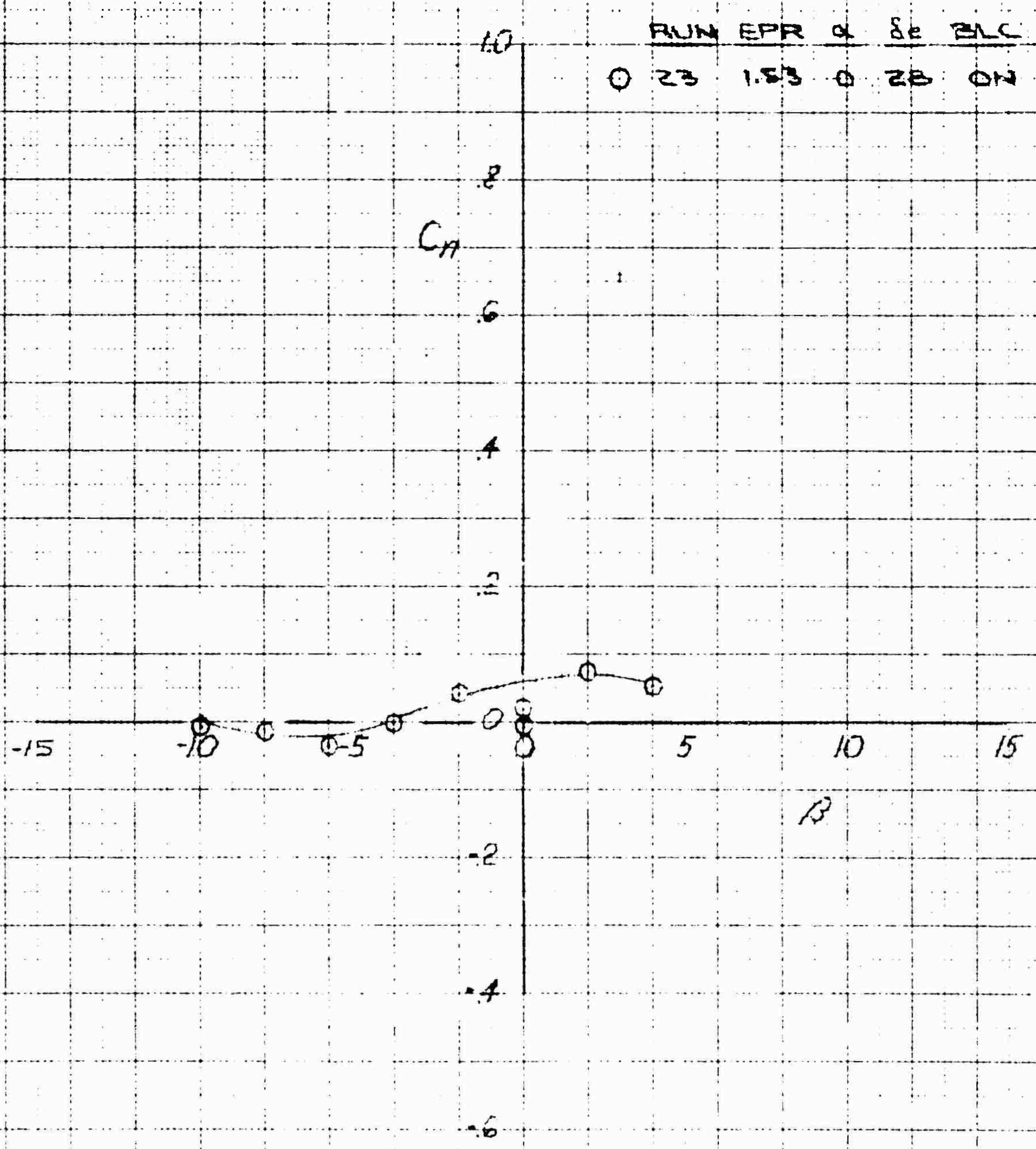

XV-4A
FULL SCALE WIND TUNNEL TEST 215
ROLLING MOMENT COEFFICIENT IN PHASE I FLIGHT AT 20 KNOTS

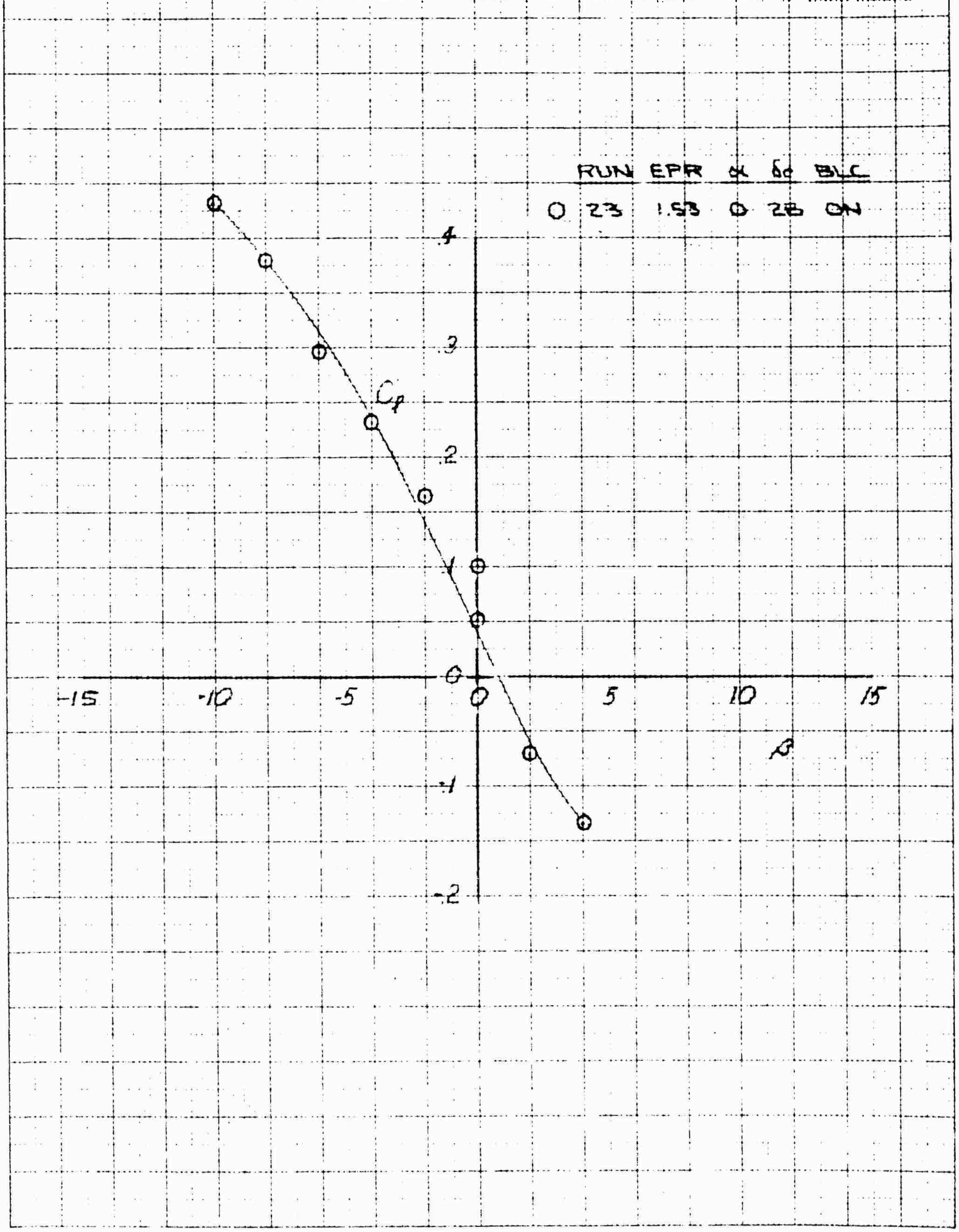

XV-4A
FULL SCALE WIND TUNNEL TEST 216
ELEVATOR EFFECT ON LIFT COEFFICIENT IN PHASE I FLIGHT AT 20 KNOTS

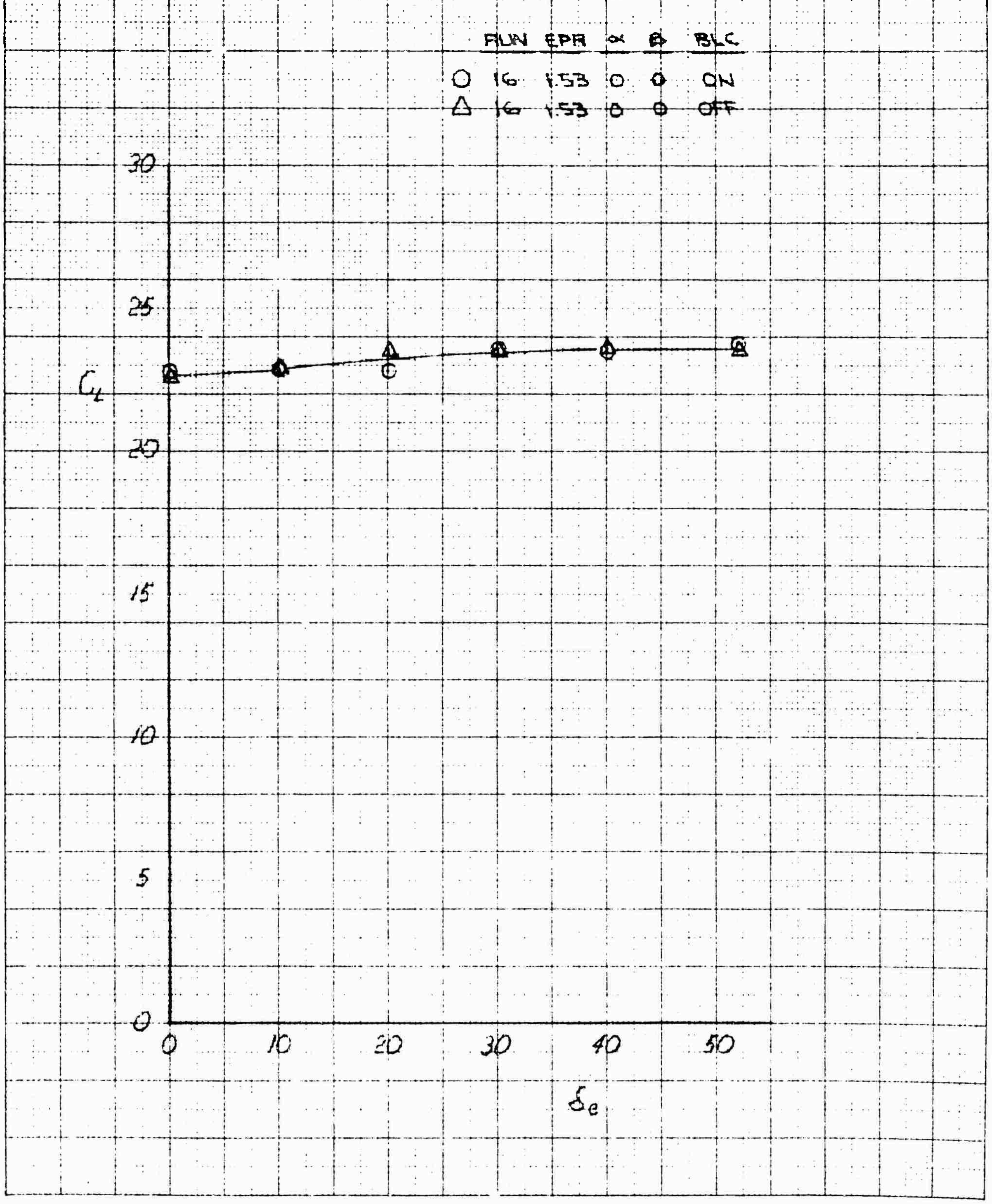

XV-4A
FULL SCALE WIND TUNNEL TEST 215
ELEVATOR EFFECT ON DRAG COEFFICIENT IN PHASE I FLIGHT AT 20 KNOTS

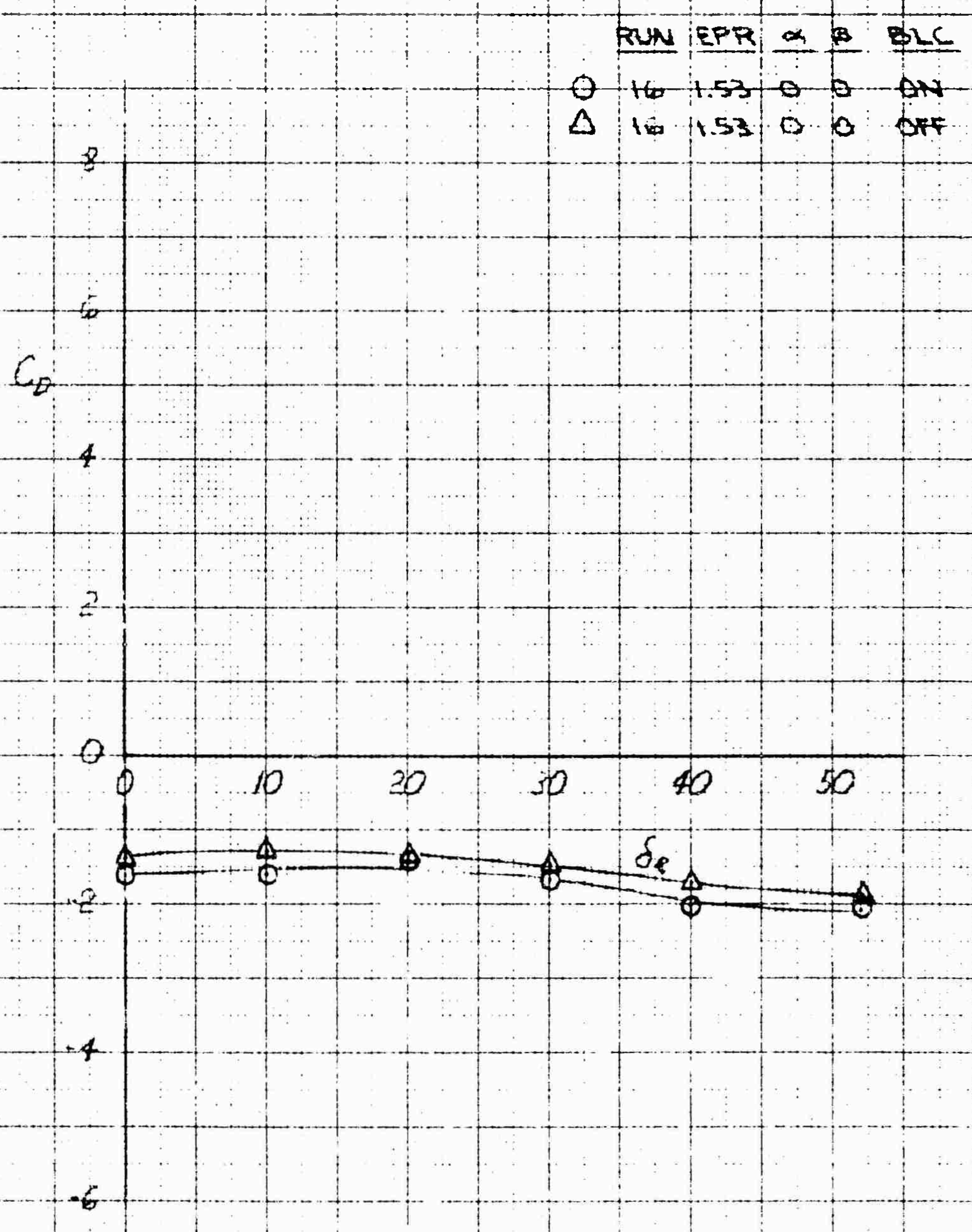

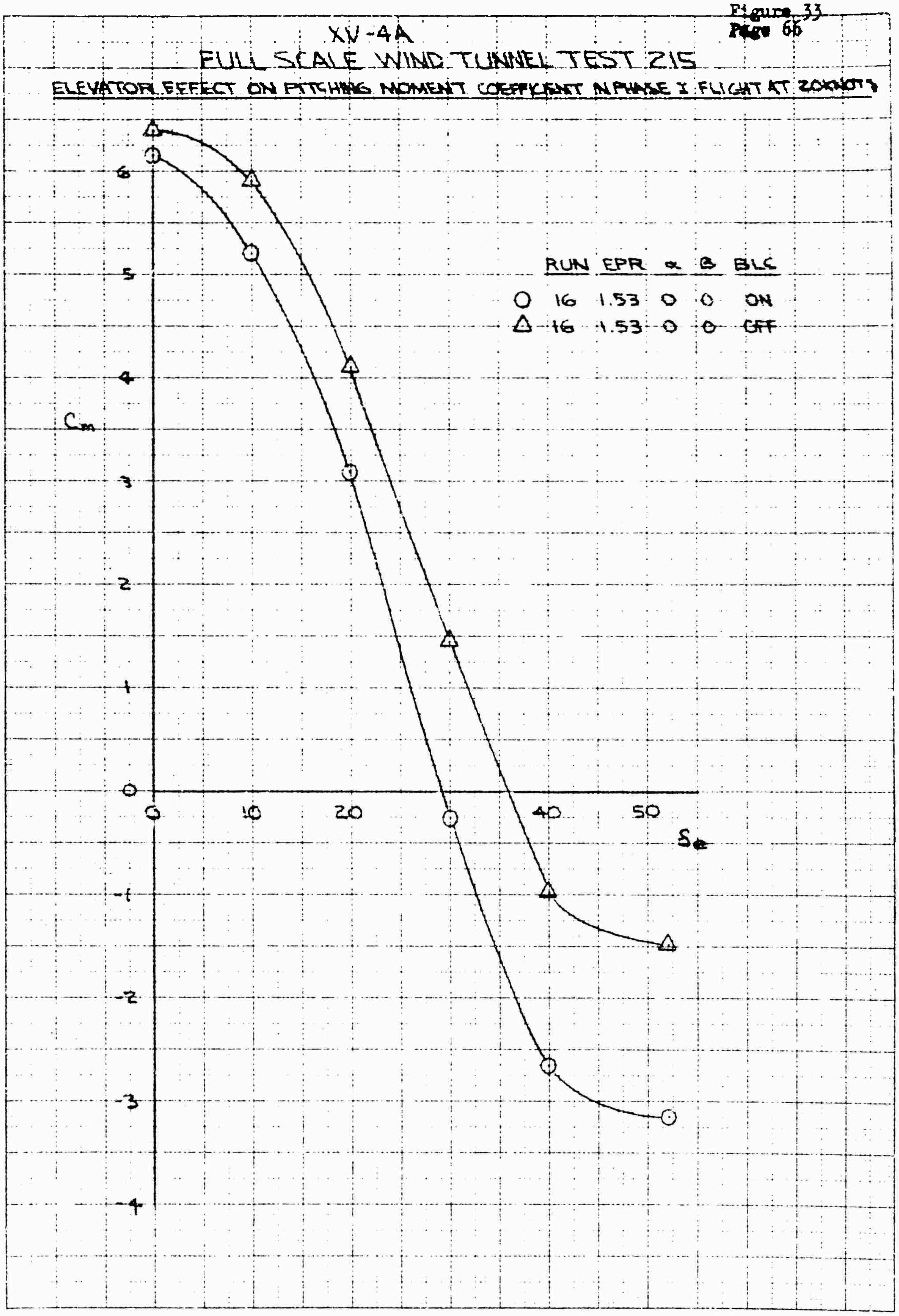
XV-4A
FULL SCALE WIND TUNNEL TEST 215
ELEVATOR EFFECT ON PITCHING MOMENT COEFFICIENT IN PHASE I FLIGHT AT 20 KNOTS
RUN EPR α β BLC
○ 16 1.53 0 0 ON
△ 16 1.53 0 0 OFF
Cm
δe
6
5
4
3
2
1
0
-1
-2
-3
-4
0
10
20
40
50

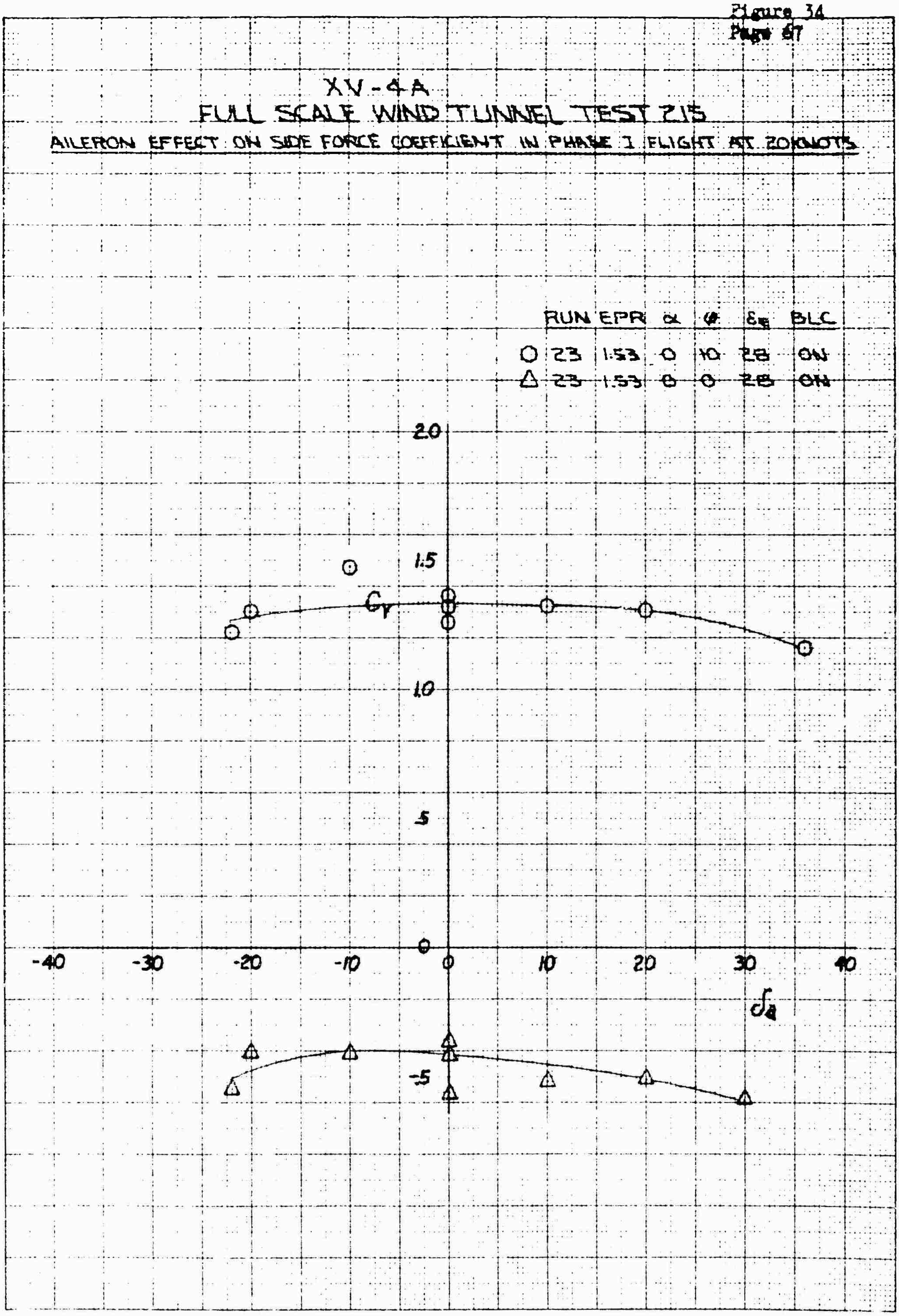
XV-4A
FULL SCALE WIND TUNNEL TEST 215
AILERON EFFECT ON SIDE FORCE COEFFICIENT IN PHASE I FLIGHT AT 20 KNOTS
RUN EPR α ψ δ_E BLC
○ 23 1.53 0 10 28 ON
△ 23 1.53 0 0 28 ON
2.0
1.5
1.0
.5
0
-.5
-40
-30
-20
-10
0
10
20
30
40
C_Y
δ_a

XV-4A
FULL SCALE WIND TUNNEL TEST 215
AILERON EFFECT ON YAWING MOMENT COEFFICIENT IN PHASE I FLIGHT AT 20 KNOTS

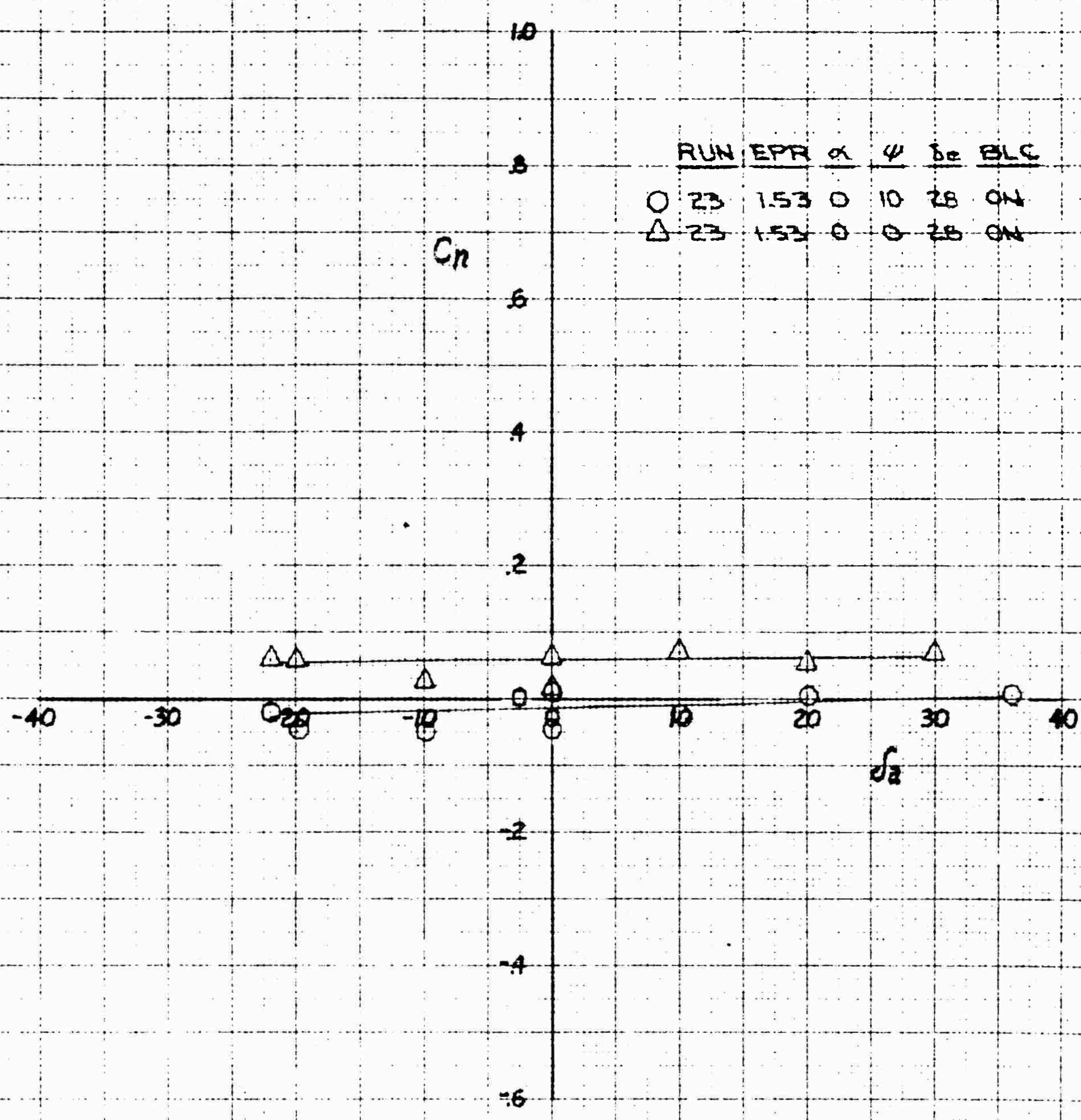

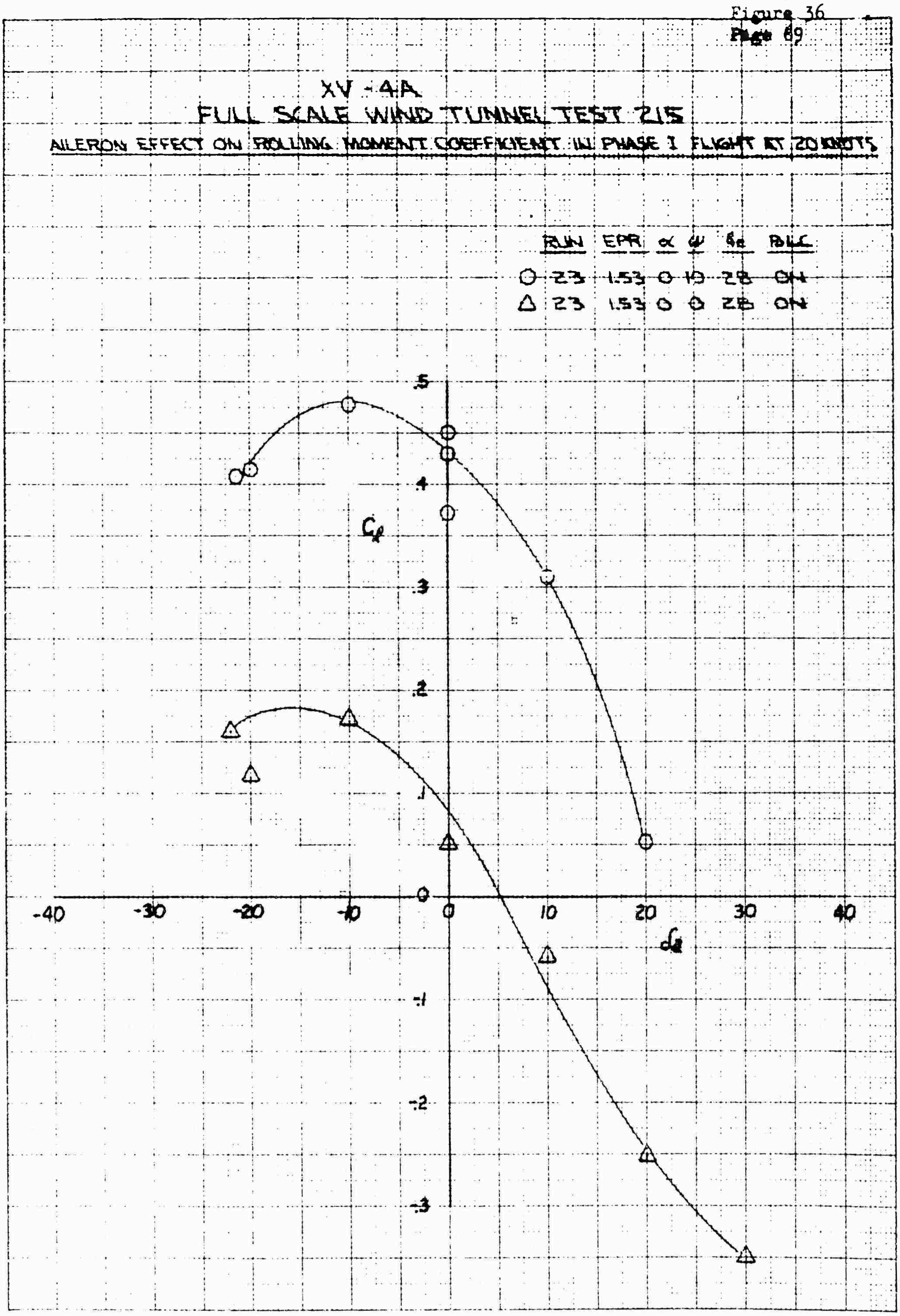
XV-4A
FULL SCALE WIND TUNNEL TEST 215
AILERON EFFECT ON ROLLING MOMENT COEFFICIENT IN PHASE I FLIGHT AT 20 KNOTS
RUN EPR α ψ δe BLC
○ 23 1.53 0 10 28 ON
△ 23 1.53 0 0 28 ON
C_ℓ
δ_a
.5
.4
.3
.2
.1
0
-.1
-.2
-.3
-40
-30
-20
-10
0
10
20
30
40

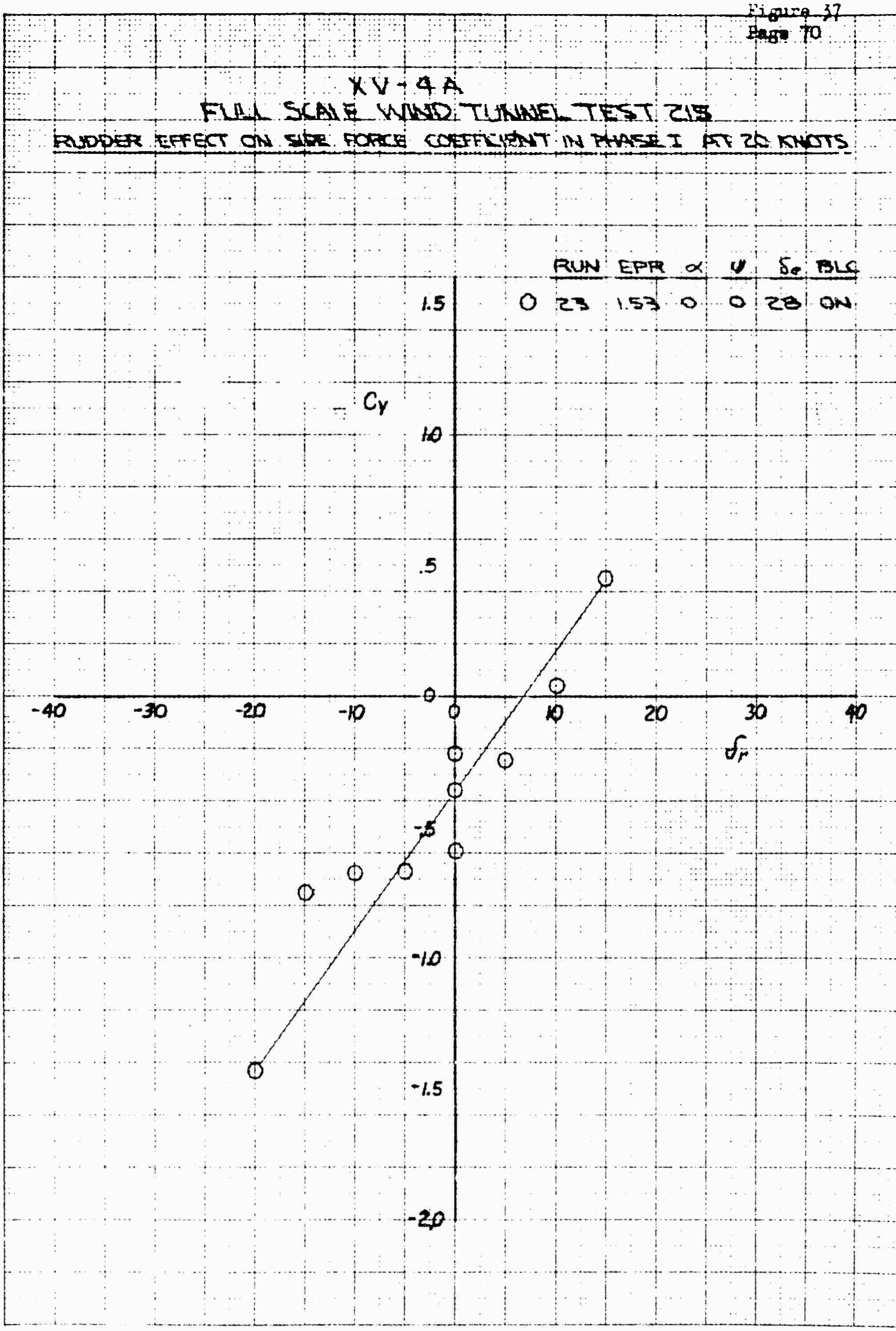
XV-4A
FULL SCALE WIND TUNNEL TEST 213
RUDDER EFFECT ON SIDE FORCE COEFFICIENT IN PHASE I AT 20 KNOTS
RUN EPR α ψ δe BLC
○ 23 1.53 0 0 28 ON
Cy
1.5
1.0
.5
0
-.5
-1.0
-1.5
-2.0
-40
-30
-20
-10
0
10
20
30
40
δr

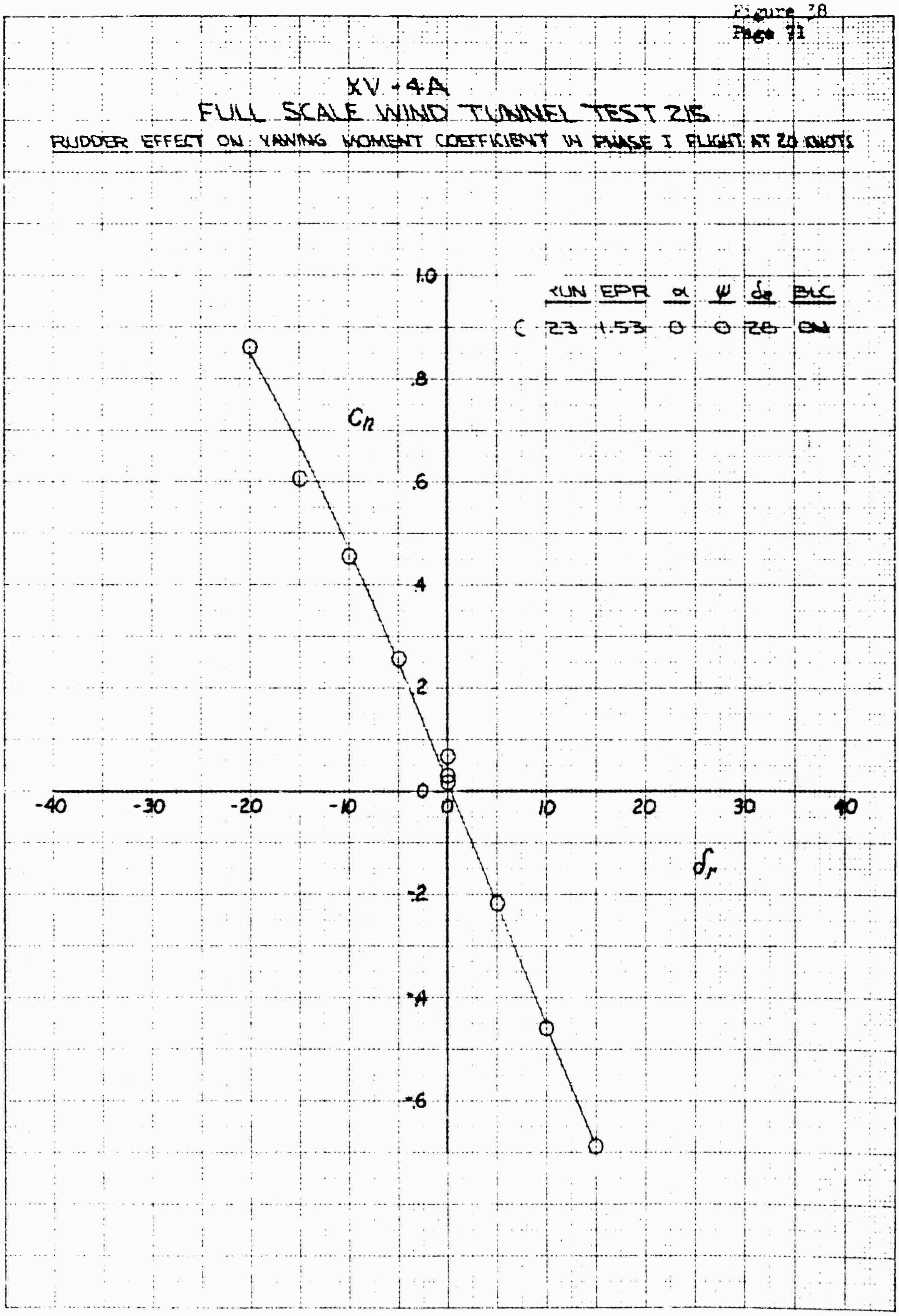
XV-4A
FULL SCALE WIND TUNNEL TEST 215
RUDDER EFFECT ON YAWING MOMENT COEFFICIENT IN PHASE I FLIGHT AT 20 KNOTS
RUN EPR α ψ δe BLC
23 1.53 0 0 26 ON
Cn
δr
1.0
.8
.6
.4
.2
0
-.2
-.4
-.6
-40
-30
-20
-10
0
10
20
30
40

XV-4A
FULL SCALE WIND TUNNEL TEST 215
RUDDER EFFECT ON ROLLING MOMENT COEFFICIENT IN PHASE I FLIGHT AT 20 KNOTS

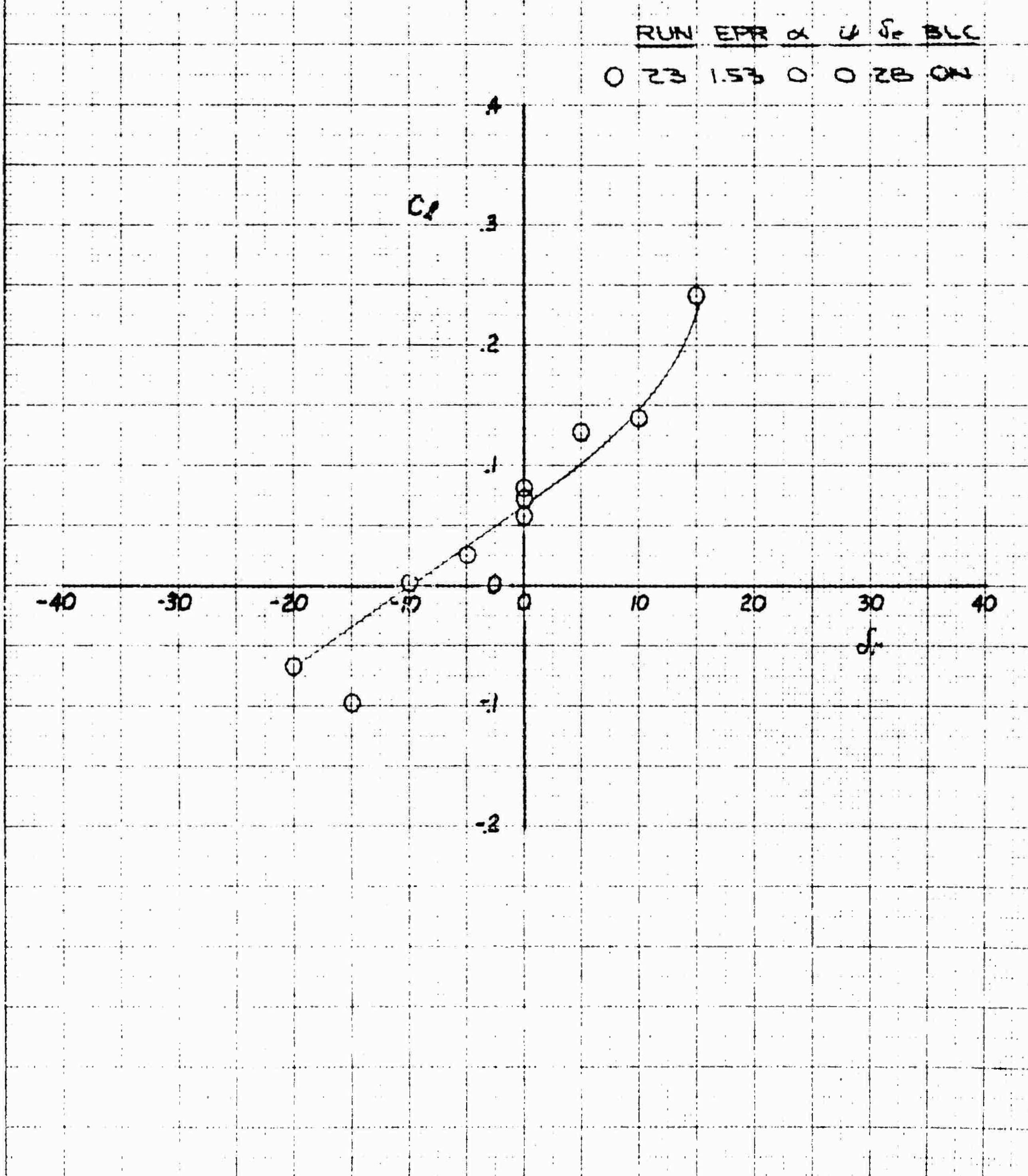

XV-4A
FULL SCALE WIND TUNNEL TEST 215
RUDDER EFFECT ON SIDE FORCE COEFFICIENT IN PHASE I AT 20 KNOTS

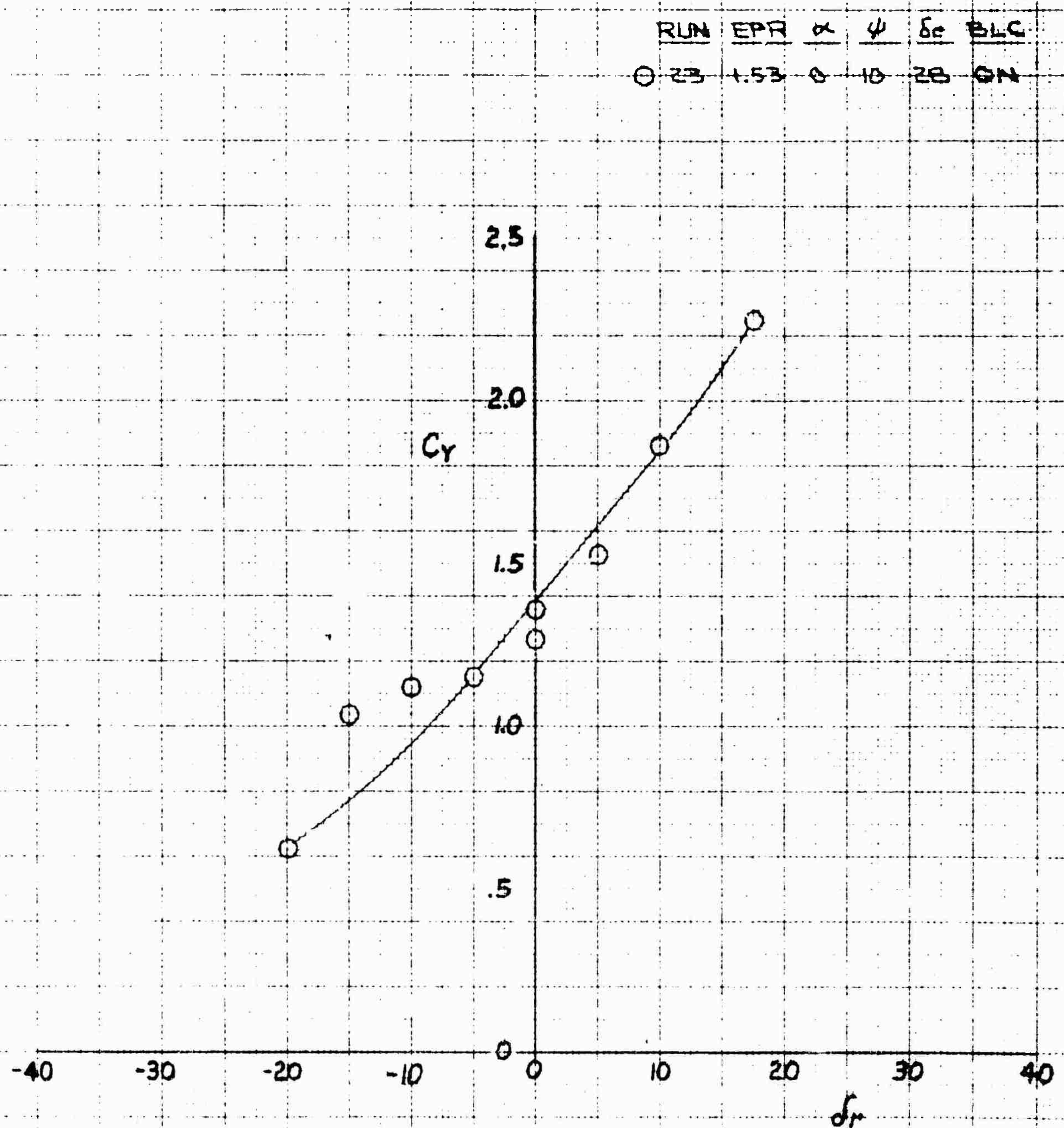

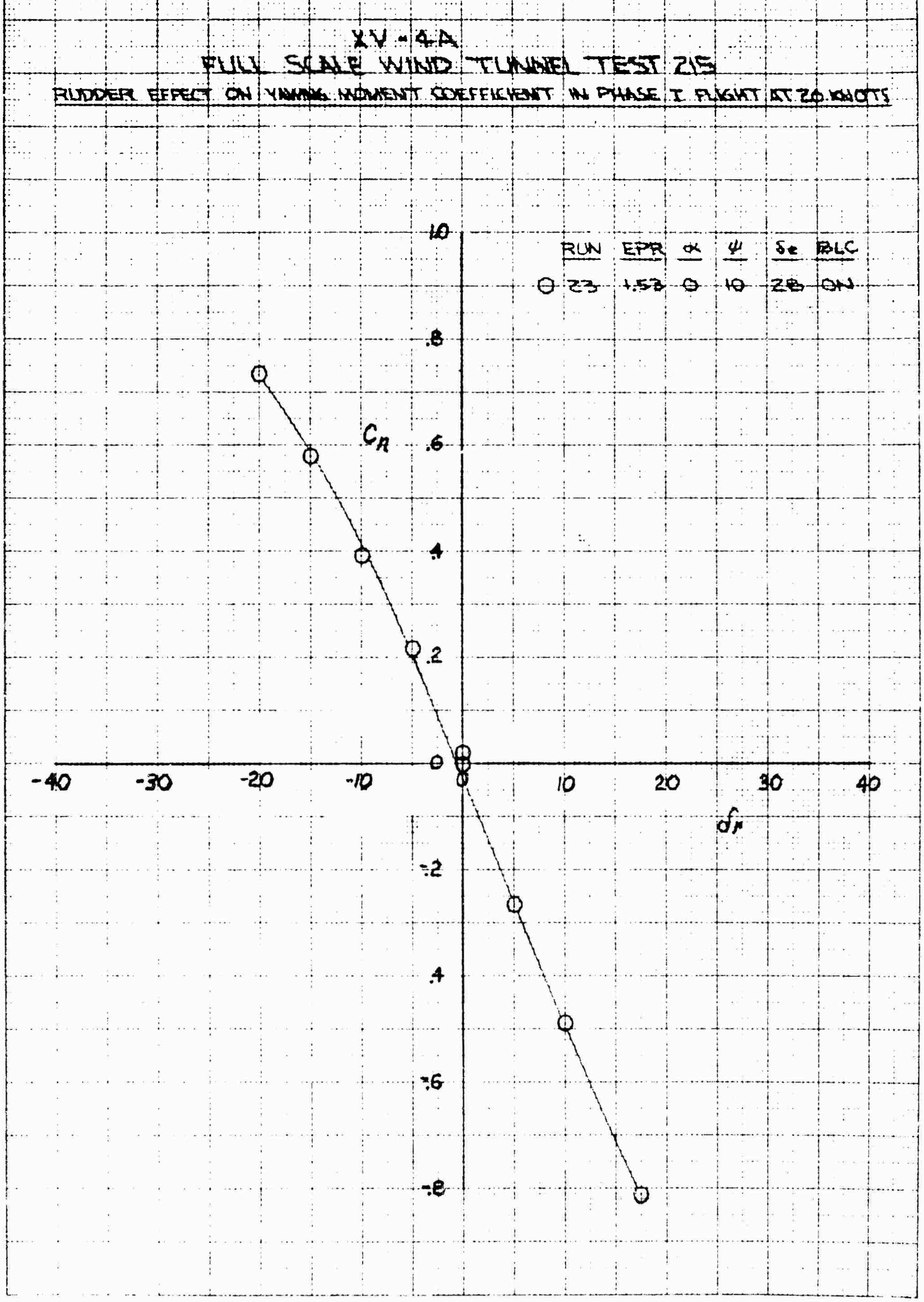
XV-4A
FULL SCALE WIND TUNNEL TEST 215
RUDDER EFFECT ON YAWING MOMENT COEFFICIENT IN PHASE I FLIGHT AT 20 KNOTS
RUN EPR α ψ δe BLC
23 1.53 0 10 28 ON
C_n
1.0
.8
.6
.4
.2
0
-.2
-.4
-.6
-.8
-40 -30 -20 -10 0 10 20 30 40
δ_r

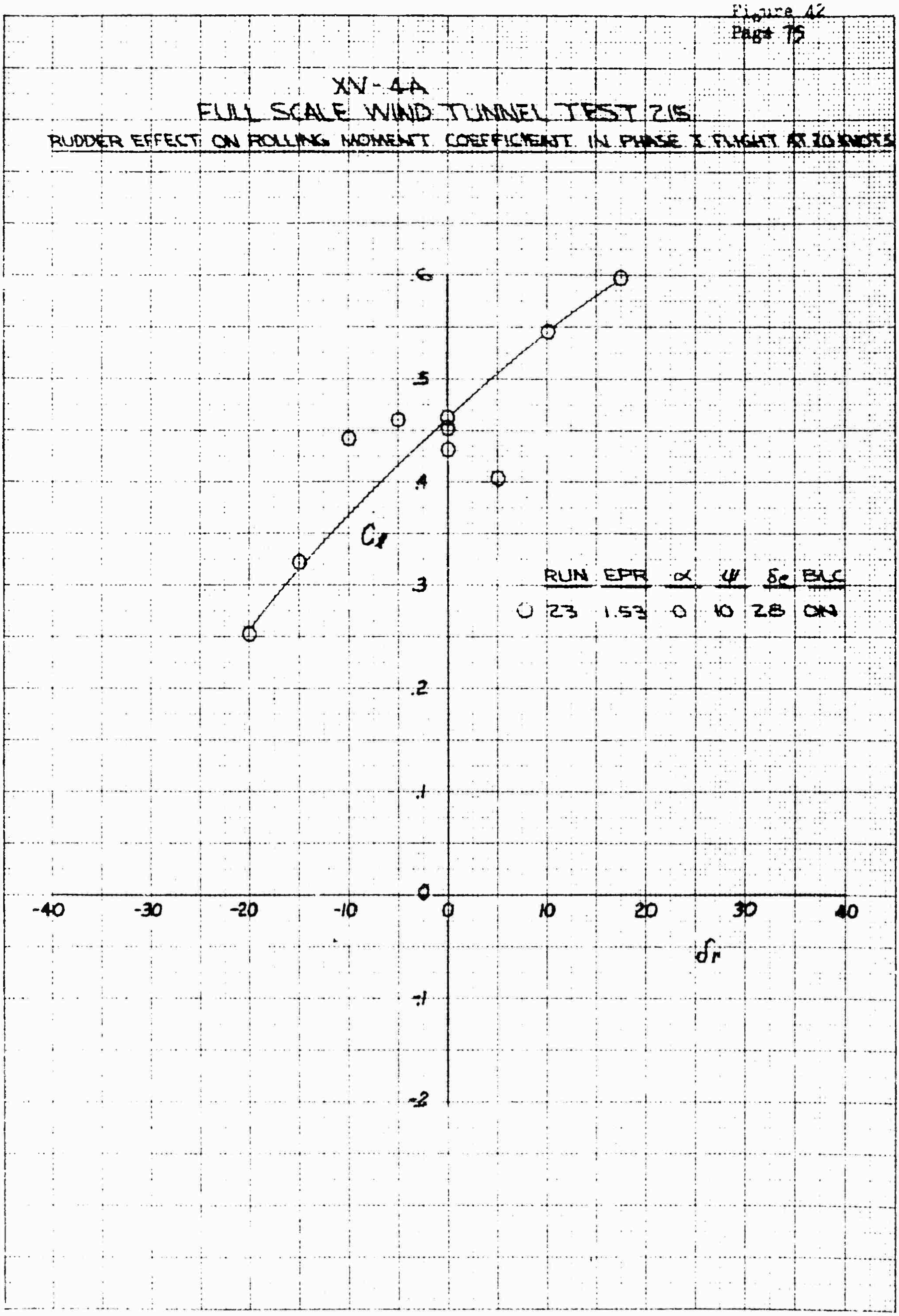
XV-4A
FULL SCALE WIND TUNNEL TEST 215
RUDDER EFFECT ON ROLLING MOMENT COEFFICIENT IN PHASE I FLIGHT AT 10 KNOTS
C_l
δ_r
RUN EPR α ψ δe BLC
23 1.53 0 10 28 ON
.6
.5
.4
.3
.2
.1
0
-.1
-.2
-40
-30
-20
-10
0
10
20
30
40

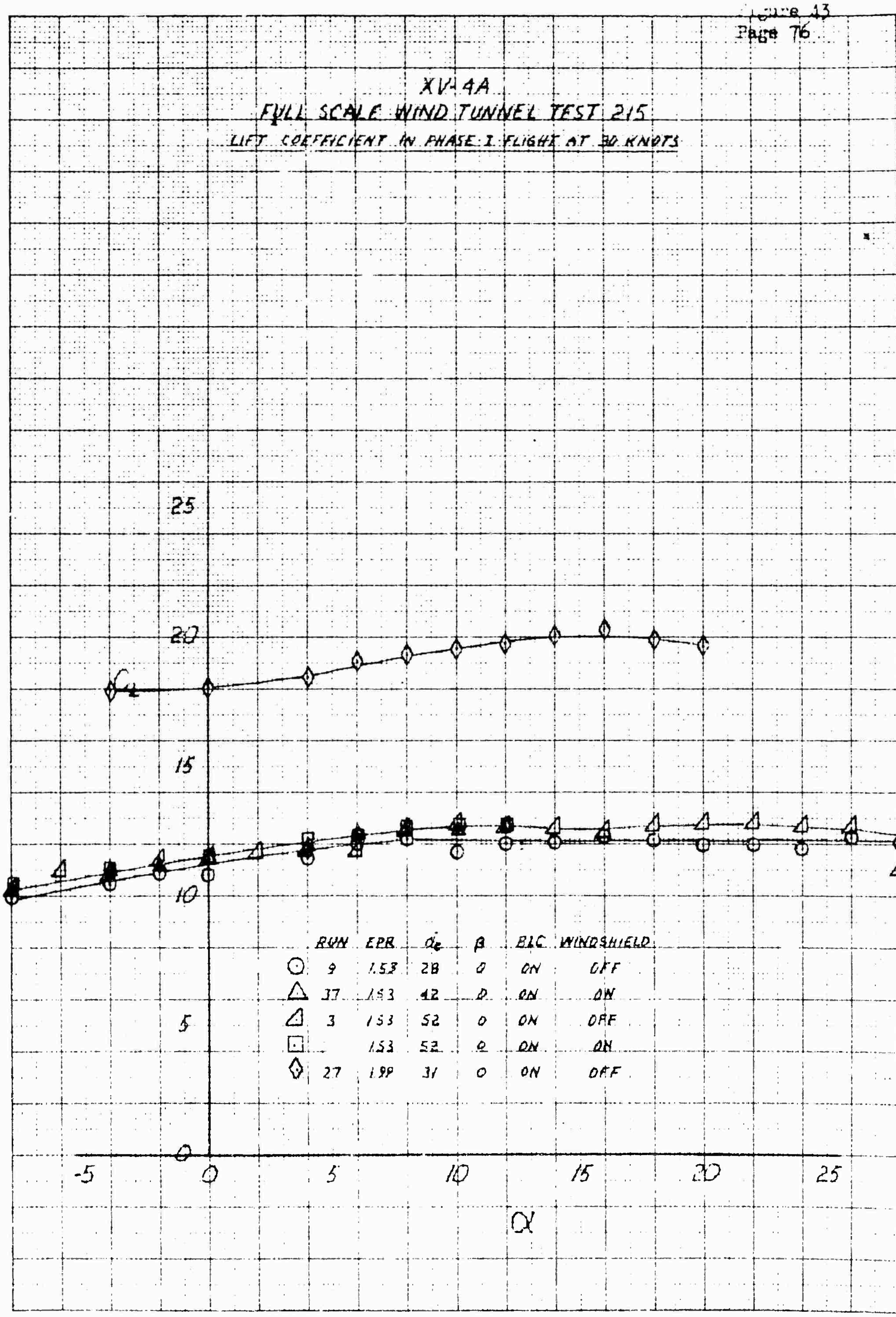
XV-4A
FULL SCALE WIND TUNNEL TEST 215
LIFT COEFFICIENT IN PHASE I FLIGHT AT 30 KNOTS
25
20
15
10
5
0
C_L
-5
0
5
10
15
20
25
α
RUN EPR α_c β BLC WINDSHIELD
9 1.53 28 0 ON OFF
37 1.53 42 0 ON ON
3 1.53 52 0 ON OFF
1.53 52 0 ON ON
27 1.99 31 0 ON OFF

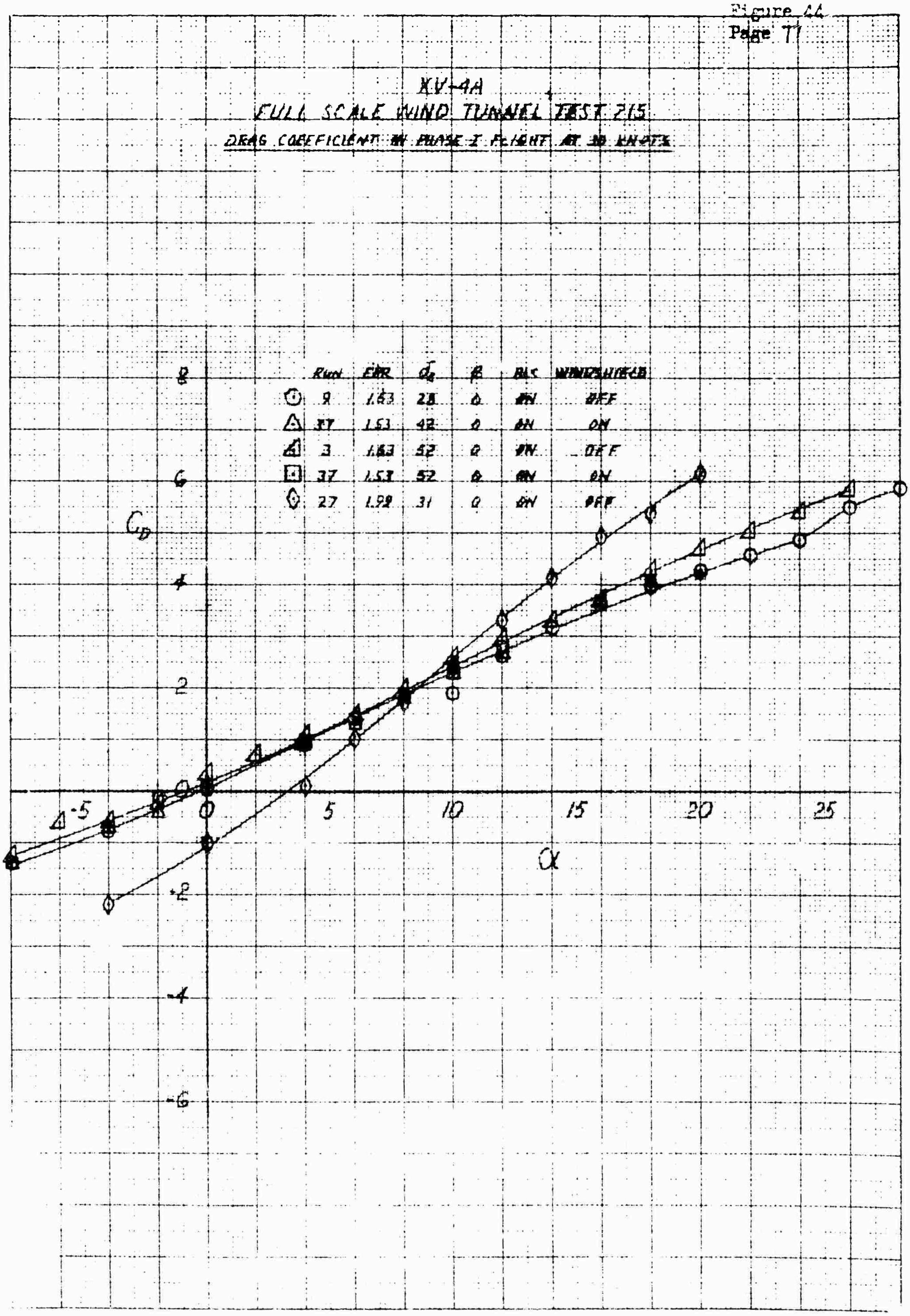
XV-4A
FULL SCALE WIND TUNNEL TEST 215
DRAG COEFFICIENT IN PHASE I FLIGHT AT 30 KNOTS
Run EPR δ β BLC WINDSHIELD
9 1.63 28 0 ON OFF
37 1.53 42 0 ON ON
3 1.63 52 0 ON OFF
37 1.53 52 0 ON ON
27 1.92 31 0 ON OFF
C_D
.8
.6
.4
.2
-.2
-.4
-.6
-5
0
5
10
15
20
25
α

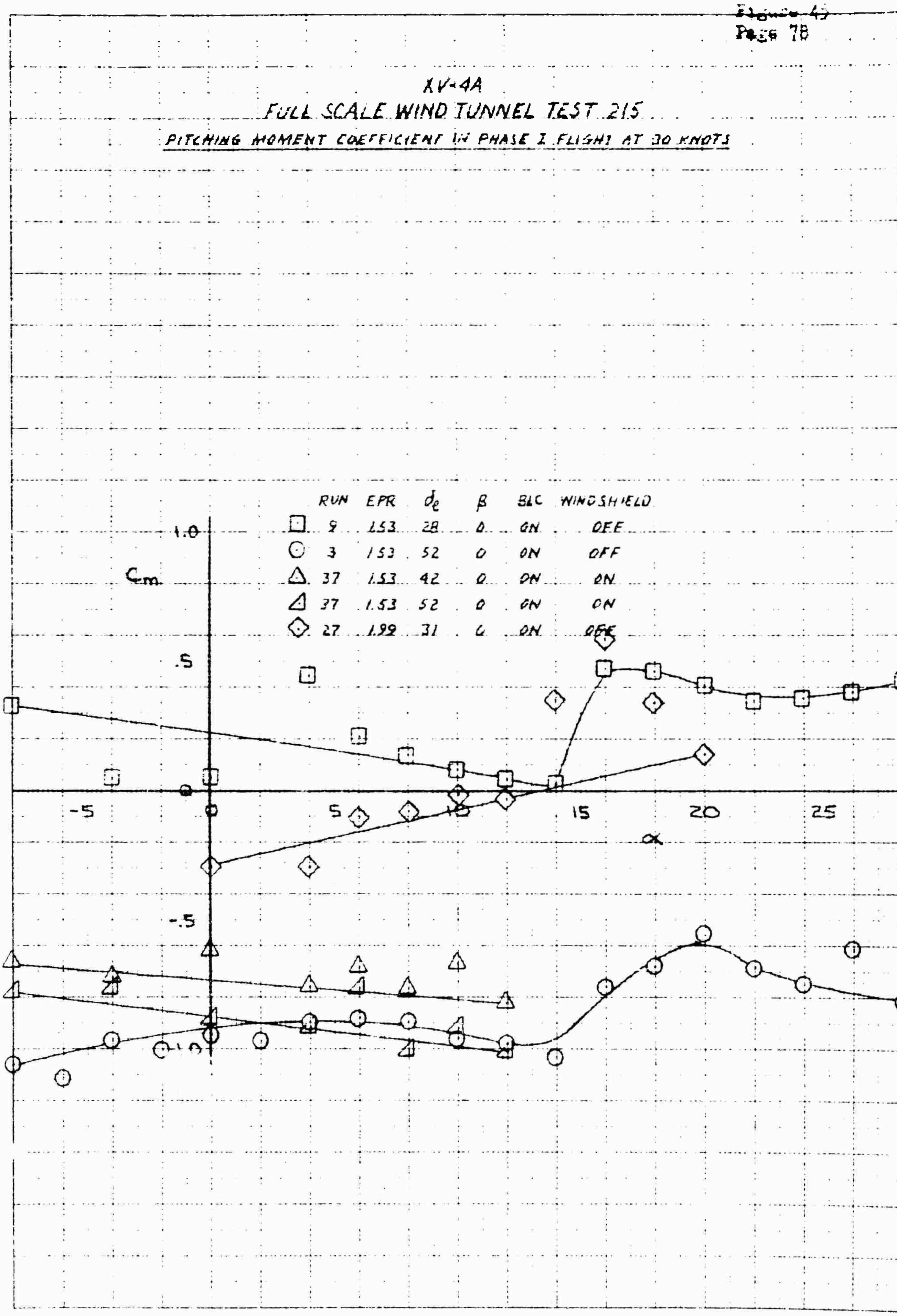
XV-4A
FULL SCALE WIND TUNNEL TEST 215
PITCHING MOMENT COEFFICIENT IN PHASE I FLIGHT AT 30 KNOTS
RUN EPR δ_e β BLC WINDSHIELD
9 1.53 28 0 ON OFF
3 1.53 52 0 ON OFF
37 1.53 42 0 ON ON
37 1.53 52 0 ON ON
27 1.99 31 0 ON OFF
Cm
1.0
.5
-.5
-1.0
-5
0
5
10
15
20
25
α

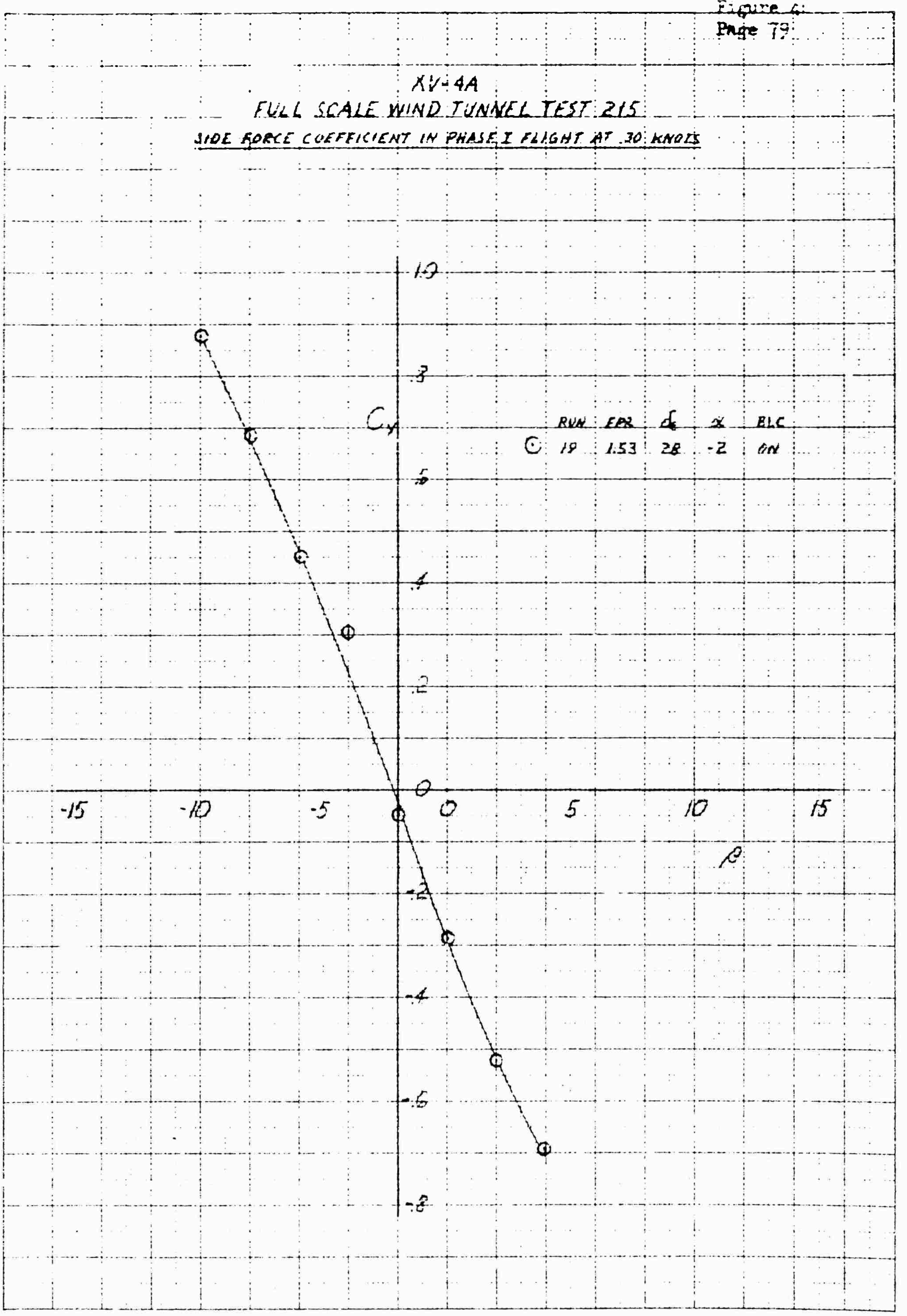
XV-4A
FULL SCALE WIND TUNNEL TEST 215
SIDE FORCE COEFFICIENT IN PHASE I FLIGHT AT 30 KNOTS
C_Y
RUN EPR δ_f α BLC
19 1.53 28 -2 ON
1.0
.8
.6
.4
.2
0
-.2
-.4
-.6
-.8
-15 -10 -5 0 5 10 15
β

XV-4A

FULL SCALE WIND TUNNEL TEST 215

YAWING MOMENT COEFFICIENT IN PHASE I FLIGHT AT 36 KNOTS

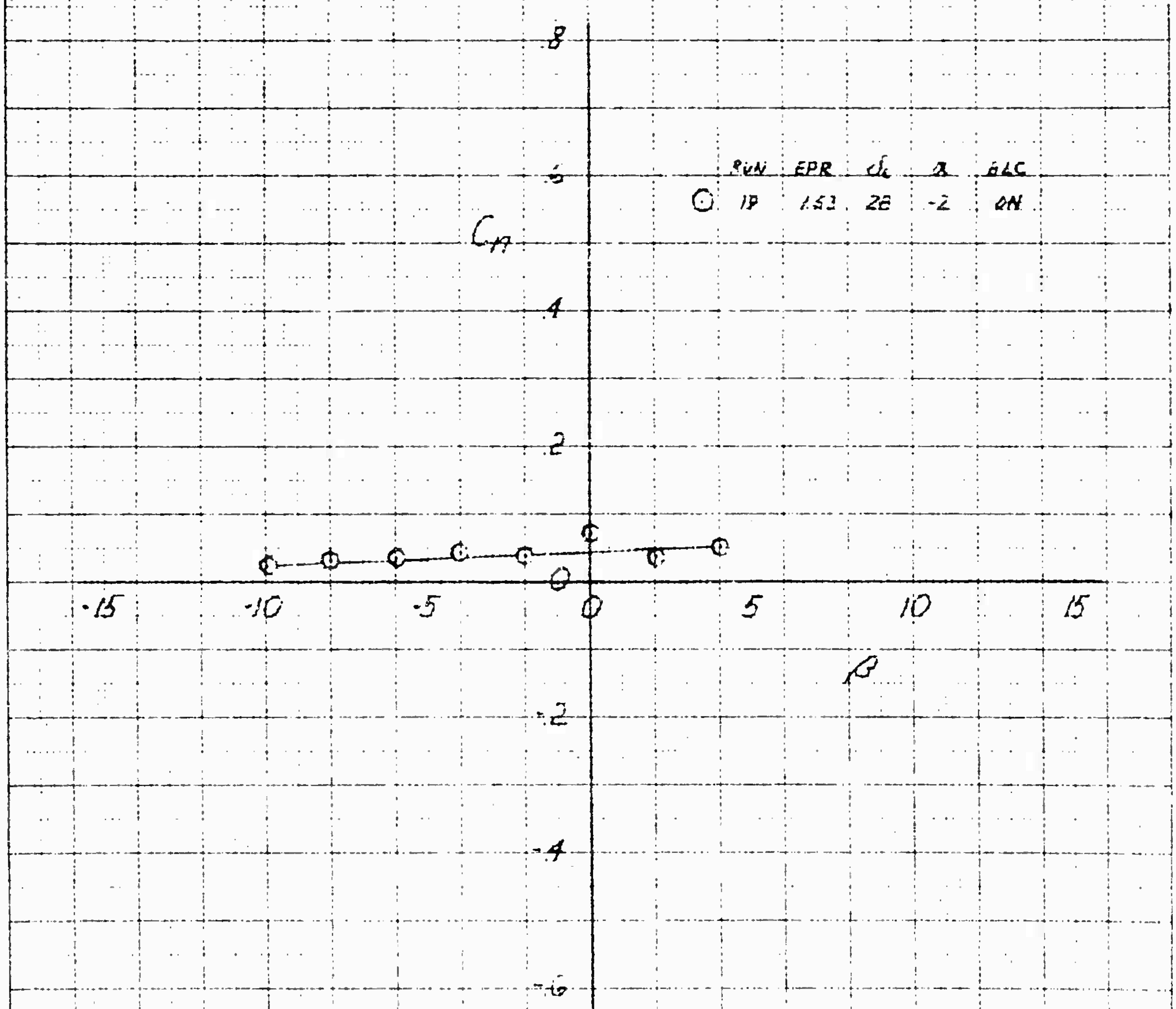

XV-4A
FULL SCALE WIND TUNNEL TEST 215
ROLLING MOMENT COEFFICIENT IN PHASE 2 FLIGHT AT 30 KNOTS

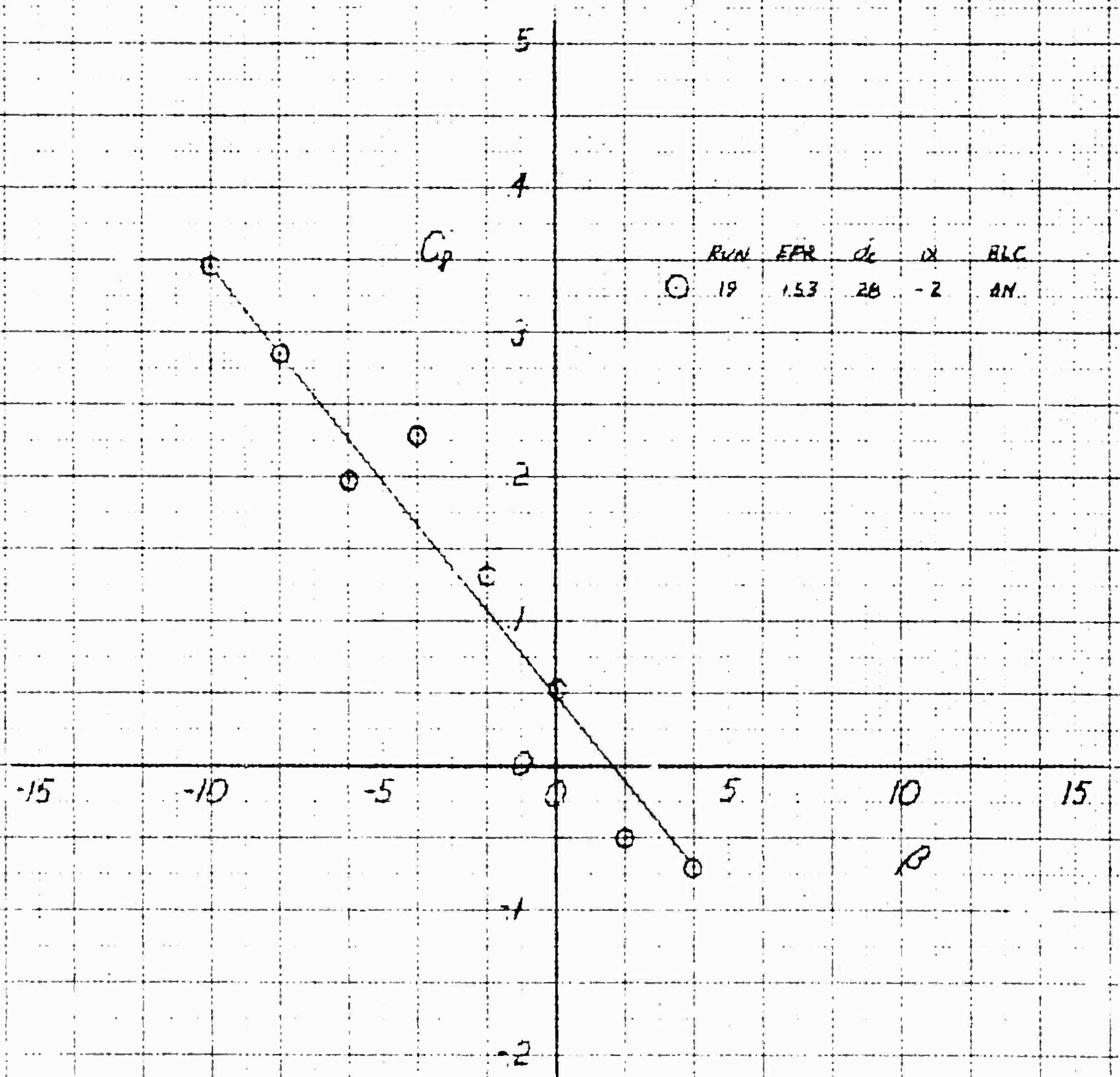

XV-4A

FULL SCALE WIND TUNNEL TEST 215

ELEVATOR EFFECT ON LIFT COEFFICIENT IN PHASE I FLIGHT AT 30 KNOTS

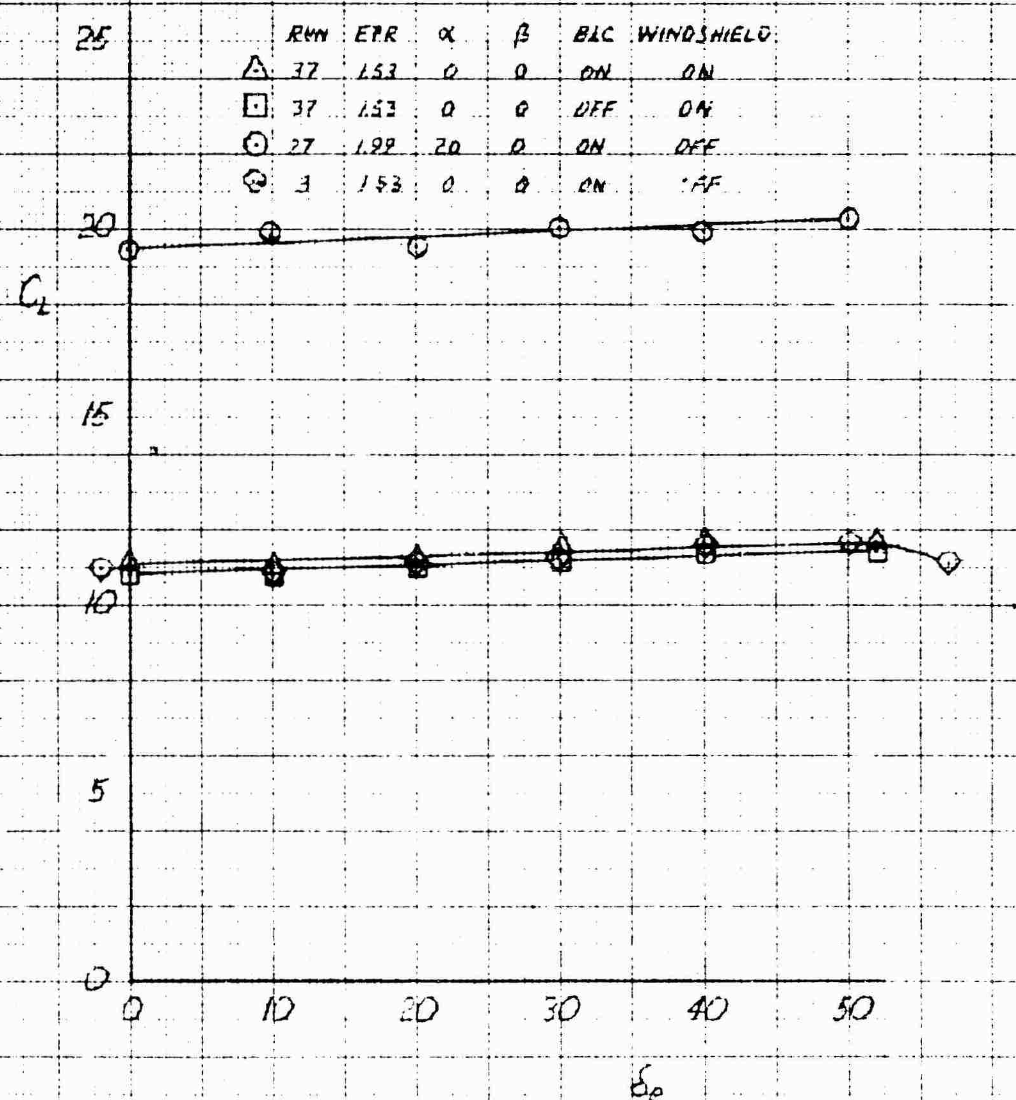

XV-4A

FULL SCALE WIND TUNNEL TEST 215

ELEVATOR EFFECT ON DRAG COEFFICIENT IN PHASE I FLIGHT AT 30 KNOTS

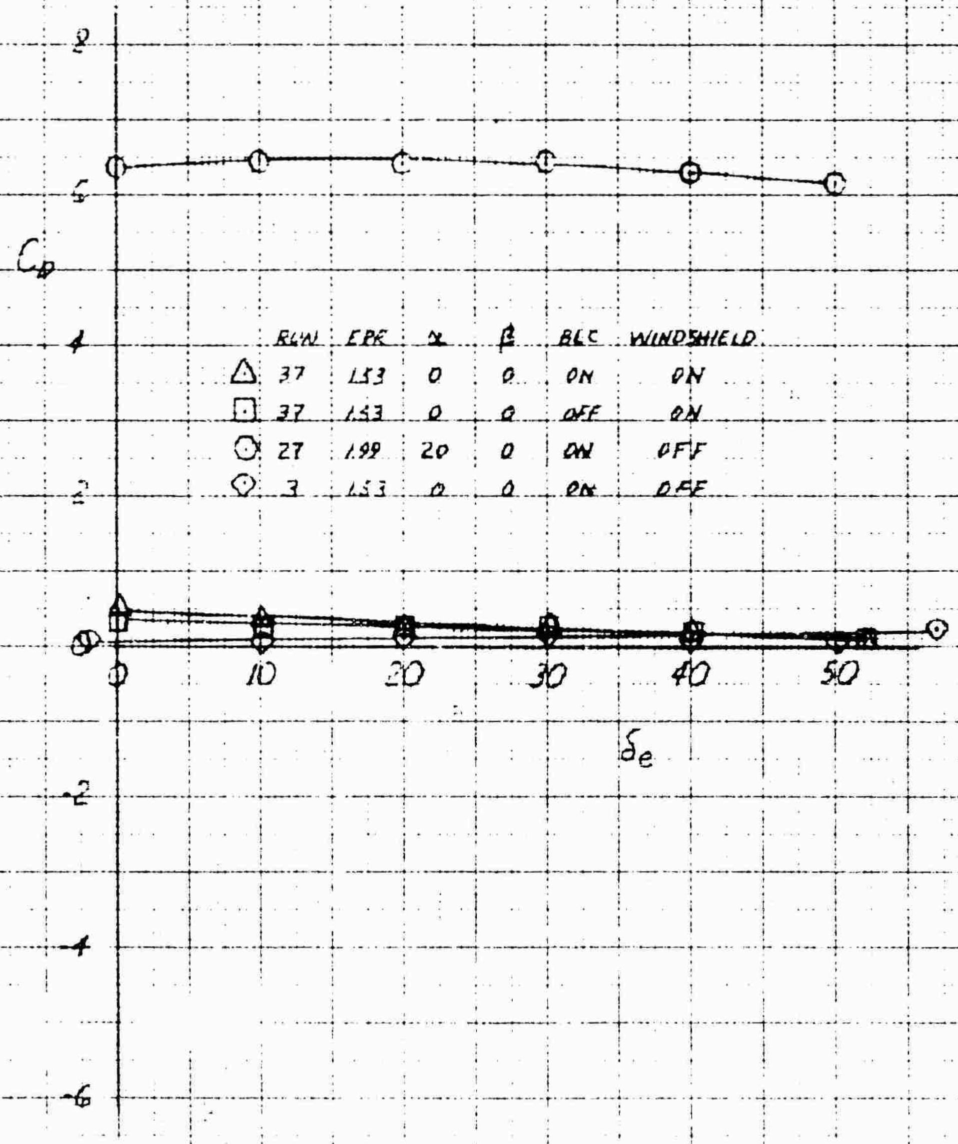

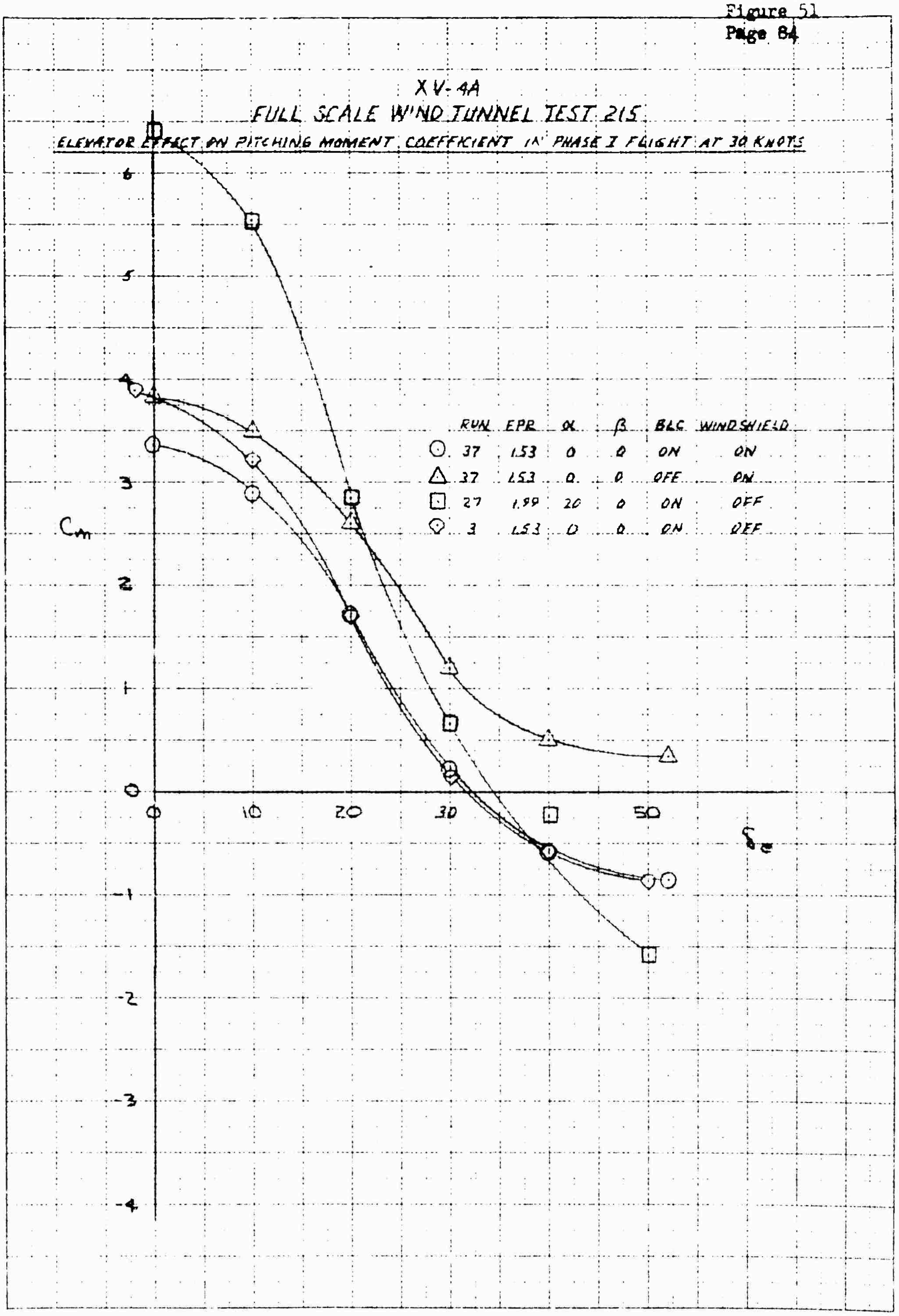
XV-4A
FULL SCALE WIND TUNNEL TEST 215
ELEVATOR EFFECT ON PITCHING MOMENT COEFFICIENT IN PHASE I FLIGHT AT 30 KNOTS
RUN EPR α β BLC WINDSHIELD
37 1.53 0 0 ON ON
37 1.53 0 0 OFF ON
27 1.99 20 0 ON OFF
3 1.53 0 0 ON OFF
Cm
δe
6
5
4
3
2
1
0
-1
-2
-3
-4
0
10
20
30
50

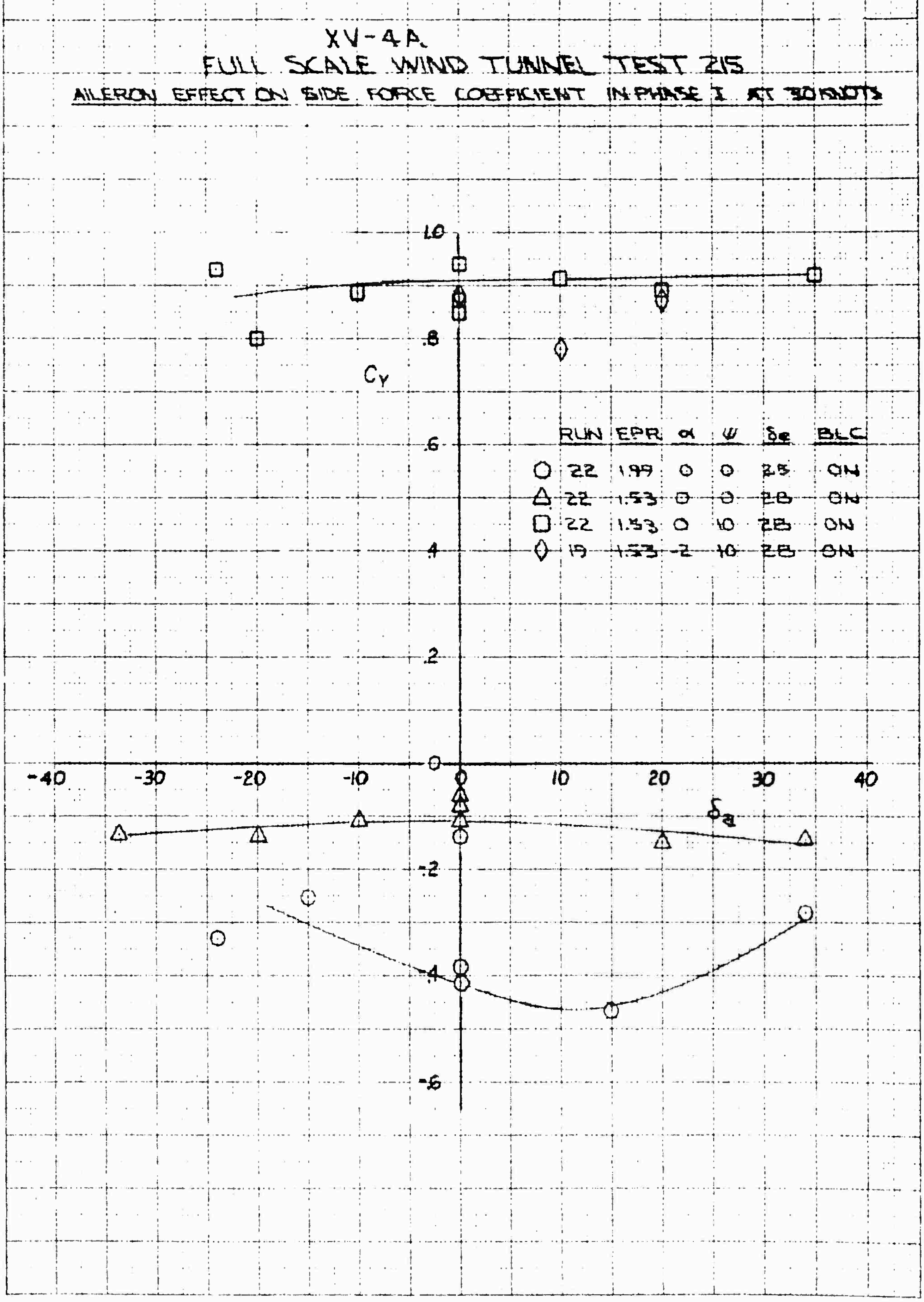
XV-4A
FULL SCALE WIND TUNNEL TEST 215
AILERON EFFECT ON SIDE FORCE COEFFICIENT IN PHASE I AT 30 KNOTS
1.0
.8
.6
.4
.2
0
-.2
-.4
-.6
C_Y
-40
-30
-20
-10
10
20
30
40
δ_a
RUN EPR α ψ δe BLC
○ 22 1.99 0 0 28 ON
△ 22 1.53 0 0 28 ON
□ 22 1.53 0 10 28 ON
◇ 19 1.53 -2 10 28 ON

XV-4A
FULL SCALE WIND TUNNEL TEST 215
AILERON EFFECT ON YAWING MOMENT COEFFICIENT IN PHASE I AT 30 KNOTS

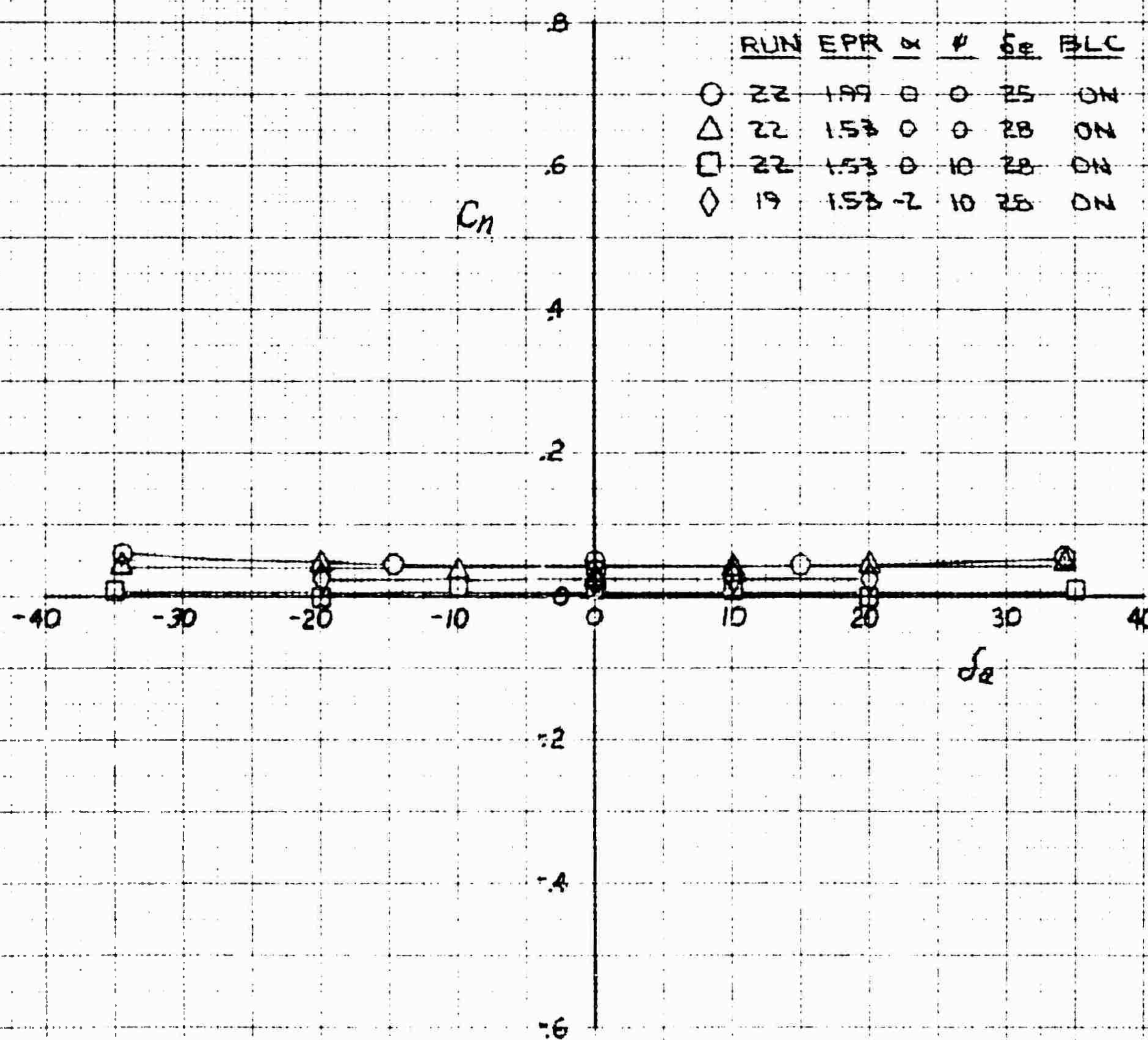

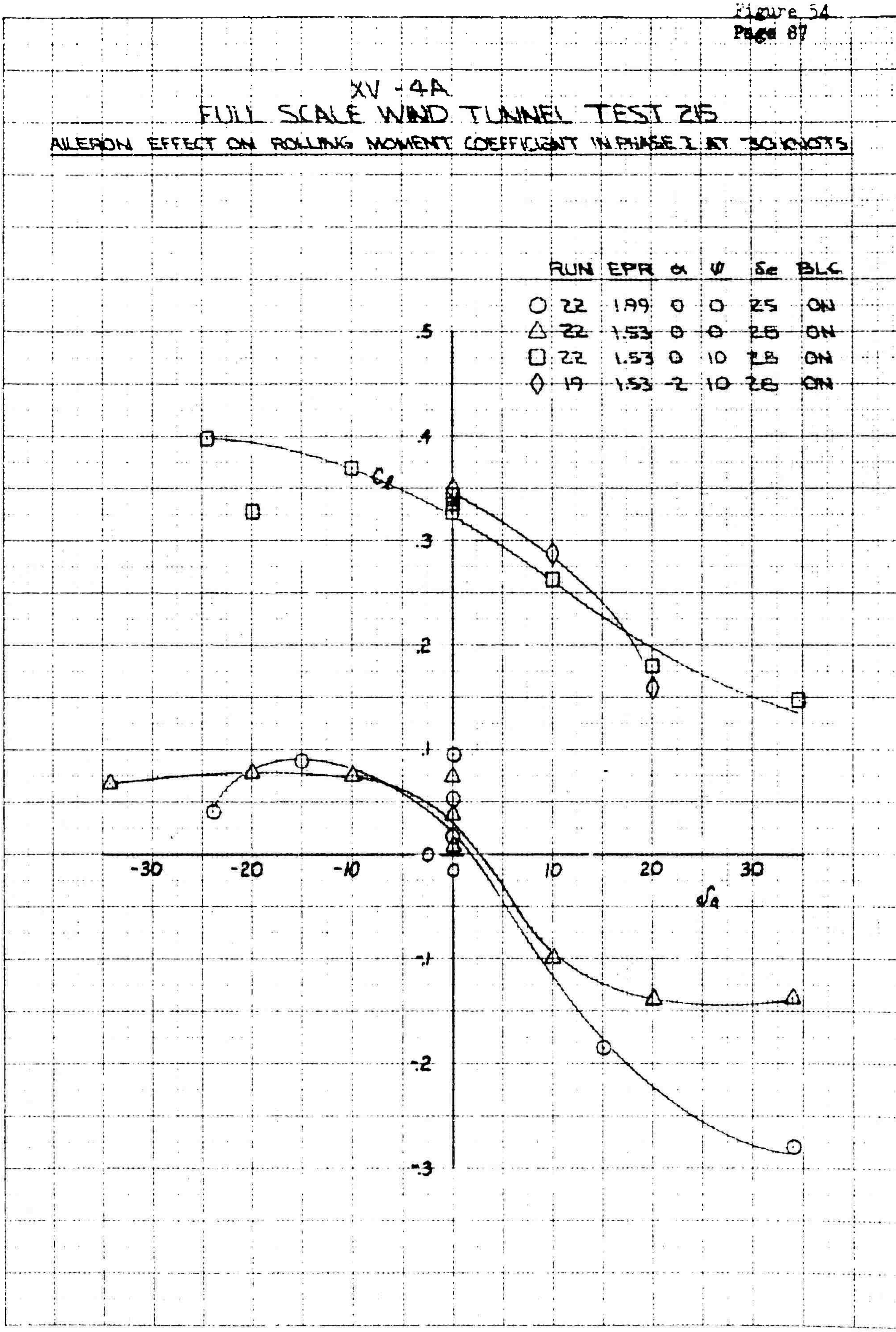
XV - 4A
FULL SCALE WIND TUNNEL TEST 215
AILERON EFFECT ON ROLLING MOMENT COEFFICIENT IN PHASE I AT 30 KNOTS
RUN EPR α ψ δe BLC
○ 22 1.99 0 0 25 ON
△ 22 1.53 0 0 25 ON
□ 22 1.53 0 10 28 ON
◇ 19 1.53 -2 10 28 ON
Cℓ
.5
.4
.3
.2
.1
0
-.1
-.2
-.3
-30
-20
-10
0
10
20
30
δa

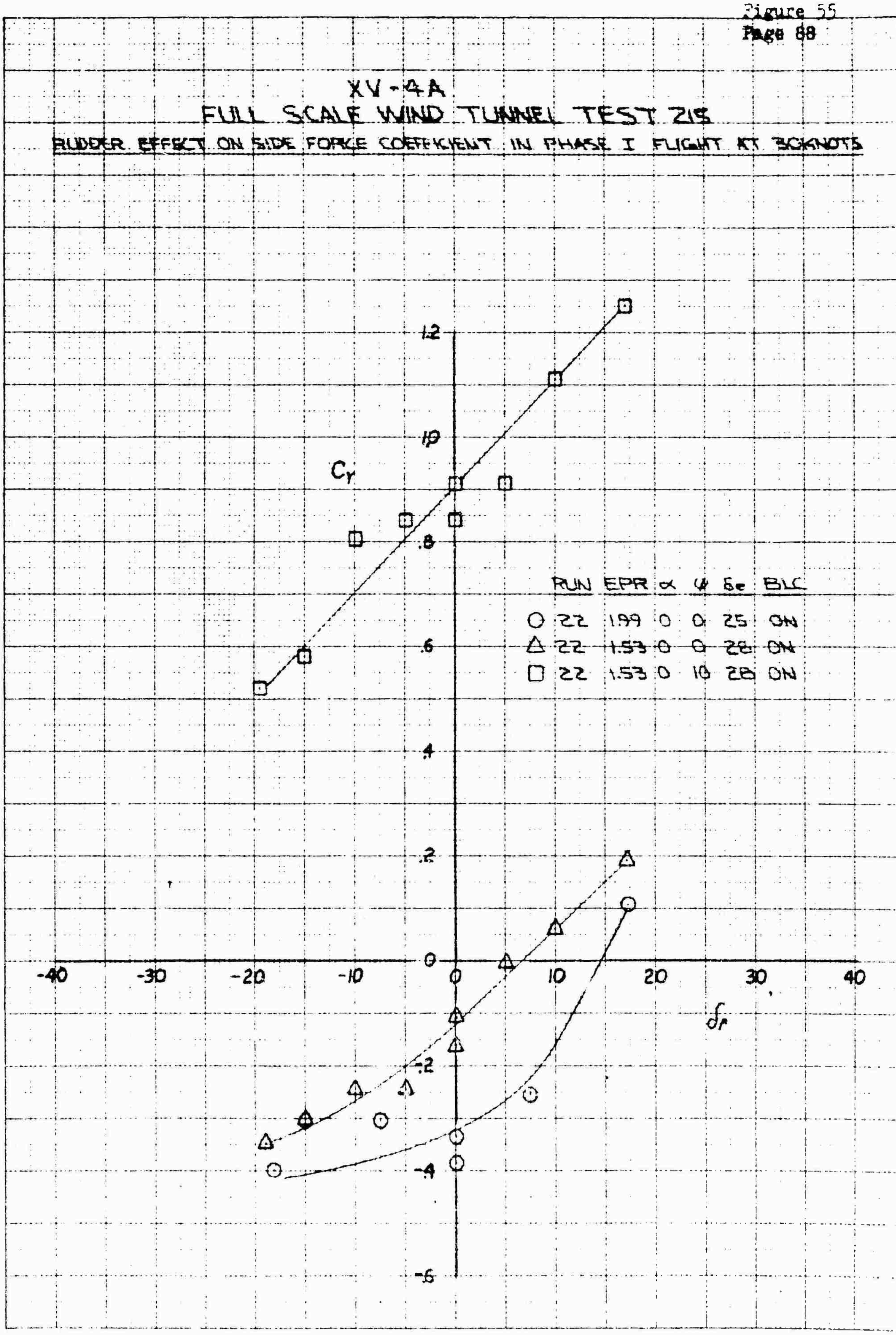
XV-4A
FULL SCALE WIND TUNNEL TEST 215
RUDDER EFFECT ON SIDE FORCE COEFFICIENT IN PHASE I FLIGHT AT 30KNOTS
C_Y
1.2
1.0
.8
.6
.4
.2
0
-.2
-.4
-.6
-40
-30
-20
-10
0
10
20
30
40
δ_r
RUN EPR α ψ δe BLC
○ 22 1.99 0 0 25 ON
△ 22 1.53 0 0 28 ON
□ 22 1.53 0 10 28 ON

ER-7634
Figure 56
Page 89

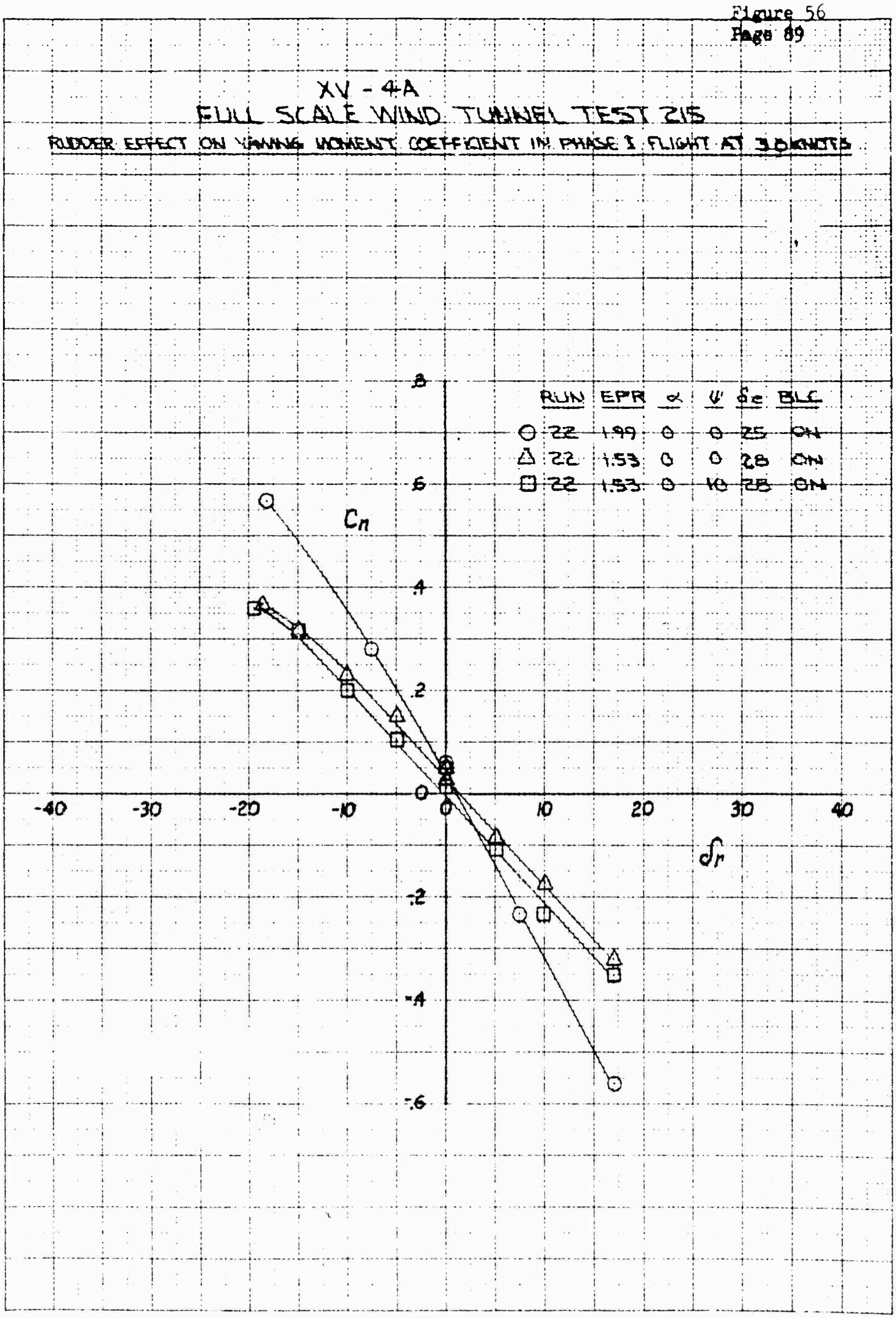

XV-4A

FULL SCALE WIND TUNNEL TEST 215

RUDDER EFFECT ON ROLLING MOMENT COEFFICIENT IN PHASE I FLIGHT AT 30 KNOTS

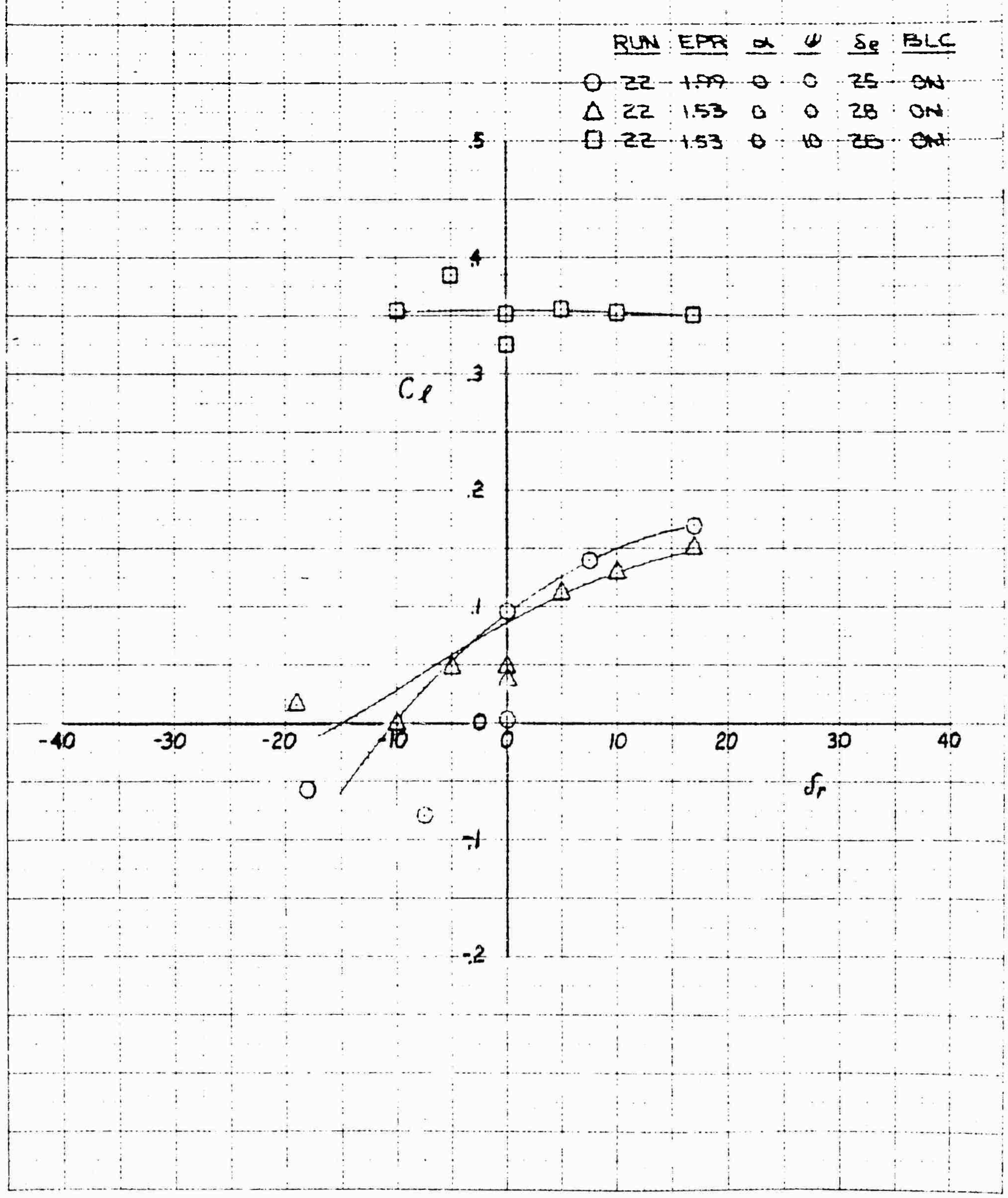

STABILITY AND CONTROL COMPARISON IN CONV

FULL SCALE DATA AMES 40' X 80'

Run No.		28	29	30	31	33	34
Ejector Doors		Closed	Closed	Closed	Closed	Closed	Cl
Flap Deflection (δ_f)	Deg.	40	40	40	0	40	40
Engines		Wind-milling	Wind-milling	Wind-milling	Wind-milling	Var. EPR	Var. EPR
Equivalent Airspeed	Knots	80	40	80	80	80	40
q	Lb/Ft^2	21.70	5.43	21.70	21.70	21.70	5.4
α	Deg.	Var.	Var.	0	Var.	Var.	0
β	Deg.	0	0	Var.	Var.	0	0
δ_e	Deg.	Var.	0	-18	Var.	Var.	0
δ_a	Deg.	Var.	0	Var.	Var.	0	0
δ_r	Deg.	Var.	0	Var.	Var.	0	0
C_{L_α}	1/Deg.	.090	.093	-	.088	.108	-
$C_{L\delta_e}$	1/Deg.	+.0044	-	-	+.0048	+.0070	-
α (C_L = 0)	Deg.	-6.4	-6.5	-	-.6	-6.4	-
C_L (α = 0)		.58	.54	-	+.05	.76	-
$C_{L_{Max}}$		1.42	1.35	-	1.10	1.77	-
dC_M/dC_L		-.112	0	-	-.139	-.045	-
C_M (C_L = δ_e = 0)		-.205	-.30	-	-.160	-.33	-
$C_{M\delta_e}$	1/Deg.	-.018	-	-	-.018	-.025	-

A

STABILITY AND CONTROL COMPARISON IN CONVENTIONAL FLIGHT

FULL SCALE DATA AMES 40' X 80'						EST. FROM SMALL SCALE DATA COMPARISON WITH RUN NO.			
29	30	31	33	34	35	28 & 30	31	33	35
Closed	Closed	Closed	Closed	Closed	Open	Closed	Closed	Closed	Open
40	40	0	40	40	40	40	0	40	40
Wind-milling	Wind-milling	Wind-milling	Var. EPR	Var. EPR	Wind-milling	Off	Off	EPR = 1.53	Off
40	80	80	80	40	80	-	-	80	-
5.43	21.70	21.70	21.70	5.43	21.70	-	-	21.70	-
Var.	0	Var.	Var.	0	Var.	-	-	-	-
0	Var.	Var.	0	0	Var.	-	-	-	-
0	-18	Var.	Var.	0	0	-	-	-	-
0	Var.	Var.	0	0	0	-	-	-	-
0	Var.	Var.	0	0	0	-	-	-	-
.093	-	.088	.108	-	.070	.089	.0863	.107	.070
-	-	+.0048	+.0070	-	-	+.00715	+.00715	+.00715	+.00715
-6.5	-	-.6	-6.4	-	-9.5	-6.6	+.245	-6.4	-8.35
.54	-	+.05	.76	-	.67	.60	-.021	.685	.585
1.35	-	1.10	1.77	-	1.52	1.82	1.20	1.75	1.62
0	-	-.139	-.045	-	-.432	-.078	-.147	-.0416	-.545
-.30	-	-.160	-.33	-	-.035	-.065	+.0615	.0282	.310
-	-	-.018	-.025	-	-	-.0252	-.0252	-.0252	-.0252

STABILITY AND CONTROL COMPARISON IN CONV

FULL SCALE DATA AMES 40' X 80'

Run No.		28	29	30	31	33	34
C_Y ($\delta_a = \delta_r = \beta = 0$)		-.008	-	-.018	-.008	-	-
C_{Y_β}	1/Deg.	-	-	-.020	-.020	-	-
$C_{Y_{\delta_a}}$	1/Deg.	0	-	0	0	-	-
$C_{Y_{\delta_r}}$	1/Deg.	+.0053	-	+.0053	+.0053	-	-
C_n ($\delta_a = \delta_r = \beta = 0$)		-.0020	-	-.0030	-.0020	-	-
C_{n_β}	1/Deg.	-	-	+.0045	+.0045	-	-
$C_{n_{\delta_a}}$	1/Deg.	-.00013	-	-.00013	-.00013	-	-
$C_{n_{\delta_r}}$	1/Deg.	-.0033	-	-.0033	-.0033	-	-
C_l ($\delta_a = \delta_r = \beta = 0$)		+..027	-	+.016	+.014	-	-
C_{l_β}	1/Deg.	-	-	-.0018	-.0018	-	-
$C_{l_{\delta_a}}$	1/Deg.	-.0011	-	-.0011	-.0011	-	-
$C_{l_{\delta_r}}$	1/Deg.	+.0008	-	+.0008	+.0008	-	-
$dC_M/dEPR$		-	-	-	-	+.270	+.2
$dC_L/dEPR$		-	-	-	-	+.035	-.1

A

STABILITY AND CONTROL COMPARISON IN CONVENTIONAL FLIGHT

E[illegible]-7034
Fig. [illegible] (Cont'd)
Page 190A

FULL SCALE DATA AMES 40' X 80'

EST. FROM SMALL SCALE DATA COMPARISON WITH RUN NO.

29	30	31	33	34	35	28 & 30	31	33	35
-	-.018	-.008	-	-	-.010	0	0	0	-
-	-.020	-.020	-	-	-.019 (α = 0) -.016 (α = 8)	-.0196	-.0196	-.0[illegible]	-
-	0	0	-	-	-	0	0	0	-
-	+.0053	+.0053	-	-	-	+.0040	+.0040	+.0040	-
-	-.0030	-.0020	-	-	+.0010	0	0	0	-
-	+.0045	+.0045	-	-	+.0014 (α = 0) -.0011 (α = 8)	+.0030	+.0030	+.0030	-
-	-.00013	-.00013	-	-	-	Neg.	Neg.	Neg.	-
-	-.0033	-.0033	-	-	-	-.00212	-.00212	-.00212	-
-	+.016	+.014	-	-	+.003	0	0	0	-
-	-.0018	-.0018	-	-	-.0026 (α = 0) -.0008 (α = 8)	-.0026	-.0026	-.0026	-
-	-.0011	-.0011	-	-	-	-.00082	-.00082	-.00082	-
-	+.0008	+.0008	-	-	-	+.00076	+.00076	+.00076	-
-	-	-	+.270	+.250	-	-	-	-	-
-	-	-	+.035	-.150	-	-	-	-	-

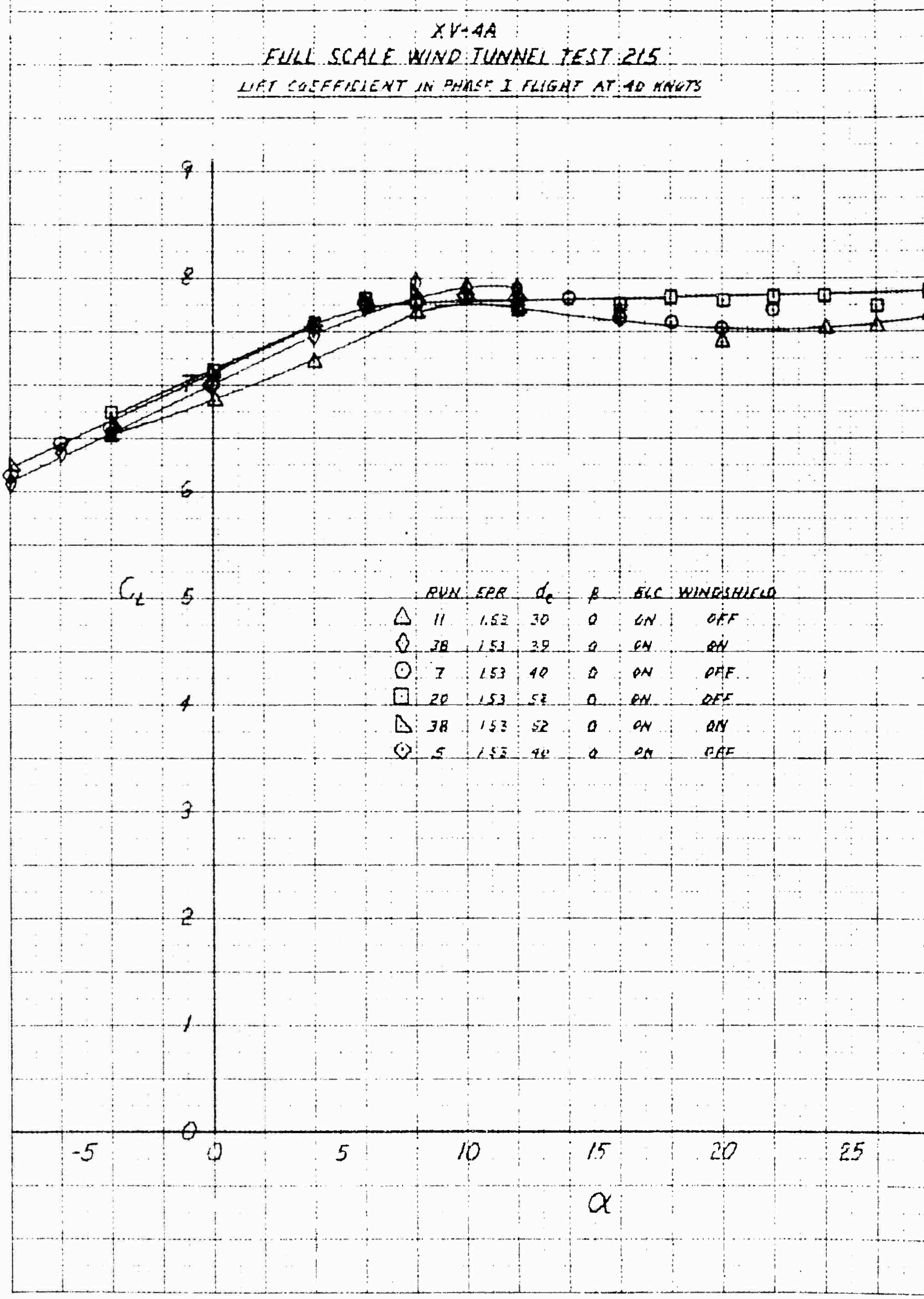
XV-4A
FULL SCALE WIND TUNNEL TEST 215
LIFT COEFFICIENT IN PHASE I FLIGHT AT 40 KNOTS
RUN EPR d_e β BLC WINDSHIELD
11 1.52 30 0 ON OFF
38 1.53 39 0 ON ON
7 1.53 40 0 ON OFF
20 1.53 52 0 ON OFF
38 1.53 52 0 ON ON
5 1.53 40 0 ON OFF
C_L
0
1
2
3
4
5
6
8
9
-5
0
5
10
15
20
25
α

XV-4A
FULL SCALE WIND TUNNEL TEST 215
DRAG COEFFICIENT IN PHASE I FLIGHT AT 40 KNOTS

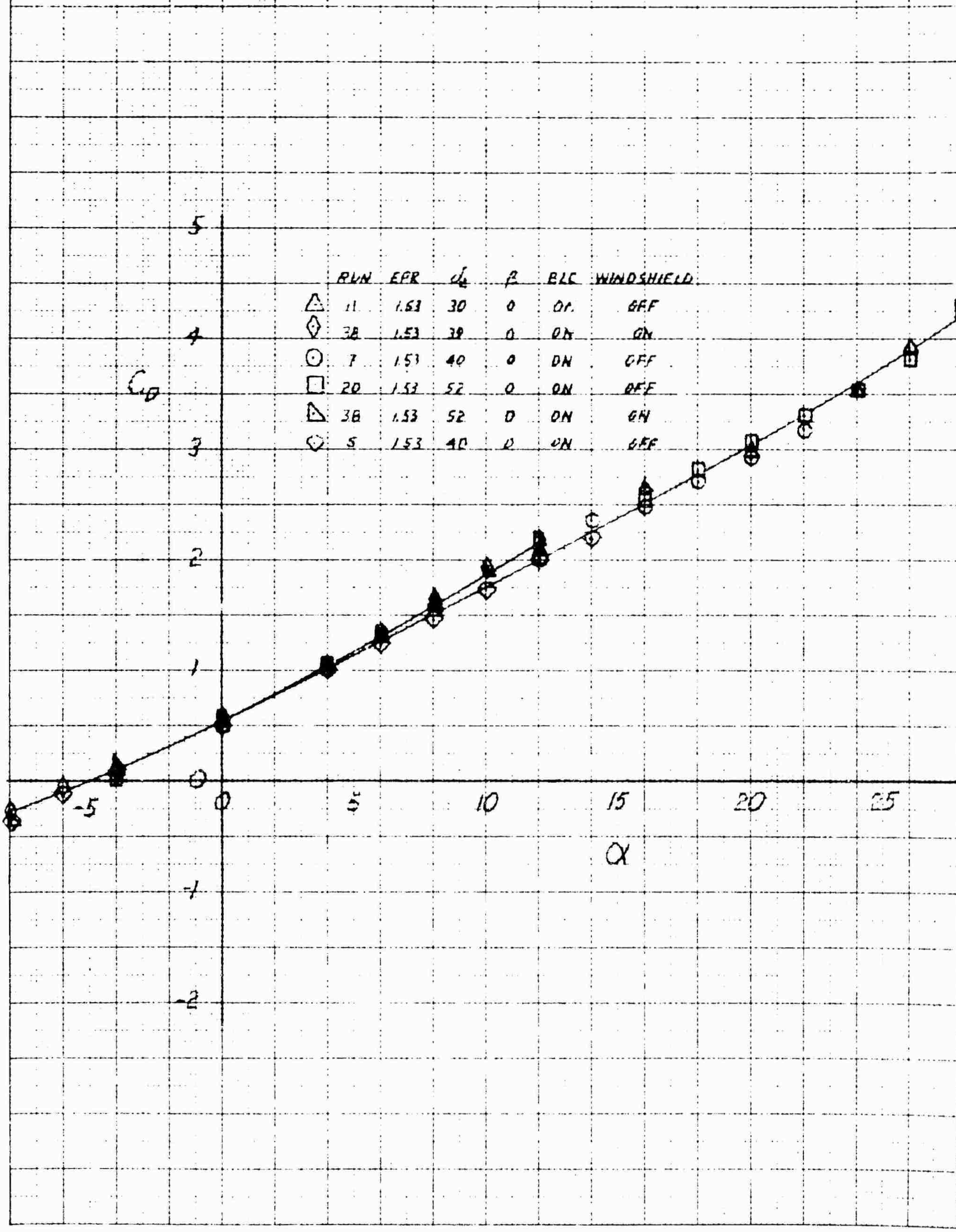

XV-4A

FULL SCALE WIND TUNNEL TEST 215

PITCHING MOMENT COEFFICIENT IN PHASE I FLIGHT AT 40 KNOTS

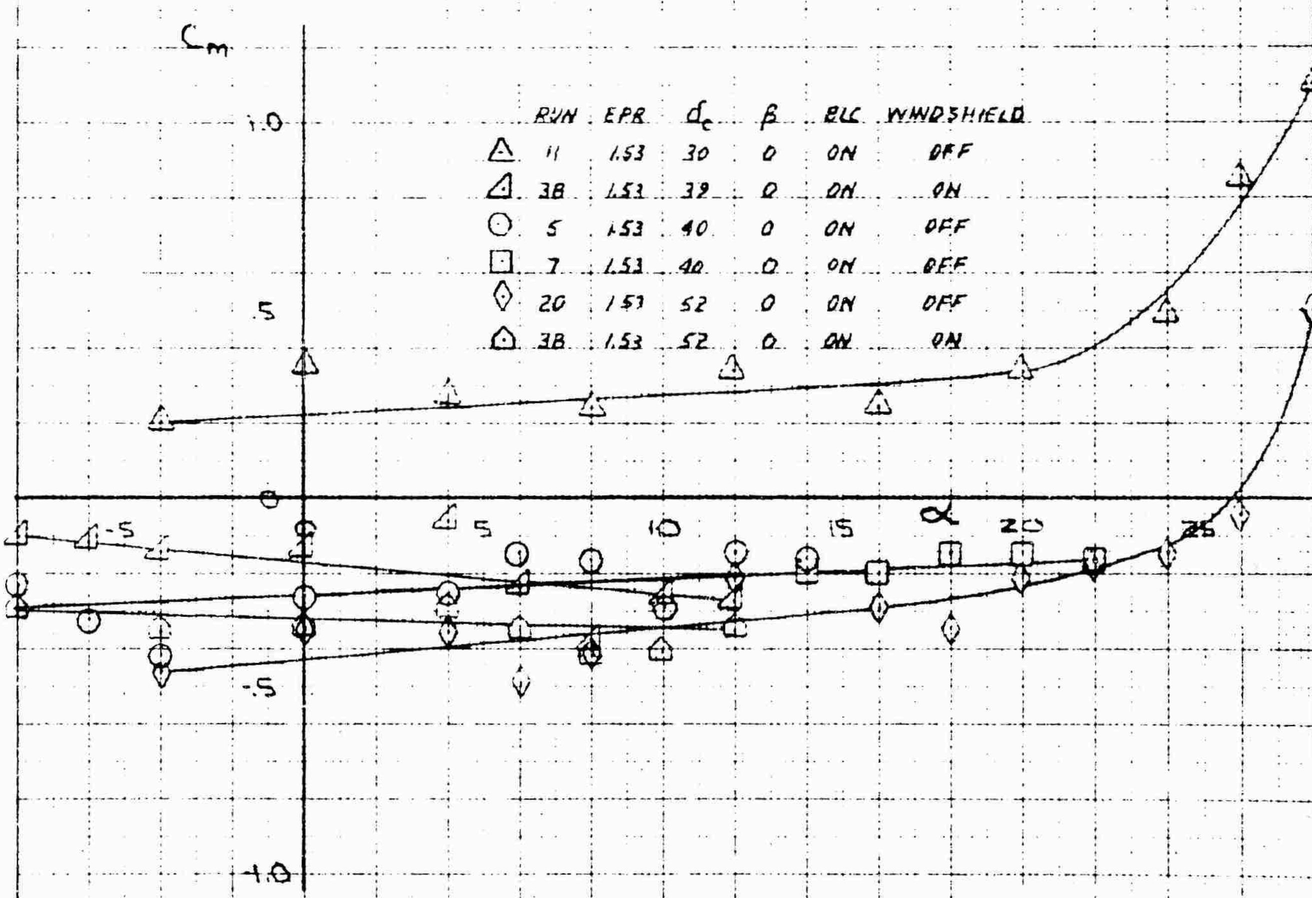

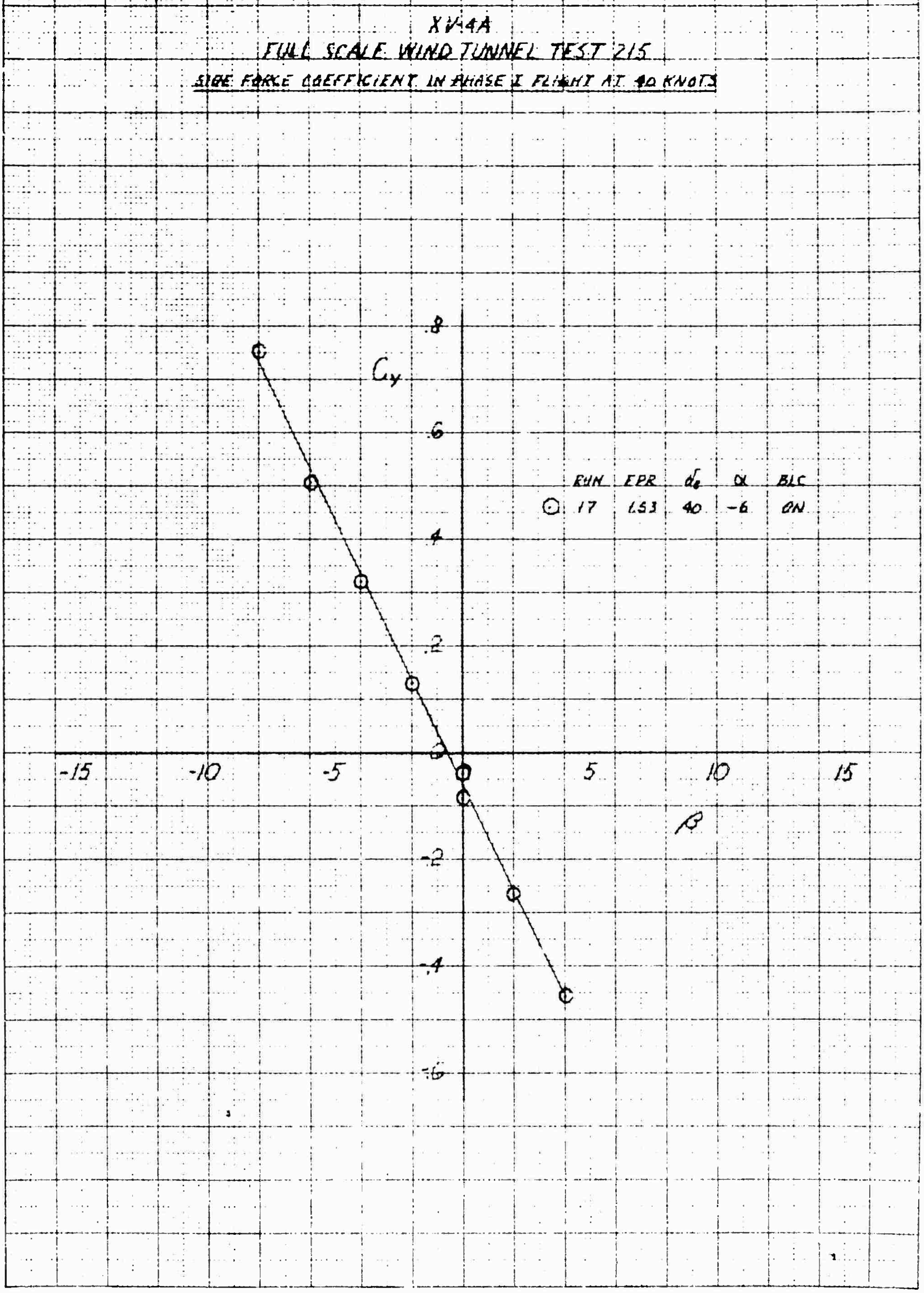
XV-4A
FULL SCALE WIND TUNNEL TEST 215
SIDE FORCE COEFFICIENT IN PHASE I FLIGHT AT 40 KNOTS
C_y
.8
.6
.4
.2
-.2
-.4
-.6
-15
-10
-5
5
10
15
β
RUN EPR δ_e α BLC
17 1.53 40 -6 ON

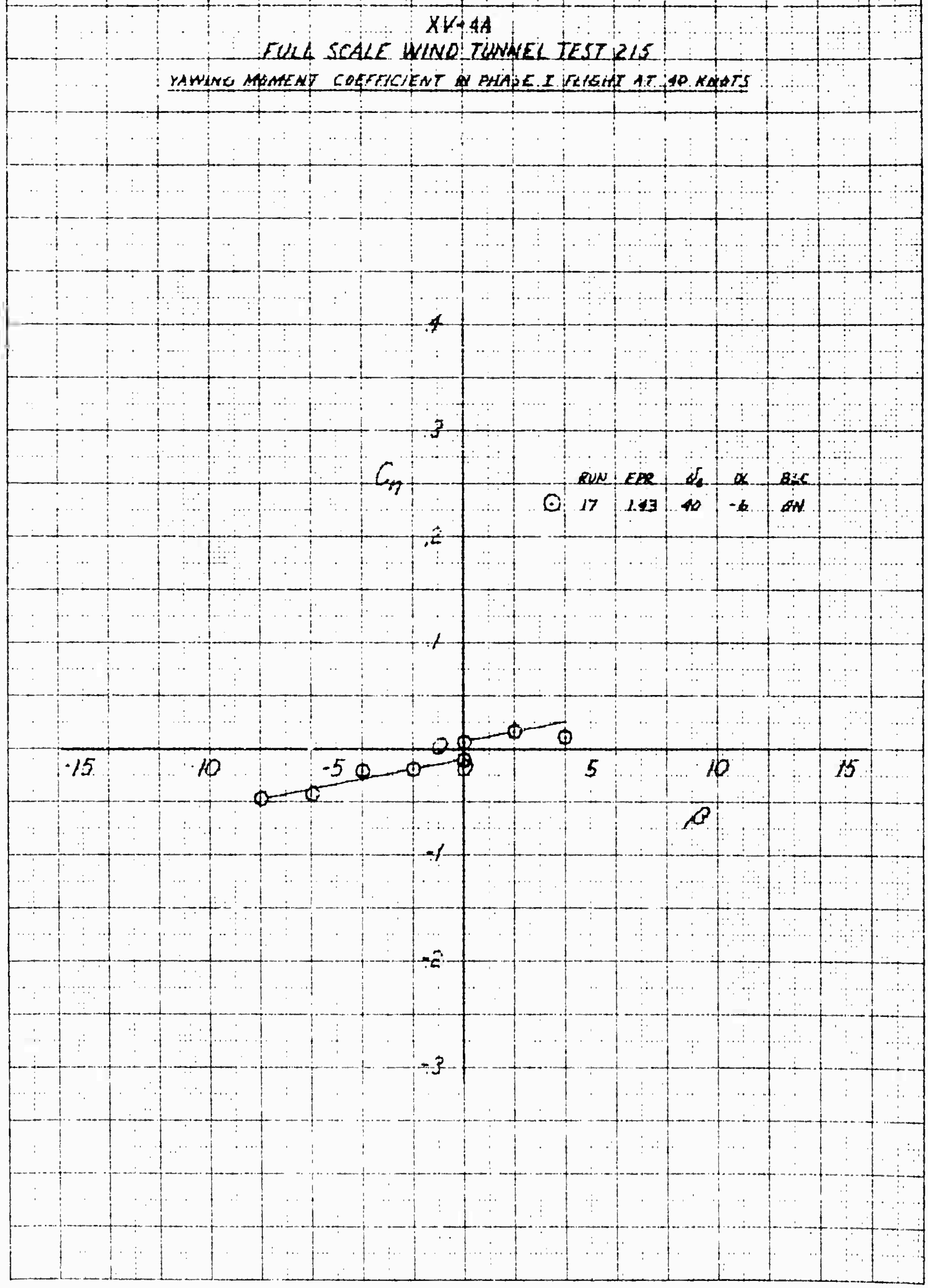
XV-4A
FULL SCALE WIND TUNNEL TEST 215
YAWING MOMENT COEFFICIENT IN PHASE I FLIGHT AT 40 KNOTS
.4
.3
.2
.1
-.1
-.2
-.3
C_n
RUN EPR δ_f α BLC
17 1.43 40 -6 ON
-15
10
-5
5
10
15
β

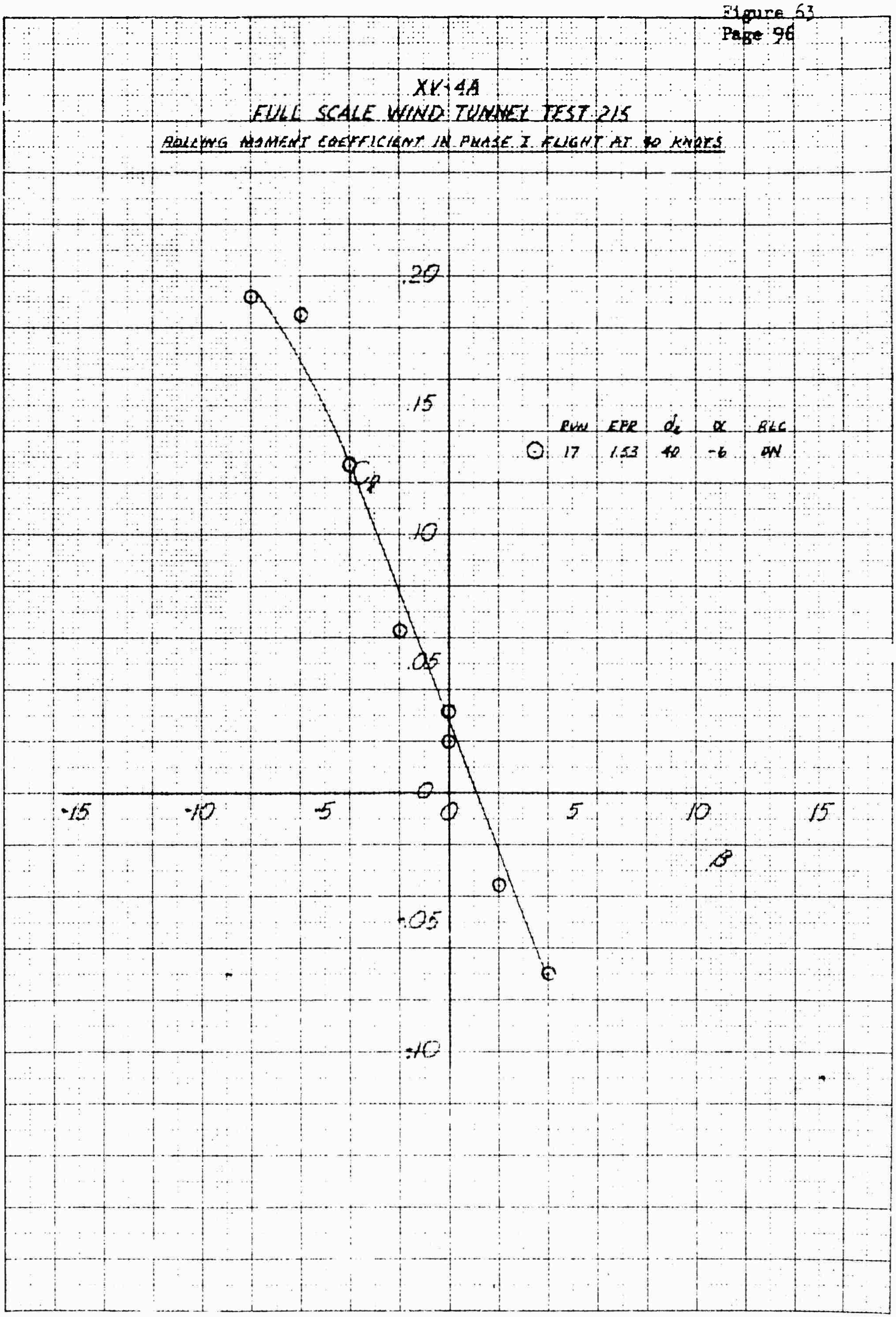
XV-4A
FULL SCALE WIND TUNNEL TEST 215
ROLLING MOMENT COEFFICIENT IN PHASE I FLIGHT AT 40 KNOTS
.20
.15
.10
.05
0
-.05
-.10
C_ℓ
-15
-10
-5
0
5
10
15
β
RUN
EPR
δ_f
α
BLC
17
1.53
40
-6
ON

XVF-4A

FULL SCALE WIND TUNNEL TEST 215

ELEVATOR EFFECT ON LIFT COEFFICIENT IN PHASE I FLIGHT AT [illegible] KNOTS

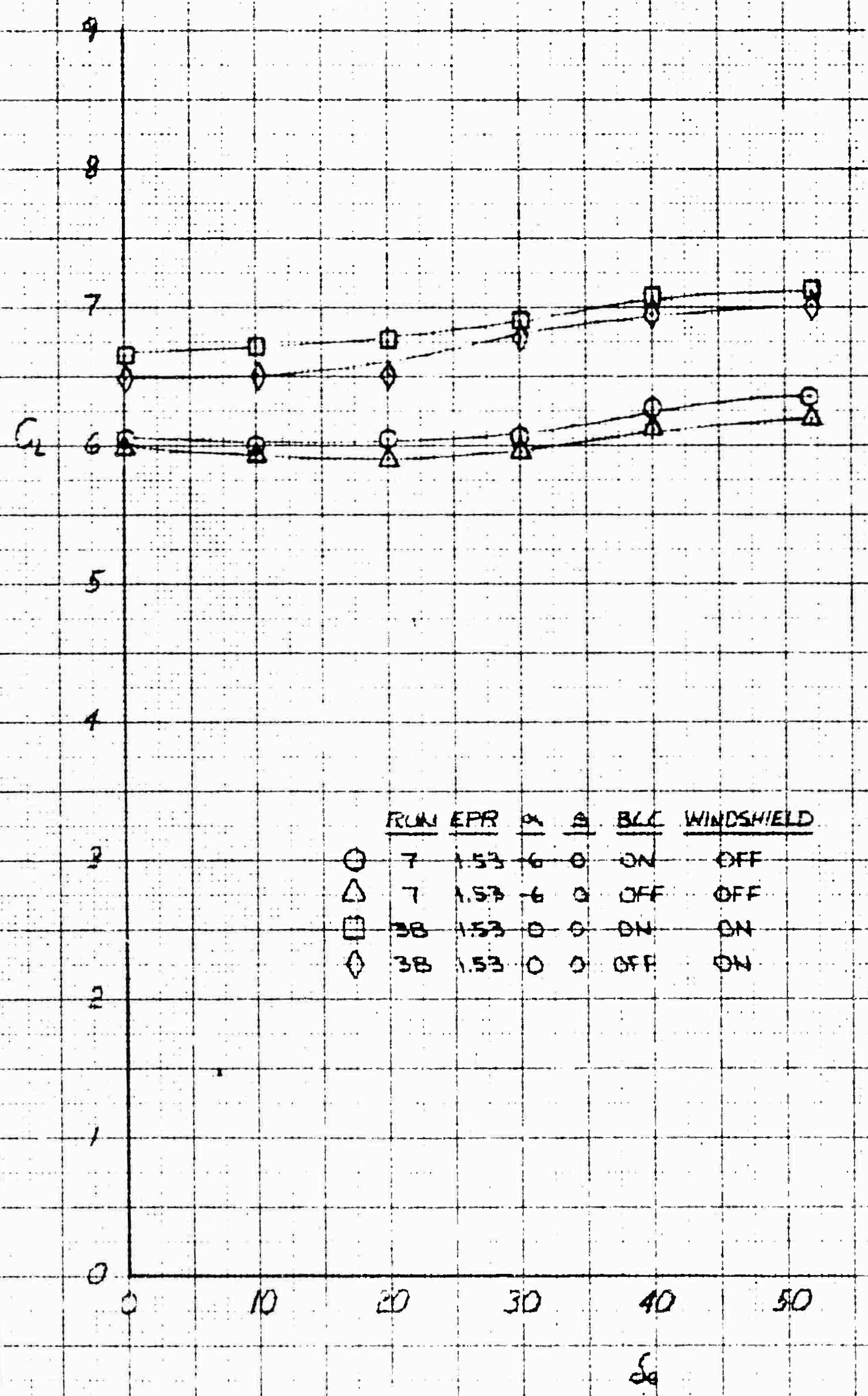

XV-4A
FULL SCALE WIND TUNNEL TEST 215
ELEVATOR EFFECT ON DRAG COEFFICIENT IN PHASE I FLIGHT AT 40 KNOTS

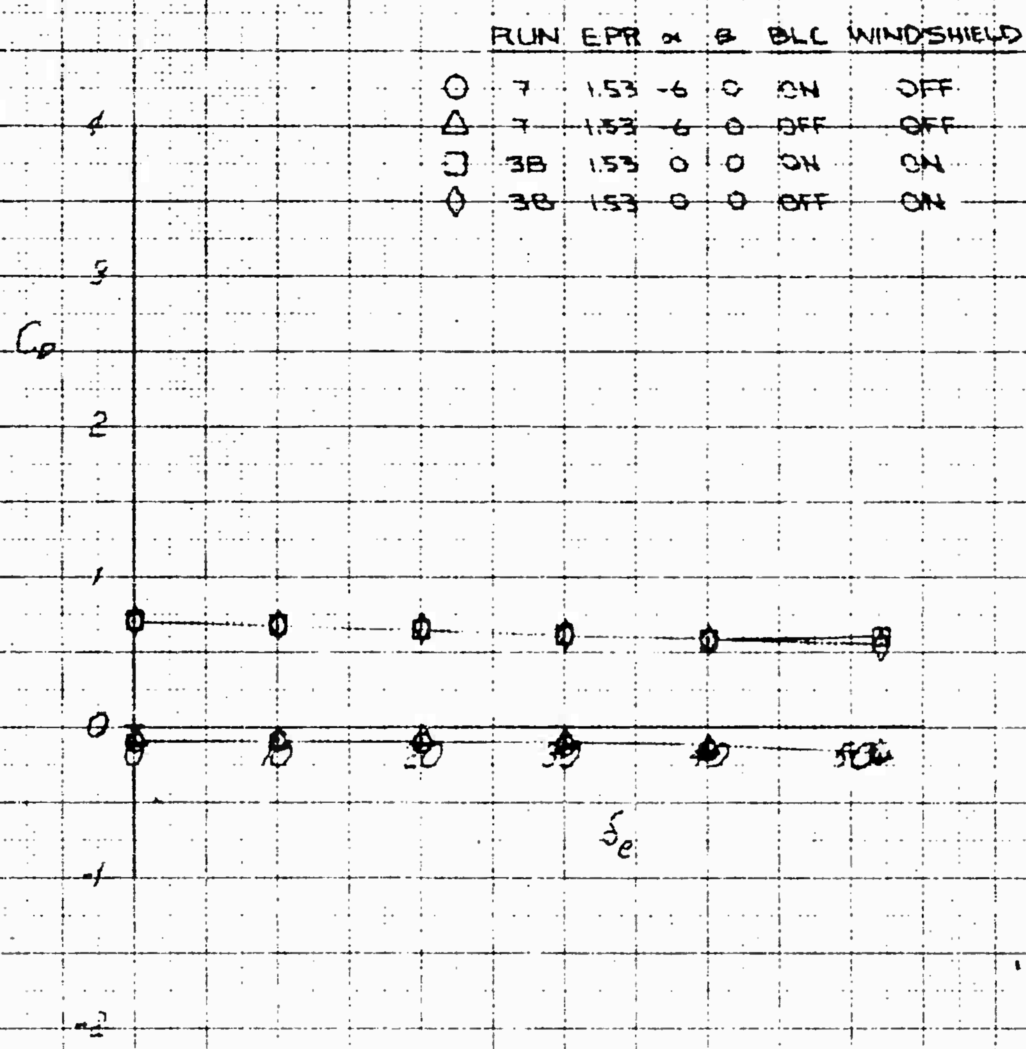

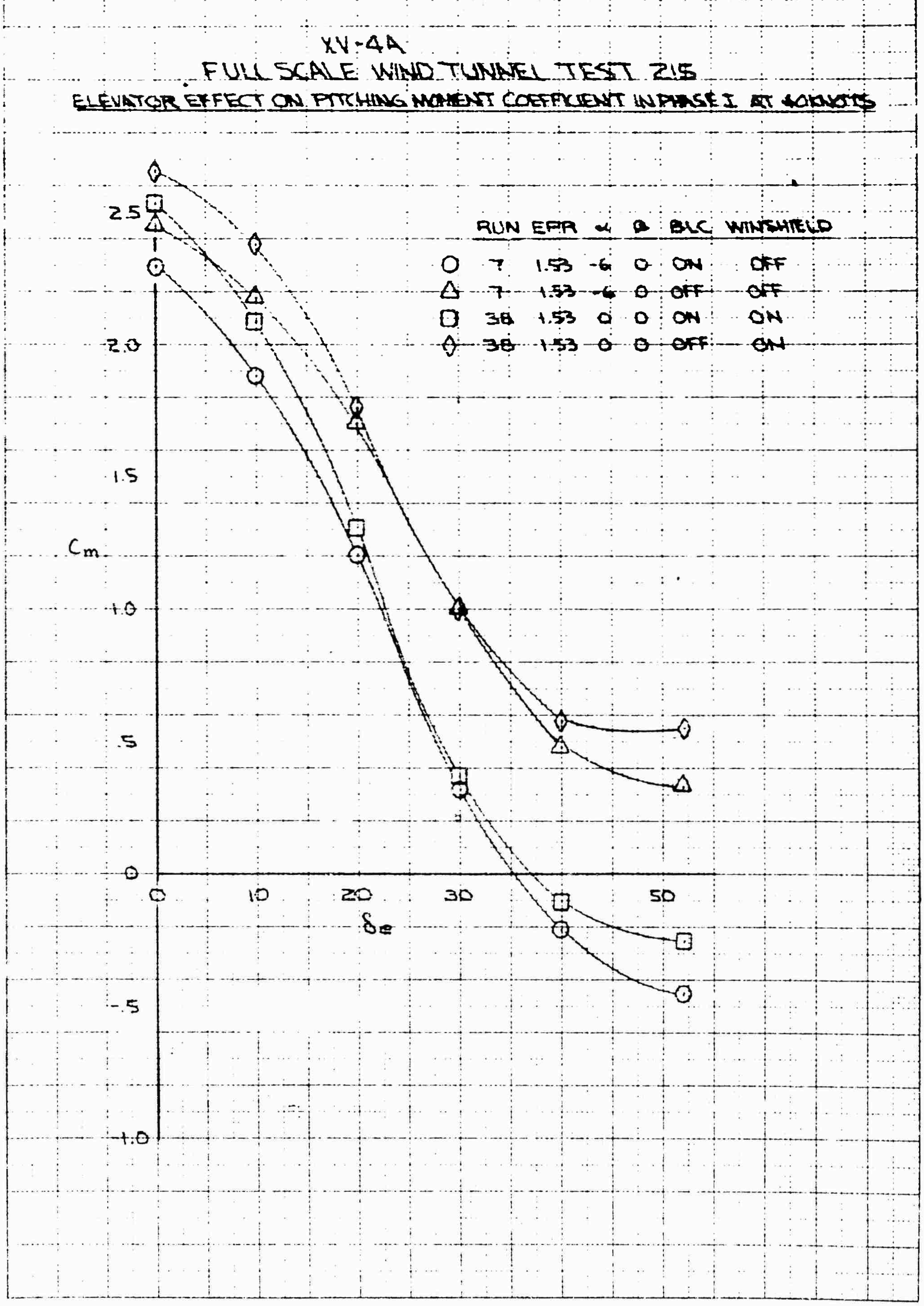
XV-4A
FULL SCALE WIND TUNNEL TEST 215
ELEVATOR EFFECT ON PITCHING MOMENT COEFFICIENT IN PHASE I AT 40 KNOTS
RUN EPR α β BLC WINSHIELD
○ 7 1.53 -6 0 ON OFF
△ 7 1.53 -6 0 OFF OFF
□ 38 1.53 0 0 ON ON
◇ 38 1.53 0 0 OFF ON
Cm
2.5
2.0
1.5
1.0
.5
0
-.5
-1.0
0
10
20
30
50
δe

XV-4A
FULL SCALE WIND TUNNEL TEST 215
AILERON EFFECT ON SIDE FORCE COEFFICIENT IN PHASE I FLIGHT AT 40 KNOTS

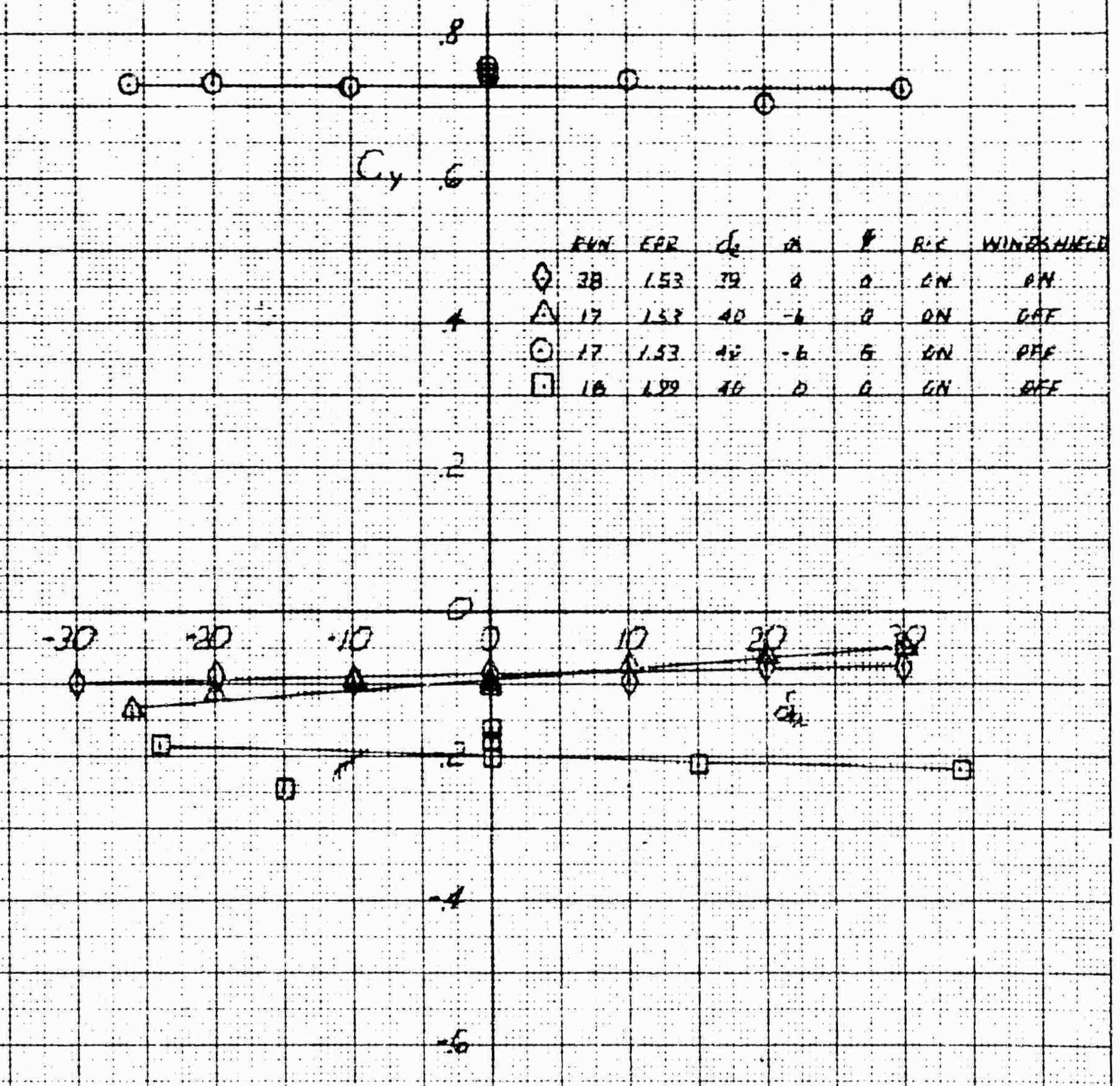

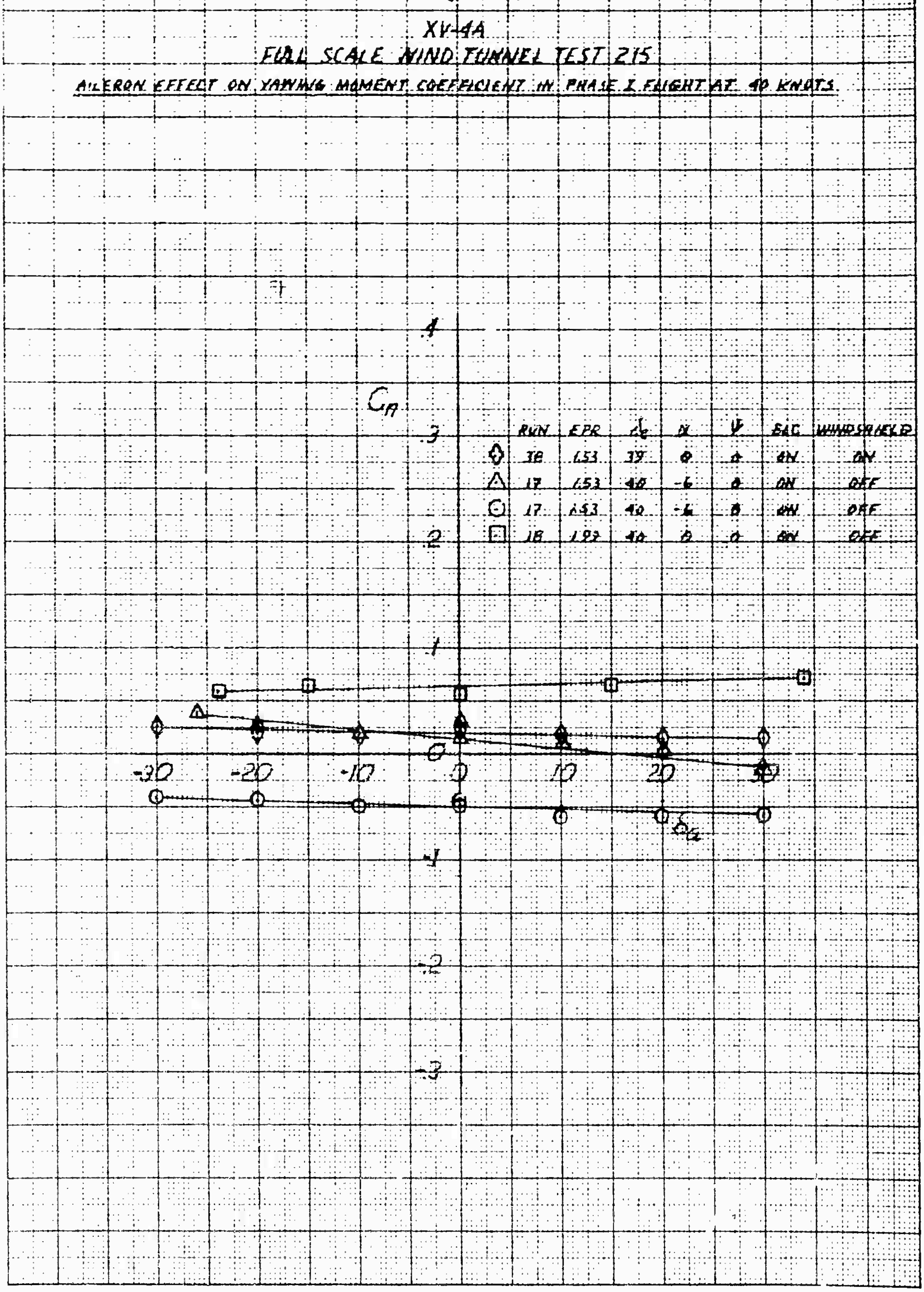
XV-4A
FULL SCALE WIND TUNNEL TEST 215
AILERON EFFECT ON YAWING MOMENT COEFFICIENT IN PHASE I FLIGHT AT 40 KNOTS
C_n
.4
.3
.2
.1
0
-.1
-.2
-.3
-30
-20
-10
0
10
20
30
δ_a
RUN EPR i_w α ψ EAC WINDSHIELD
38 1.53 39 0 0 ON ON
17 1.53 40 -6 0 ON OFF
17 1.53 40 -6 0 ON OFF
18 1.97 40 0 0 ON OFF

XV-4A
FULL SCALE WIND TUNNEL TEST 215
AILERON EFFECT ON ROLLING MOMENT COEFFICIENT IN PHASE I FLIGHT AT 40 KNOTS

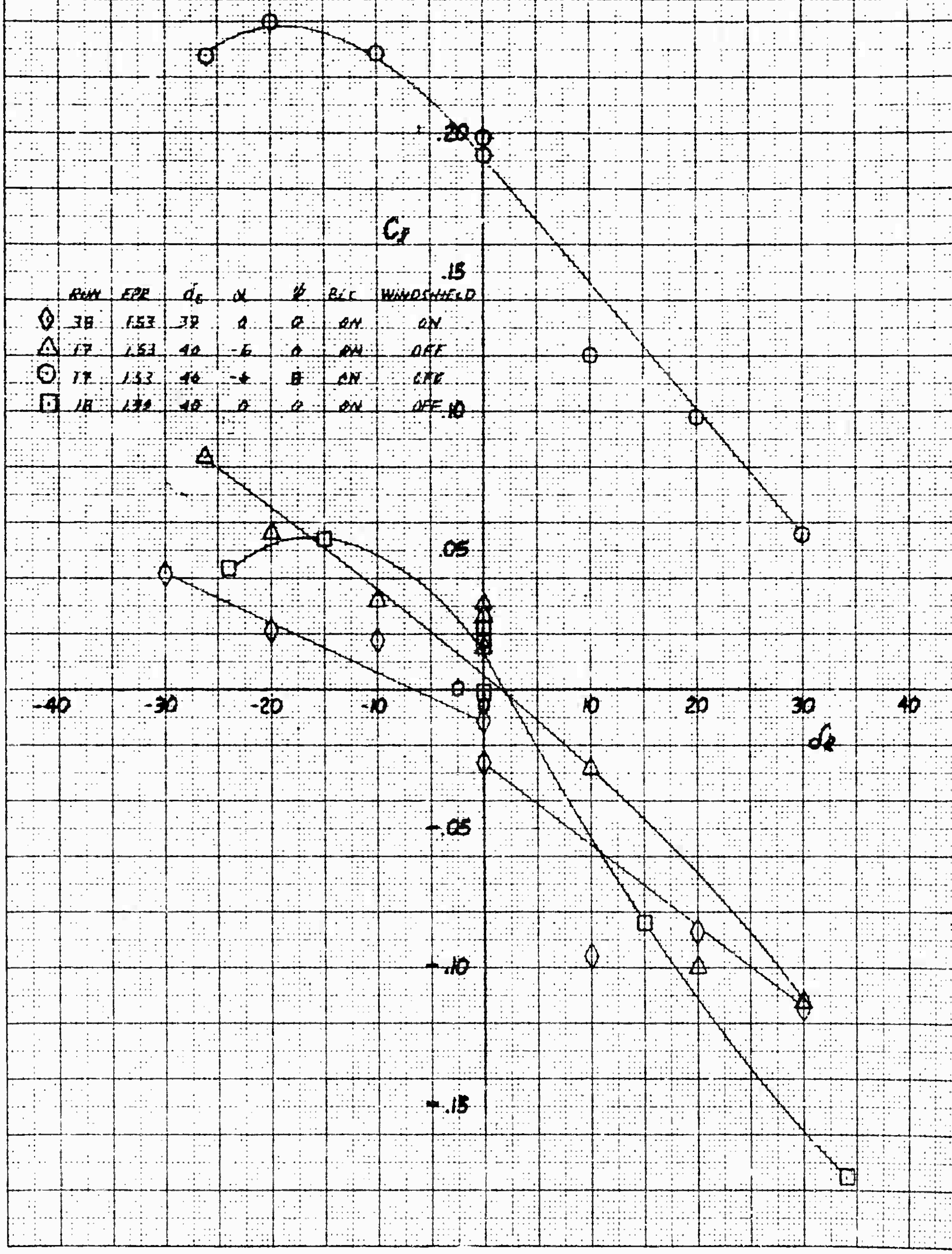

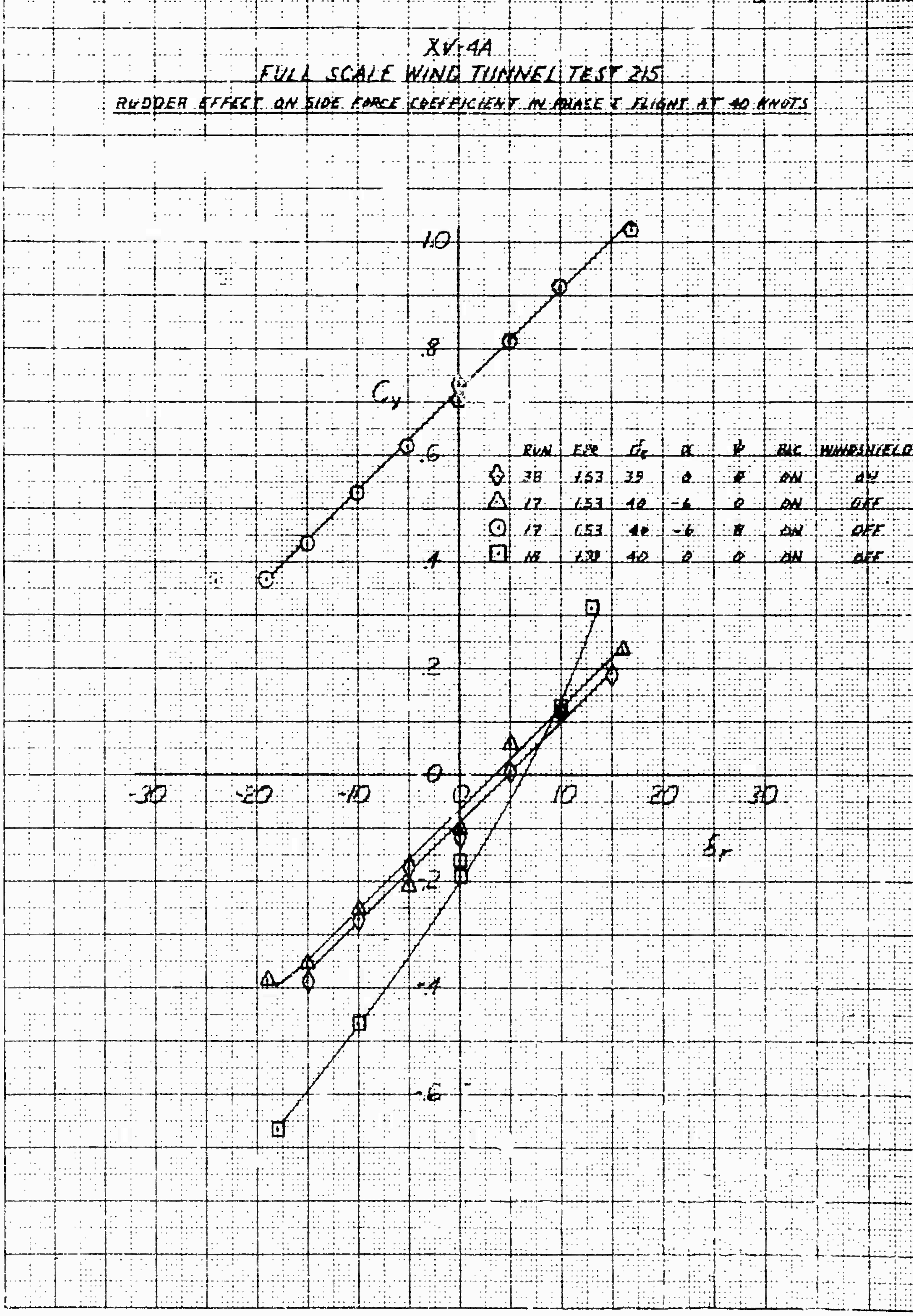
XV-4A
FULL SCALE WIND TUNNEL TEST 215
RUDDER EFFECT ON SIDE FORCE COEFFICIENT IN PHASE I FLIGHT AT 40 KNOTS
C_y
δ_r
1.0
.8
.6
.4
.2
0
-.2
-.4
-.6
-30
-20
-10
0
10
20
30
RUN
B/C
WINDSHIELD
38 1.53 39 0 ON
17 1.53 40 -6 0 ON OFF
17 1.53 -6 ON OFF
18 40 0 0 ON OFF

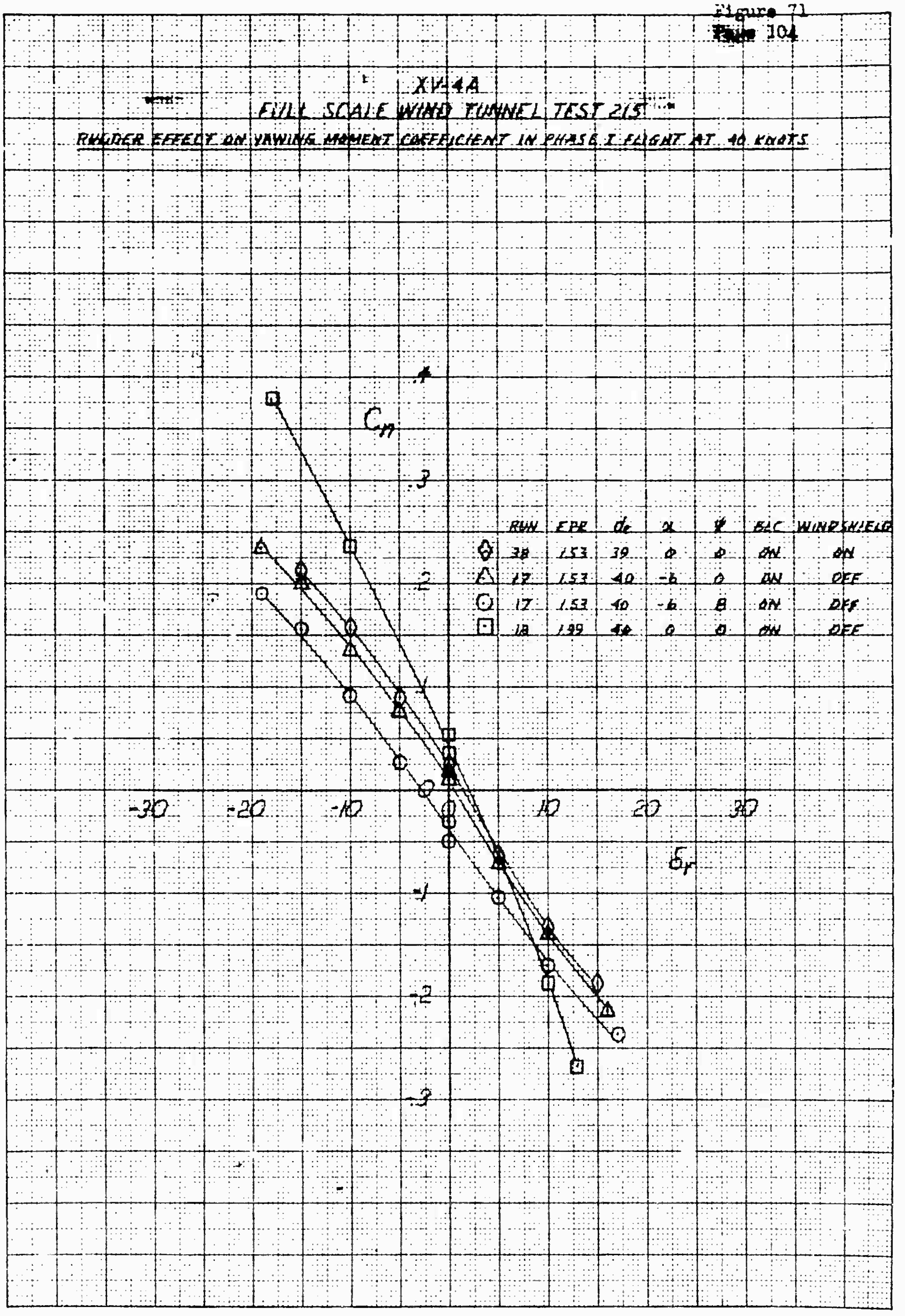

XV-4A
FULL SCALE WIND TUNNEL TEST 215
RUDDER EFFECT ON YAWING MOMENT COEFFICIENT IN PHASE I FLIGHT AT 40 KNOTS

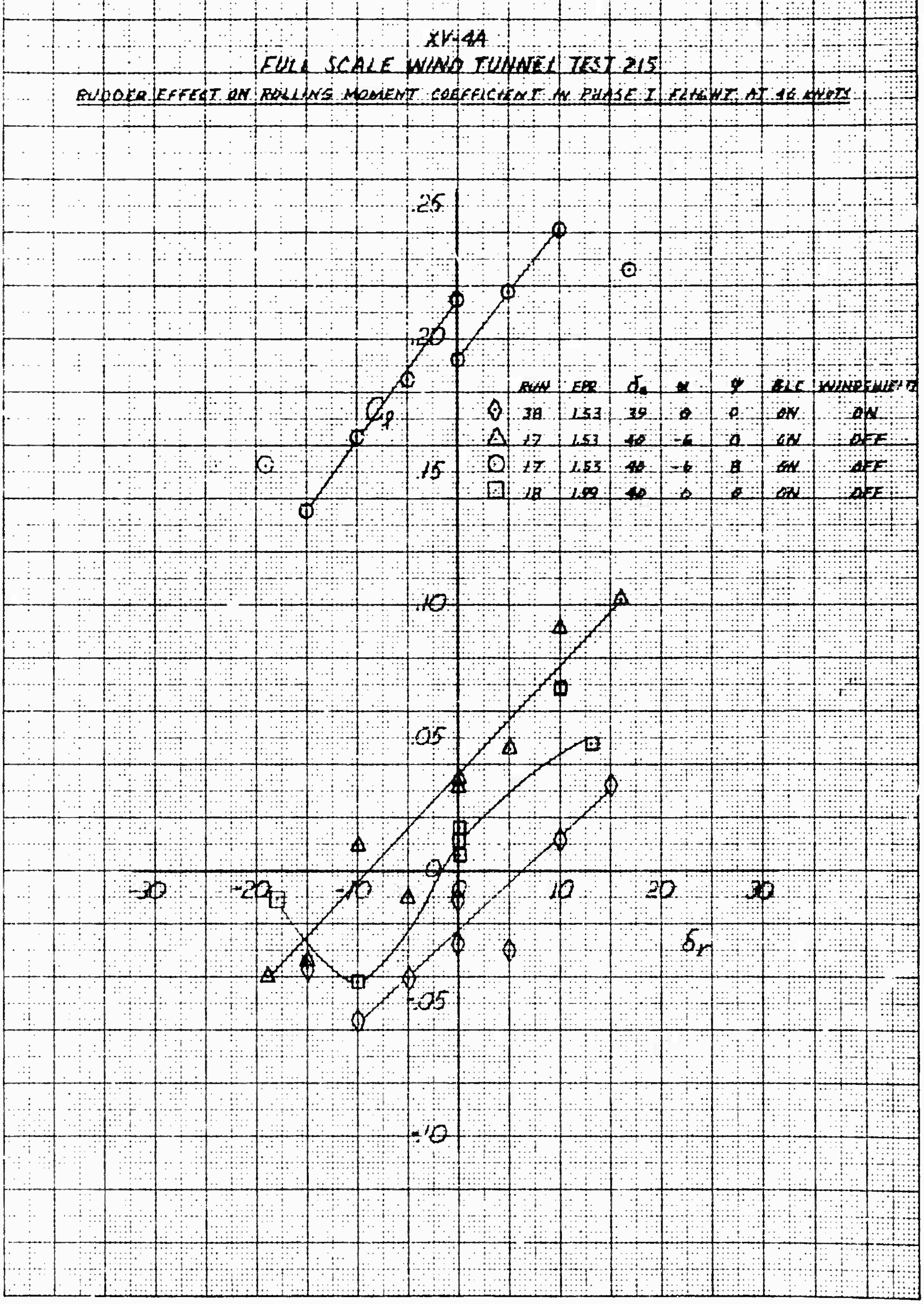
XV-4A
FULL SCALE WIND TUNNEL TEST 215
.25
.20
.15
.10
.05
-.05
-.10
C_ℓ
-30
-20
-10
0
10
20
30
δ_r
RUN
38
17
17
18

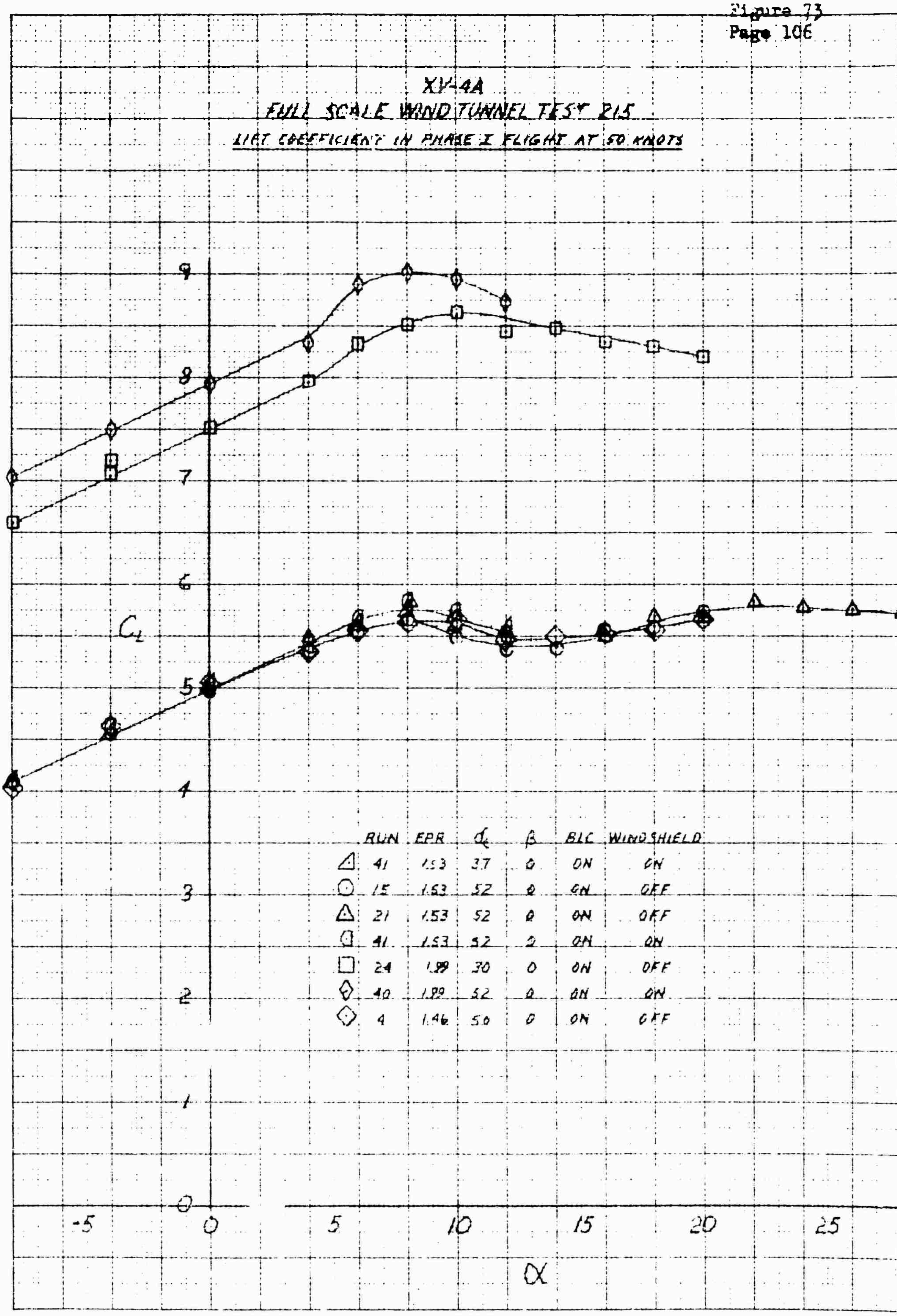
XV-4A
FULL SCALE WIND TUNNEL TEST 215
LIFT COEFFICIENT IN PHASE I FLIGHT AT 50 KNOTS
C_L
α
RUN EPR α_c β BLC WINDSHIELD
41 1.53 37 0 ON ON
15 1.53 52 0 ON OFF
21 1.53 52 0 ON OFF
41 1.53 52 0 ON ON
24 1.99 30 0 ON OFF
40 1.99 52 0 ON ON
4 1.46 50 0 ON OFF

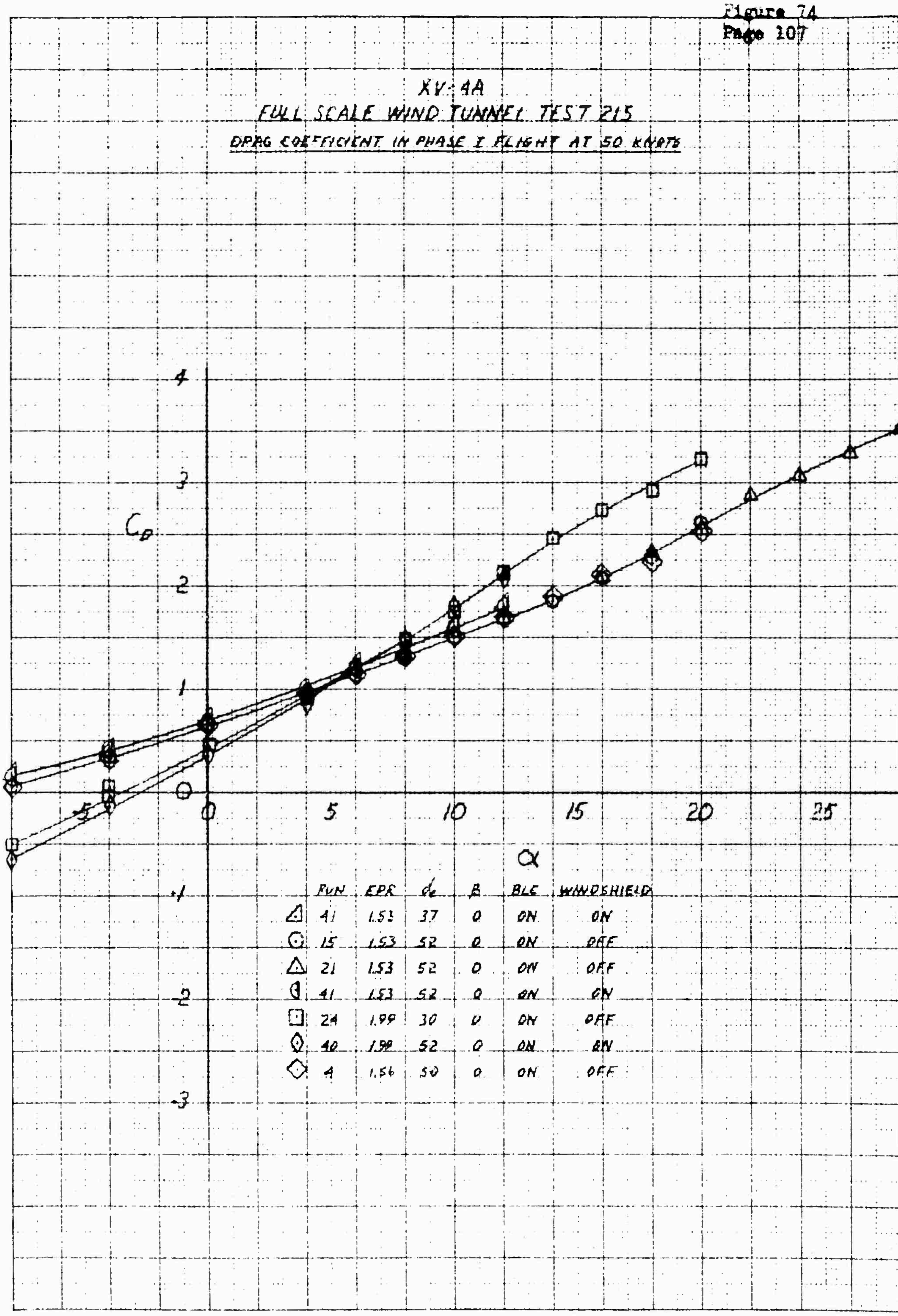
XV-4A
FULL SCALE WIND TUNNEL TEST 215
DRAG COEFFICIENT IN PHASE I FLIGHT AT 50 KNOTS
C_D
4
3
2
1
-1
-2
-3
-5
0
5
10
15
20
25
α
RUN EPR δ_e β BLC WINDSHIELD
41 1.53 37 0 ON ON
15 1.53 52 0 ON OFF
21 1.53 52 0 ON OFF
41 1.53 52 0 ON ON
24 1.99 30 0 ON OFF
40 1.99 52 0 ON ON
4 1.56 50 0 ON OFF

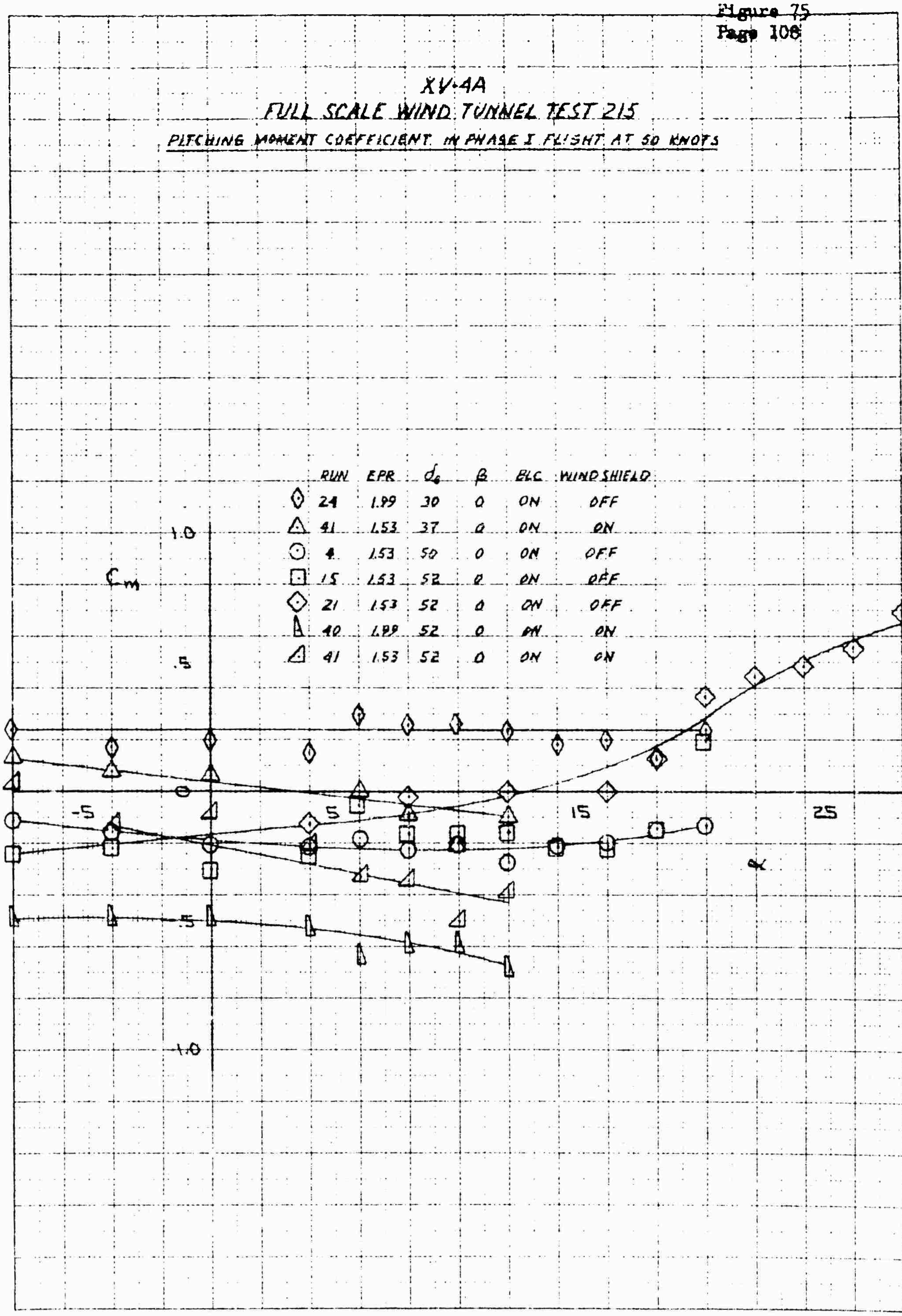
XV-4A
FULL SCALE WIND TUNNEL TEST 215
PITCHING MOMENT COEFFICIENT IN PHASE I FLIGHT AT 50 KNOTS
RUN
EPR
β
BLC
WINDSHIELD
24
1.99
30
0
ON
OFF
41
1.53
37
0
ON
ON
4
1.53
50
0
ON
OFF
15
1.53
52
0
ON
OFF
21
1.53
52
0
ON
OFF
40
1.99
52
0
ON
ON
41
1.53
52
0
ON
ON
1.0
Cm
.5
-5
5
15
25
α
-.5
-1.0

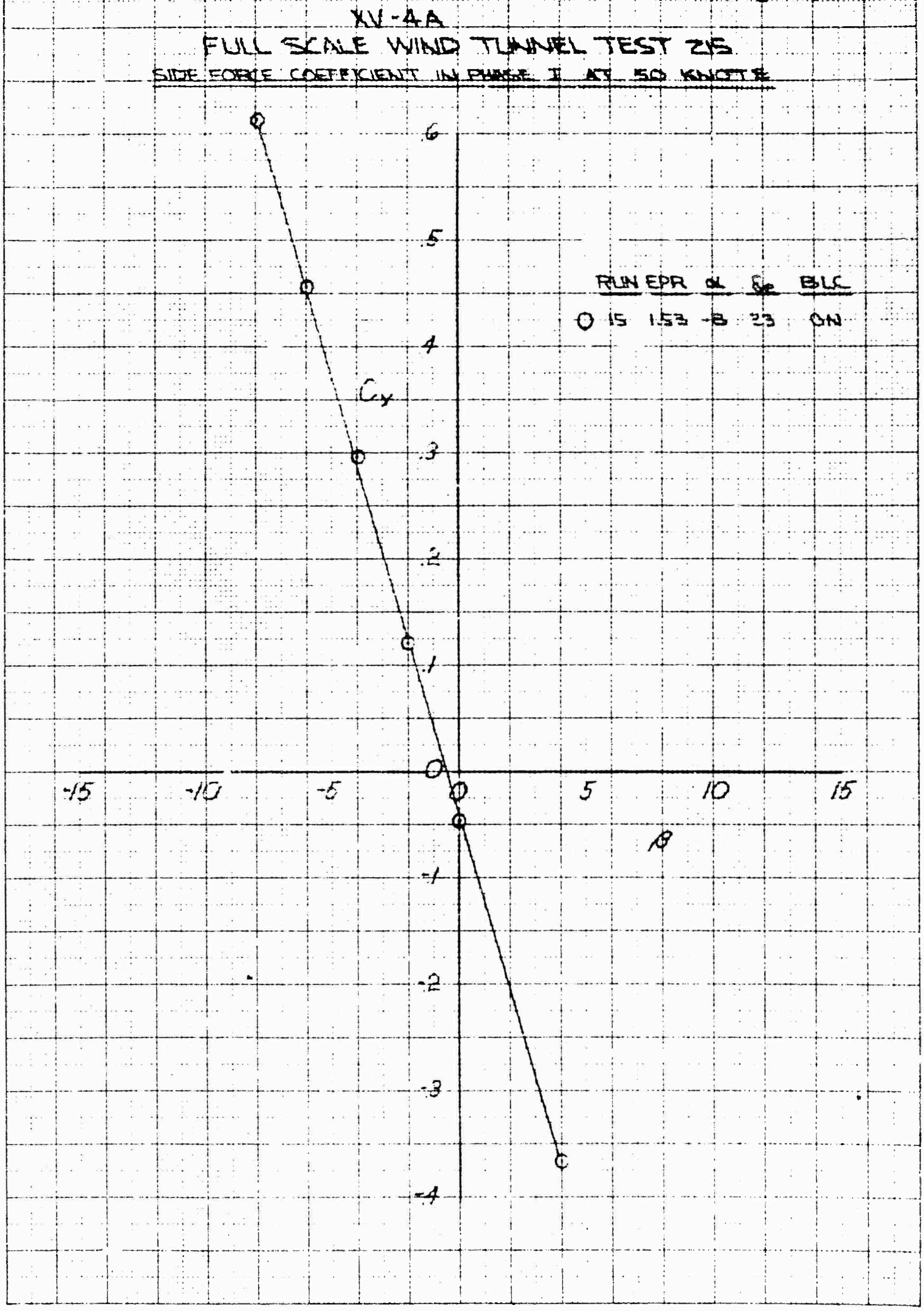
XV-4A
FULL SCALE WIND TUNNEL TEST 215
SIDE FORCE COEFFICIENT IN PHASE I AT 50 KNOTS
RUN EPR α δe BLC
15 1.53 -8 23 ON
Cy
β
.6
.5
.4
.3
.2
.1
0
-.1
-.2
-.3
-.4
-15
-10
-5
0
5
10
15

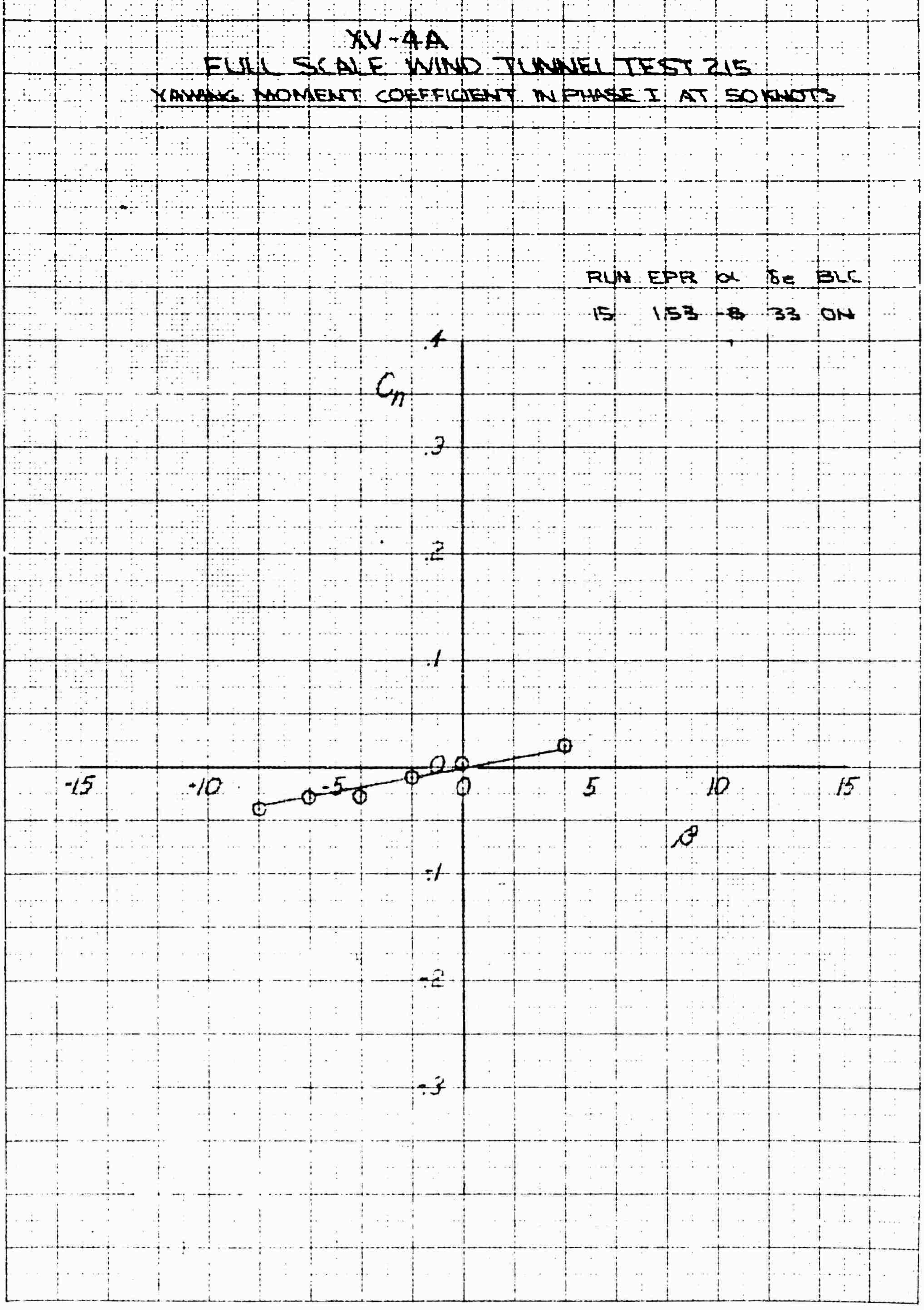
XV-4A
FULL SCALE WIND TUNNEL TEST 215
YAWING MOMENT COEFFICIENT IN PHASE I AT 50 KNOTS
RUN EPR α δe BLC
15 1.53 -8 33 ON
C_n
.4
.3
.2
.1
-.1
-.2
-.3
-15
-10
-5
0
5
10
15
β

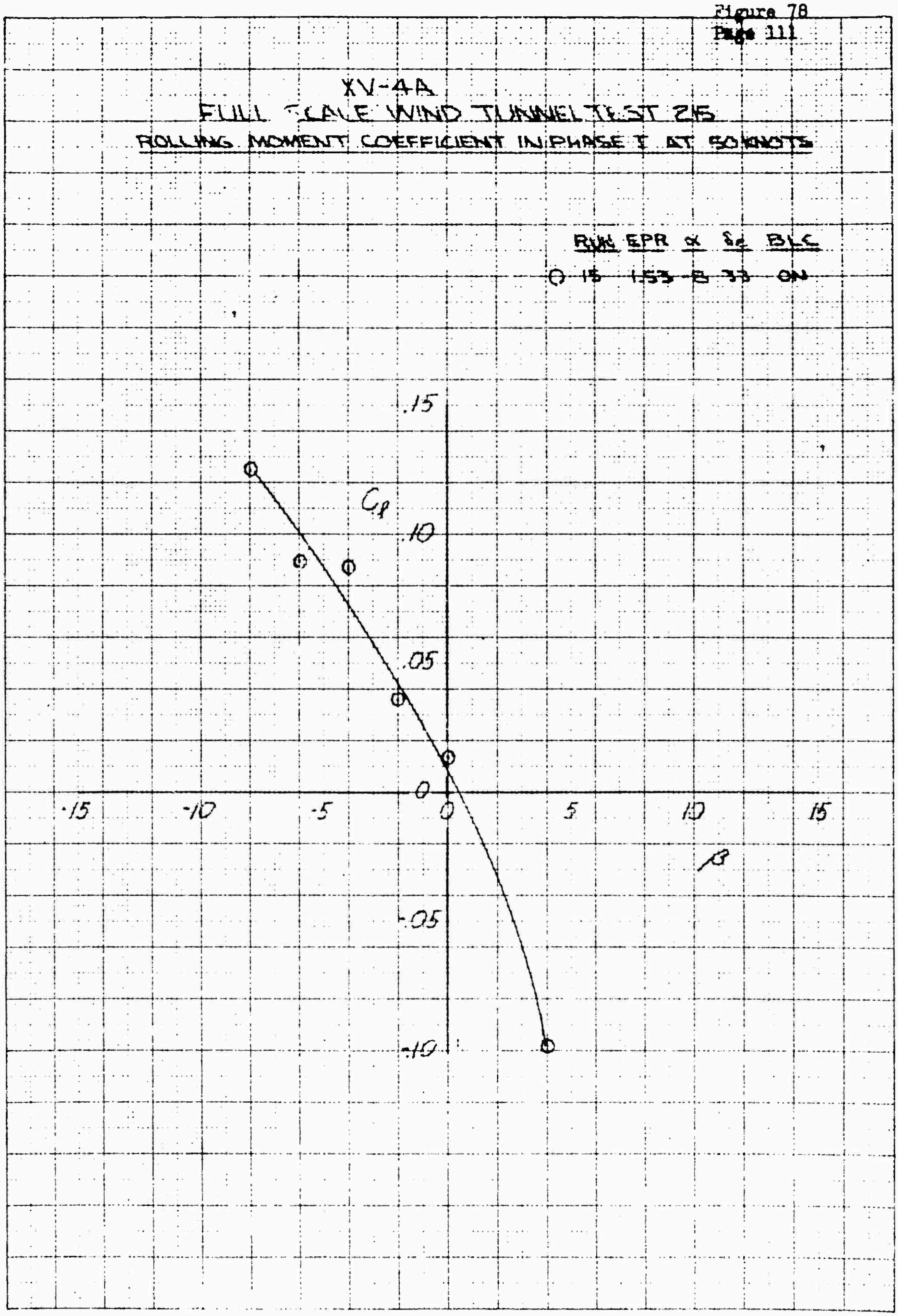
XV-4A
FULL SCALE WIND TUNNEL TEST 215
ROLLING MOMENT COEFFICIENT IN PHASE I AT 50 KNOTS
RUN EPR α δe BLC
15 1.53 -8 33 ON
.15
.10
.05
0
-.05
-.10
C_ℓ
-15
-10
-5
0
5
10
15
β

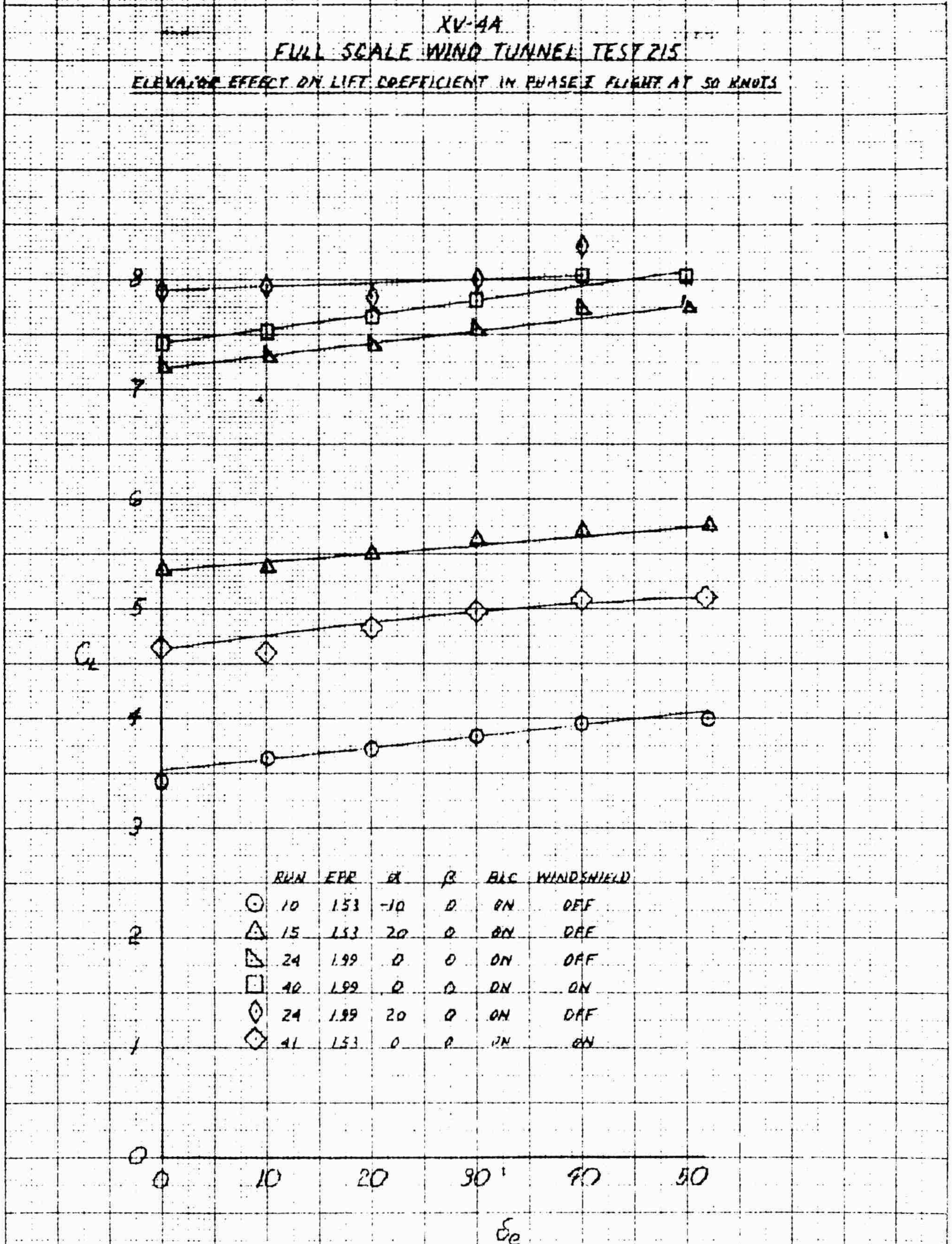
XV-4A
FULL SCALE WIND TUNNEL TEST 215
ELEVATOR EFFECT ON LIFT COEFFICIENT IN PHASE I FLIGHT AT 50 KNOTS
C_L
δ_e
0
1
2
3
4
5
6
7
8
0
10
20
30
40
50
RUN EPR α β BLC WINDSHIELD
10 1.53 -10 0 ON OFF
15 1.53 20 0 ON OFF
24 1.99 0 0 ON OFF
40 1.99 0 0 ON ON
24 1.99 20 0 ON OFF
41 1.53 0 0 ON ON

XV-4A

FULL SCALE WIND TUNNEL TEST 215

ELEVATOR EFFECT ON DRAG COEFFICIENT IN PHASE I FLIGHT AT 0 KNOTS

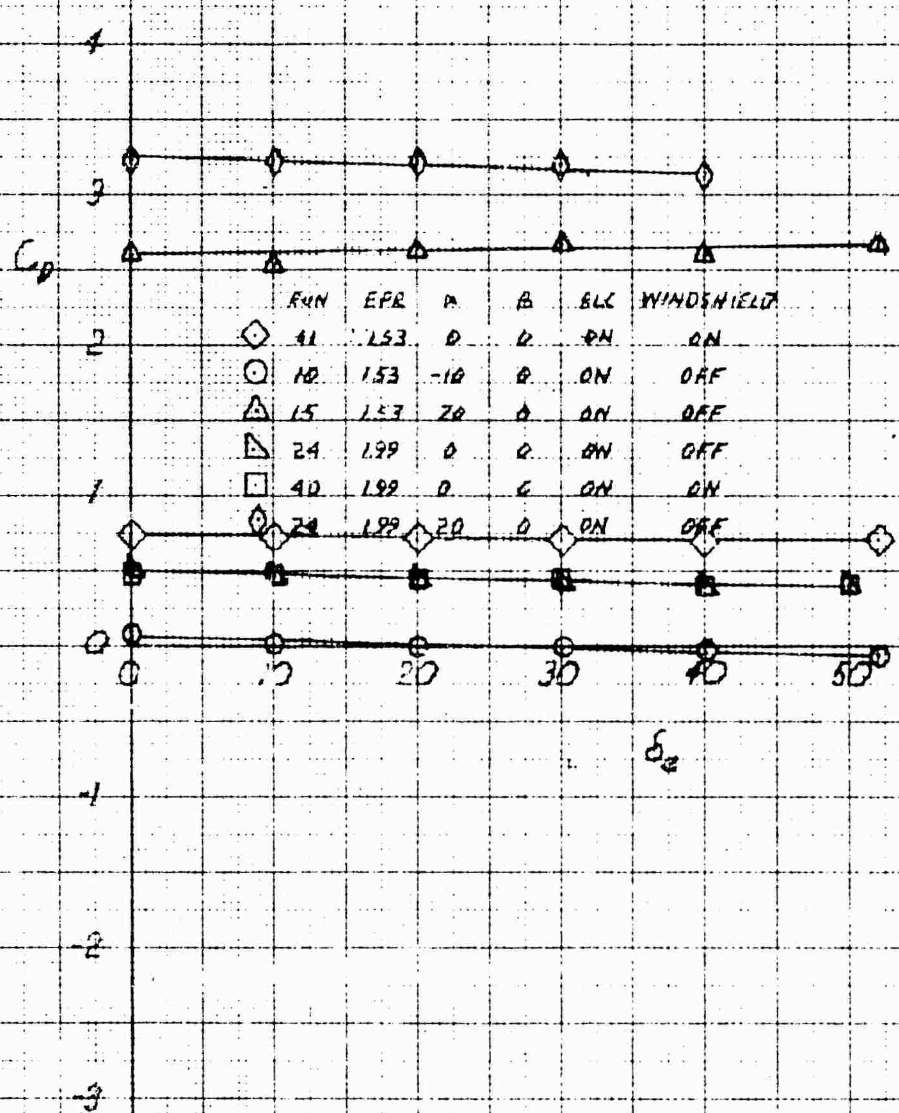

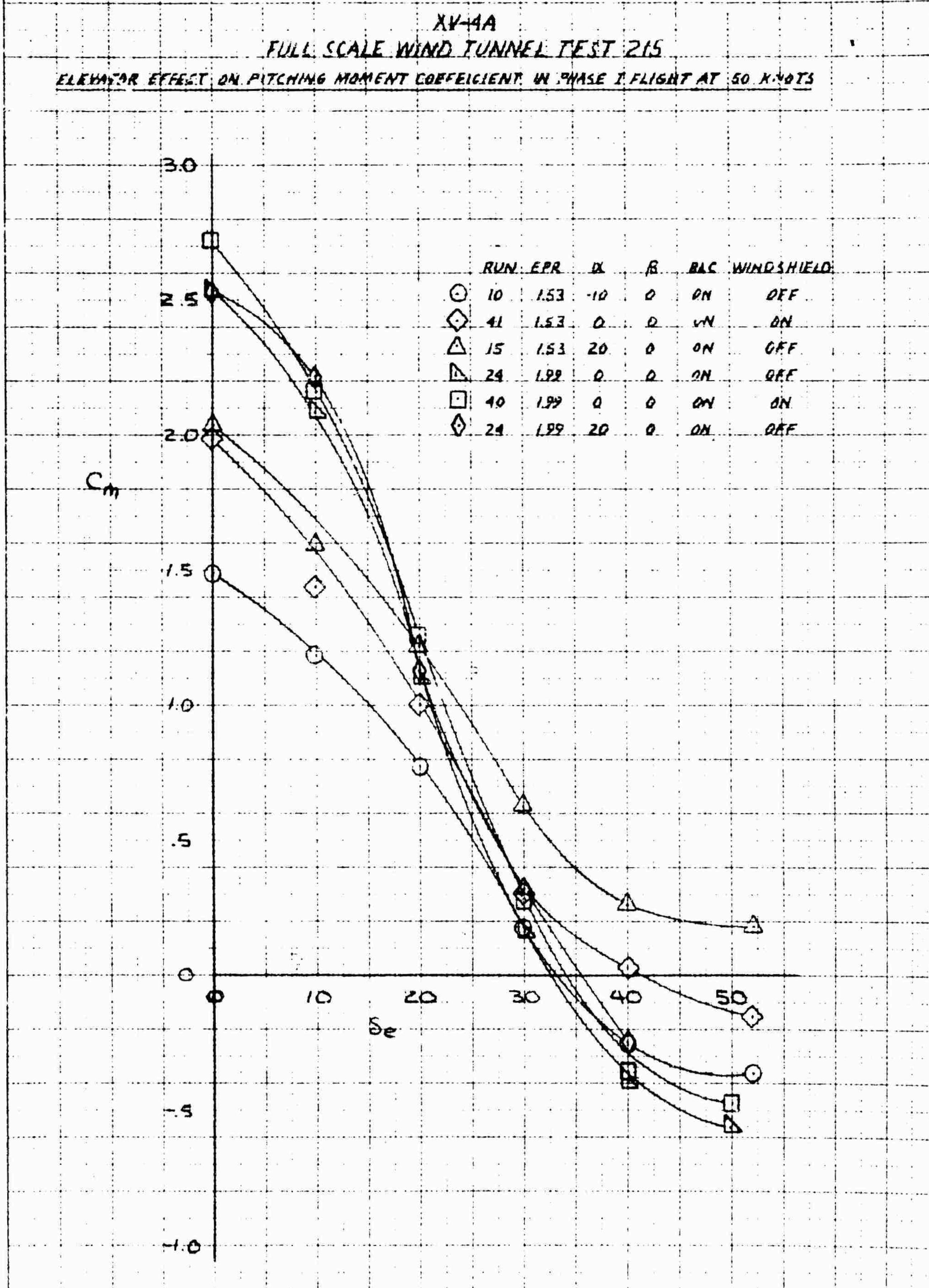
XV-4A
FULL SCALE WIND TUNNEL TEST 215
ELEVATOR EFFECT ON PITCHING MOMENT COEFFICIENT IN PHASE I FLIGHT AT 50 KNOTS
RUN EPR α β BLC WINDSHIELD
10 1.53 -10 0 ON OFF
41 1.53 0 0 ON ON
15 1.53 20 0 ON OFF
24 1.99 0 0 ON OFF
40 1.99 0 0 ON ON
24 1.99 20 0 ON OFF
3.0
2.5
2.0
1.5
1.0
.5
0
-.5
-1.0
Cm
0
10
20
30
40
50
δe

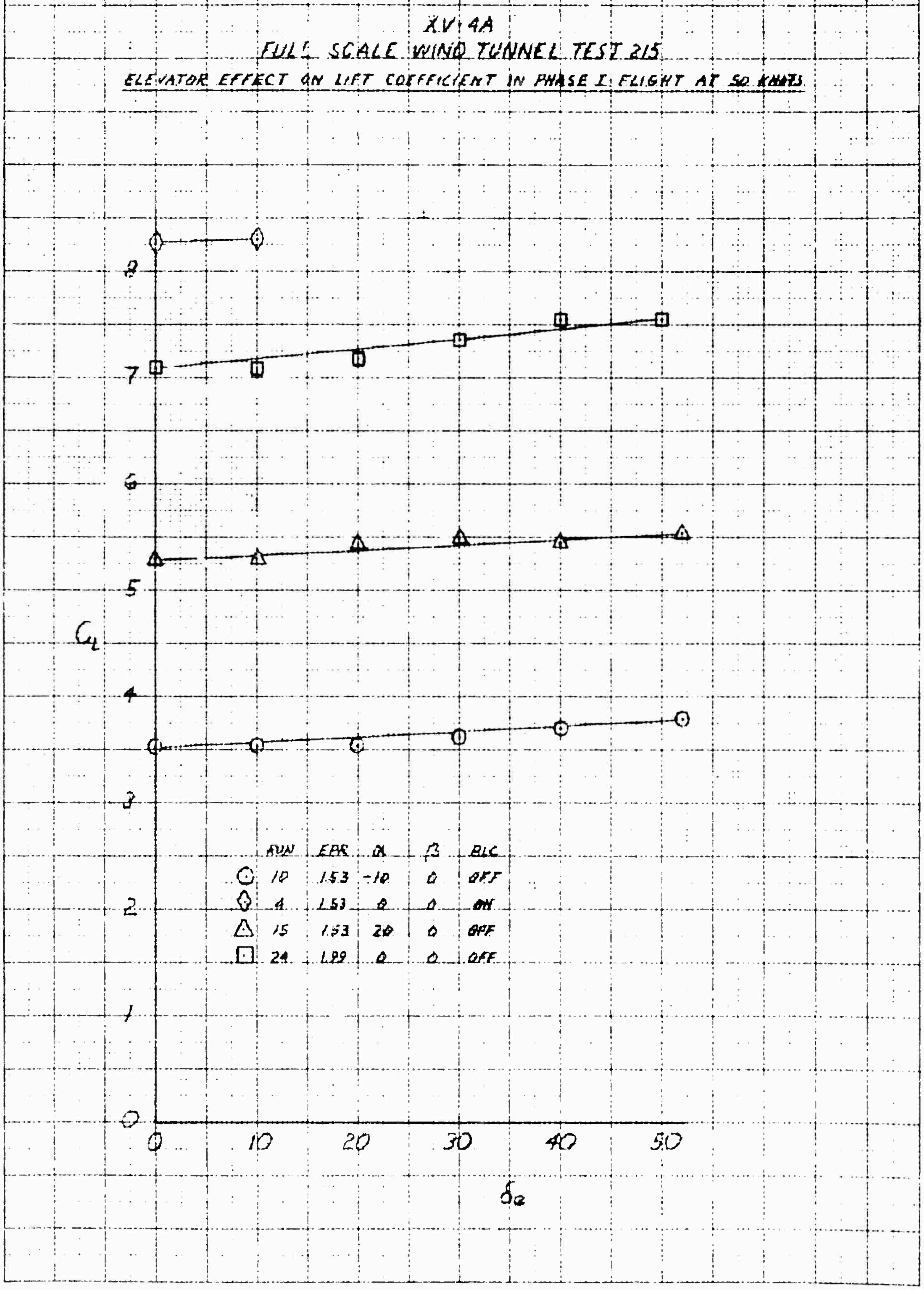
XV-4A
FULL SCALE WIND TUNNEL TEST 215
ELEVATOR EFFECT ON LIFT COEFFICIENT IN PHASE I FLIGHT AT 50 KNOTS
C_L
0
1
2
3
4
5
6
7
8
0
10
20
30
40
50
δ_e
RUN EPR α β BLC
10 1.53 -10 0 OFF
4 1.53 0 0 ON
15 1.53 20 0 OFF
24 1.99 0 0 OFF

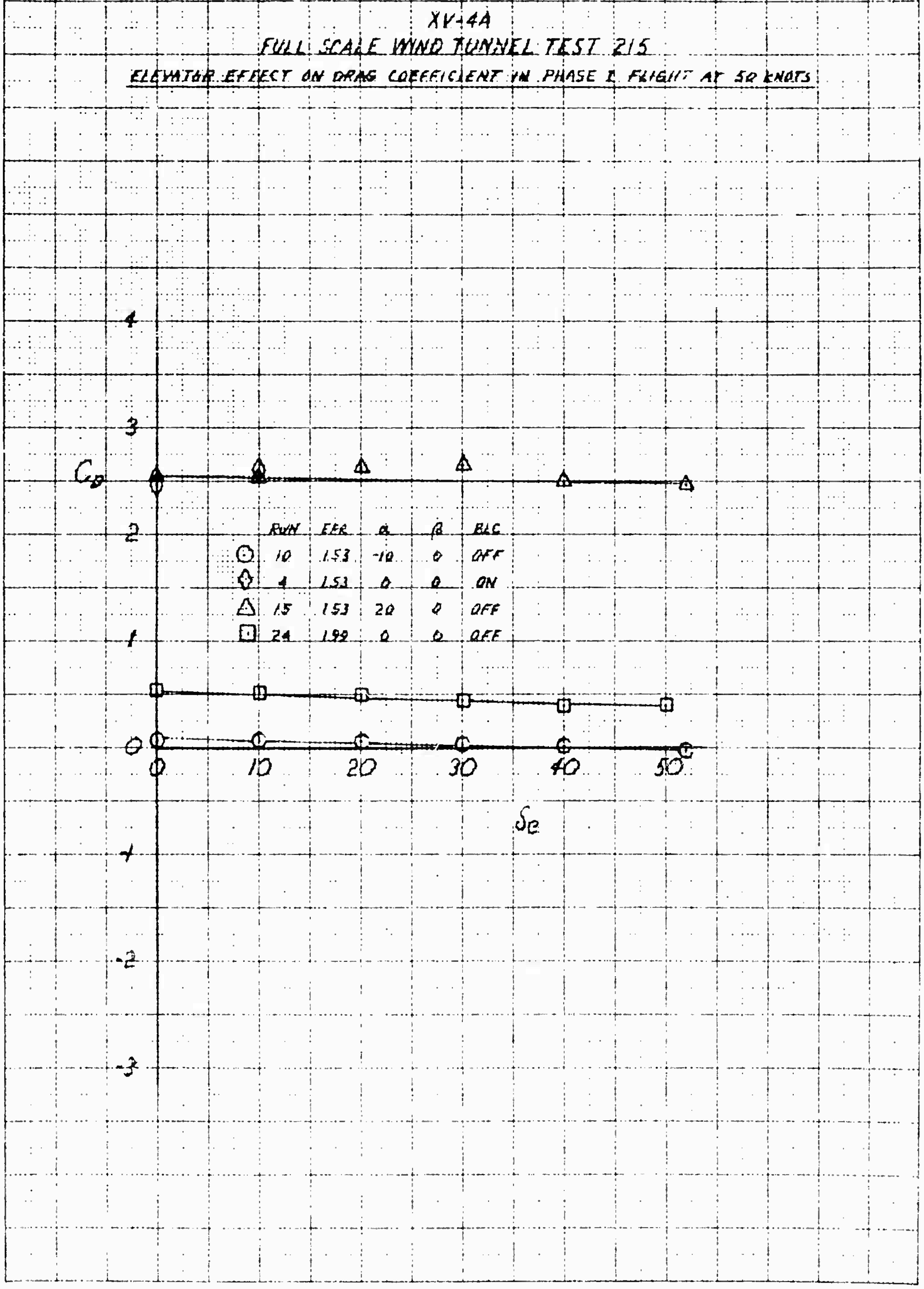
XV-4A
FULL SCALE WIND TUNNEL TEST 215
ELEVATOR EFFECT ON DRAG COEFFICIENT IN PHASE I FLIGHT AT 50 KNOTS
RUN EFR α β BLC
10 1.53 -10 0 OFF
4 1.53 0 0 ON
15 1.53 20 0 OFF
24 1.99 0 0 OFF
C_D
δ_e
4
3
2
1
0
-1
-2
-3
0 10 20 30 40 50

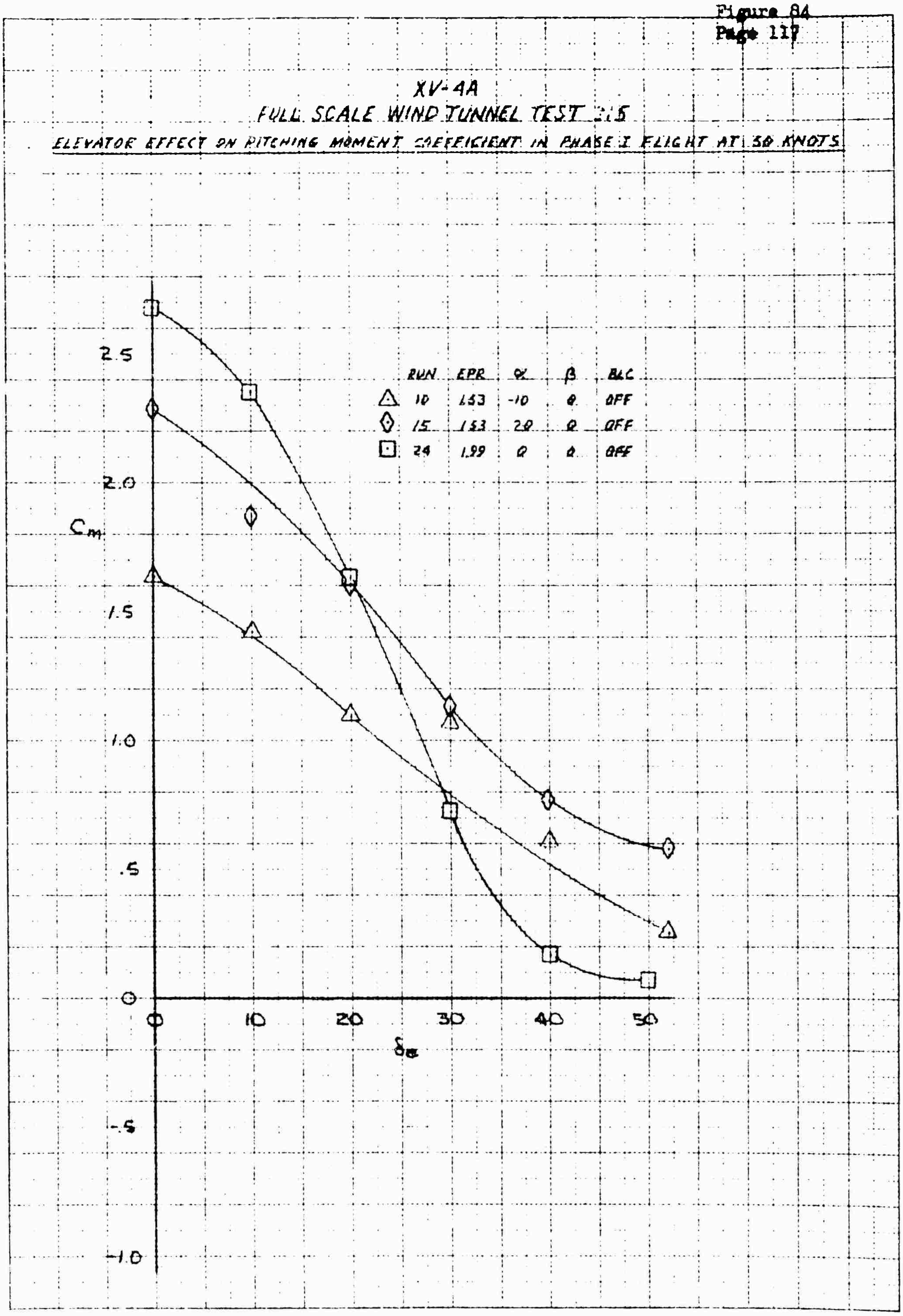
XV-4A
FULL SCALE WIND TUNNEL TEST 215
ELEVATOR EFFECT ON PITCHING MOMENT COEFFICIENT IN PHASE I FLIGHT AT 50 KNOTS
RUN EPR α β BLC
10 1.53 -10 0 OFF
15 1.53 20 0 OFF
24 1.99 0 0 OFF
2.5
2.0
C_m
1.5
1.0
.5
0
-.5
-1.0
0
10
20
30
40
50
δ_e

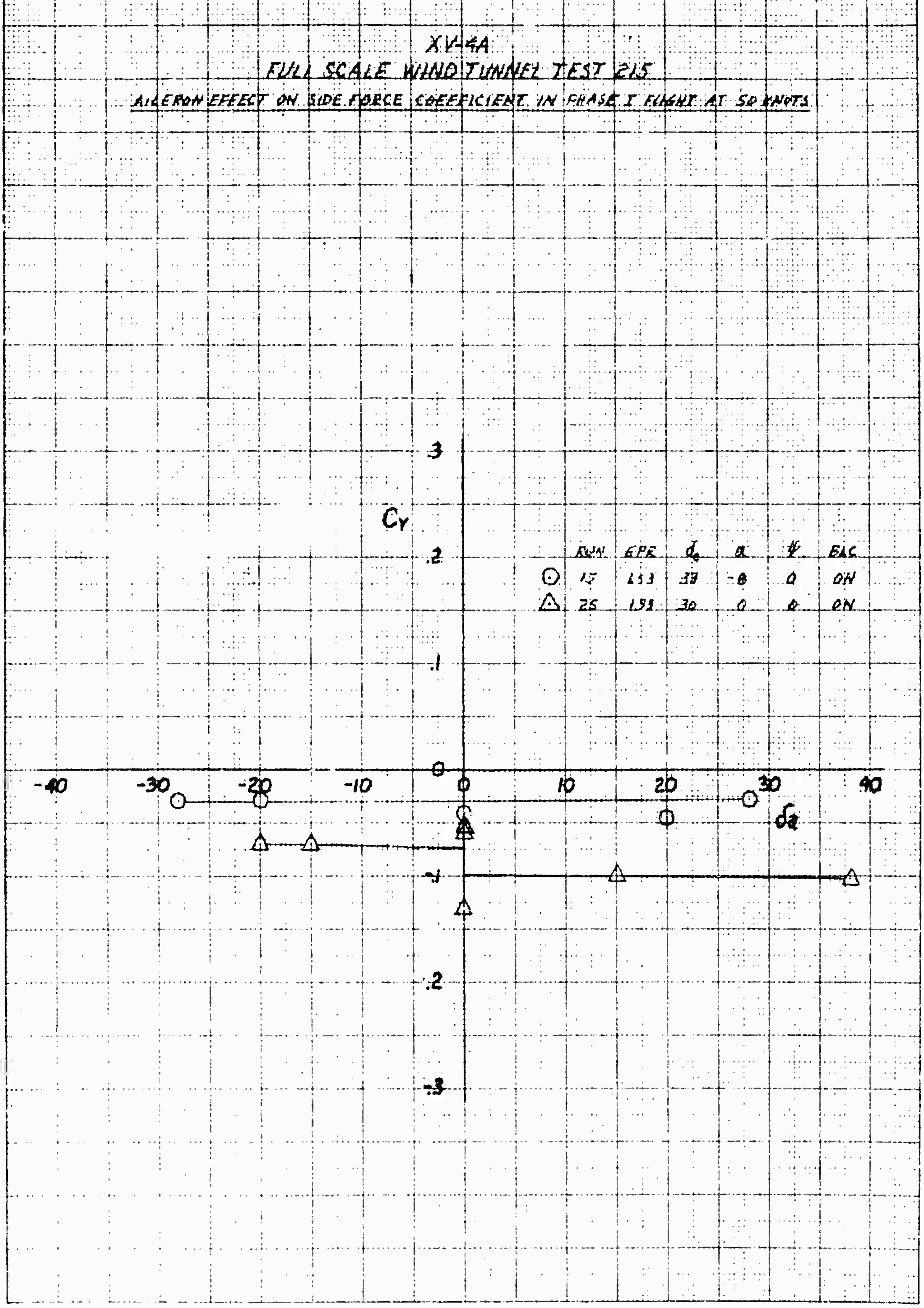
XV-4A
FULL SCALE WIND TUNNEL TEST 215
AILERON EFFECT ON SIDE FORCE COEFFICIENT IN PHASE I FLIGHT AT 50 KNOTS
C_Y
.3
.2
.1
0
-.1
-.2
-.3
-40
-30
-20
-10
0
10
20
30
40
δ_a
RUN EPE δ_e α ψ EAC
15 153 30 -8 0 ON
25 193 30 0 0 ON

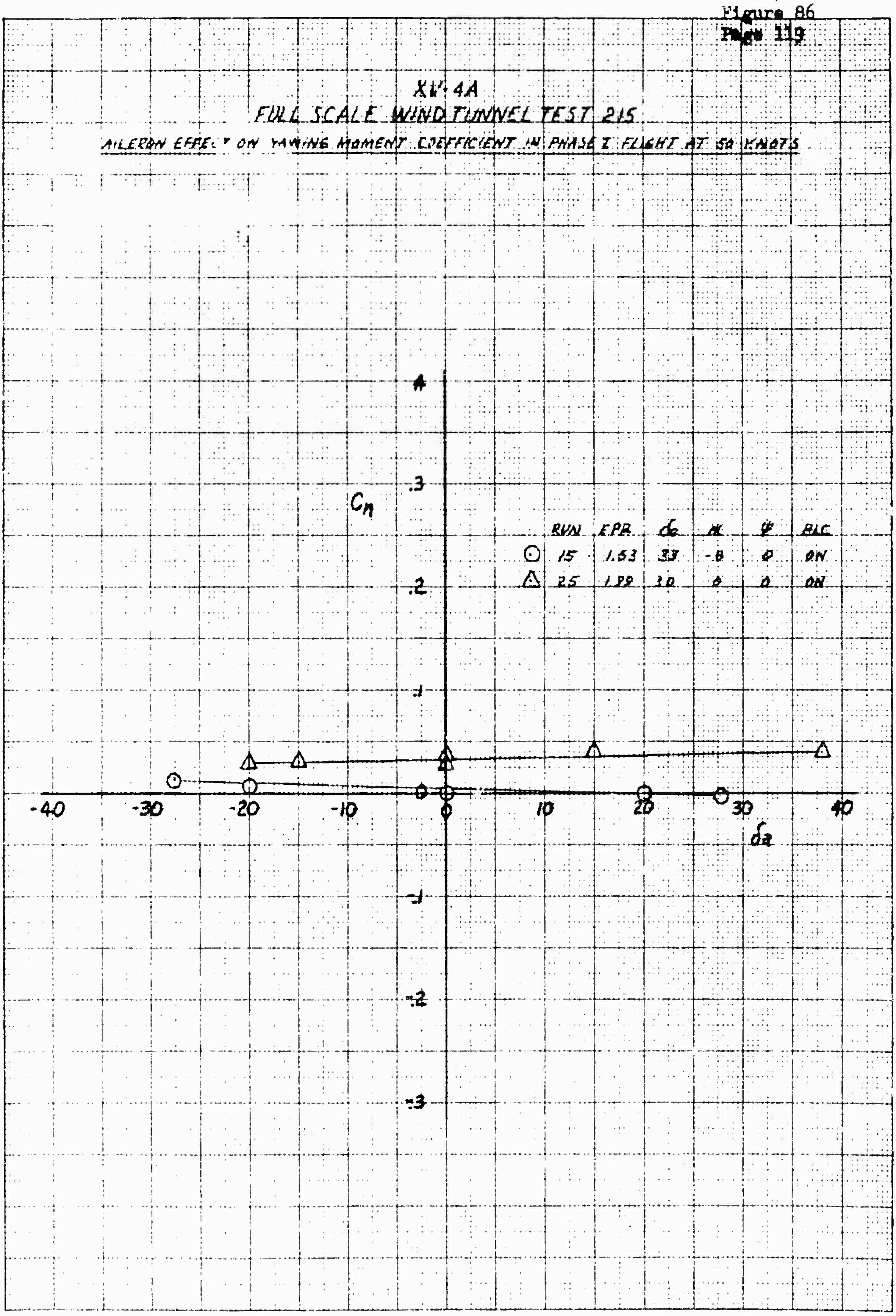
XV-4A
FULL SCALE WIND TUNNEL TEST 215
AILERON EFFECT ON YAWING MOMENT COEFFICIENT IN PHASE I FLIGHT AT 50 KNOTS
RUN EPR δo α ψ BLC
15 1.53 33 -8 0 ON
25 1.98 30 0 0 ON
Cn
.4
.3
.2
.1
-.1
-.2
-.3
-40
-30
-20
-10
0
10
20
30
40
δa

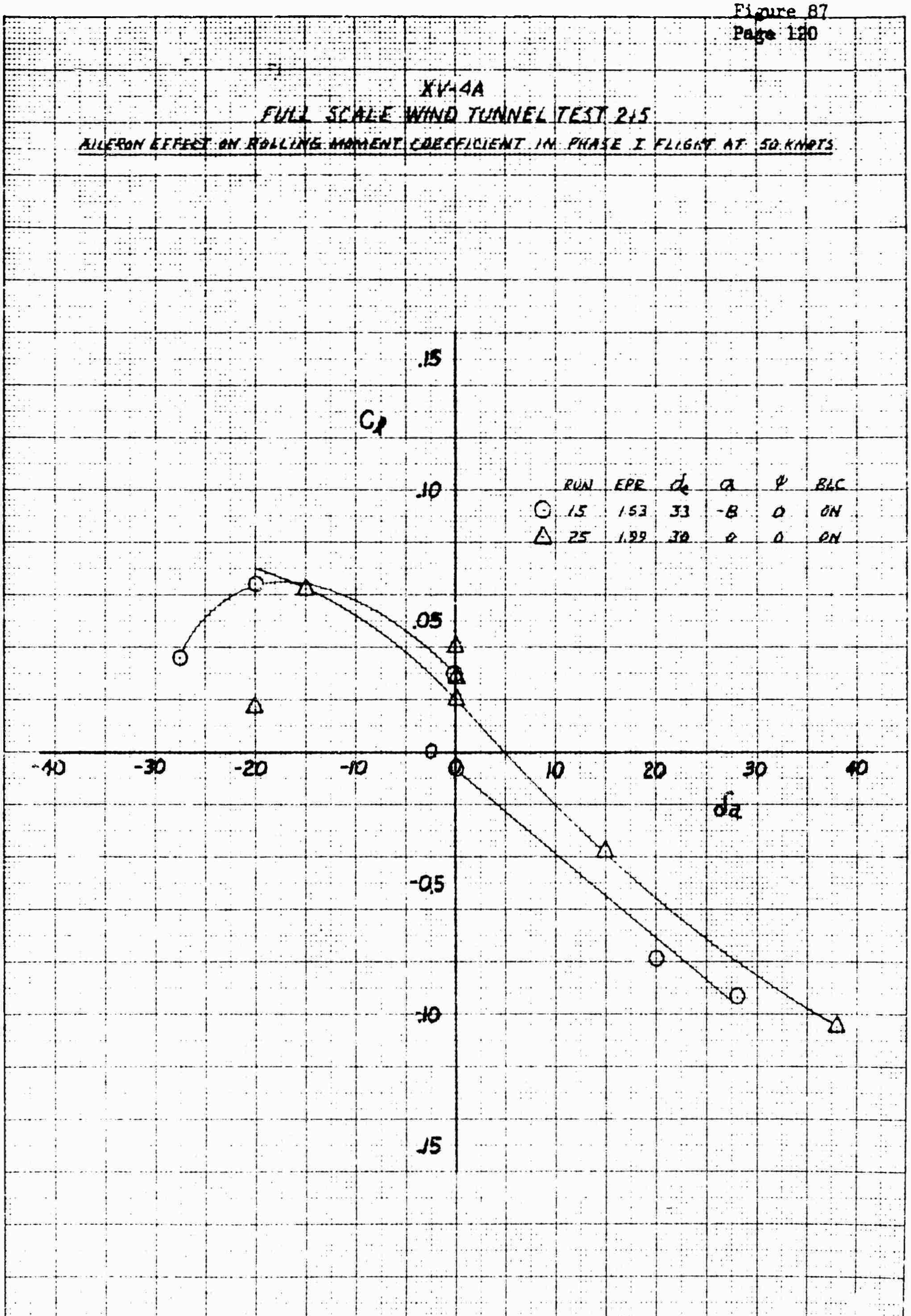
XV-4A
FULL SCALE WIND TUNNEL TEST 215
AILERON EFFECT ON ROLLING MOMENT COEFFICIENT IN PHASE I FLIGHT AT 50 KNOTS
RUN EPE δe α ψ BLC
○ 15 1.53 33 -8 0 ON
△ 25 1.99 30 0 0 ON
Cl
.15
.10
.05
0
-.05
-.10
-.15
-40
-30
-20
-10
0
10
20
30
40
δa

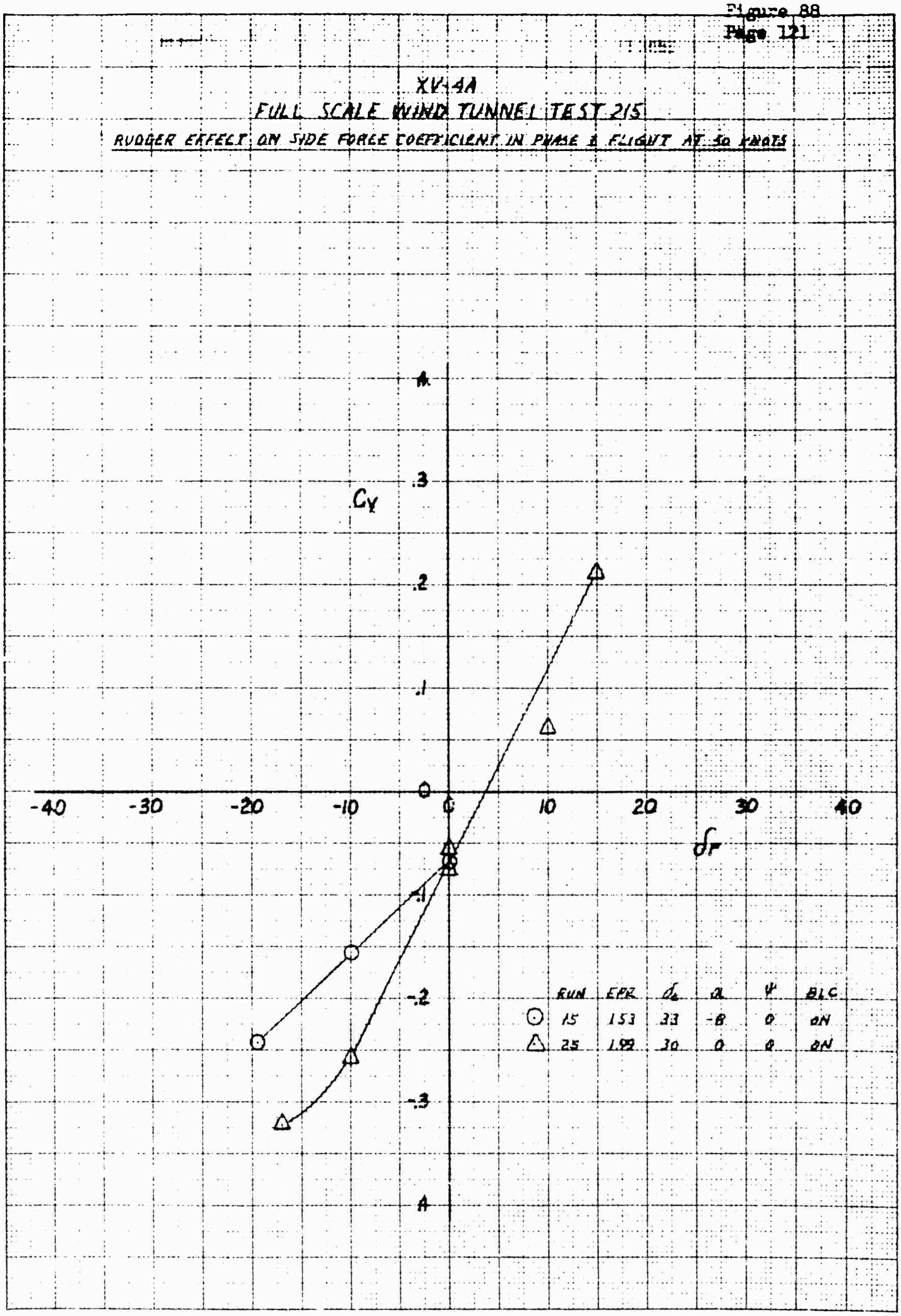
XV-4A
FULL SCALE WIND TUNNEL TEST 215
RUDDER EFFECT ON SIDE FORCE COEFFICIENT IN PHASE 3 FLIGHT AT 50 KNOTS
C_Y
.4
.3
.2
.1
0
-.1
-.2
-.3
-.4
-40
-30
-20
-10
0
10
20
30
40
δ_r
RUN EPR δ_e α ψ BLC
15 1.53 33 -8 0 ON
25 1.99 30 0 0 ON

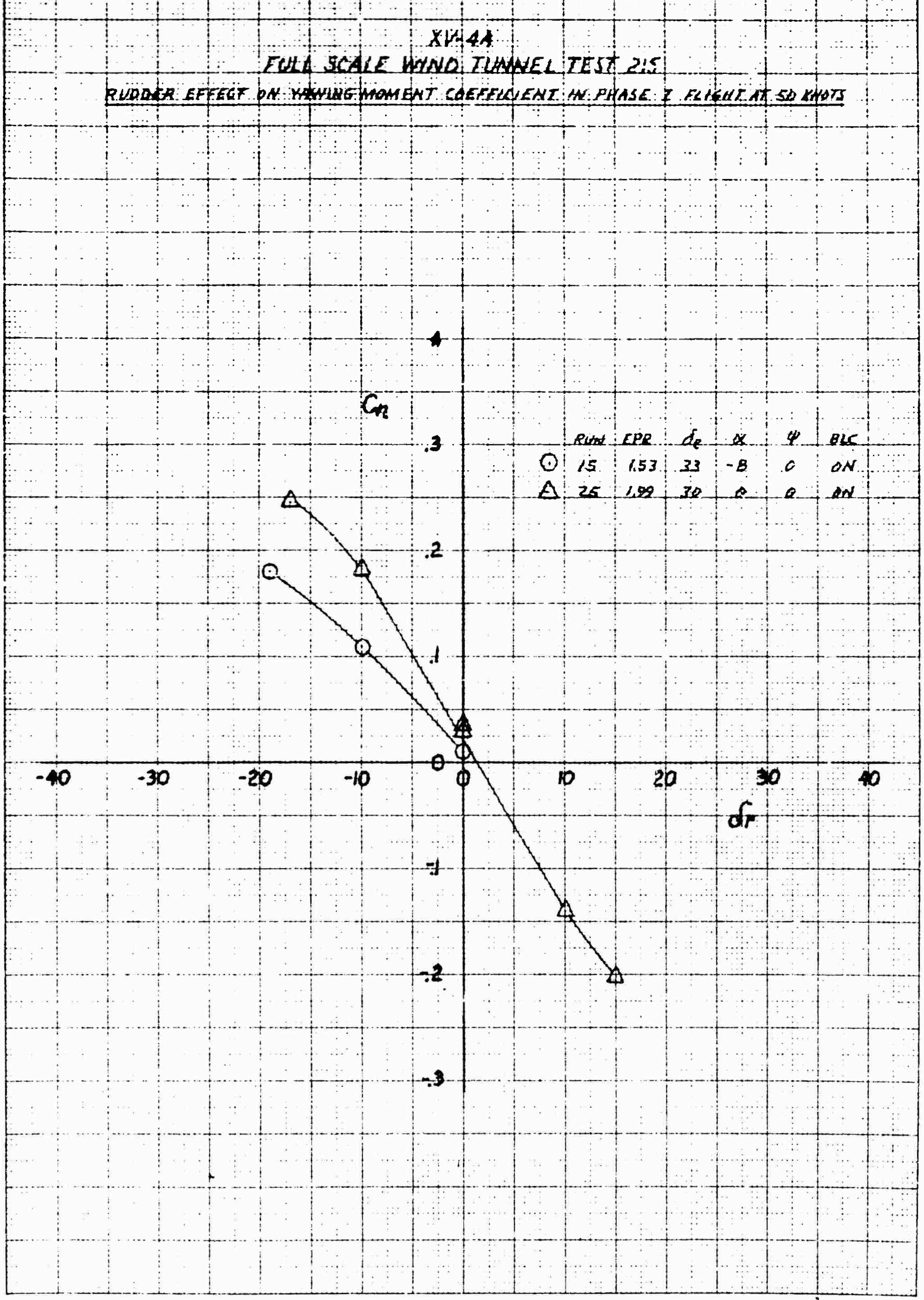
XV-4A
FULL SCALE WIND TUNNEL TEST 215
RUDDER EFFECT ON YAWING MOMENT COEFFICIENT IN PHASE I FLIGHT AT 50 KNOTS
Run EPR δe α ψ BLC
15 1.53 33 -8 0 ON
25 1.99 30 0 0 ON
Cn
.4
.3
.2
.1
0
-.1
-.2
-.3
-40
-30
-20
-10
0
10
20
30
40
δr

XV-4A
FULL SCALE WIND TUNNEL TEST 215
RUDDER EFFECT ON ROLLING MOMENT COEFFICIENT IN PHASE I FLIGHT AT 50 KNOTS

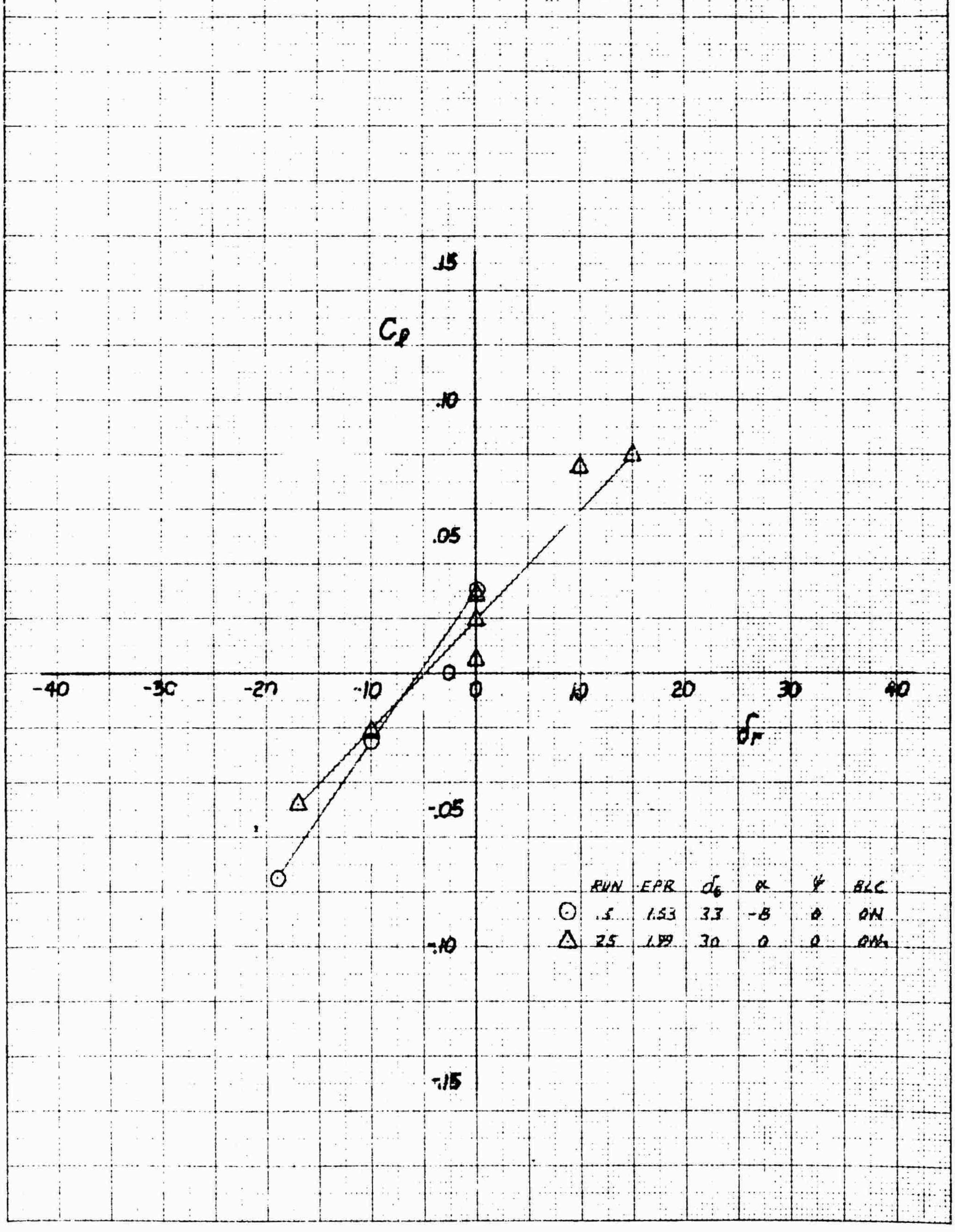

ER-7634
Figure 91
Page 124

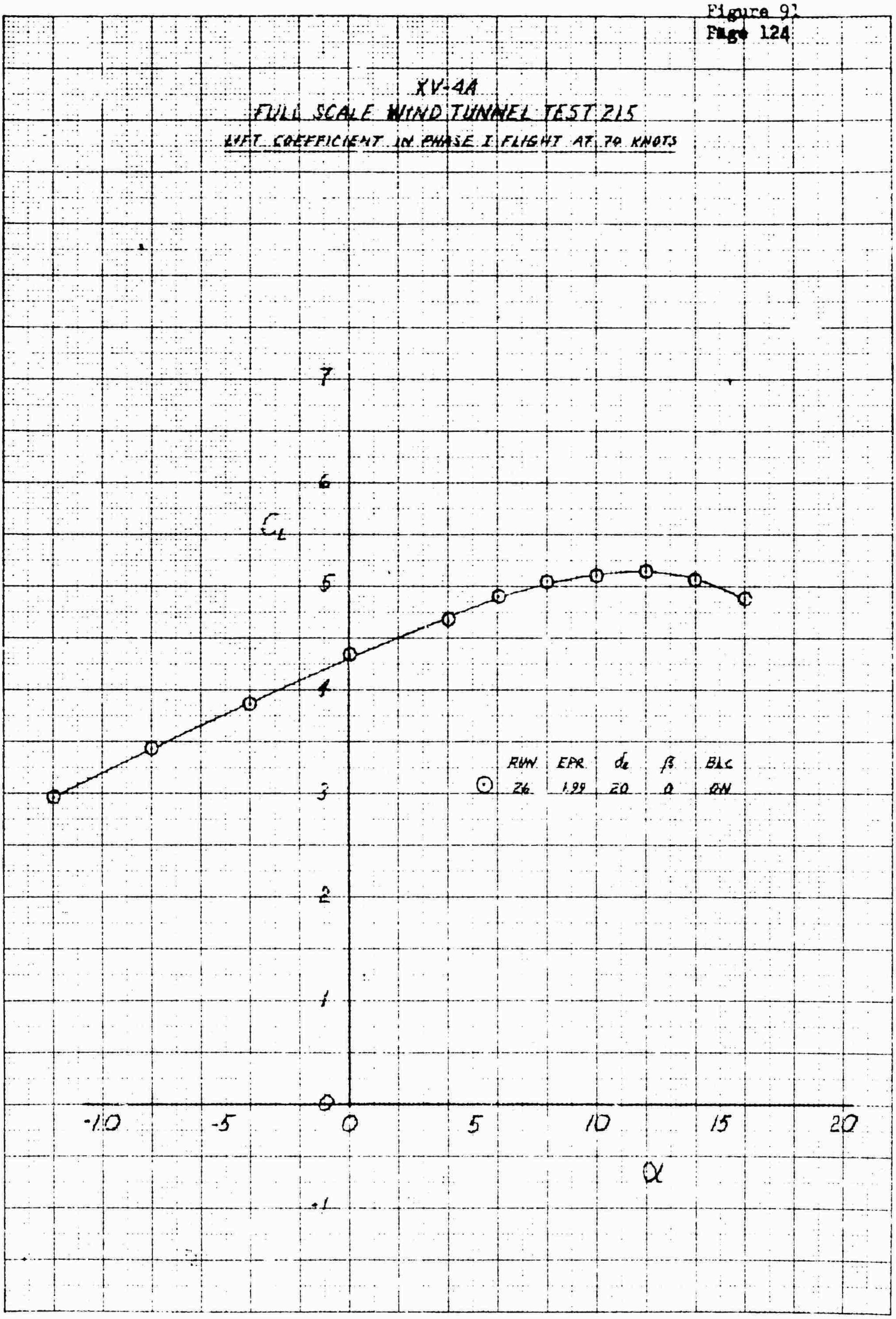

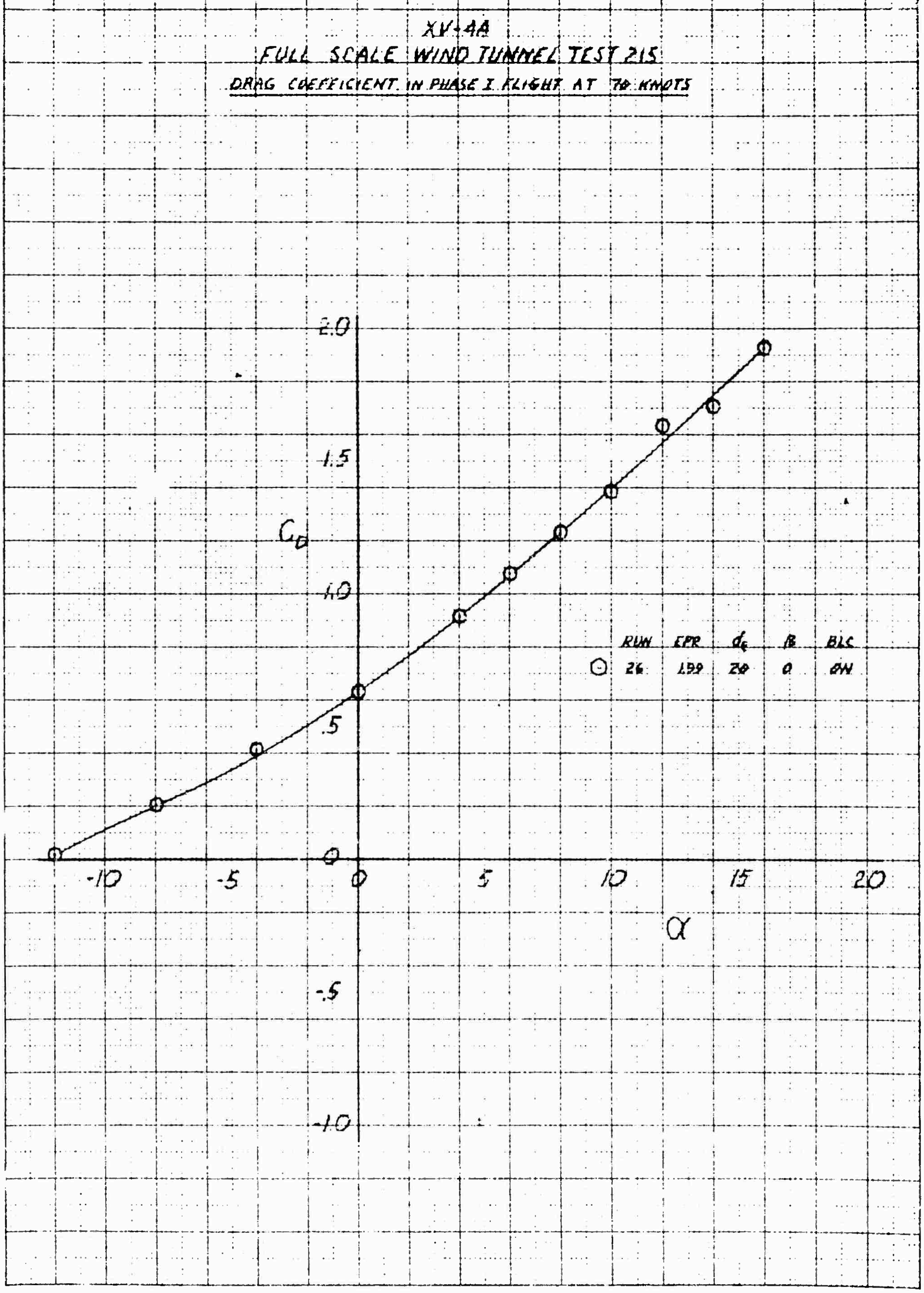
XV-4A
FULL SCALE WIND TUNNEL TEST 215
DRAG COEFFICIENT IN PHASE I FLIGHT AT 70 KNOTS
2.0
1.5
1.0
.5
0
-.5
-1.0
C_D
-10
-5
0
5
10
15
20
α
RUN
EPR
d_f
β
BLC
26
1.99
20
0
ON

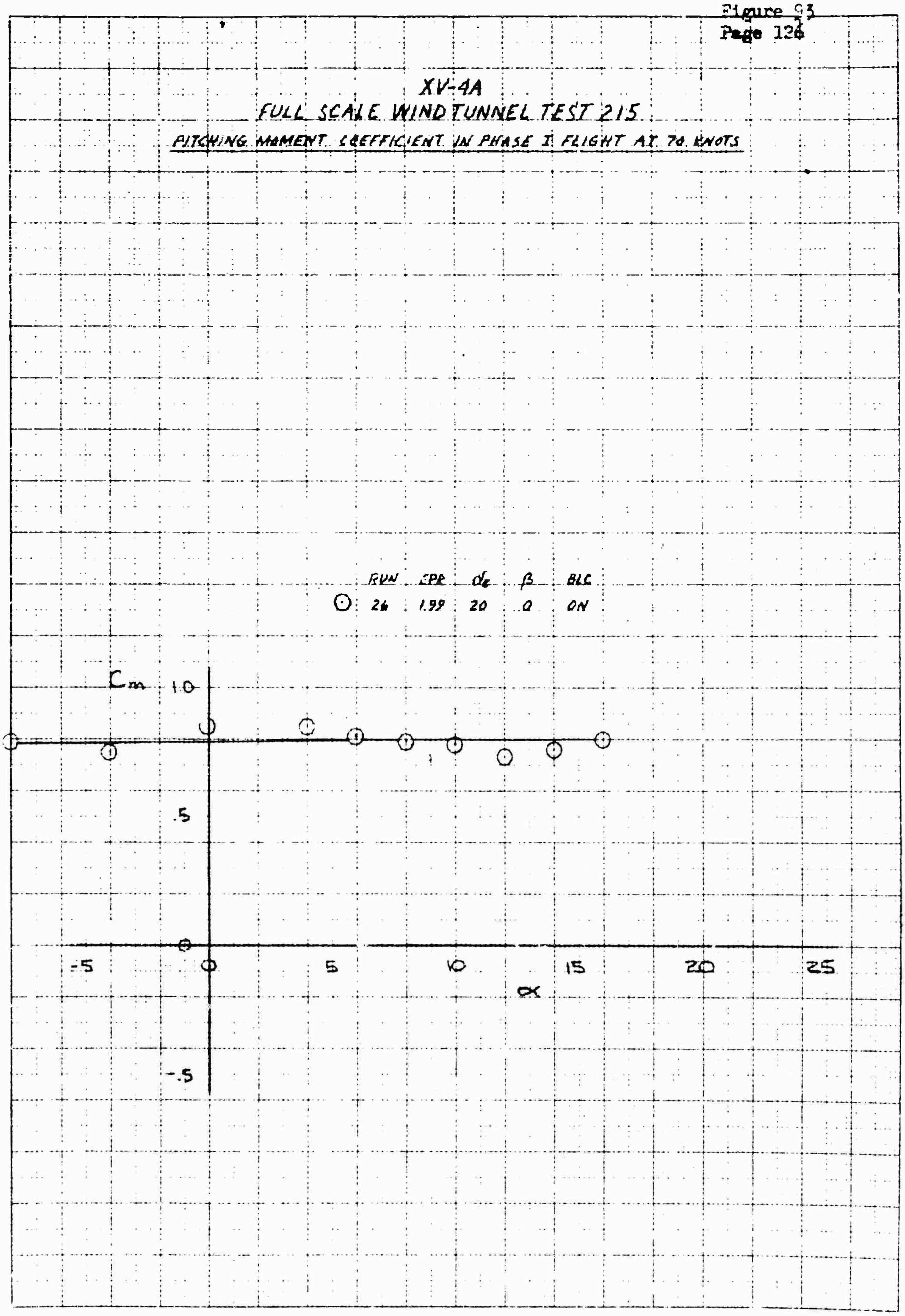
XV-4A
FULL SCALE WIND TUNNEL TEST 215
PITCHING MOMENT COEFFICIENT IN PHASE I FLIGHT AT 70 KNOTS
RUN CPR δε β BLC
26 1.99 20 0 ON
Cm
1.0
.5
-.5
-5
0
5
10
15
20
25
α

XV-4A
FULL SCALE WIND TUNNEL TEST 215
ELEVATOR EFFECT ON LIFT COEFFICIENT IN PHASE I FLIGHT AT 70 KNOTS

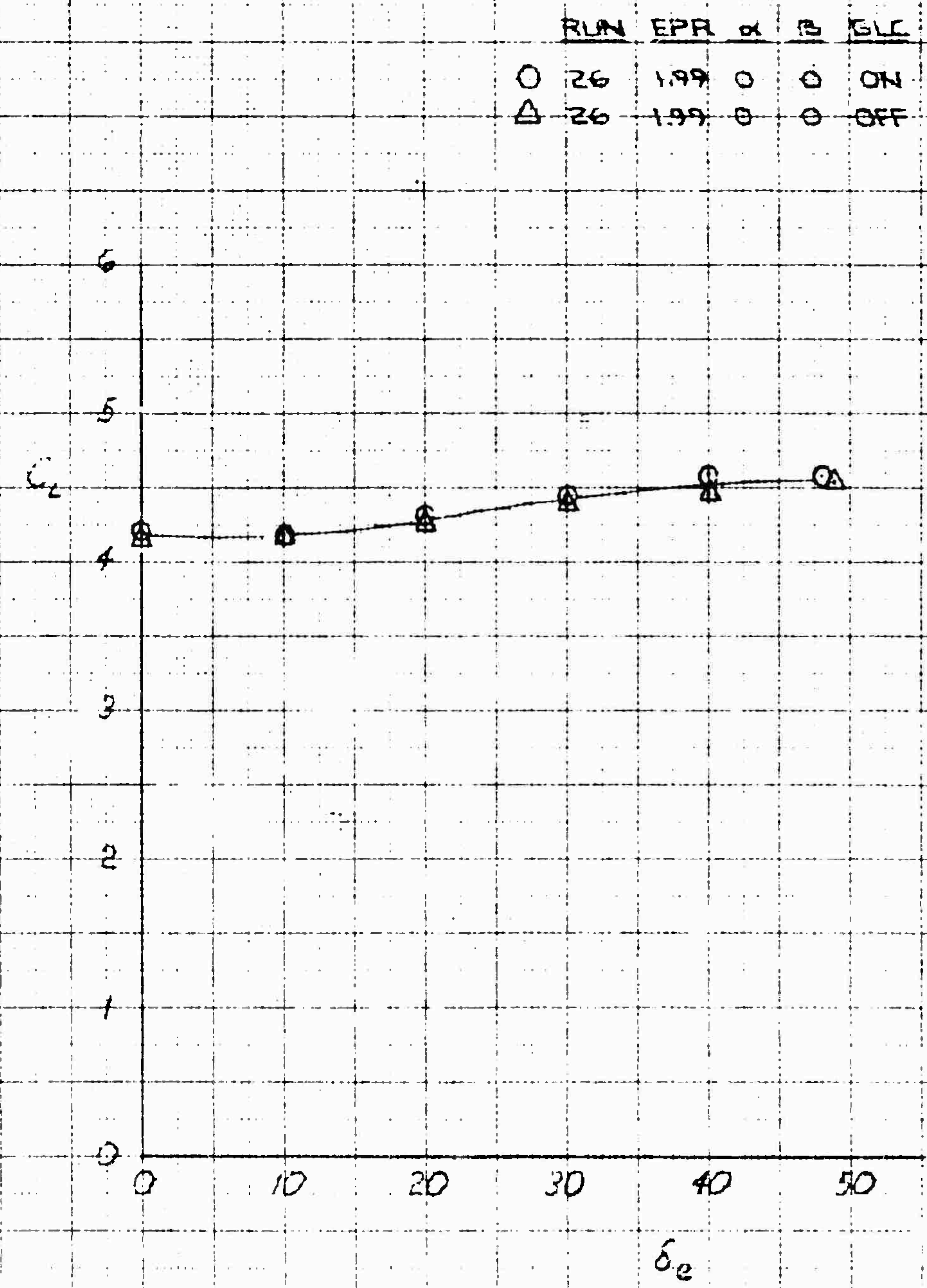

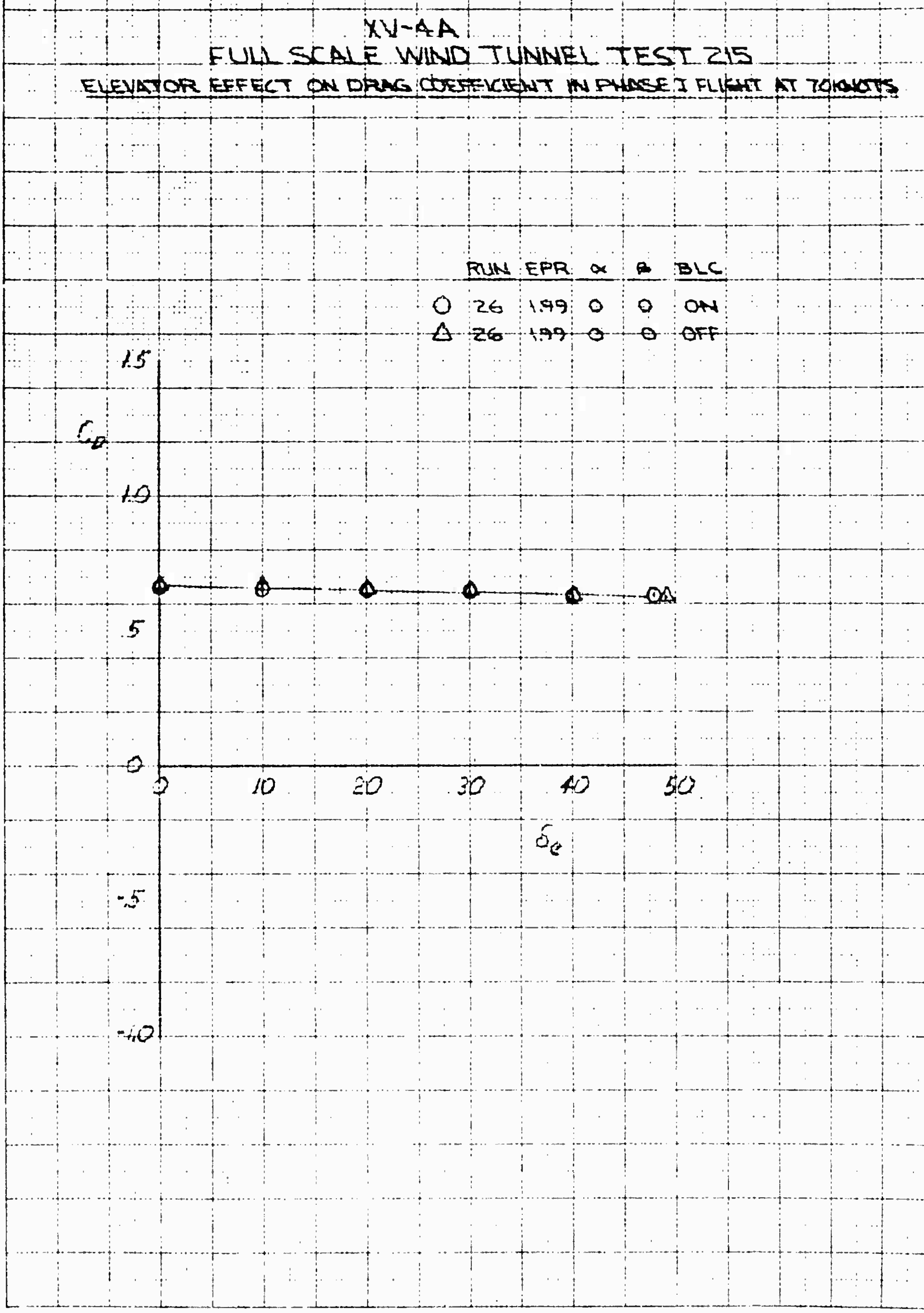
XV-4A
FULL SCALE WIND TUNNEL TEST 215
ELEVATOR EFFECT ON DRAG COEFFICIENT IN PHASE I FLIGHT AT 70 KNOTS
RUN EPR α β BLC
○ 26 1.99 0 0 ON
△ 26 1.99 0 0 OFF
C_D
1.5
1.0
.5
0
-.5
-1.0
0
10
20
30
40
50
δ_e

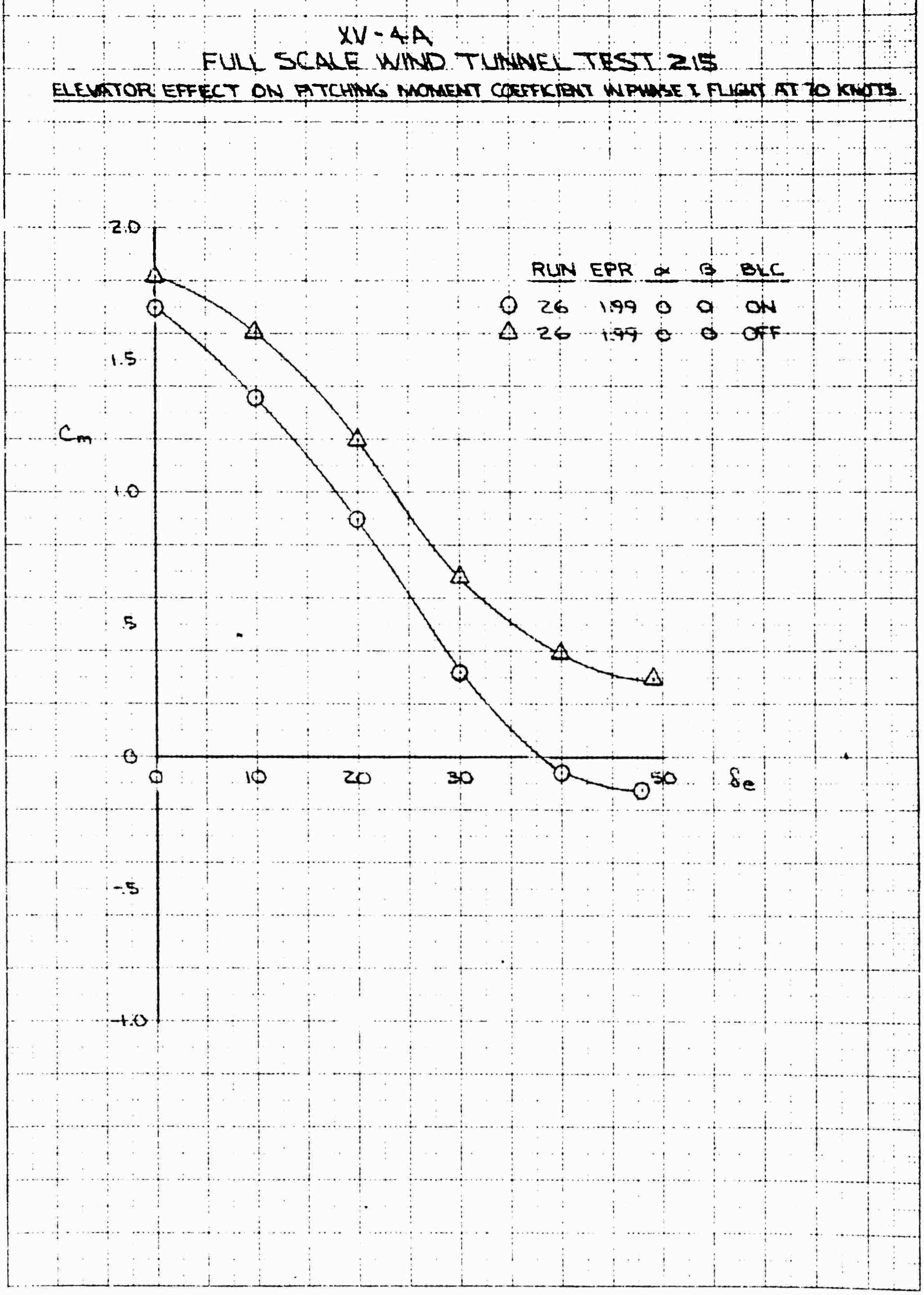
XV-4A
FULL SCALE WIND TUNNEL TEST 215
ELEVATOR EFFECT ON PITCHING MOMENT COEFFICIENT IN PHASE I FLIGHT AT 70 KNOTS
RUN EPR α β BLC
26 1.99 0 0 ON
26 1.99 0 0 OFF
2.0
1.5
1.0
.5
0
-.5
-1.0
Cm
0
10
20
30
50
δe

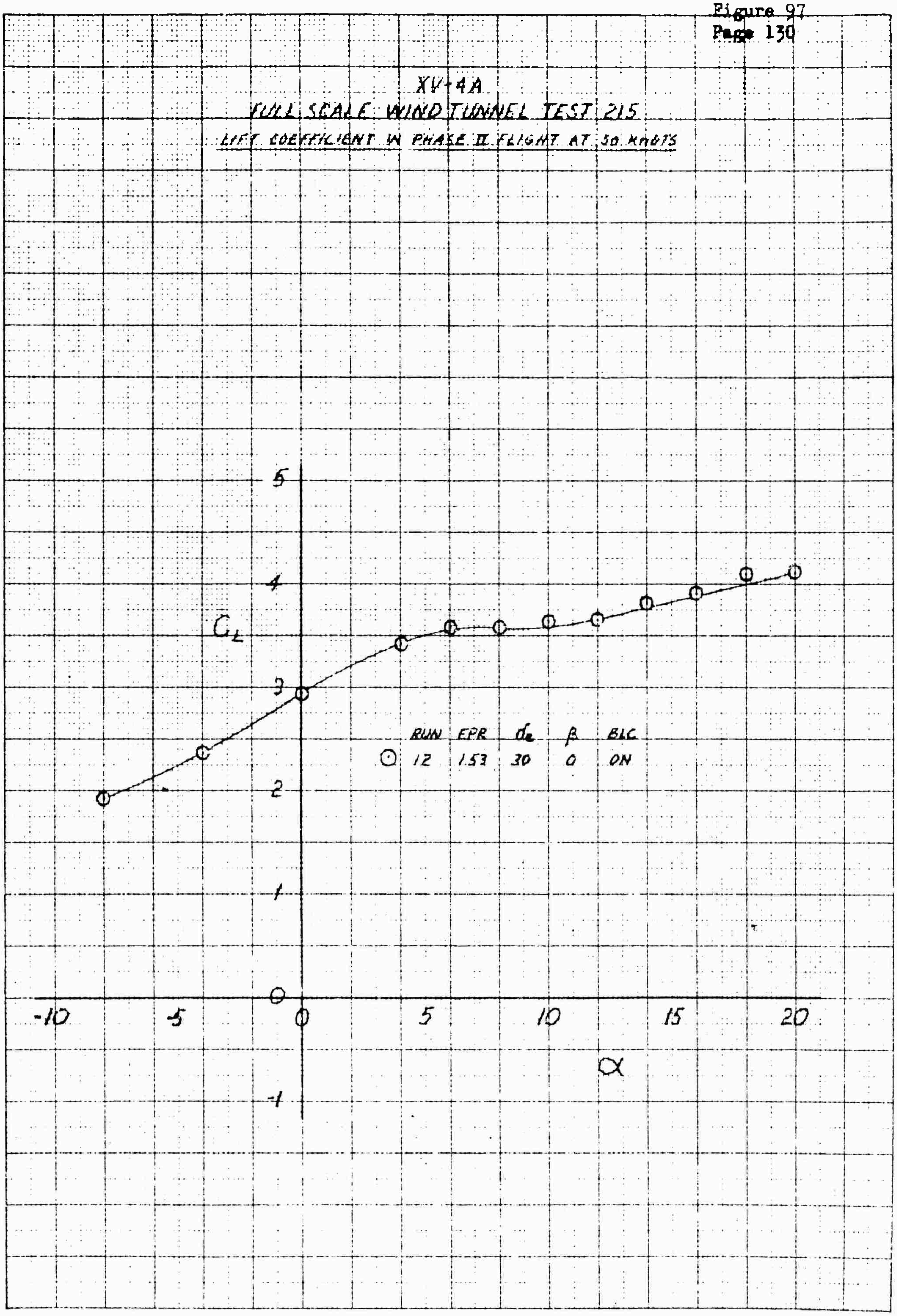
XV-4A
FULL SCALE WIND TUNNEL TEST 215
LIFT COEFFICIENT IN PHASE II FLIGHT AT 50 KNOTS
C_L
5
4
3
2
1
0
-1
-10
-5
0
5
10
15
20
α
RUN EPR δ_e β BLC
12 1.53 30 0 ON

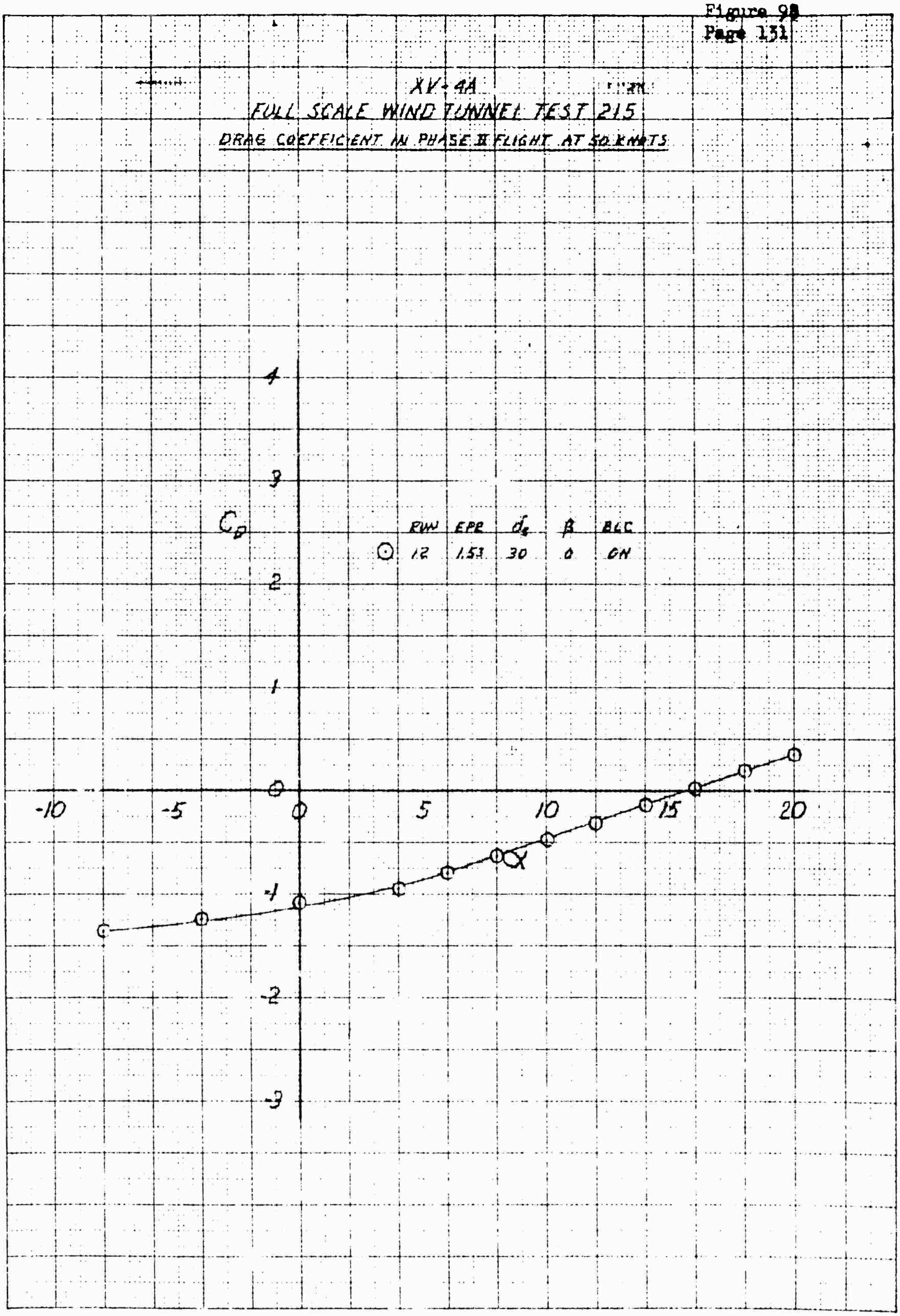
XV-4A
FULL SCALE WIND TUNNEL TEST 215
DRAG COEFFICIENT IN PHASE II FLIGHT AT 50 KNOTS
C_D
RW
EPR
δ_f
β
BLC
12
1.53
30
0
ON
4
3
2
1
-1
-2
-3
-10
-5
0
5
10
15
20
α

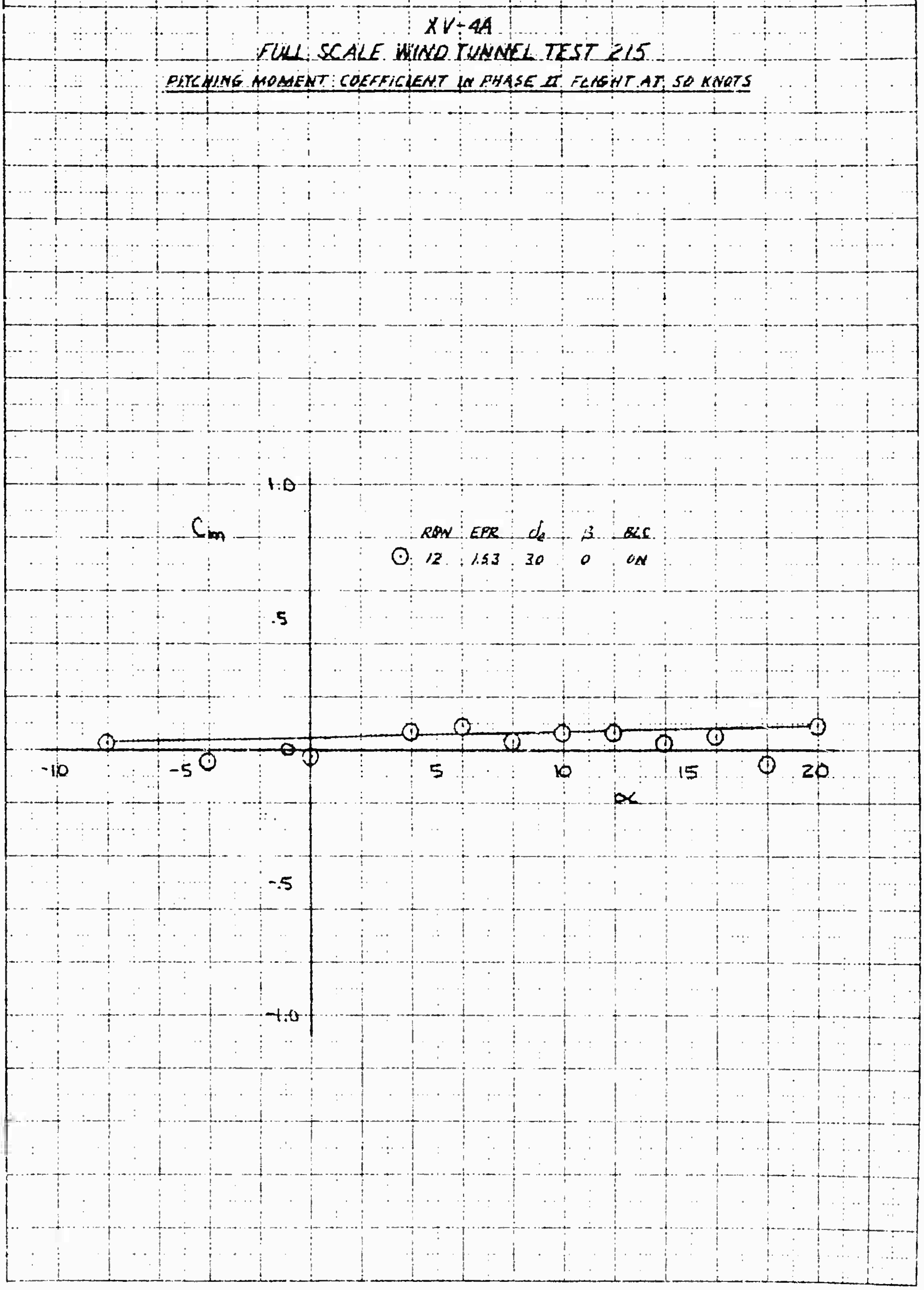
XV-4A
FULL SCALE WIND TUNNEL TEST 215
PITCHING MOMENT COEFFICIENT IN PHASE II FLIGHT AT 50 KNOTS
RPM EPR δe β BLC
12 1.53 30 0 ON
Cm
1.0
.5
-.5
-1.0
-10
-5
5
10
15
20
α

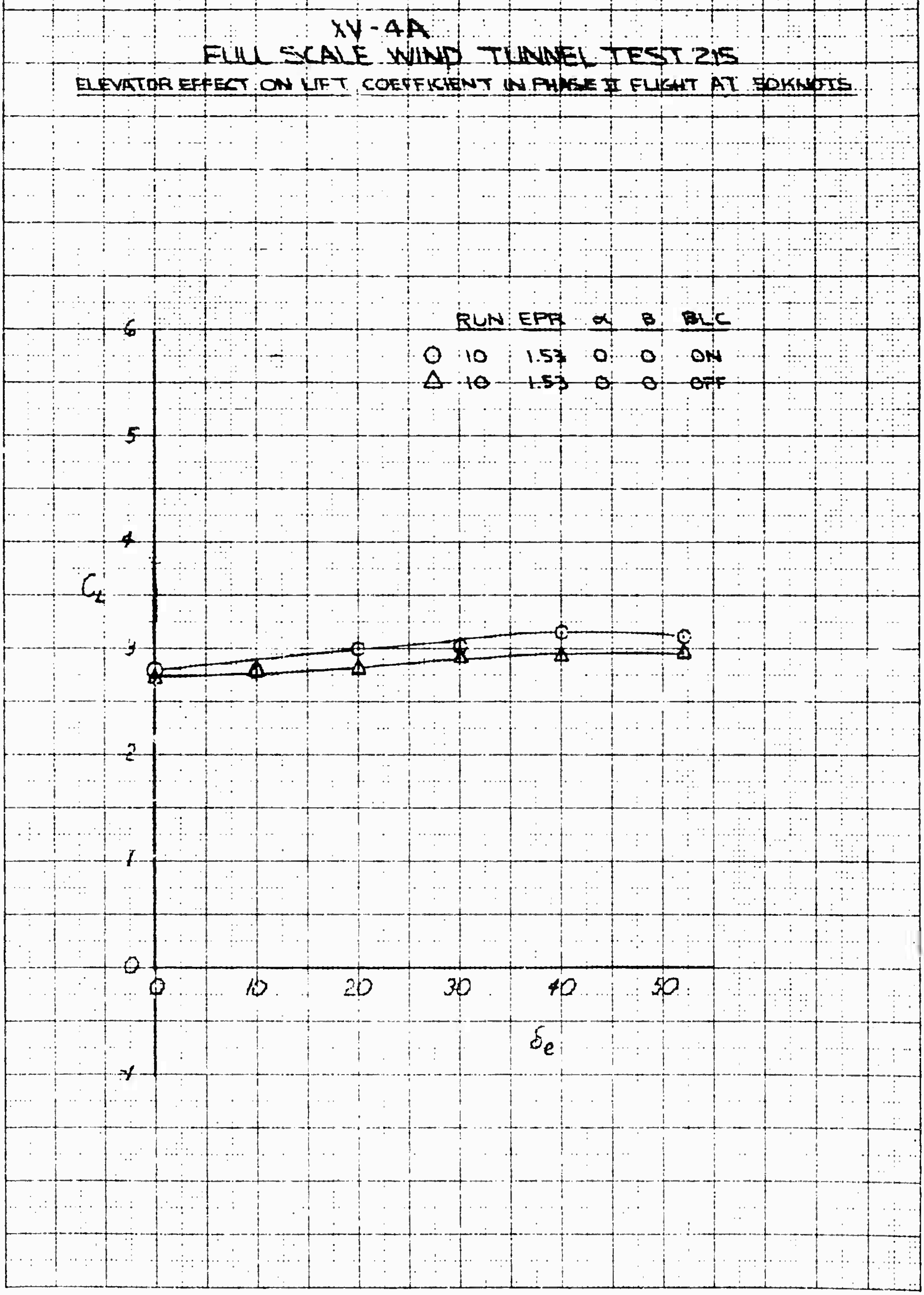
XV-4A
FULL SCALE WIND TUNNEL TEST 215
ELEVATOR EFFECT ON LIFT COEFFICIENT IN PHASE II FLIGHT AT 50KNOTS
RUN EPR α β BLC
○ 10 1.53 0 0 ON
△ 10 1.53 0 0 OFF
C_L
6
5
4
3
2
1
0
-1
0 10 20 30 40 50
δ_e

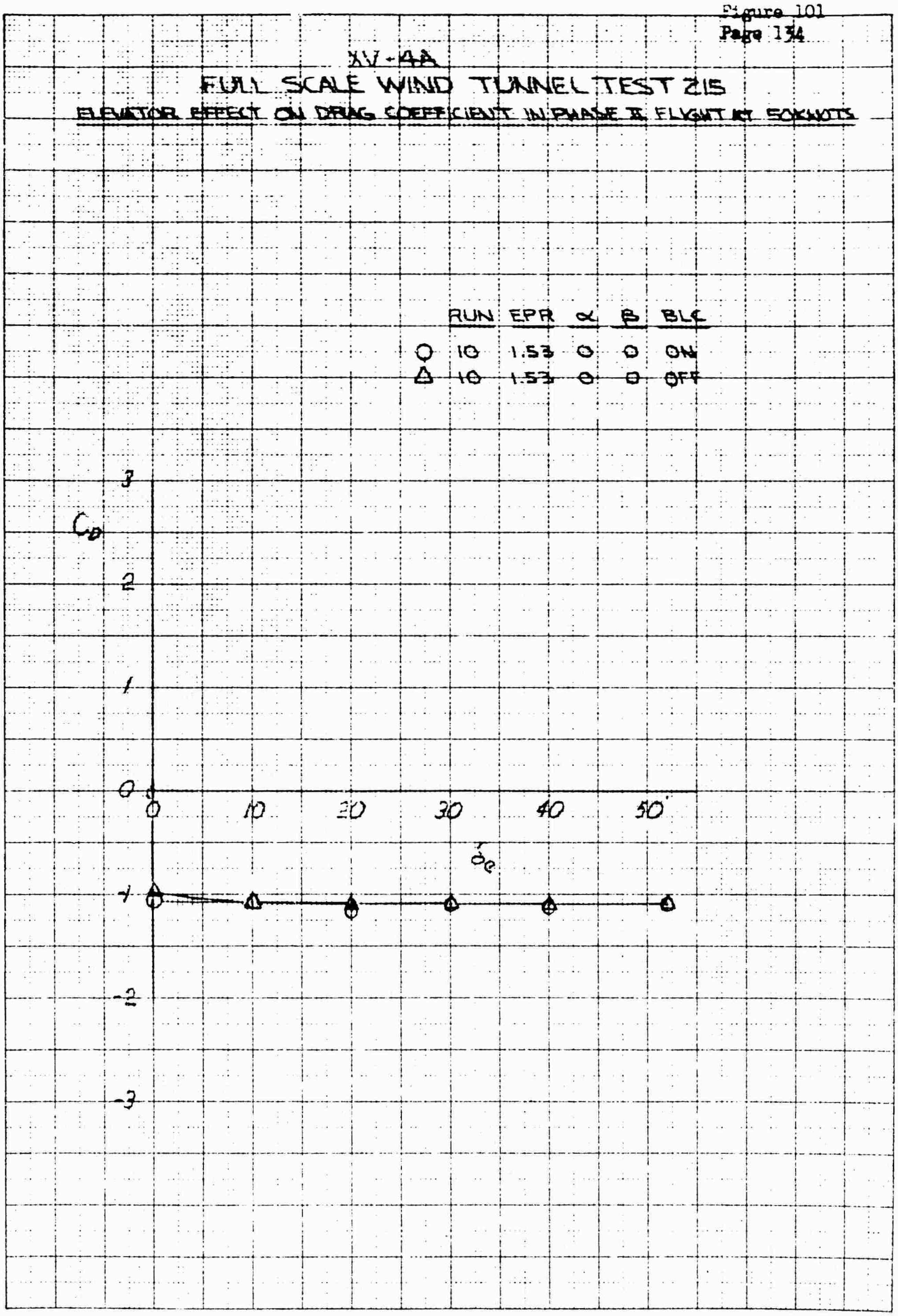
XV-4A
FULL SCALE WIND TUNNEL TEST 215
ELEVATOR EFFECT ON DRAG COEFFICIENT IN PHASE II FLIGHT AT 50 KNOTS
RUN EPR α β BLC
10 1.53 0 0 ON
10 1.53 0 0 OFF
C_D
3
2
1
0
-1
-2
-3
0
10
20
30
40
50
δ_e

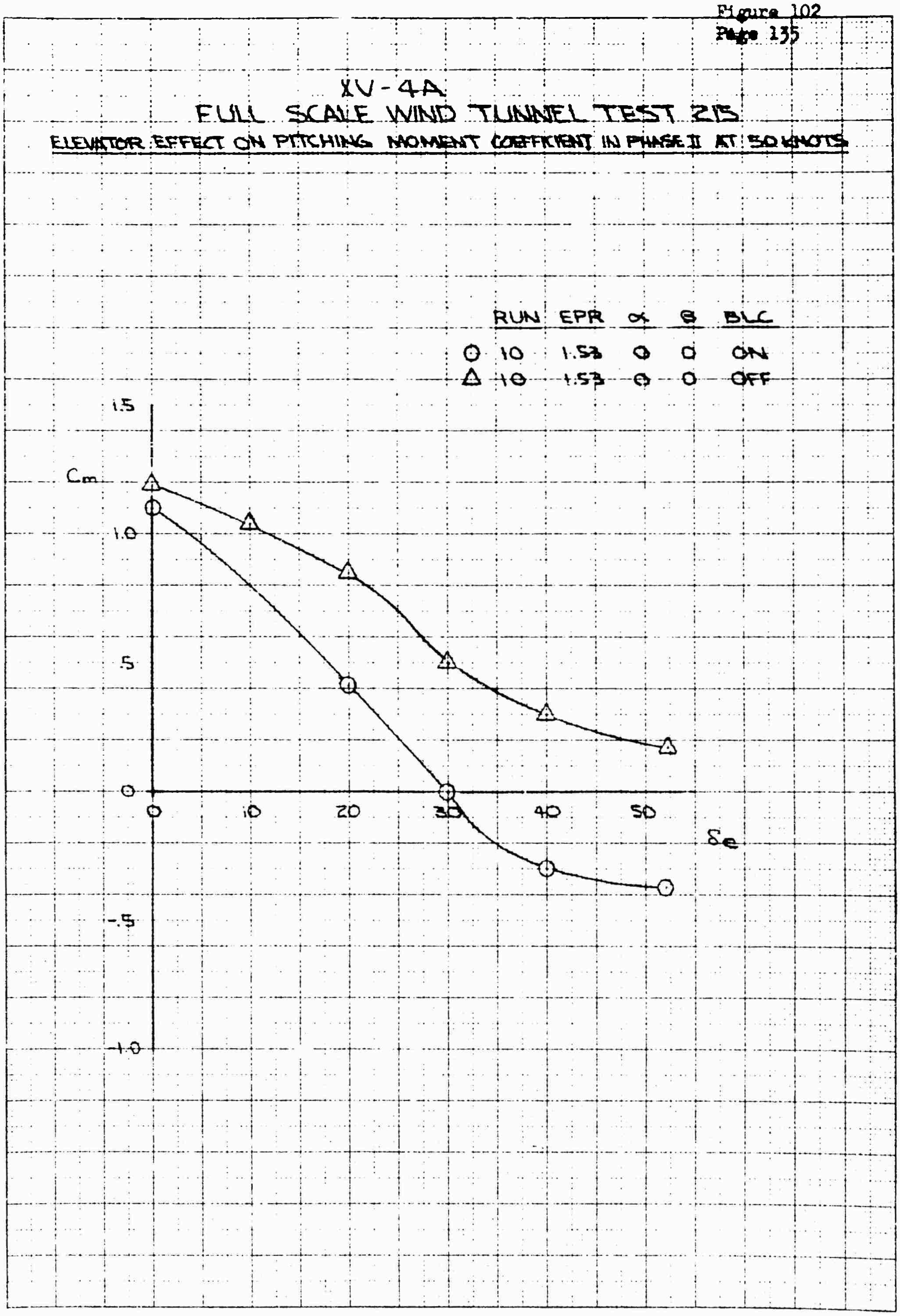
XV-4A
FULL SCALE WIND TUNNEL TEST 215
ELEVATOR EFFECT ON PITCHING MOMENT COEFFICIENT IN PHASE II AT 50 KNOTS
RUN EPR α θ BLC
○ 10 1.53 0 0 ON
△ 10 1.53 0 0 OFF
Cm
1.5
1.0
.5
0
-.5
-1.0
0
10
20
30
40
50
δe

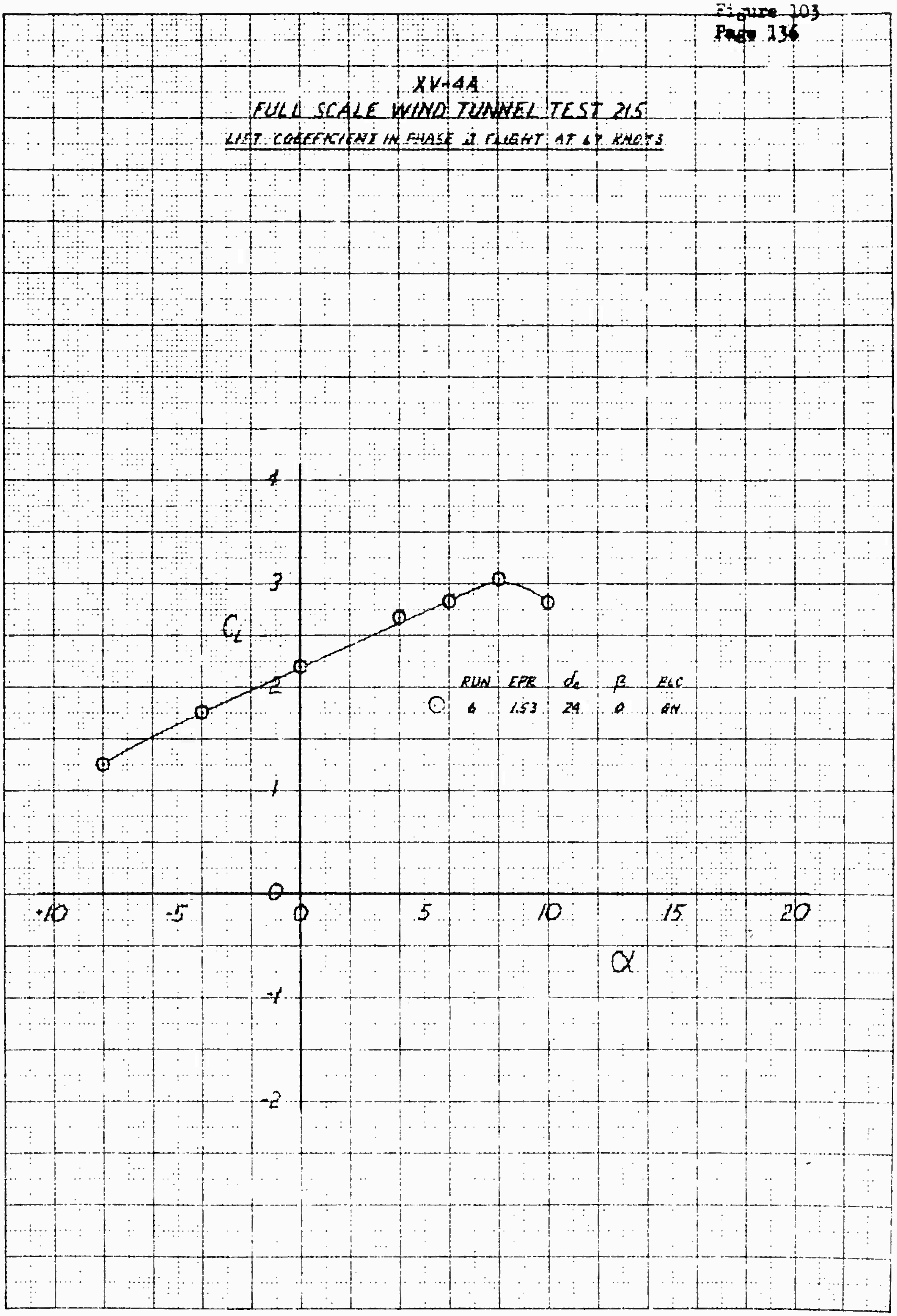
XV-4A
FULL SCALE WIND TUNNEL TEST 215
LIFT COEFFICIENT IN PHASE II FLIGHT AT 67 KNOTS
C_L
α
4
3
2
1
0
-1
-2
-10
-5
0
5
10
15
20
RUN EPR δ_e β ELC
6 1.53 24 0 ON

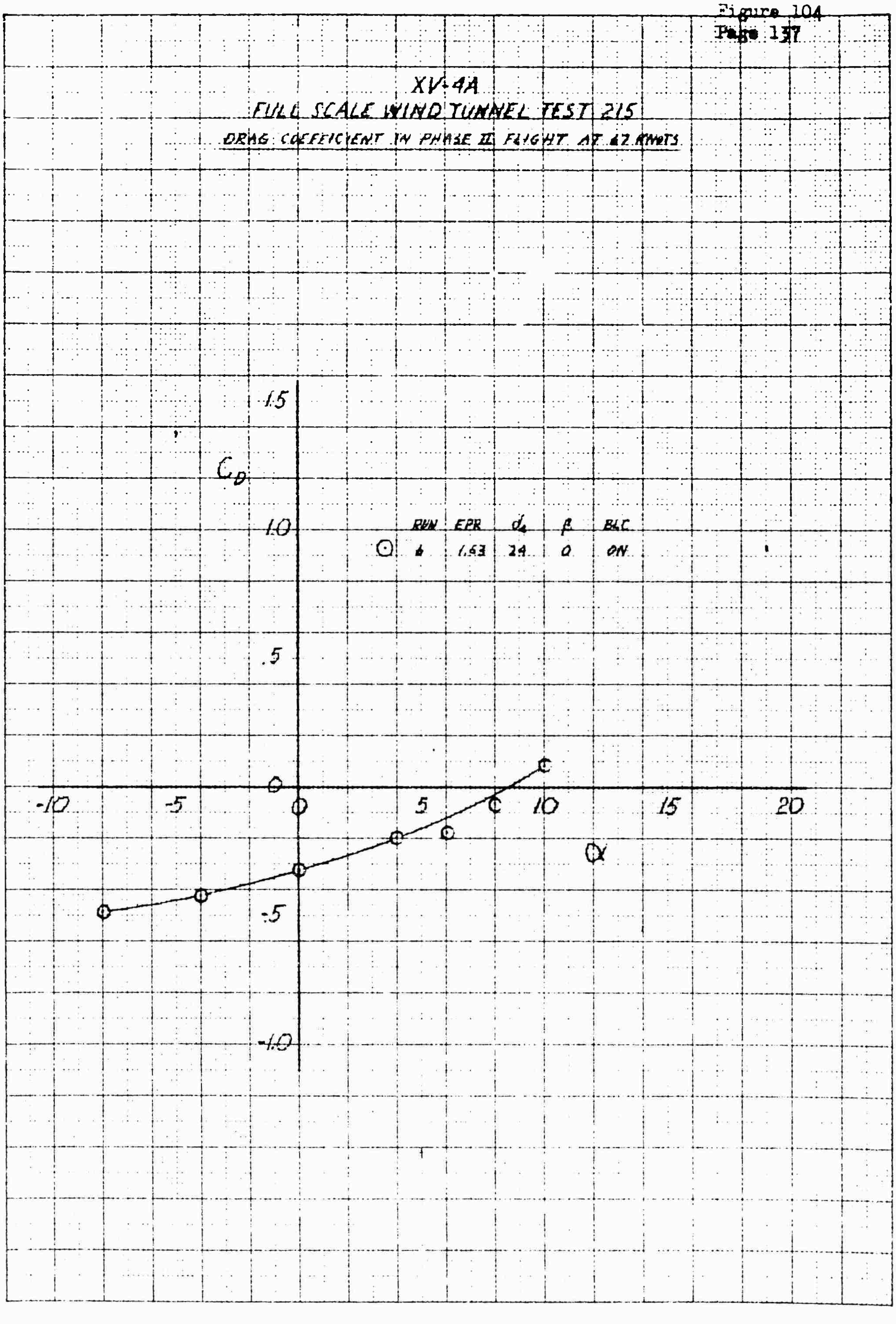
XV-4A
FULL SCALE WIND TUNNEL TEST 215
DRAG COEFFICIENT IN PHASE II FLIGHT AT 62 KNOTS
C_D
1.5
1.0
.5
0
-.5
-1.0
-10
-5
0
5
10
15
20
α
RUN EPR d_4 β BLC
6 1.63 24 0 ON

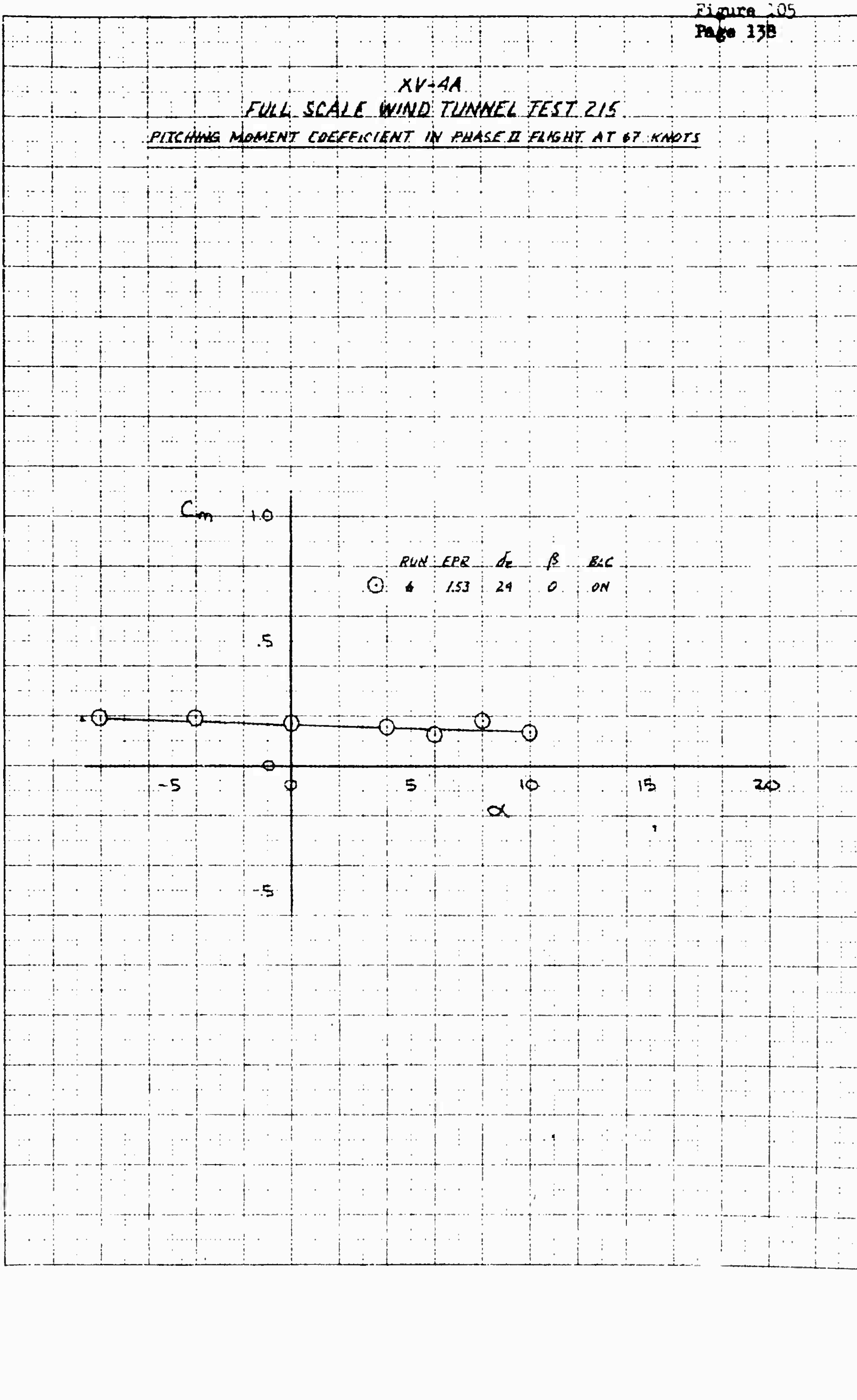
XV-4A
FULL SCALE WIND TUNNEL TEST 215
PITCHING MOMENT COEFFICIENT IN PHASE II FLIGHT AT 67 KNOTS
Cm
1.0
.5
-.5
-5
0
5
10
15
20
α
RUN EPR δe β BLC
6 1.53 24 0 ON

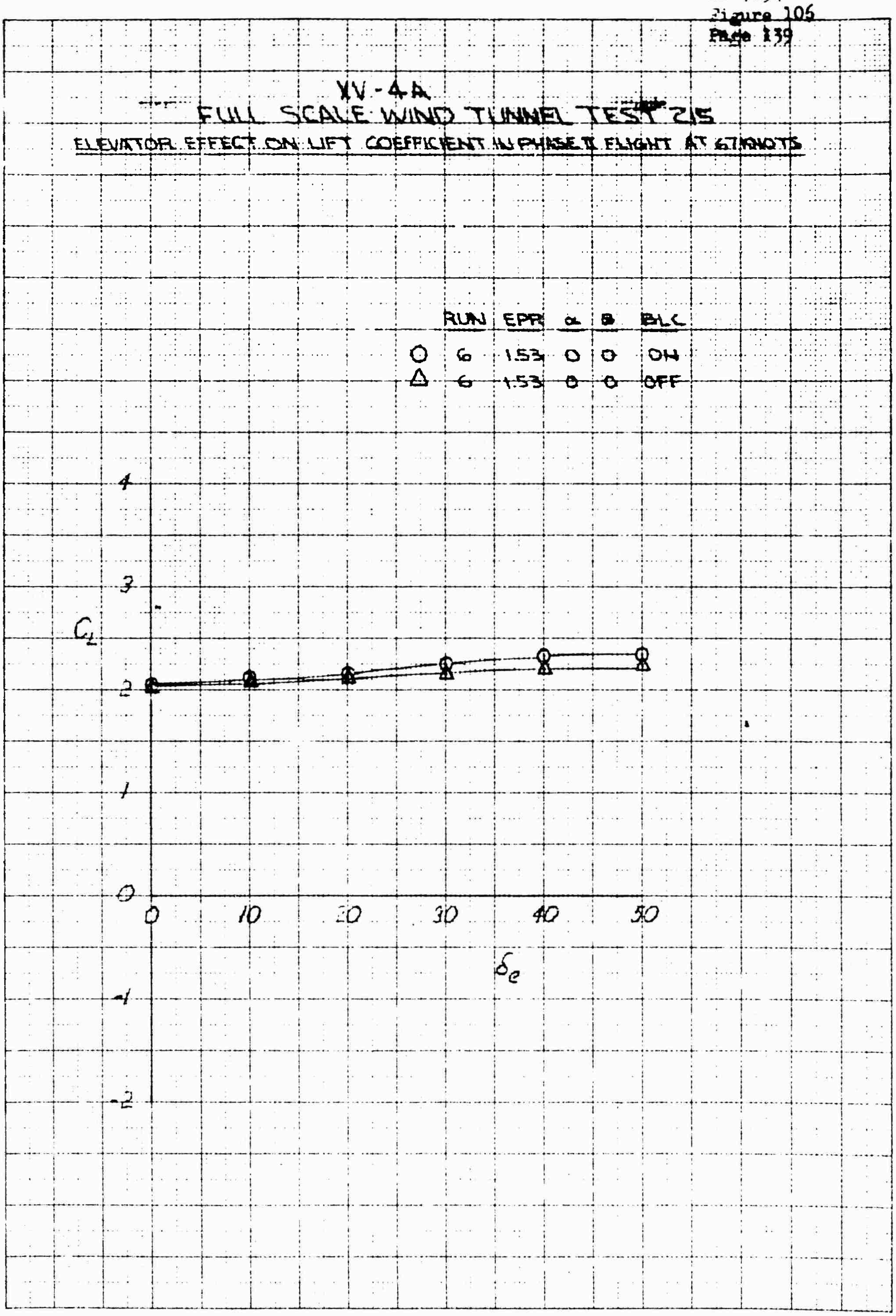
XV-4A
FULL SCALE WIND TUNNEL TEST 215
ELEVATOR EFFECT ON LIFT COEFFICIENT IN PHASE II FLIGHT AT 67 KNOTS
RUN EPR α β BLC
○ 6 1.53 0 0 ON
△ 6 1.53 0 0 OFF
C_L
4
3
2
1
0
-1
-2
0
10
20
30
40
50
δ_e

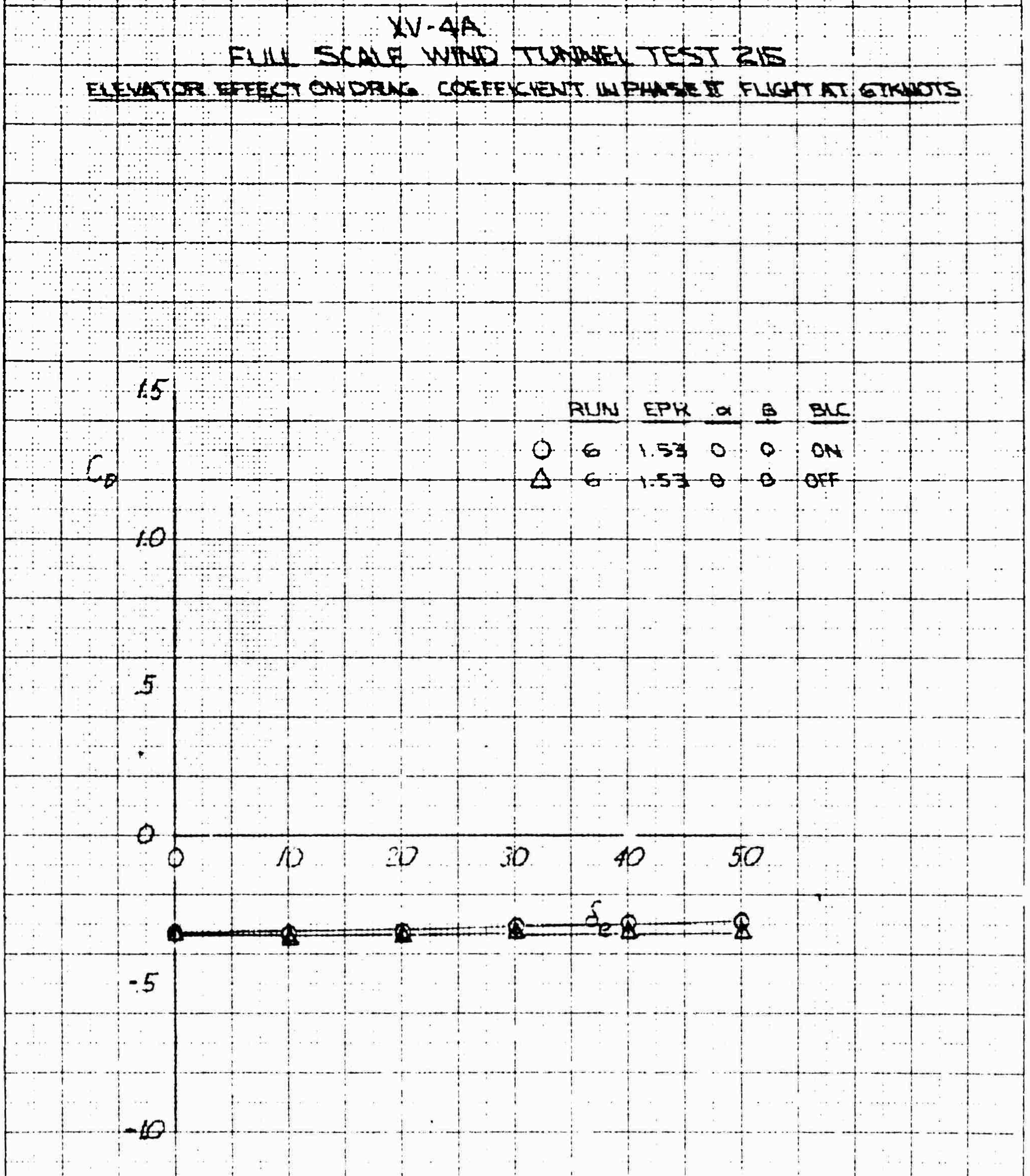
XV-4A
FULL SCALE WIND TUNNEL TEST 215
ELEVATOR EFFECT ON DRAG COEFFICIENT IN PHASE II FLIGHT AT 67KNOTS
RUN EPR α β BLC
6 1.53 0 0 ON
6 1.53 0 0 OFF
C_D
1.5
1.0
.5
0
-.5
-1.0
0 10 20 30 40 50
δ_e

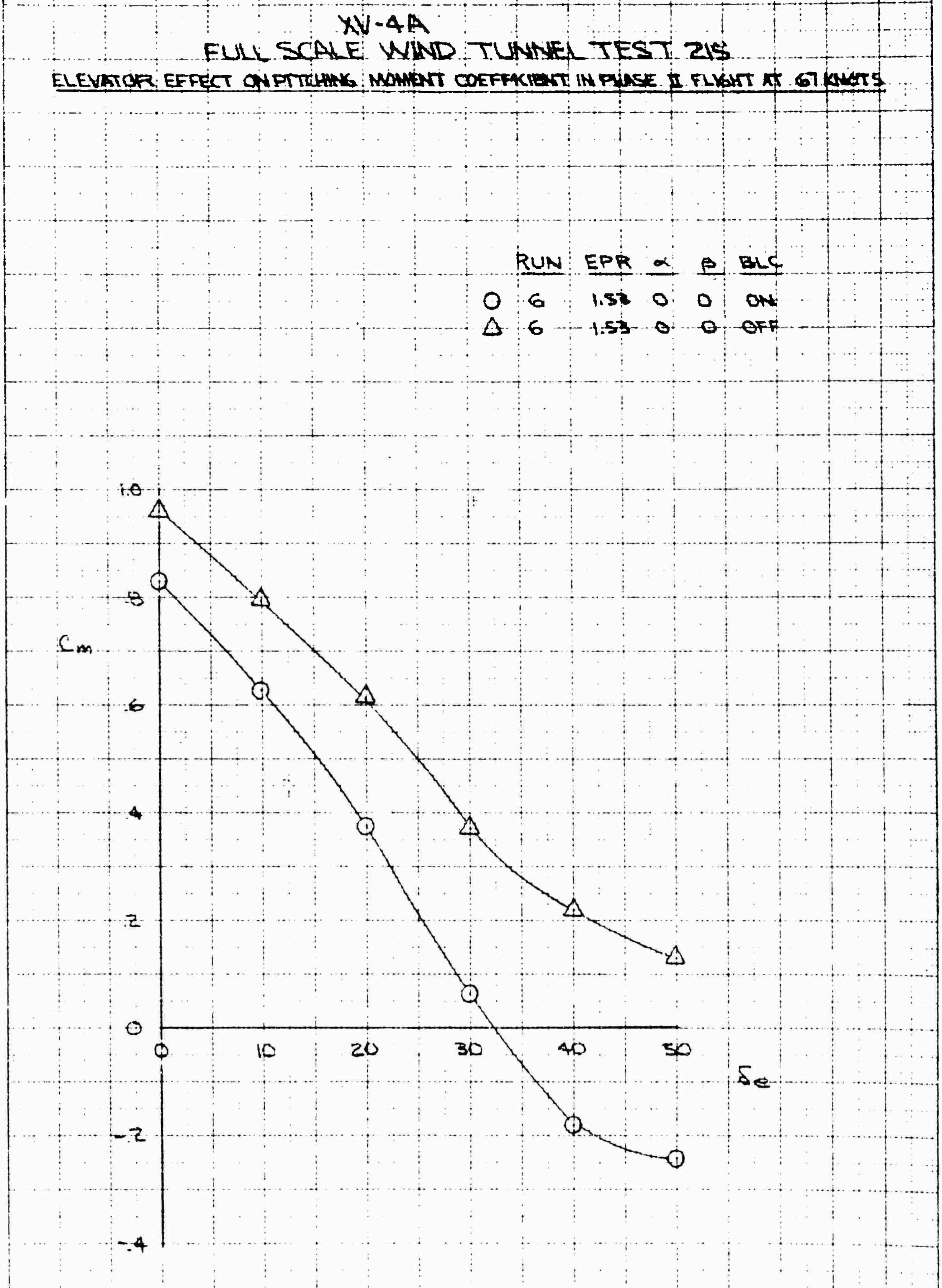
XV-4A
FULL SCALE WIND TUNNEL TEST 215
ELEVATOR EFFECT ON PITCHING MOMENT COEFFICIENT IN PHASE II FLIGHT AT 67 KNOTS
RUN EPR α β BLC
○ 6 1.53 0 0 ON
△ 6 1.53 0 0 OFF
Cm
1.0
.8
.6
.4
.2
0
-.2
-.4
0
10
20
30
40
50
δe

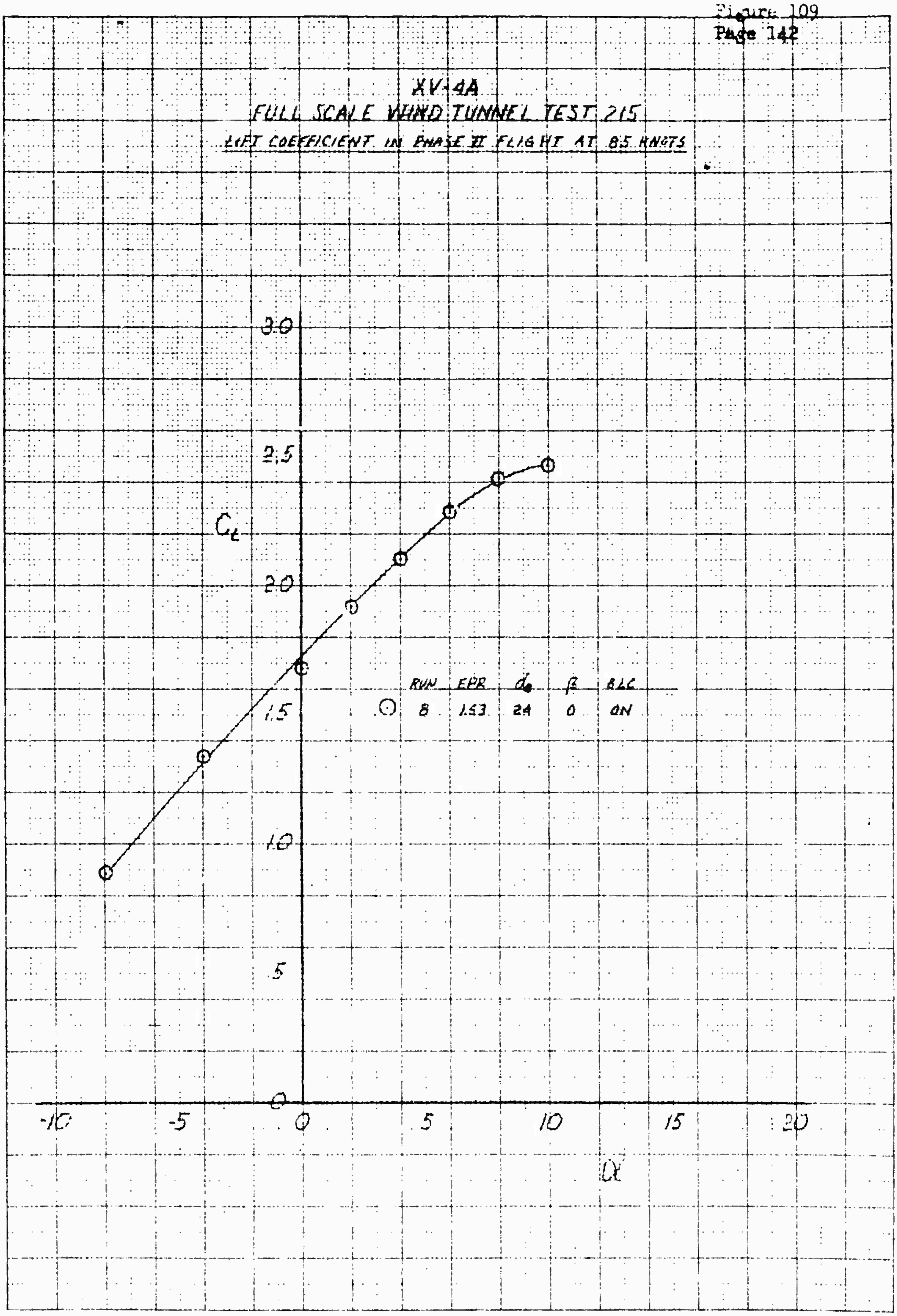
XV-4A
FULL SCALE WIND TUNNEL TEST 215
LIFT COEFFICIENT IN PHASE II FLIGHT AT 85 KNOTS
3.0
2.5
2.0
1.5
1.0
.5
0
C_L
-10
-5
0
5
10
15
20
α
RUN
EPR
δ_e
β
BLC
8
1.53
24
0
ON

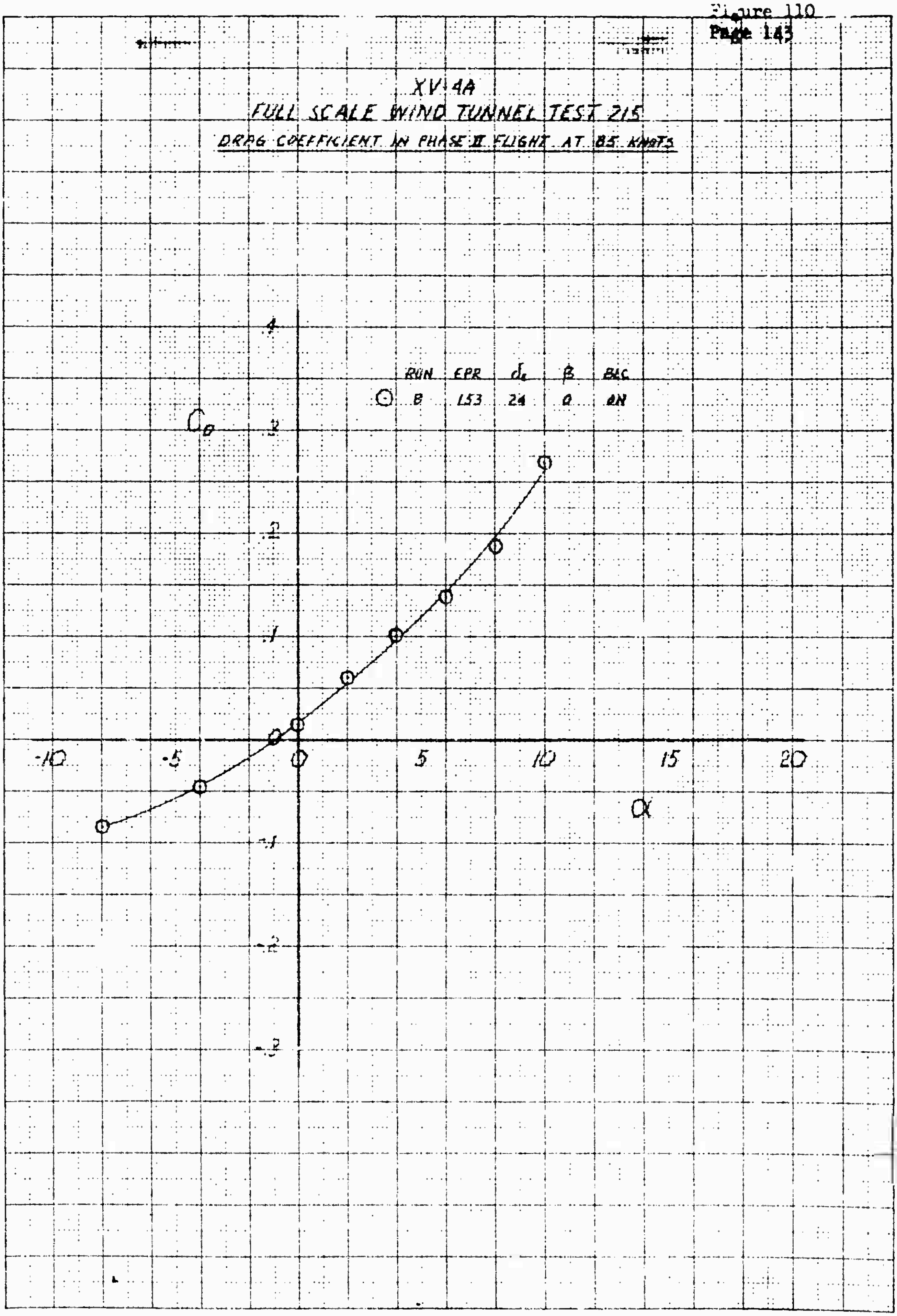
XV-4A
FULL SCALE WIND TUNNEL TEST 215
DRAG COEFFICIENT IN PHASE II FLIGHT AT 85 KNOTS
RUN EPR δe β BLC
B 1.53 24 0 ON
C_D
.4
.3
.2
.1
-.1
-.2
-.3
-10
-5
0
5
10
15
20
α

XV-4A
FULL SCALE WIND TUNNEL TEST 215
PITCHING MOMENT COEFFICIENT IN PHASE II FLIGHT AT 85 KNOTS

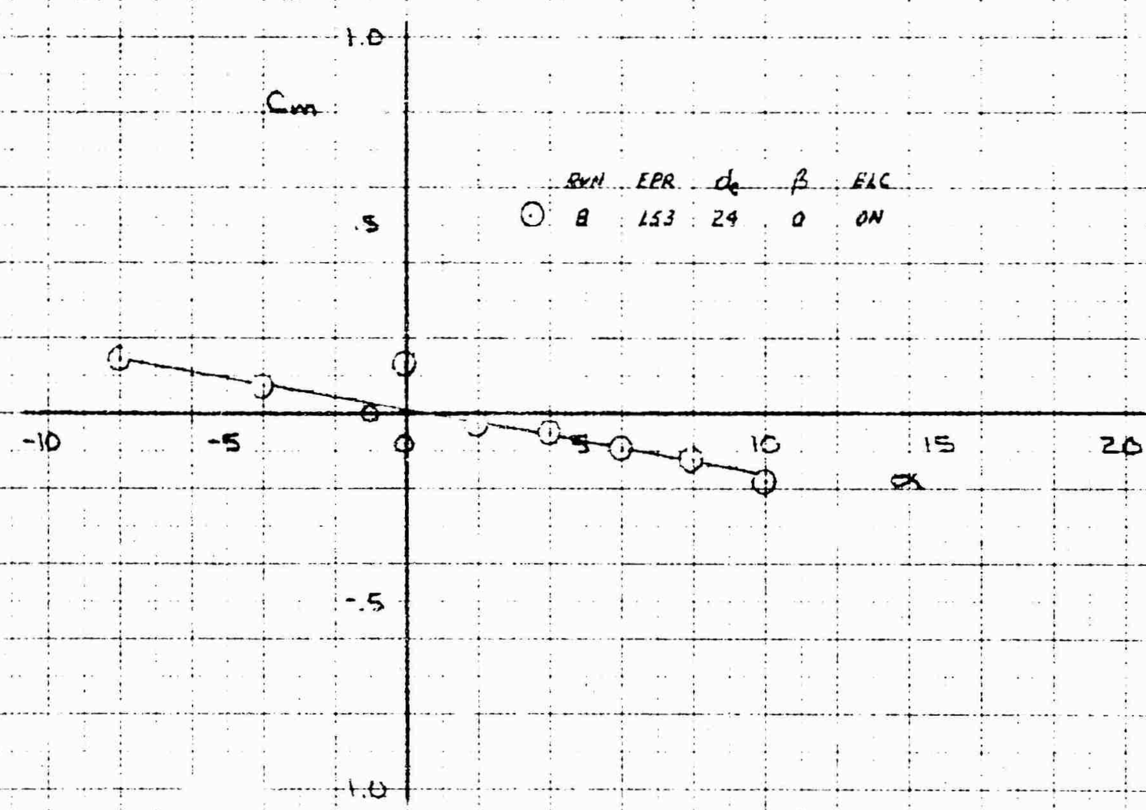

XV-4A
FULL SCALE WIND TUNNEL TEST 215
ELEVATOR EFFECT ON LIFT COEFFICIENT IN PHASE II FLIGHT AT 85KNOTS

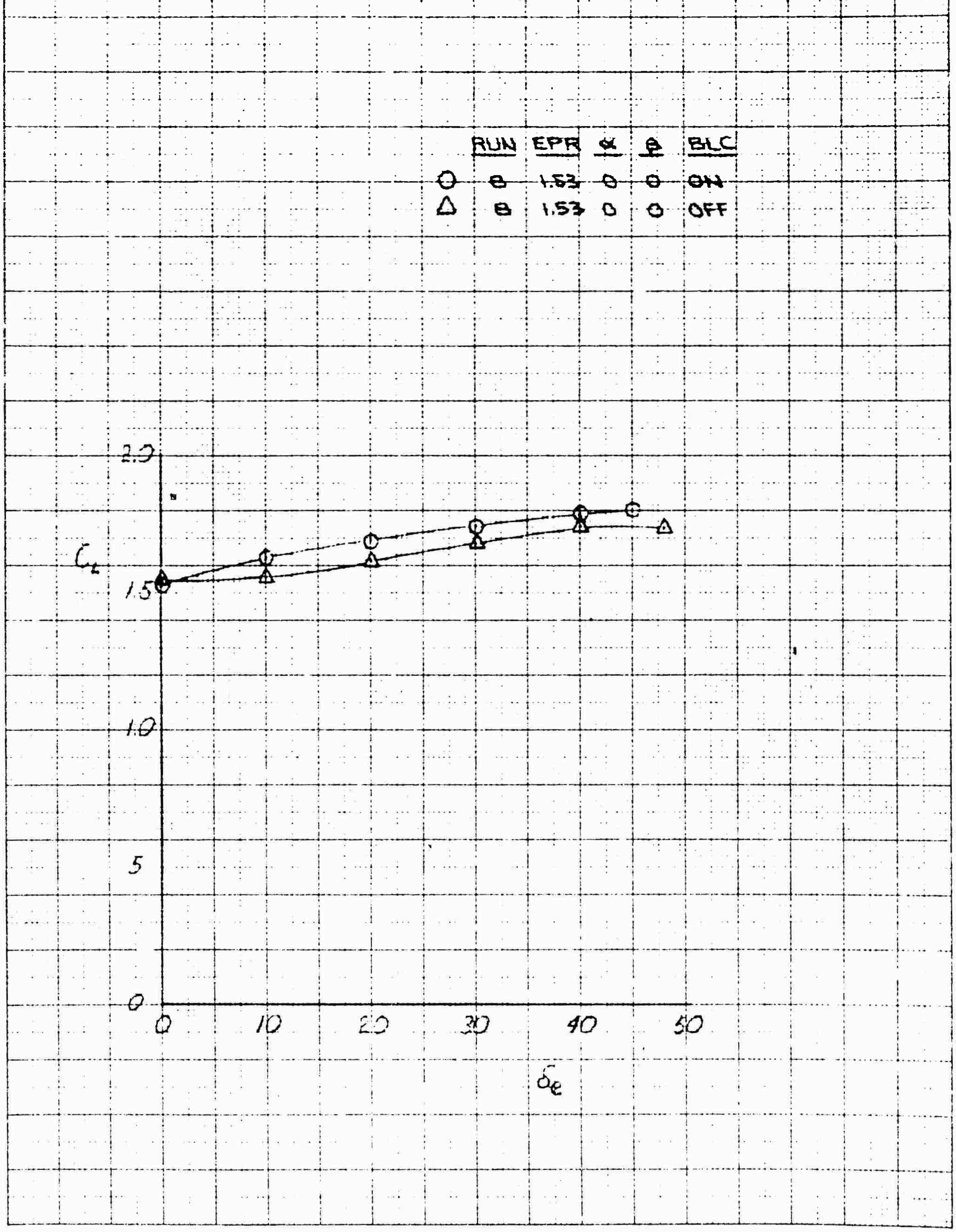

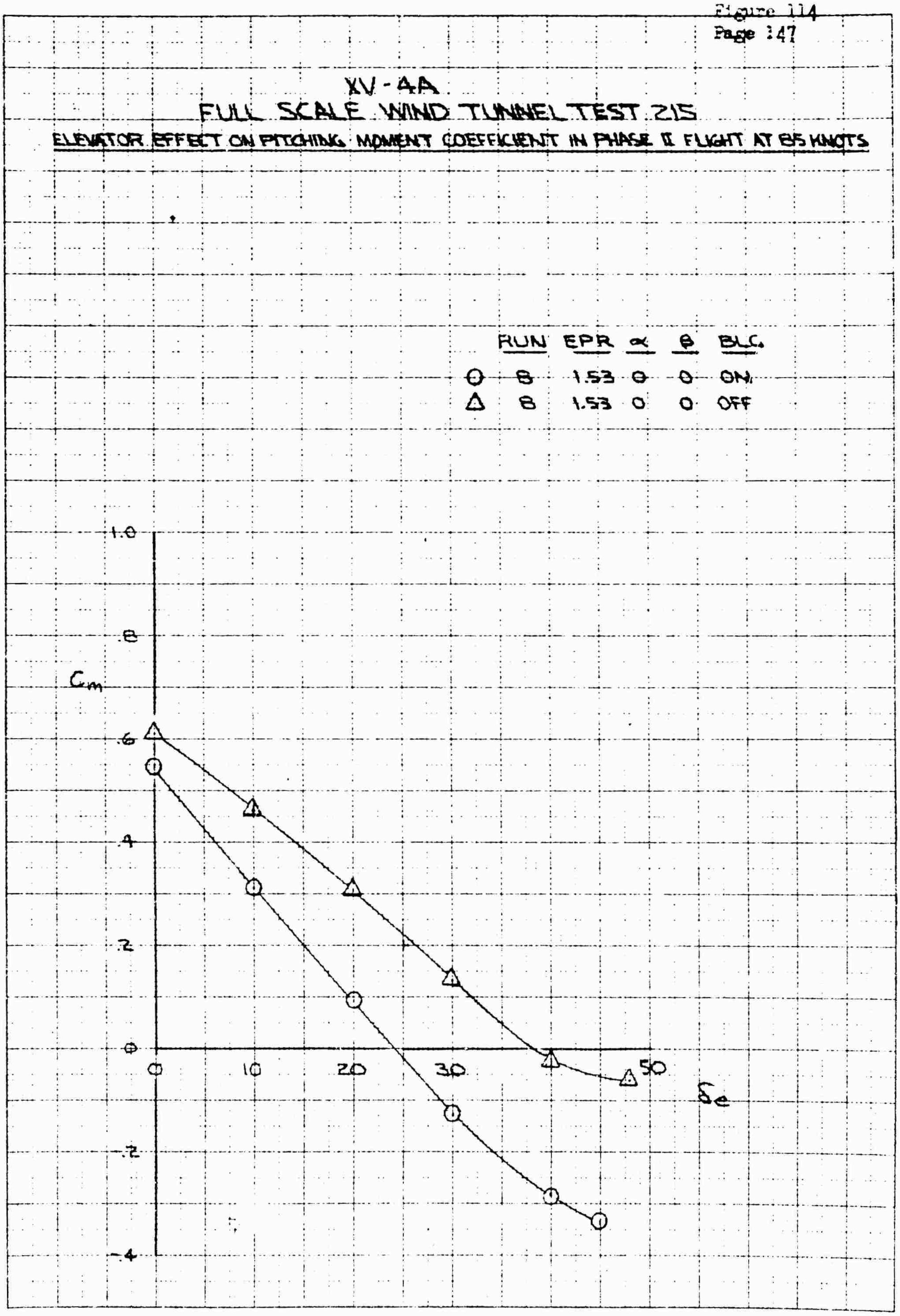
XV-4A
FULL SCALE WIND TUNNEL TEST 215
ELEVATOR EFFECT ON PITCHING MOMENT COEFFICIENT IN PHASE II FLIGHT AT 85 KNOTS
RUN EPR α β BLC
8 1.53 0 0 ON
8 1.53 0 0 OFF
1.0
.8
.6
.4
.2
0
-.2
-.4
C_m
0
10
20
30
50
δ_e

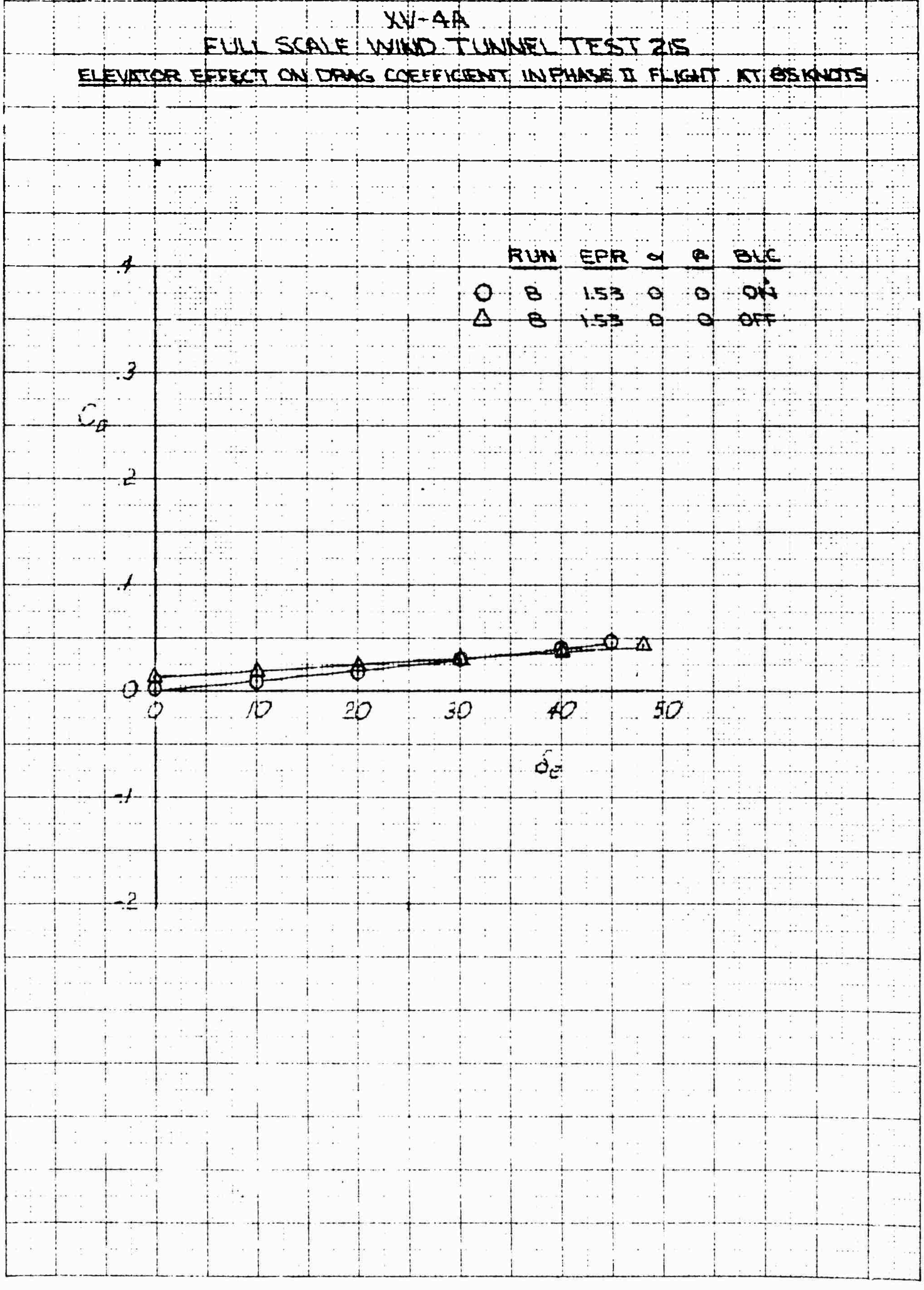
XV-4A
FULL SCALE WIND TUNNEL TEST 215
ELEVATOR EFFECT ON DRAG COEFFICIENT IN PHASE II FLIGHT AT 85 KNOTS
RUN EPR α β BLC
○ 8 1.53 0 0 ON
△ 8 1.53 0 0 OFF
C_D
.4
.3
.2
.1
0
-.1
-.2
0
10
20
30
40
50
δ_e

XV-4A

FULL SCALE WIND TUNNEL TEST 215

LIFT COEFFICIENT IN PHASE II FLIGHT AT 100 KNOTS

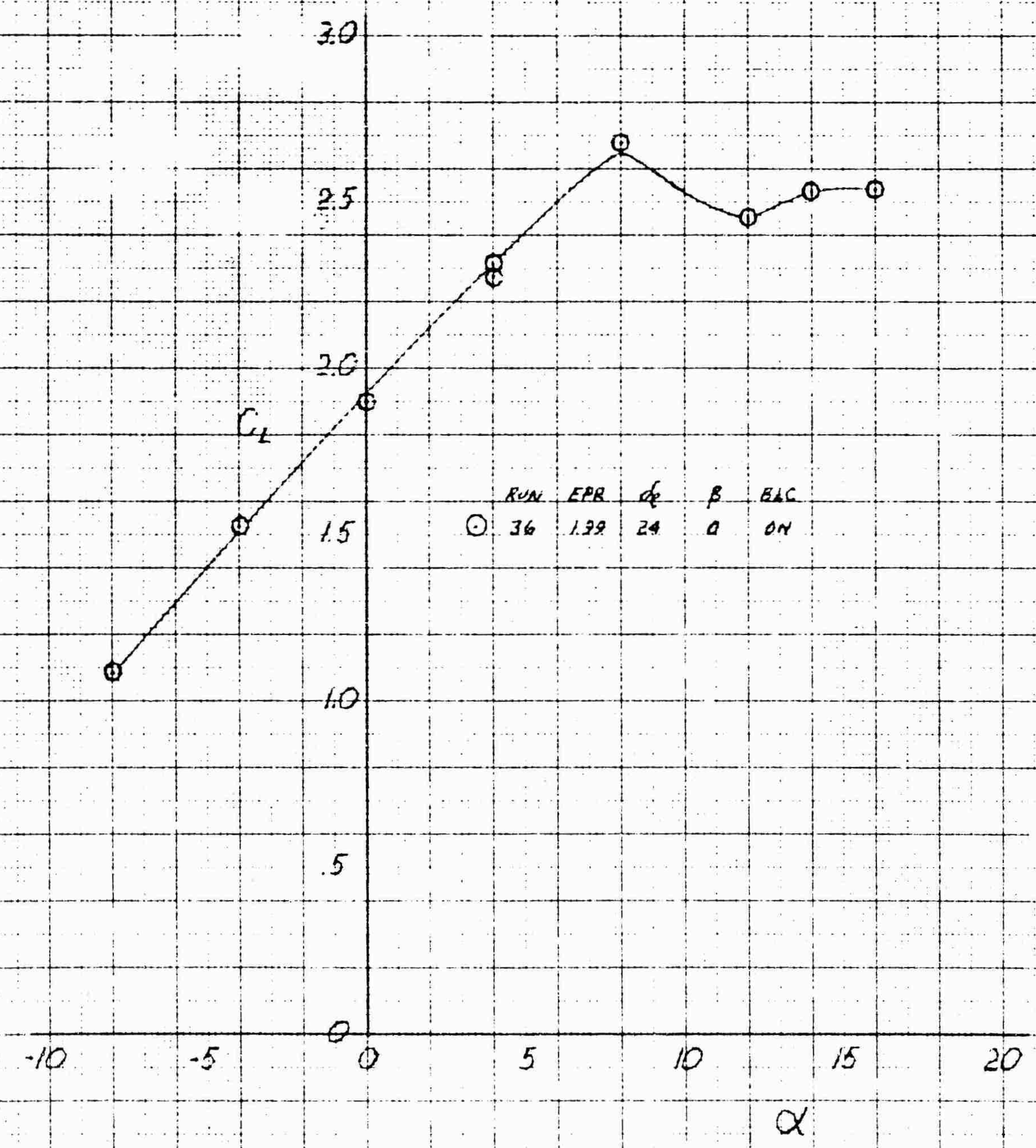

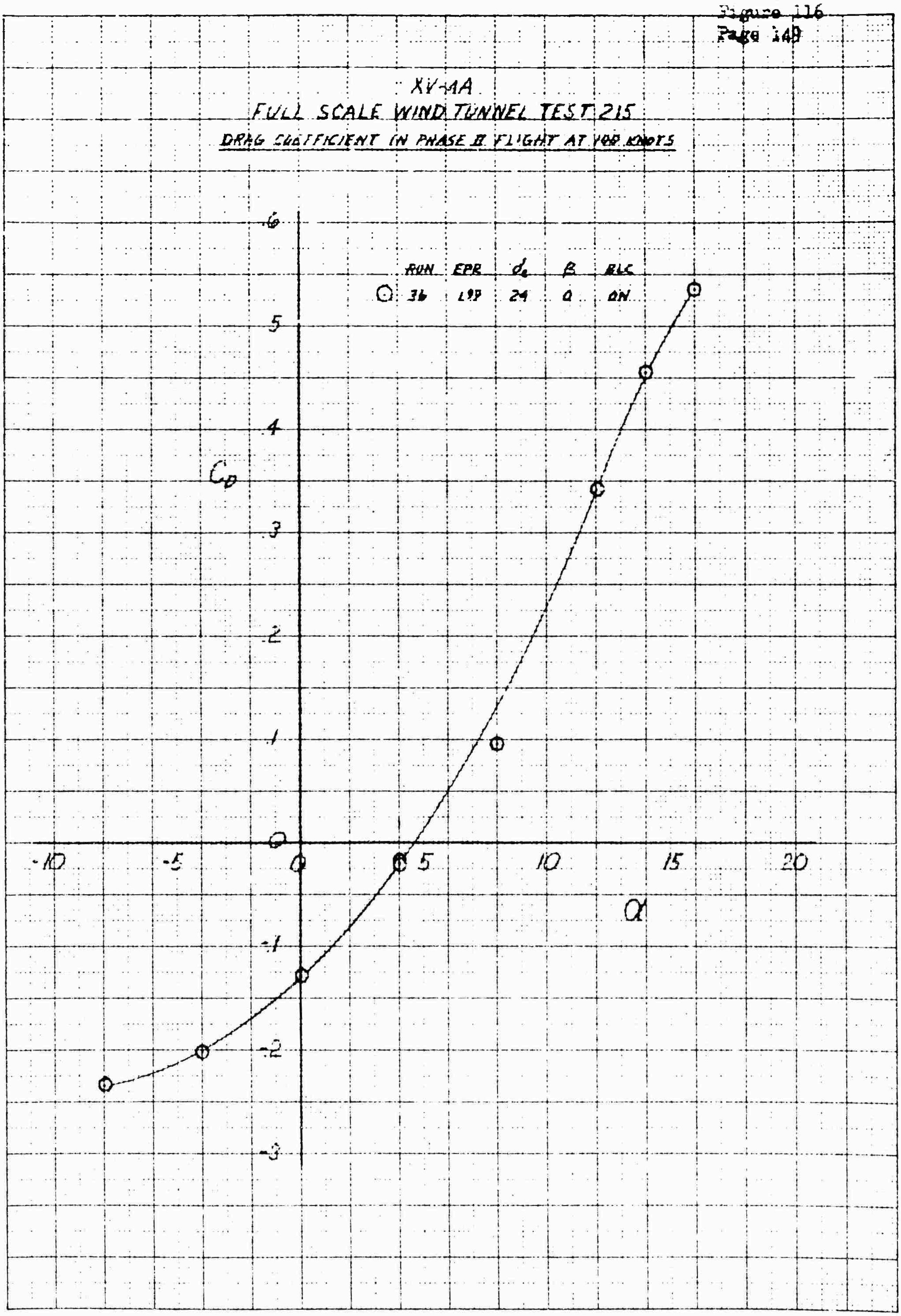
XV-4A
FULL SCALE WIND TUNNEL TEST 215
DRAG COEFFICIENT IN PHASE II FLIGHT AT 100 KNOTS
RUN EPR δ_a β BLC
36 1.97 24 0 ON
C_D
.6
.5
.4
.3
.2
.1
0
-.1
-.2
-.3
-10
-5
0
5
10
15
20
α

XV-4A
FULL SCALE WIND TUNNEL TEST 215
PITCHING MOMENT COEFFICIENT IN PHASE II FLIGHT AT 100 KNOTS

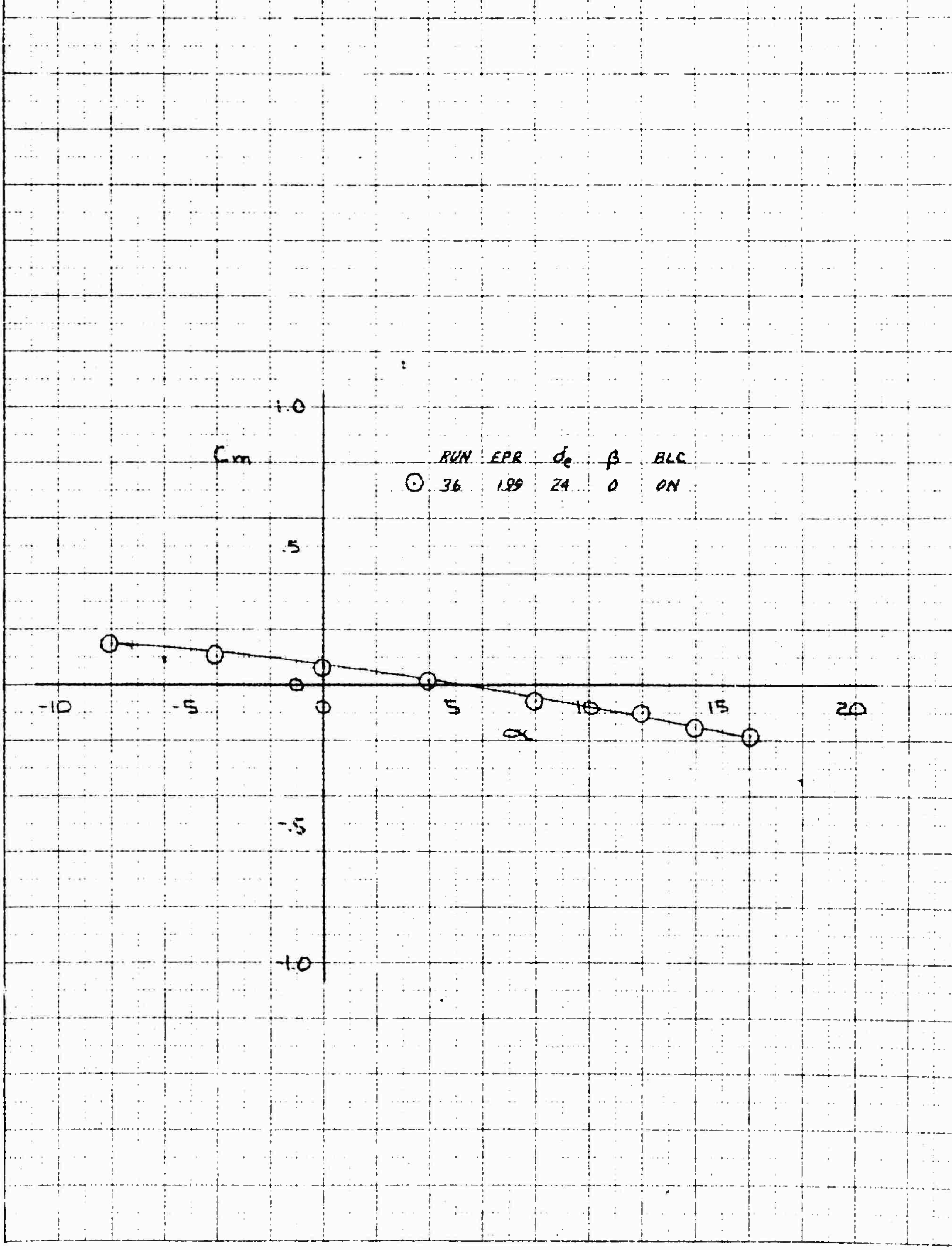

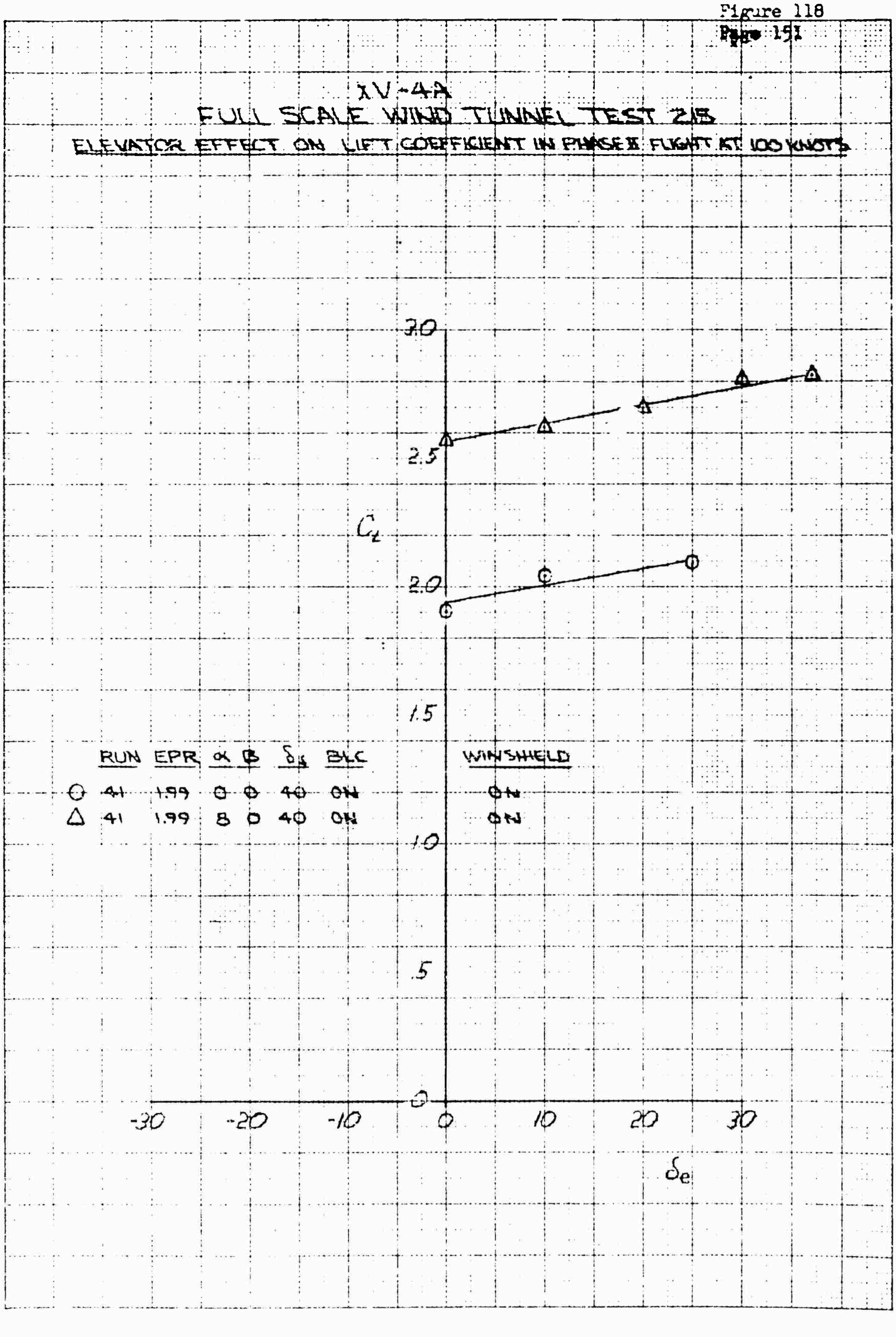
XV-4A
FULL SCALE WIND TUNNEL TEST 215
ELEVATOR EFFECT ON LIFT COEFFICIENT IN PHASE II FLIGHT AT 100 KNOTS
3.0
2.5
C_L
2.0
1.5
1.0
.5
0
-30
-20
-10
0
10
20
30
δ_e
RUN EPR α β $\delta_{\tilde{s}}$ BLC WINSHIELD
○ 41 1.99 0 0 40 ON ON
△ 41 1.99 8 0 40 ON ON

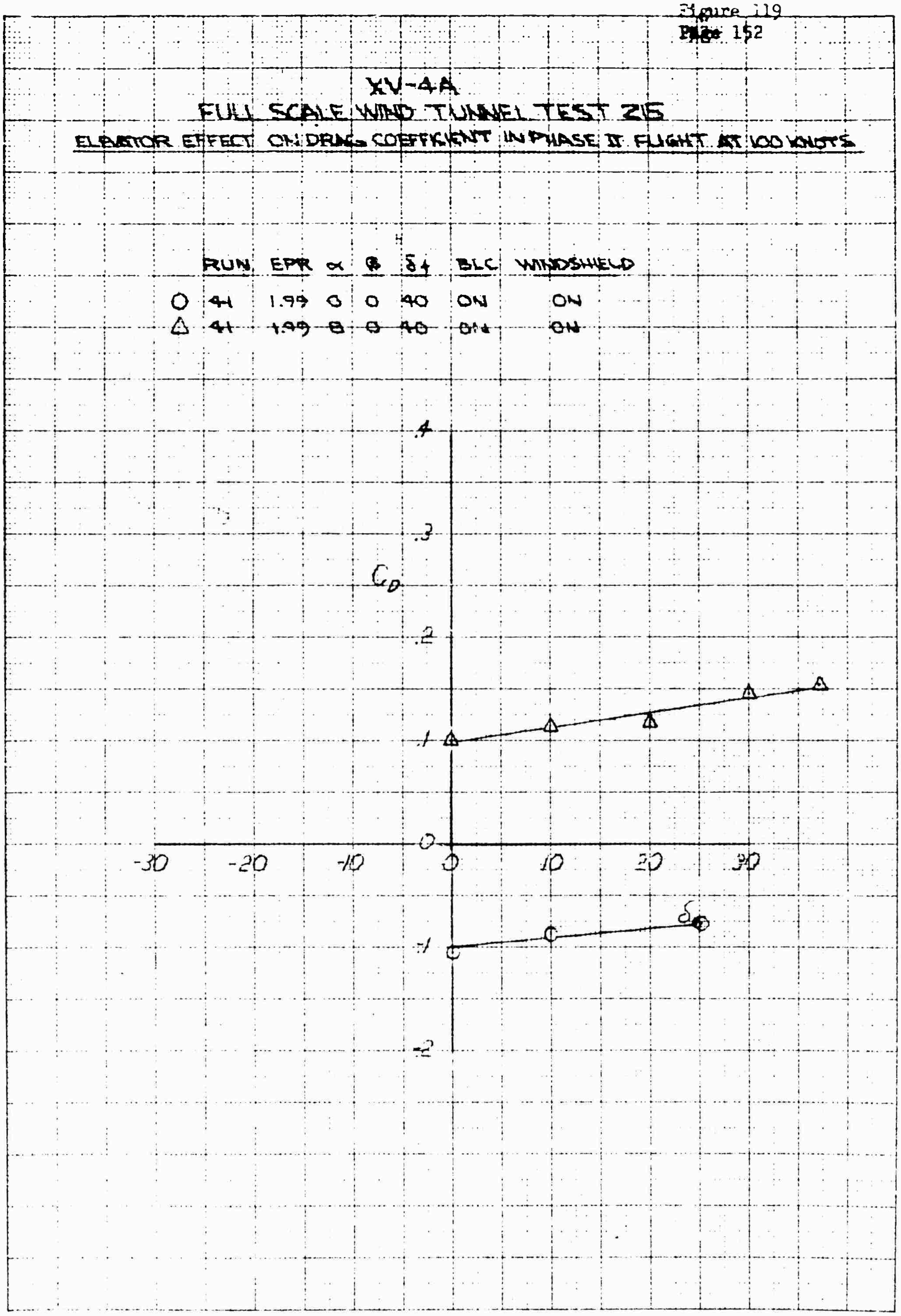
XV-4A
FULL SCALE WIND TUNNEL TEST 215
ELEVATOR EFFECT ON DRAG COEFFICIENT IN PHASE II FLIGHT AT 100 KNOTS
RUN EPR α β δf BLC WINDSHIELD
41 1.99 0 0 40 ON ON
41 1.99 8 0 40 ON ON
.4
.3
CD
.2
.1
0
-.1
-.2
-30
-20
-10
0
10
20
30
δe

XV-4A
FULL SCALE WIND TUNNEL TEST 215
ELEVATOR EFFECT ON PITCHING MOMENT COEFFICIENT IN PHASE II FLIGHT AT 100 KNOTS

	RUN	EPR	α	β	δ_f	BLC	WINDSHIELD
○	41	1.99	0	0	40	ON	ON
△	41	1.99	8	0	40	ON	ON

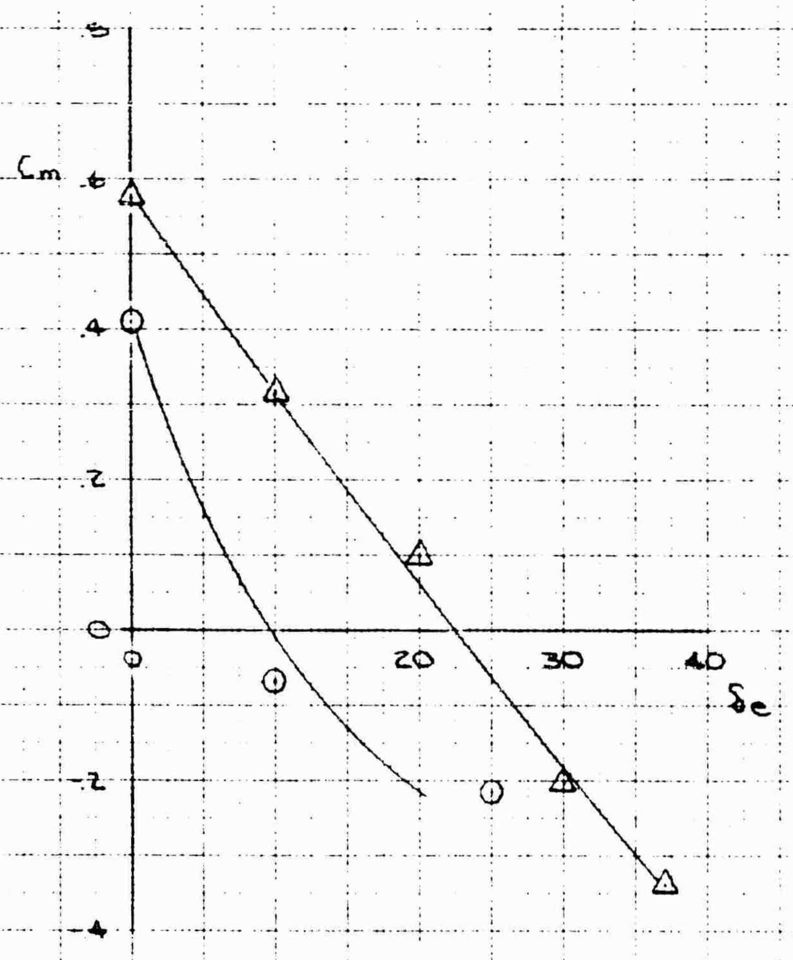

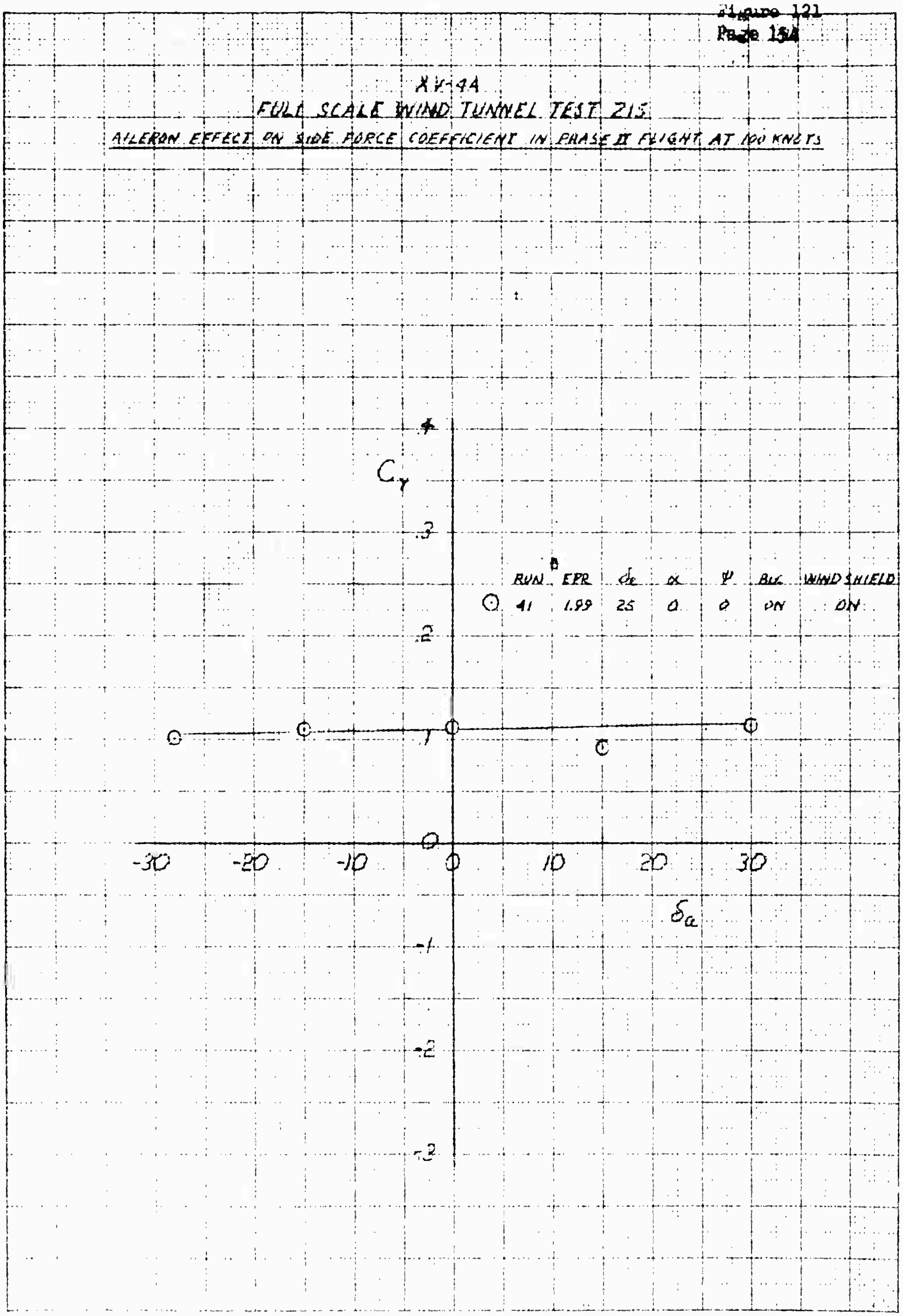
XV-4A
FULL SCALE WIND TUNNEL TEST 215
AILERON EFFECT ON SIDE FORCE COEFFICIENT IN PHASE II FLIGHT AT 100 KNOTS
C_Y
.4
.3
.2
.1
0
-.1
-.2
-.3
-30
-20
-10
0
10
20
30
δ_a
RUN EPR δ_E α ψ B.L.C. WINDSHIELD
41 1.99 25 0 0 ON ON

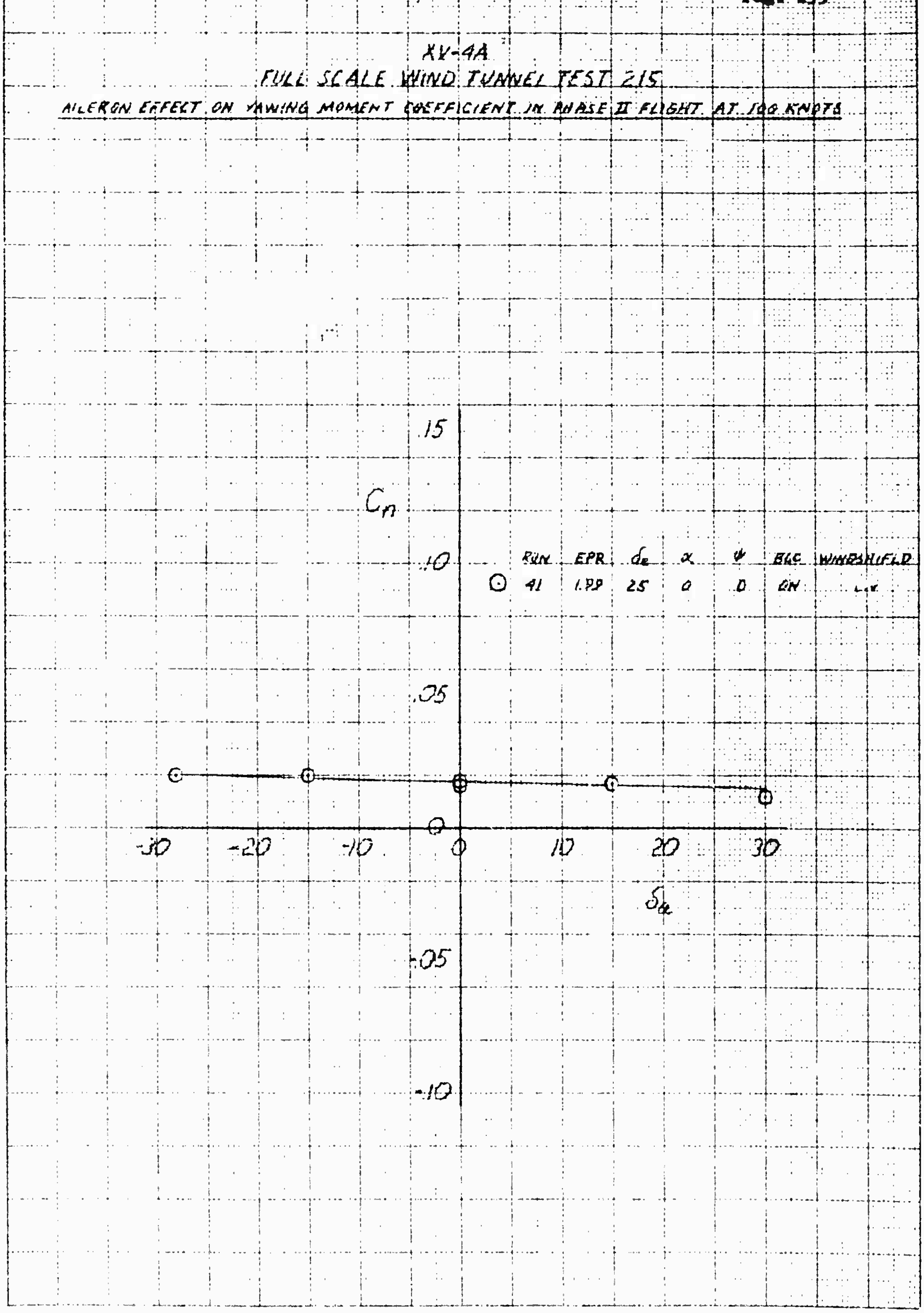
XV-4A
FULL SCALE WIND TUNNEL TEST 215
AILERON EFFECT ON YAWING MOMENT COEFFICIENT IN PHASE II FLIGHT AT 100 KNOTS
Cn
.15
.10
.05
-.05
-.10
RUN EPR δe α ψ BLC WINDSHIELD
41 1.99 25 0 0 ON
-30 -20 -10 0 10 20 30
δa

XV-4A

FULL SCALE WIND TUNNEL TEST 215

AILERON EFFECT ON ROLLING MOMENT COEFFICIENT IN PHASE II FLIGHT AT 100 KNOTS

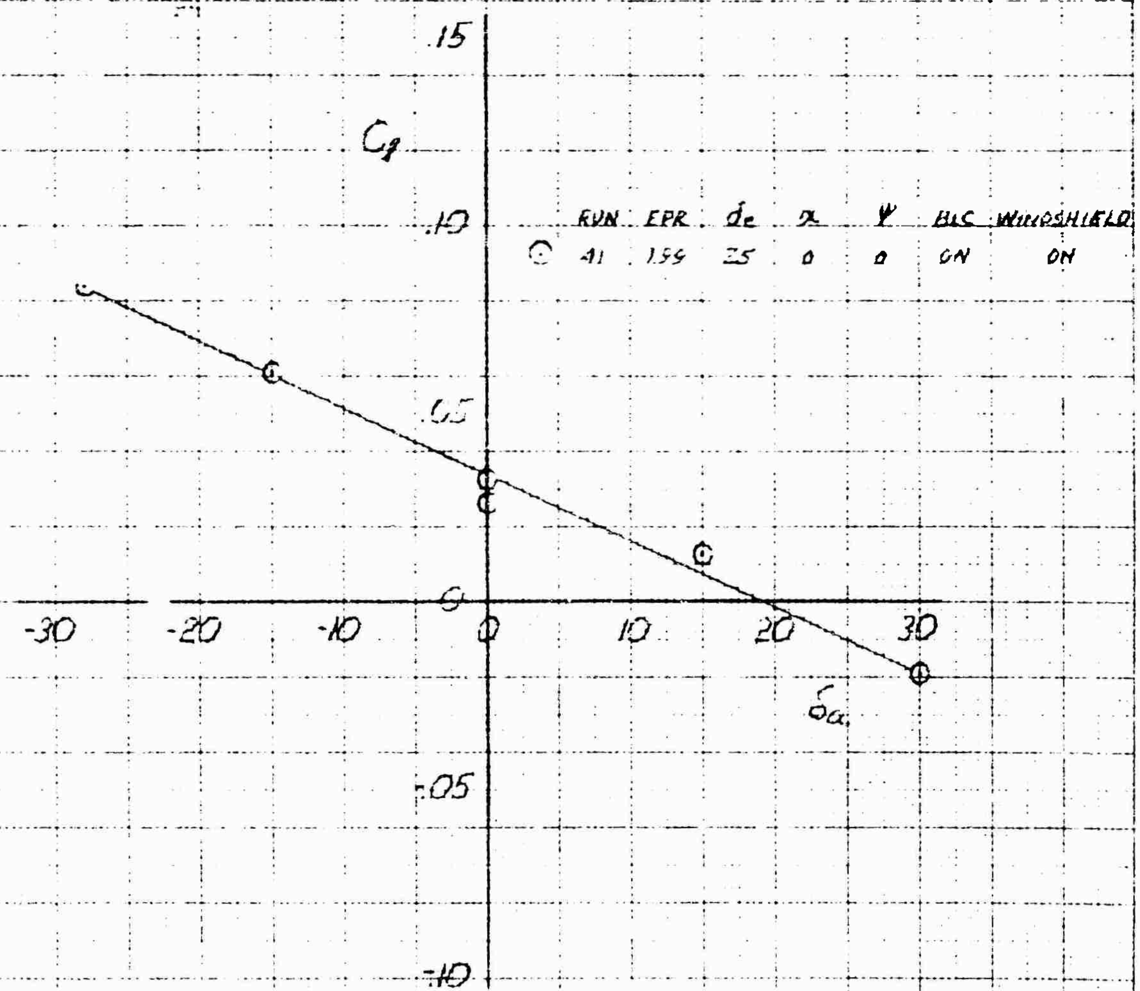

XV-4A

FULL SCALE WIND TUNNEL TEST 215

RUDDER EFFECT ON SIDE FORCE COEFFICIENT IN PHASE II FLIGHT AT 40 KNOTS

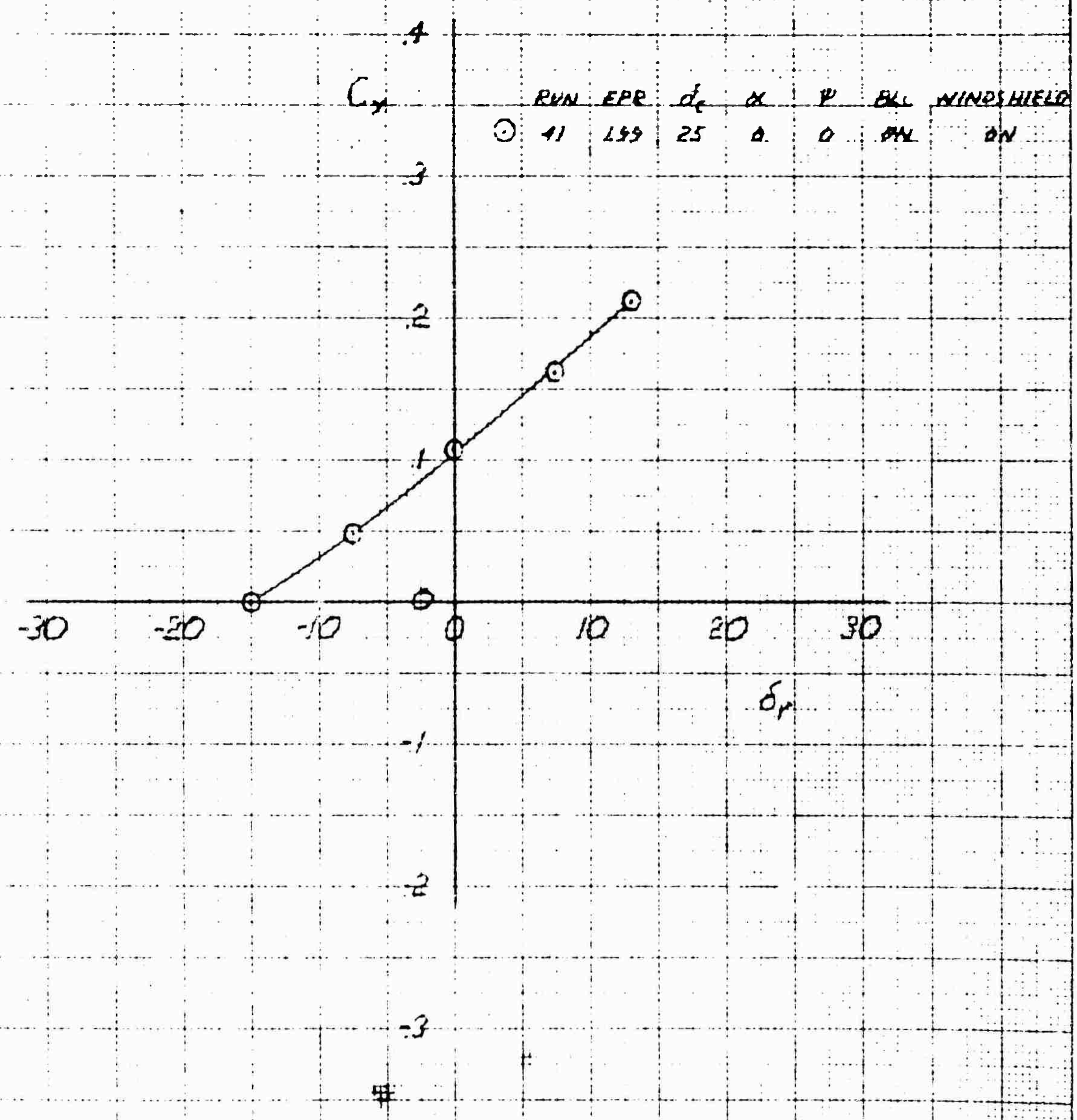

XV-4A
FULL SCALE WIND TUNNEL TEST 215
RUDDER EFFECT ON YAWING MOMENT COEFFICIENT IN PHASE II FLIGHT AT 100 KNOTS

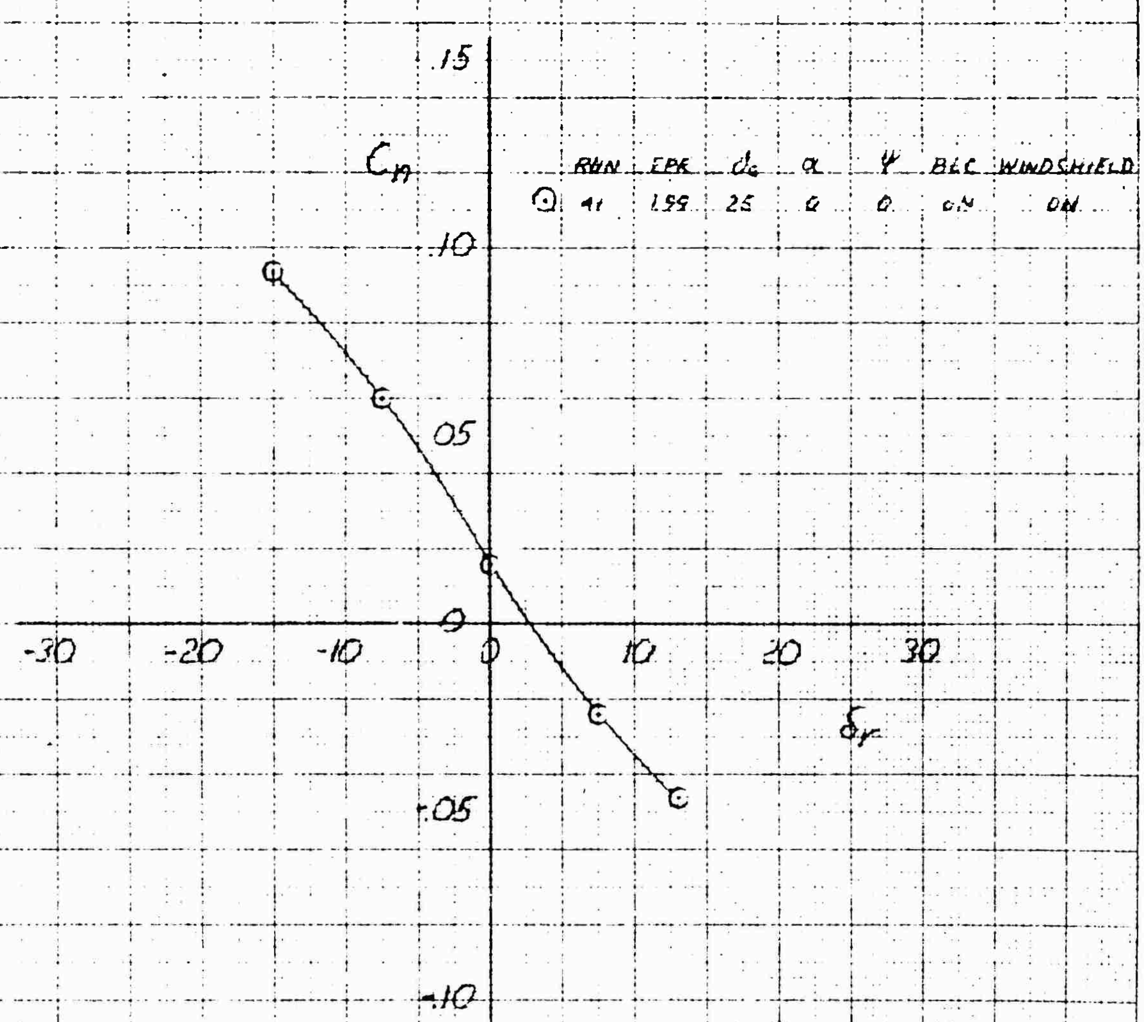

XV-4A

FULL SCALE WIND TUNNEL TEST 215

RUDDER EFFECT ON ROLLING MOMENT COEFFICIENT IN PHASE II FLIGHT AT 100 KNOTS

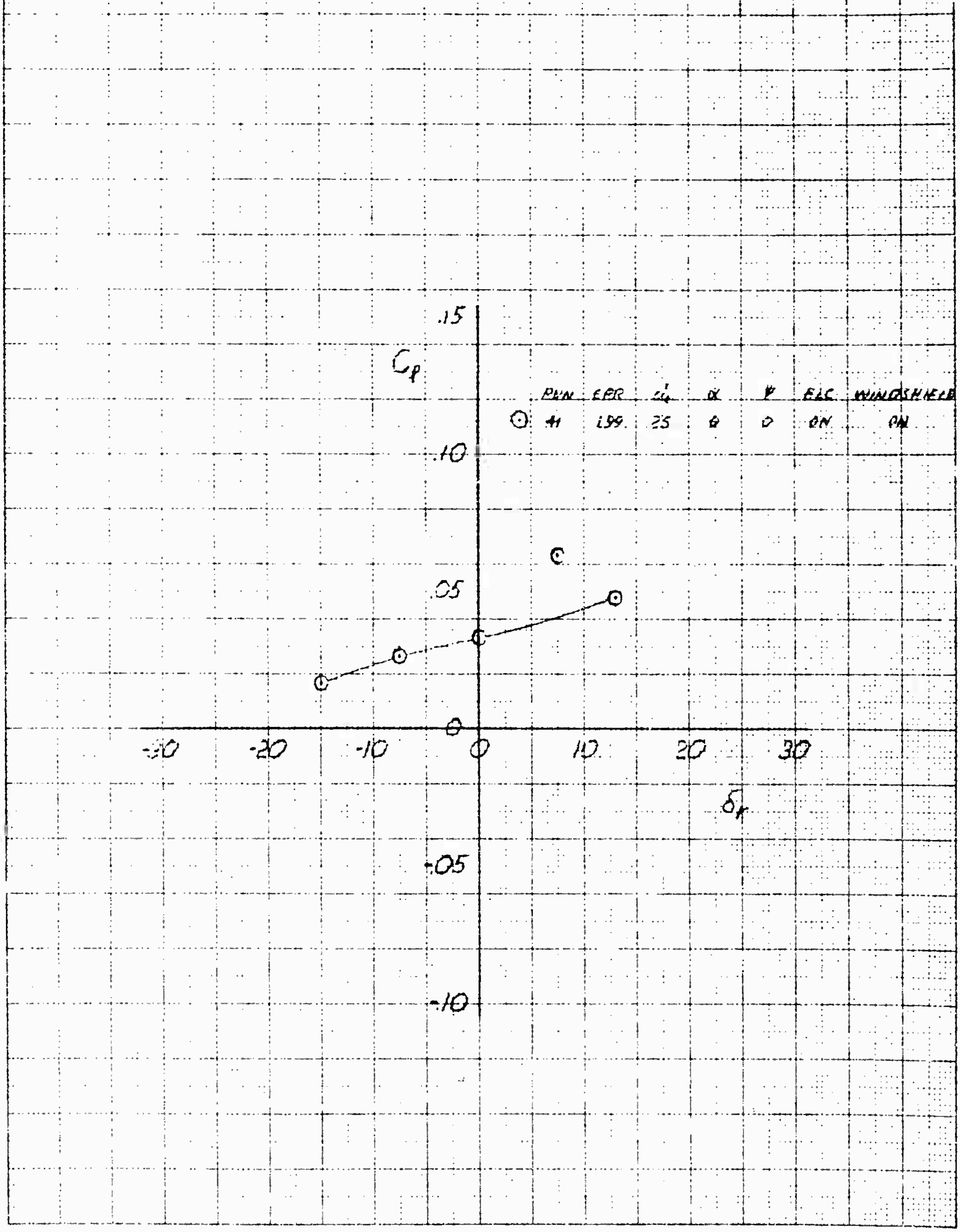

XV-4A
FULL SCALE WIND TUNNEL TEST 215
LIFT COEFFICIENT IN PHASE III FLIGHT AT 80 KNOTS

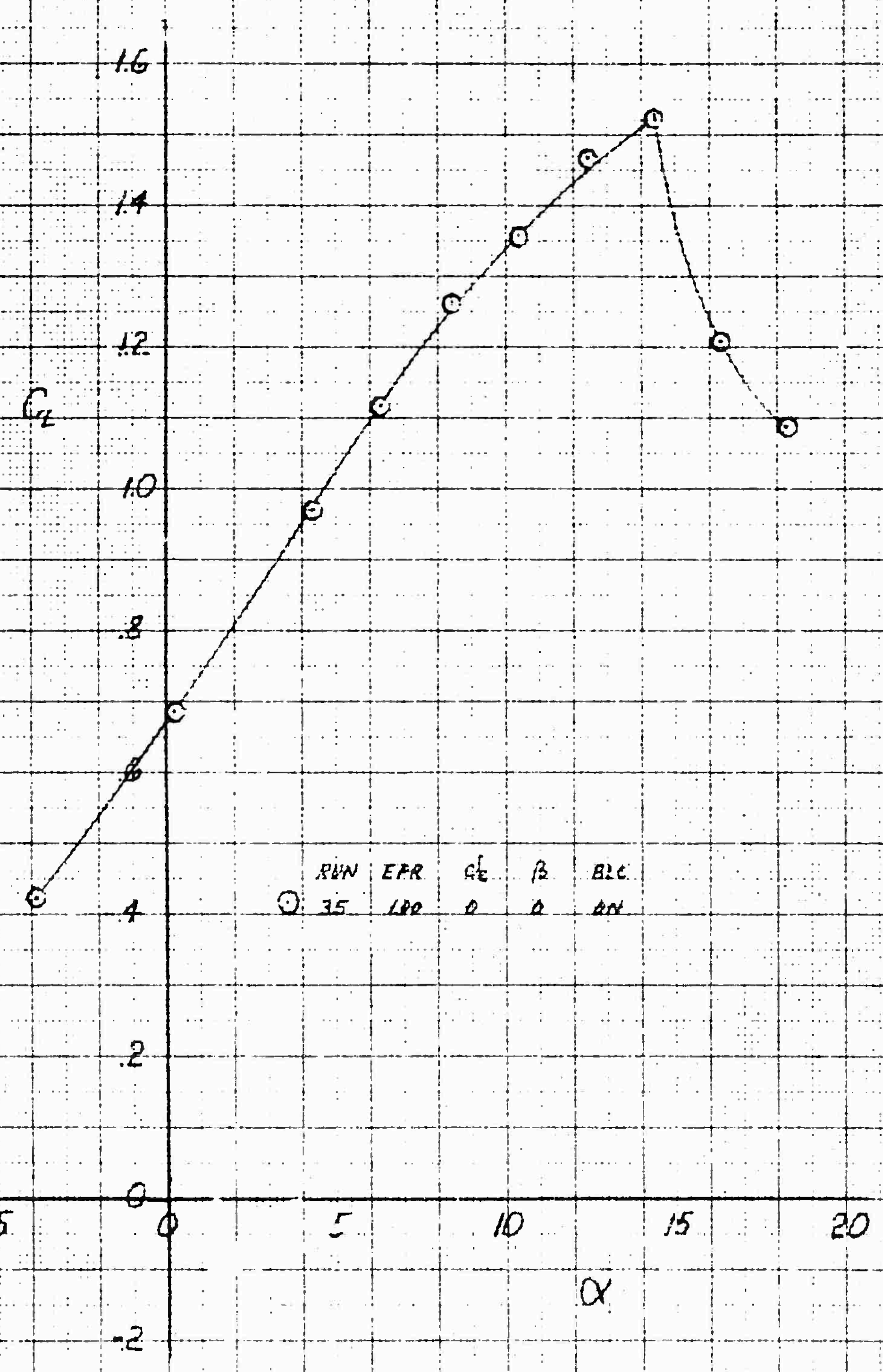

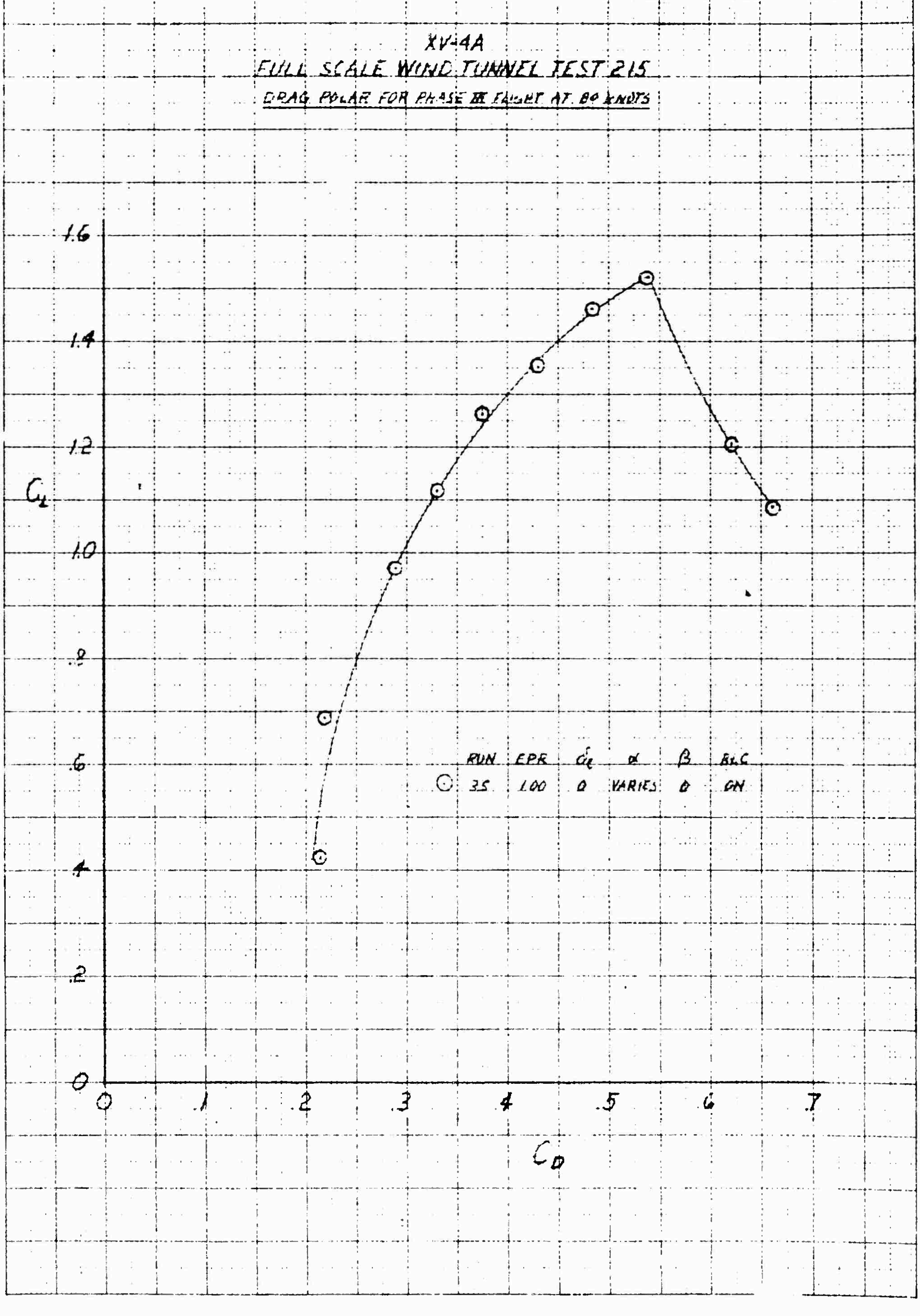
XV-4A
FULL SCALE WIND TUNNEL TEST 215
DRAG POLAR FOR PHASE III FLIGHT AT 80 KNOTS
1.6
1.4
1.2
C_L
1.0
.8
.6
.4
.2
0
0
.1
.2
.3
.4
.5
.6
.7
C_D
RUN EPR δ_e α β BLC
35 1.00 0 VARIES 0 ON

XV-4A
FULL SCALE WIND TUNNEL TEST 215
PITCHING MOMENT CHARACTERISTICS IN PHASE III FLIGHT AT 80 KNOTS

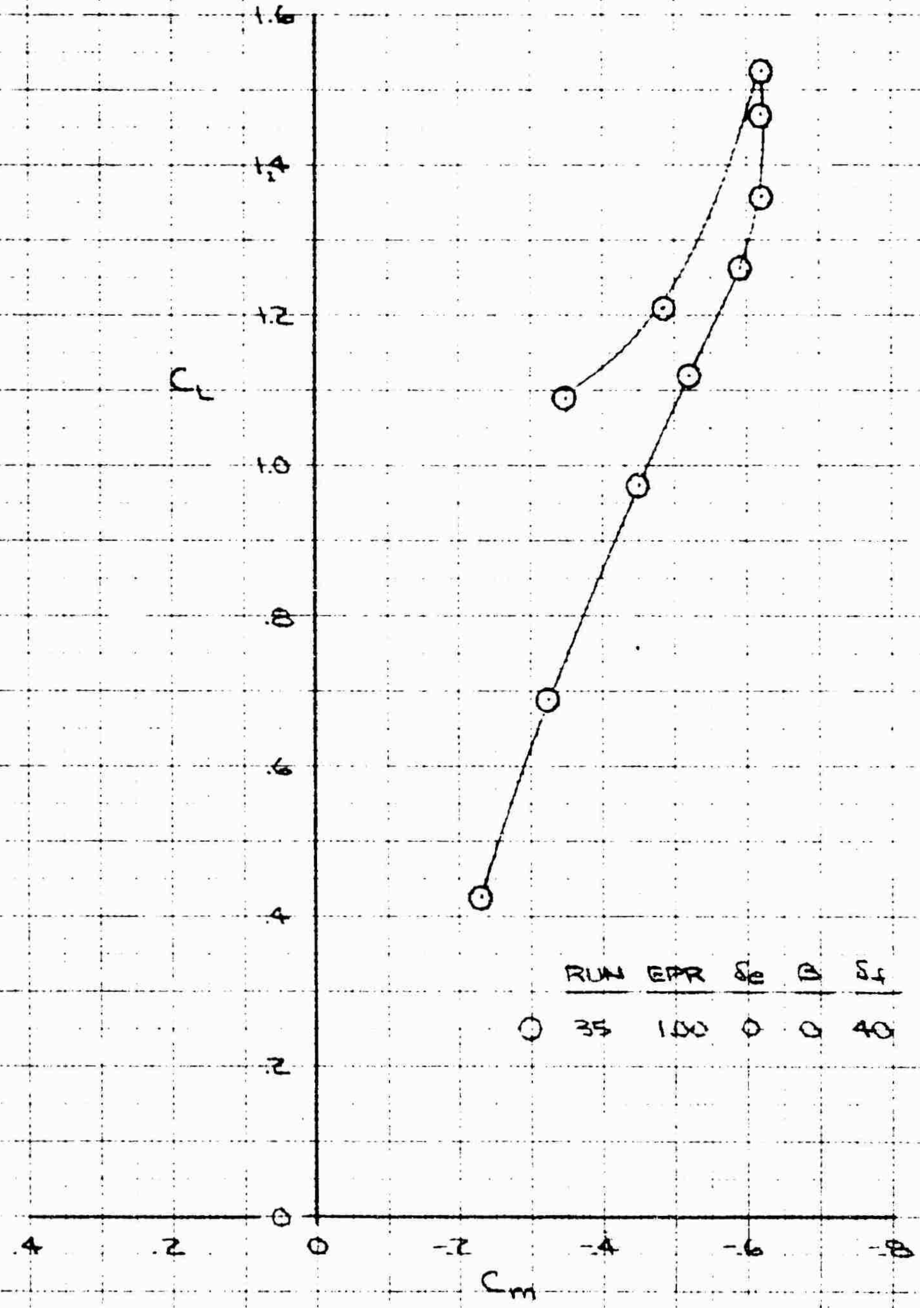

XV-4A

FULL SCALE WIND TUNNEL TEST 215

SIDE FORCE COEFFICIENT IN PHASE III FLIGHT AT 80 KNOTS

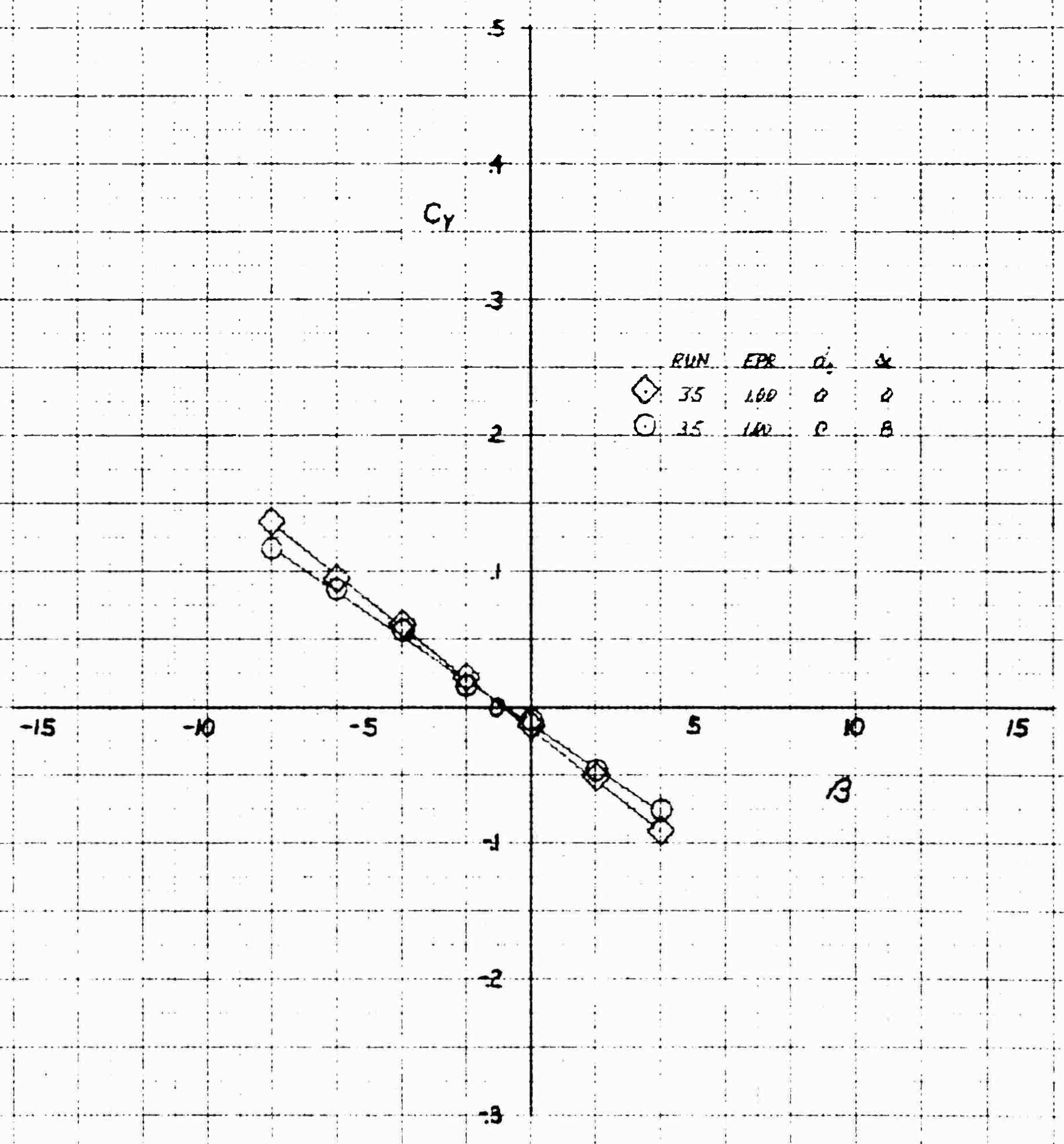

XV-4A

FULL SCALE WIND TUNNEL TEST 215

YAWING MOMENT COEFFICIENT IN PHASE III FLIGHT AT 80 KNOTS

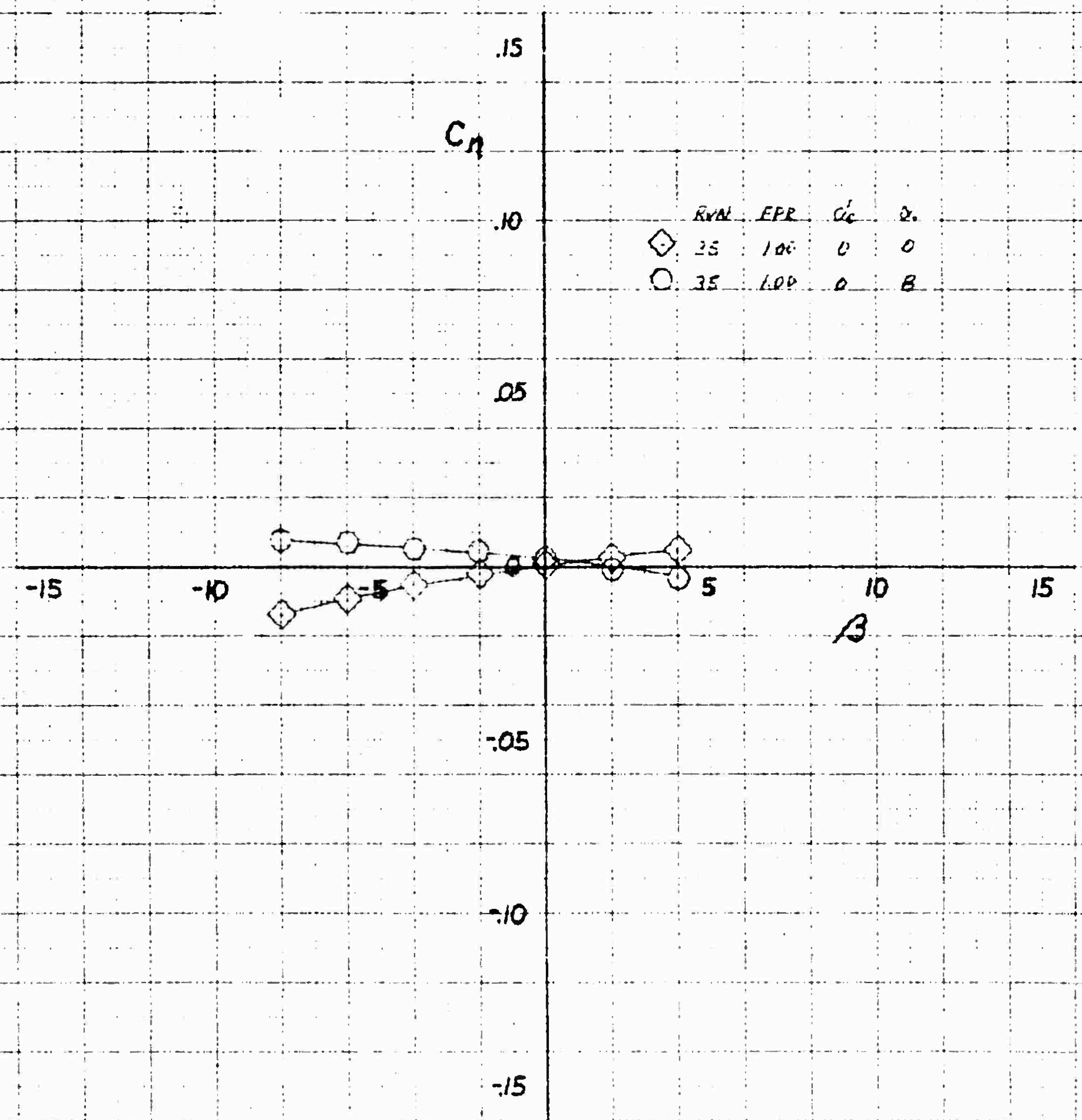

XV-4A

FULL SCALE WIND TUNNEL TEST 215

ROLLING MOMENT COEFFICIENT IN PHASE III FLIGHT AT 80 KNOTS

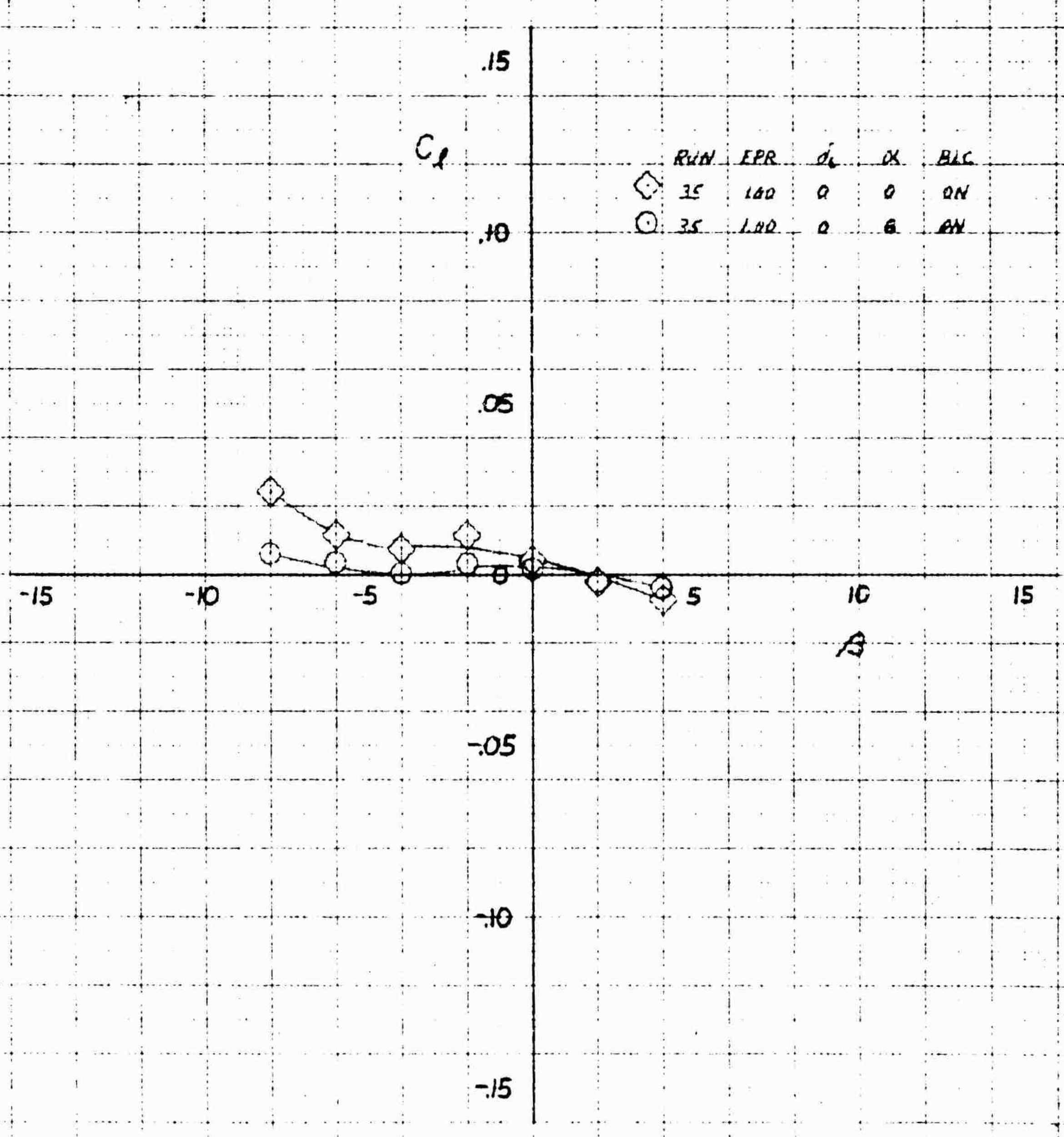

XV-4A
FULL SCALE WIND TUNNEL TEST 215
LIFT COEFFICIENT IN CONVENTIONAL FLIGHT AT 40 KNOTS

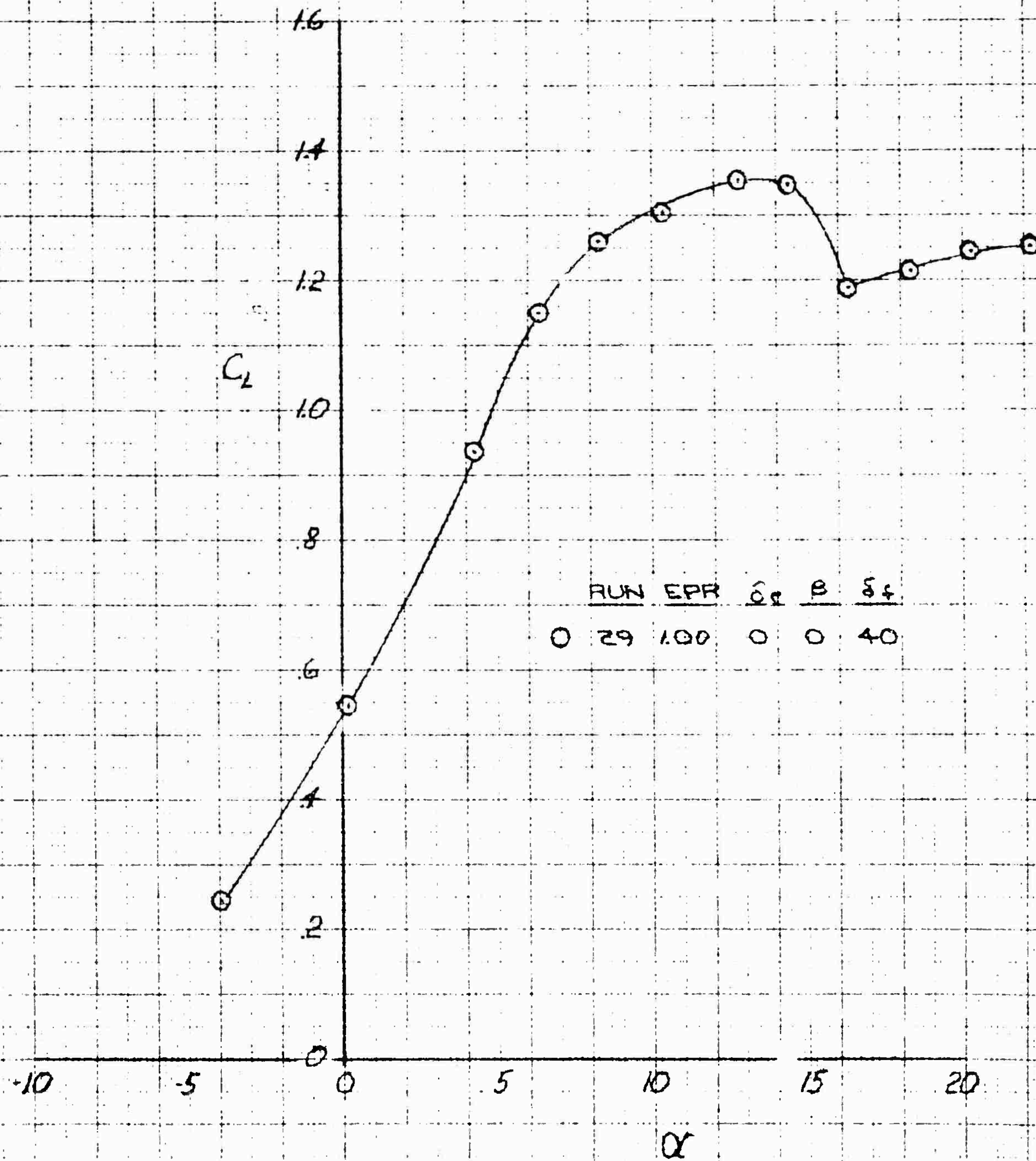

XV-4A
FULL SCALE WIND TUNNEL TEST 215
DRAG POLAR IN CONVENTIONAL FLIGHT AT 40 KNOTS

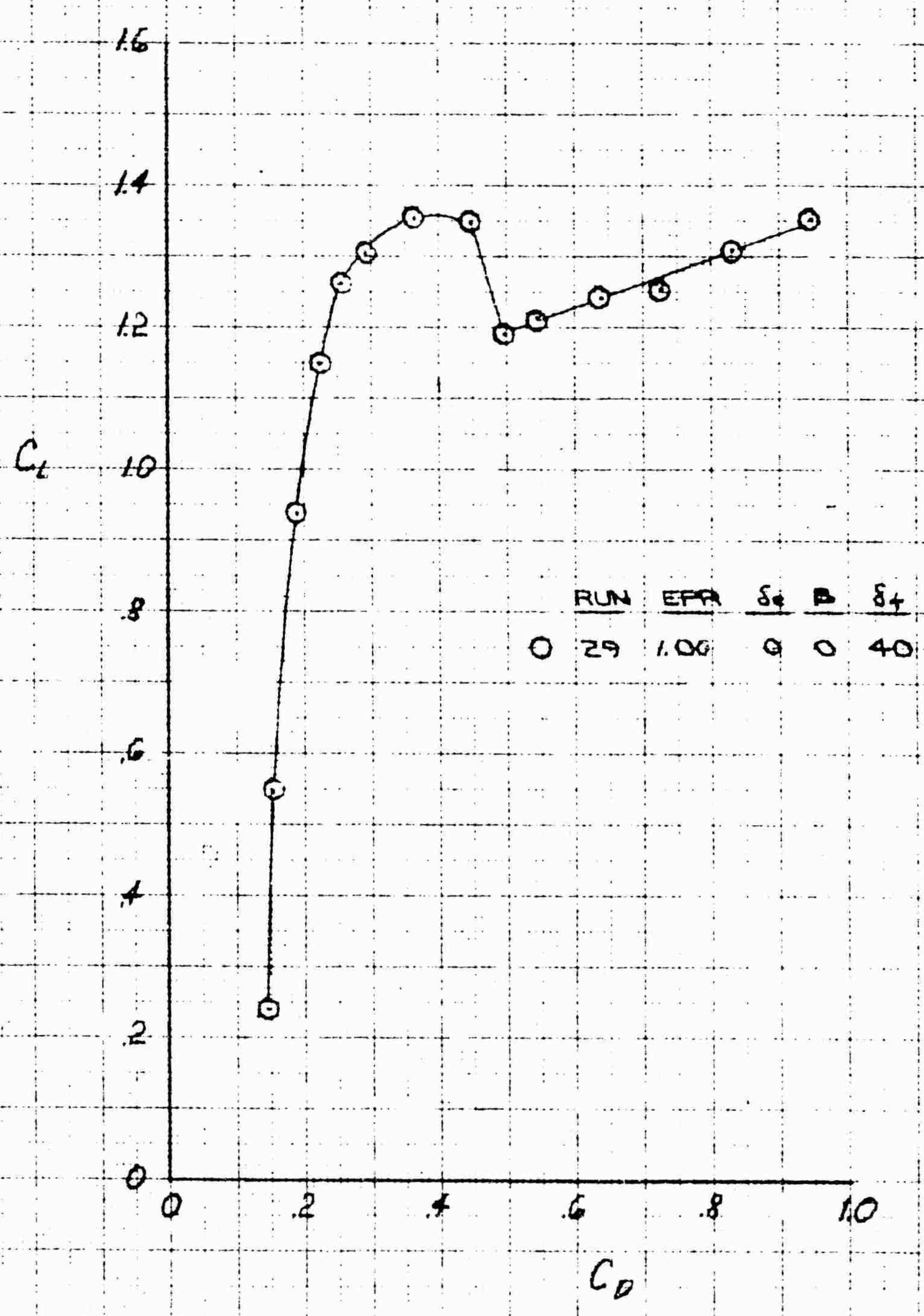

XV-4A
FULL SCALE WIND TUNNEL TEST 215
PITCHING MOMENT CHARACTERISTICS IN CONVENTIONAL FLIGHT AT 40 KNOTS

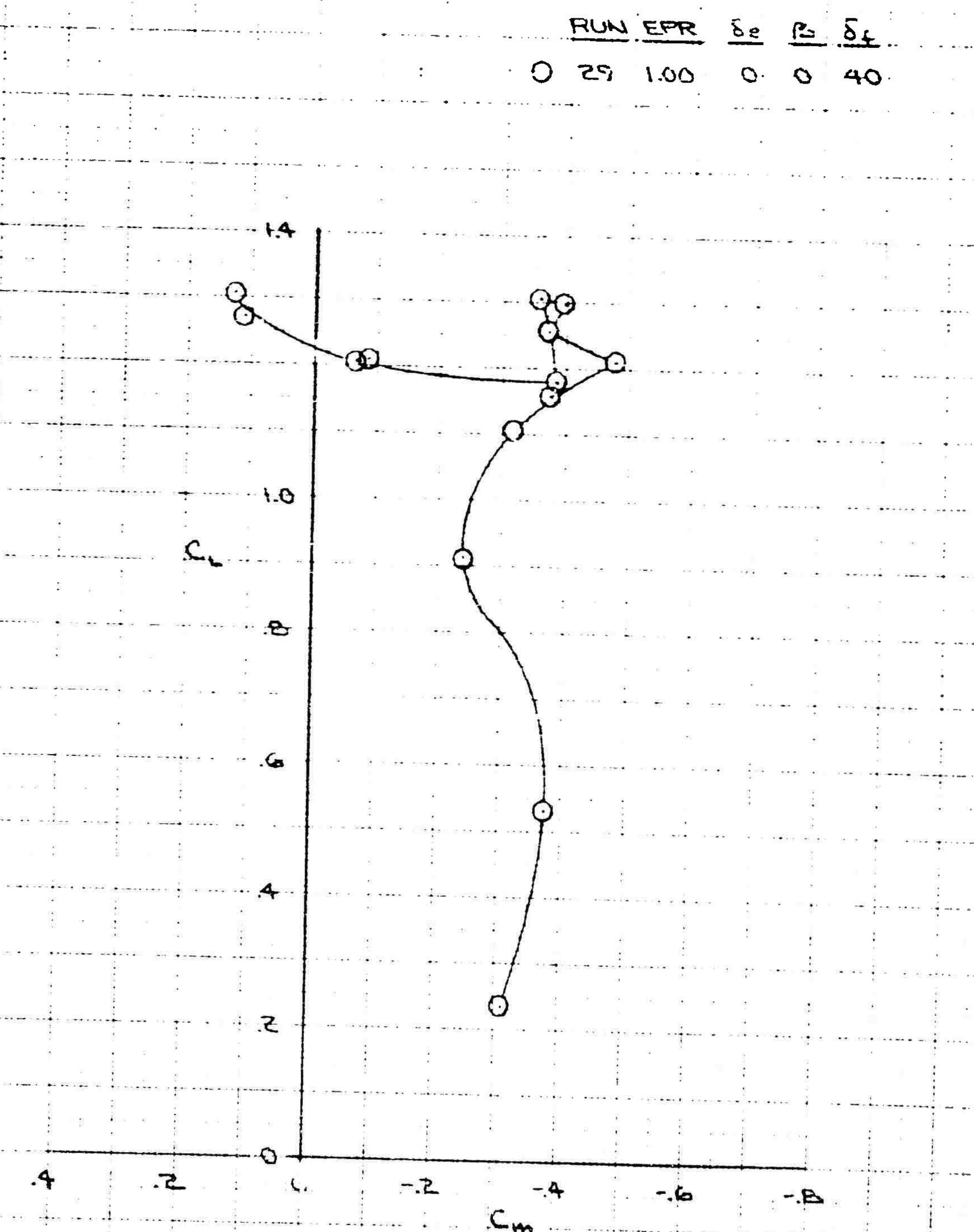

XV-4A
FULL SCALE WIND TUNNEL TEST 215
LIFT COEFFICIENT IN CONVENTIONAL FLIGHT AT 80 KNOTS

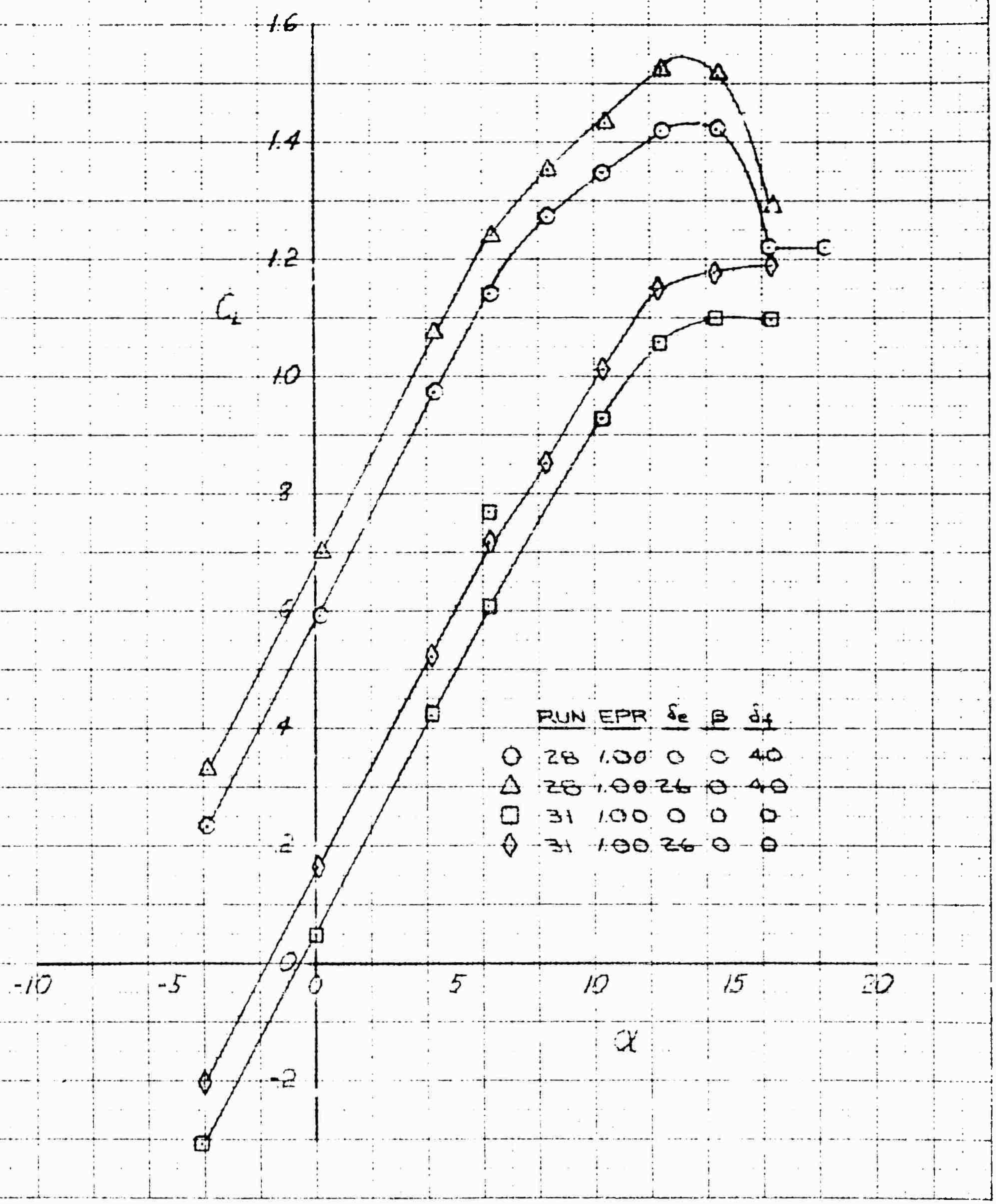

XV-4A

FULL SCALE WIND TUNNEL TEST 215

DRAG POLAR IN CONVENTIONAL FLIGHT AT 80 KNOTS

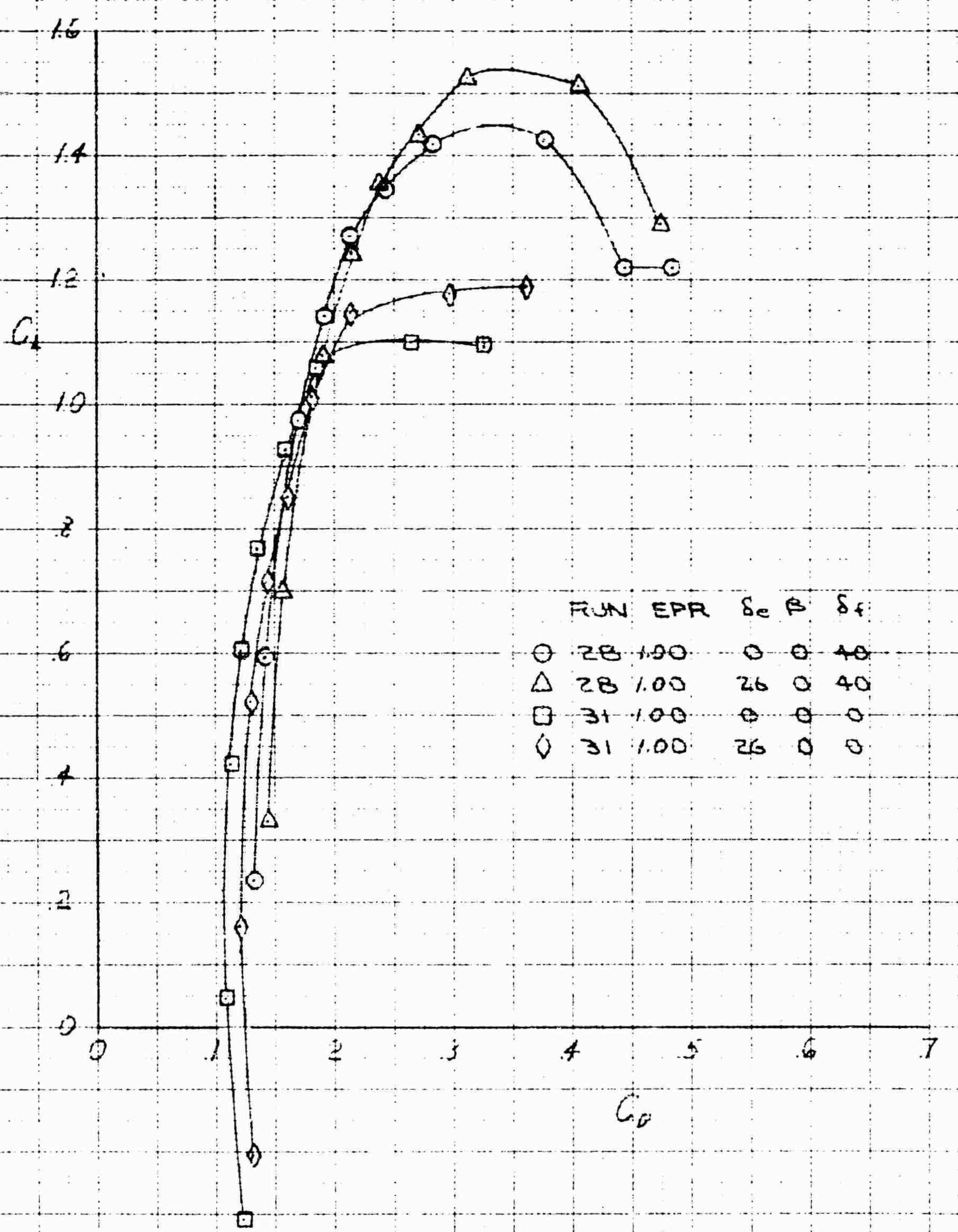

XV-4A
FULL SCALE WIND TUNNEL TEST 215
PITCHING MOMENT CHARACTERISTICS IN CONVENTIONAL FLIGHT AT 80 KNOTS

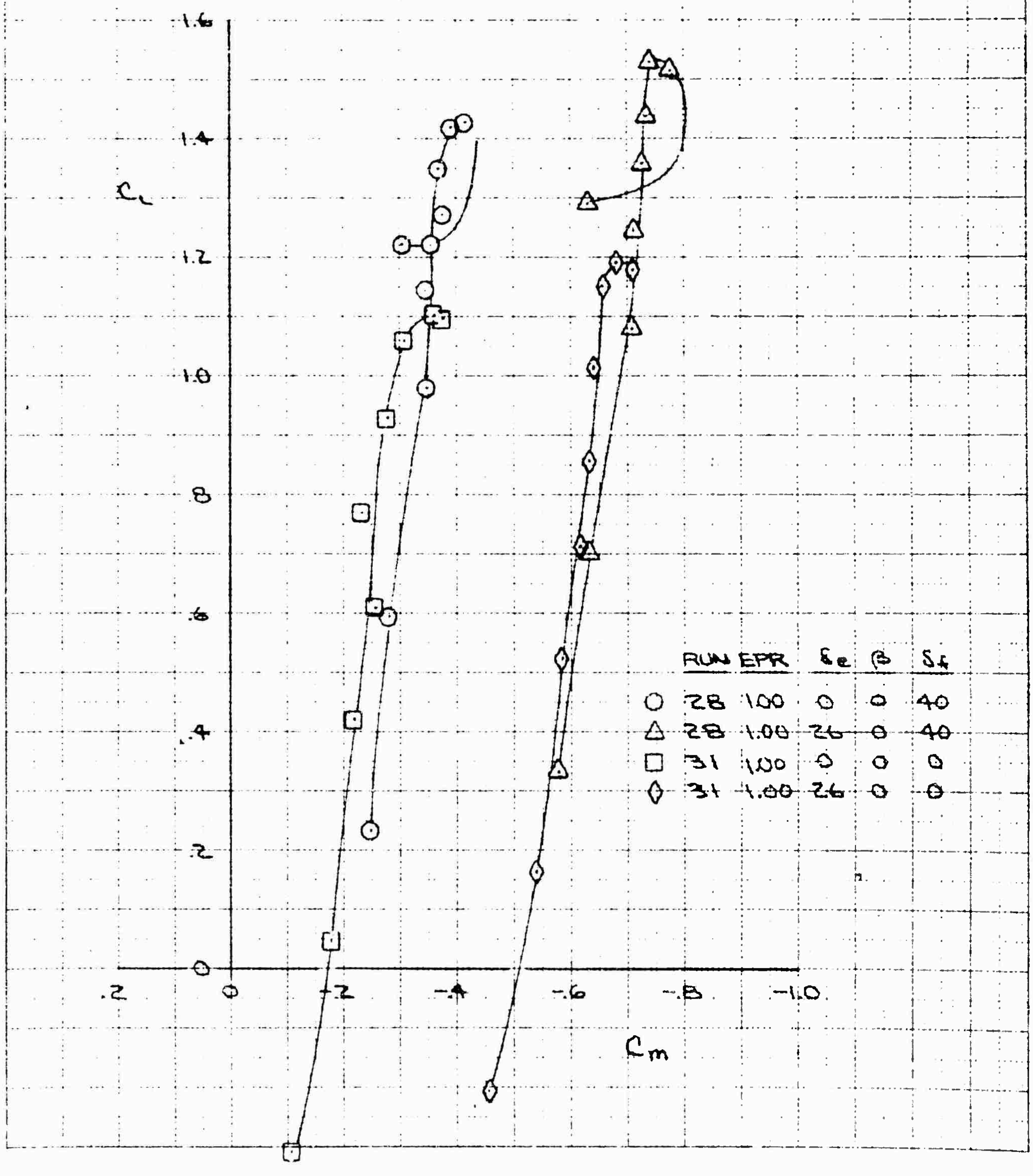

XV-4A
FULL SCALE WIND TUNNEL TEST 215
SIDE FORCE COEFFICIENT IN CONVENTIONAL FLIGHT AT 80 KNOTS

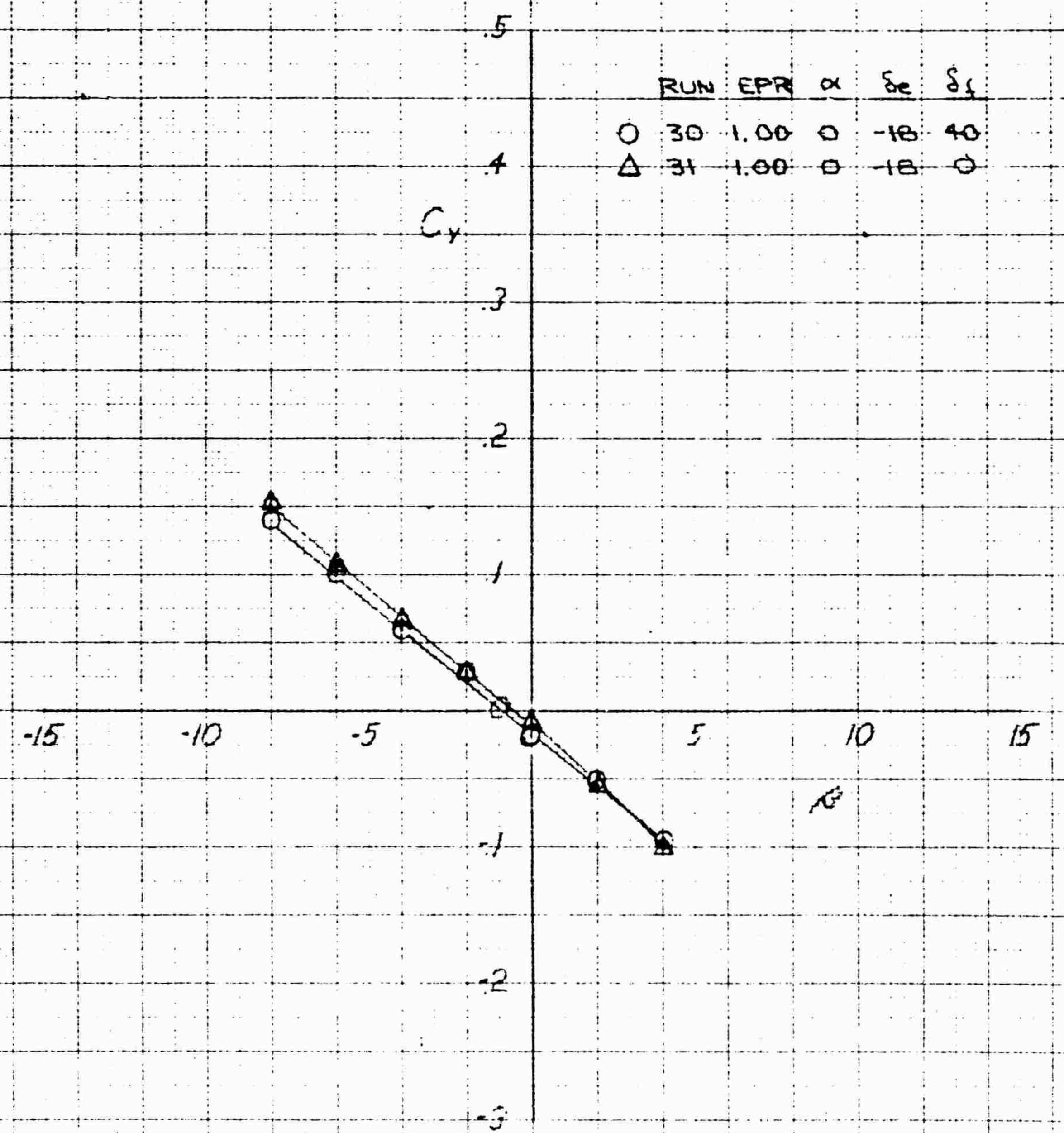

XV-4A
FULL SCALE WIND TUNNEL TEST 215
YAWING MOMENT COEFFICIENT IN CONVENTIONAL FLIGHT AT 80 KNOTS

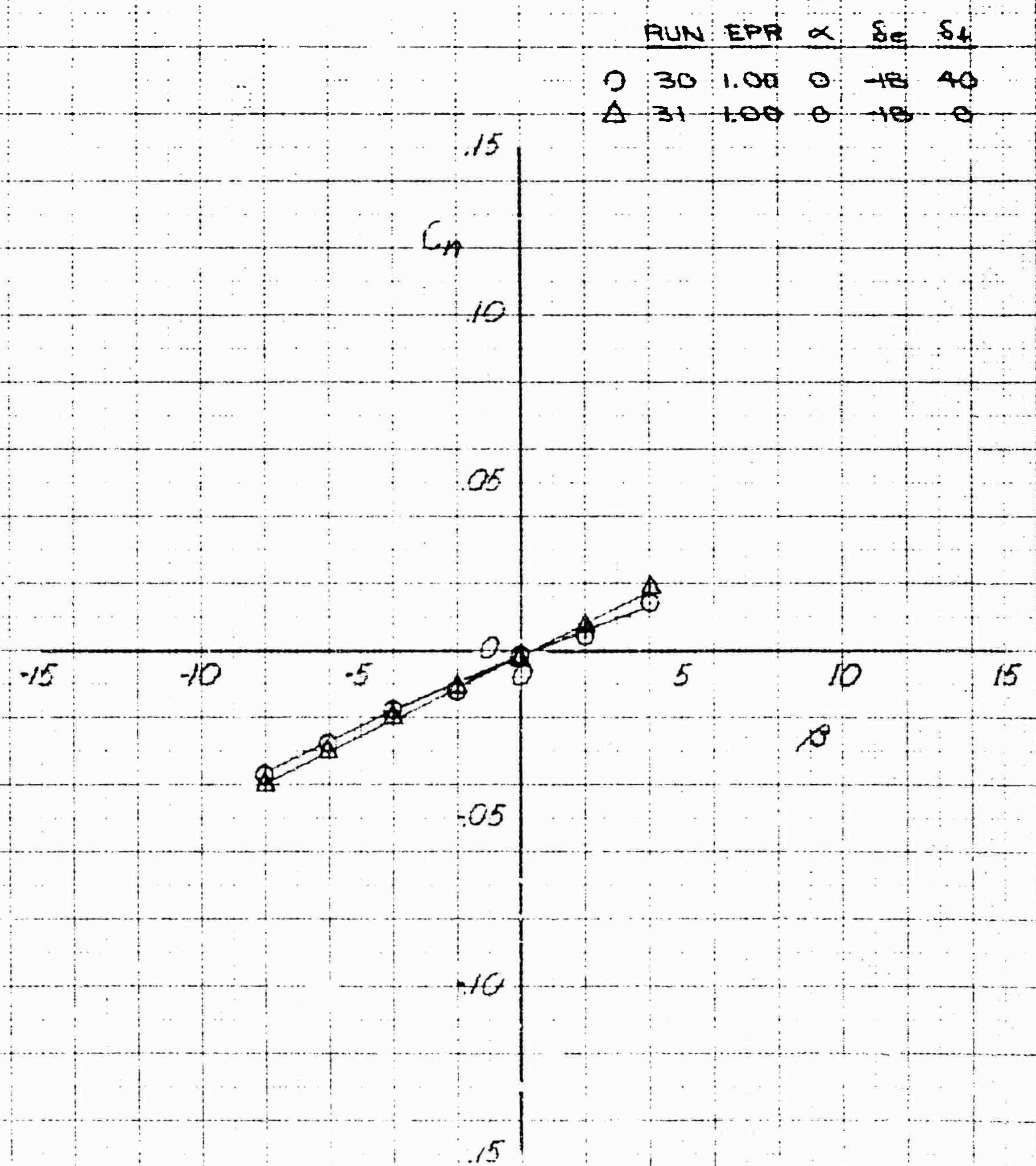

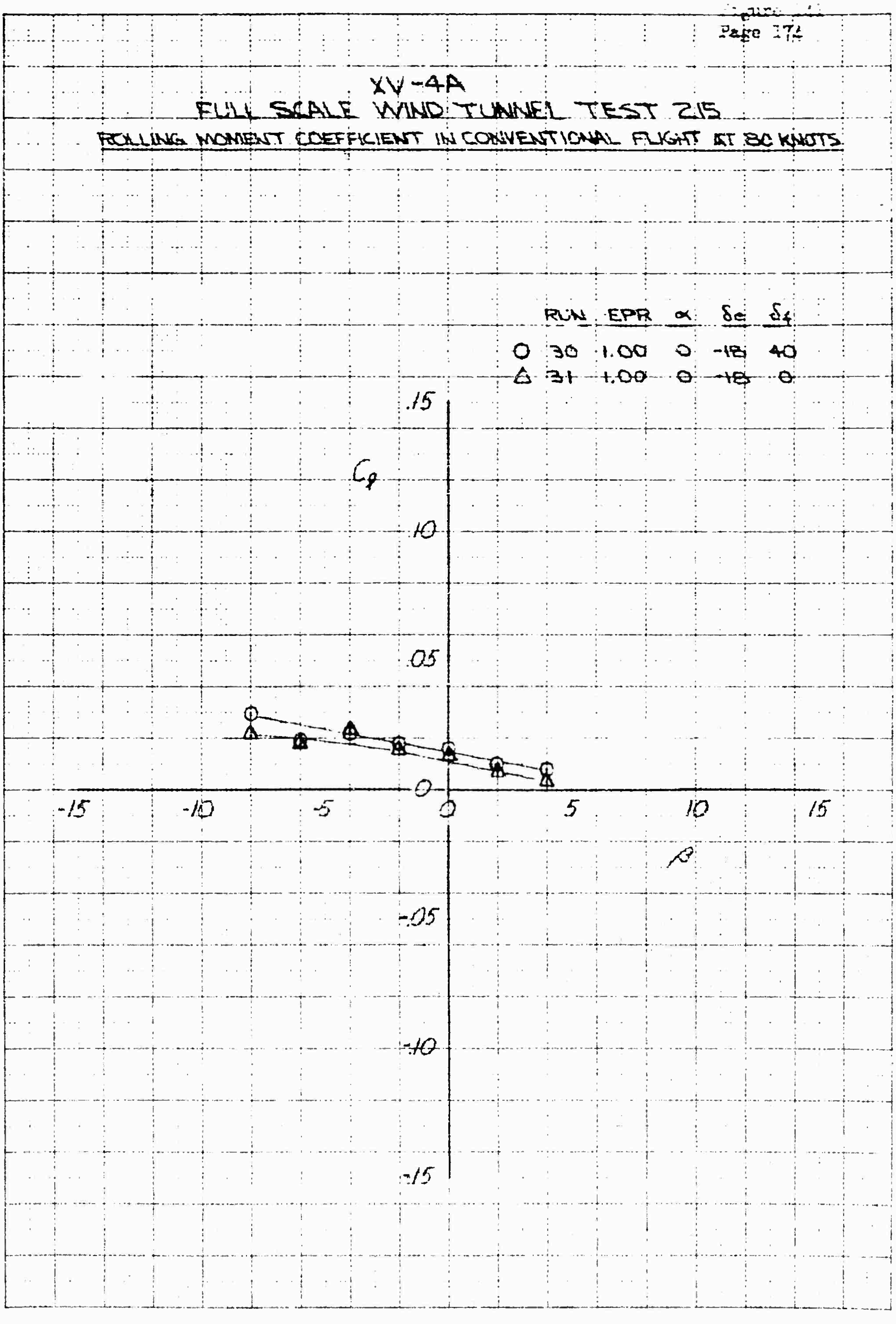
XV-4A
FULL SCALE WIND TUNNEL TEST 215
ROLLING MOMENT COEFFICIENT IN CONVENTIONAL FLIGHT AT 80 KNOTS
RUN EPR α δe δf
30 1.00 0 -18 40
31 1.00 0 -18 0
Cl
β
.15
.10
.05
0
-.05
-.10
-.15
-15
-10
-5
0
5
10
15

XV-4A
FULL SCALE WIND TUNNEL TEST 215
ELEVATOR EFFECT ON LIFT COEFFICIENT IN CONVENTIONAL FLIGHT AT 80KNOTS

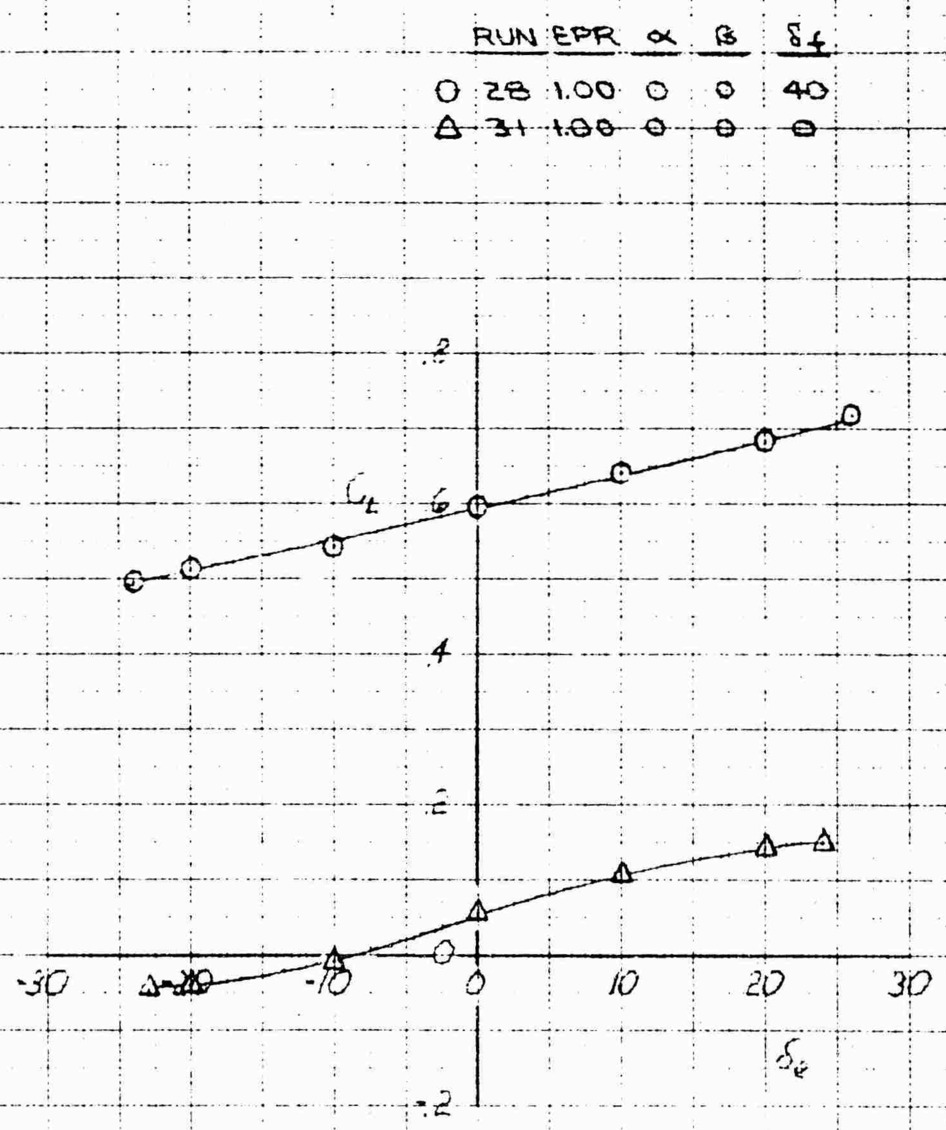

XV-4A
FULL SCALE WIND TUNNEL TEST 215
ELEVATOR EFFECT ON DRAG COEFFICIENT IN CONVENTIONAL FLIGHT AT 80 KNOTS

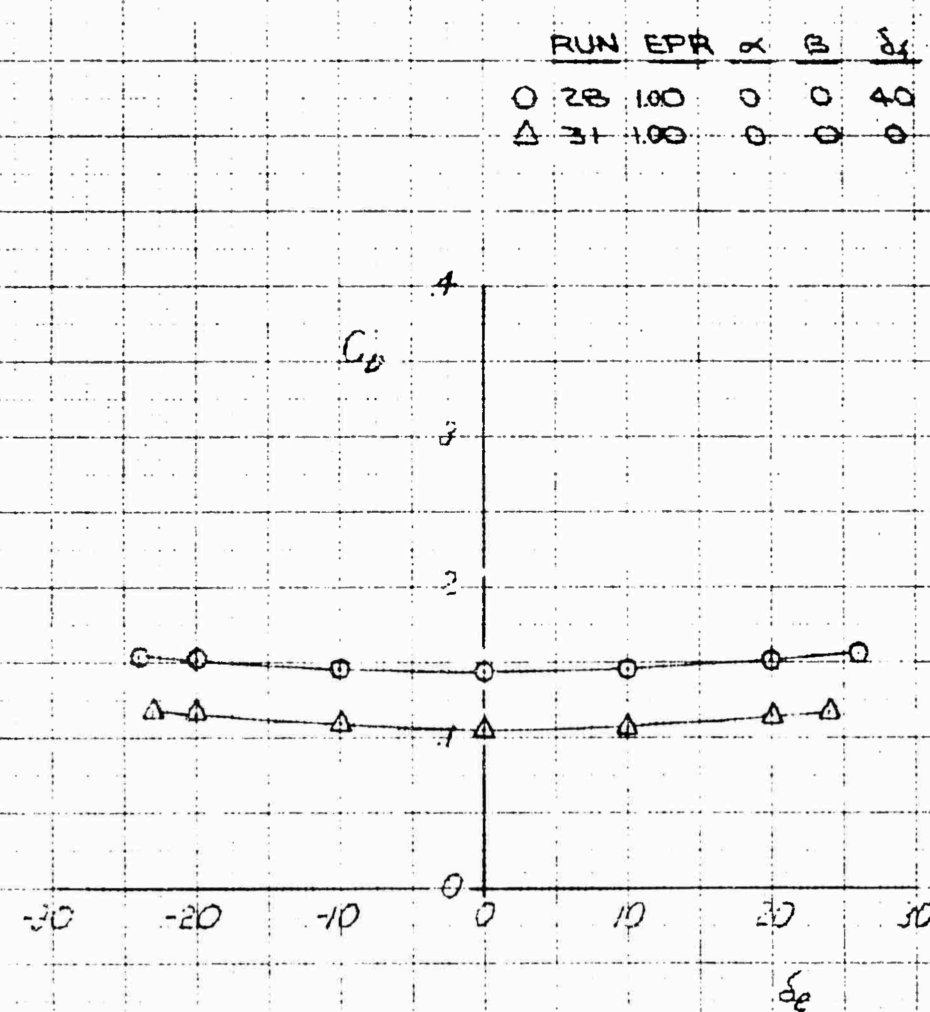

XV-4A
FULL SCALE WIND TUNNEL TEST 215
ELEVATOR EFFECT ON PITCHING MOMENT COEFFICIENT IN CONVENTIONAL FLIGHT AT 80 KNOTS

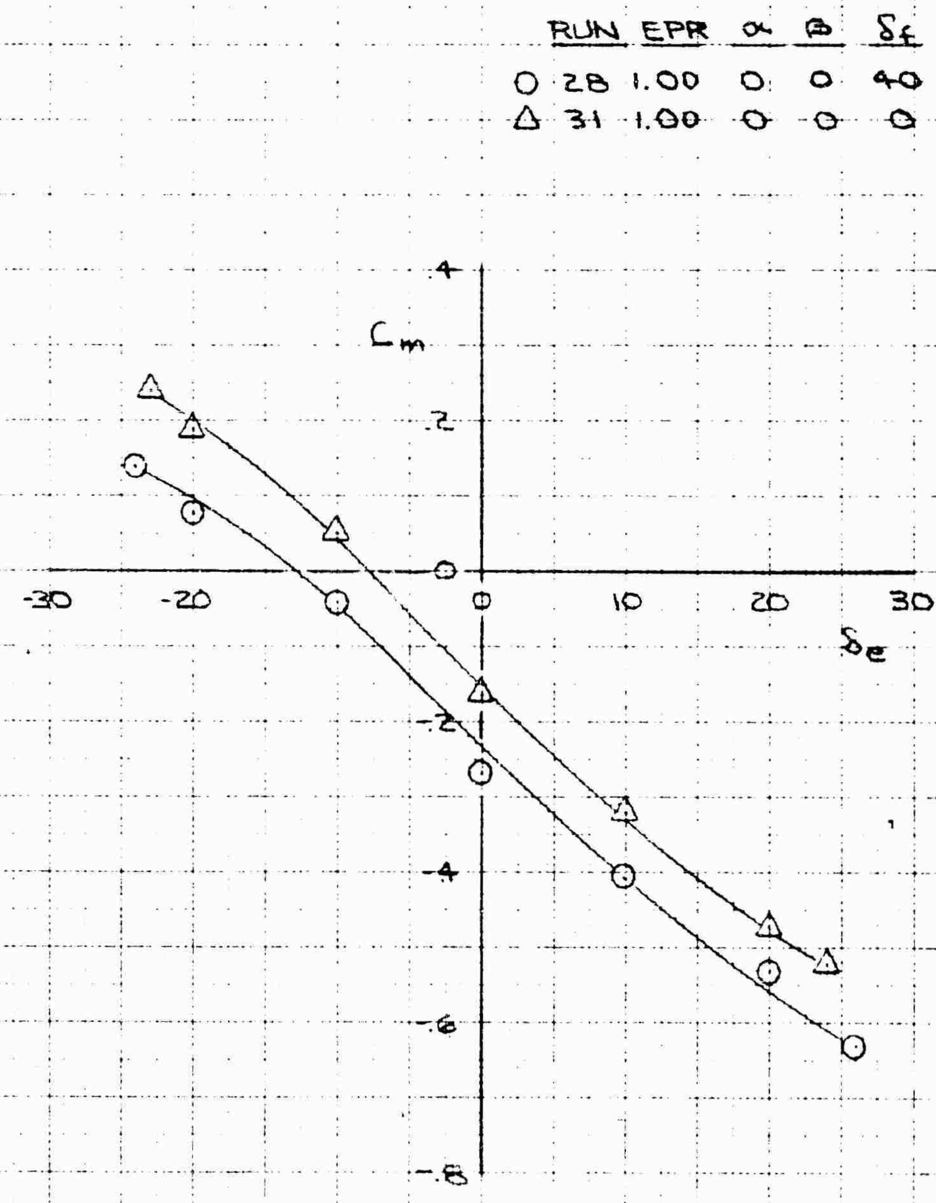

XV-4A
FULL SCALE WIND TUNNEL TEST 215
AILERON EFFECT ON SIDE FORCE COEFFICIENT IN CONVENTIONAL FLIGHT AT 80 KNOTS

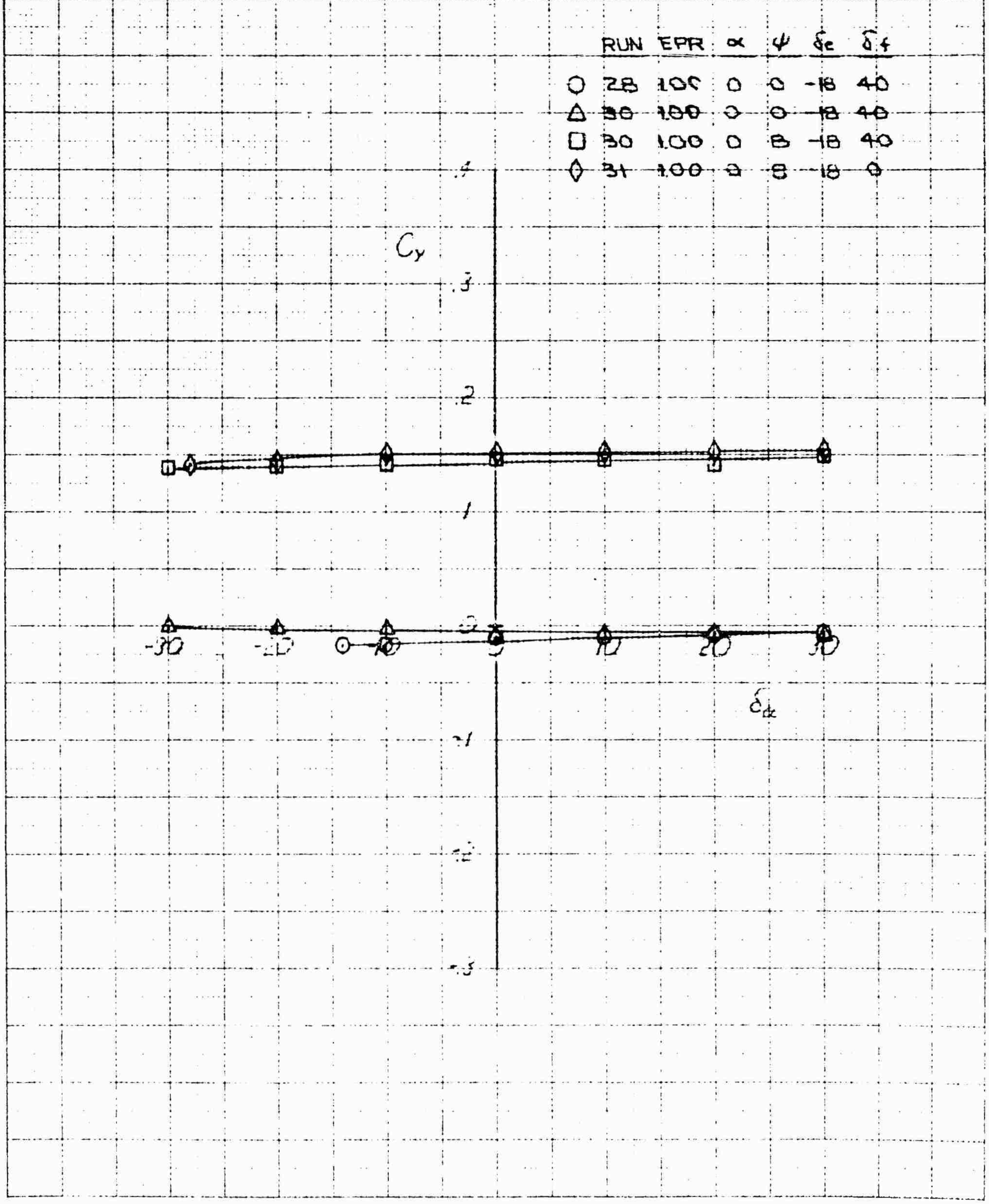

XV-4A
FULL SCALE WIND TUNNEL TEST 215
AILERON EFFECT ON YAWING MOMENT COEFFICIENT IN CONVENTIONAL FLIGHT AT 80 KNOTS

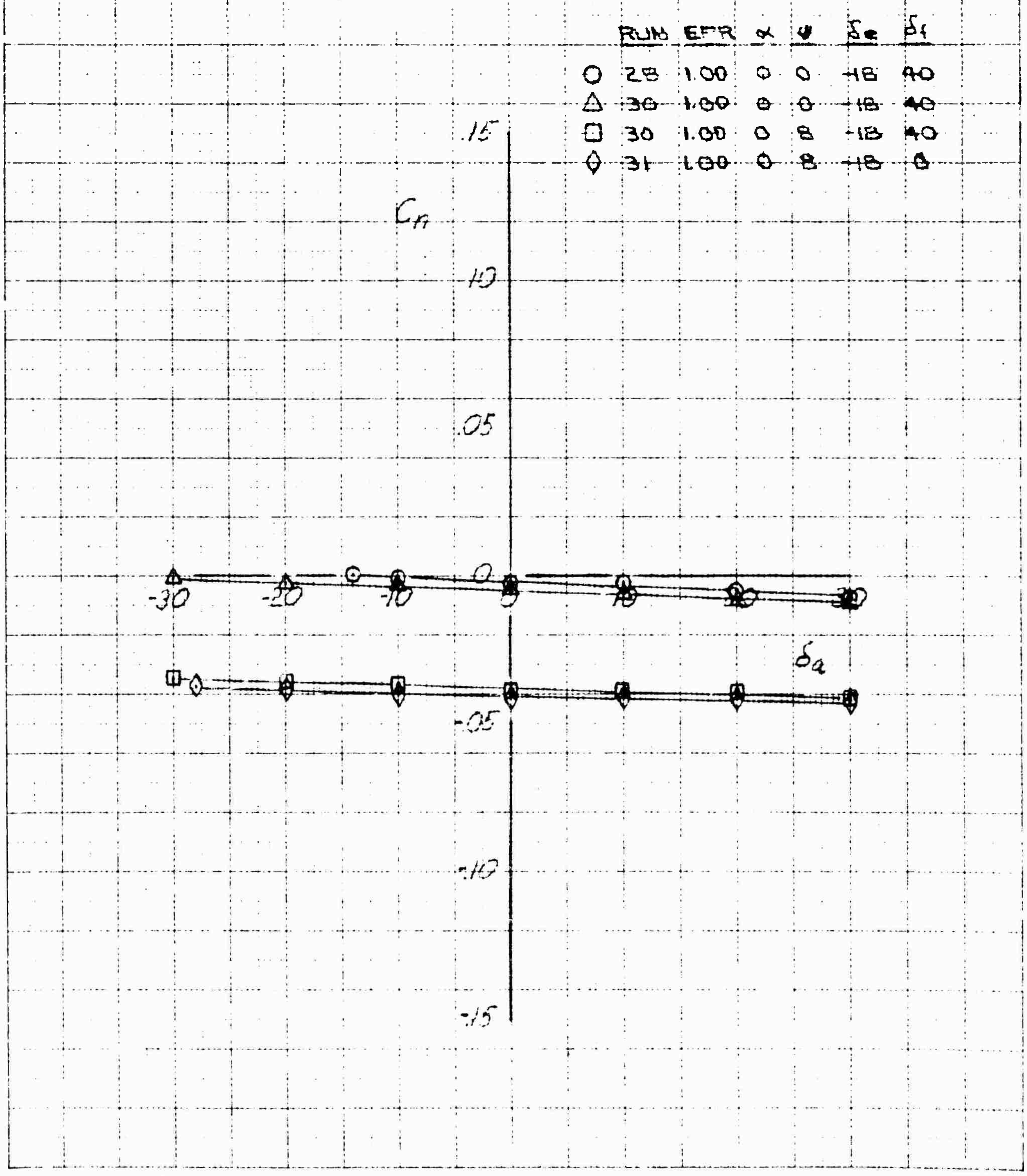

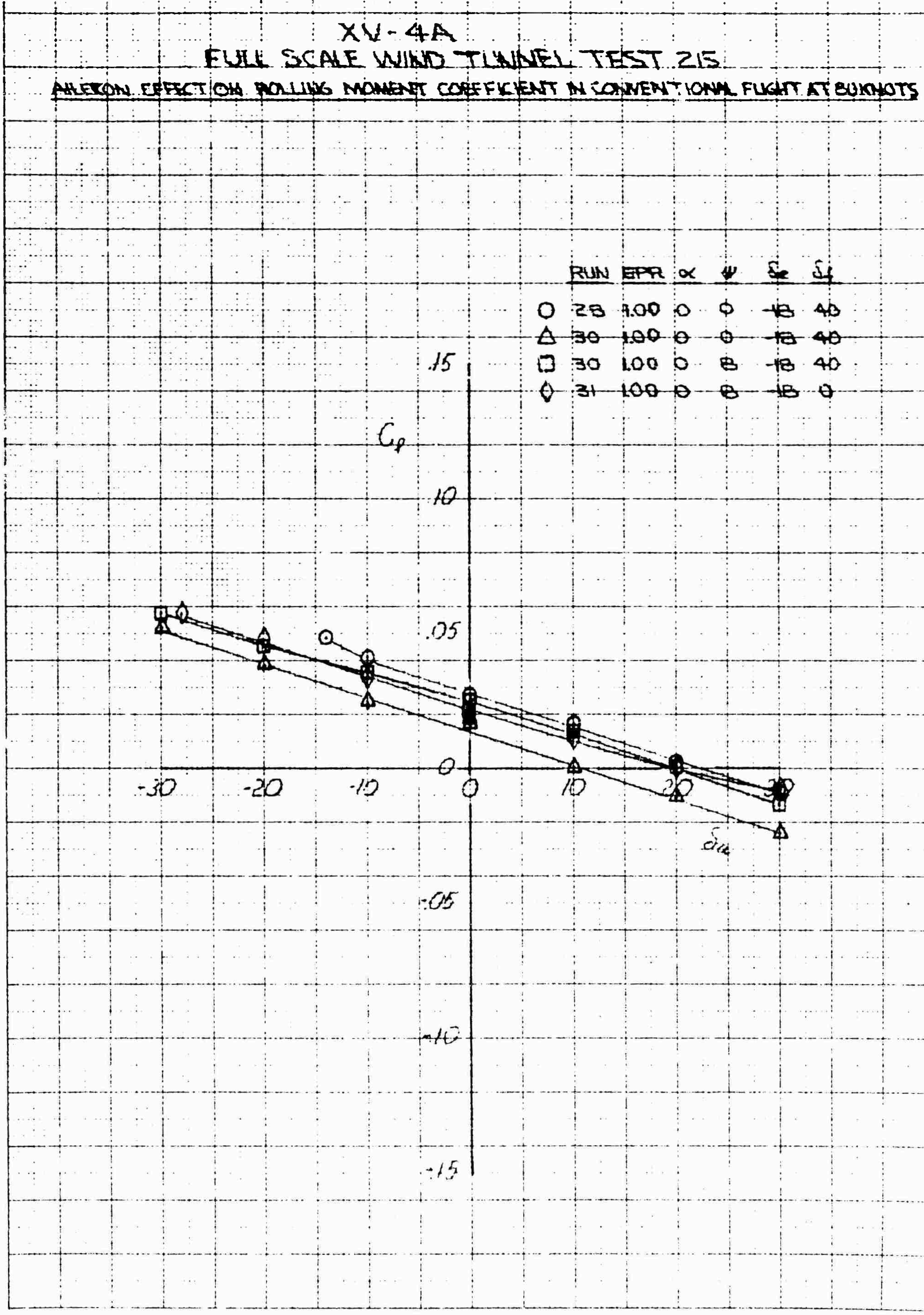
XV-4A
FULL SCALE WIND TUNNEL TEST 215
AILERON EFFECT ON ROLLING MOMENT COEFFICIENT IN CONVENTIONAL FLIGHT AT 80 KNOTS
RUN EPR α ψ δe δf
28 1.00 0 0 -18 40
30 1.00 0 0 -18 40
30 1.00 0 8 -18 40
31 1.00 0 8 -18 0
Cℓ
.15
.10
.05
0
-.05
-.10
-.15
-30
-20
-10
0
10
20
30
δa

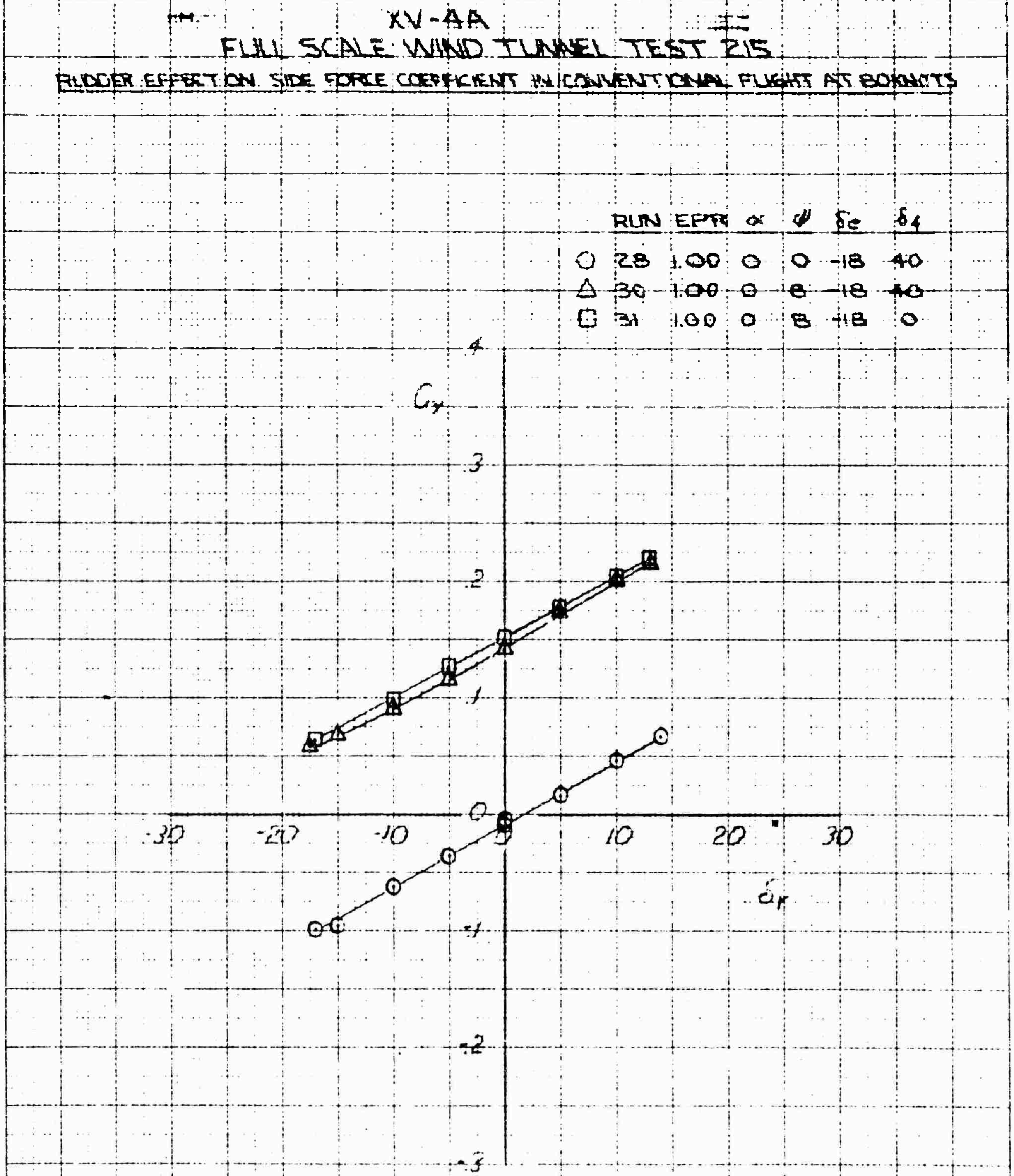
XV-4A
FULL SCALE WIND TUNNEL TEST 215
RUDDER EFFECT ON SIDE FORCE COEFFICIENT IN CONVENTIONAL FLIGHT AT 80 KNOTS
RUN EPR α ψ δe δf
28 1.00 0 0 -18 40
30 1.00 0 8 -18 40
31 1.00 0 8 +18 0
C_y
.4
.3
.2
.1
0
-.1
-.2
-.3
-30
-20
-10
0
10
20
30
δ_r

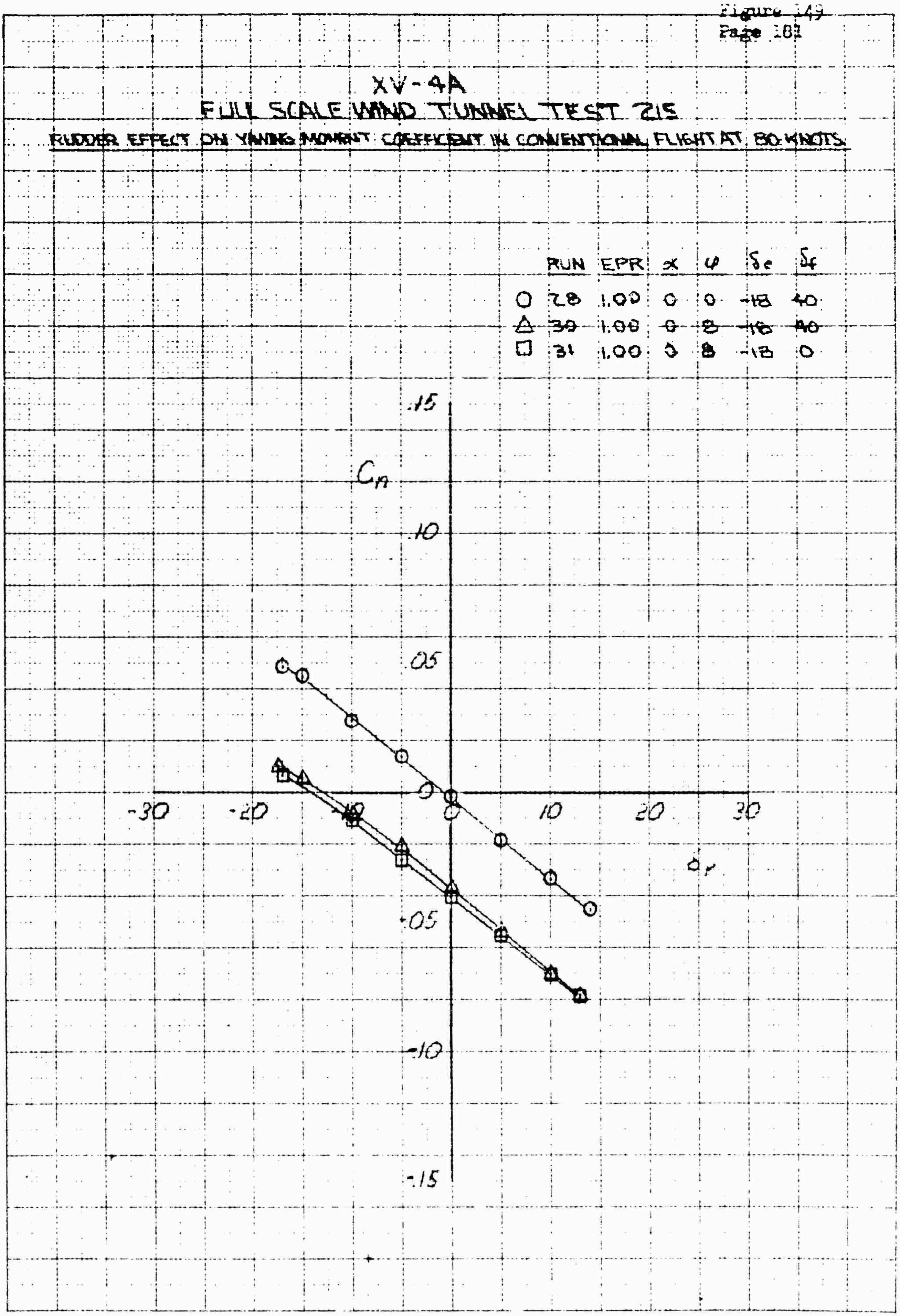
XV-4A
FULL SCALE WIND TUNNEL TEST 215
RUDDER EFFECT ON YAWING MOMENT COEFFICIENT IN CONVENTIONAL FLIGHT AT 80 KNOTS
RUN EPR α ψ δe δf
28 1.00 0 0 -18 40
30 1.00 0 8 -18 40
31 1.00 0 8 -18 0
Cn
.15
.10
.05
-.05
-.10
-.15
-30
-20
-10
0
10
20
30
δr

XV-4A

FULL SCALE WIND TUNNEL TEST 215

RUDDER EFFECT ON ROLLING MOMENT COEFFICIENT IN CONVENTIONAL FLIGHT AT 80 KNOTS

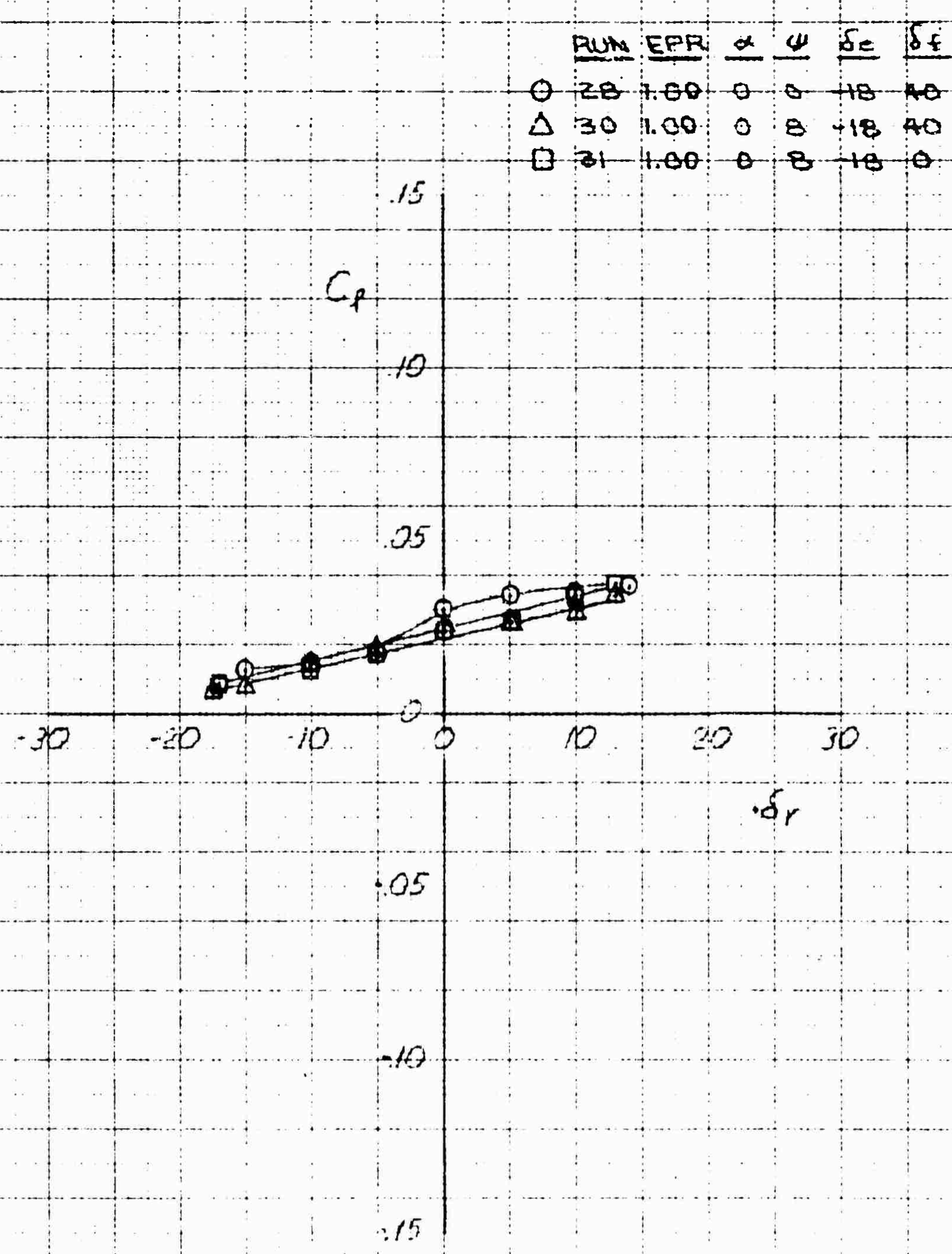

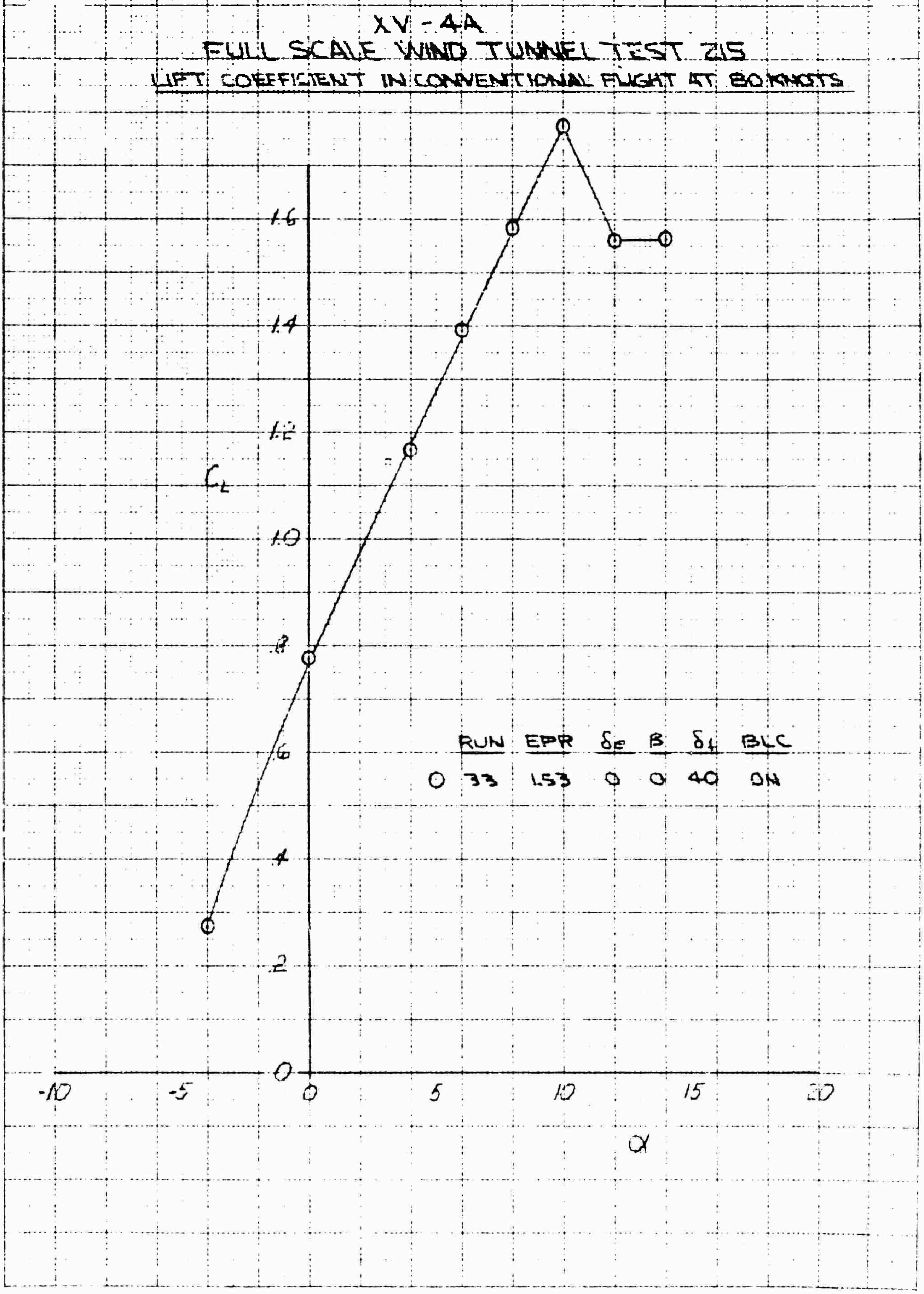
XV-4A
FULL SCALE WIND TUNNEL TEST 215
LIFT COEFFICIENT IN CONVENTIONAL FLIGHT AT 80 KNOTS
C_L
1.6
1.4
1.2
1.0
.8
.6
.4
.2
0
-10
-5
0
5
10
15
20
α
RUN EPR δ_E β δ_f BLC
○ 33 1.53 0 0 40 ON

XV-4A
FULL SCALE WIND TUNNEL TEST 215
DRAG POLAR IN CONVENTIONAL FLIGHT AT 80 KNOTS

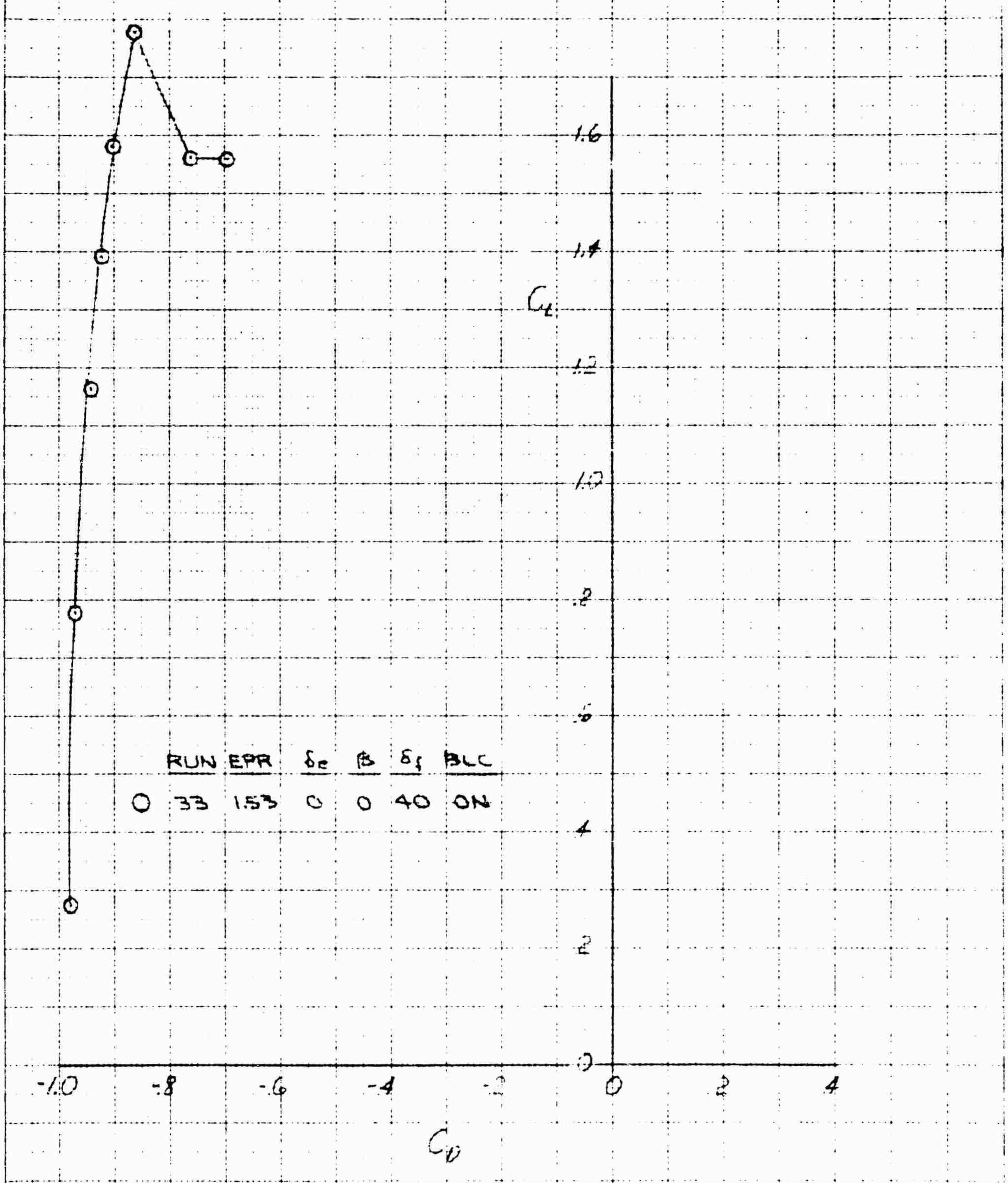

XV-4A
FULL SCALE WIND TUNNEL TEST 215
PITCHING MOMENT CHARACTERISTICS IN CONVENTIONAL FLIGHT AT 80 KNOTS

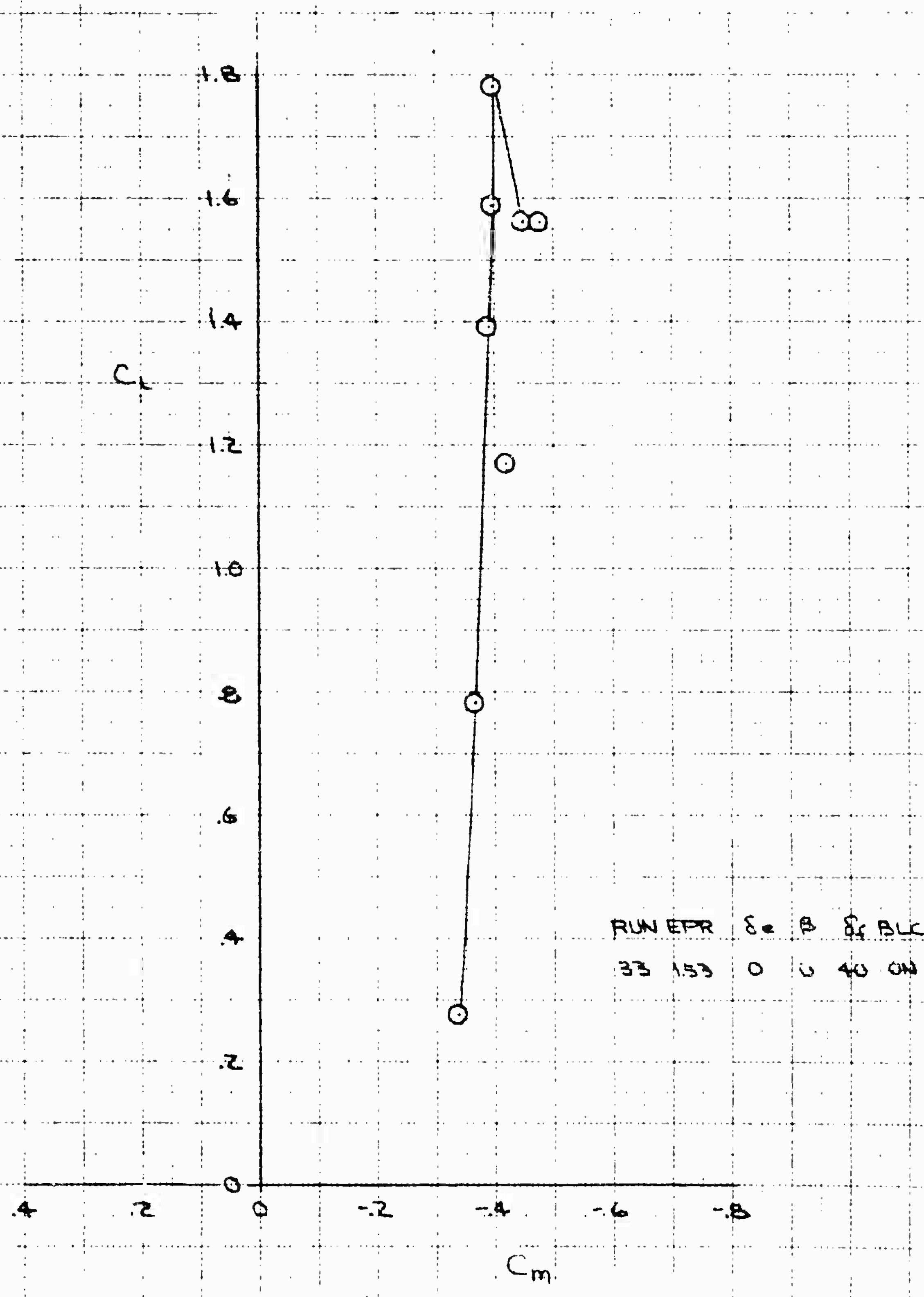

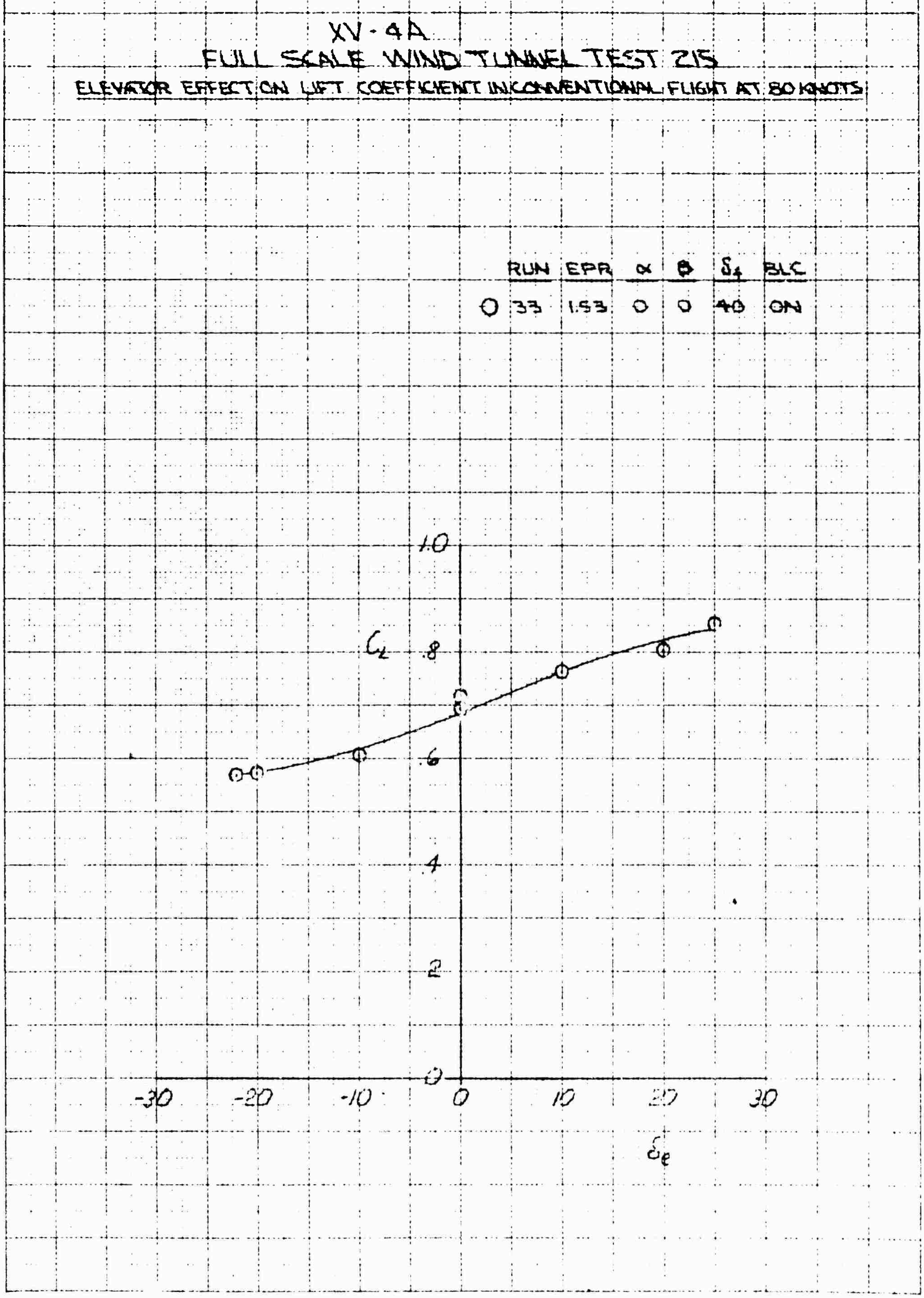
XV-4A
FULL SCALE WIND TUNNEL TEST 215
ELEVATOR EFFECT ON LIFT COEFFICIENT IN CONVENTIONAL FLIGHT AT 80 KNOTS
RUN EPR α β δf BLC
33 1.53 0 0 40 ON
CL
1.0
.8
.6
.4
.2
0
-30
-20
-10
0
10
20
30
δe

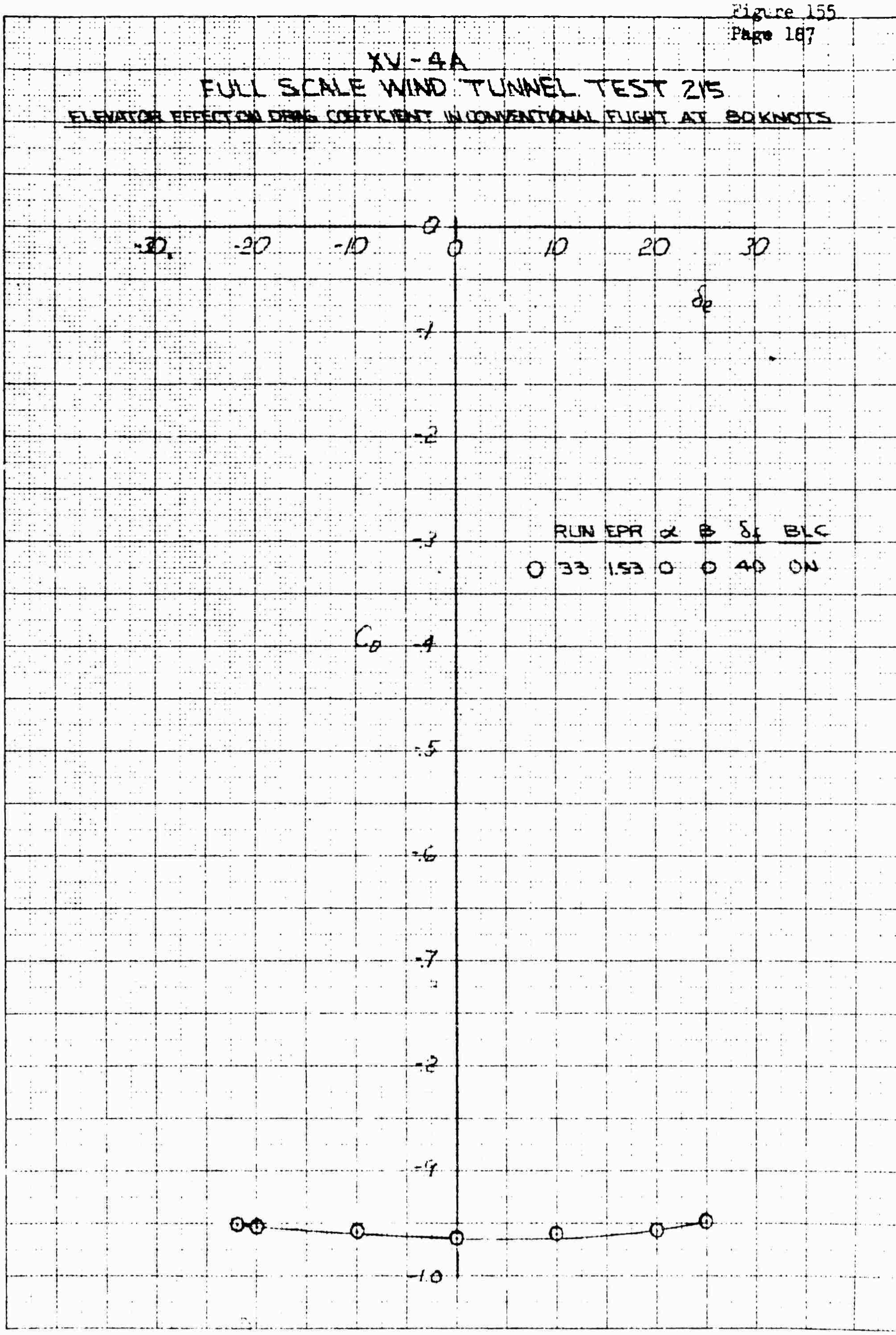
XV-4A
FULL SCALE WIND TUNNEL TEST 215
ELEVATOR EFFECT ON DRAG COEFFICIENT IN CONVENTIONAL FLIGHT AT 80 KNOTS
-30
-20
-10
0
10
20
30
δ_e
-.1
-.2
-.3
-.4
-.5
-.6
-.7
-.8
-.9
-1.0
C_D
RUN EPR α β δ_f BLC
O 33 1.53 0 0 40 ON

XV-4A
FULL SCALE WIND TUNNEL TEST 215
ELEVATOR EFFECT ON PITCHING MOMENT COEFFICIENT IN CONVENTIONAL FLIGHT AT 80 KNOTS

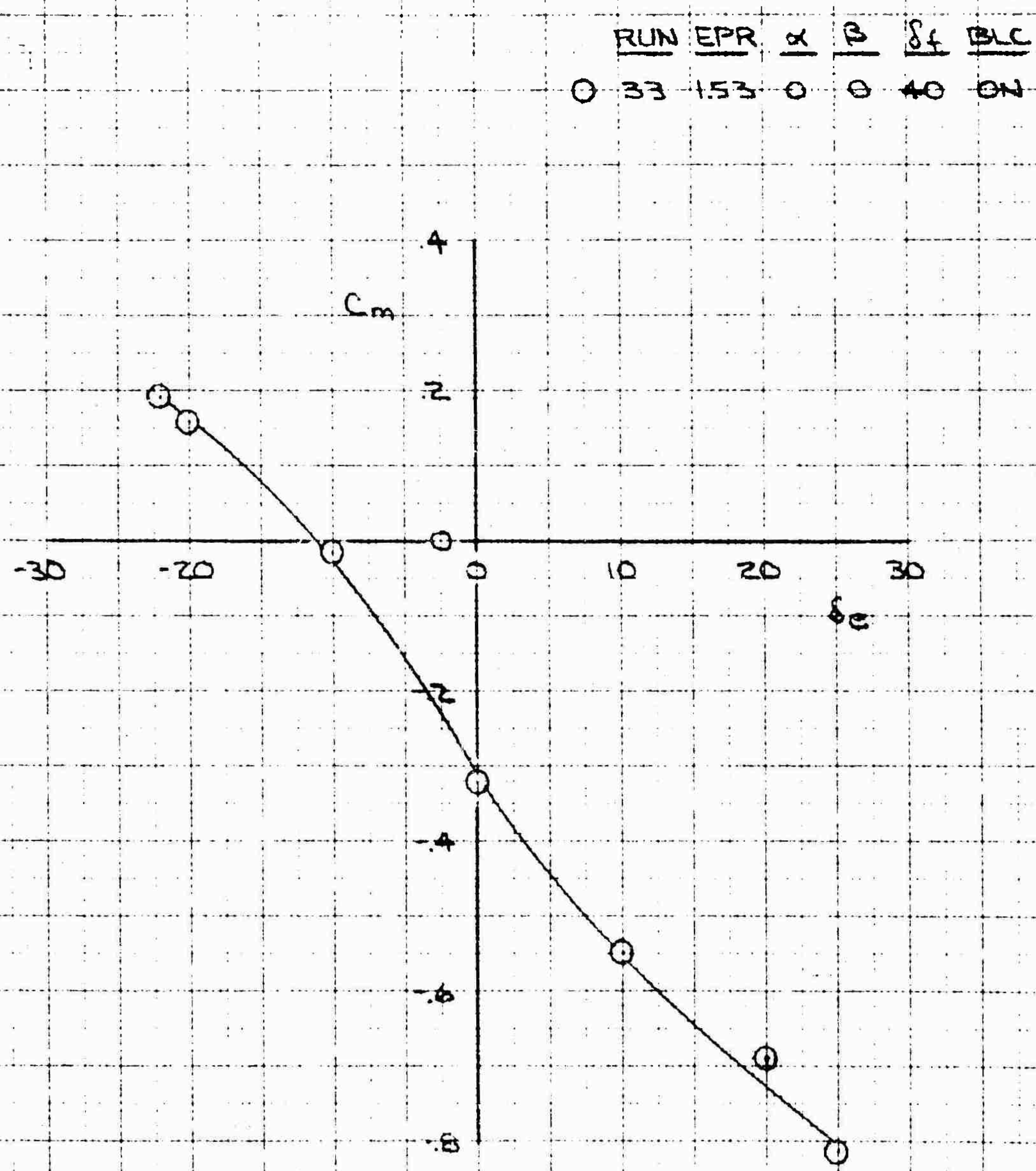

XV-4A
FULL SCALE WIND TUNNEL TEST 215
TUNNEL DYNAMIC PRESSURE EFFECT ON DATA PRESENTATION

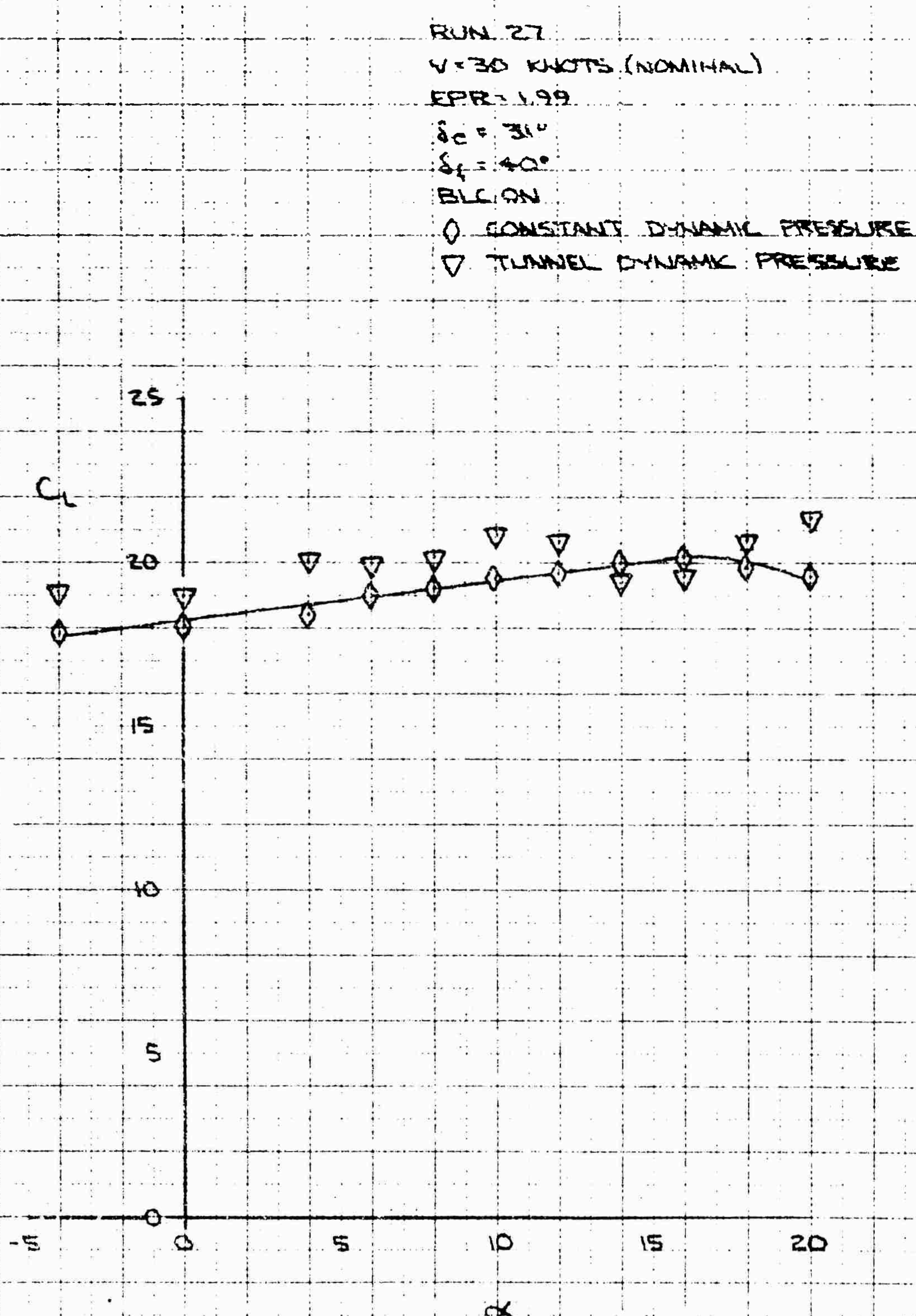

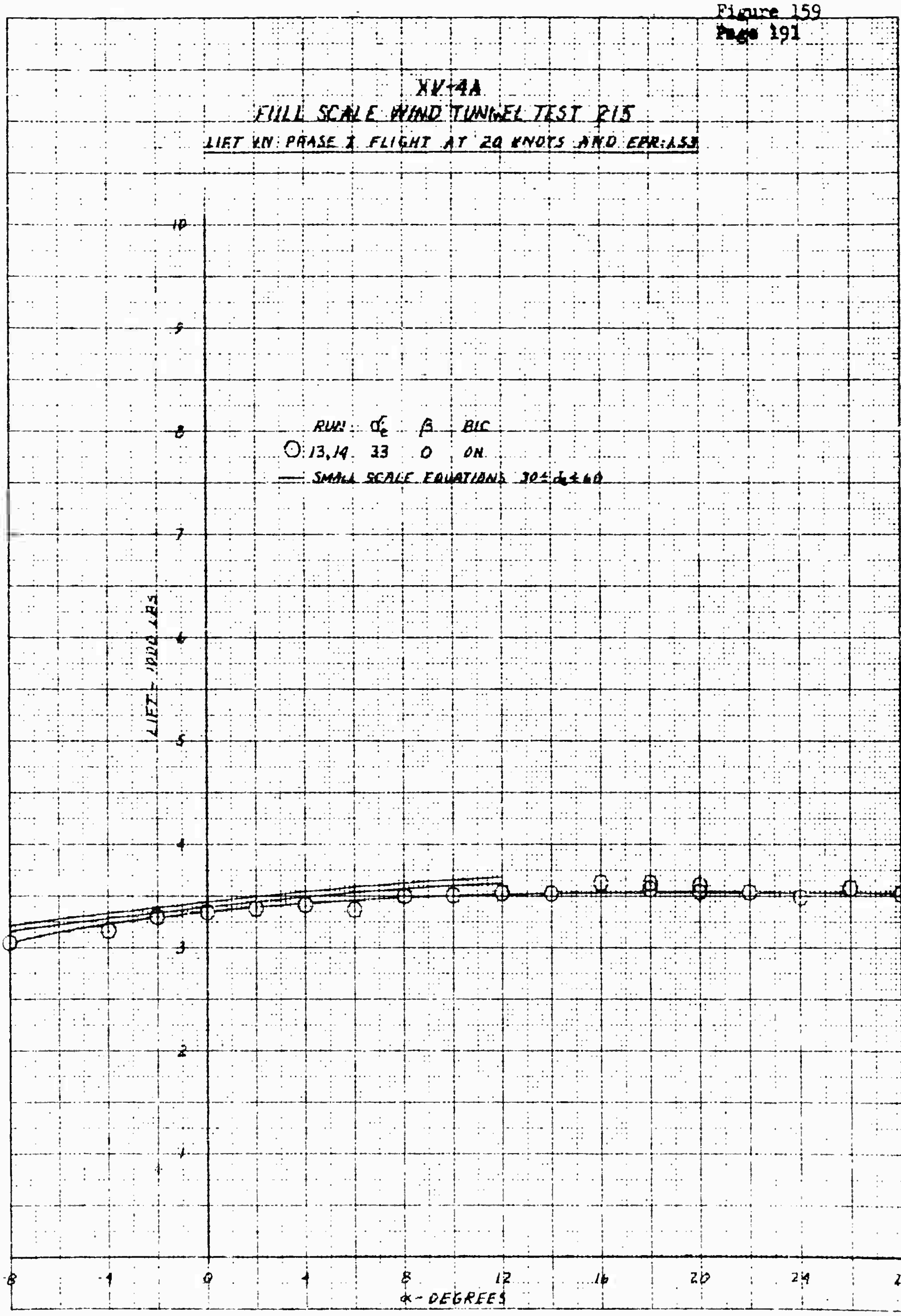
XV-4A
FULL SCALE WIND TUNNEL TEST 215
RUN β BIC
13,14 33 0 ON
SMALL SCALE EQUATIONS
LIFT - 1000 LBS
α - DEGREES
-8
-4
0
4
8
12
16
20
24
1
2
3
4
5
6
7
8
9
10

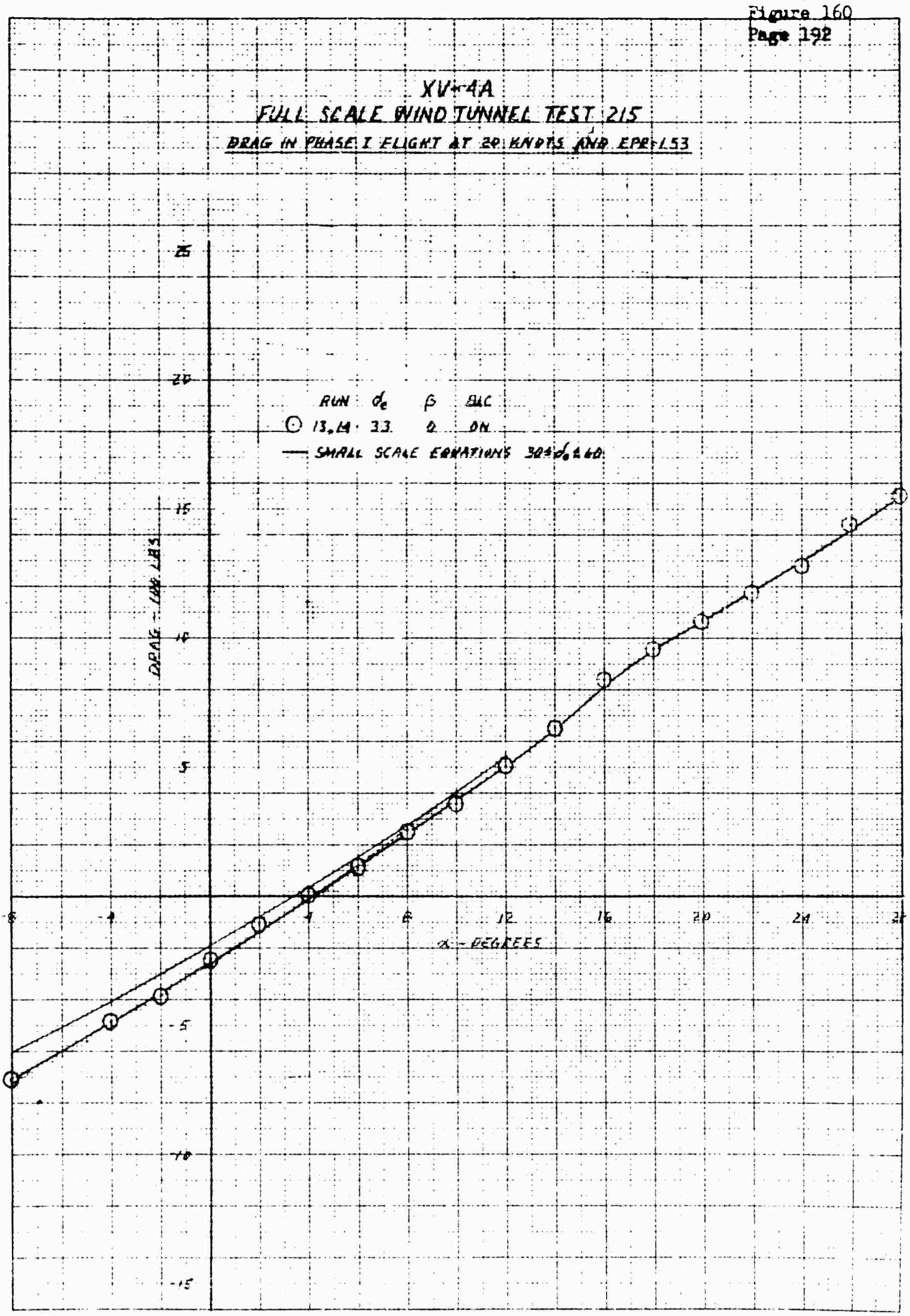
XV-4A
FULL SCALE WIND TUNNEL TEST 215
DRAG IN PHASE I FLIGHT AT 20 KNOTS AND EPR-1.53
RUN δ_e β BLC
13, 14 33 0 ON
SMALL SCALE EQUATIONS
DRAG - 100 LBS
α - DEGREES

XV-4A
FULL SCALE WIND TUNNEL TEST 215
PITCHING MOMENT IN PHASE 2 FLIGHT AT 20 KNOTS AND EPR=1.53

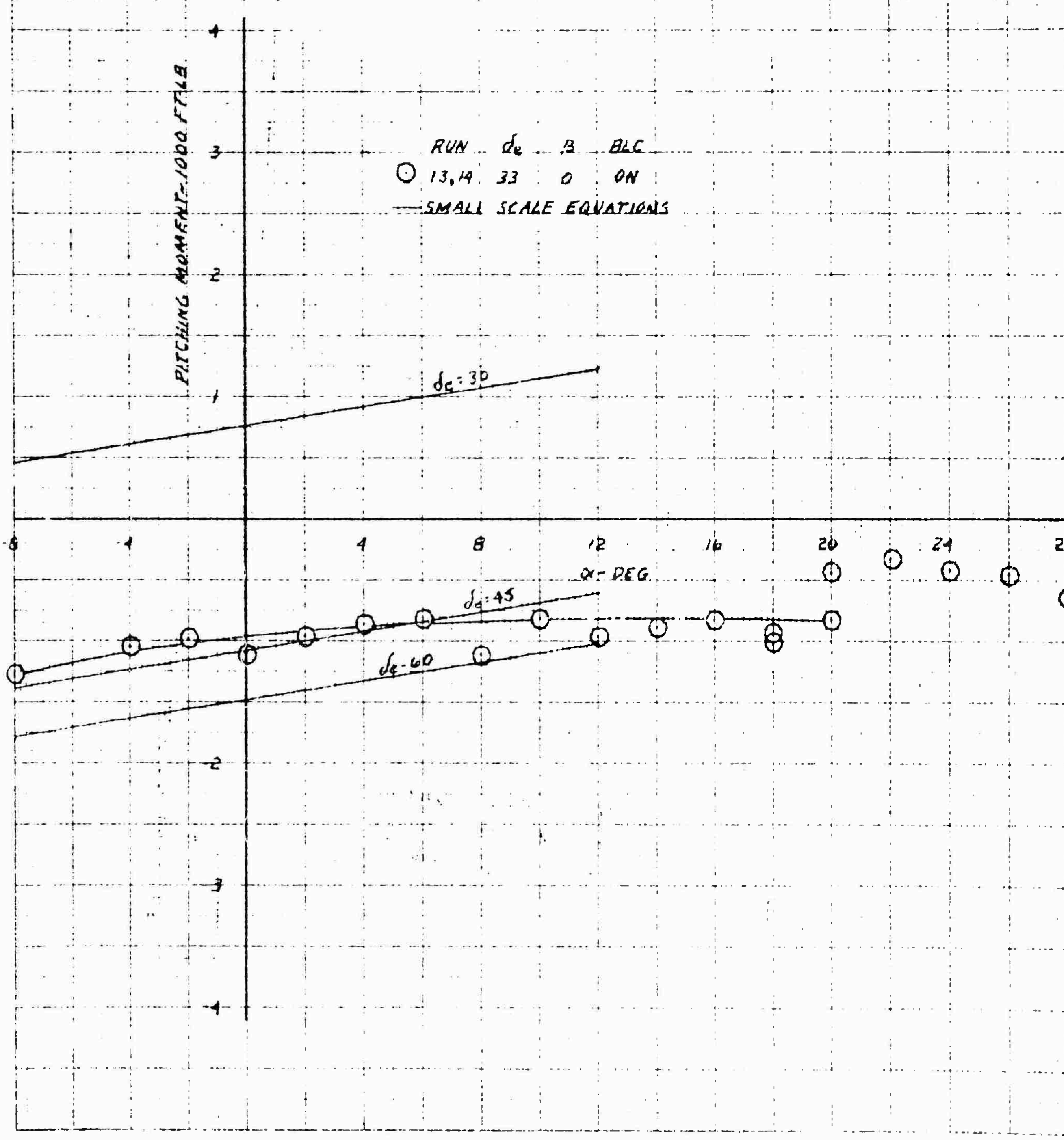

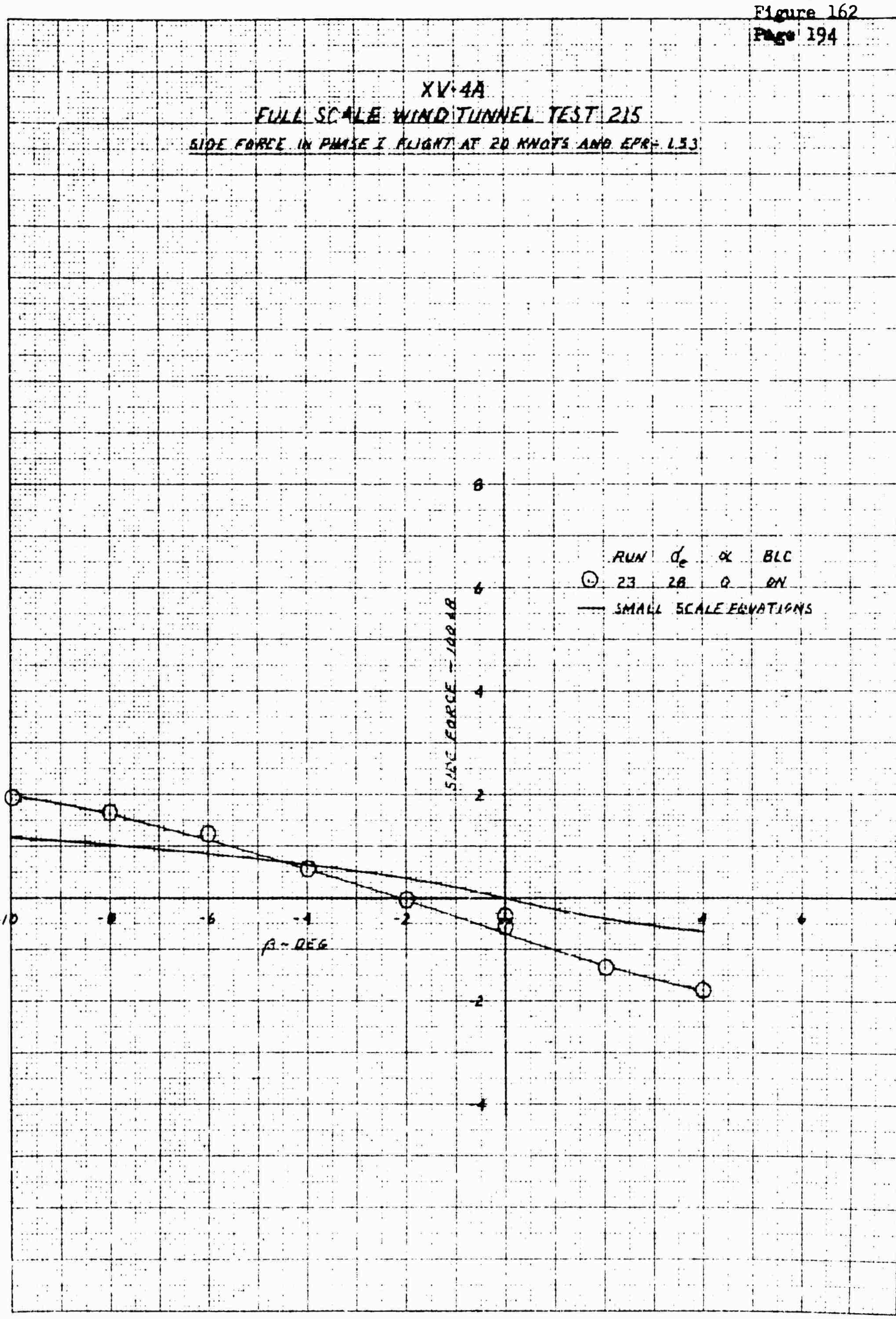
XV-4A
FULL SCALE WIND TUNNEL TEST 215
SIDE FORCE IN PHASE I FLIGHT AT 20 KNOTS AND EPR = 1.53
RUN
δ_e
α
BLC
23
28
0
ON
SMALL SCALE EQUATIONS
SIDE FORCE — 100 LB
β ~ DEG

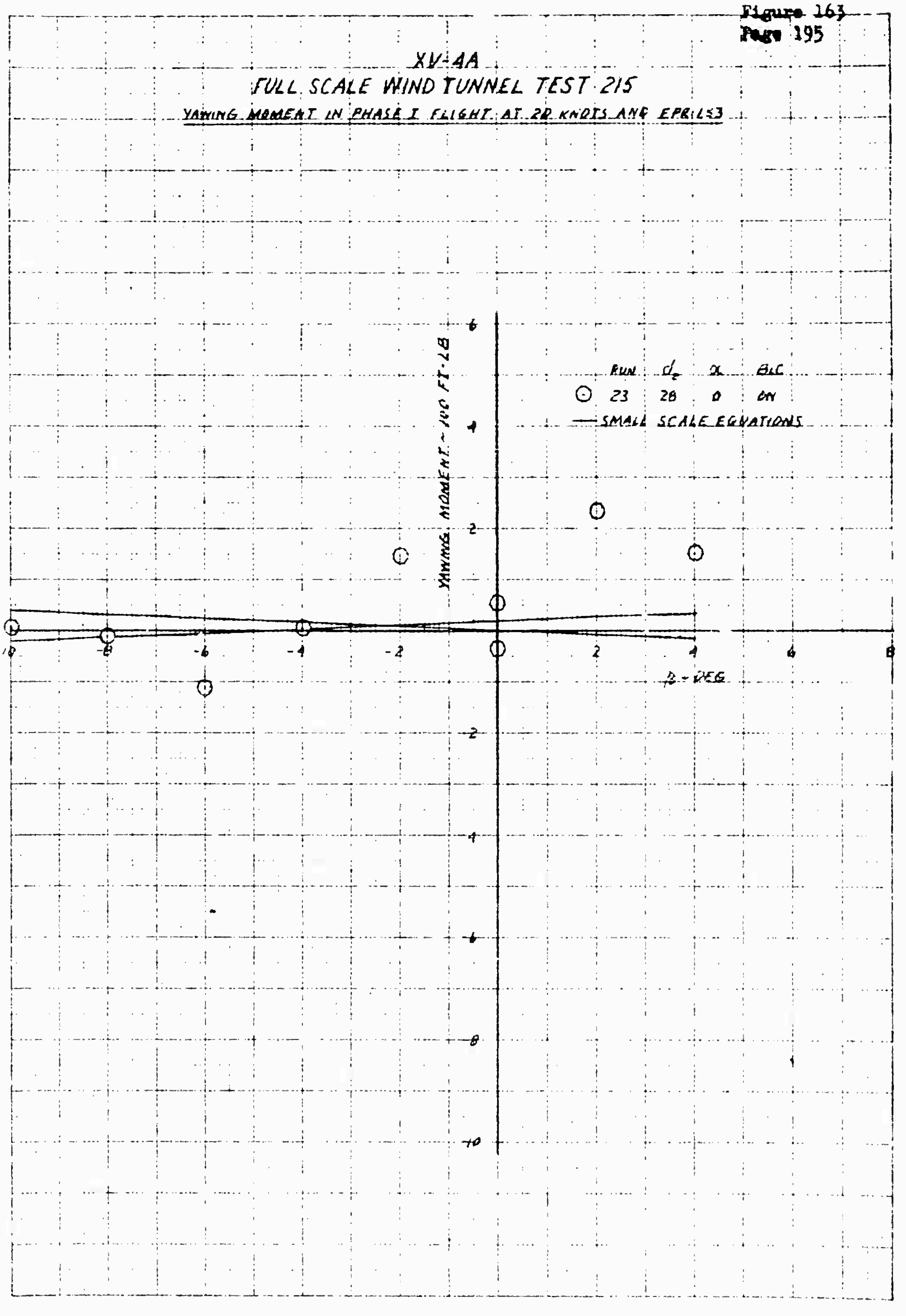
XV-4A
FULL SCALE WIND TUNNEL TEST 215
YAWING MOMENT IN PHASE I FLIGHT AT 20 KNOTS AND EPR≤1.3
RUN
δ_e
α
BLC
23
28
0
ON
SMALL SCALE EQUATIONS
YAWING MOMENT ~ 100 FT-LB
β - DEG
6
4
2
-2
-4
-6
-8
-10
-10
-8
-6
-4
-2
2
4
6
8

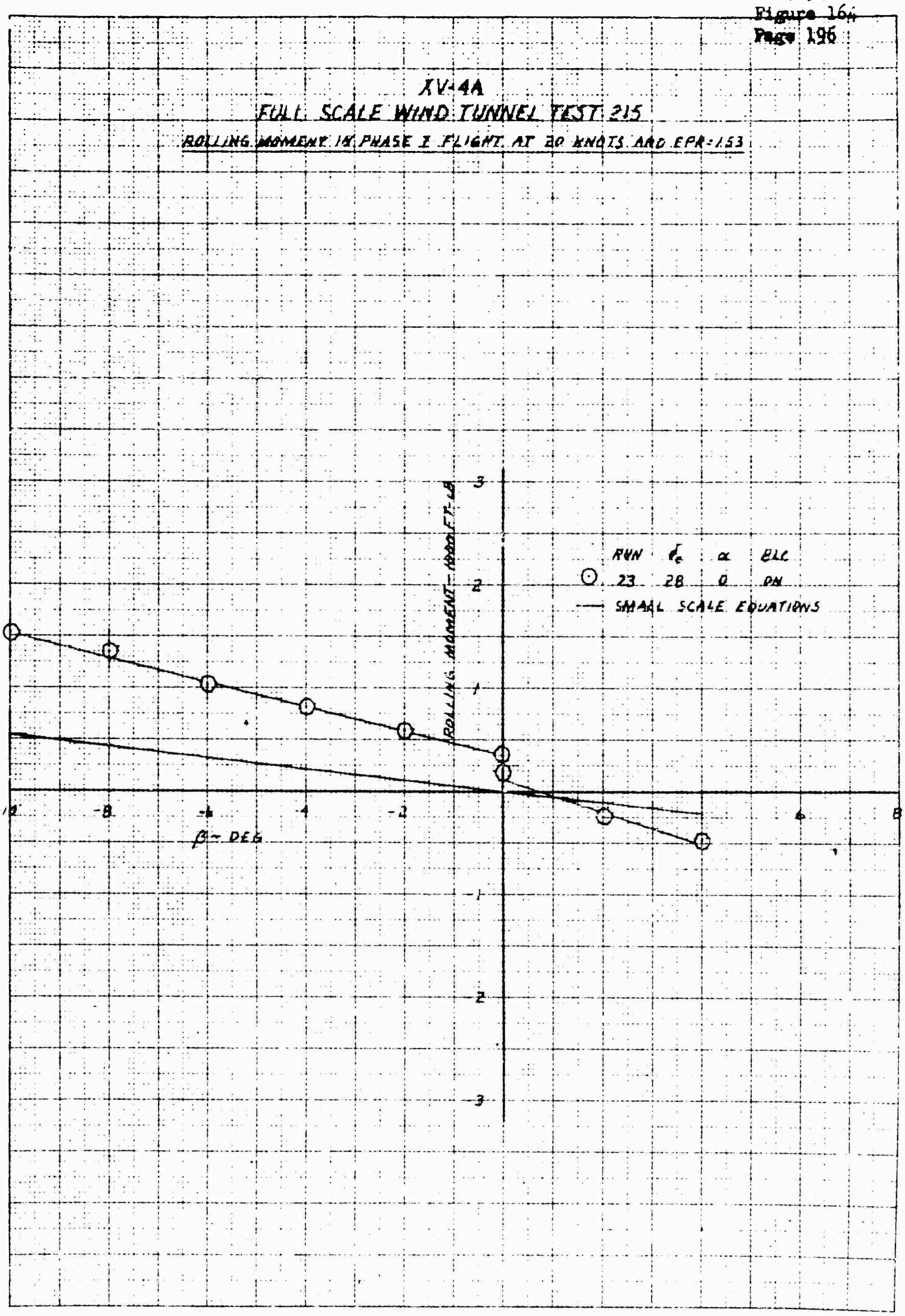
XV-4A
FULL SCALE WIND TUNNEL TEST 215
ROLLING MOMENT IN PHASE I FLIGHT AT 20 KNOTS AND EPR=1.53
ROLLING MOMENT~1000 FT-LB
β ~ DEG
RUN
α
BLC
23
28
0
ON
SMALL SCALE EQUATIONS

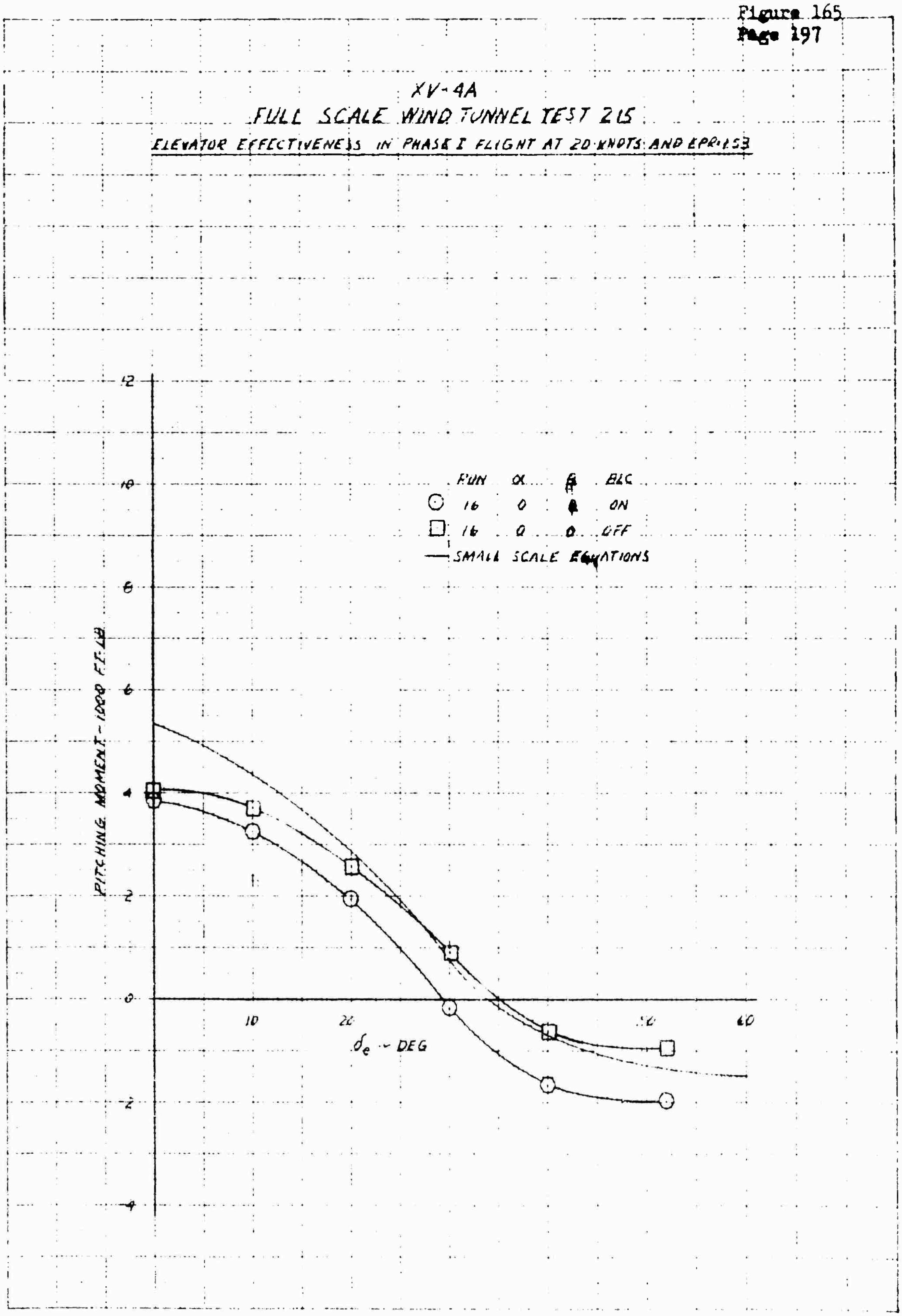
XV-4A
FULL SCALE WIND TUNNEL TEST 215
ELEVATOR EFFECTIVENESS IN PHASE I FLIGHT AT 20 KNOTS AND EPR=1.53
RUN α β BLC
16 0 0 ON
16 0 0 OFF
SMALL SCALE EQUATIONS
PITCHING MOMENT - 1000 FT-LB
12
10
8
6
4
2
0
-2
-4
10
20
30
40
50
60
δ_e ~ DEG

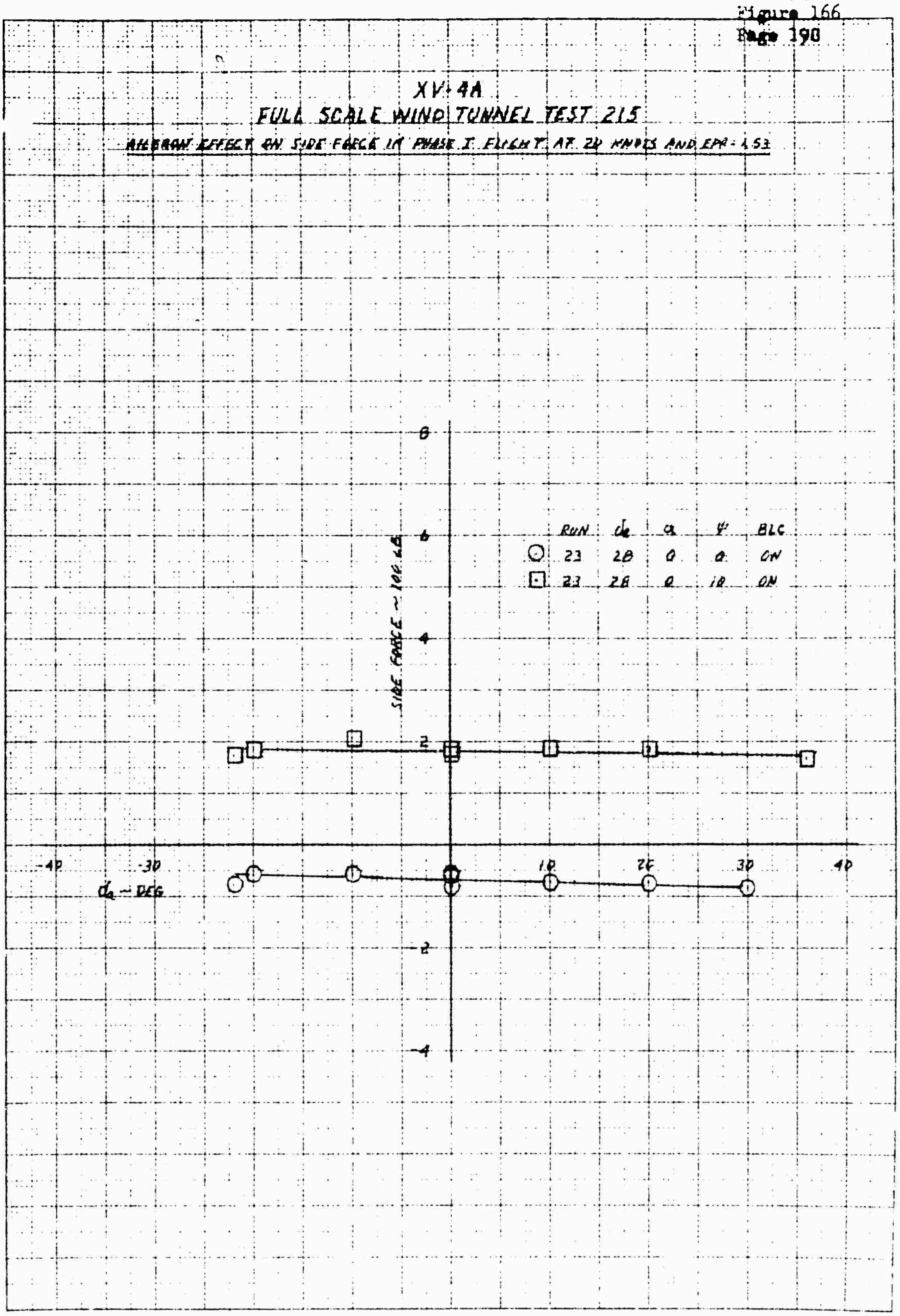
XV-4A
FULL SCALE WIND TUNNEL TEST 215
AILERON EFFECT ON SIDE FORCE IN PHASE I FLIGHT AT 20 KNOTS AND EPR = 1.53
RUN δ_e α ψ BLC
23 28 0 0 ON
23 28 0 10 ON
SIDE FORCE ~ 100 LB
8
6
4
2
-2
-4
-40
-30
10
20
30
40
δ_a ~ DEG

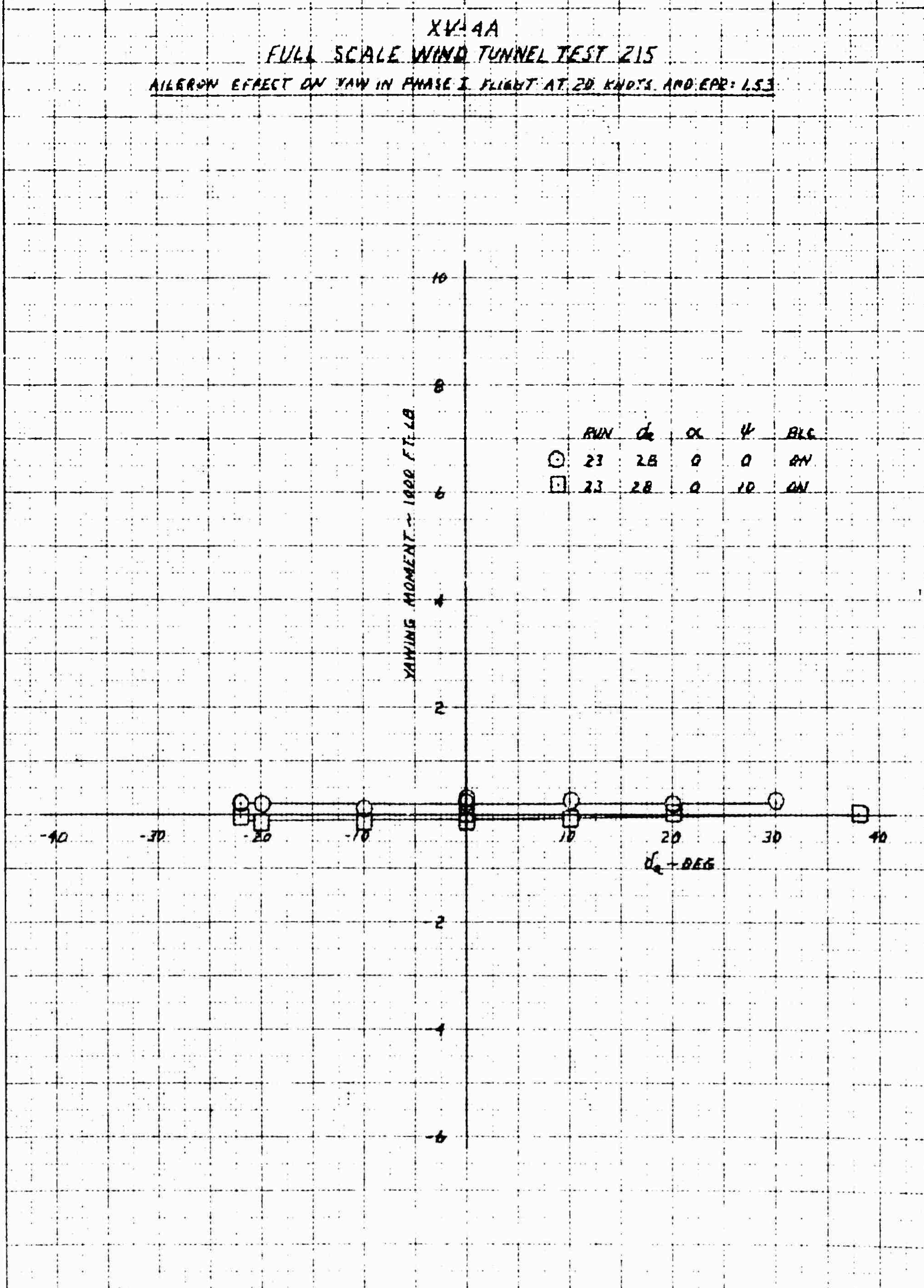
XV-4A
FULL SCALE WIND TUNNEL TEST 215
AILERON EFFECT ON YAW IN PHASE I FLIGHT AT 20 KNOTS AND EPR: 1.53
RUN δ_a α ψ BLC
23 28 0 0 ON
23 28 0 10 ON
YAWING MOMENT ~ 1000 FT-LB
δ_a ~ DEG
10
8
6
4
2
-2
-4
-6
-40
-30
-20
-10
10
20
30
40

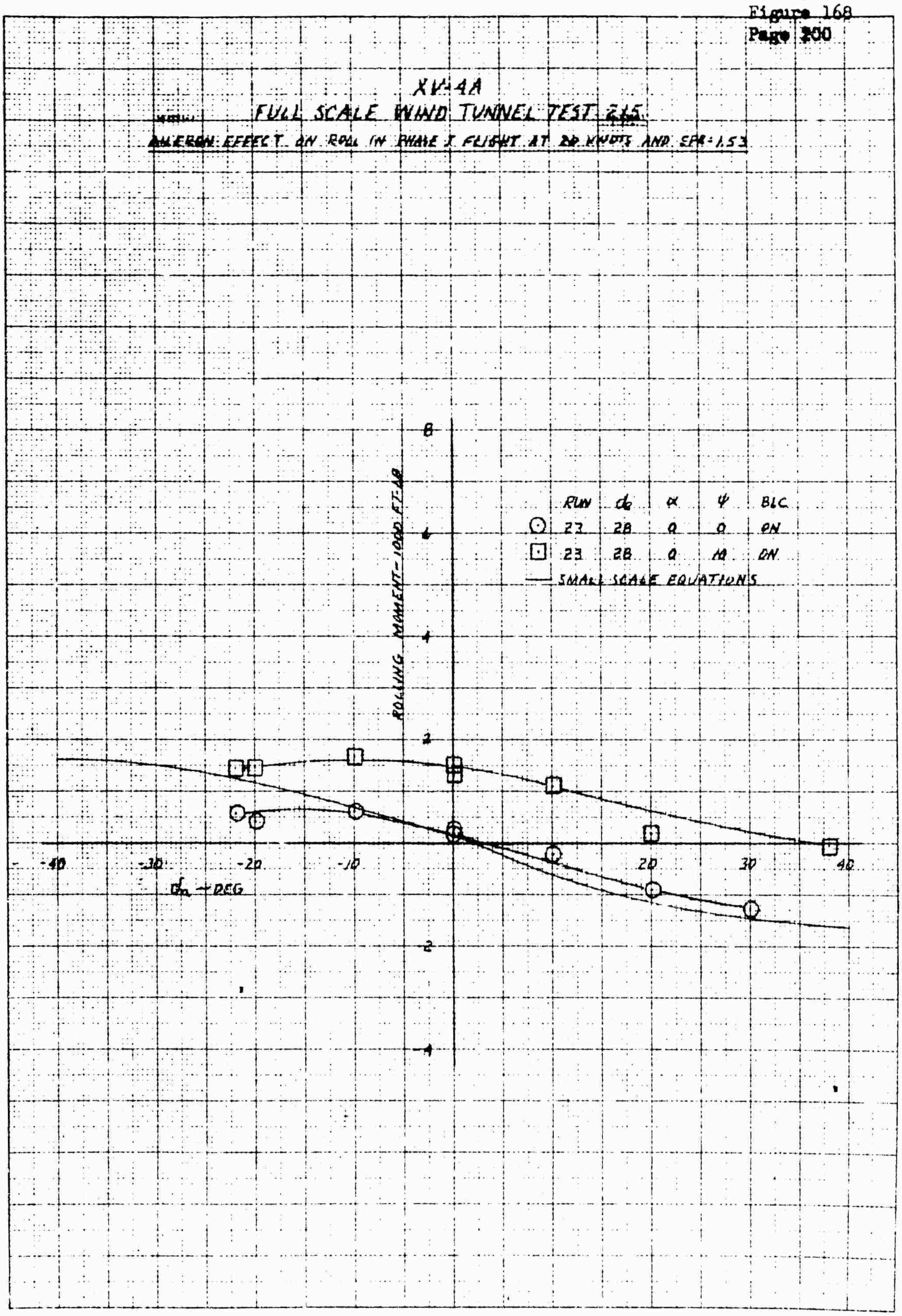
XV-4A
FULL SCALE WIND TUNNEL TEST 215
AILERON EFFECT ON ROLL IN PHASE I FLIGHT AT KNOTS AND EPR=1.53
ROLLING MOMENT-1000 FT-LB
δa - DEG
RUN δe α ψ BLC
23 28 0 0 ON
23 28 0 10 ON
SMALL SCALE EQUATIONS
8
6
4
2
-2
-4
-40
-30
-20
-10
20
30
40

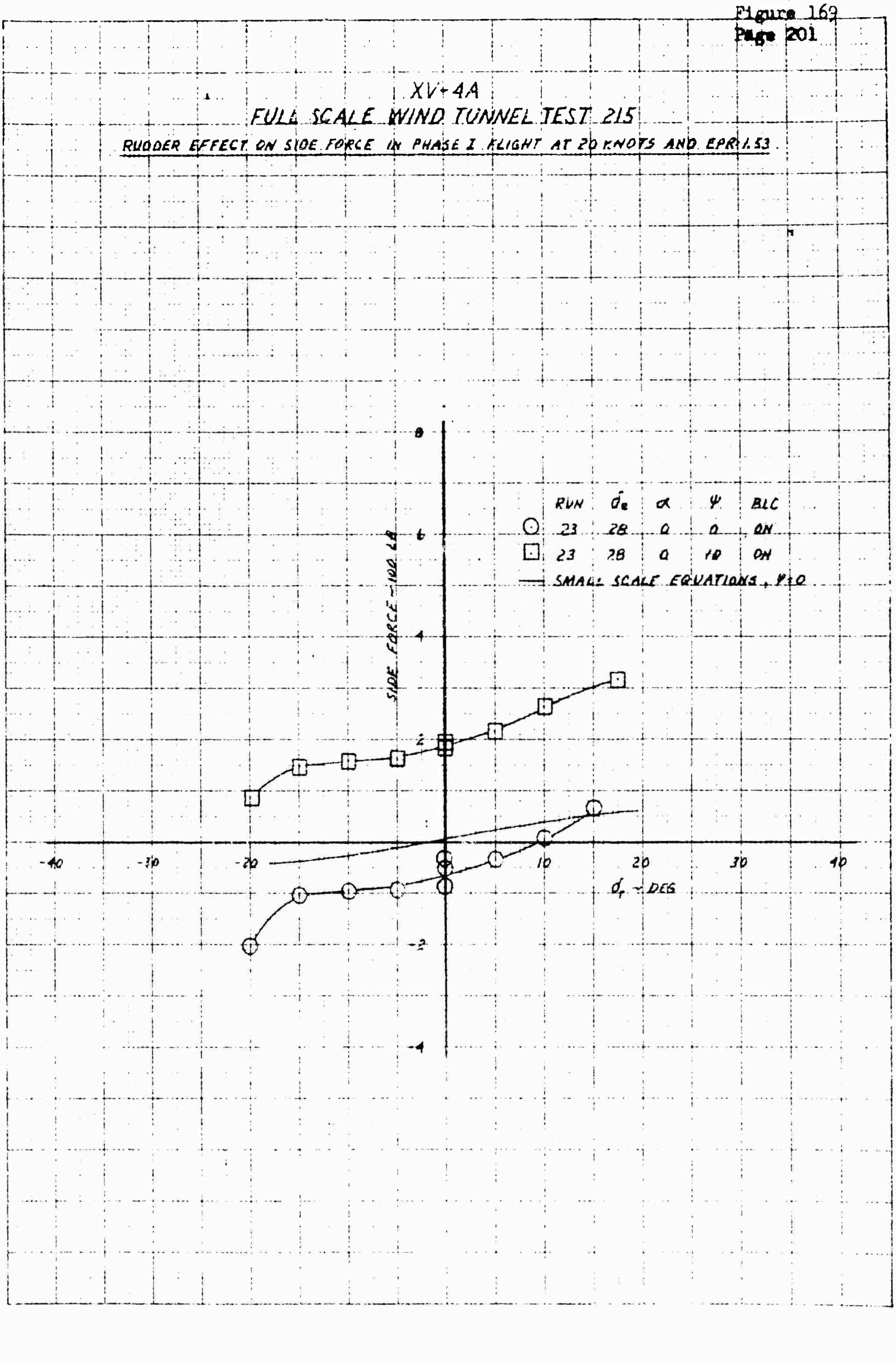
XV-4A
FULL SCALE WIND TUNNEL TEST 215
RUDDER EFFECT ON SIDE FORCE IN PHASE I FLIGHT AT 20 KNOTS AND EPR 1.53
RUN
δe
α
ψ
BLC
23
28
0
0
ON
23
28
0
10
ON
SMALL SCALE EQUATIONS, ψ=0
SIDE FORCE ~ 100 LB
δr ~ DEG
-40
-30
-20
10
20
30
40
8
6
4
2
-2
-4

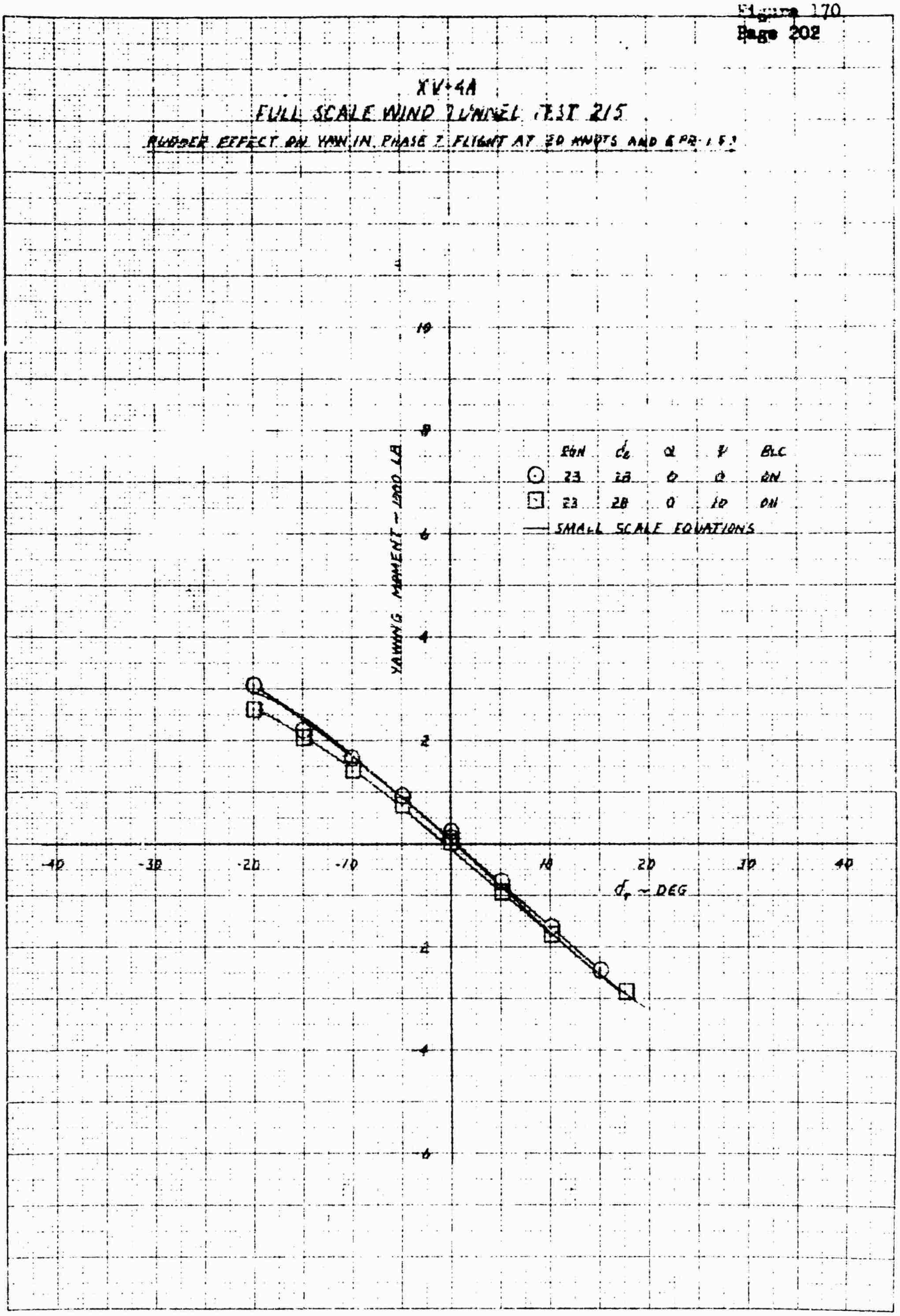
XV-4A
FULL SCALE WIND TUNNEL TEST 215
RUDDER EFFECT ON YAW IN PHASE 2 FLIGHT AT 20 KNOTS AND EPR 1.53
RGN
23
23
28
28
0
0
0
10
BLC
ON
ON
SMALL SCALE EQUATIONS
YAWING MOMENT ~ 1000 LB
10
8
6
4
2
-2
-4
-6
-40
-30
-20
-10
10
20
30
40
DEG

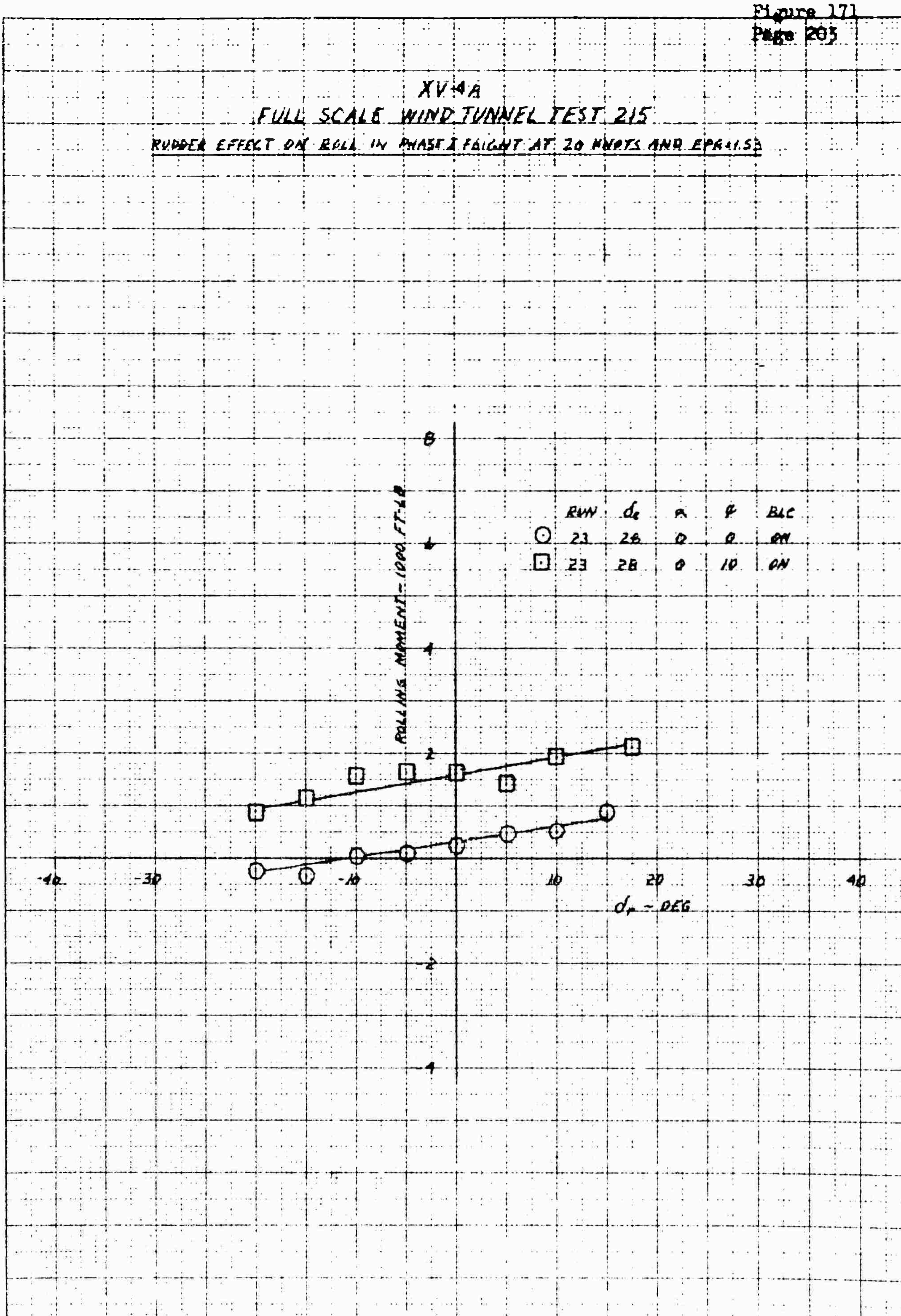
XV-4A
FULL SCALE WIND TUNNEL TEST 215
RUDDER EFFECT ON ROLL IN PHASE I FLIGHT AT 20 KNOTS AND EPR=1.53
ROLLING MOMENT - 1000 FT-LB
8
6
4
2
-2
-4
-40
-30
-10
10
20
30
40
δ_r - DEG
RUN
δ_e
α
ϕ
BLC
23
28
0
0
ON
23
28
0
10
ON

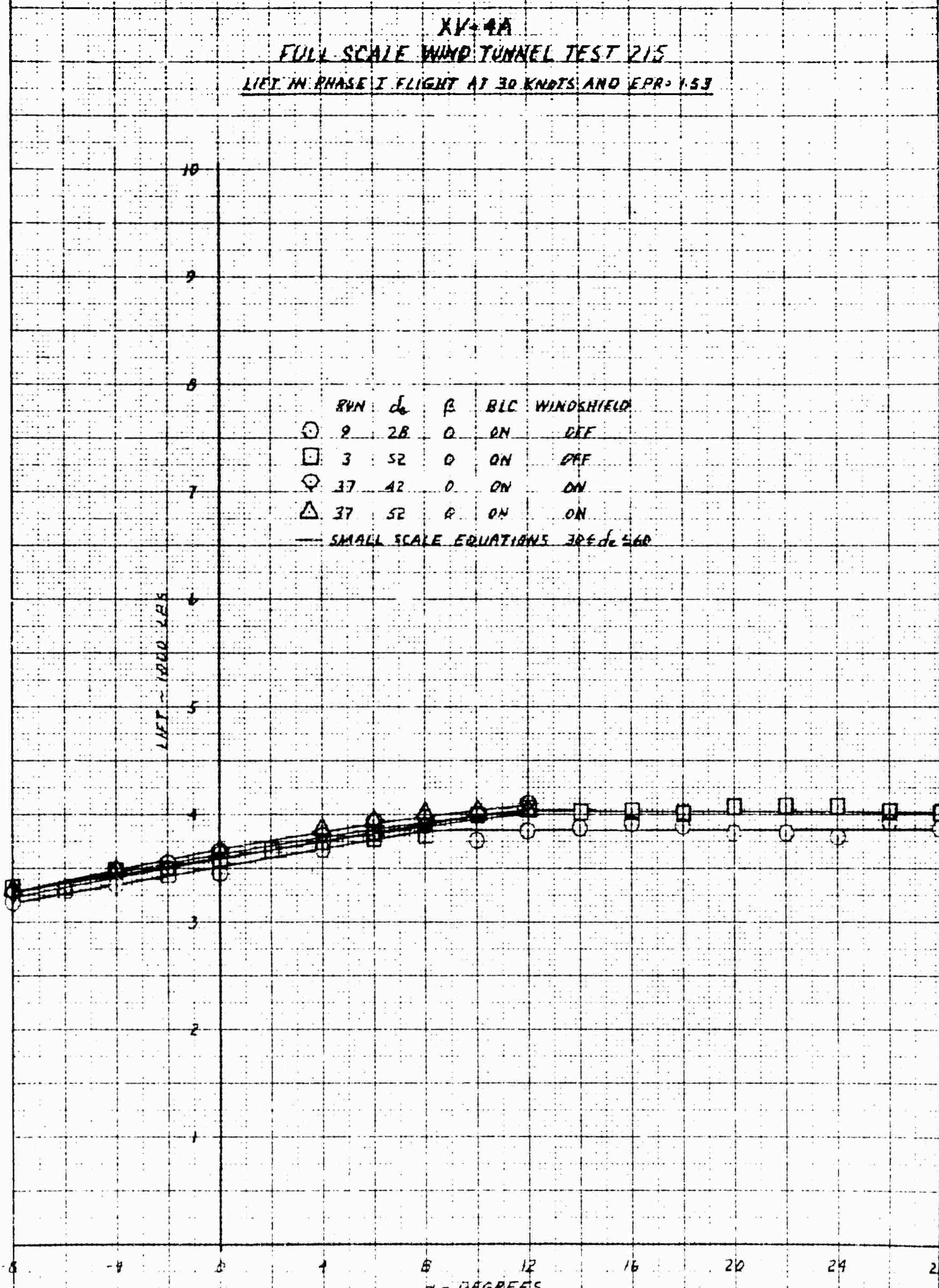
XV-4A
FULL SCALE WIND TUNNEL TEST 215
LIFT IN PHASE I FLIGHT AT 30 KNOTS AND EPR=1.53
RUN δe β BLC WINDSHIELD
9 28 0 ON OFF
3 52 0 ON OFF
37 42 0 ON ON
37 52 0 ON ON
SMALL SCALE EQUATIONS 38≤δe≤60
LIFT ~ 1000 LBS
α - DEGREES
10
9
8
7
6
5
4
3
2
1
-8
-4
0
4
8
12
16
20
24
28

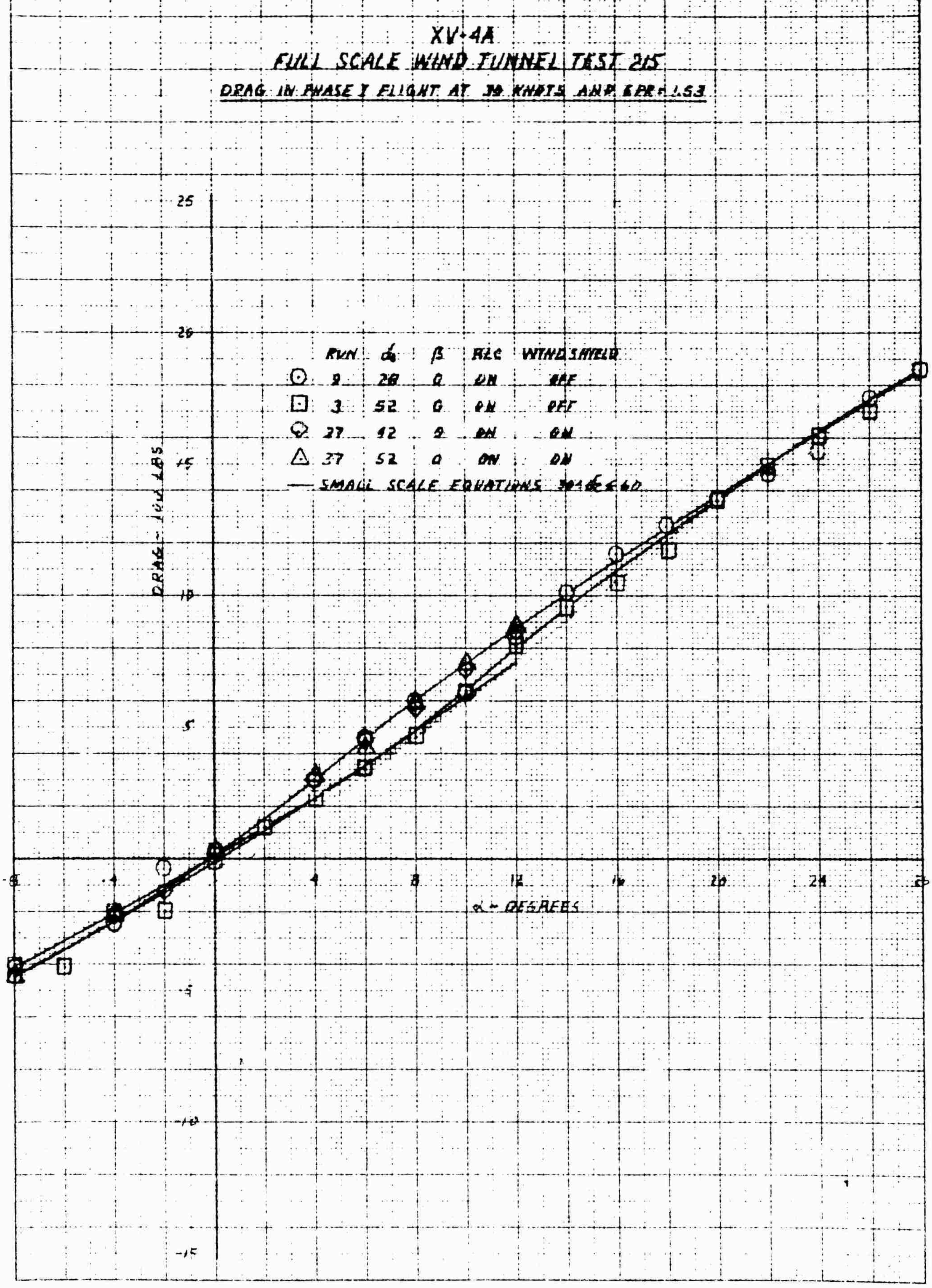
XV-4A
FULL SCALE WIND TUNNEL TEST 215
RUN
β
WINDSHIELD
9
3
52
37
42
52
ON
OFF
SMALL SCALE EQUATIONS
α - DEGREES
25
20
15
10
5
-5
-10
-15
4
8
12
16
20
24

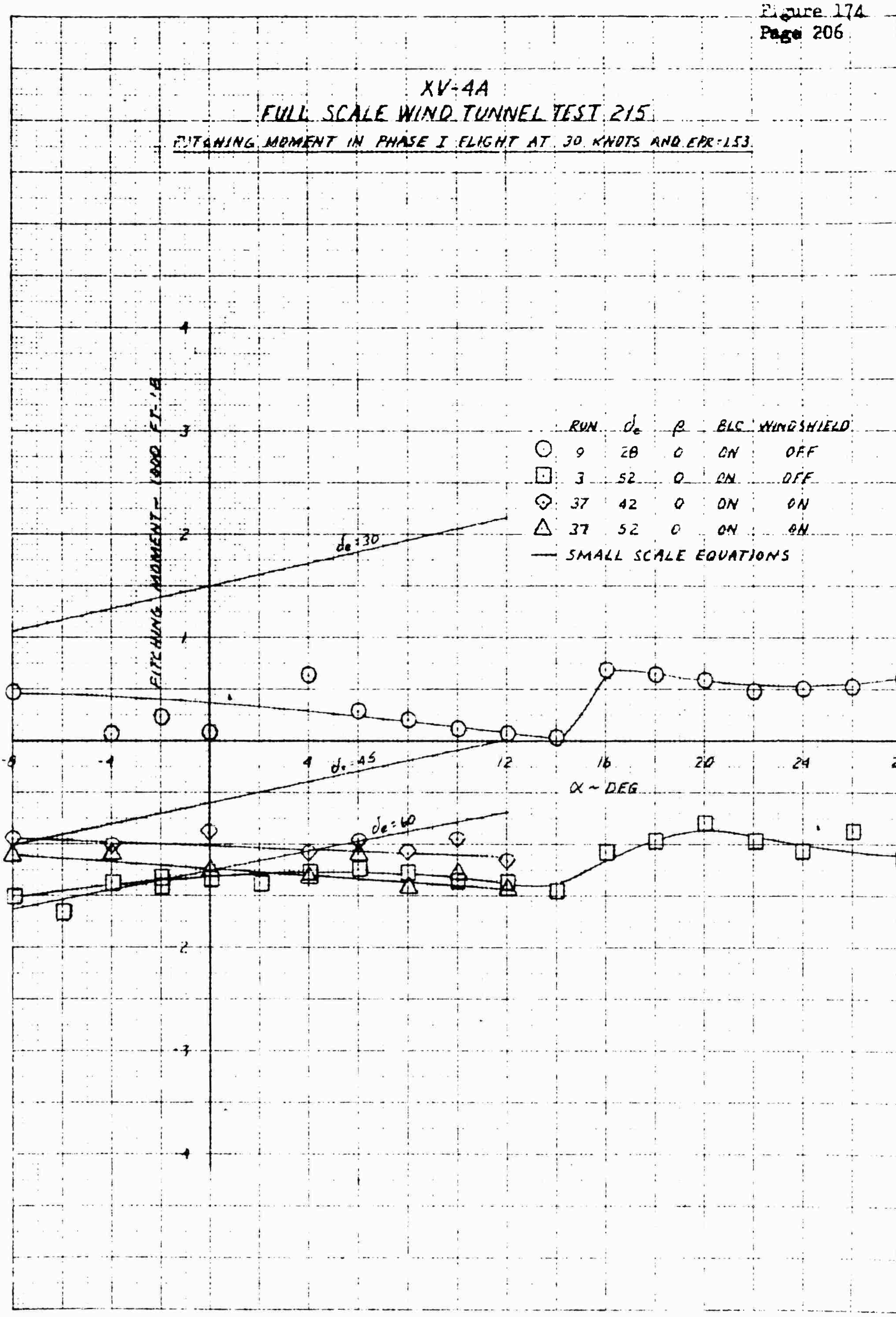
XV-4A
FULL SCALE WIND TUNNEL TEST 215
PITCHING MOMENT IN PHASE I FLIGHT AT 30 KNOTS AND EPR-1.53
PITCHING MOMENT - 1000 FT-LB
α ~ DEG
RUN δe β BLC WINDSHIELD
9 28 0 ON OFF
3 52 0 ON OFF
37 42 0 ON ON
37 52 0 ON ON
— SMALL SCALE EQUATIONS
δe=30
δe=45
δe=60

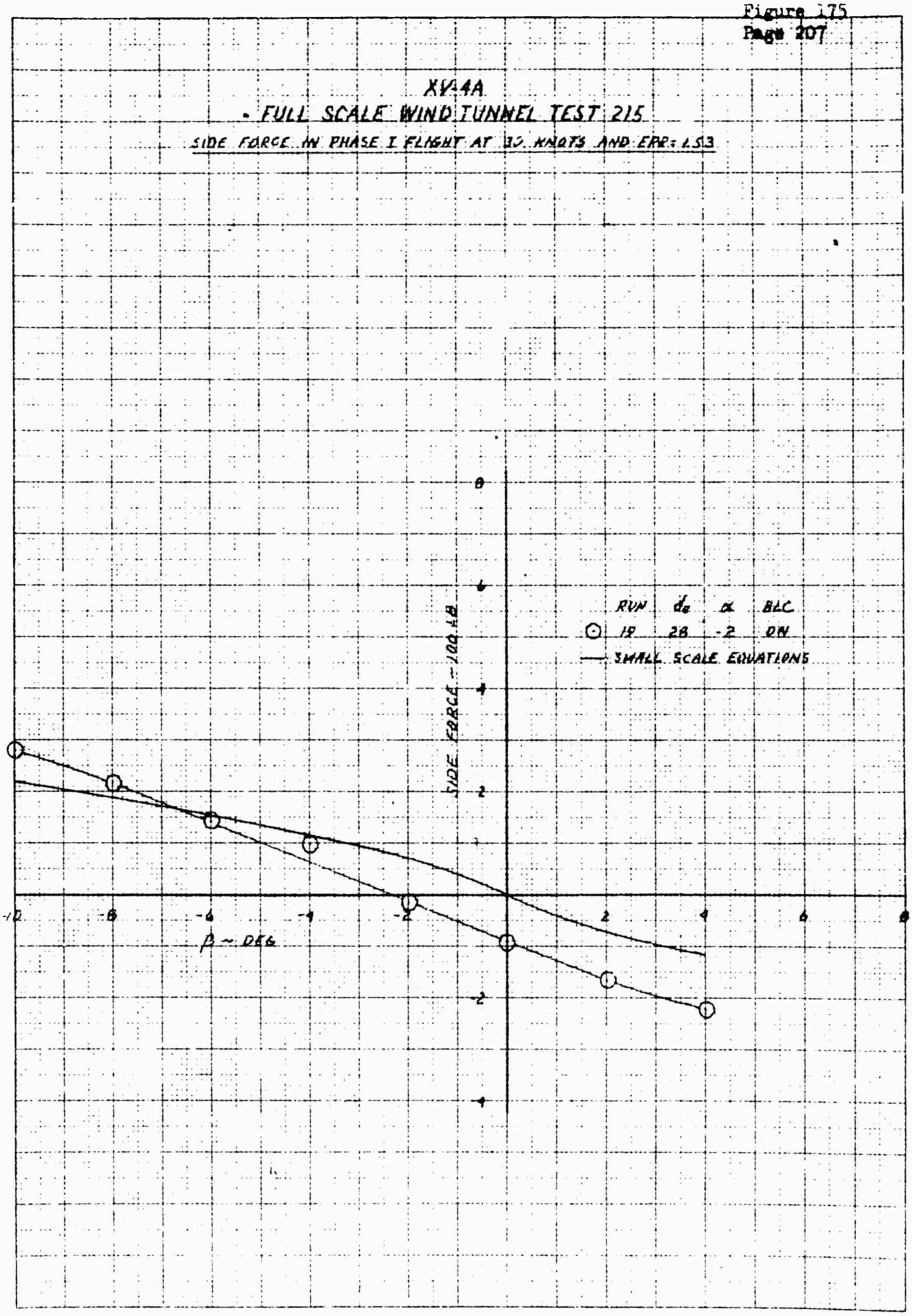
XV-4A
FULL SCALE WIND TUNNEL TEST 215
SIDE FORCE IN PHASE I FLIGHT AT 35 KNOTS AND EPR: 1.53
RUN
δ_e
α
BLC
19
28
-2
ON
SMALL SCALE EQUATIONS
SIDE FORCE ~ 100 LB
β ~ DEG
-10
-8
-6
-4
-2
2
4
6
8
8
6
4
2
-2
-4

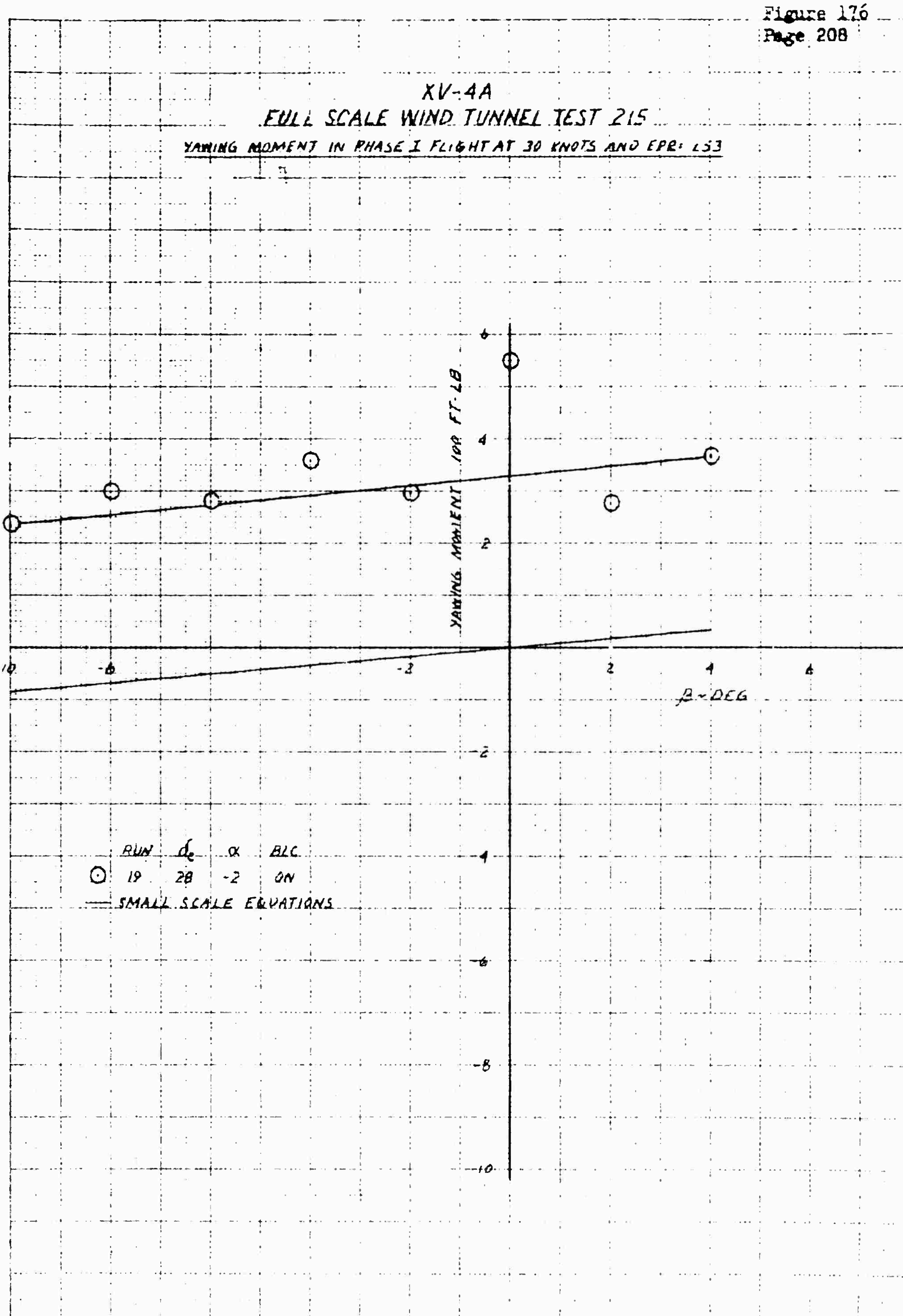
XV-4A
FULL SCALE WIND TUNNEL TEST 215
YAWING MOMENT IN PHASE I FLIGHT AT 30 KNOTS AND EPR: 1.53
YAWING MOMENT 1000 FT-LB
β ~ DEG
RUN δe α BLC
19 28 -2 ON
SMALL SCALE EQUATIONS

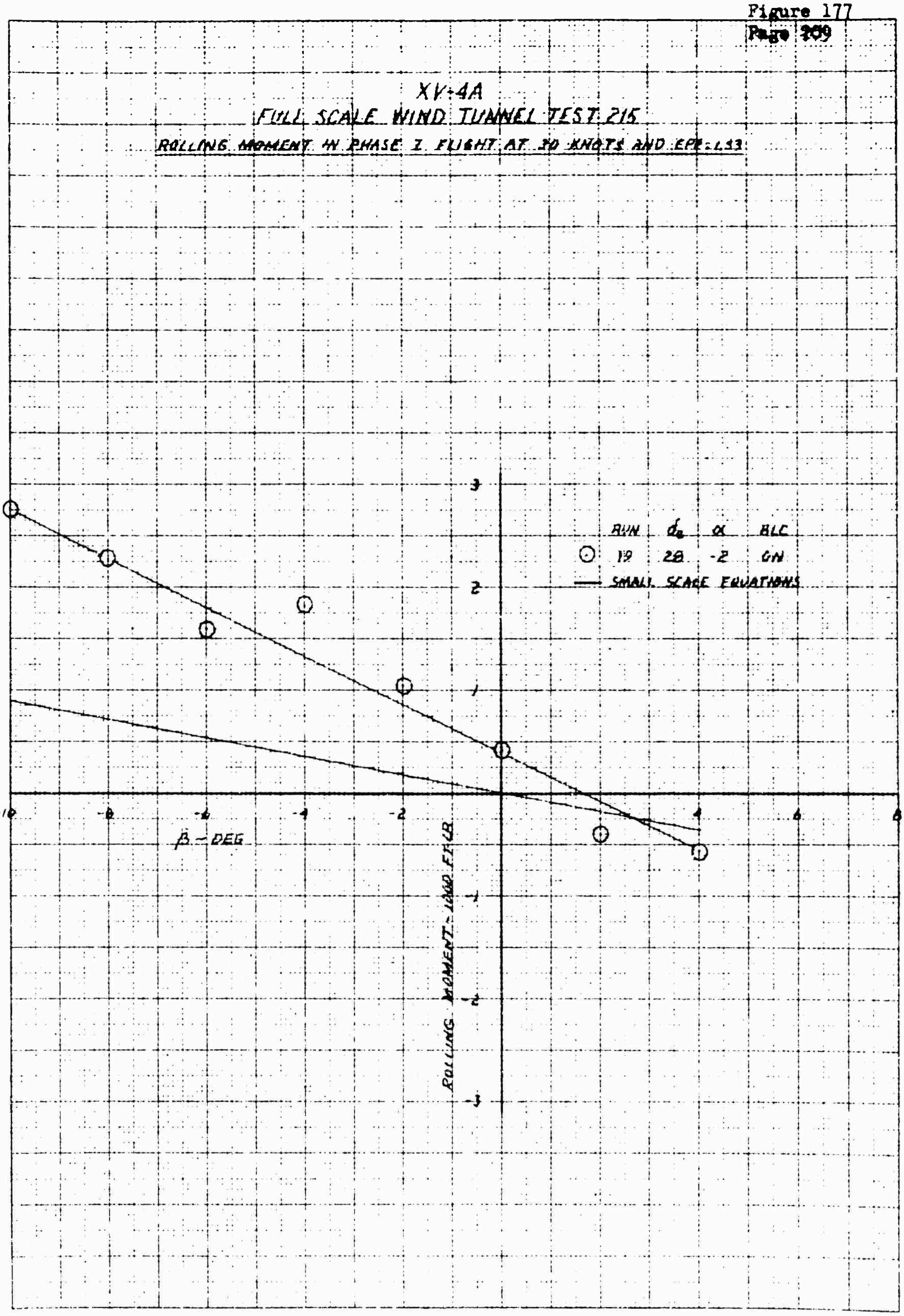
XV-4A
FULL SCALE WIND TUNNEL TEST 215
ROLLING MOMENT IN PHASE I FLIGHT AT 30 KNOTS AND EPR=1.33
RUN δ_a α BLC
19 28 -2 ON
SMALL SCALE EQUATIONS
β – DEG
ROLLING MOMENT – 1000 FT-LB
-10
-8
-6
-4
-2
4
6
8
3
2
1
-1
-2
-3

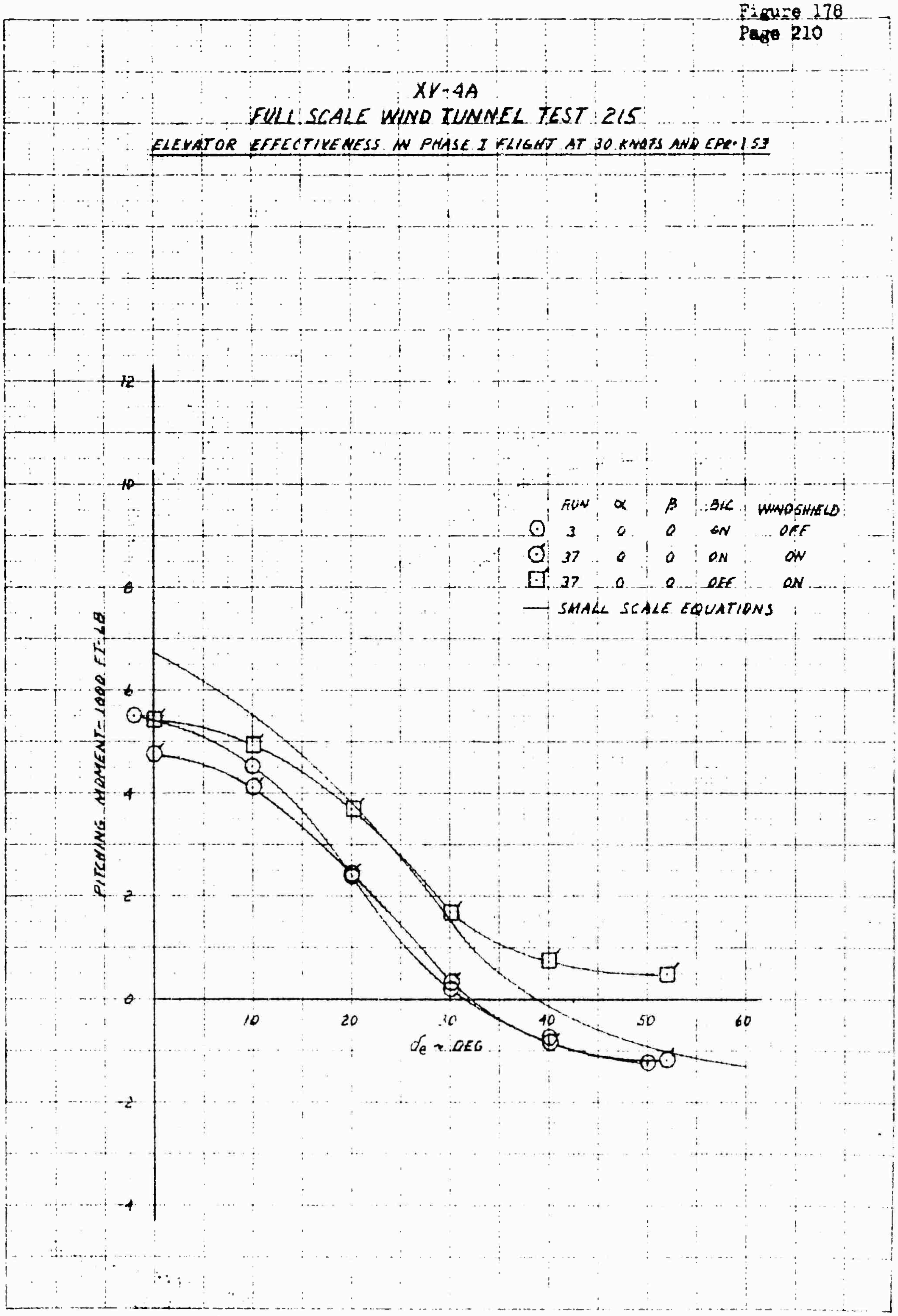
XV-4A
FULL SCALE WIND TUNNEL TEST 215
ELEVATOR EFFECTIVENESS IN PHASE I FLIGHT AT 30 KNOTS AND EPR 1.53
RUN α β BLC WINDSHIELD
3 0 0 ON OFF
37 0 0 ON ON
37 0 0 OFF ON
SMALL SCALE EQUATIONS
PITCHING MOMENT - 1000 FT-LB
12
10
8
6
4
2
0
-2
-4
10
20
30
40
50
60
δe ~ DEG

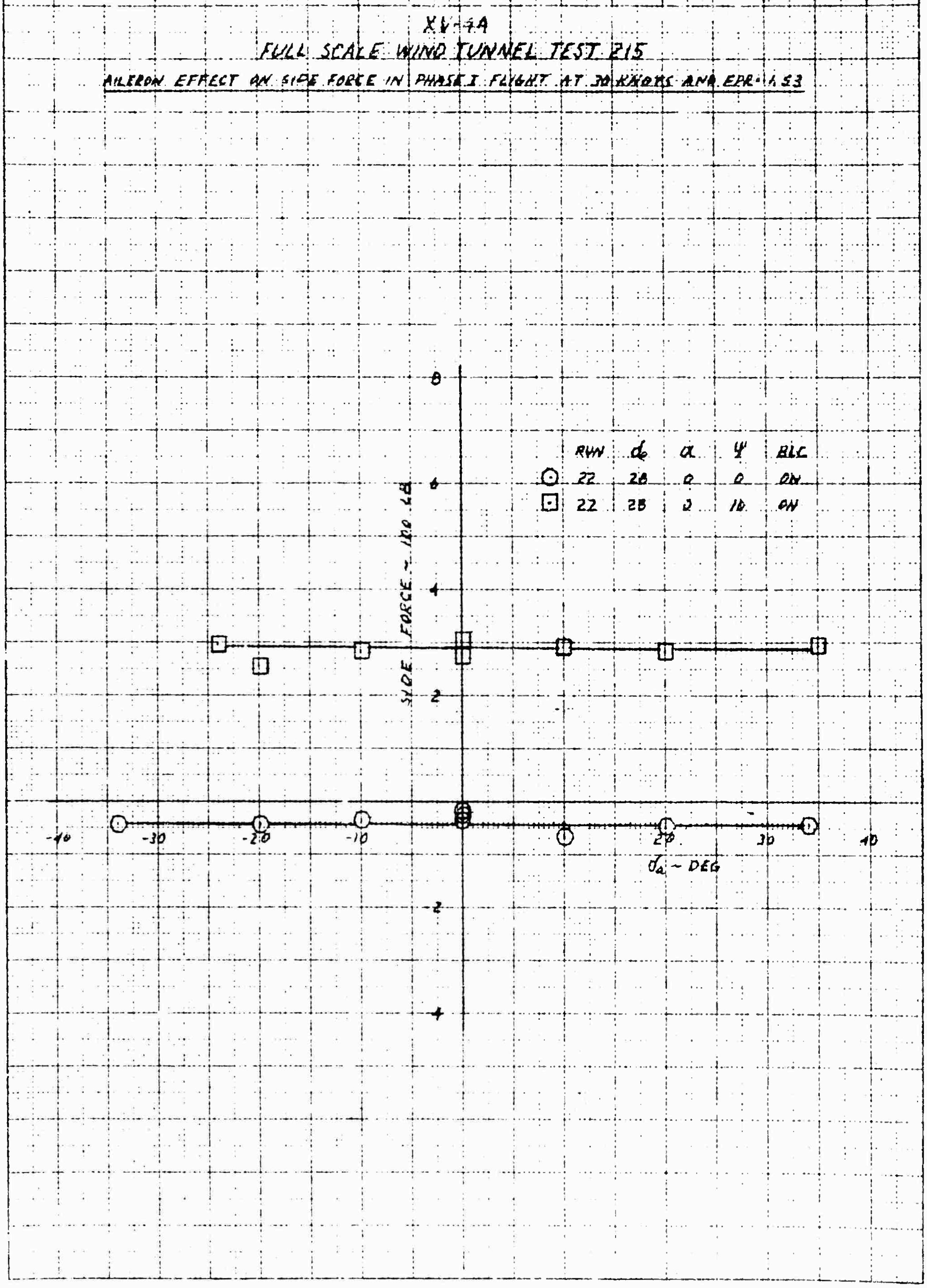
XV-4A
FULL SCALE WIND TUNNEL TEST 215
AILERON EFFECT ON SIDE FORCE IN PHASE I FLIGHT AT 30 KNOTS AND EPR = 1.53
RUN
δ_e
α
ψ
BLC
22
28
0
0
ON
22
28
0
10
ON
SIDE FORCE ~ 100 LB
8
6
4
2
-2
-4
-40
-30
-20
-10
20
30
40
δ_a ~ DEG

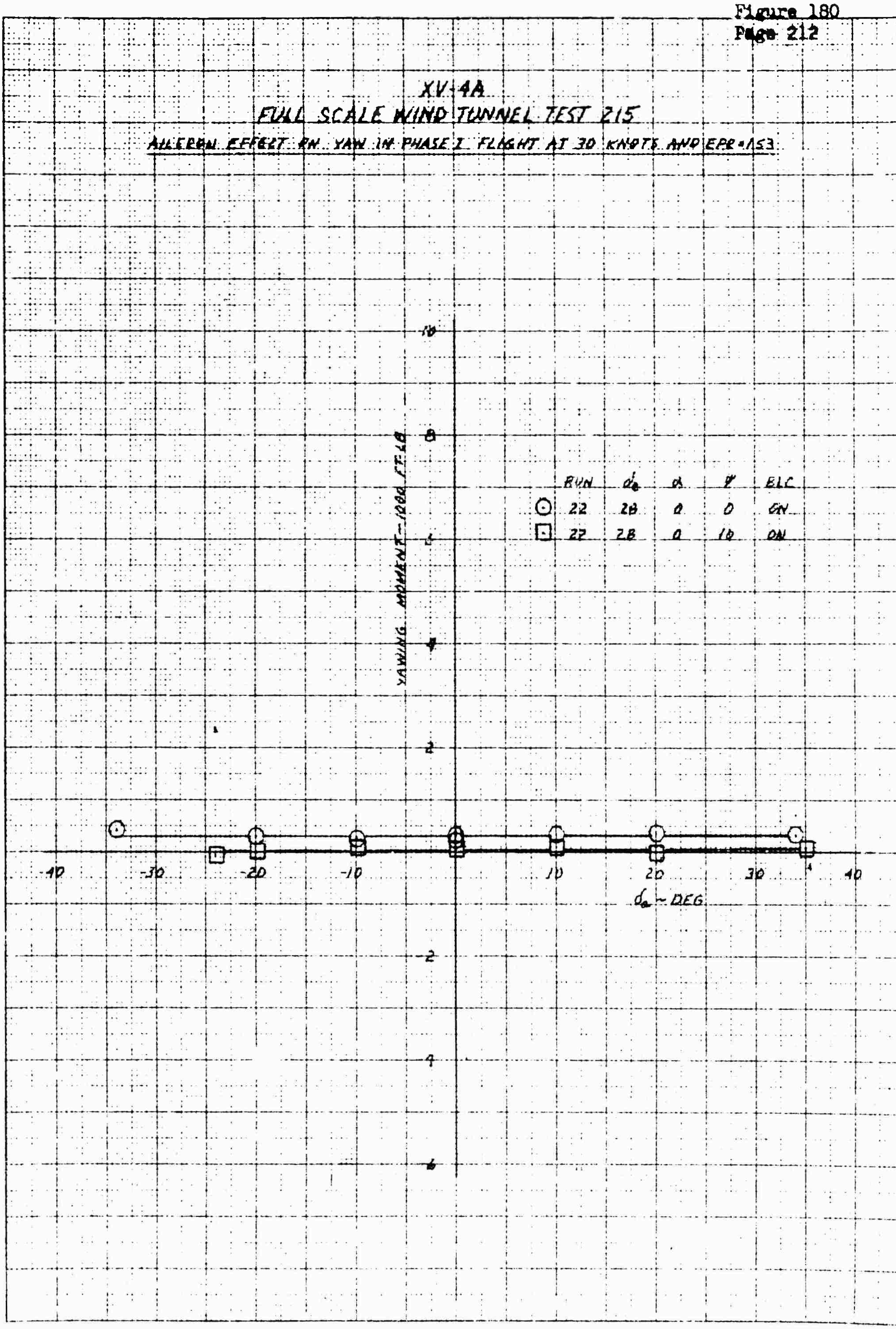
XV-4A
FULL SCALE WIND TUNNEL TEST 215
AILERON EFFECT ON YAW IN PHASE I FLIGHT AT 30 KNOTS AND EPR=1.53
YAWING MOMENT—1000 FT-LB
δa ~ DEG
RUN δe α ψ BLC
22 28 0 0 ON
22 28 0 10 ON

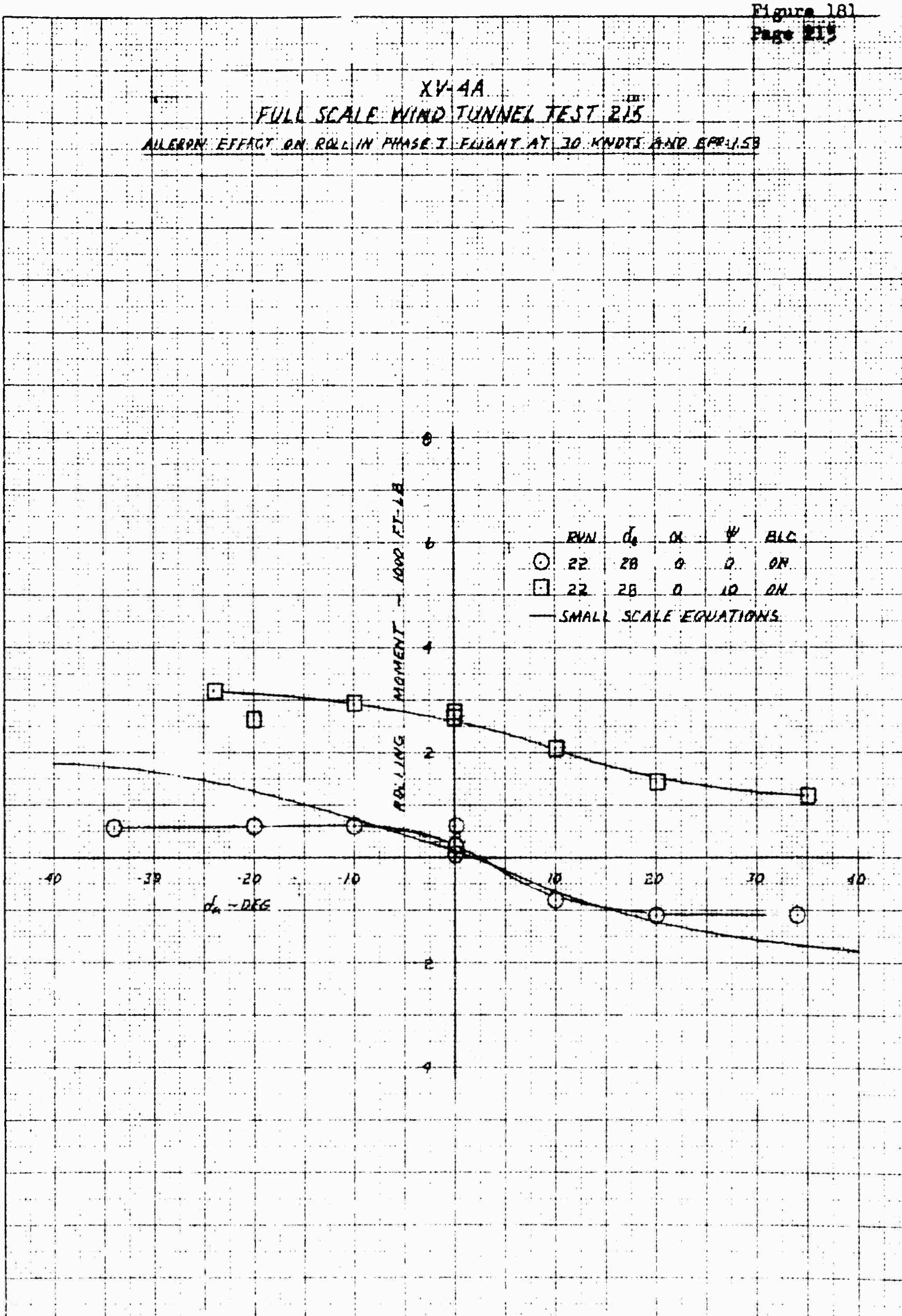
XV-4A
FULL SCALE WIND TUNNEL TEST 215
AILERON EFFECT ON ROLL IN PHASE I FLIGHT AT 30 KNOTS AND EPR=1.58
RUN
22
22
28
28
0
0
0
10
BLC
ON
ON
SMALL SCALE EQUATIONS
ROLLING MOMENT - 1000 FT-LB
8
6
4
2
2
4
-40
-30
-20
-10
10
20
30
40
δa - DEG

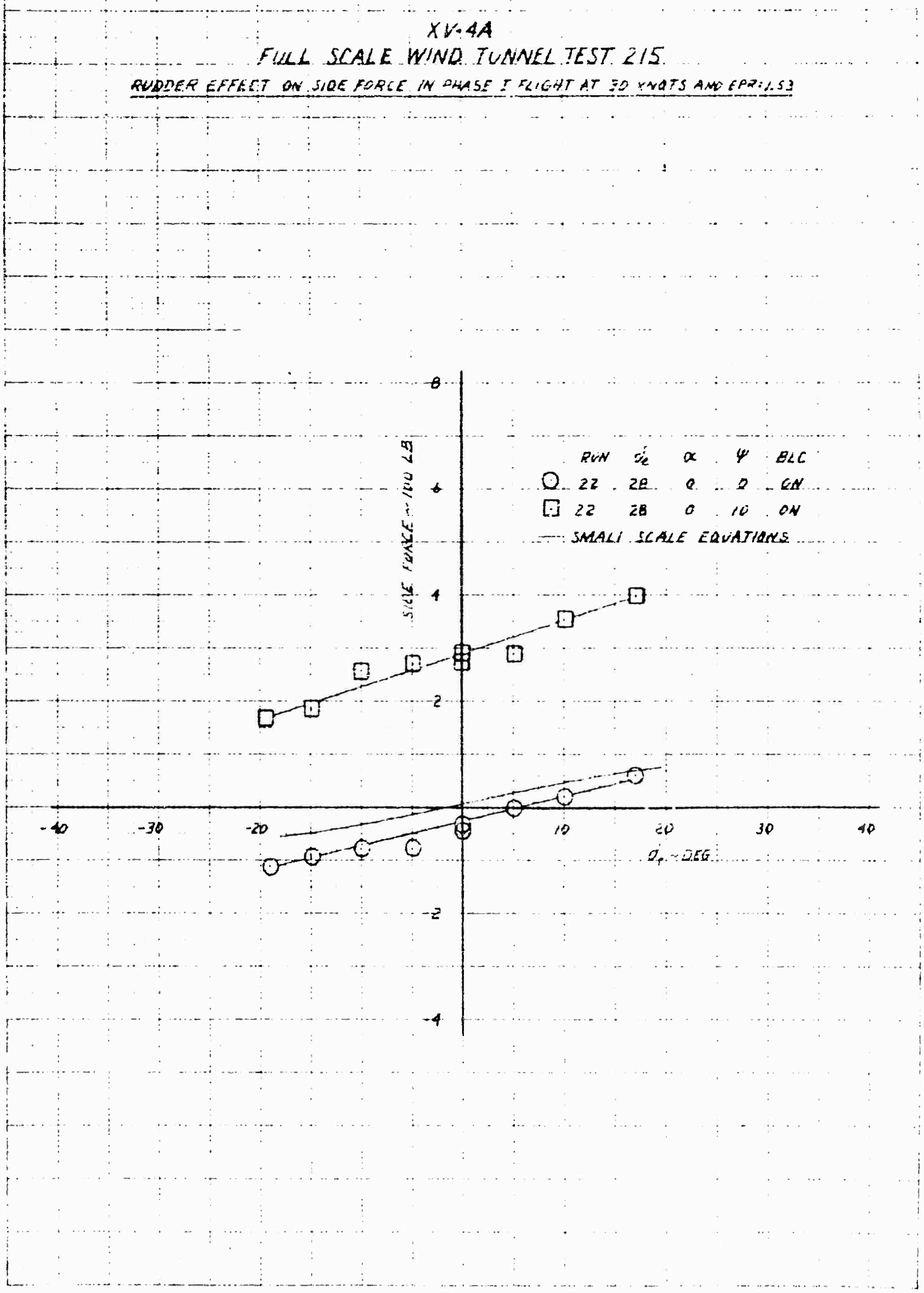
XV-4A
FULL SCALE WIND TUNNEL TEST 215
RUDDER EFFECT ON SIDE FORCE IN PHASE I FLIGHT AT 30 KNOTS AND EPR=1.53
RUN δ α ψ BLC
22 28 0 0 ON
22 28 0 10 ON
SMALL SCALE EQUATIONS
SIDE FORCE ~ 100 LB
δr ~ DEG
8
6
4
2
-2
-4
-40
-30
-20
10
20
30
40

XV-4A

FULL SCALE WIND TUNNEL TEST 215

RUDDER EFFECT ON YAW IN PHASE I FLIGHT AT 30 KNOTS AND EPR=1.53

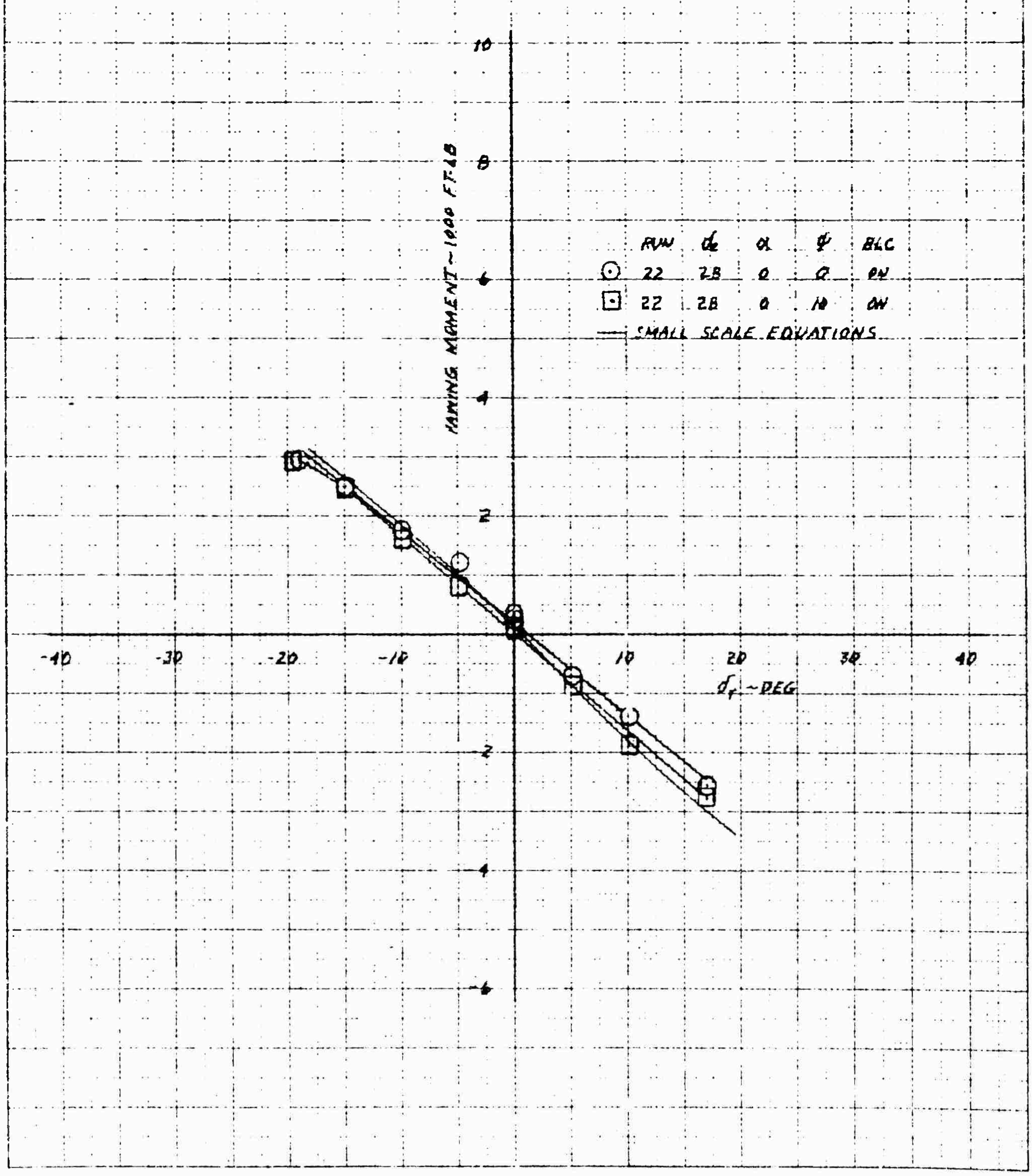

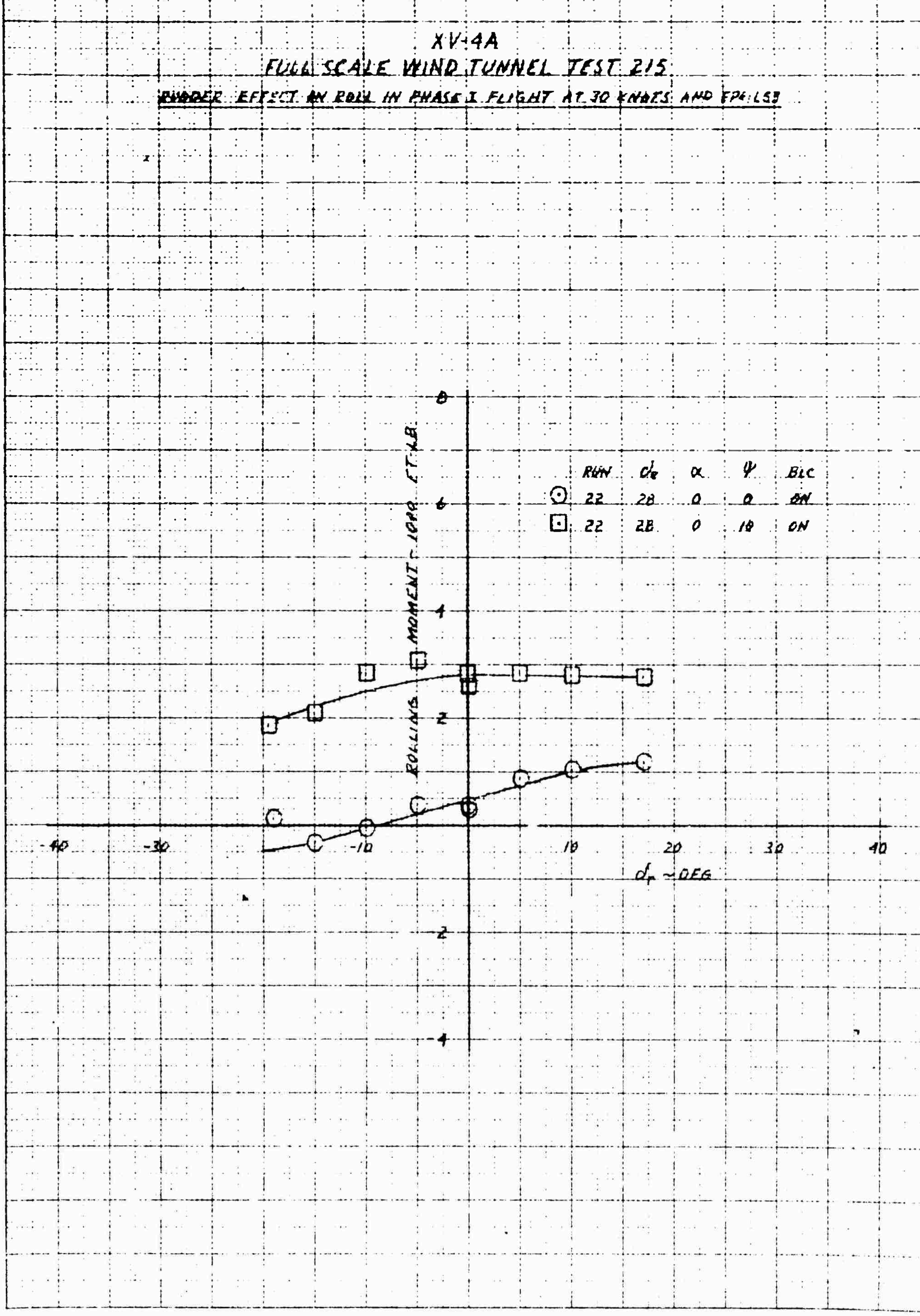
XV-4A
FULL SCALE WIND TUNNEL TEST 215
RUDDER EFFECT ON ROLL IN PHASE I FLIGHT AT 30 KNOTS AND EPI LS3
ROLLING MOMENT ~ 1000 FT-LB
RUN
22
22
28
28
0
0
0
10
BLC
ON
ON
8
6
4
2
-2
-4
-40
-30
-10
10
20
30
40
~ DEG

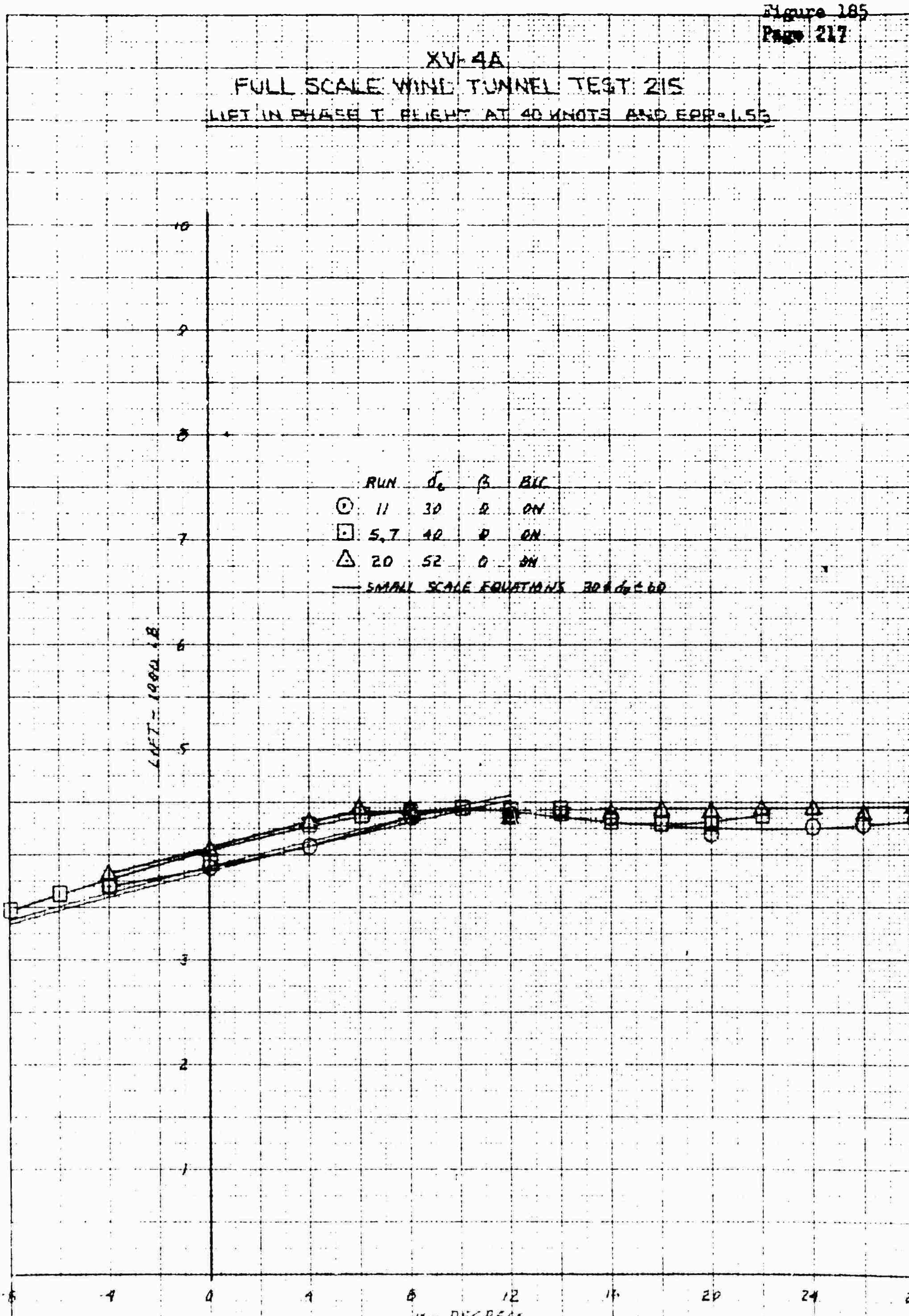
XV-4A
FULL SCALE WIND TUNNEL TEST 215
LIFT IN PHASE I FLIGHT AT 40 KNOTS AND EPR=1.55
RUN
δ
β
BLC
11
30
0
ON
5,7
40
0
ON
20
52
0
ON
SMALL SCALE EQUATIONS 30≤δ≤60
LIFT - 1000 LB
10
9
8
7
6
5
3
2
1
-8
-4
0
4
8
12
16
20
24
28
α ~ DEGREES

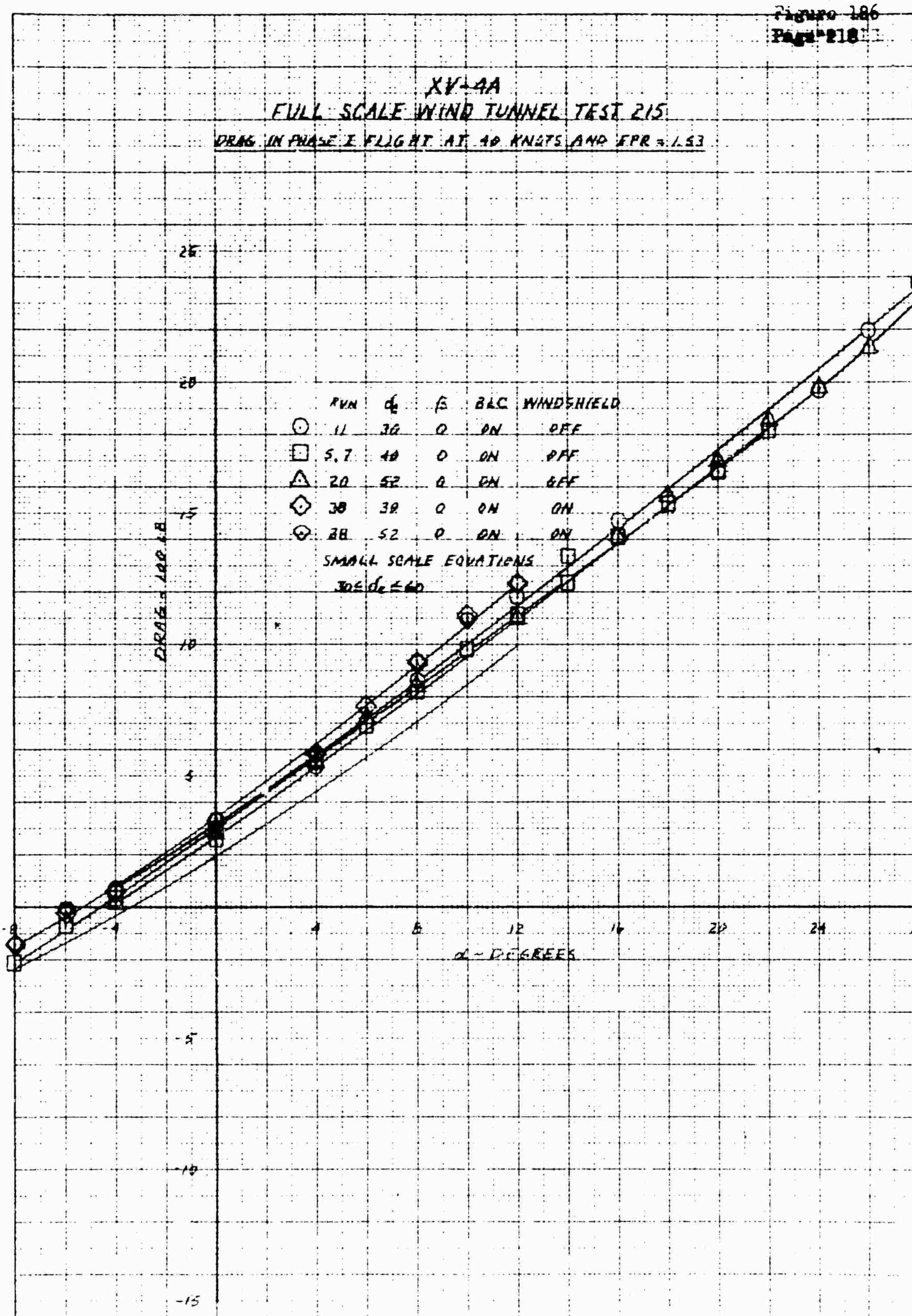
XV-4A
FULL SCALE WIND TUNNEL TEST 215
DRAG IN PHASE I FLIGHT AT 40 KNOTS AND EPR = 1.53
RUN
11
5, 7
20
38
38
30
40
52
30
52
0
BLC
ON
WINDSHIELD
OFF
SMALL SCALE EQUATIONS
DRAG ~ 100 LB
α ~ DEGREES

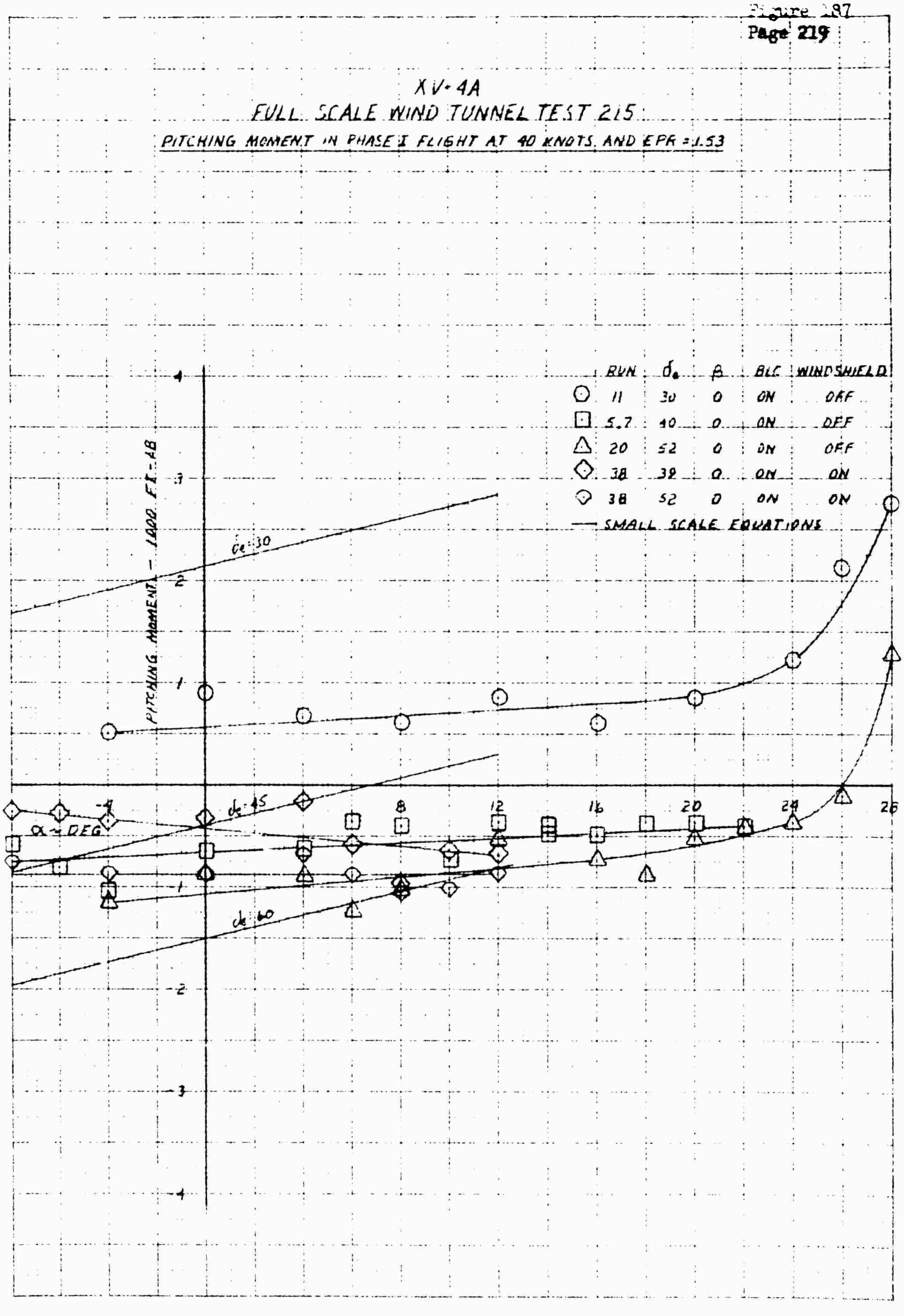
XV-4A
FULL SCALE WIND TUNNEL TEST 215
PITCHING MOMENT IN PHASE I FLIGHT AT 40 KNOTS AND EPR = 1.53
PITCHING MOMENT - 1000 FT-LB
α ~ DEG
RUN
δe
β
BLC
WINDSHIELD
11
30
0
ON
OFF
5,7
40
0
ON
OFF
20
52
0
ON
OFF
38
39
0
ON
ON
38
52
0
ON
ON
SMALL SCALE EQUATIONS
δe=30
δe=45
δe=60

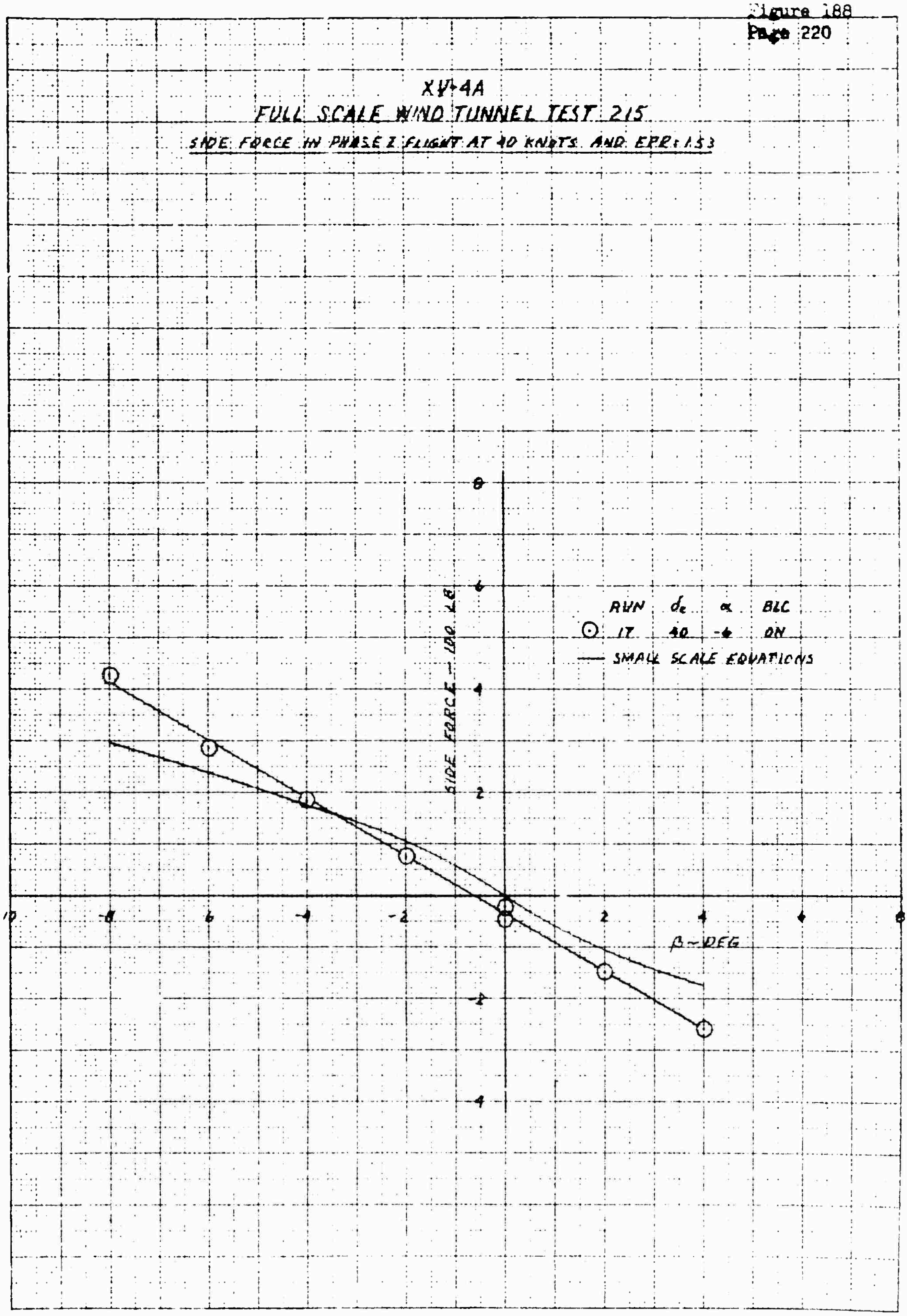
XV-4A
FULL SCALE WIND TUNNEL TEST 215
SIDE FORCE IN PHASE I FLIGHT AT 40 KNOTS AND EPR = 1.53
RUN δe α BLC
17 40 -6 ON
SMALL SCALE EQUATIONS
SIDE FORCE – 100 LB
β ~ DEG

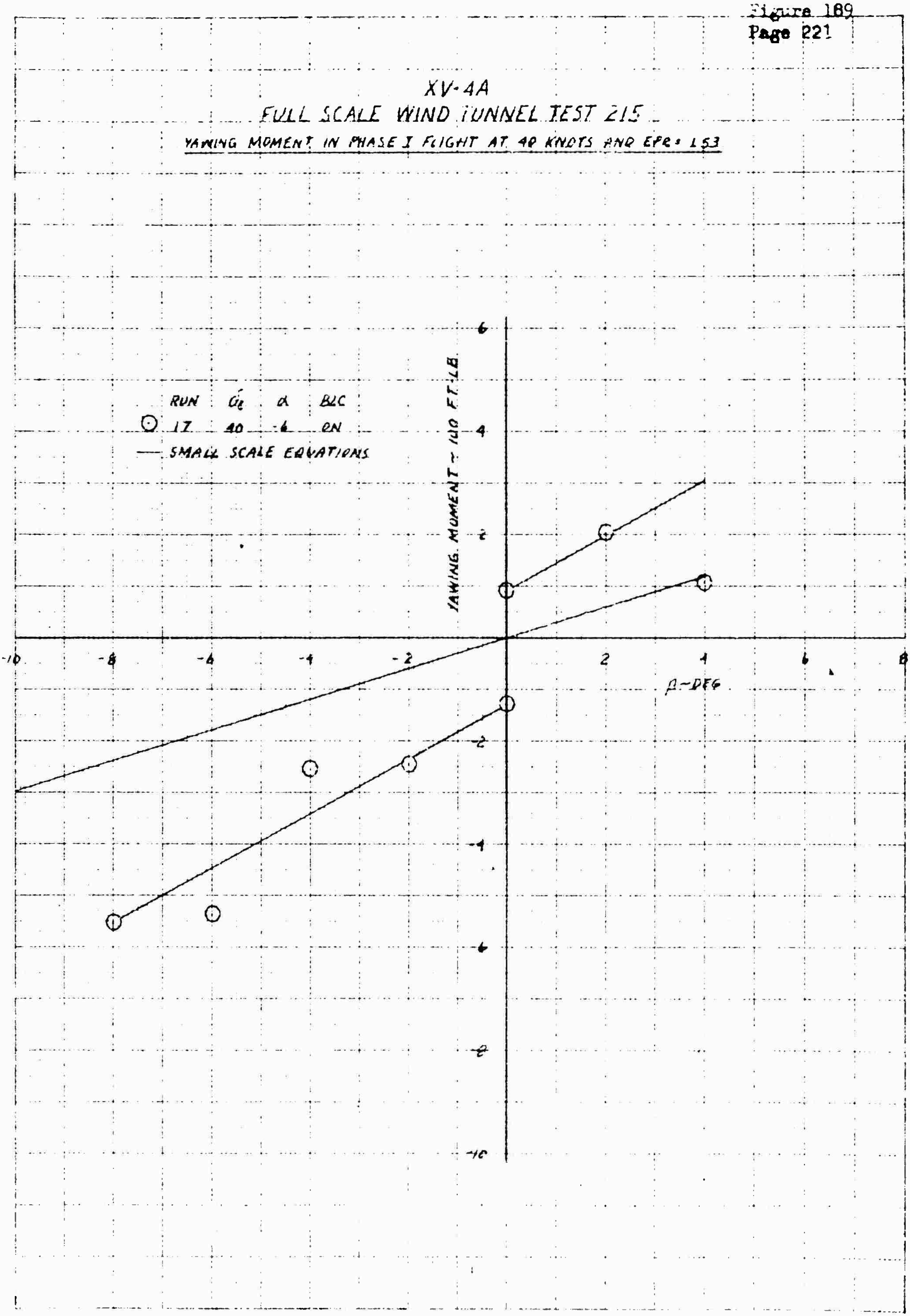
XV-4A
FULL SCALE WIND TUNNEL TEST 215
YAWING MOMENT IN PHASE I FLIGHT AT 40 KNOTS AND EPR = 1.53
RUN
δ_e
α
BLC
17
40
-6
ON
SMALL SCALE EQUATIONS
YAWING MOMENT ~ 100 FT-LB
β ~ DEG
-10
-8
-6
-4
-2
2
4
6
8
-10

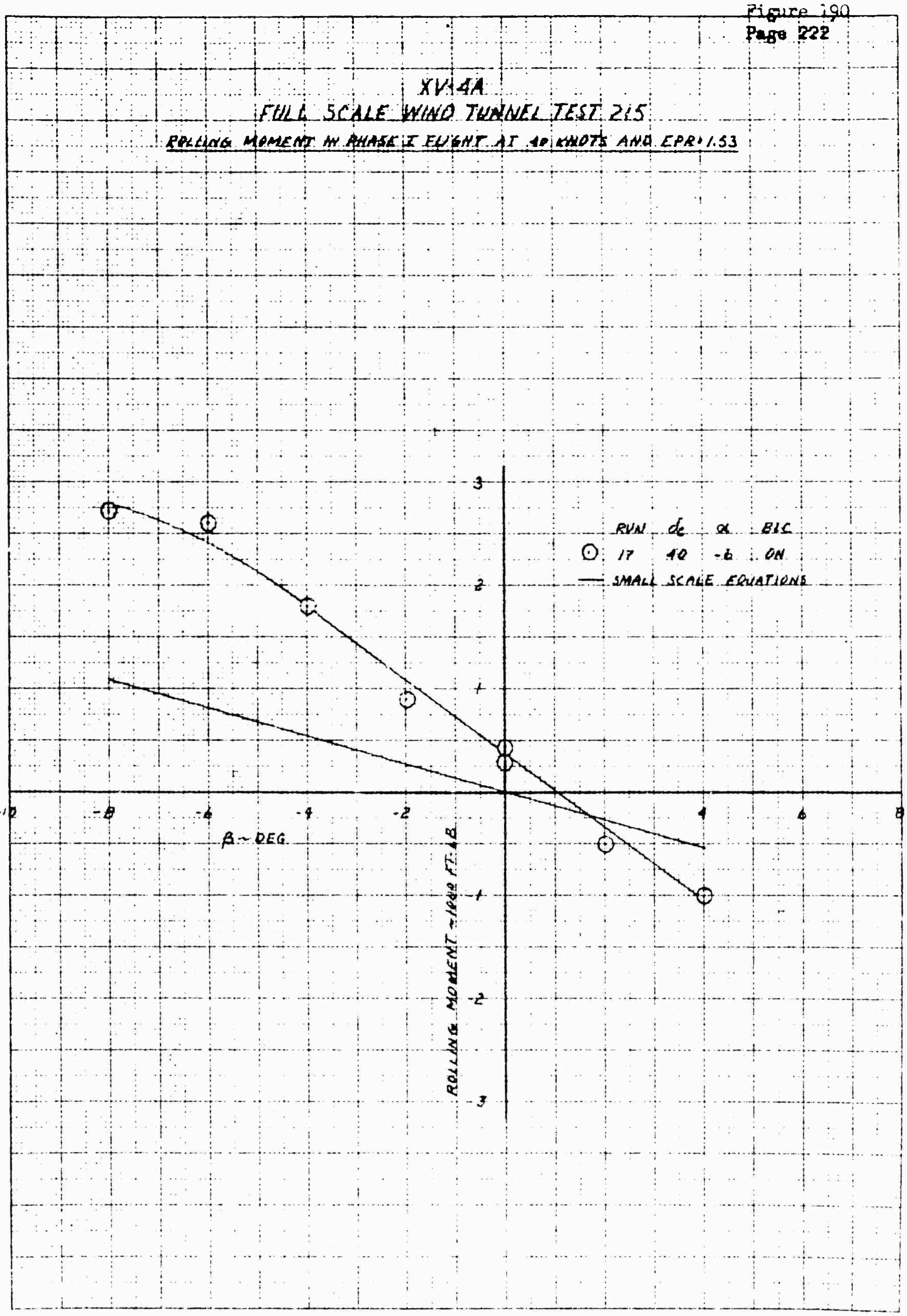
XV-4A
FULL SCALE WIND TUNNEL TEST 215
ROLLING MOMENT IN PHASE I FLIGHT AT 40 KNOTS AND EPR 1.53
RUN δe α BLC
17 40 -6 ON
SMALL SCALE EQUATIONS
β ~ DEG
ROLLING MOMENT ~1000 FT-LB
3
2
1
-1
-2
-3
-10
-8
-6
-4
-2
4
6
8

XV-4A
FULL SCALE WIND TUNNEL TEST 215
ELEVATOR EFFECTIVENESS IN PHASE I FLIGHT AT 40 KNOTS AND EPR=1.53

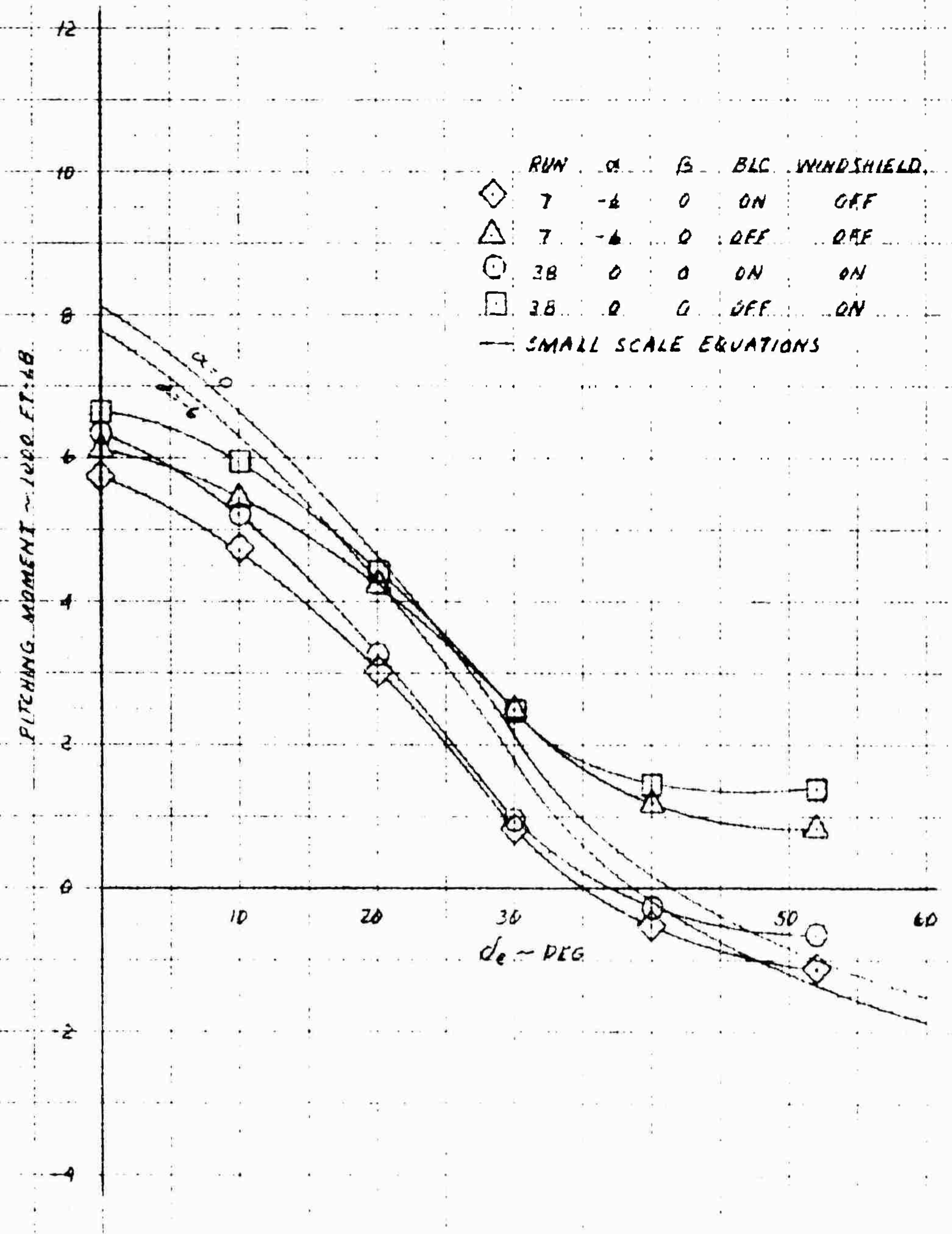

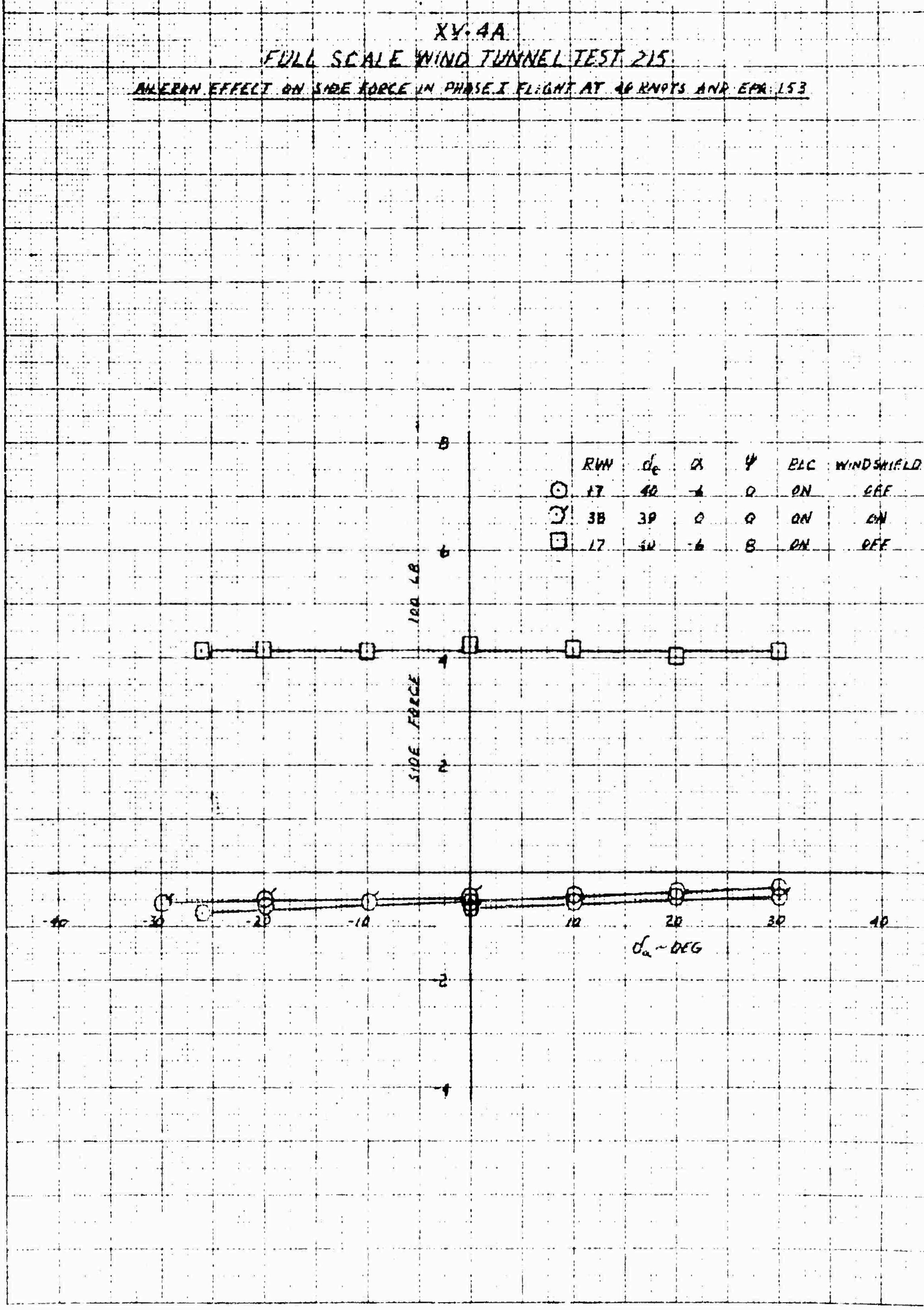
XV-4A
FULL SCALE WIND TUNNEL TEST 215
AILERON EFFECT ON SIDE FORCE IN PHASE I FLIGHT AT 40 KNOTS AND EPR 1.53
RUN
δ_e
α
ψ
BLC
WINDSHIELD
17 40 -6 0 ON OFF
38 39 0 0 ON ON
17 40 -6 8 ON OFF
SIDE FORCE 100 LB
8
6
4
2
-2
-4
-40
-30
-20
-10
10
20
30
40
δ_a ~ DEG

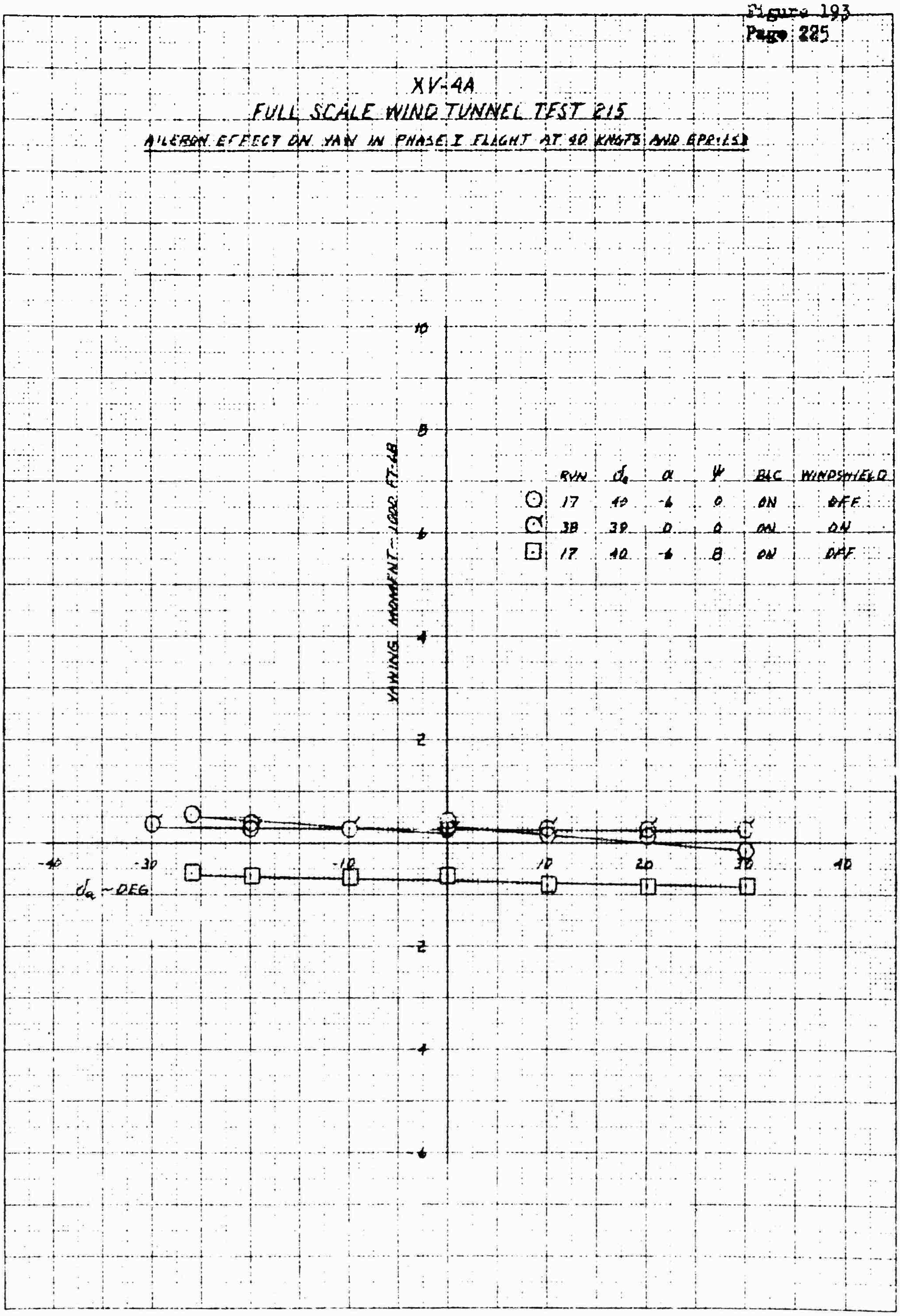
XV-4A
FULL SCALE WIND TUNNEL TEST 215
AILERON EFFECT ON YAW IN PHASE I FLIGHT AT 40 KNOTS AND EPR:1.5
RUN δa α ψ BLC WINDSHIELD
17 40 -6 0 ON OFF
38 39 0 0 ON ON
17 40 -6 8 ON OFF
YAWING MOMENT ~ 1000 FT-LB
10
8
6
4
2
-2
-4
-6
-40
-30
-10
10
20
30
40
δa ~ DEG

XV-4A
FULL SCALE WIND TUNNEL TEST 215
AILERON EFFECT ON ROLL IN PHASE I FLIGHT AT 40 KNOTS AND EFR-153

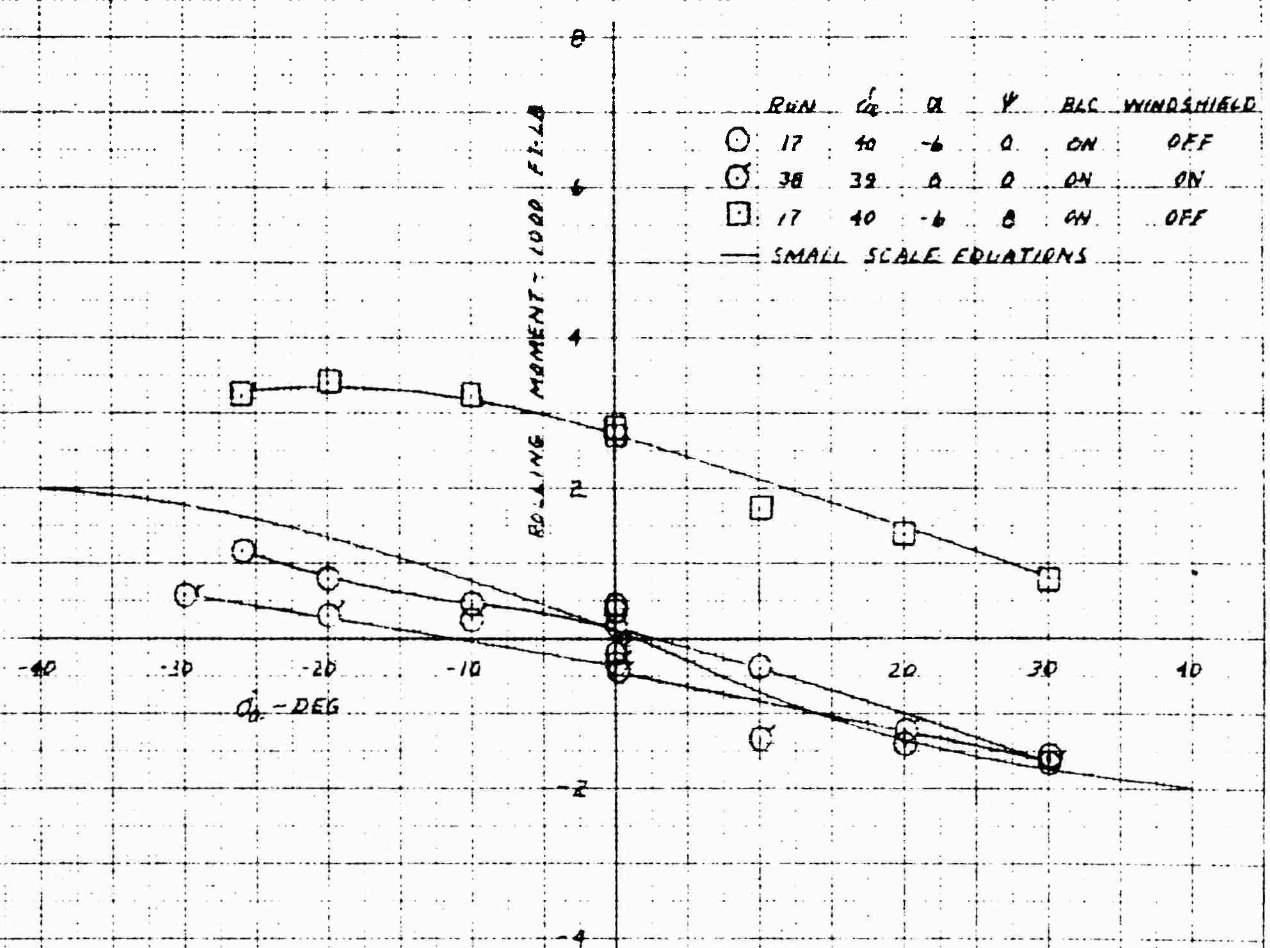

XV-4A
FULL SCALE WIND TUNNEL TEST 215
RUDDER EFFECT ON SIDE FORCE IN PHASE I FLIGHT AT 40 KNOTS AND EPR 1.53

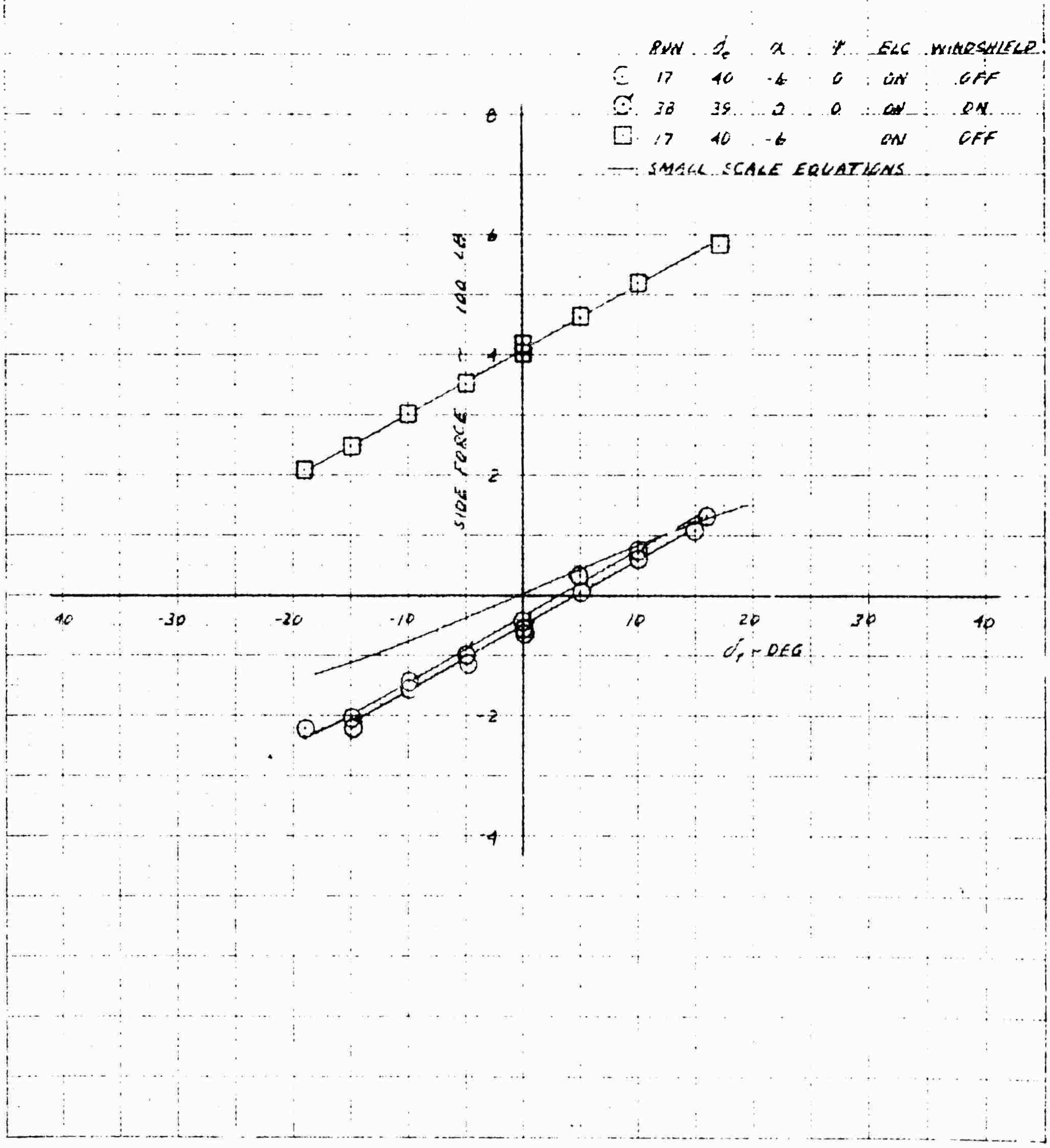

XV-4A

FULL SCALE WIND TUNNEL TEST 215

RUDDER EFFECT ON YAW IN PHASE I FLIGHT AT 40 KNOTS AND EPR=1.53

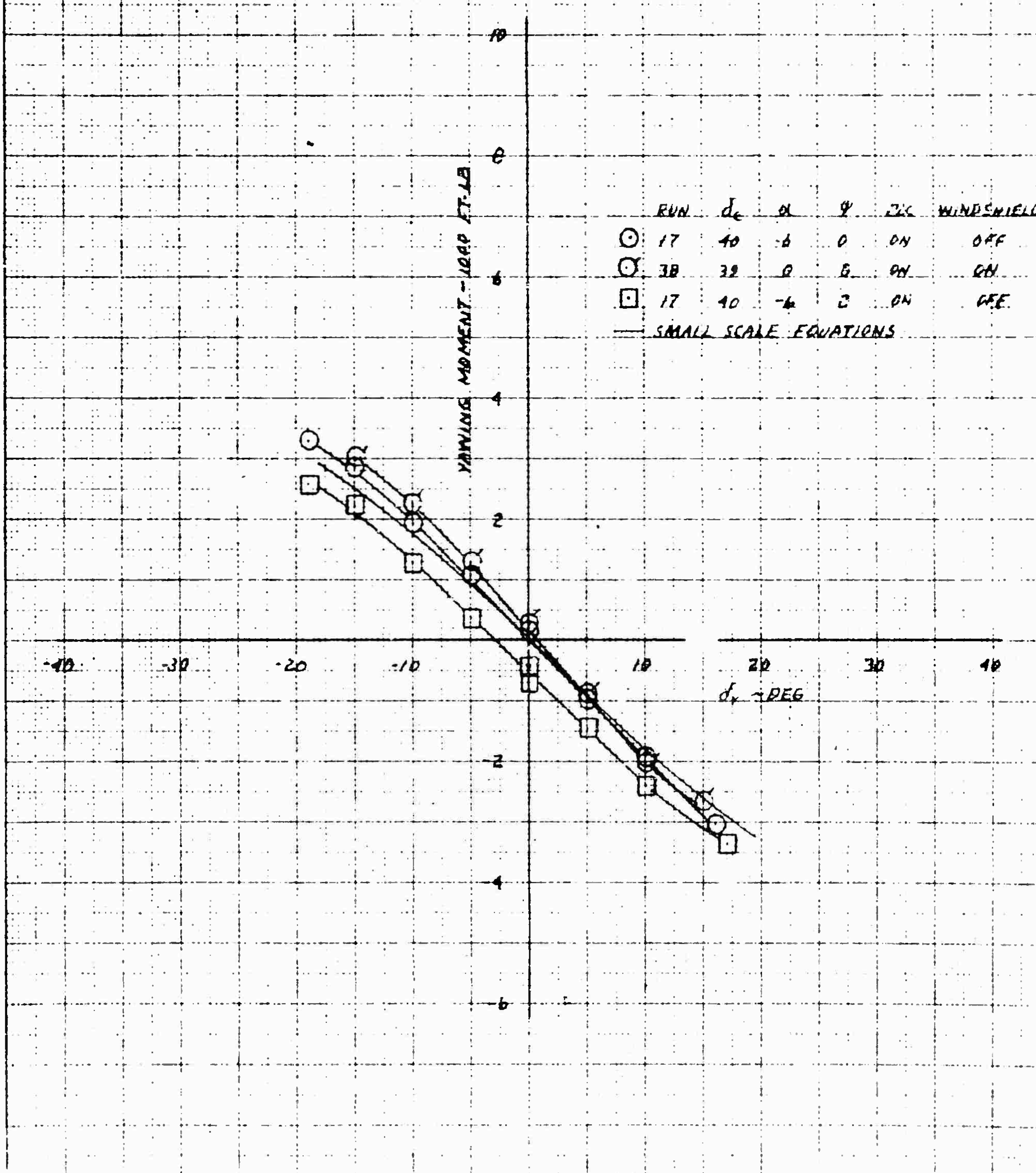

XV-4A
FULL SCALE WIND TUNNEL TEST 215
RUDDER EFFECT ON ROLL IN PHASE I FLIGHT AT 40 KNOTS AND EPR 1.53

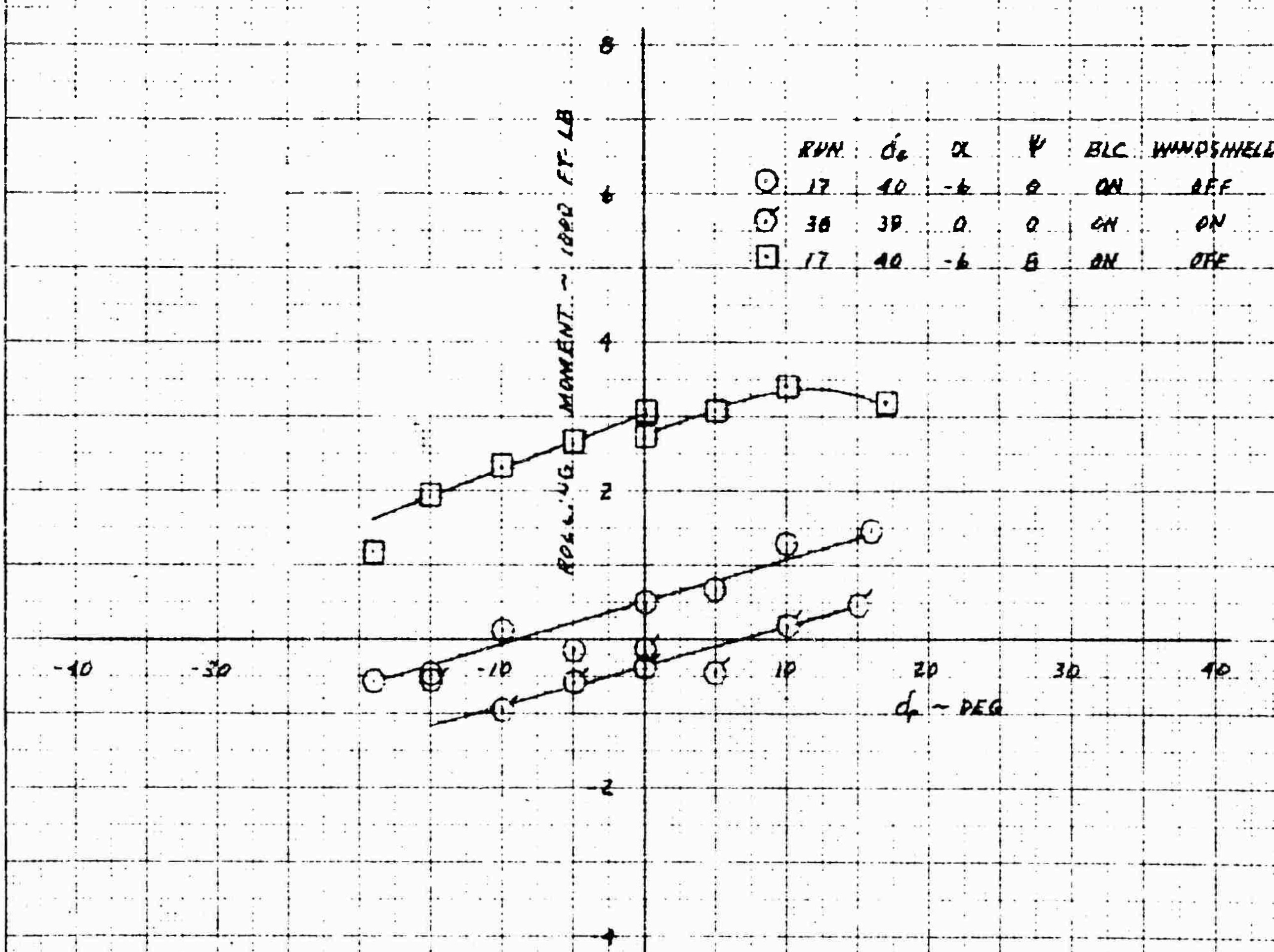

XV-4A
FULL SCALE WIND TUNNEL TEST 215
LIFT IN PHASE I FLIGHT AT 50 KNOTS AND EPR = 1.53

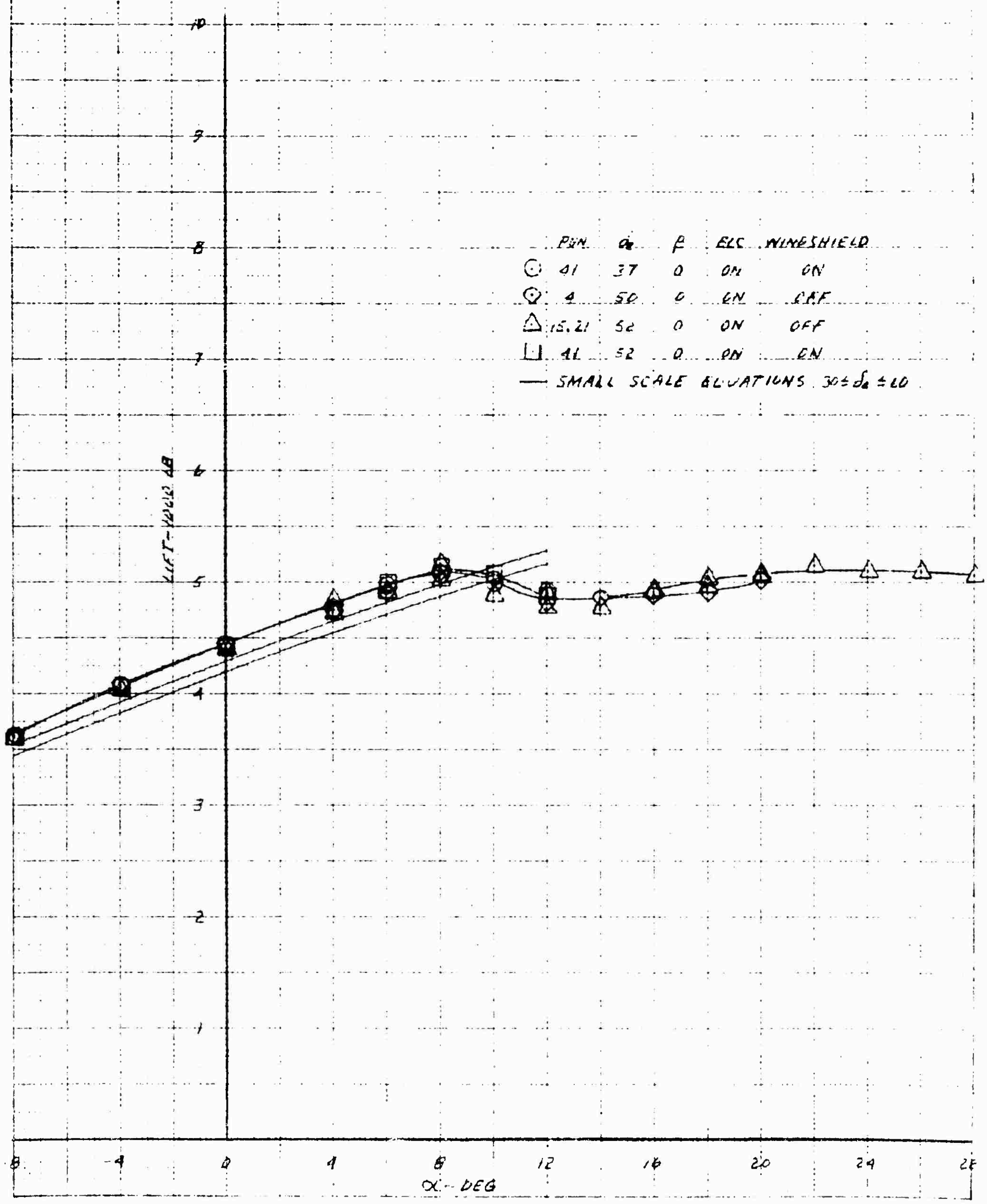

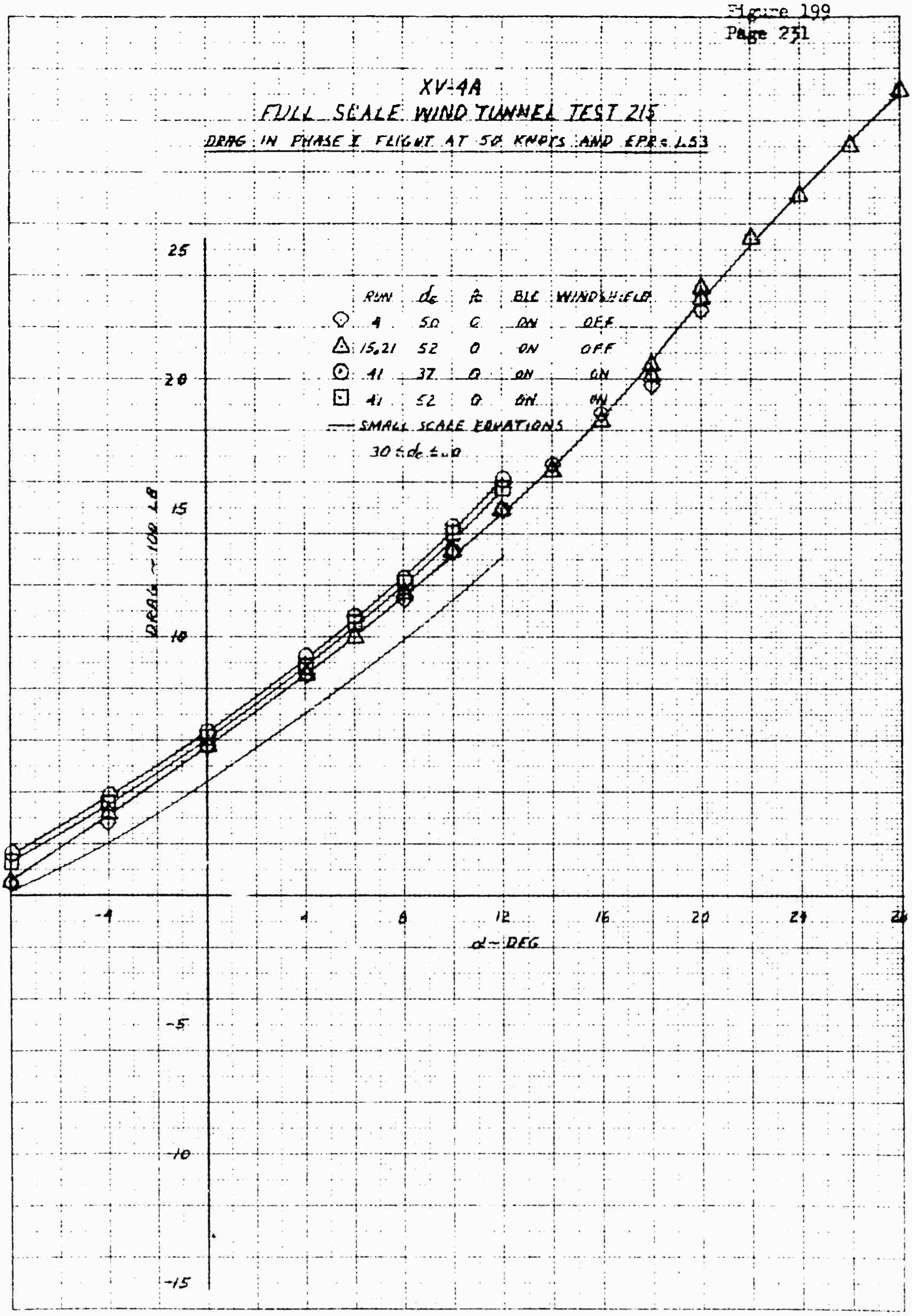
XV-4A
FULL SCALE WIND TUNNEL TEST 215
DRAG IN PHASE I FLIGHT AT 50 KNOTS AND EPR = 1.53
RUN
4
15,21
41
41
50
52
37
52
0
0
0
0
ON
ON
ON
ON
WINDSHIELD
OFF
OFF
ON
ON
SMALL SCALE EQUATIONS
DRAG ~ 100 LB
25
20
15
10
-5
-10
-15
-4
4
8
12
16
20
24
α ~ DEG

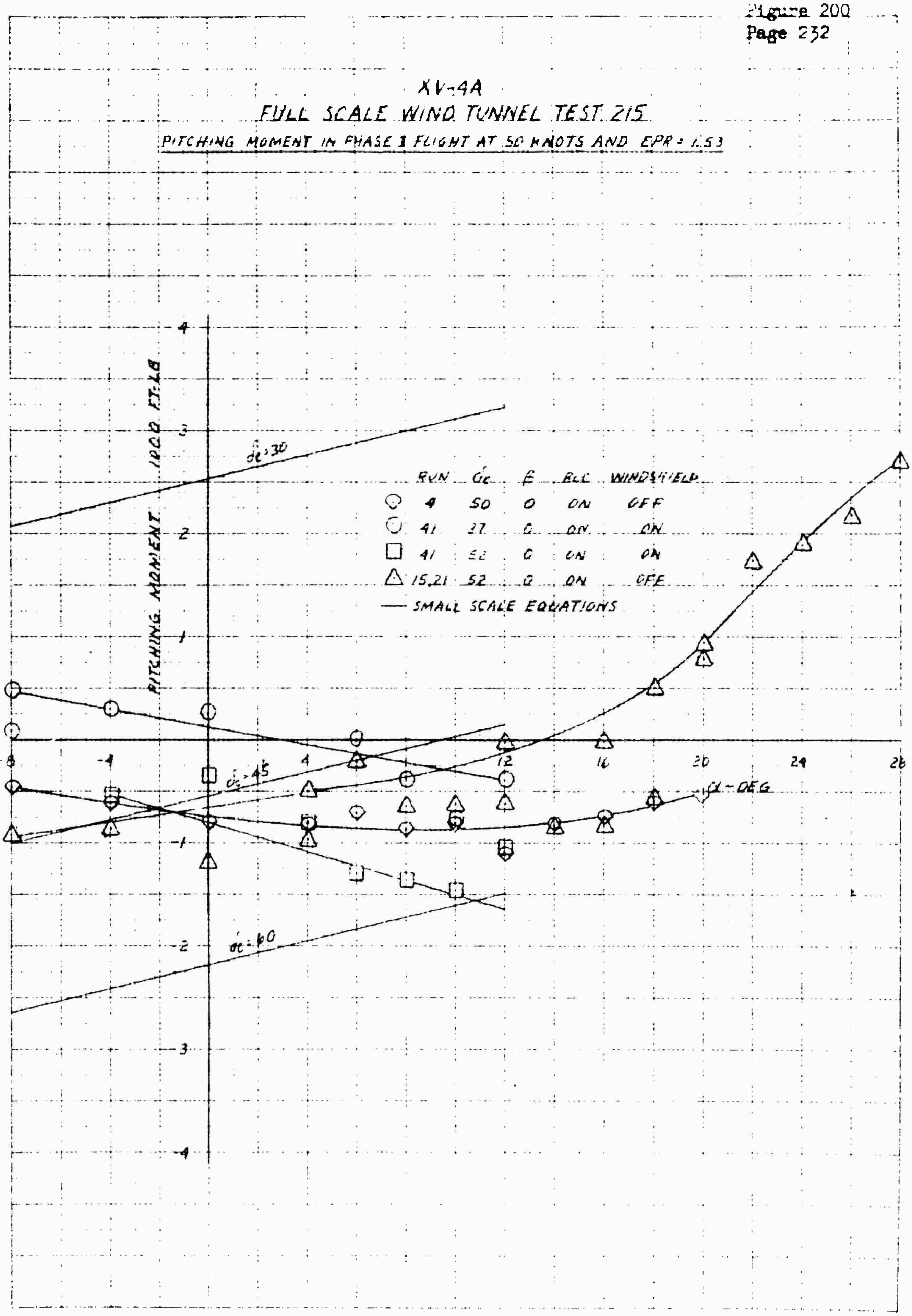
XV-4A
FULL SCALE WIND TUNNEL TEST 215
PITCHING MOMENT IN PHASE I FLIGHT AT 50 KNOTS AND EPR = 1.53
PITCHING MOMENT 1000 FT-LB
RUN
4
41
41
15,21
50
37
52
52
0
0
0
0
BLC
ON
ON
ON
ON
WINDSHIELD
OFF
ON
ON
OFF
SMALL SCALE EQUATIONS
α ~ DEG

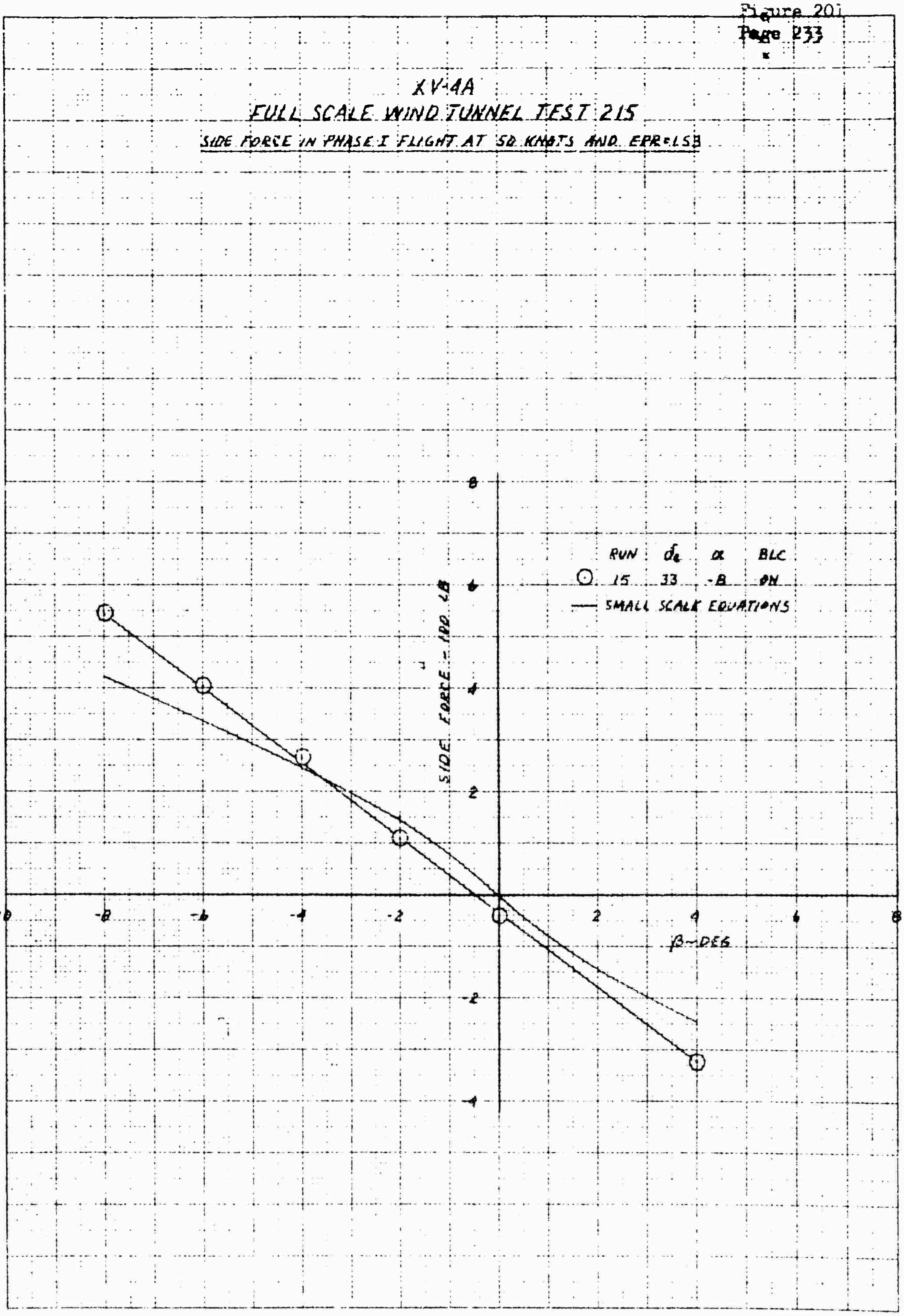
XV-4A
FULL SCALE WIND TUNNEL TEST 215
SIDE FORCE IN PHASE I FLIGHT AT 50 KNOTS AND EPR=1.53
RUN
15
33
-8
ON
BLC
SMALL SCALE EQUATIONS
SIDE FORCE - 100 LB
β - DEG
8
6
4
2
-2
-4
-10
-8
-6
-4
-2
2
4
6
8

XV-4A

FULL SCALE WIND TUNNEL TEST 215

YAWING MOMENT IN PHASE I FLIGHT AT 50 KNOTS AND EPR=1.53

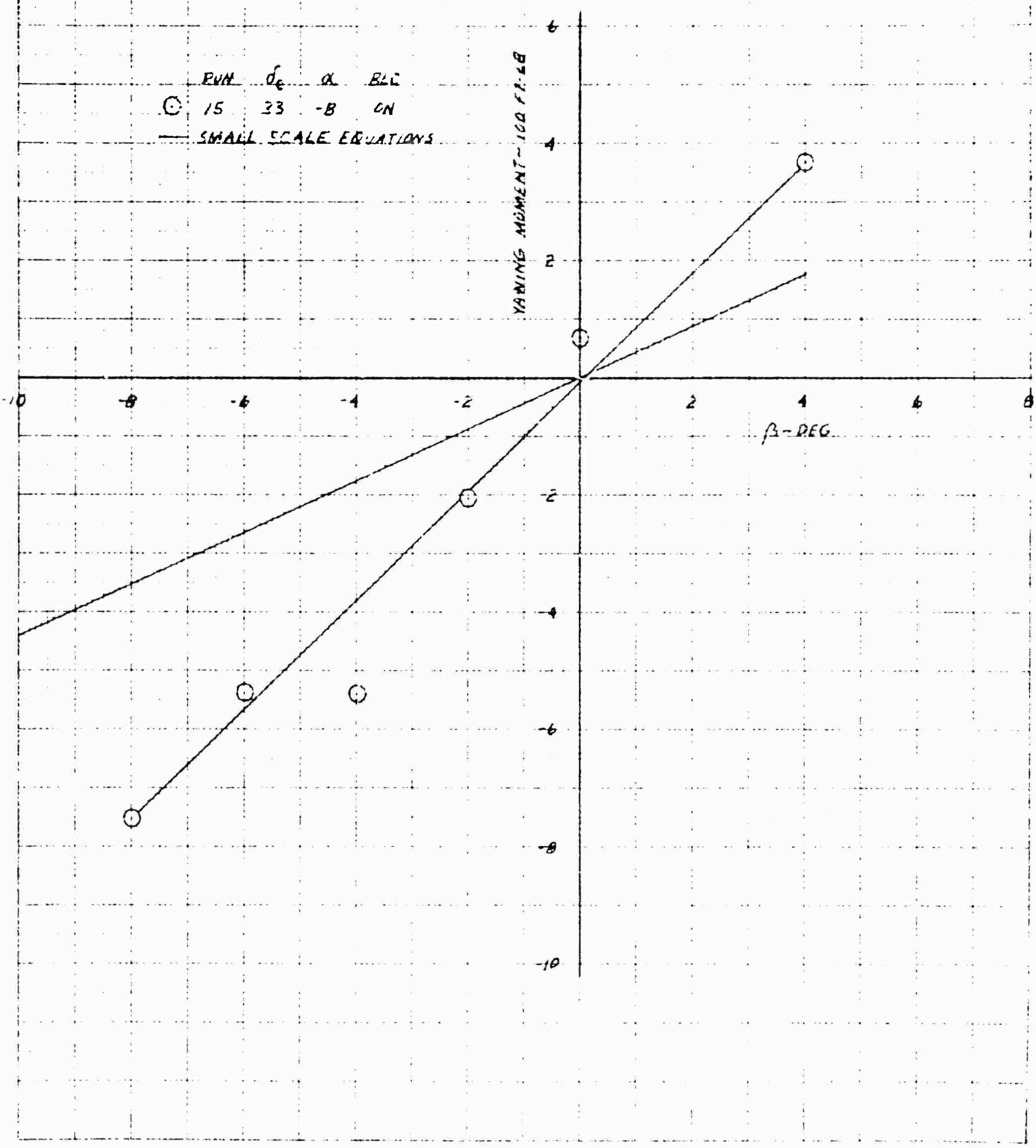

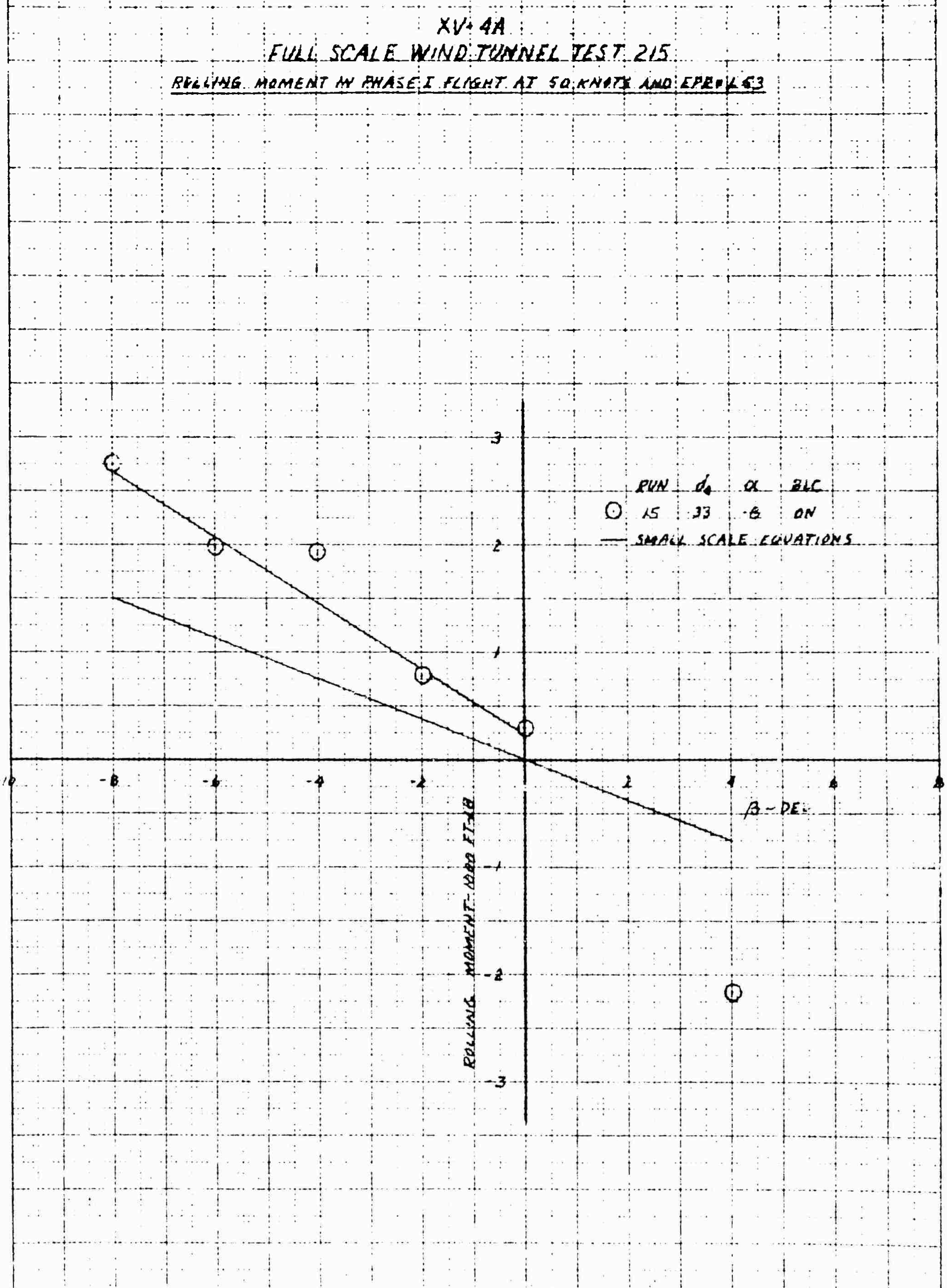
XV-4A
FULL SCALE WIND TUNNEL TEST 215
ROLLING MOMENT IN PHASE I FLIGHT AT 50 KNOTS AND EPR = 1.63
RUN
15
SMALL SCALE EQUATIONS
ON
BLC
-10
-8
-6
-4
-2
2
4
6
8
β ~ DEG
3
2
1
-1
-2
-3
ROLLING MOMENT-1000 FT-LB

XV-4A
FULL SCALE WIND TUNNEL TEST 215
ELEVATOR EFFECTIVENESS IN PHASE I FLIGHT AT 50 KNOTS AND EPF 1.33

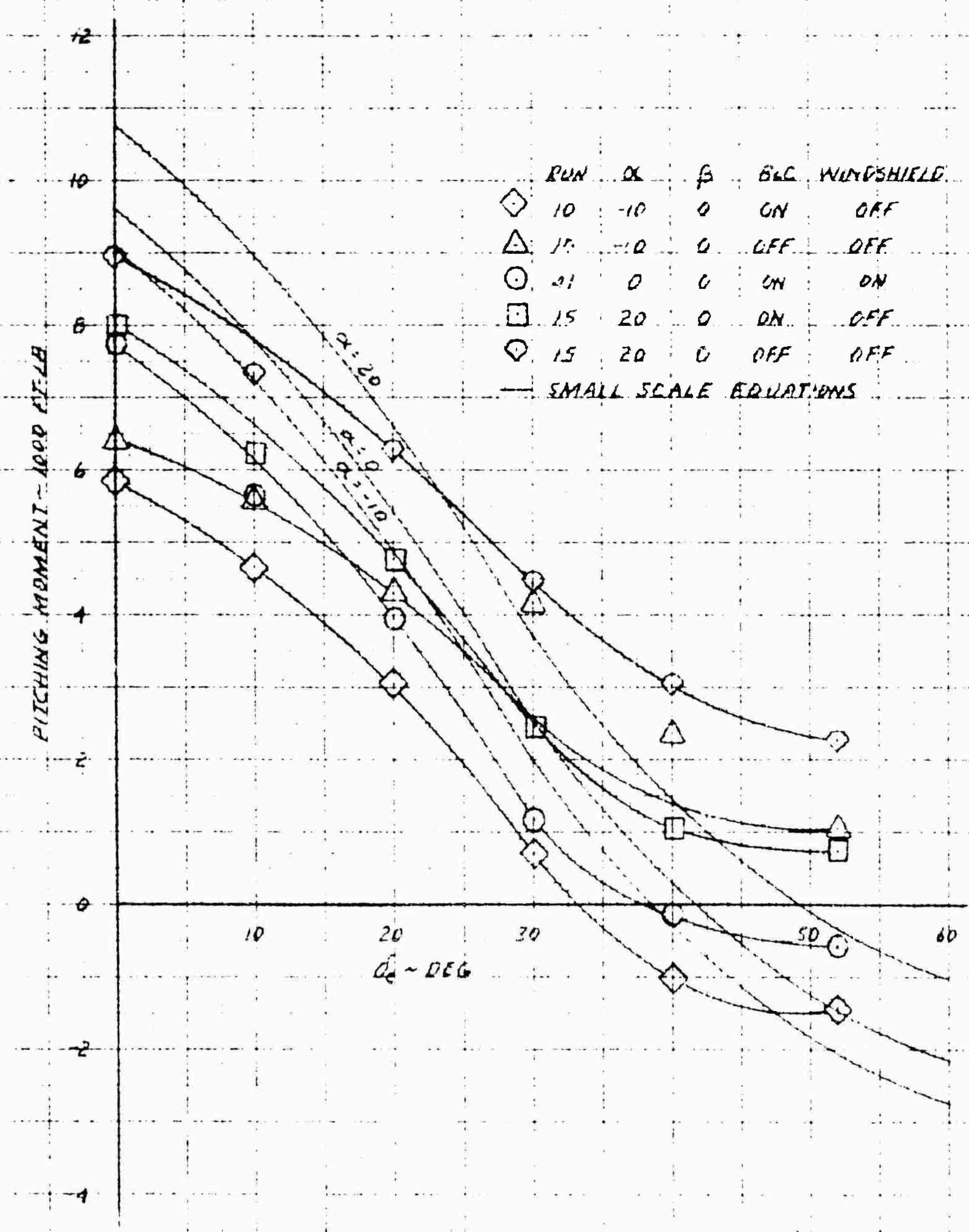

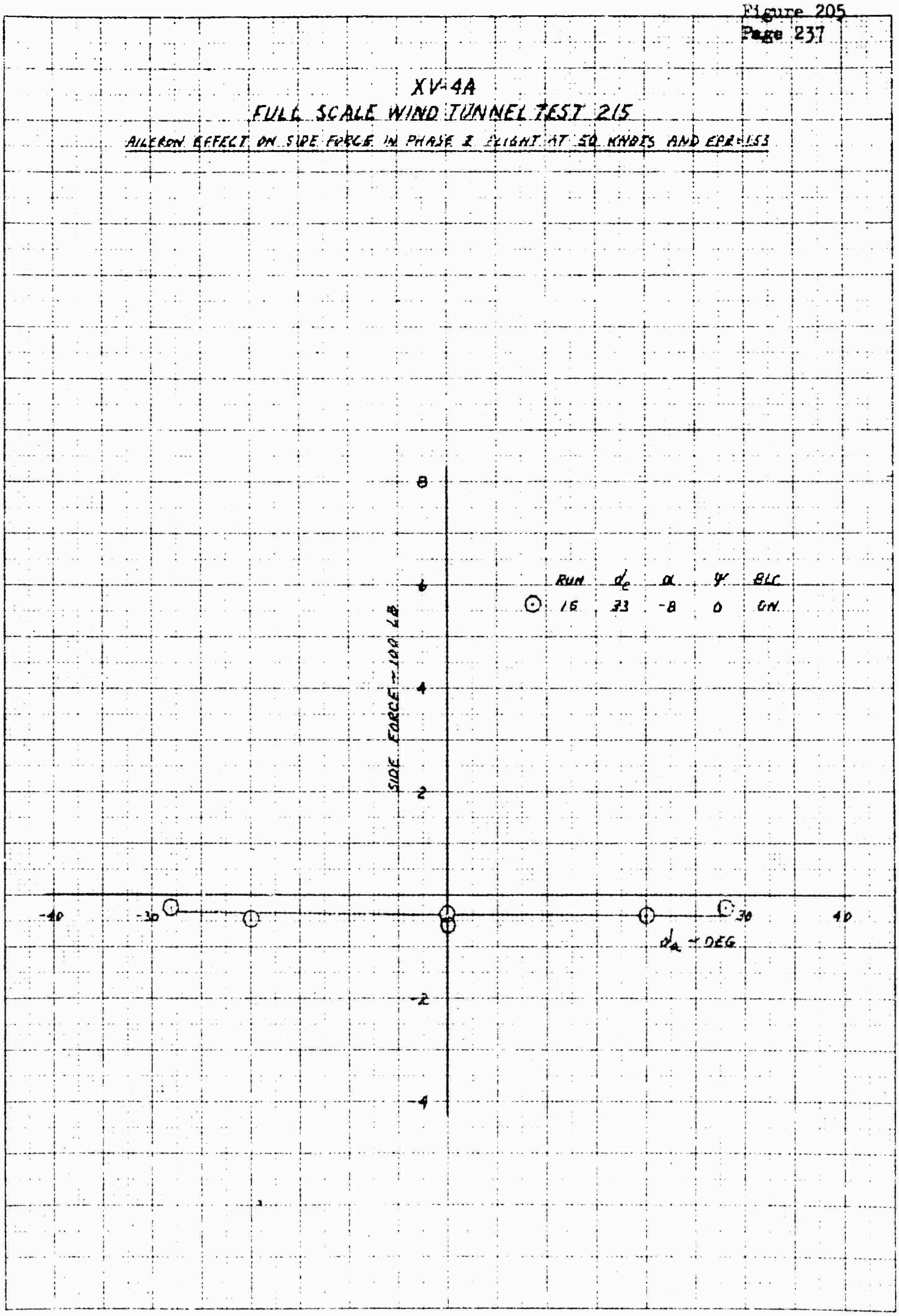
XV-4A
FULL SCALE WIND TUNNEL TEST 215
AILERON EFFECT ON SIDE FORCE IN PHASE I FLIGHT AT 50 KNOTS AND EPR=1.53
RUN
16
33
-8
0
ON
BLC
SIDE FORCE ~ 100 LB
8
6
4
2
-2
-4
-40
-30
30
40
DEG

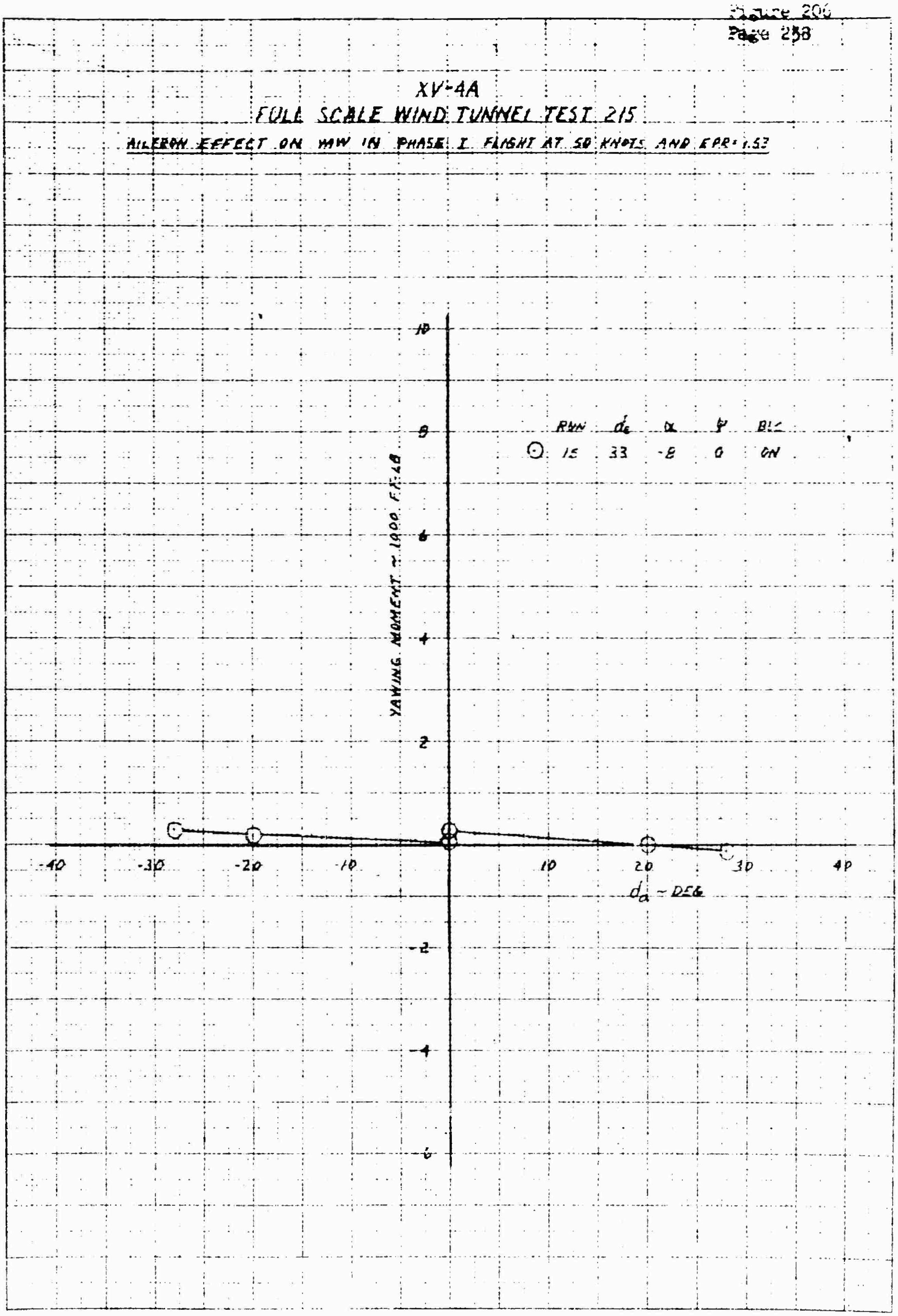
XV-4A
FULL SCALE WIND TUNNEL TEST 215
AILERON EFFECT ON YAW IN PHASE I FLIGHT AT 50 KNOTS AND EPR=1.53
RUN δ_e α ψ BLC
15 33 -8 0 ON
YAWING MOMENT ~ 1000 FT-LB
10
8
6
4
2
-2
-4
-6
-40
-30
-20
-10
10
20
30
40
δ_a ~ DEG

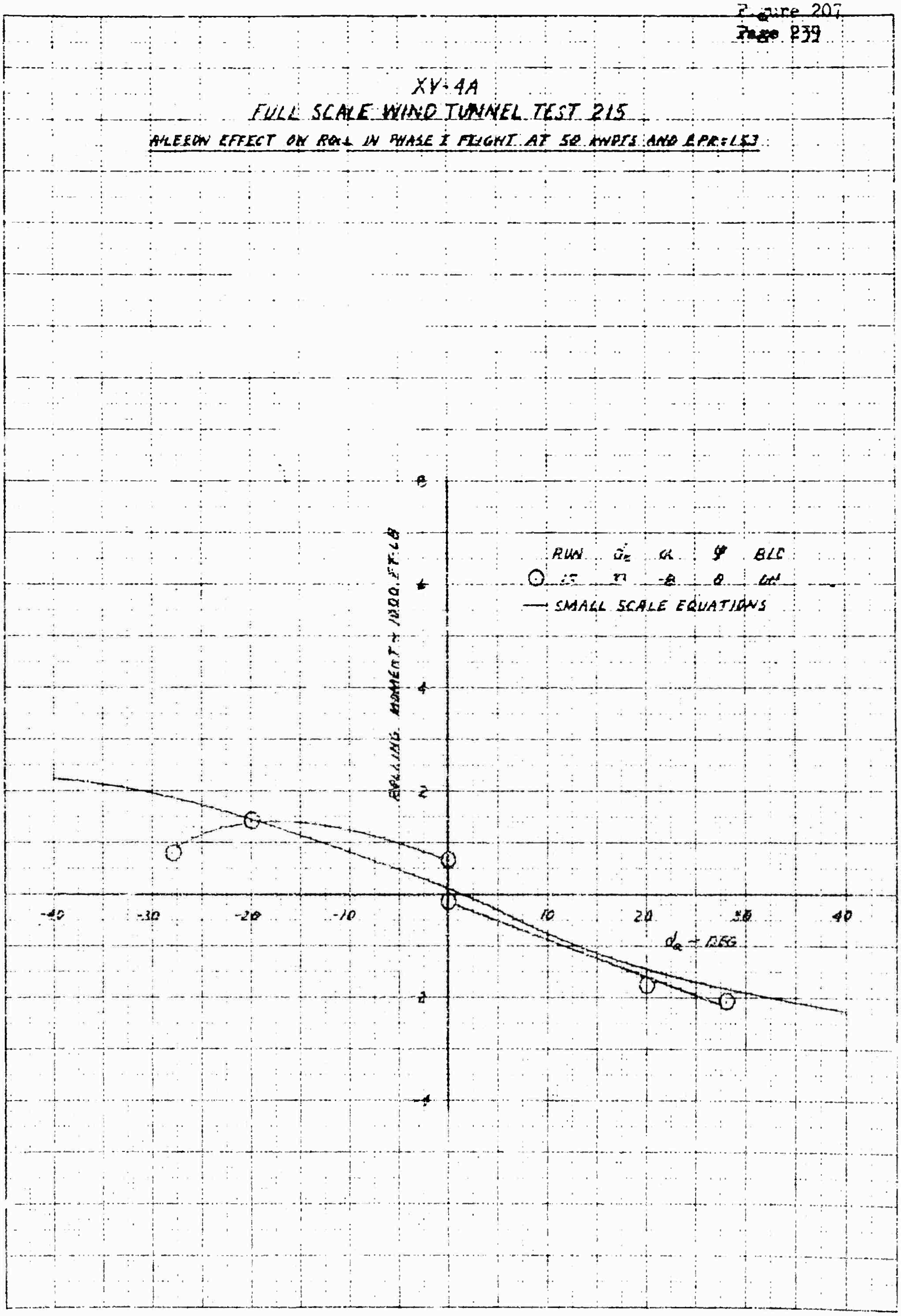
XV-4A
FULL SCALE WIND TUNNEL TEST 215
AILERON EFFECT ON ROLL IN PHASE I FLIGHT AT 50 KNOTS AND EPR=1.53
RUN
α
BLC
-8
0
SMALL SCALE EQUATIONS
ROLLING MOMENT ~ 1000 FT-LB
8
6
4
2
-2
-4
-40
-30
-20
-10
10
20
30
40
δ_a ~ DEG

XV-4A
FULL SCALE WIND TUNNEL TEST 215
ELEVATOR EFFECTIVENESS IN HOVER AT EPR = 1.99

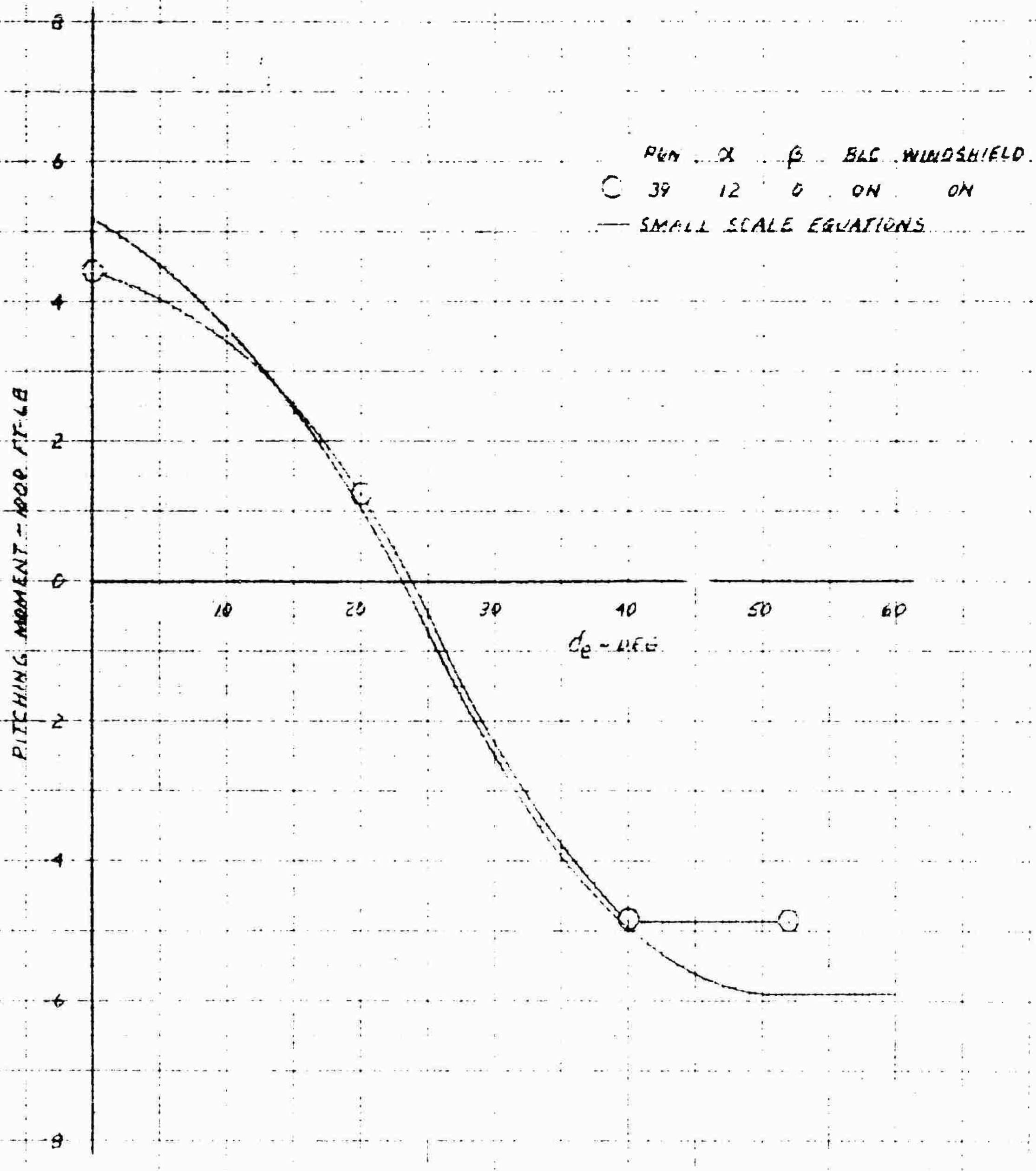

XV-4A

FULL SCALE WIND TUNNEL TEST 215

AILERON EFFECT ON SIDE FORCE IN HOVER AT EPR = 1.99

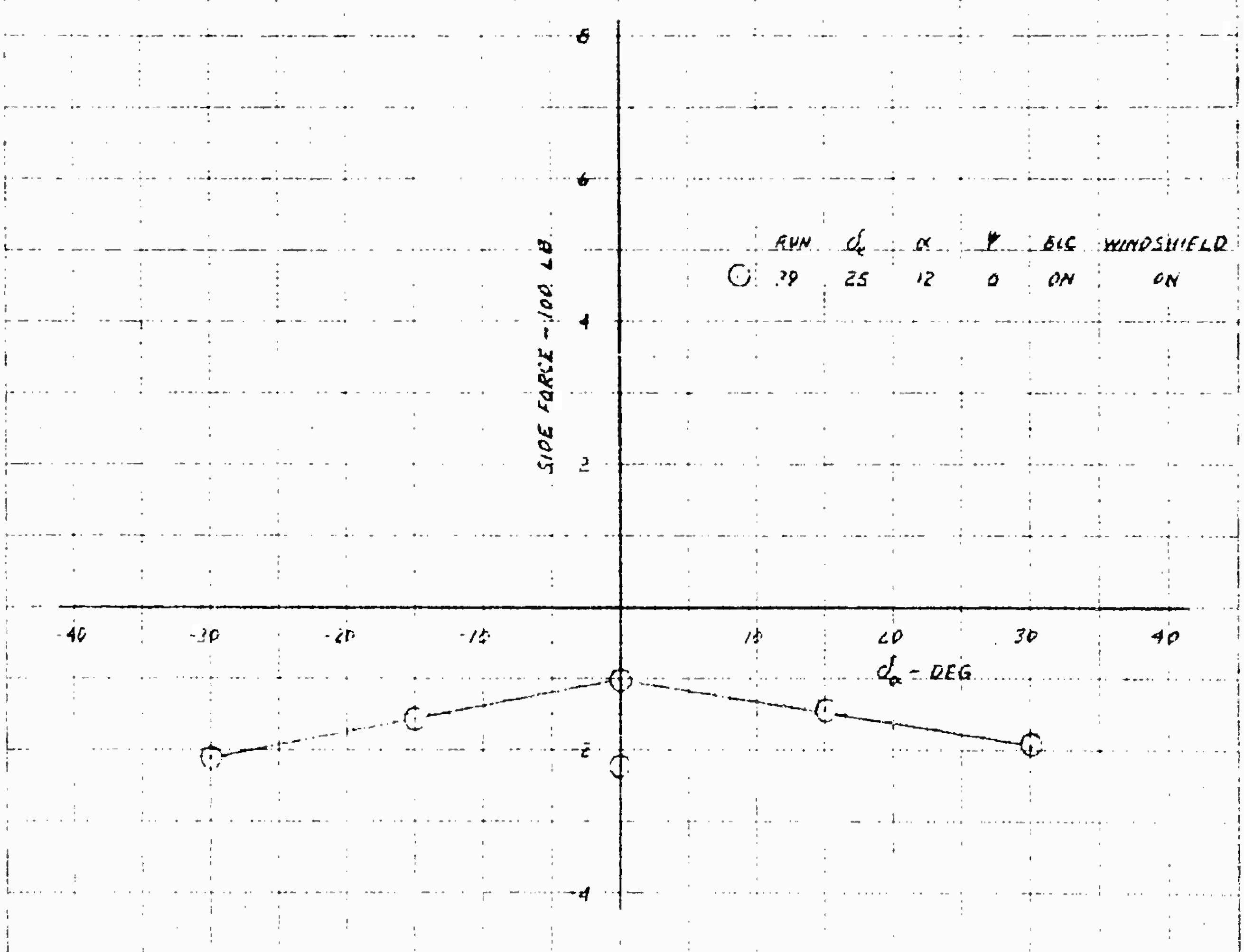

XV-4A
FULL SCALE WIND TUNNEL TEST 215
AILERON EFFECT ON YAW IN HOVER AT EPR: 1.99

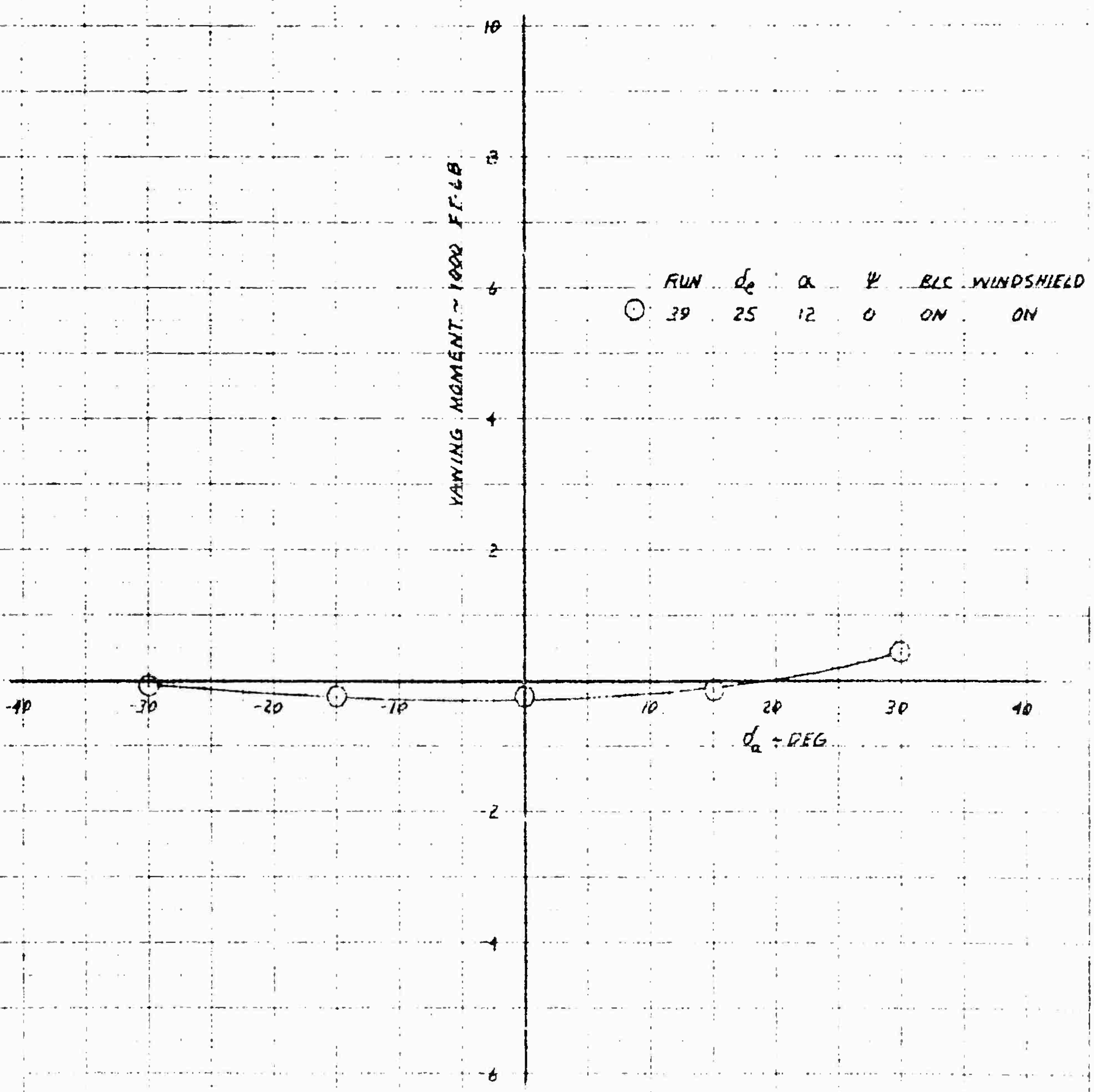

XV-4A

FULL SCALE WIND TUNNEL TEST 215

AILERON EFFECT ON ROLL IN HOVER AT EPR=1.99

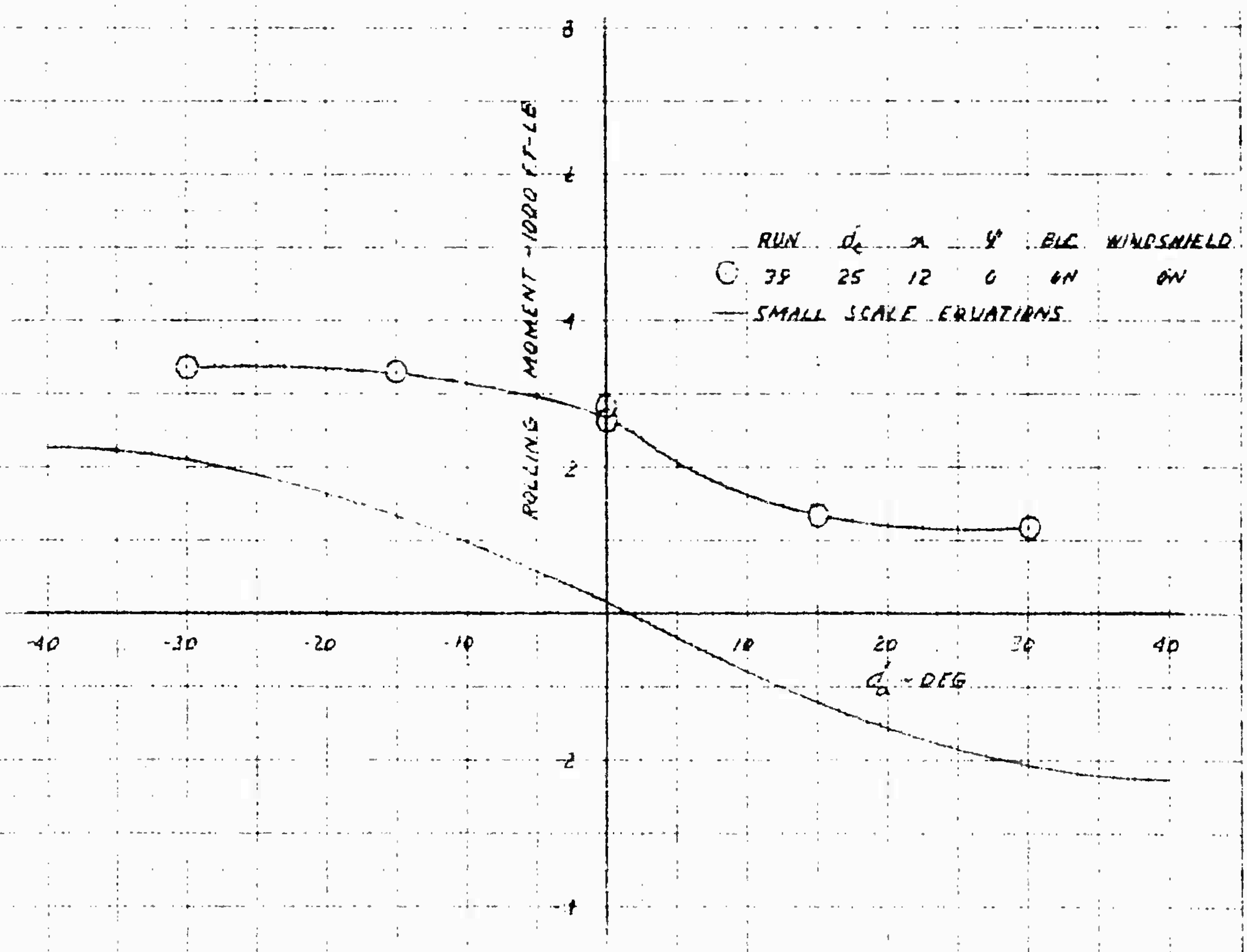

XV-4A
FULL SCALE WIND TUNNEL TEST 215
RUDDER EFFECT ON SIDE FORCE IN HOVER AT EPR = 1.99

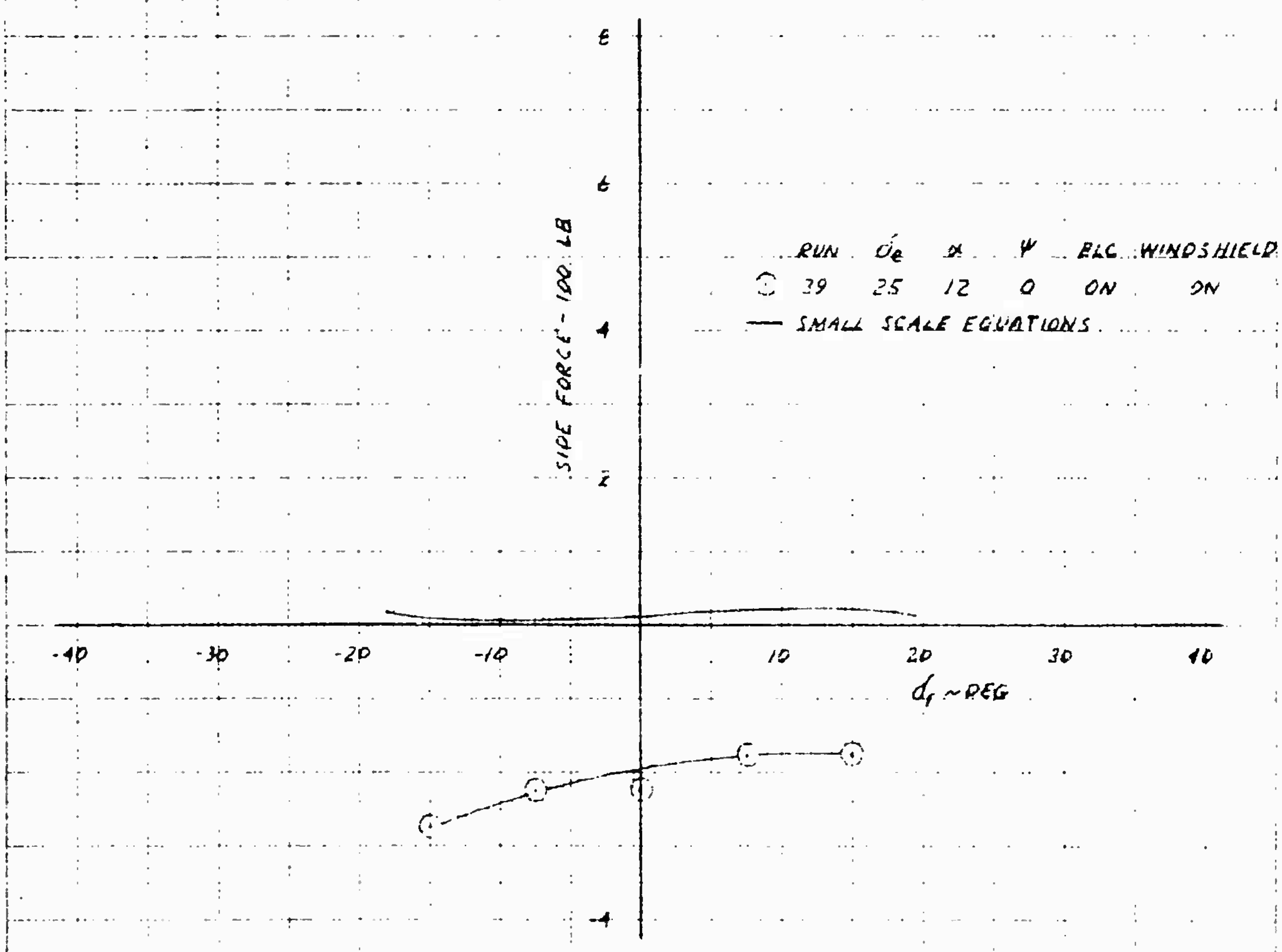

XV-4A
FULL SCALE WIND TUNNEL TEST 215
RUDDER EFFECT ON YAW IN HOVER AT EPR=1.99

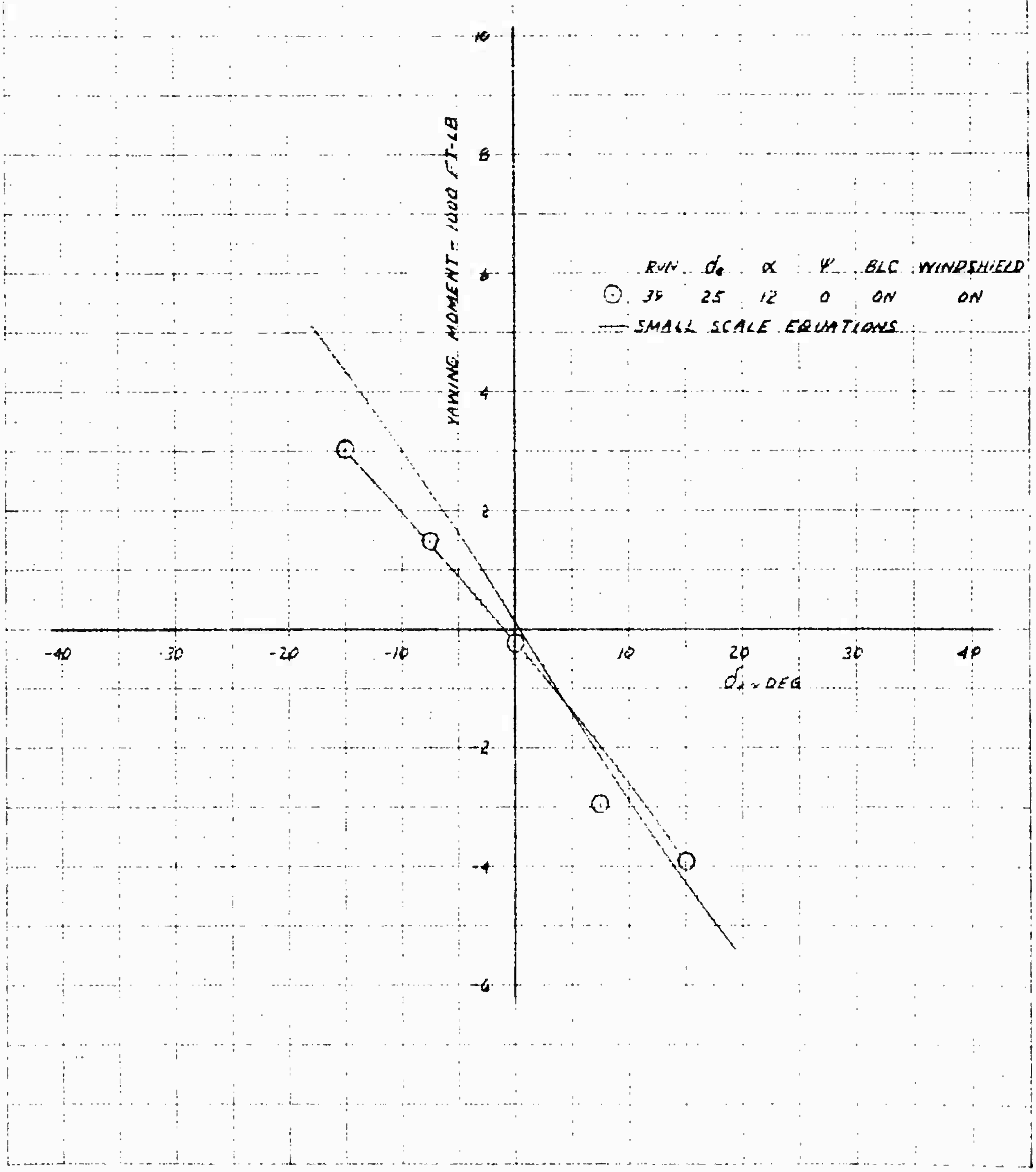

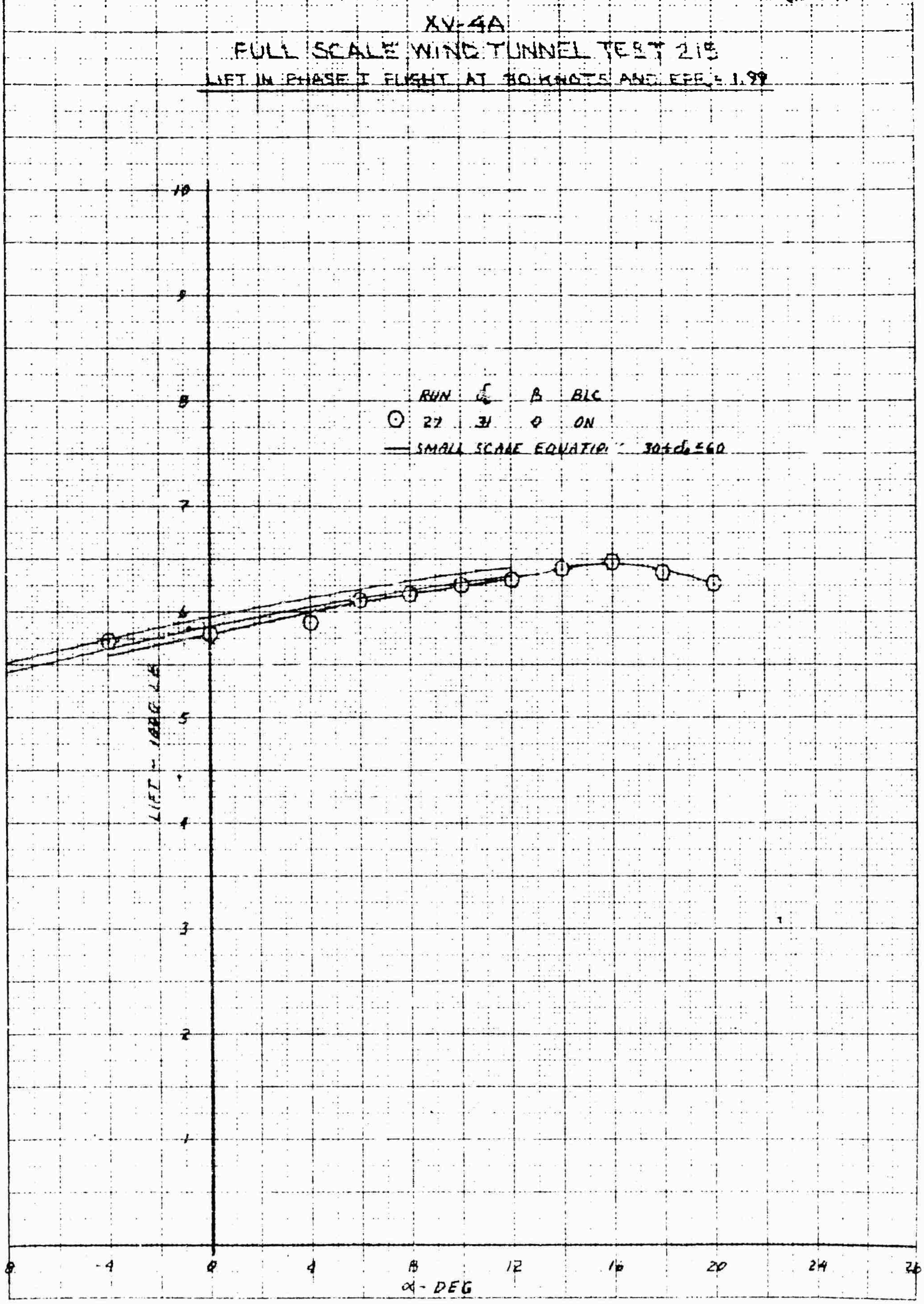
XV-4A
FULL SCALE WIND TUNNEL TEST 215
LIFT IN PHASE I FLIGHT AT 80 KNOTS AND EPR = 1.99
RUN
B
BLC
27
31
0
ON
SMALL SCALE EQUATION
LIFT - 1000 LB
α - DEG

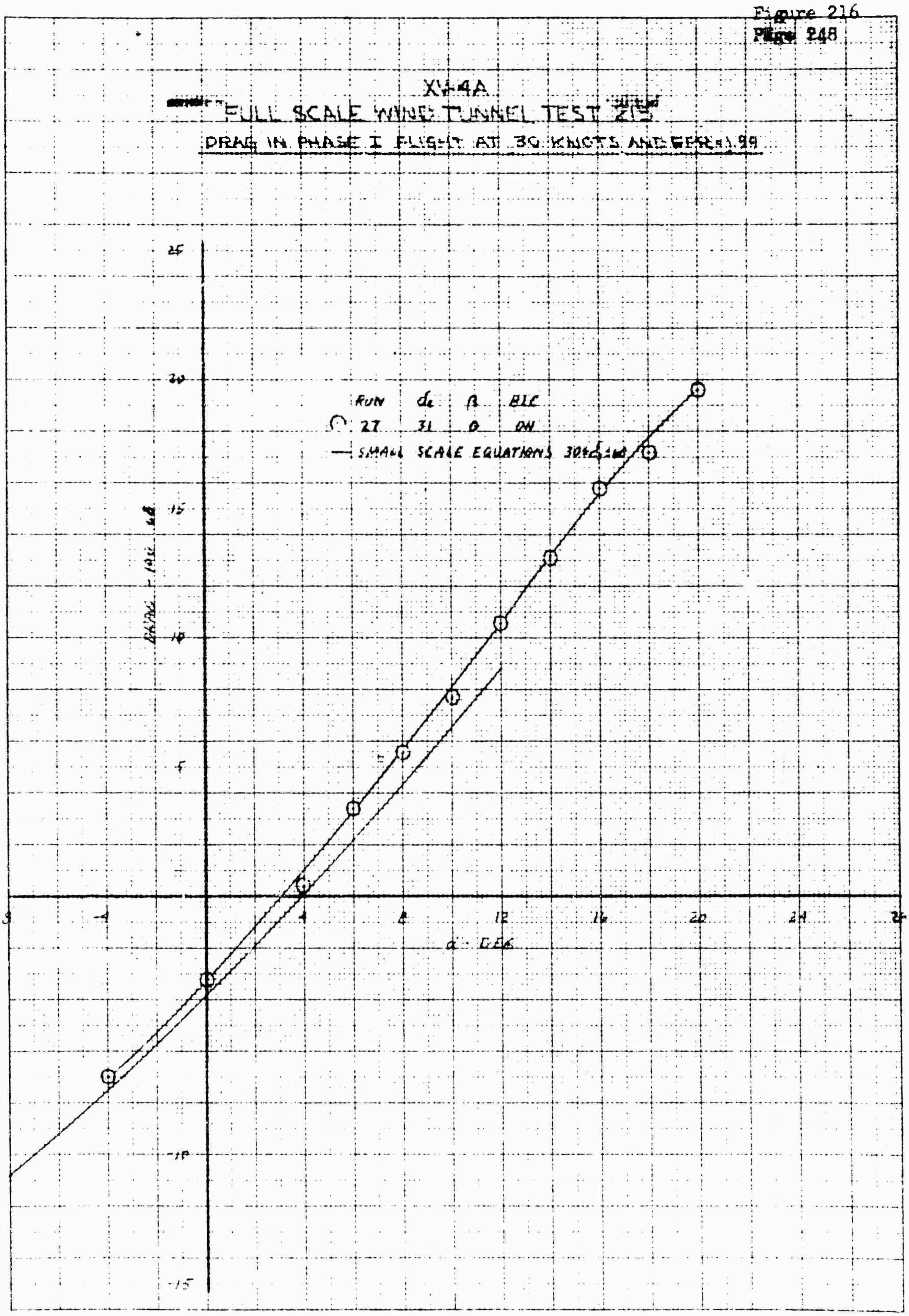
XV-4A
FULL SCALE WIND TUNNEL TEST 215
DRAG IN PHASE I FLIGHT AT 30 KNOTS AND EPR=1.99
RUN
27
31
0
ON
SMALL SCALE EQUATIONS
25
20
15
10
5
-10
-15
-8
-4
4
8
12
16
20
24
28

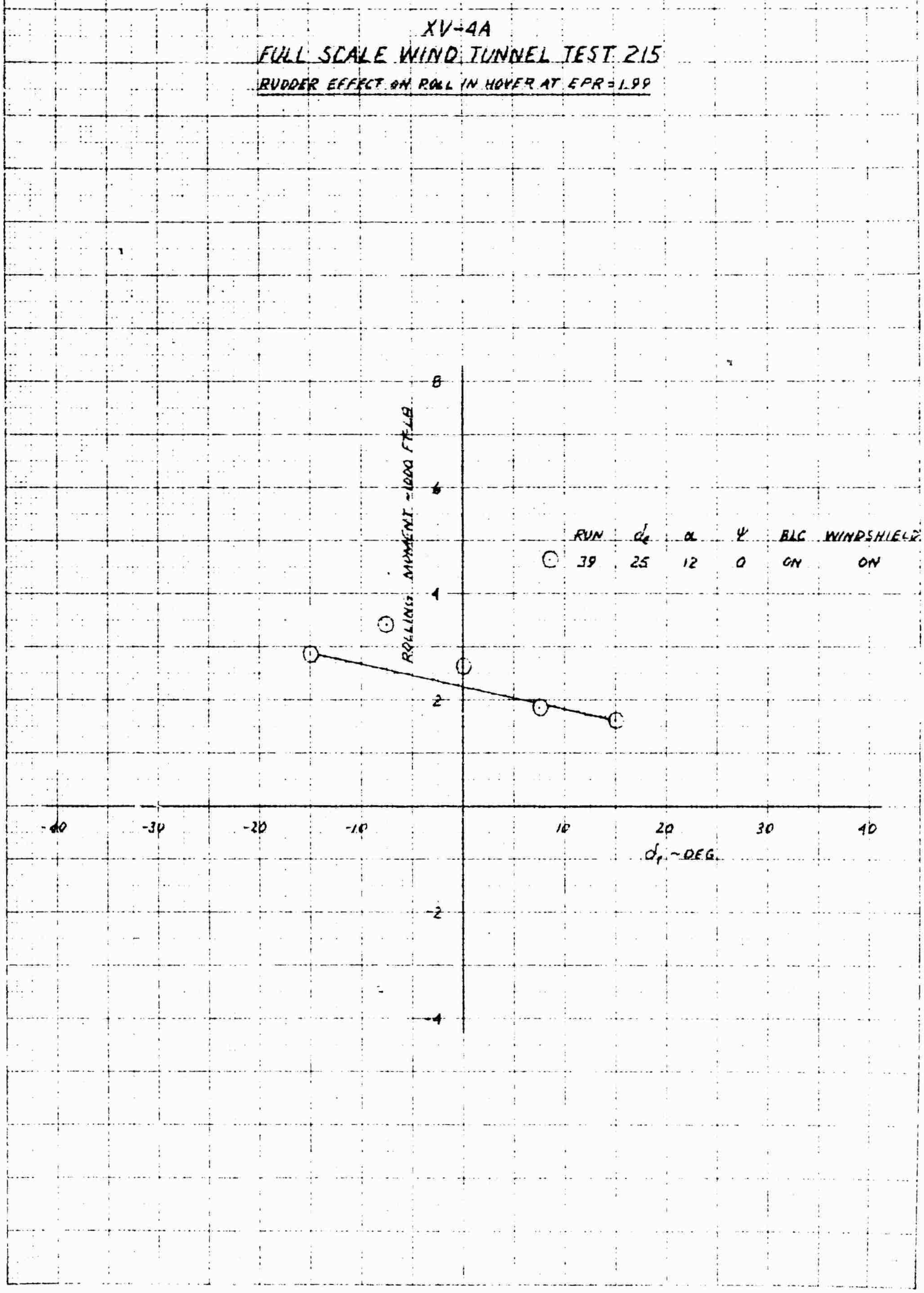
XV-4A
FULL SCALE WIND TUNNEL TEST 215
RUDDER EFFECT ON ROLL IN HOVER AT EPR = 1.99
ROLLING MOMENT ~1000 FT-LB
δ_r ~ DEG.
RUN
39
δ_e
25
α
12
ψ
0
BLC
ON
WINDSHIELD
ON
8
6
4
2
-2
-4
-40
-30
-20
-10
10
20
30
40

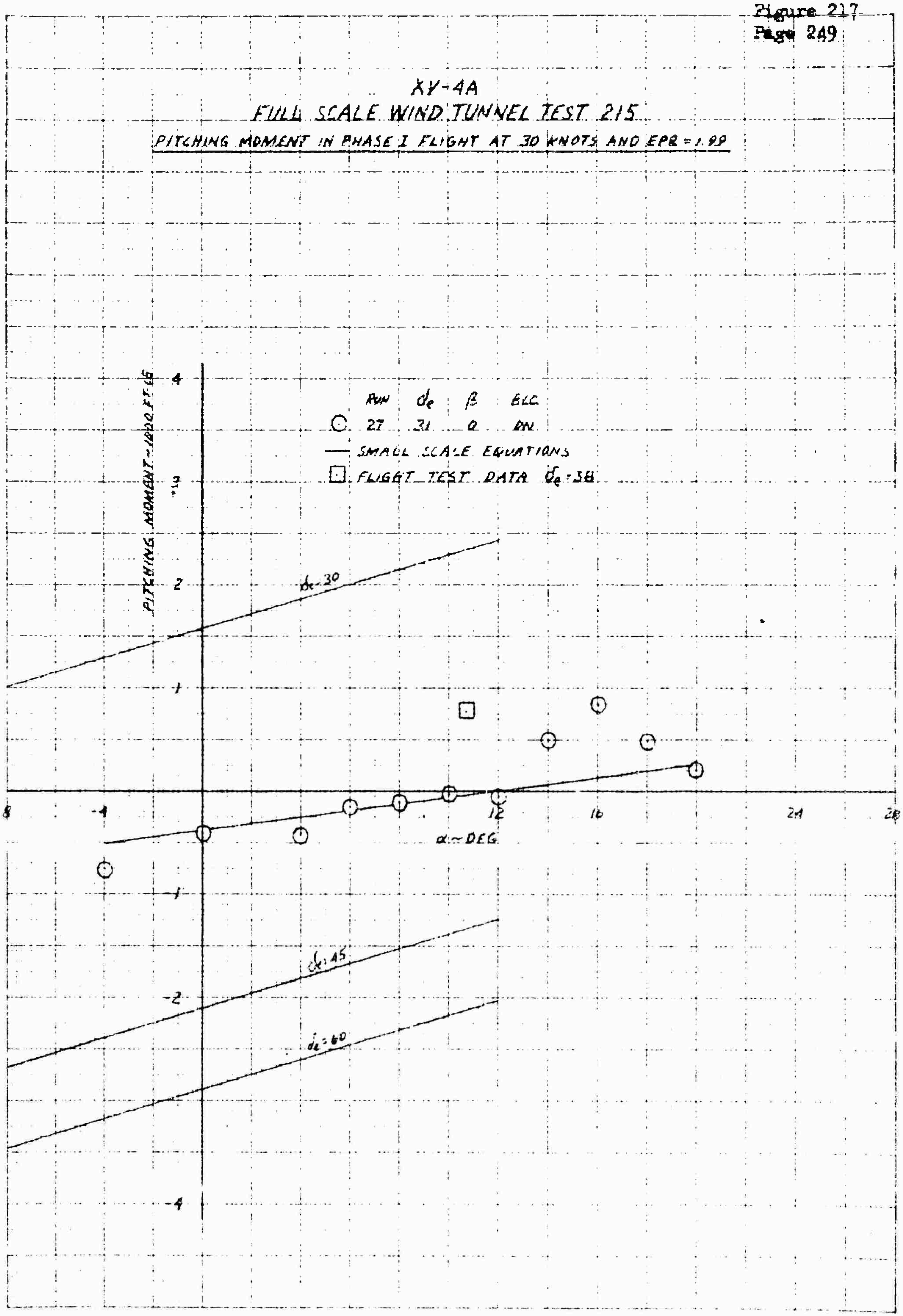
XV-4A
FULL SCALE WIND TUNNEL TEST 215
PITCHING MOMENT IN PHASE I FLIGHT AT 30 KNOTS AND EPR = 1.99
RUN
δ_e
β
BLC
27
31
0
ON
SMALL SCALE EQUATIONS
FLIGHT TEST DATA δ_e = 38
δ_e = 30
δ_e = 45
δ_e = 60
PITCHING MOMENT ~ 1000 FT-LB
α ~ DEG
4
3
2
1
-1
-2
-4
-8
-4
12
16
24
28

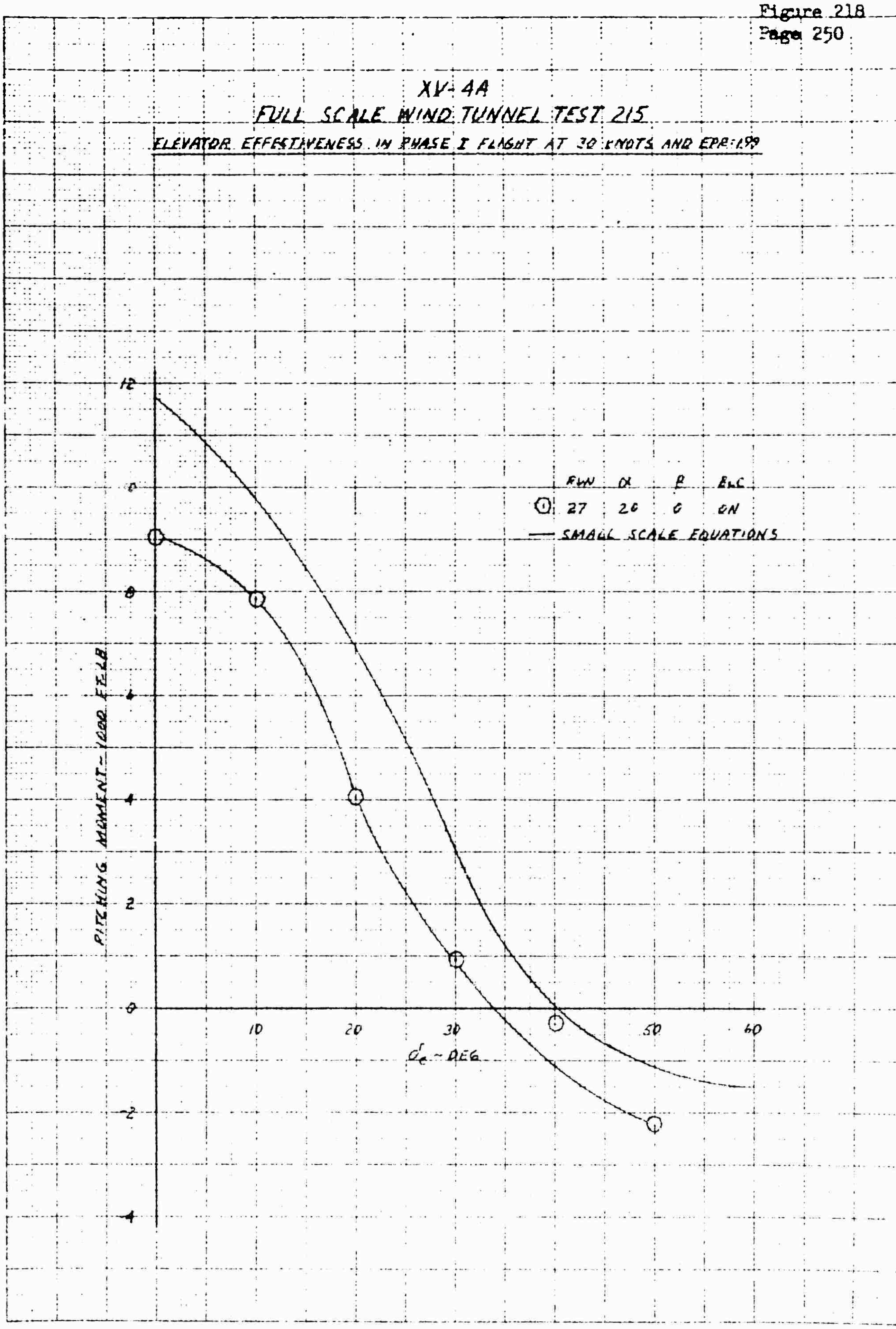
XV-4A
FULL SCALE WIND TUNNEL TEST 215
ELEVATOR EFFECTIVENESS IN PHASE I FLIGHT AT 30 KNOTS AND EPR=1.99
RUN α β ELC
27 20 0 ON
SMALL SCALE EQUATIONS
PITCHING MOMENT ~ 1000 FT-LB
δe ~ DEG
12
8
4
2
0
-2
-4
10
20
30
50
60

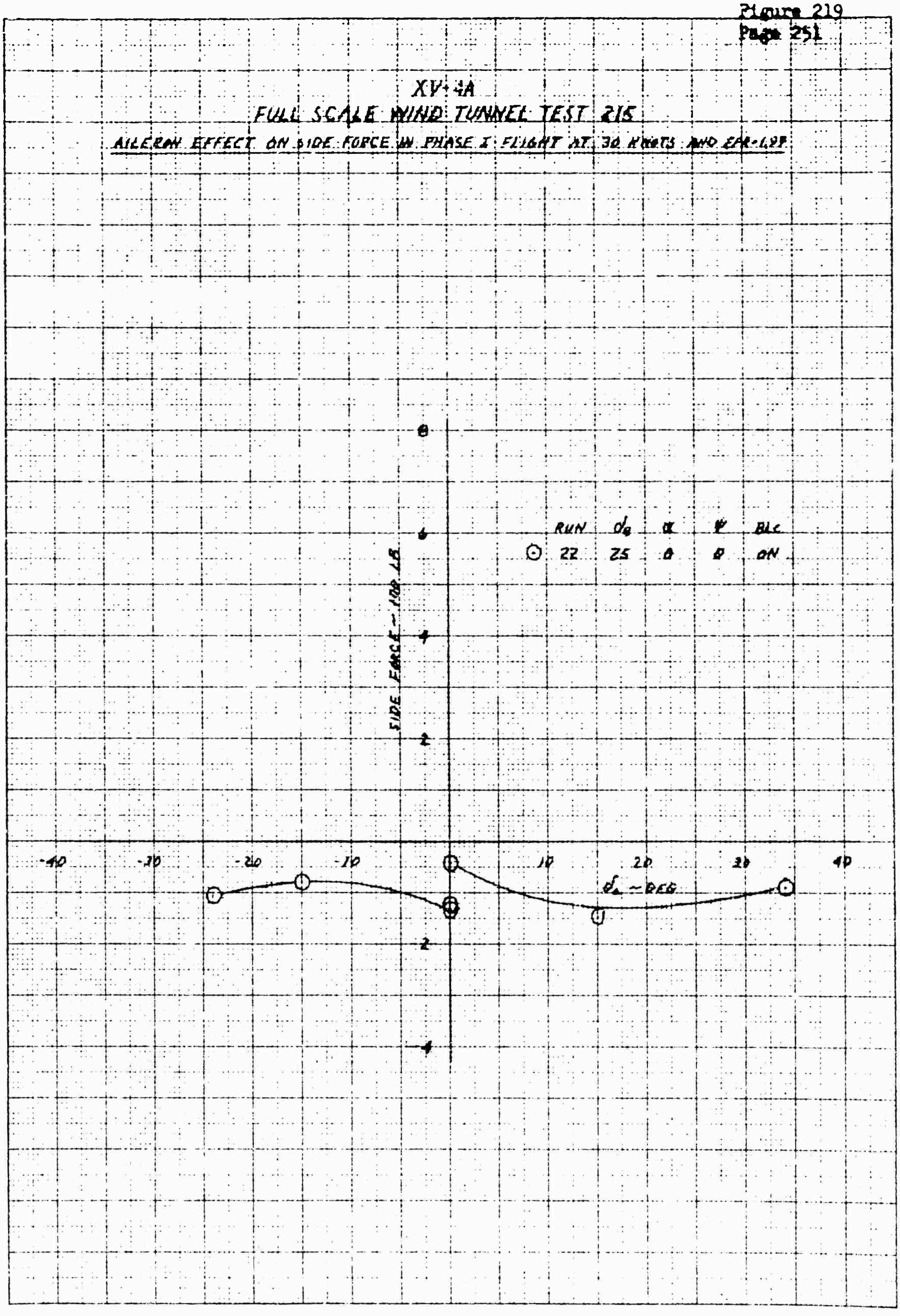
XV-4A
FULL SCALE WIND TUNNEL TEST 215
AILERON EFFECT ON SIDE FORCE IN PHASE I FLIGHT AT 30 KNOTS AND EPR-1.97
RUN
22
25
0
0
BLC
ON
SIDE FORCE ~ 100 LB
δ_a ~ DEG
-40
-30
-20
-10
10
20
30
40
8
6
4
2
-2
-4

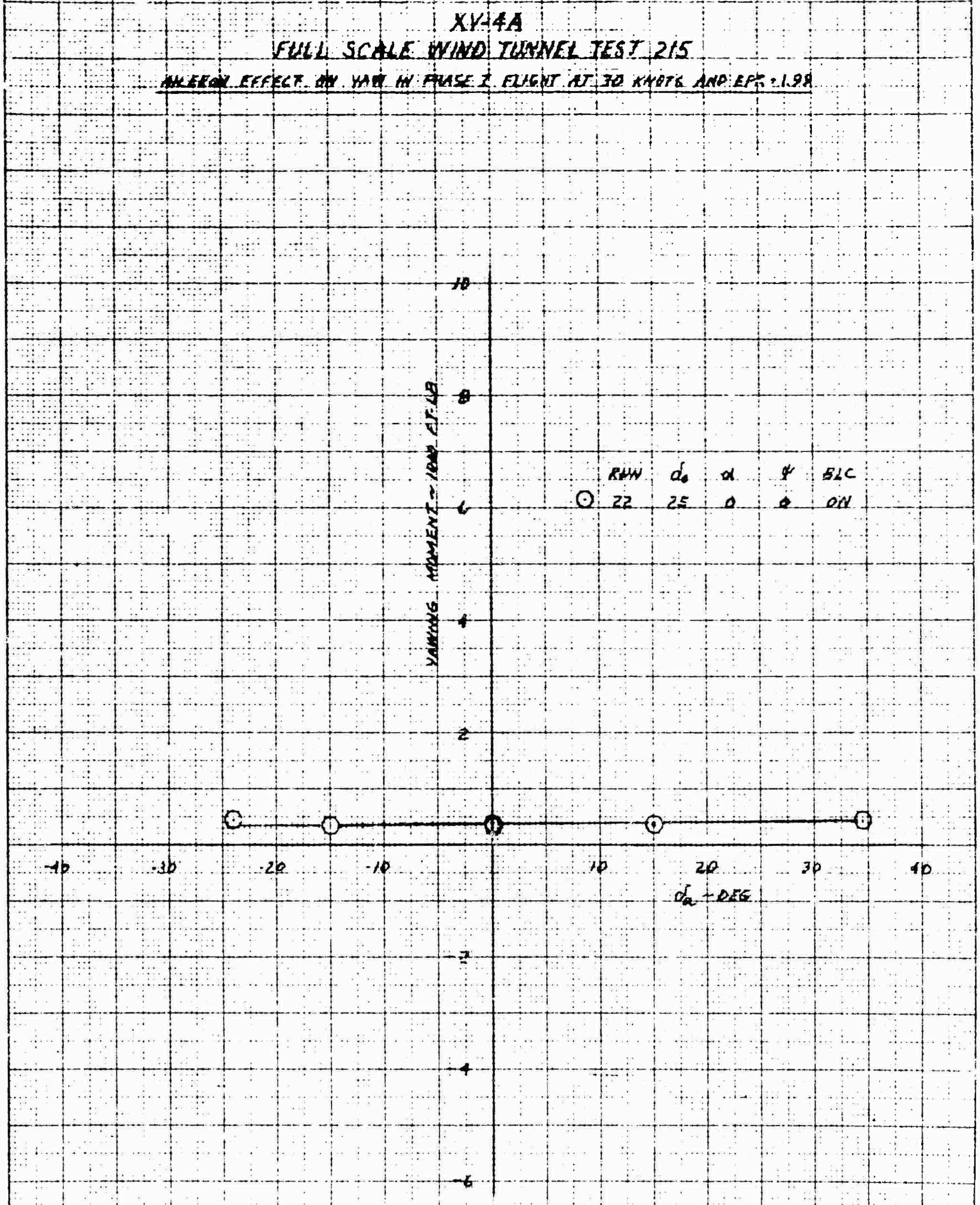
XV-4A
FULL SCALE WIND TUNNEL TEST 215
AILERON EFFECT ON YAW IN PHASE I FLIGHT AT 30 KNOTS AND EPR=1.98
YAWING MOMENT ~ 1000 FT-LB
10
8
6
4
2
-2
-4
-6
-40
-30
-20
-10
10
20
30
40
δa ~ DEG
RUN δe α ψ BLC
22 25 0 0 ON

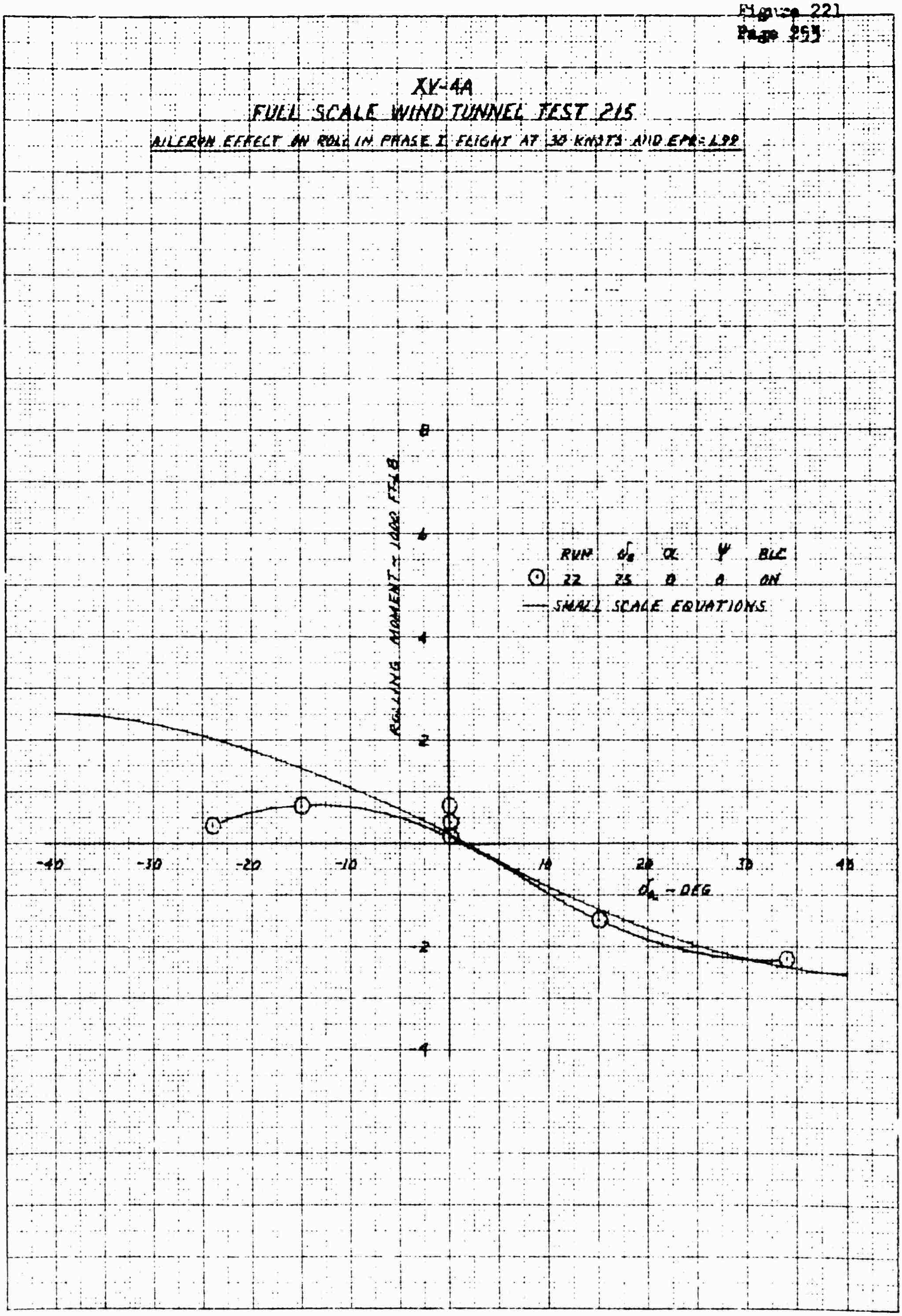
XV-4A
FULL SCALE WIND TUNNEL TEST 215
AILERON EFFECT ON ROLL IN PHASE I FLIGHT AT 30 KNOTS AND EPR=1.99
ROLLING MOMENT ~ 1000 FT-LB
8
6
4
2
-2
-4
-40
-30
-20
-10
10
20
30
40
δ_a ~ DEG
RUN
δ_f
α
ψ
BLC
22
75
0
0
ON
SMALL SCALE EQUATIONS

XV-4A
FULL SCALE WIND TUNNEL TEST 215
RUDDER EFFECT ON SIDE FORCE IN PHASE I FLIGHT AT 30 KNOTS AND EPR = 1.99

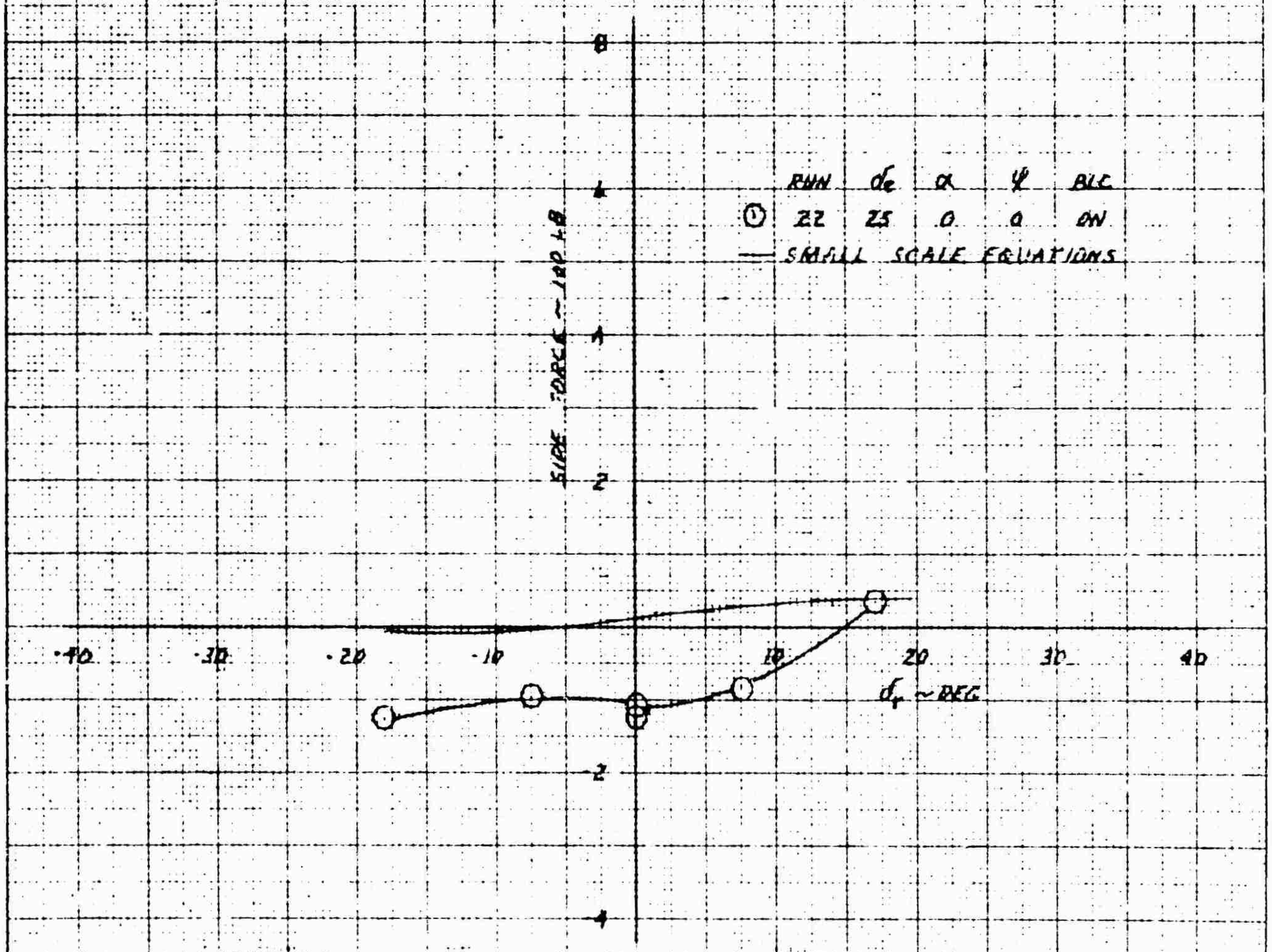

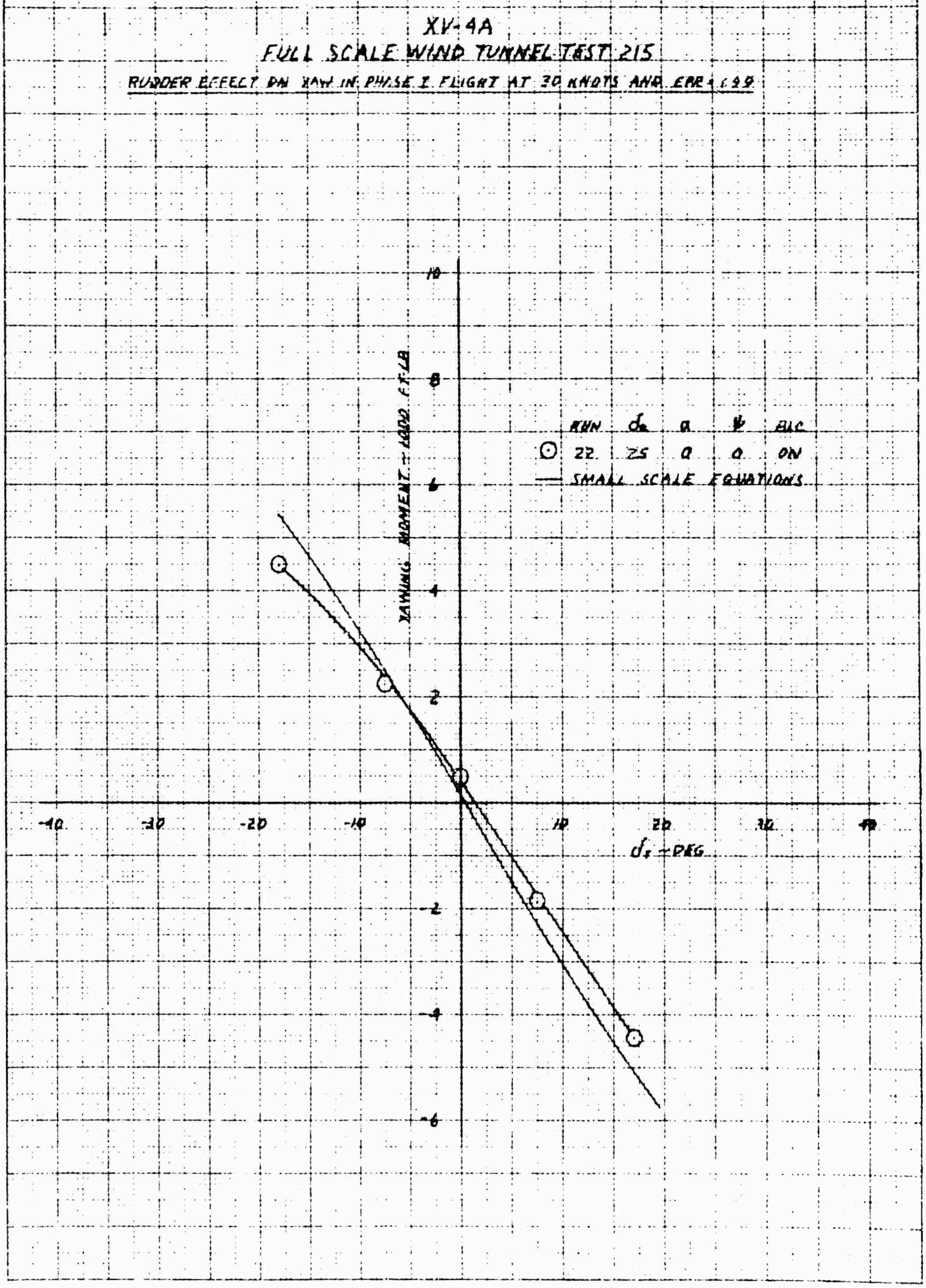
XV-4A
FULL SCALE WIND TUNNEL TEST 215
RUDDER EFFECT ON YAW IN PHASE I FLIGHT AT 30 KNOTS AND EPR
YAWING MOMENT - 1000 FT-LB
δ_r - DEG
RUN
22
25
0
0
ON
SMALL SCALE EQUATIONS

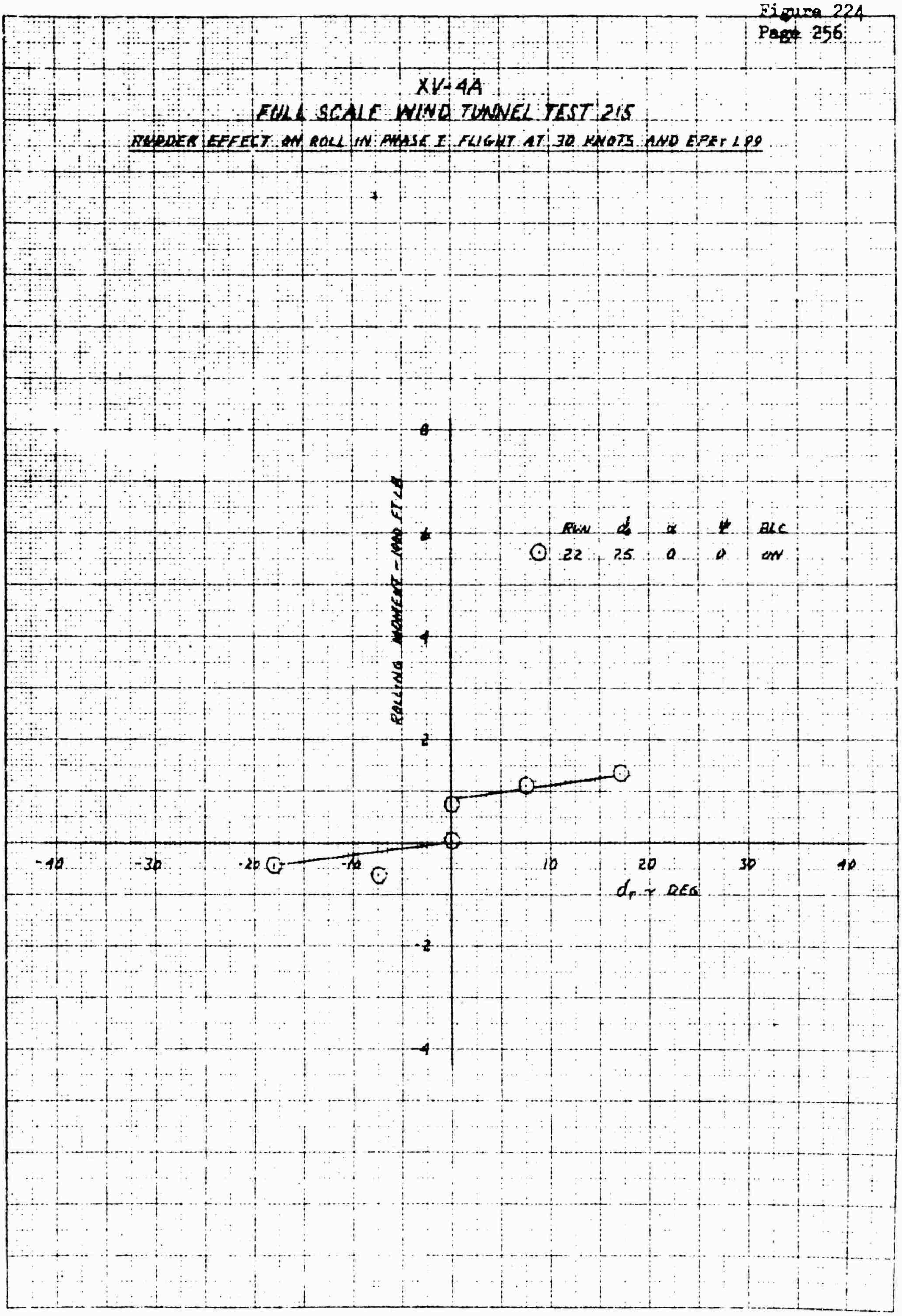
XV-4A
FULL SCALE WIND TUNNEL TEST 215
RUDDER EFFECT ON ROLL IN PHASE I FLIGHT AT 30 KNOTS AND EPE 1.99
ROLLING MOMENT – 1000 FT LB
RUN
22
25
0
0
BLC
ON
d_r ~ DEG
-40
-30
-20
-10
10
20
30
40
8
6
4
2
-2
-4

XV-4A
FULL SCALE WIND TUNNEL TEST 215
AILERON EFFECT ON SIDE FORCE IN PHASE I FLIGHT AT 40 KNOTS AND EPR=1.90

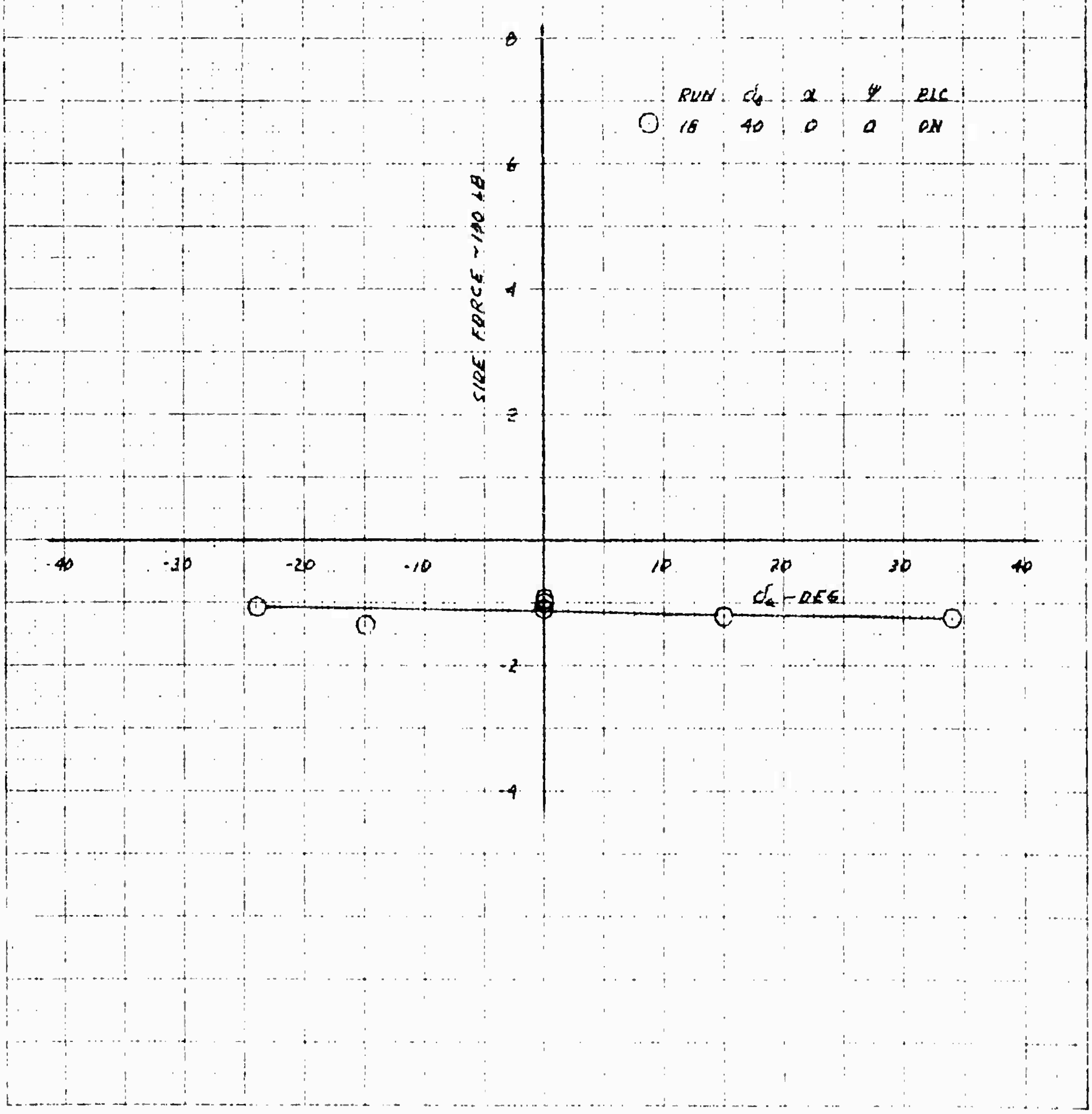

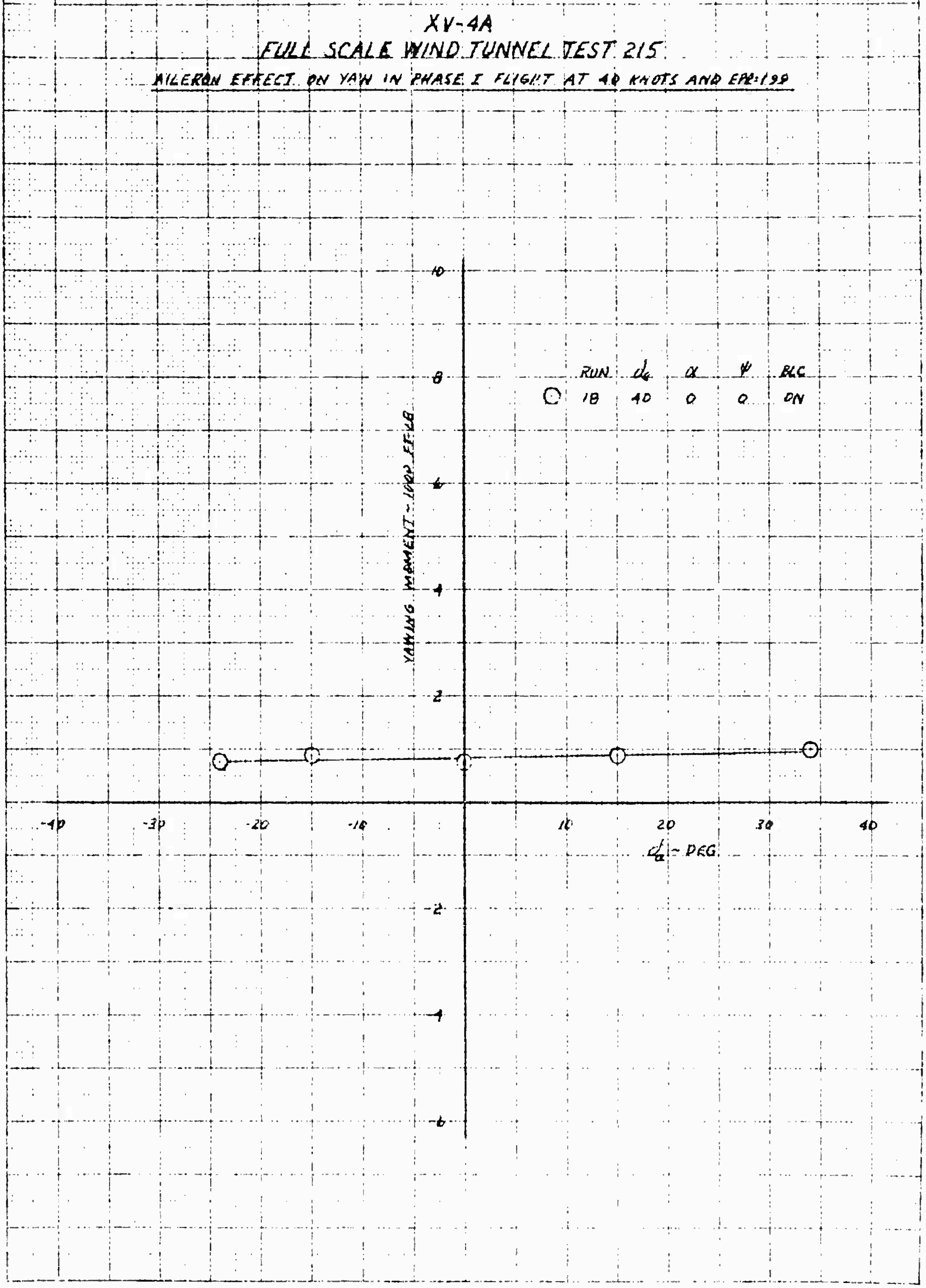
XV-4A
FULL SCALE WIND TUNNEL TEST 215
AILERON EFFECT ON YAW IN PHASE I FLIGHT AT 40 KNOTS AND EPR=1.99
RUN
δ_e
α
ψ
BLC
18
40
0
0
ON
YAWING MOMENT ~ 1000 FT-LB
10
8
6
4
2
-2
-4
-6
-40
-30
-20
-10
10
20
30
40
δ_a ~ DEG

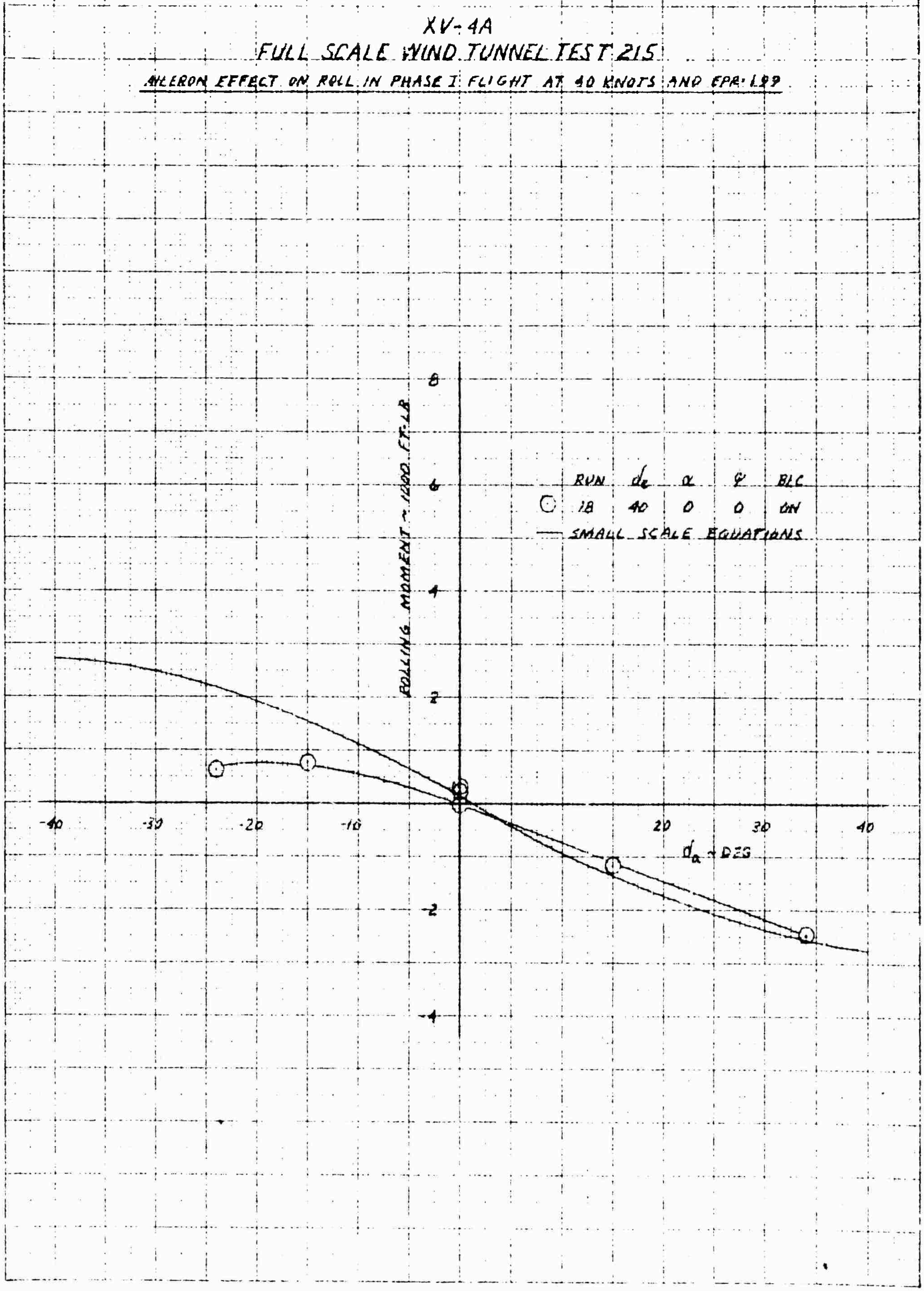
XV-4A
FULL SCALE WIND TUNNEL TEST 215
AILERON EFFECT ON ROLL IN PHASE I FLIGHT AT 40 KNOTS AND EPR-1.99
ROLLING MOMENT ~ 1000 FT-LB
8
6
4
2
-2
-4
RUN
δ_e
α
φ
BLC
18
40
0
0
ON
SMALL SCALE EQUATIONS
-40
-30
-20
-10
20
30
40
δ_a ~ DEG

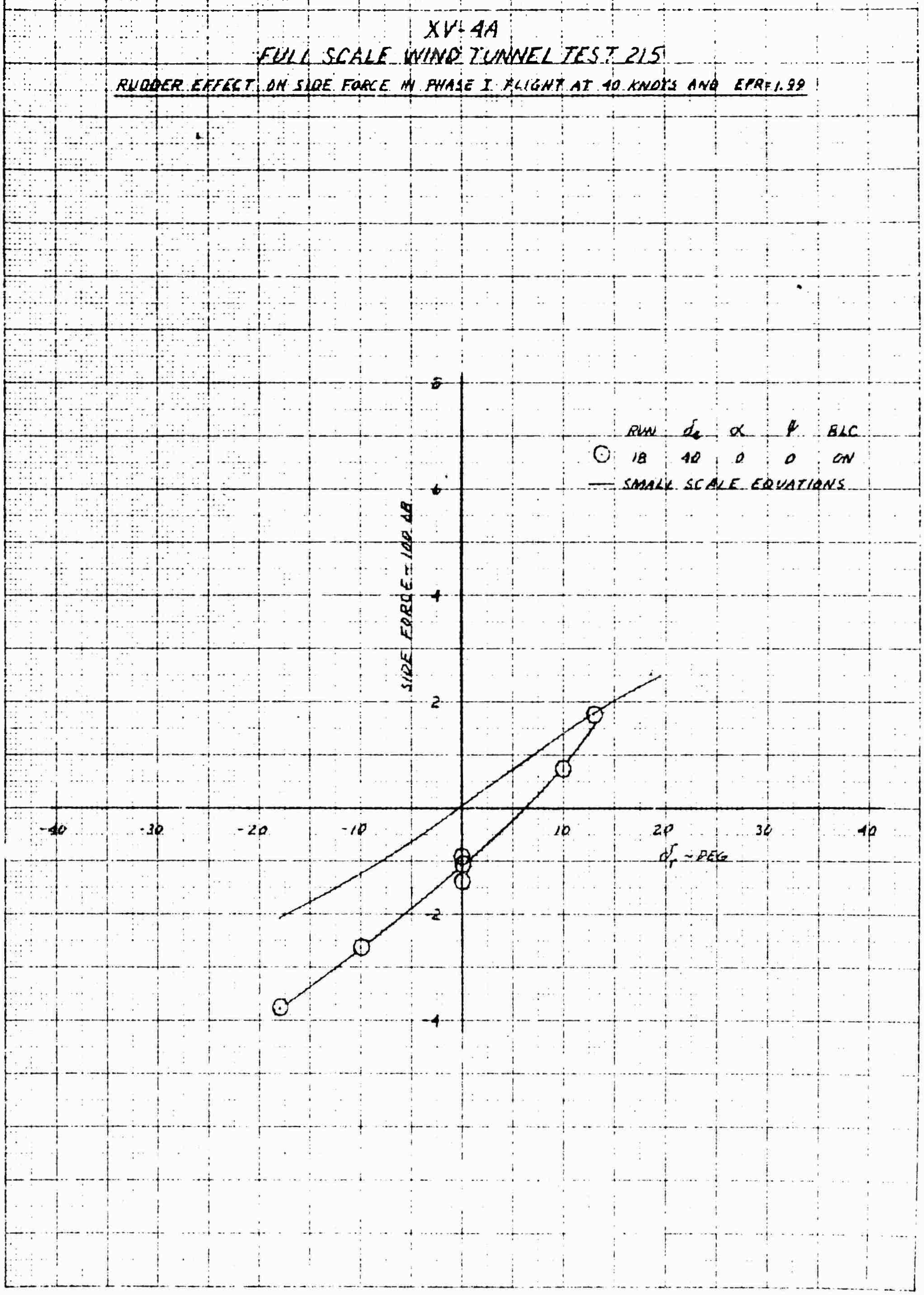
XV-4A
FULL SCALE WIND TUNNEL TEST 215
RUDDER EFFECT ON SIDE FORCE IN PHASE I FLIGHT AT 40 KNOTS AND EPR=1.99
RUN
18
40
0
0
ON
SMALL SCALE EQUATIONS
SIDE FORCE ~ 100 LB
8
6
4
2
-2
-4
-40
-30
-20
-10
10
20
30
40
~ DEG

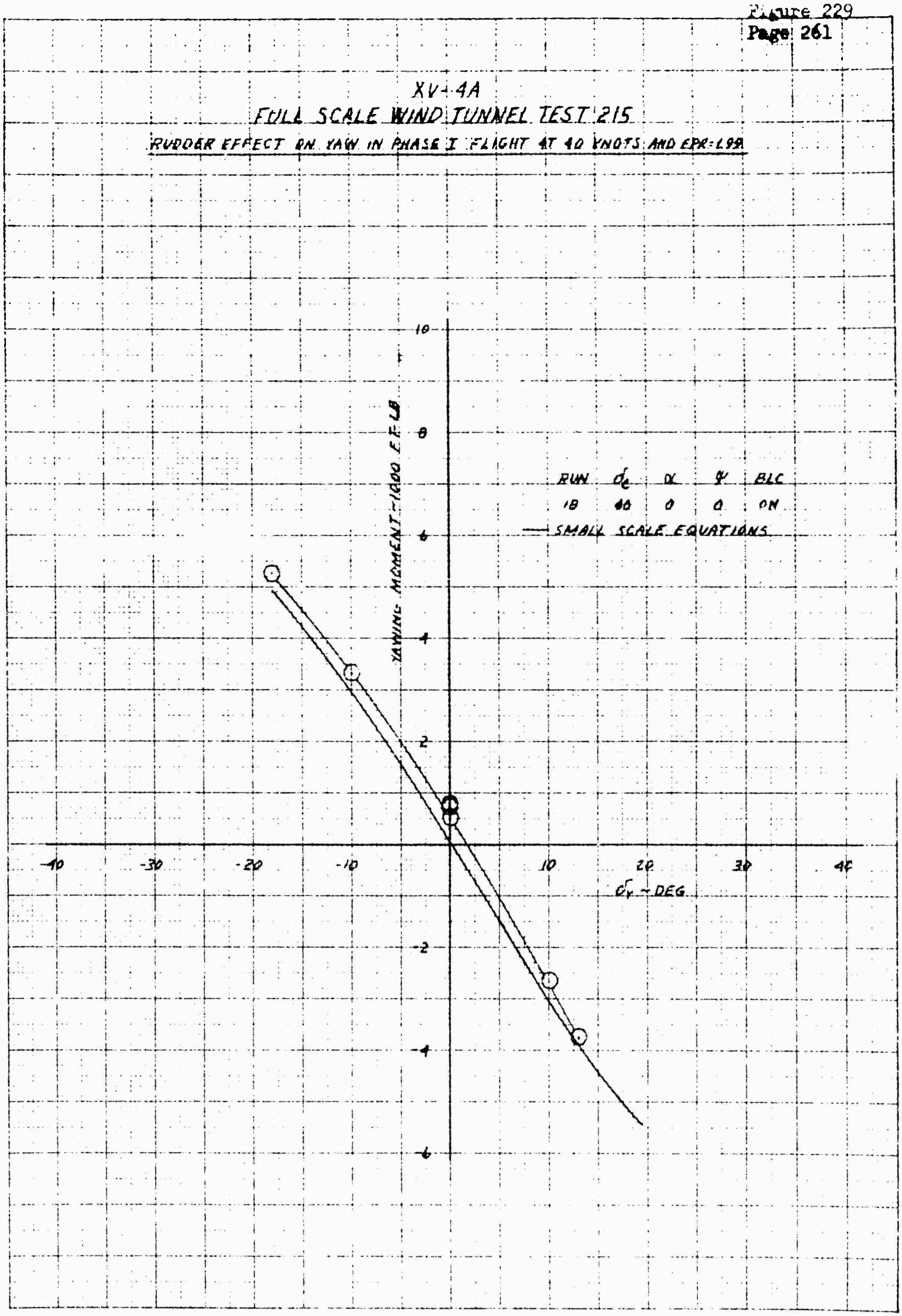
XV-4A
FULL SCALE WIND TUNNEL TEST 215
RUDDER EFFECT ON YAW IN PHASE I FLIGHT AT 40 KNOTS AND EPR=1.99
YAWING MOMENT ~1000 FT LB
10
8
6
4
2
-2
-4
-6
-40
-30
-20
-10
10
20
30
40
δ_r ~ DEG
RUN
δ_e
α
ψ
BLC
18
40
0
0
ON
SMALL SCALE EQUATIONS

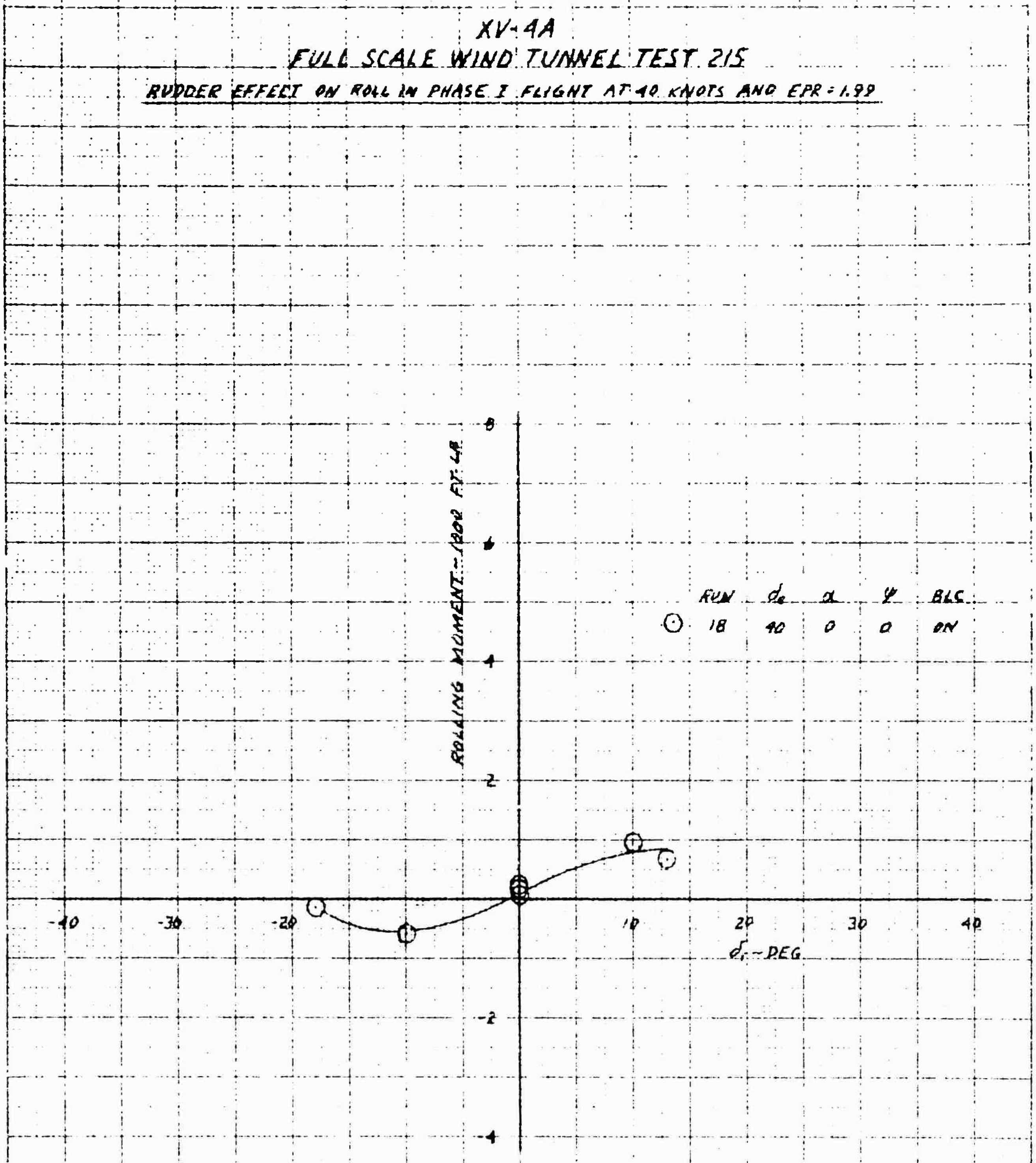
XV-4A
FULL SCALE WIND TUNNEL TEST 215
RUDDER EFFECT ON ROLL IN PHASE I FLIGHT AT 40 KNOTS AND EPR = 1.99
ROLLING MOMENT ~ 1000 FT-LB
8
6
4
2
-2
-4
-40
-30
-20
10
20
30
40
δ_r ~ DEG
RUN δ_e α ψ BLC
18 40 0 0 ON

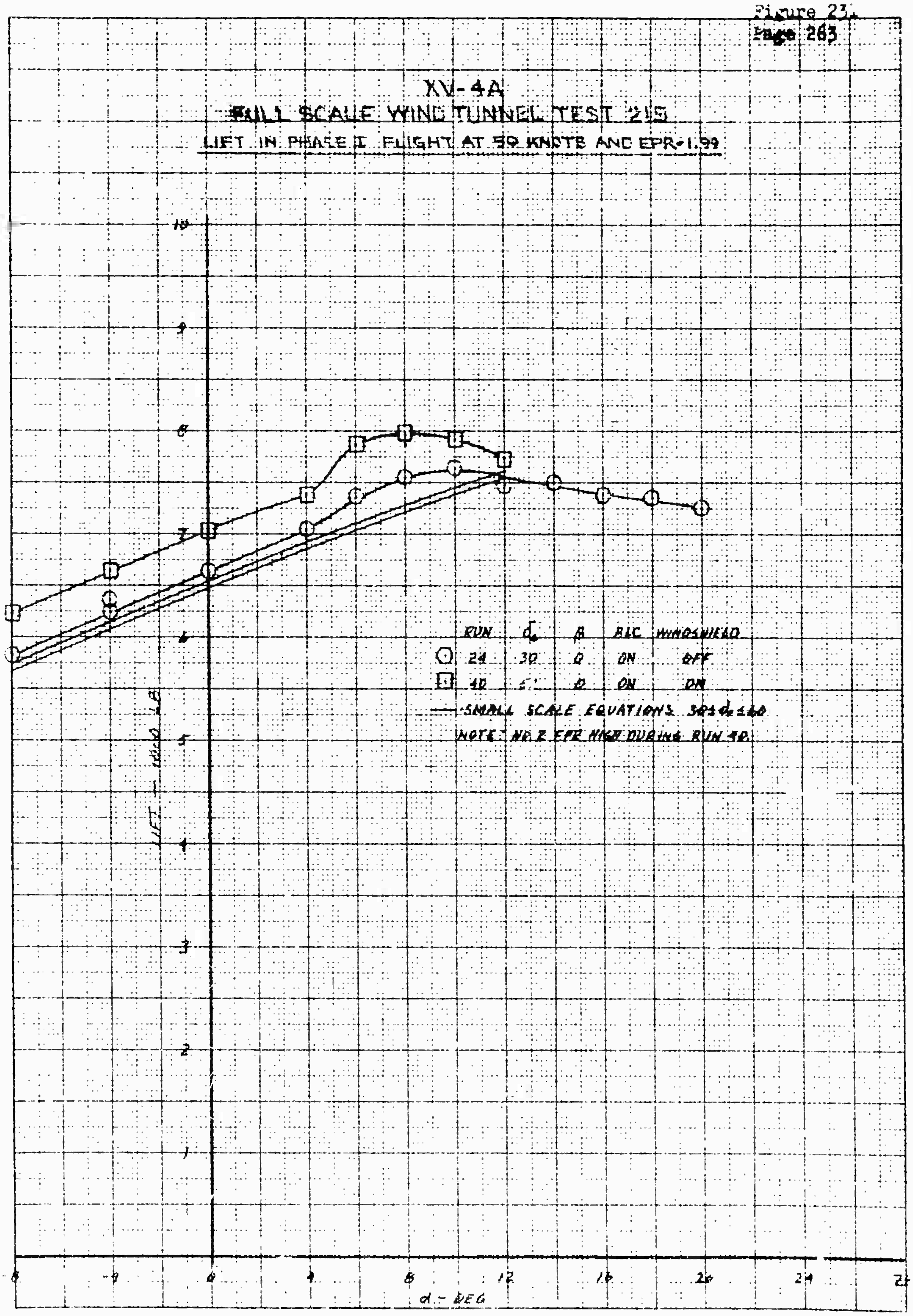
XV-4A
FULL SCALE WIND TUNNEL TEST 215
LIFT IN PHASE I FLIGHT AT 59 KNOTS AND EPR=1.99
RUN
BLC
WINDSHIELD
24
30
ON
OFF
40
ON
ON
SMALL SCALE EQUATIONS
NOTE: NO. 2 EPR HIGH DURING RUN 40.
LIFT — 1000 LB
α – DEG
-8
-4
0
4
8
12
16
20
24
1
2
3
4
5
6
7
8
9
10

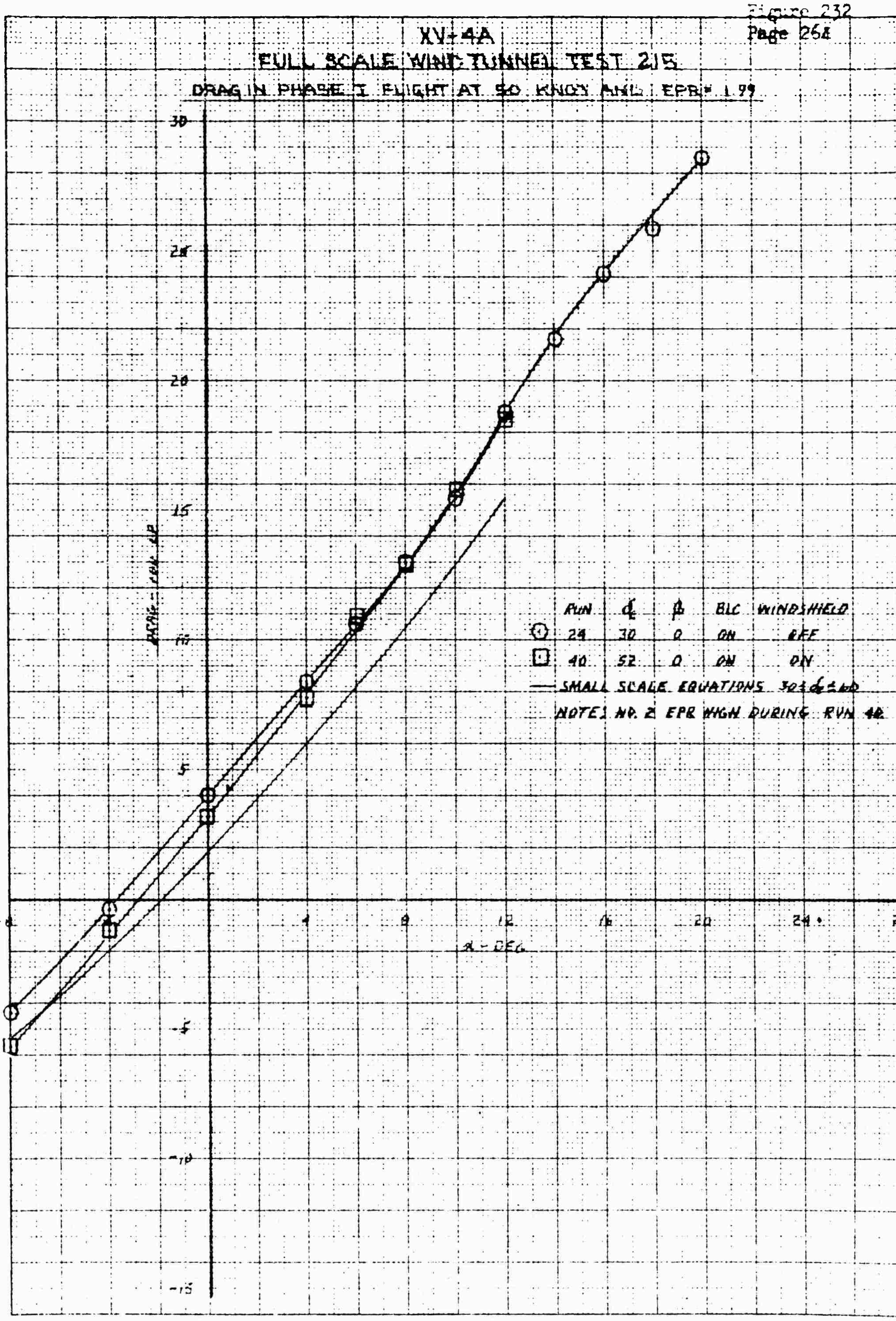
XV-4A
FULL SCALE WIND TUNNEL TEST 215
DRAG IN PHASE I FLIGHT AT 50 KNOTS AND EPR = 1.99
DRAG - 100 LB
α - DEG
RUN δf β BLC WINDSHIELD
24 30 0 ON OFF
40 52 0 ON ON
SMALL SCALE EQUATIONS 30 ≤ δf ≤ 60
NOTE: NO. 2 EPR HIGH DURING RUN 40

XV-4A

FULL SCALE WIND TUNNEL TEST 215

PITCHING MOMENT IN PHASE I FLIGHT AT 50 KNOTS AND EPR = 1.99

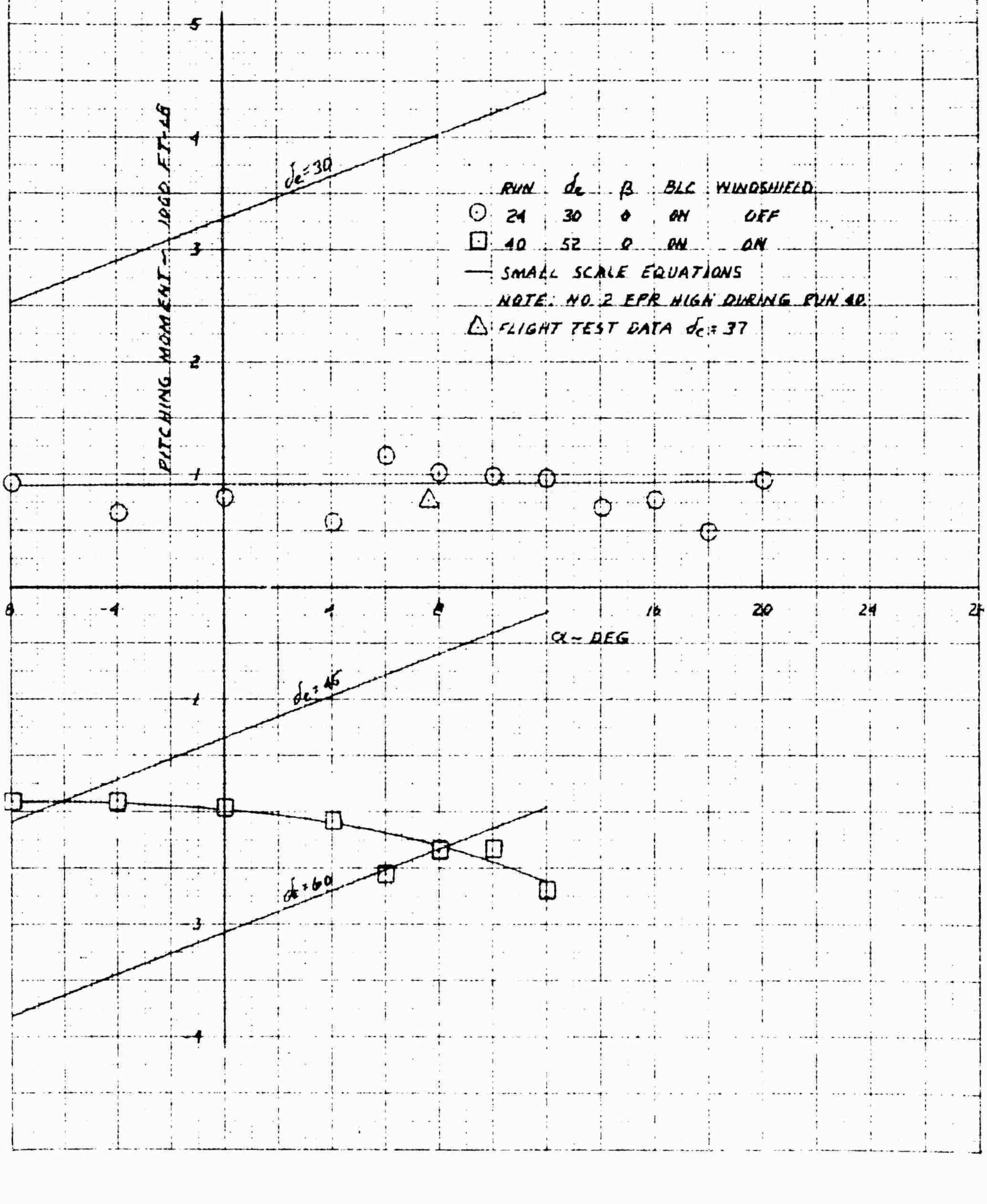

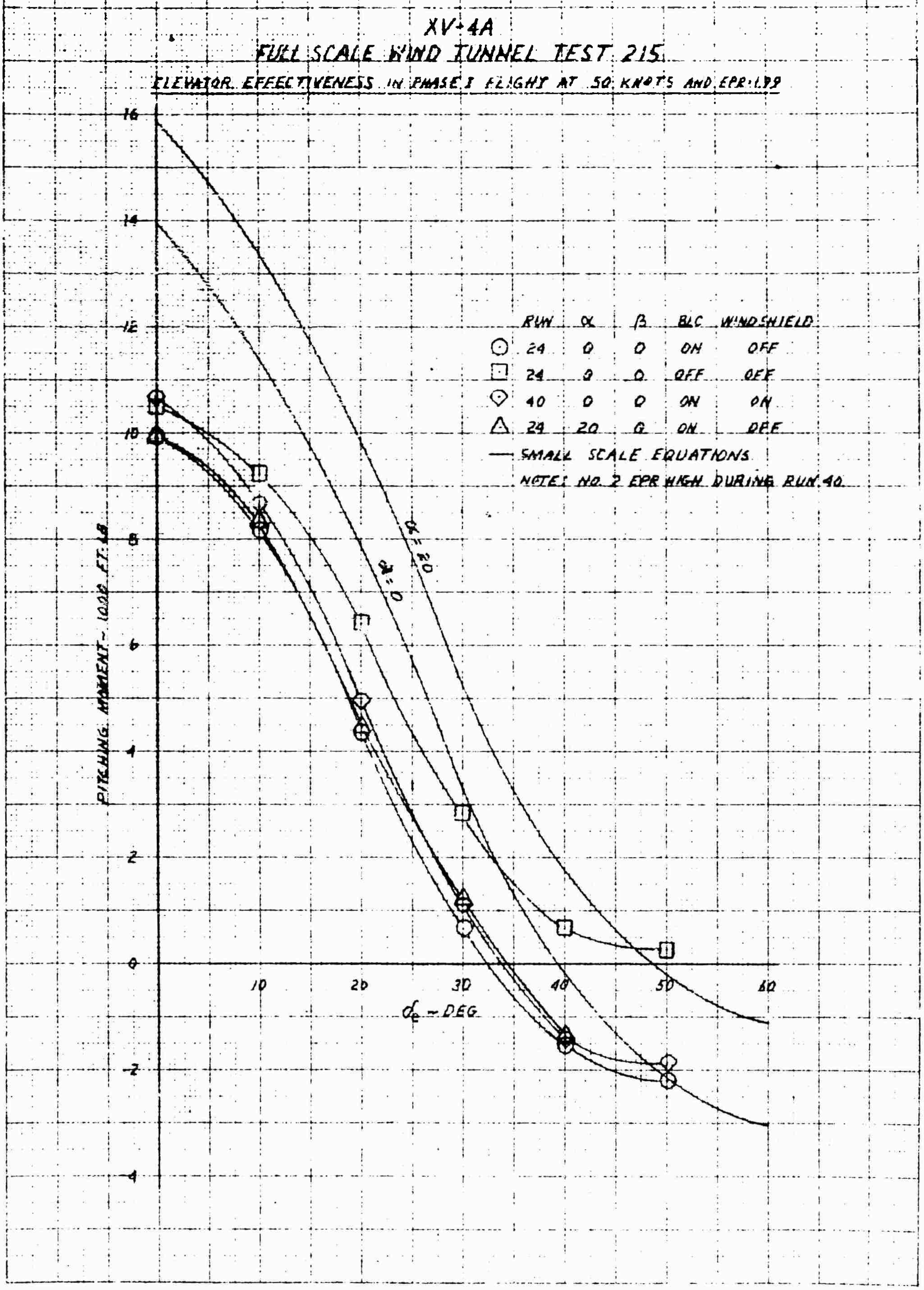
XV-4A
FULL SCALE WIND TUNNEL TEST 215
ELEVATOR EFFECTIVENESS IN PHASE I FLIGHT AT 50 KNOTS AND EPR-1.79
RUN α β BLC WINDSHIELD
24 0 0 ON OFF
24 0 0 OFF OFF
40 0 0 ON ON
24 20 0 ON OFF
SMALL SCALE EQUATIONS
NOTE: NO. 2 EPR HIGH DURING RUN 40
α = 20
α = 0
PITCHING MOMENT - 1000 FT-LB
δe - DEG
16
14
12
10
8
6
4
2
0
-2
-4
10
20
30
40
50
60

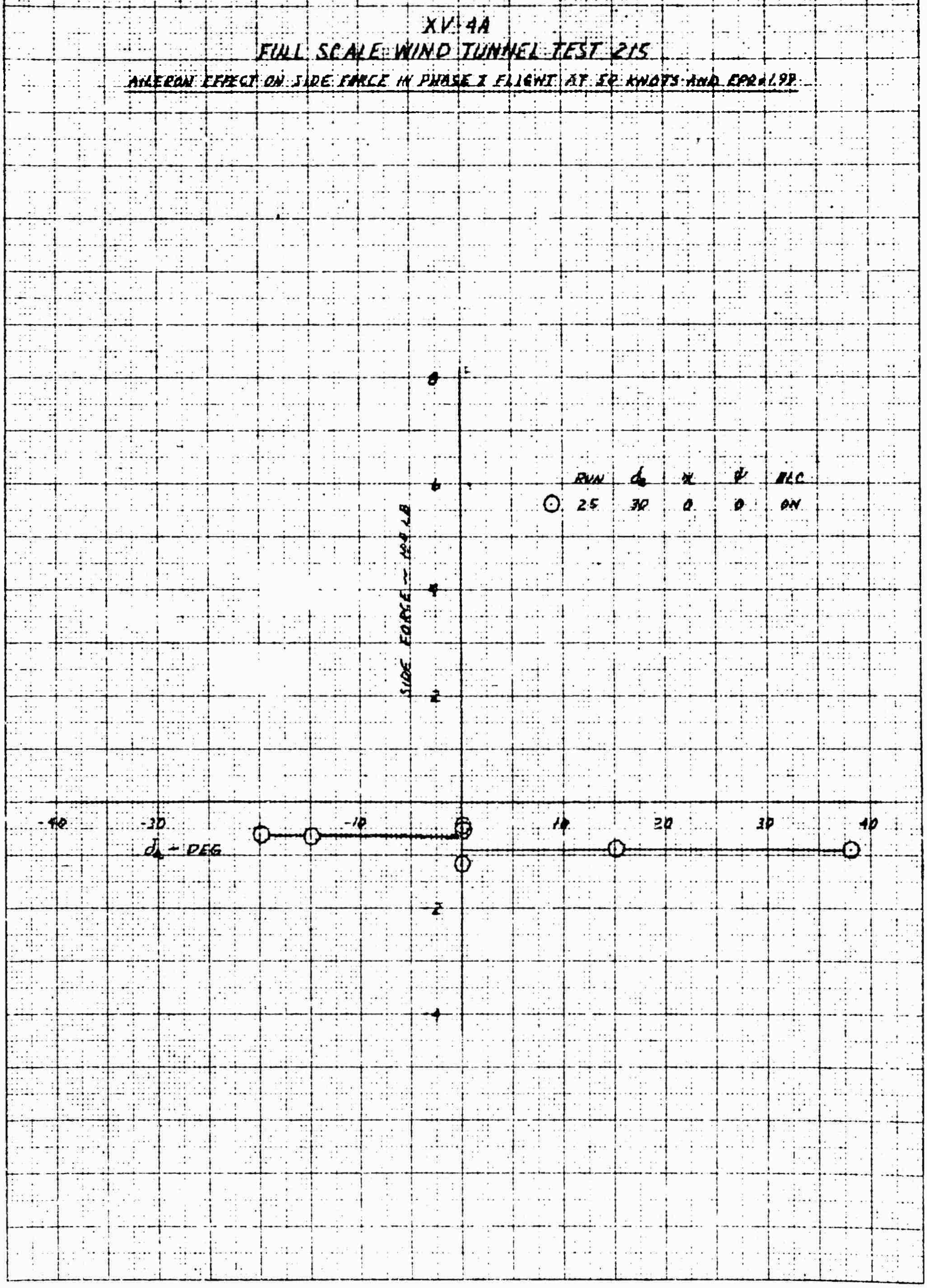
XV-4A
FULL SCALE WIND TUNNEL TEST 215
AILERON EFFECT ON SIDE FORCE IN PHASE I FLIGHT AT 50 KNOTS AND EPR=1.99
RUN
25
30
0
0
ON
SIDE FORCE ~ 10² LB
8
6
4
2
-2
-4
-40
-30
-10
10
20
30
40
δ ~ DEG

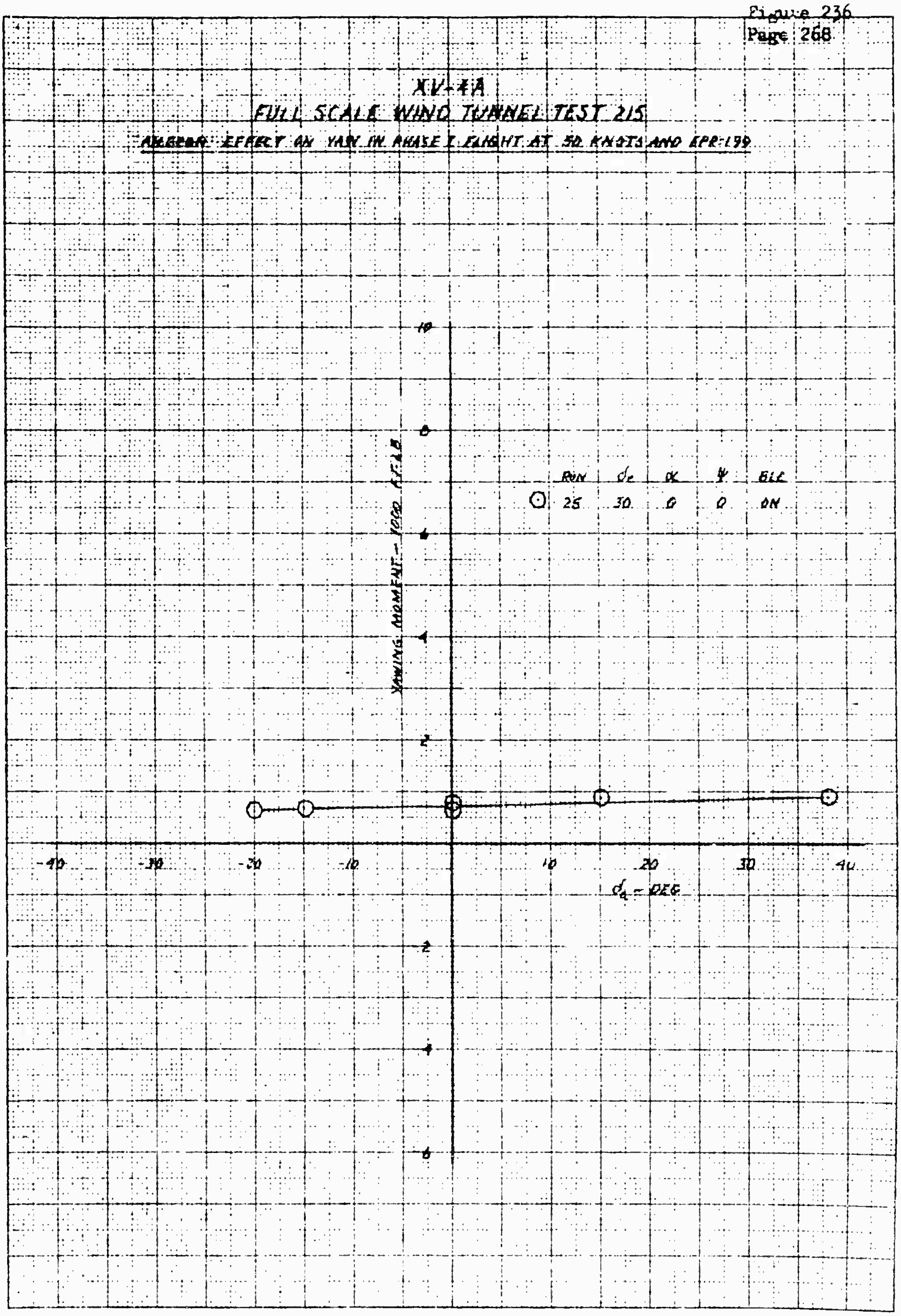
XV-4A
FULL SCALE WIND TUNNEL TEST 215
AILERON: EFFECT ON YAW IN PHASE I FLIGHT AT 50 KNOTS AND EPR-1.99
YAWING MOMENT - 1000 FT-LB
δa - DEG
RUN
δe
α
ψ
BLC
25
30
0
0
ON
10
8
6
4
2
-2
-4
-6
-40
-30
-20
-10
10
20
30
40

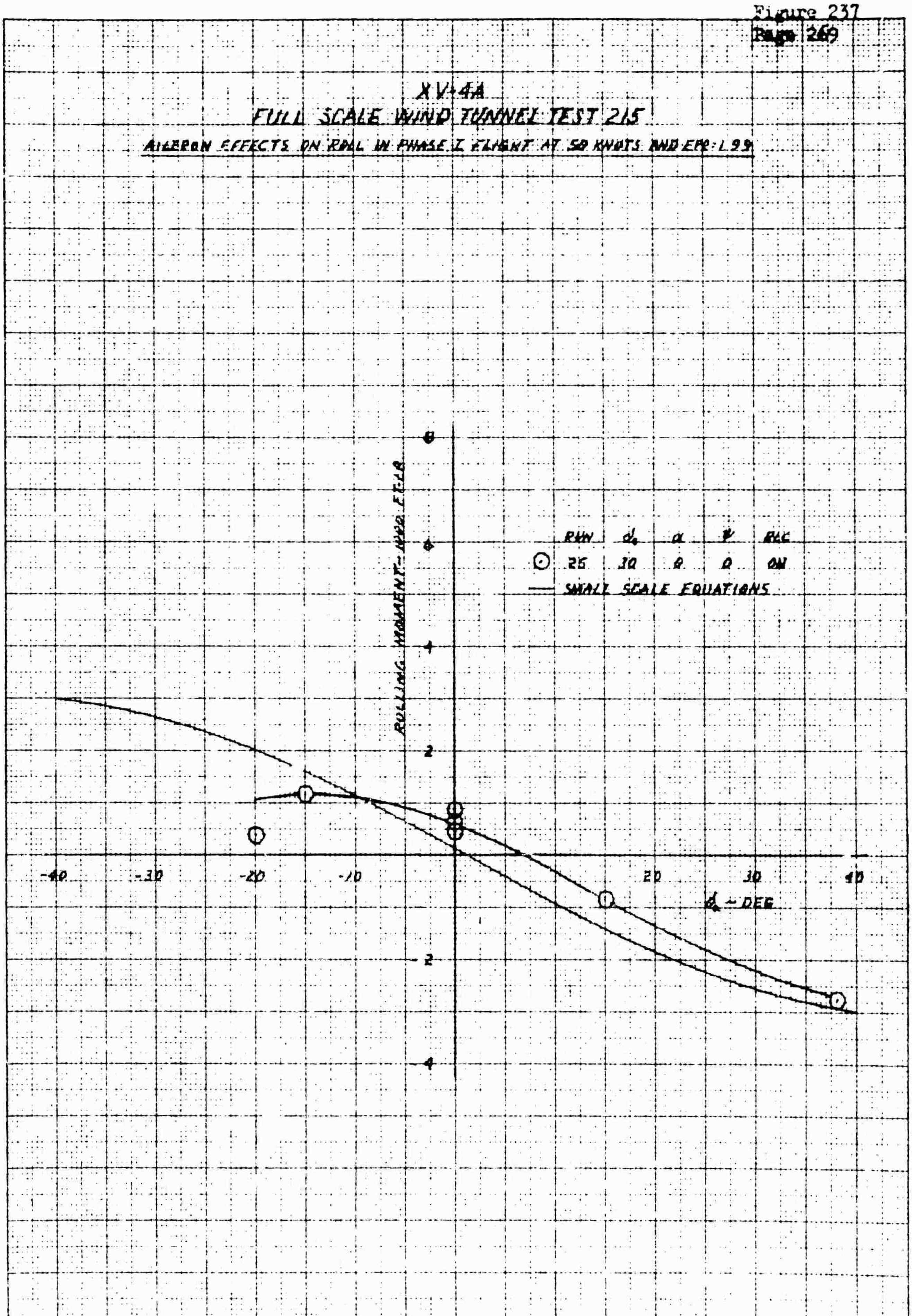
XV-4A
FULL SCALE WIND TUNNEL TEST 215
AILERON EFFECTS ON ROLL IN PHASE I FLIGHT AT 50 KNOTS AND EPR: 1.99
ROLLING MOMENT - 1000 FT-LB
RUN
25
30
0
0
ON
SMALL SCALE EQUATIONS
δ_a - DEG
-40
-30
-20
-10
20
30
40
8
6
4
2
-2
-4

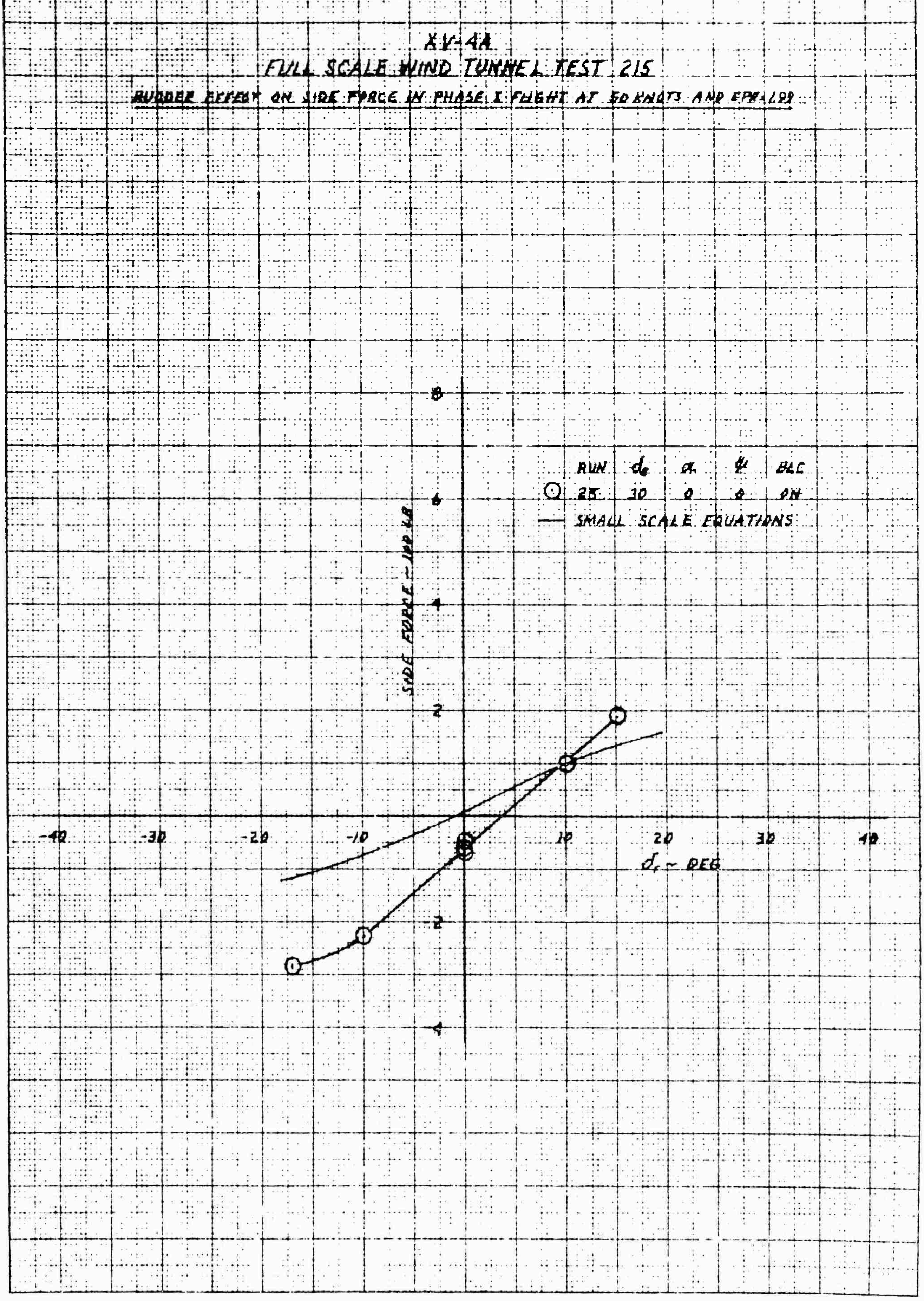
XV-4A
FULL SCALE WIND TUNNEL TEST 215
RUDDER EFFECT ON SIDE FORCE IN PHASE I FLIGHT AT 50 KNOTS AND EPR=1.99
RUN δ_e α ψ BLC
25 30 0 0 ON
SMALL SCALE EQUATIONS
SIDE FORCE ~ 100 LB
δ_r ~ DEG
-40
-30
-20
-10
10
20
30
40
8
6
4
2
-2
-4

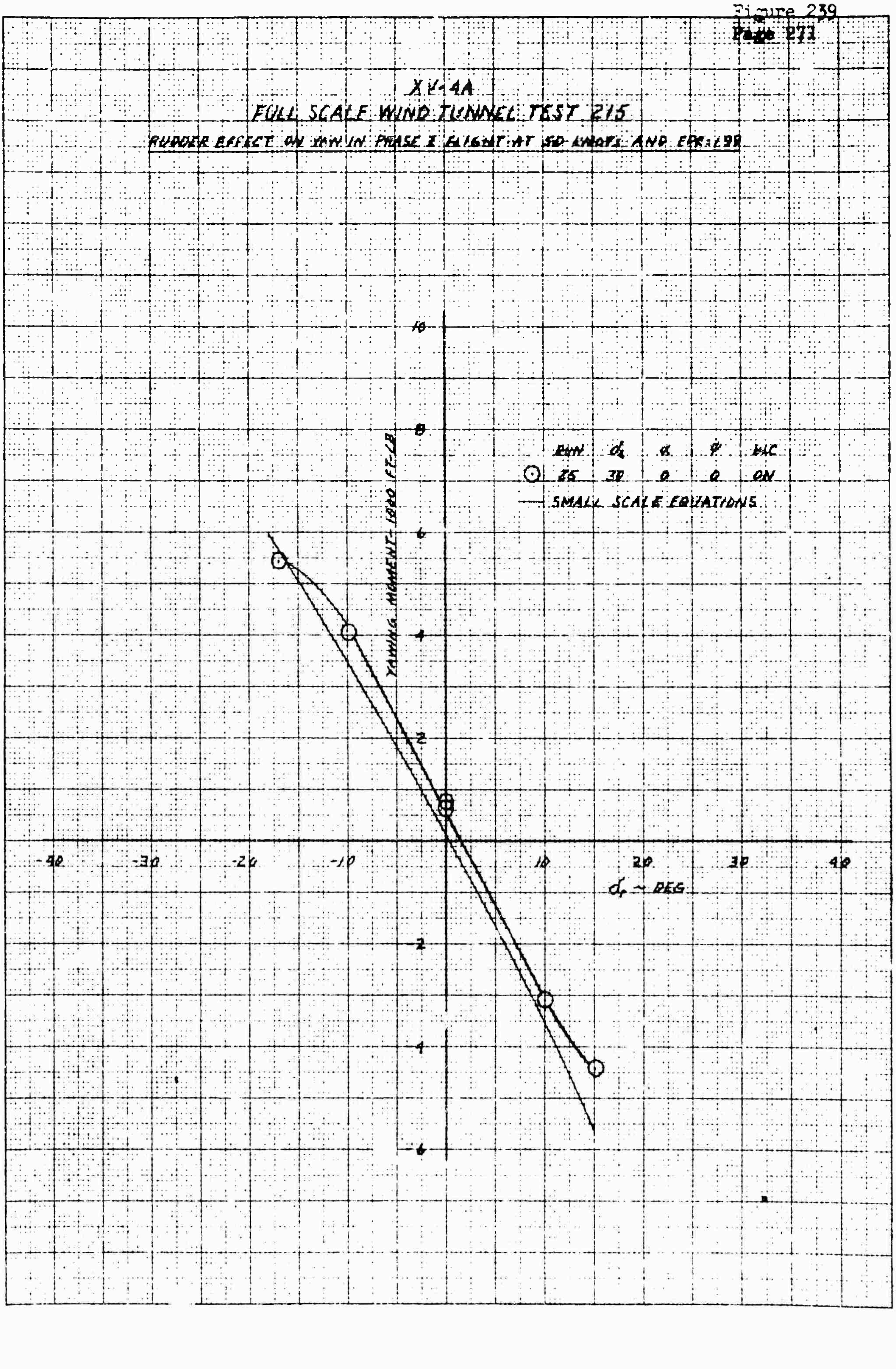
XV-4A
FULL SCALE WIND TUNNEL TEST 215
RUDDER EFFECT ON YAW IN PHASE I FLIGHT AT 50 KNOTS AND EPR=1.98
RUN δ α ψ HC
25 30 0 0 ON
SMALL SCALE EQUATIONS
YAWING MOMENT-1000 FT-LB
δr ~ DEG
10
8
6
4
2
-2
-4
-6
-40
-30
-20
-10
10
20
30
40

XV-4A

FULL SCALE WIND TUNNEL TEST 215

RUDDER EFFECT ON ROLL IN PHASE I FLIGHT AT 50 KNOTS AND EPR 1.99

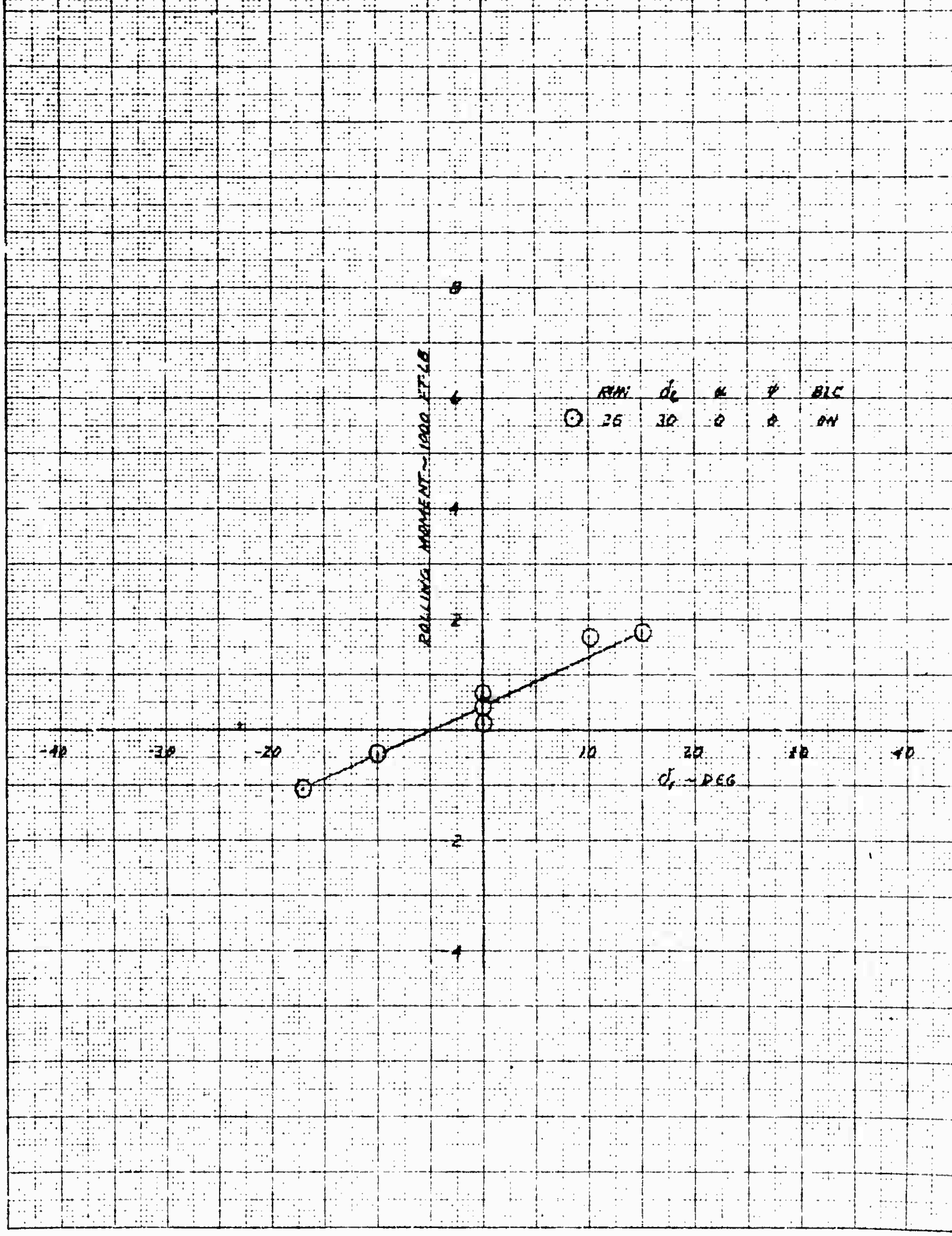

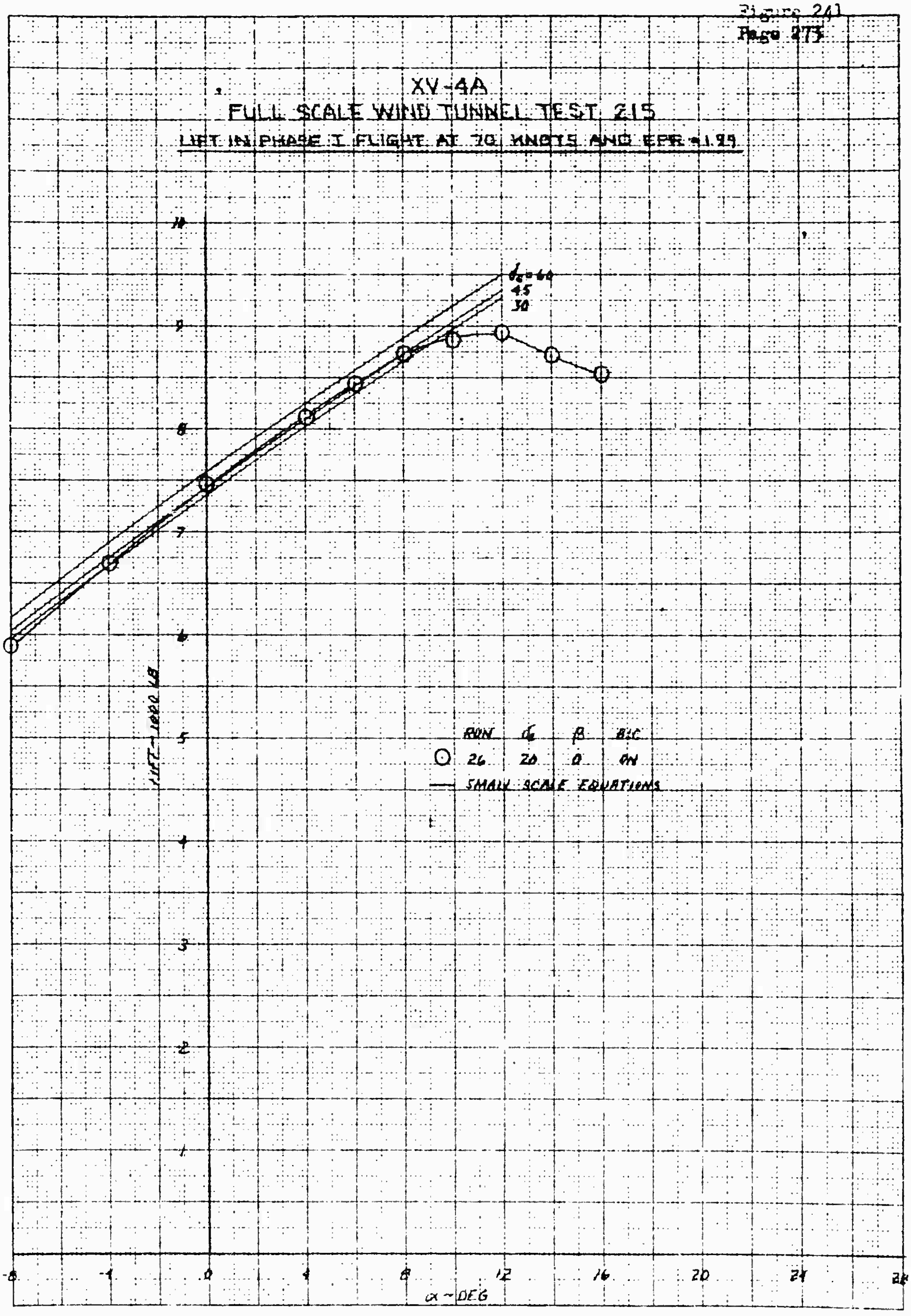
XV-4A
FULL SCALE WIND TUNNEL TEST 215
LIFT IN PHASE I FLIGHT AT 70 KNOTS AND EPR = 1.99
LIFT ~ 1000 LB
α ~ DEG
RUN
β
B.C.
26
20
0
ON
SMALL SCALE EQUATIONS
45
30

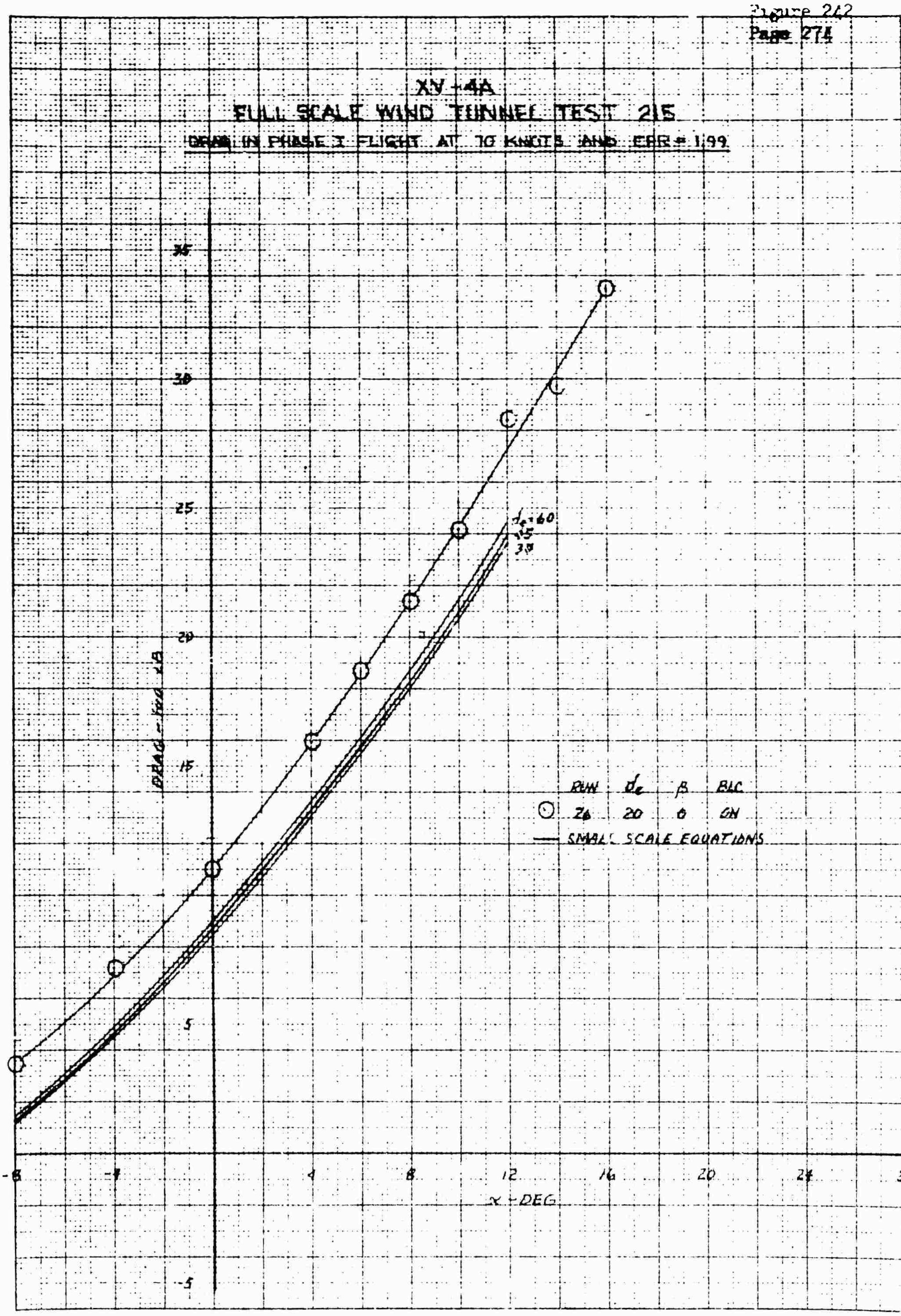
XV-4A
FULL SCALE WIND TUNNEL TEST 215
DRAG IN PHASE I FLIGHT AT 10 KNOTS AND EPR = 1.99
DRAG - 100 LB
α - DEG
RUN δe β BLC
26 20 0 ON
SMALL SCALE EQUATIONS
δe = 60
45
30
35
30
25
20
15
5
-5
-8
-4
4
8
12
16
20
24
28

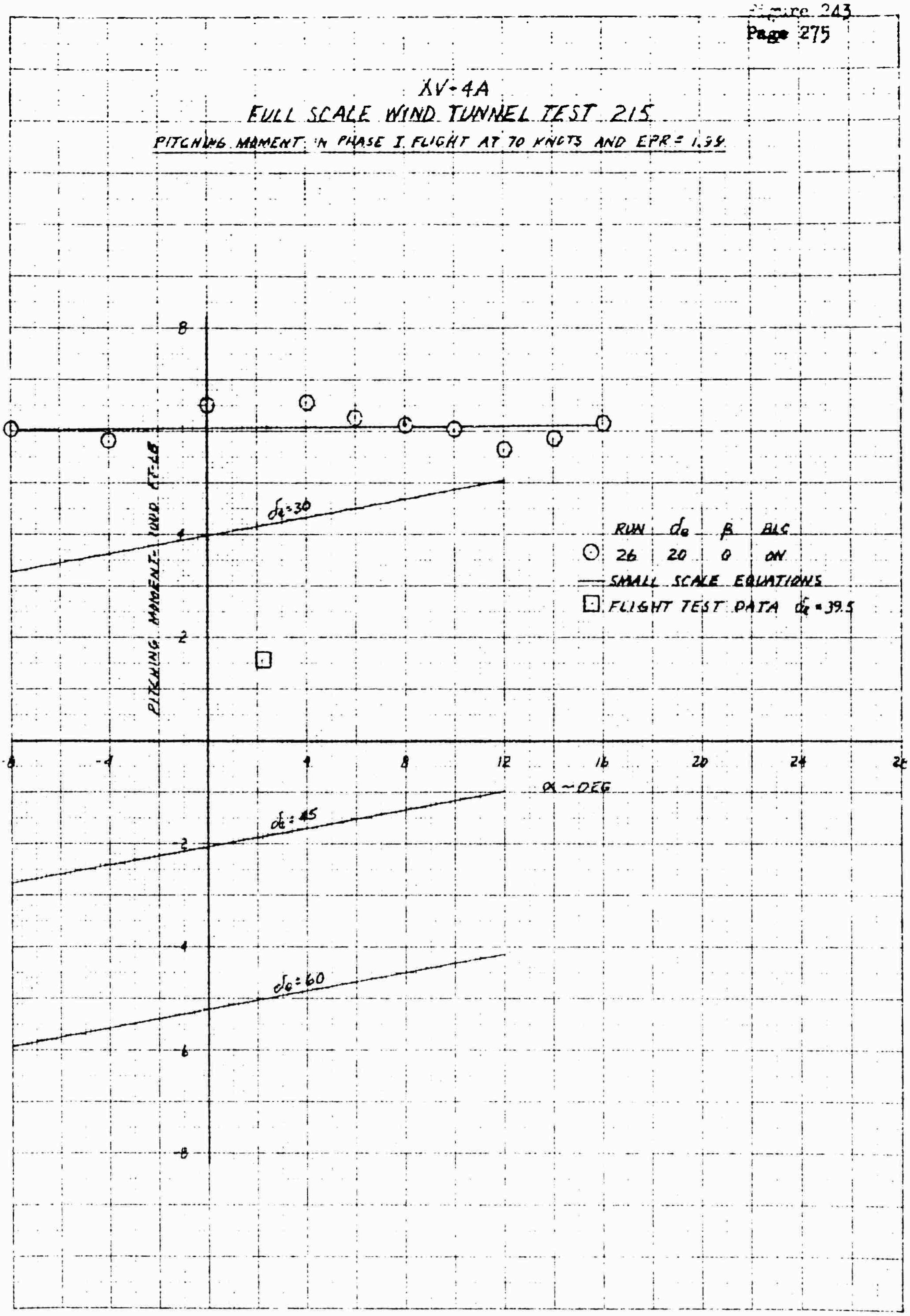
XV-4A
FULL SCALE WIND TUNNEL TEST 215
PITCHING MOMENT IN PHASE I FLIGHT AT 70 KNOTS AND EPR = 1.34
PITCHING MOMENT - 1000 FT-LB
α ~ DEG
δ_e=30
δ_e=45
δ_e=60
RUN δ_e β BLC
26 20 0 ON
SMALL SCALE EQUATIONS
FLIGHT TEST DATA δ_e = 39.5

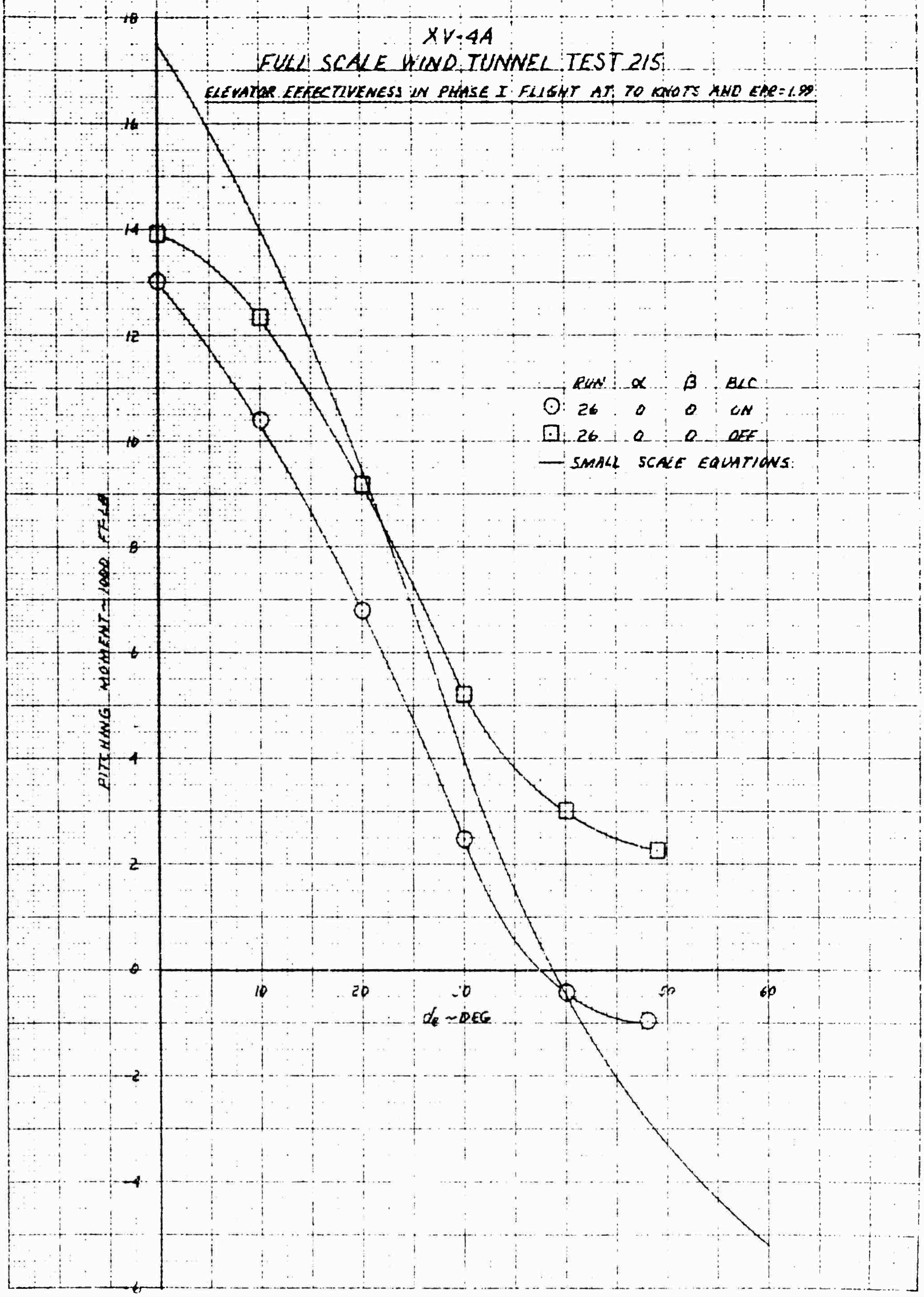
XV-4A
FULL SCALE WIND TUNNEL TEST 215
ELEVATOR EFFECTIVENESS IN PHASE I FLIGHT AT 70 KNOTS AND EPR=1.99
RUN α β BLC
26 0 0 ON
26 0 0 OFF
SMALL SCALE EQUATIONS
PITCHING MOMENT~1000 FT-LB
δ_e ~DEG
18
16
14
12
10
8
6
4
2
0
-2
-4
-6
10
20
30
50
60

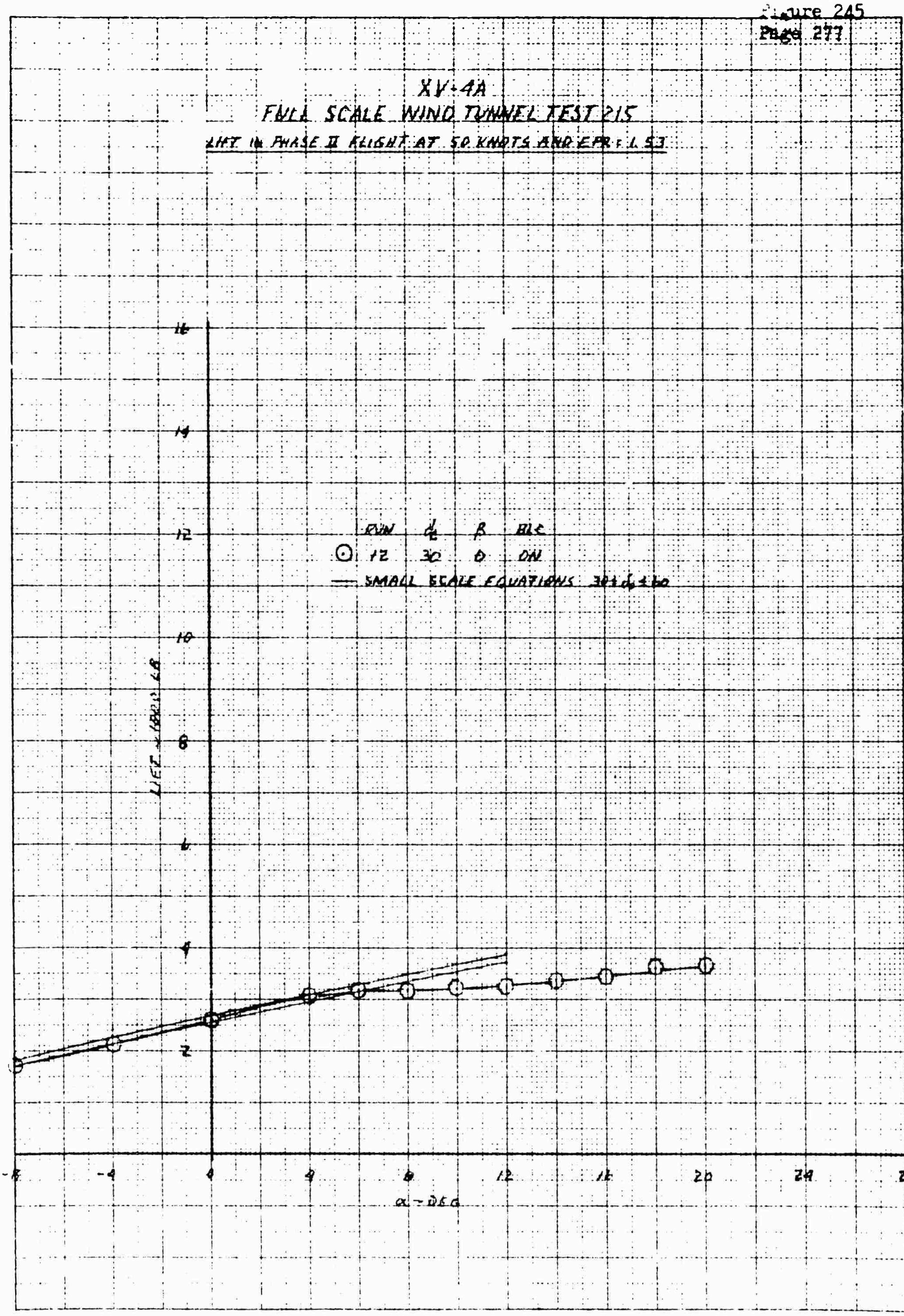
XV-4A
FULL SCALE WIND TUNNEL TEST 215
LIFT IN PHASE II FLIGHT AT 50 KNOTS AND EPR = 1.53
RUN
β
BLC
12
30
0
ON
SMALL SCALE EQUATIONS
LIFT x 1000 LB
α ~ DEG
16
14
12
10
8
6
4
2
-8
-4
0
4
8
12
16
20
24
28

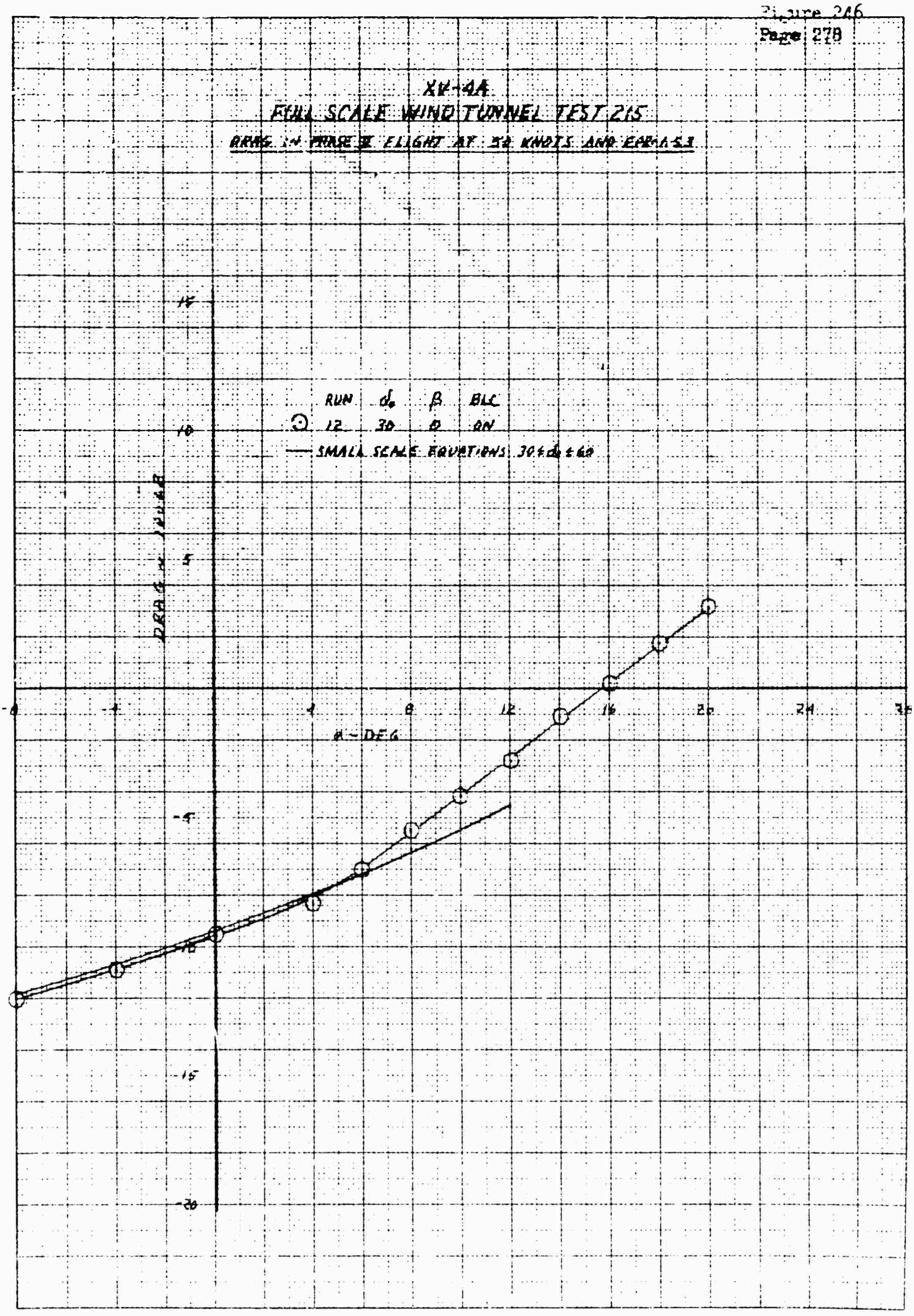
XV-4A
FULL SCALE WIND TUNNEL TEST 215
DRAG IN PHASE II FLIGHT AT 50 KNOTS AND EPR=1.53
RUN
δ_e
β
BLC
12
30
0
ON
SMALL SCALE EQUATIONS 30°≤δ_e≤60
DRAG ~ 1bs
α ~ DEG

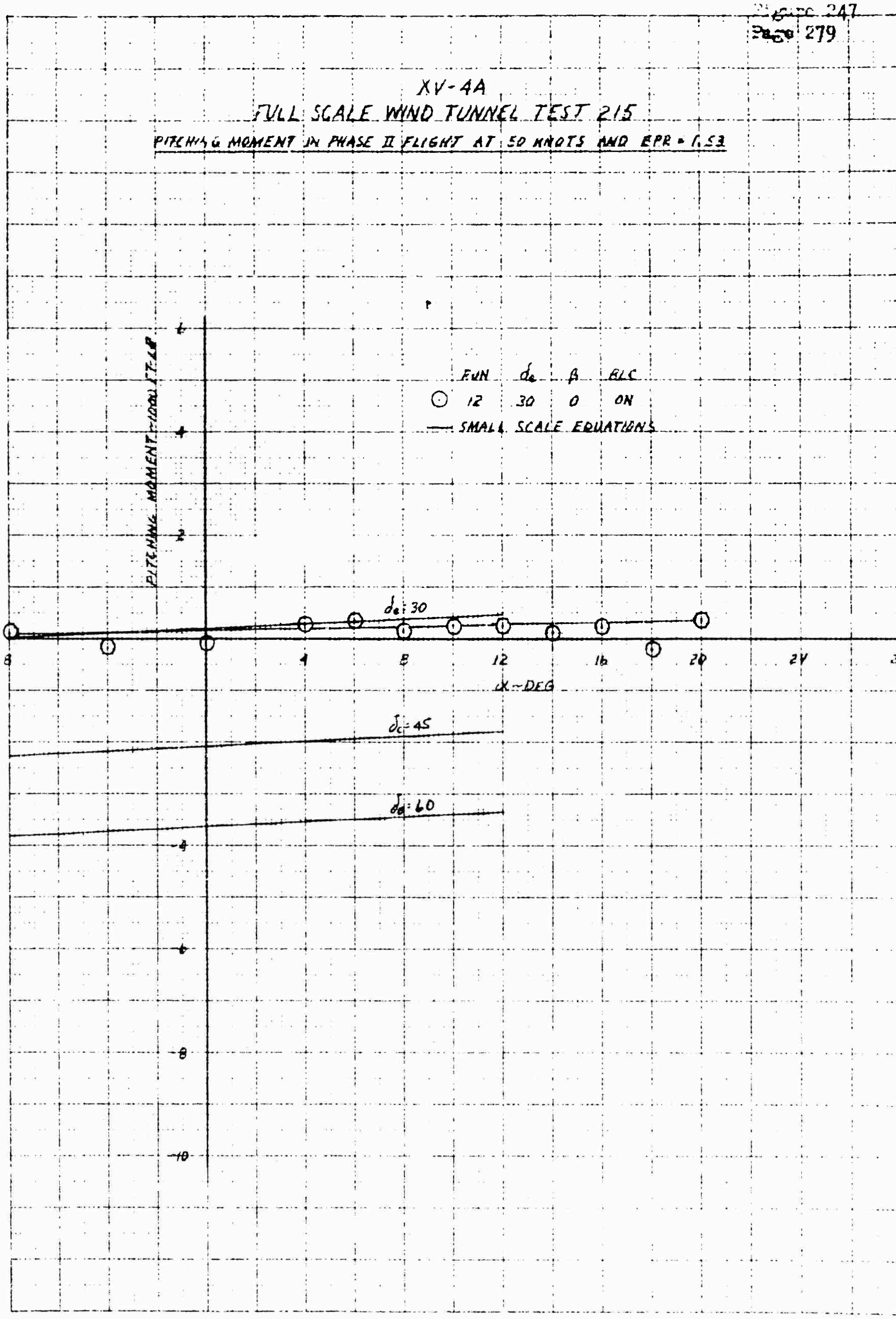
XV-4A
FULL SCALE WIND TUNNEL TEST 215
PITCHING MOMENT IN PHASE II FLIGHT AT 50 KNOTS AND EPR = 1.53
RUN
δ_e
β
BLC
12
30
0
ON
SMALL SCALE EQUATIONS
PITCHING MOMENT ~1000 FT-LB
δ_e = 30
δ_e = 45
δ_e = 60
α ~ DEG
6
4
2
-4
-6
-8
-10
4
8
12
16
20
24

XV-4A

FULL SCALE WIND TUNNEL TEST 215

ELEVATOR EFFECTIVENESS IN PHASE II FLIGHT AT 50 KNOTS AND FPE:153

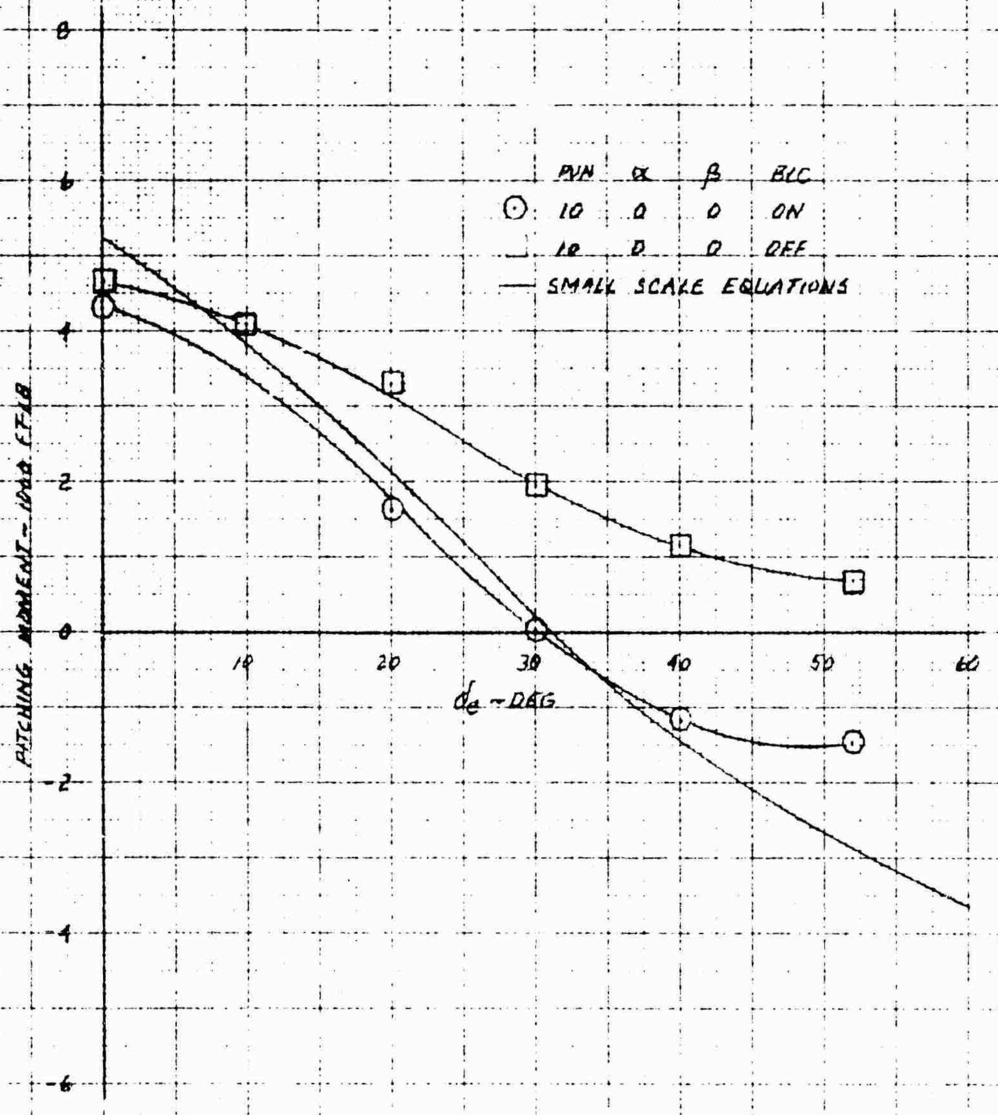

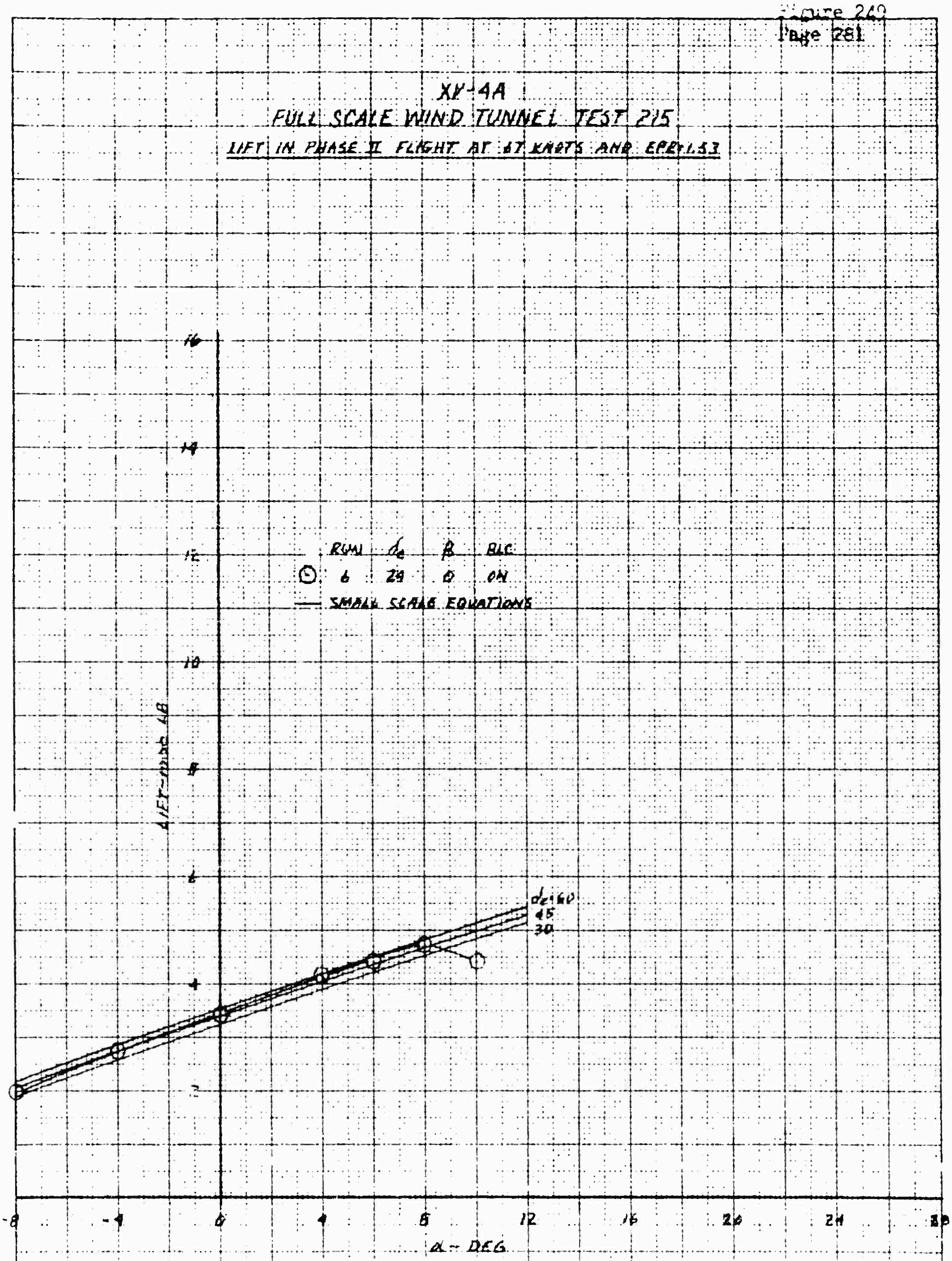
XV-4A
FULL SCALE WIND TUNNEL TEST 215
LIFT IN PHASE II FLIGHT AT 67 KNOTS AND EPR=1.53
RUN δ_e β BLC
6 29 0 ON
SMALL SCALE EQUATIONS
δ_e=60
45
30
LIFT-1000 LB
α - DEG

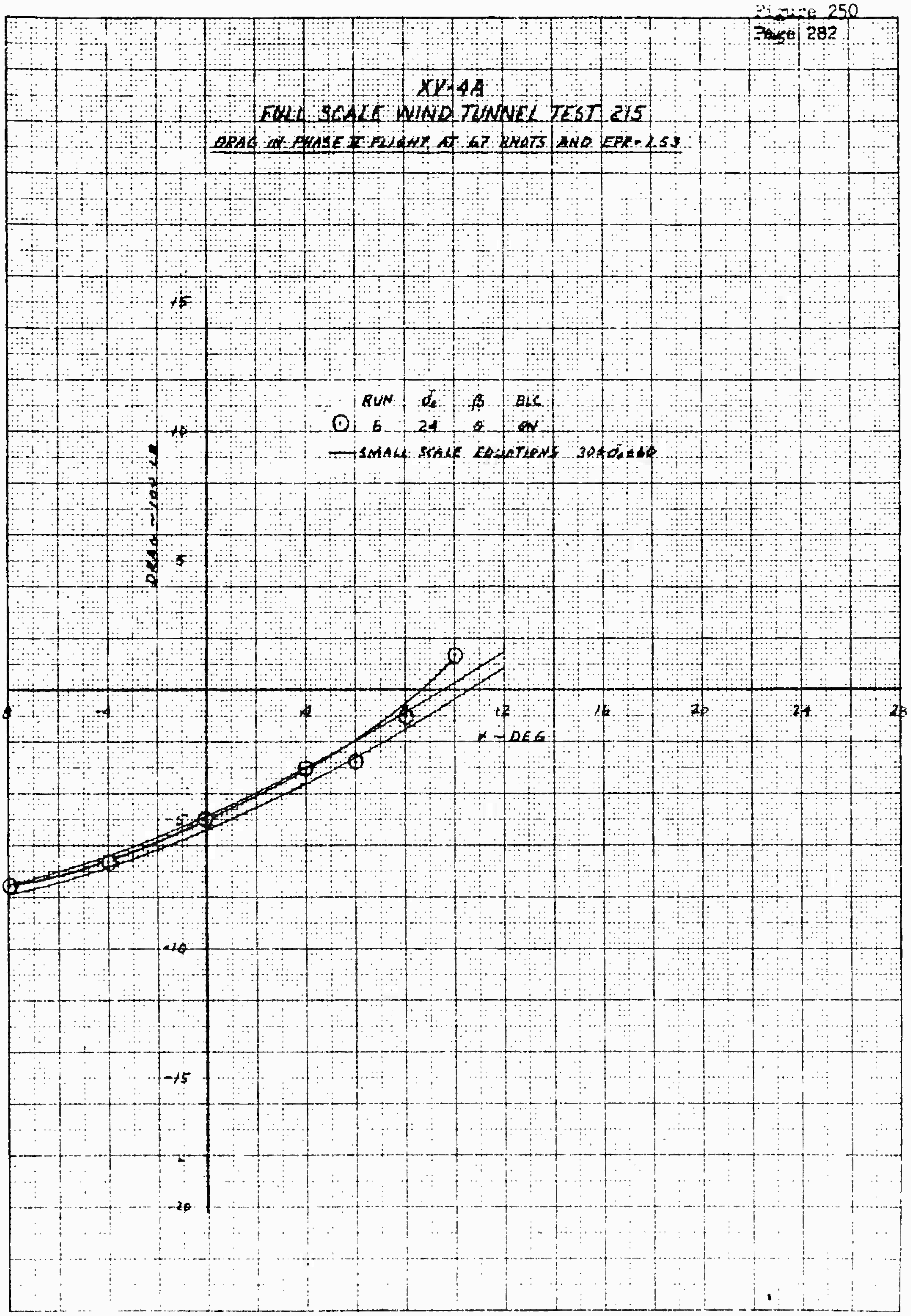
XV-4A
FULL SCALE WIND TUNNEL TEST 215
DRAG IN PHASE II FLIGHT AT 67 KNOTS AND EPR=1.53
RUN
6
24
0
ON
BLC
SMALL SCALE EQUATIONS
DRAG ~ 100 LB
α ~ DEG
15
10
5
-5
-10
-15
-20
-8
-4
4
8
12
16
20
24
28

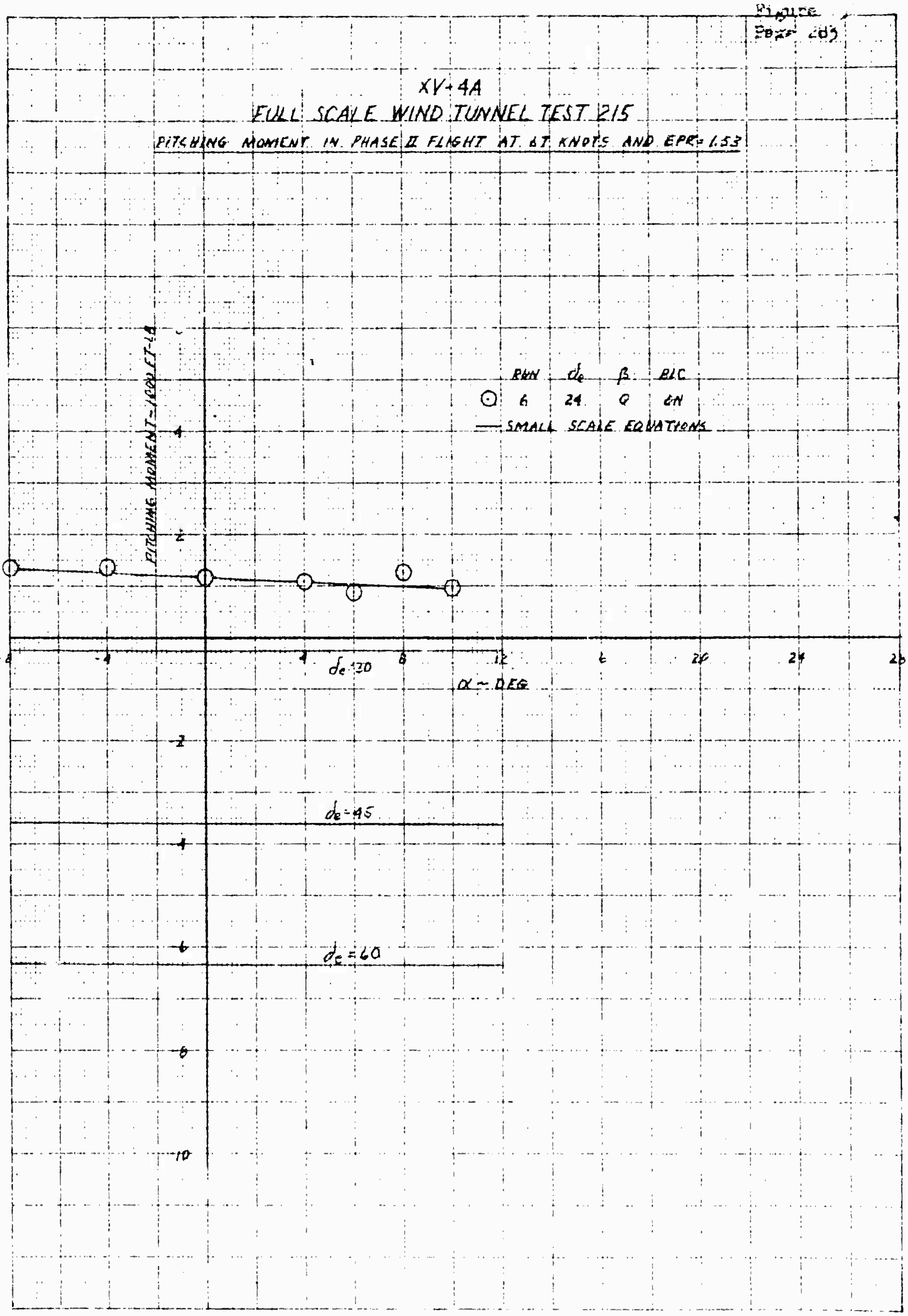
XV-4A
FULL SCALE WIND TUNNEL TEST 215
PITCHING MOMENT IN PHASE II FLIGHT AT 67 KNOTS AND EPR=1.53
RUN δe β B/C
6 24 0 ON
SMALL SCALE EQUATIONS
PITCHING MOMENT~1000 FT-LB
α ~ DEG
δe=30
δe=45
δe=60
-8
-4
4
8
12
16
20
24
28
4
2
-2
-4
-6
-8
-10

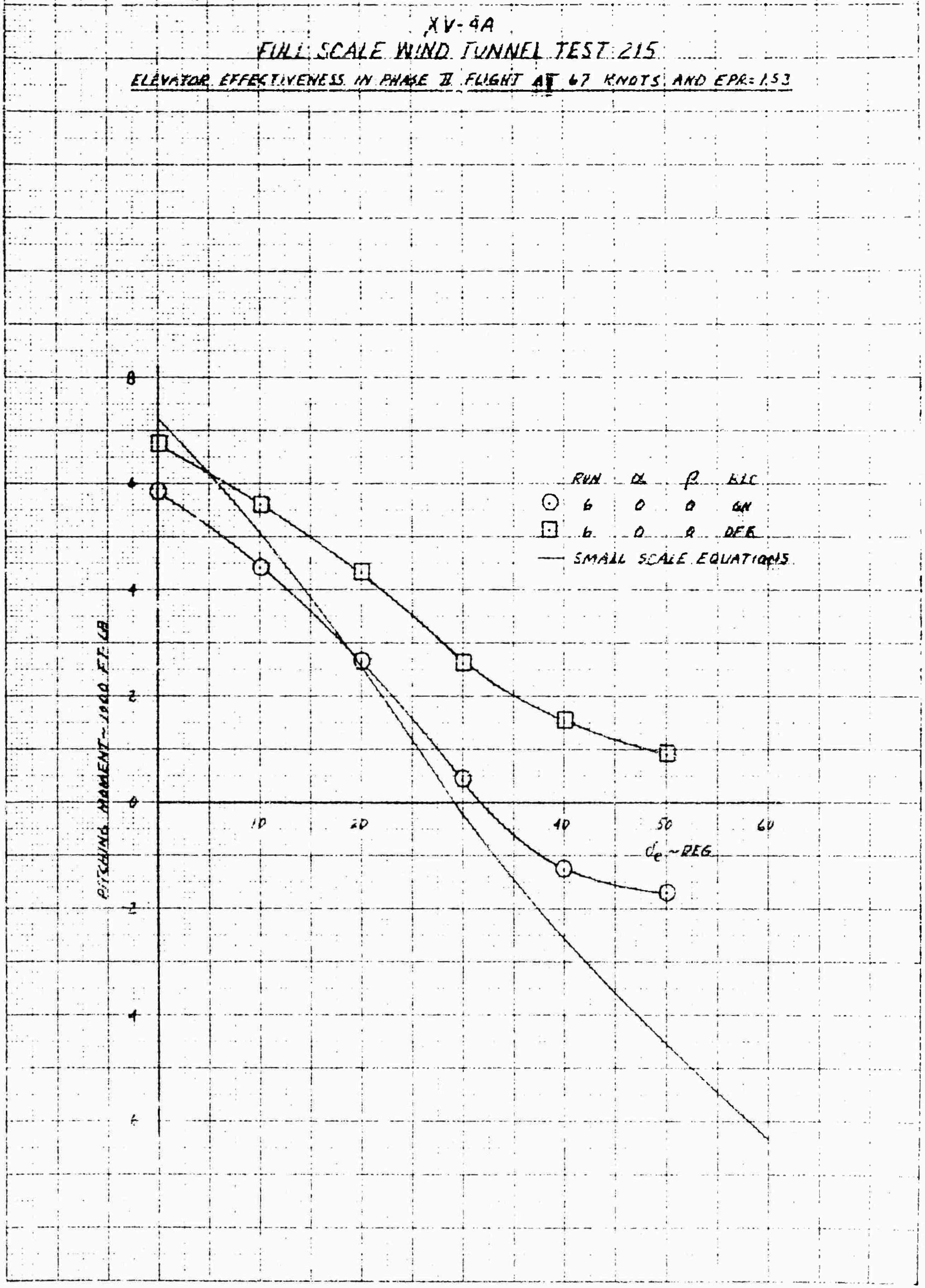
XV-4A
FULL SCALE WIND TUNNEL TEST 215
ELEVATOR EFFECTIVENESS IN PHASE II FLIGHT AT 67 KNOTS AND EPR=1.53
RUN α β BLC
6 0 0 ON
6 0 0 OFF
SMALL SCALE EQUATIONS
PITCHING MOMENT ~ 1000 FT-LB
δ_e ~ DEG

XV-4A

FULL SCALE WIND TUNNEL TEST 215

LIFT IN PHASE II FLIGHT AT 85 KNOTS AND EPR = 1.53

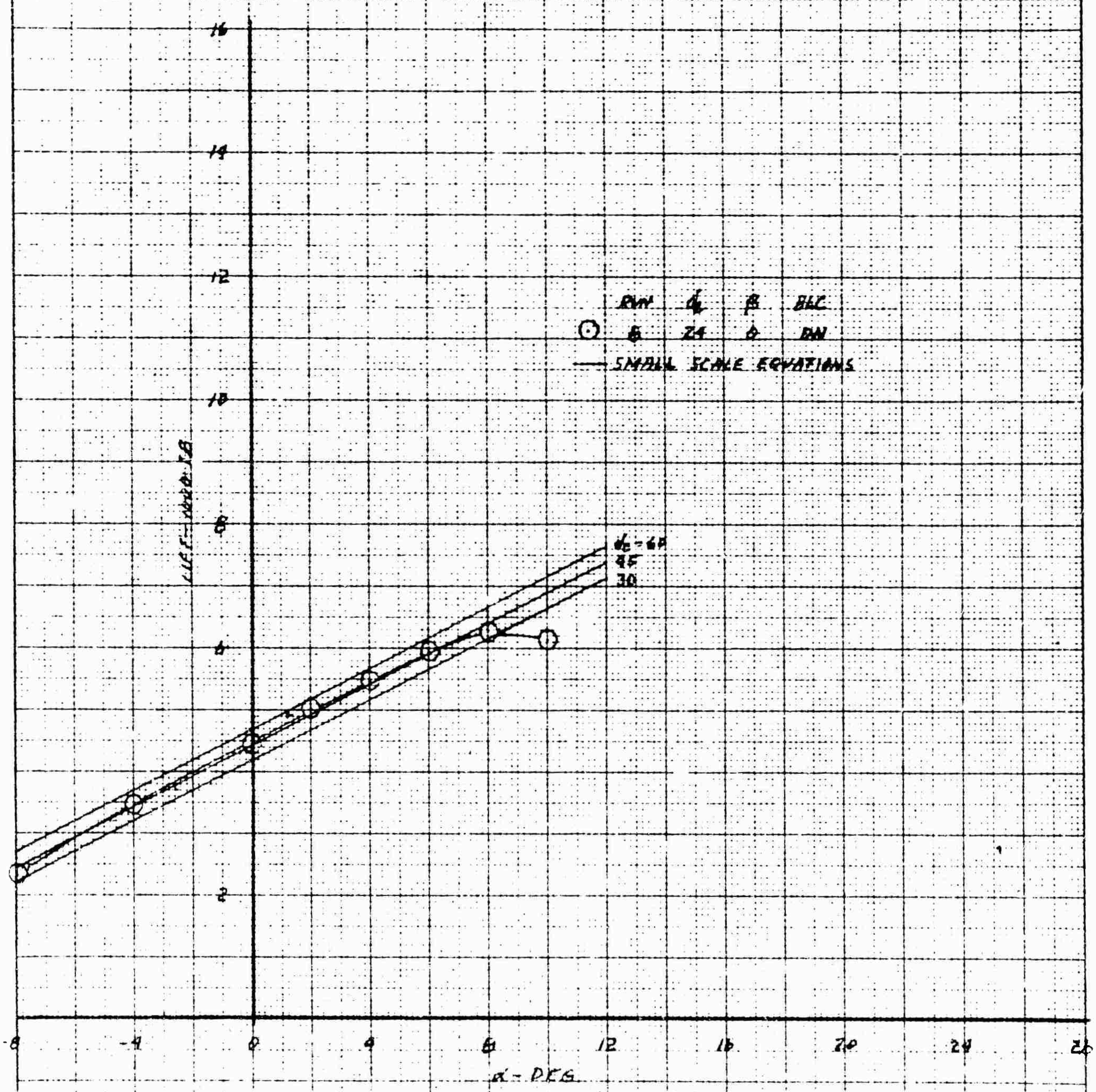

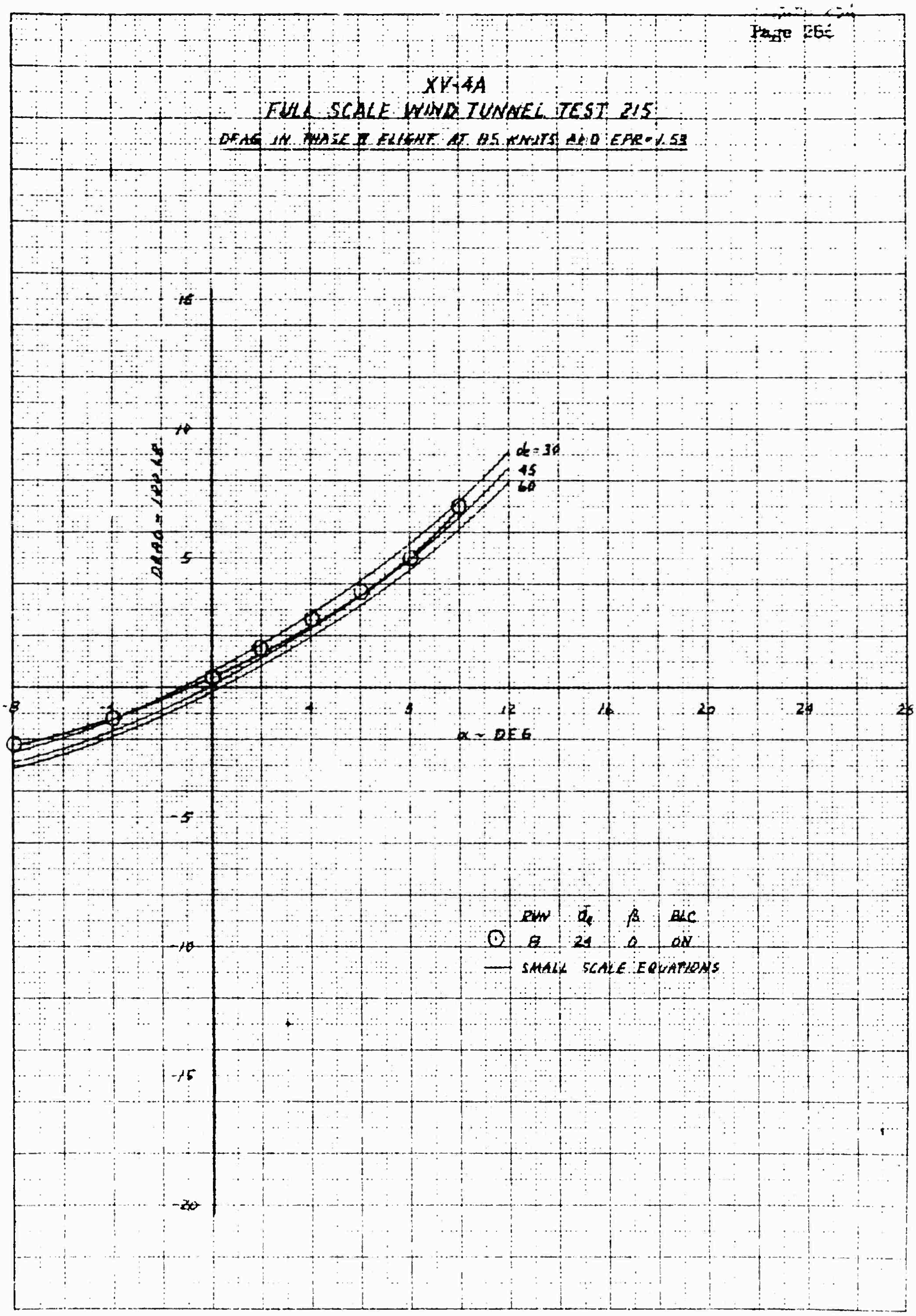
XV-4A
FULL SCALE WIND TUNNEL TEST 215
DRAG IN PHASE II FLIGHT AT 85 KNOTS AND EPR = 1.53
DRAG ~ 1000 LB
α ~ DEG
δ = 30
45
60
RUN
B
24
0
ON
SMALL SCALE EQUATIONS

XV-4A

FULL SCALE WIND TUNNEL TEST 215

PITCHING MOMENT IN PHASE II FLIGHT AT 85 KNOTS AND EPR = 1.53

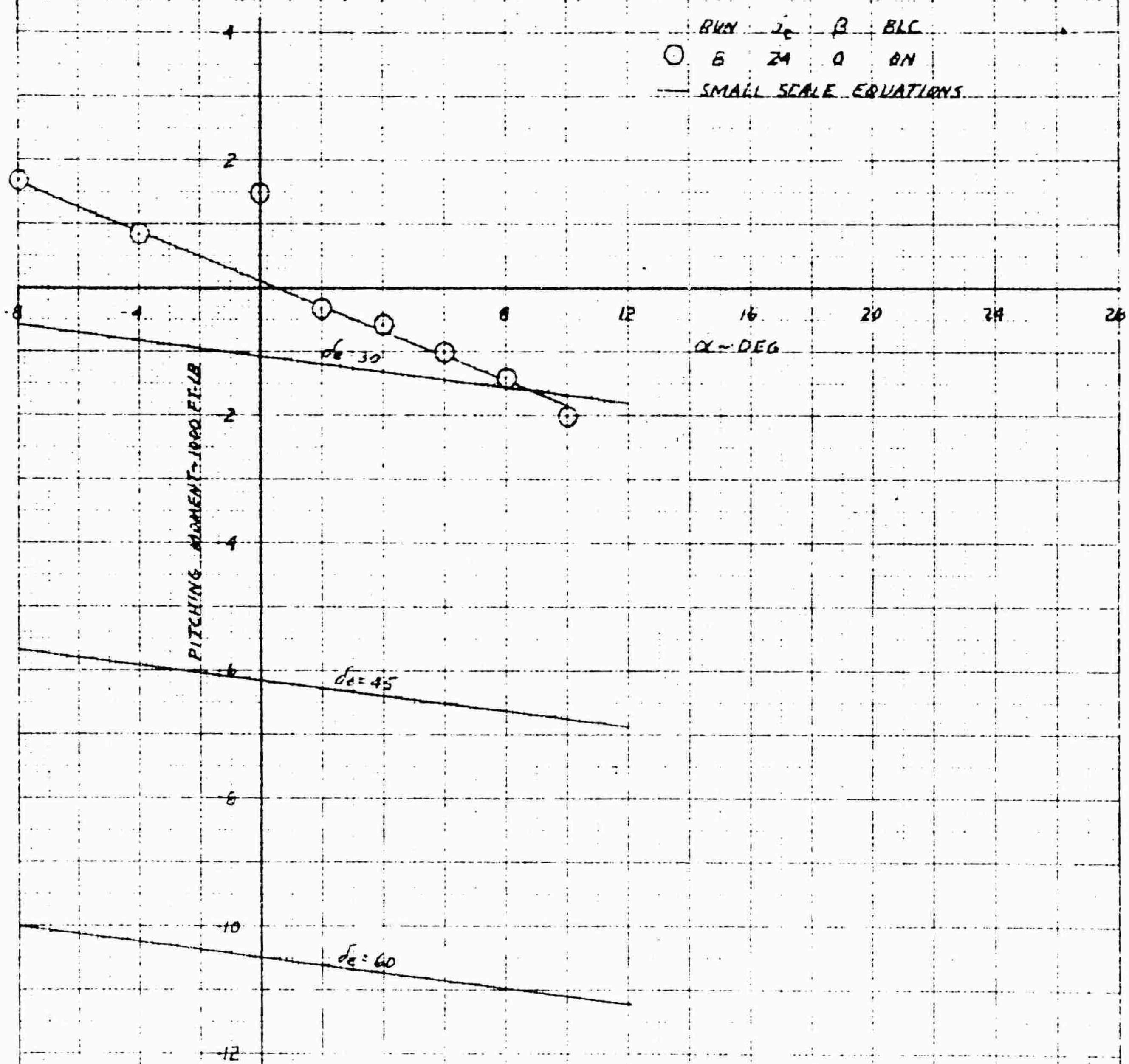

XV-4A

FULL SCALE WIND TUNNEL TEST 215

ELEVATOR EFFECTIVENESS IN PHASE II FLIGHT AT 85 KNOTS AND EPR=1.53

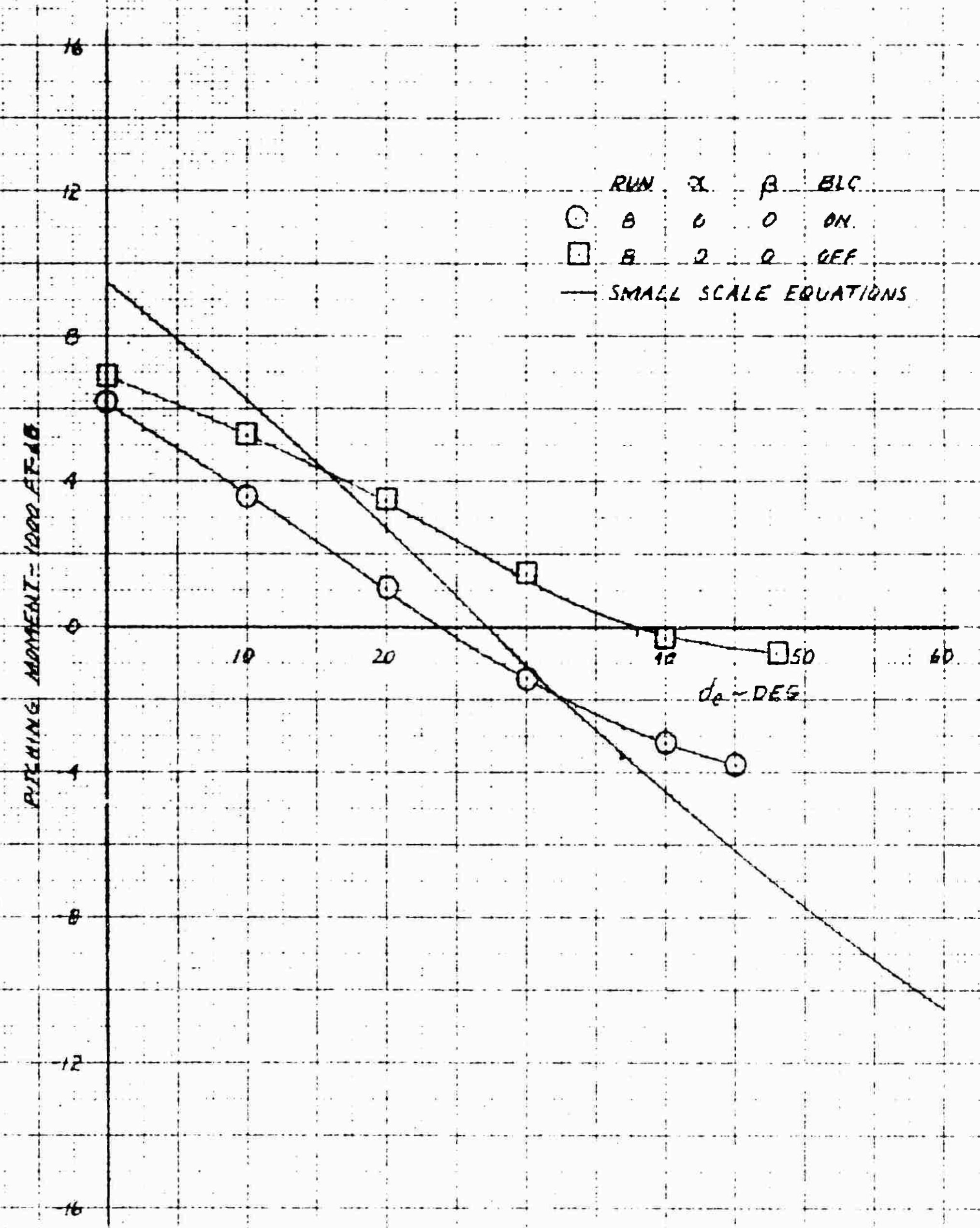

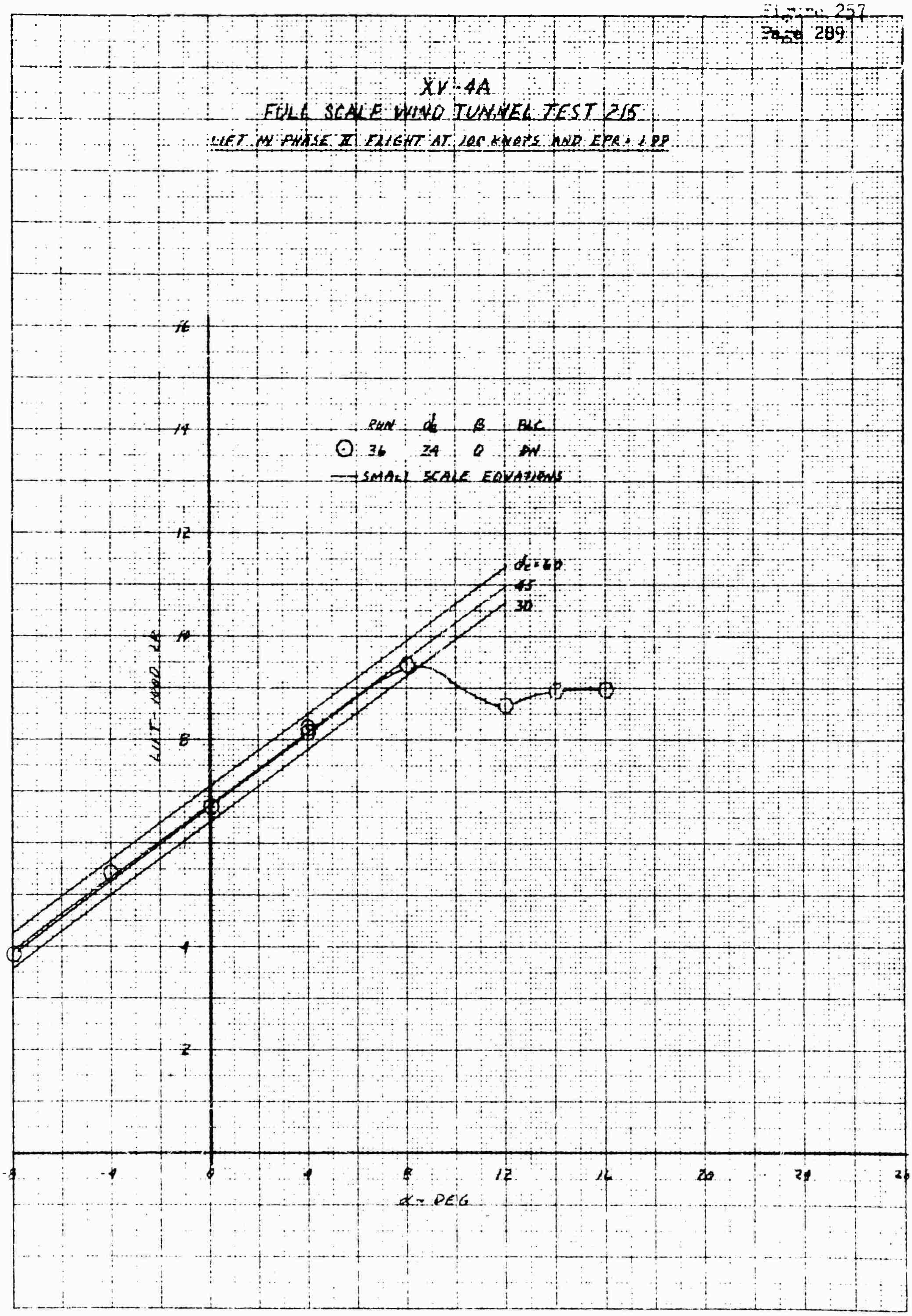
XV-4A
FULL SCALE WIND TUNNEL TEST 215
LIFT IN PHASE II FLIGHT AT 100 KNOTS AND EPR = 1.88
RUN δf β BLC
36 24 0 ON
SMALL SCALE EQUATIONS
δf = 60
45
30
LIFT - 1000 LB
16
14
12
10
8
4
2
-8
-4
0
4
8
12
16
20
24
28
α - DEG

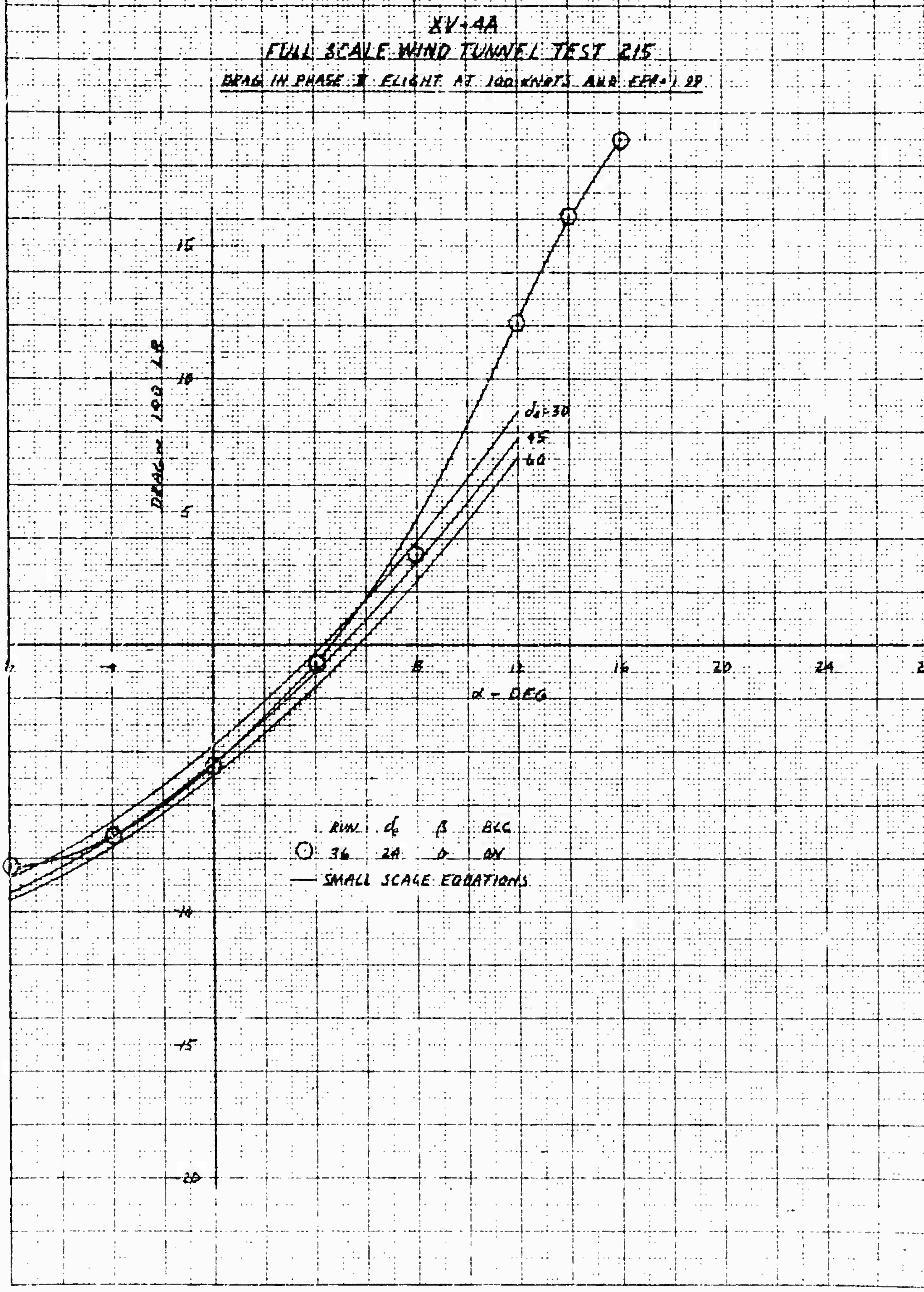
XV-4A
FULL SCALE WIND TUNNEL TEST 215
DRAG IN PHASE II FLIGHT AT 100 KNOTS AND EPR=1.09
DRAG – 100 LB
α – DEG
RUN δ β BLC
36 20 0 ON
SMALL SCALE EQUATIONS
δ=30
45
60
15
10
5
-10
-15
-20
-4
8
12
16
20
24
28

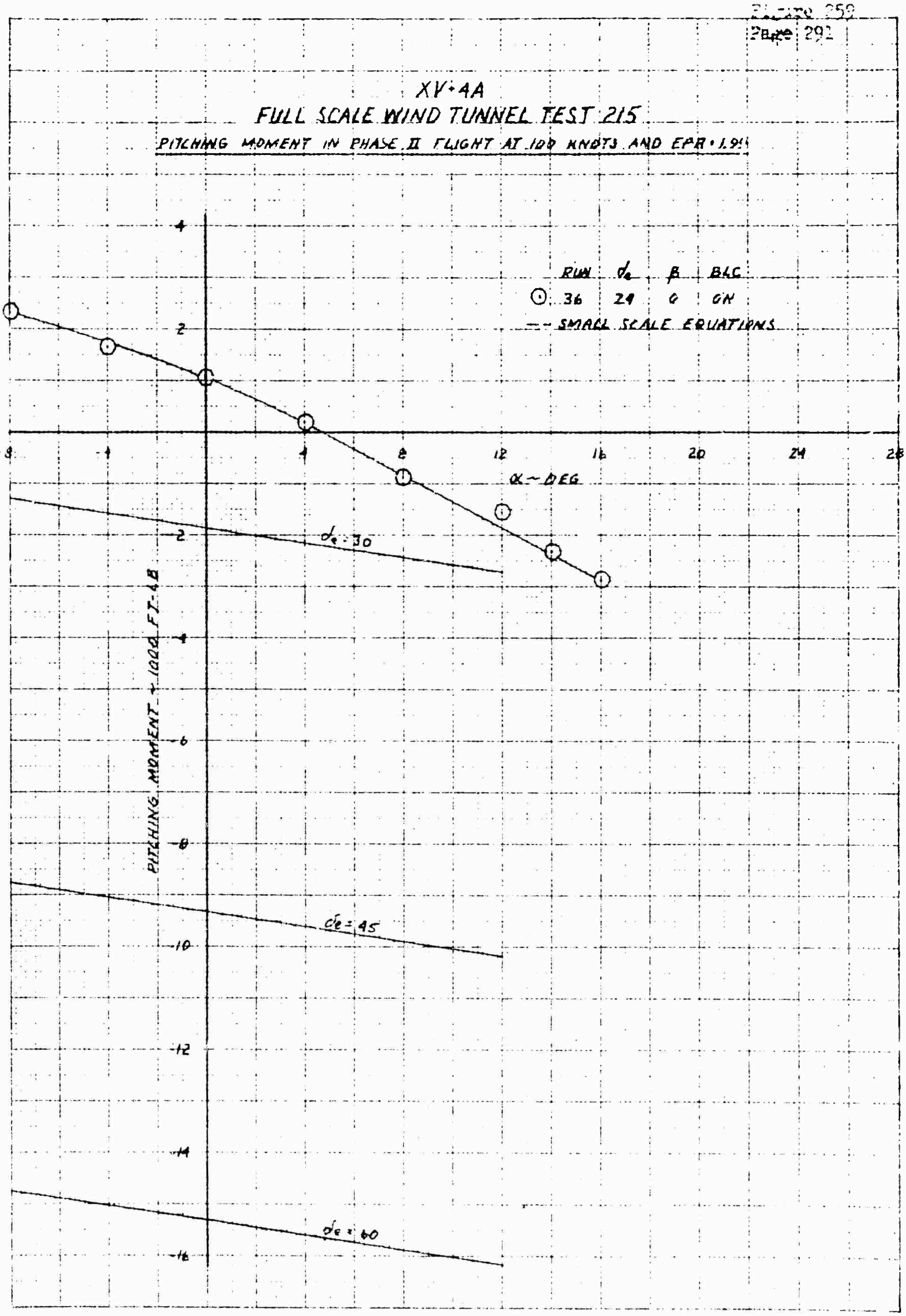
XV-4A
FULL SCALE WIND TUNNEL TEST 215
PITCHING MOMENT IN PHASE II FLIGHT AT 100 KNOTS AND EPR • 1.95
RUN
δ_e
β
BLC
36
24
0
ON
SMALL SCALE EQUATIONS
δ_e = 30
δ_e = 45
δ_e = 60
α ~ DEG
PITCHING MOMENT ÷ 1000 FT-LB

XV-4A
FULL SCALE WIND TUNNEL TEST 215
ELEVATOR EFFECTIVENESS IN PHASE II FLIGHT AT 100 KNOTS AND EPR 1.99

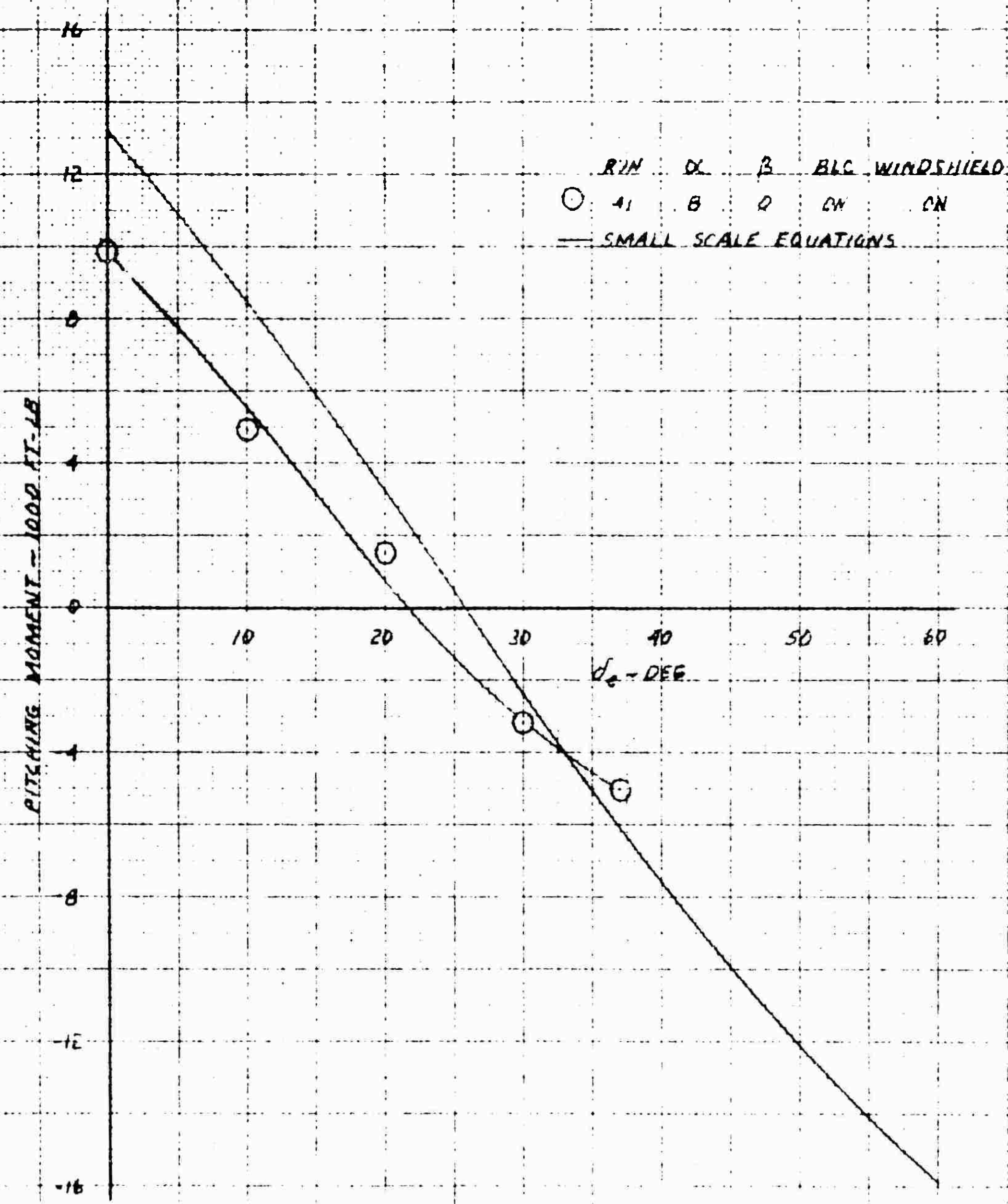

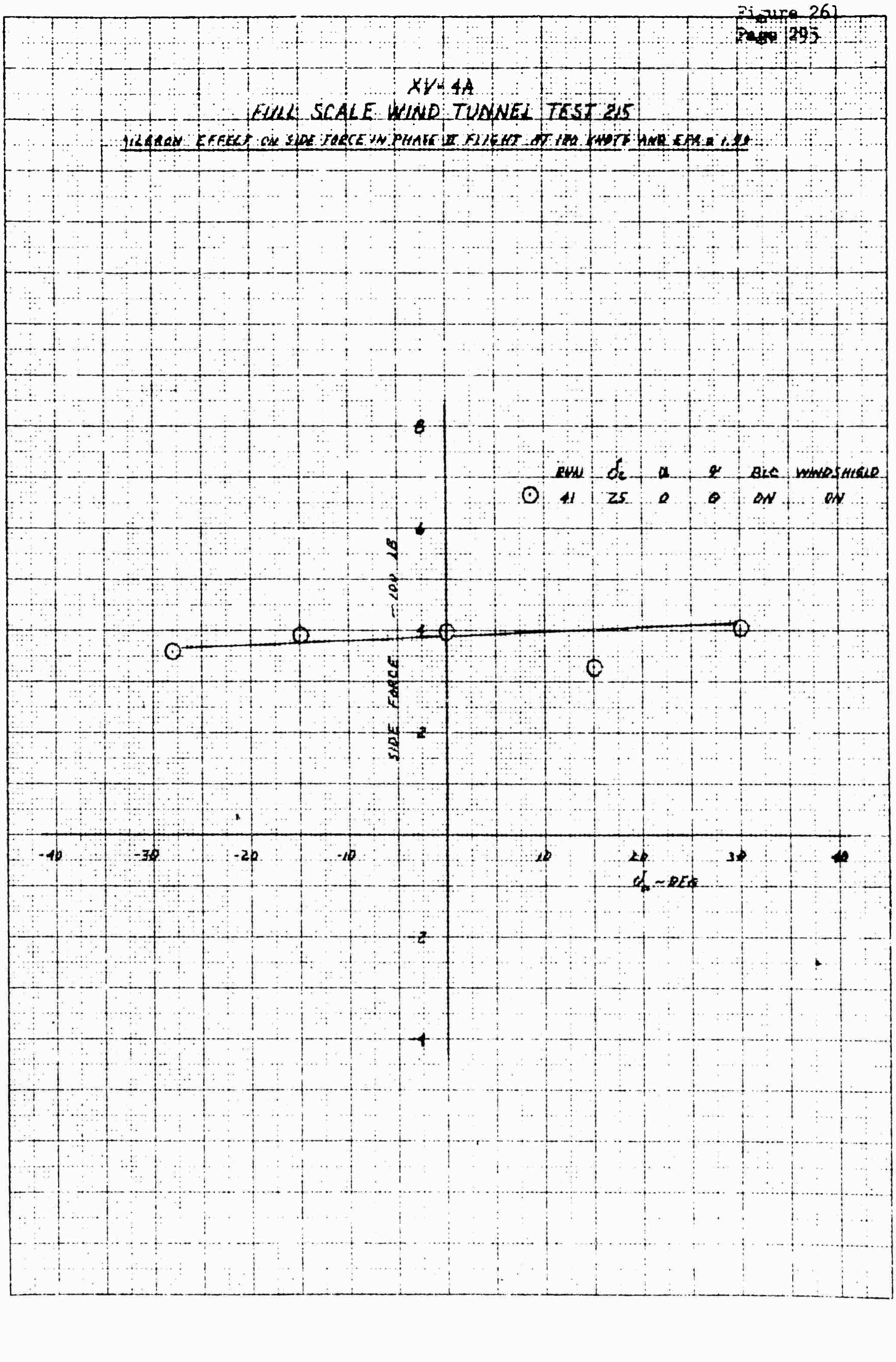
XV-4A
FULL SCALE WIND TUNNEL TEST 215
AILERON EFFECT ON SIDE FORCE IN PHASE II FLIGHT AT
RVU
25
ON
41
0
BLC
WINDSHIELD
SIDE FORCE ~100 LB
8
4
2
-2
-4
-40
-30
-20
-10
10
20
30
40
δa ~ DEG

XV-4A

FULL SCALE WIND TUNNEL TEST 215

AILERON EFFECT ON YAW IN PHASE II FLIGHT AT 180 KNOTS AND EPR= 1.99

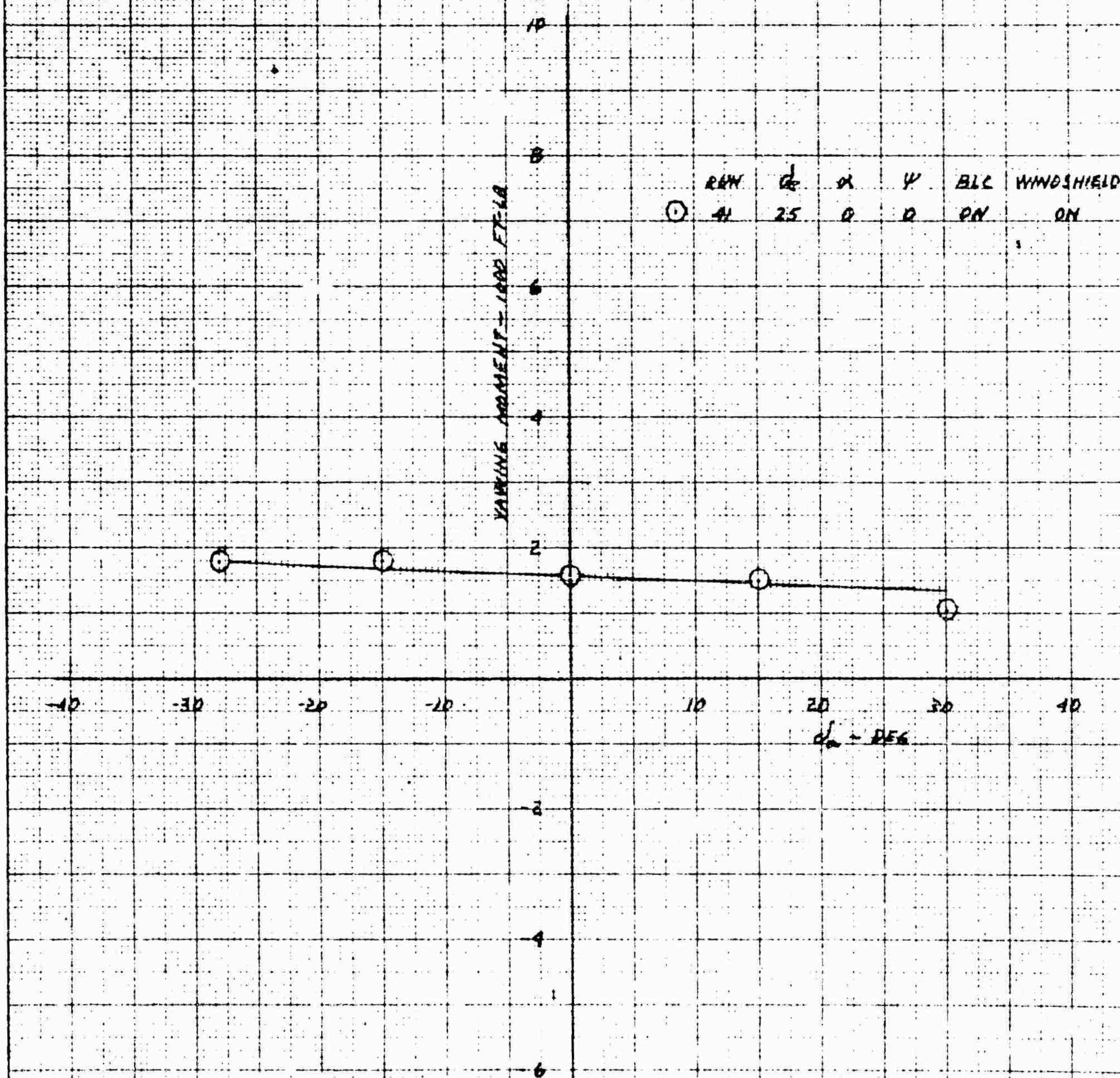

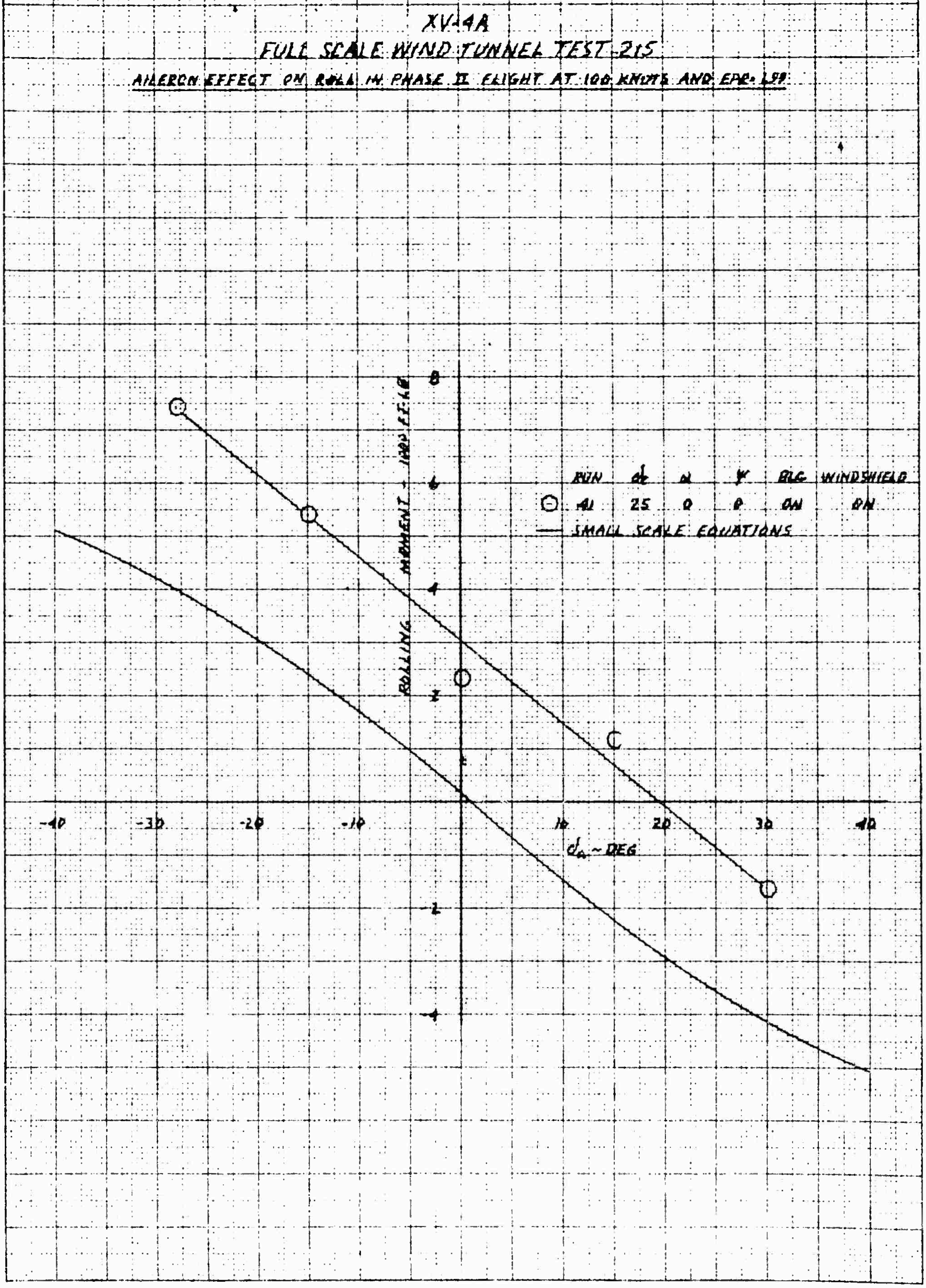
XV-4A
FULL SCALE WIND TUNNEL TEST 215
AILERON EFFECT ON ROLL IN PHASE II FLIGHT AT 100 KNOTS AND EPR=1.99
ROLLING MOMENT - 1000 FT-LB
8
6
4
2
-2
-4
-40
-30
-20
-10
10
20
30
40
δa ~ DEG
RUN
41
25
0
0
BLG
ON
WINDSHIELD
ON
SMALL SCALE EQUATIONS

XV-4A
FULL SCALE WIND TUNNEL TEST 215
RUDDER EFFECT ON SIDE FORCE IN PHASE II FLIGHT AT 140 KNOTS AND EPR = 1.99

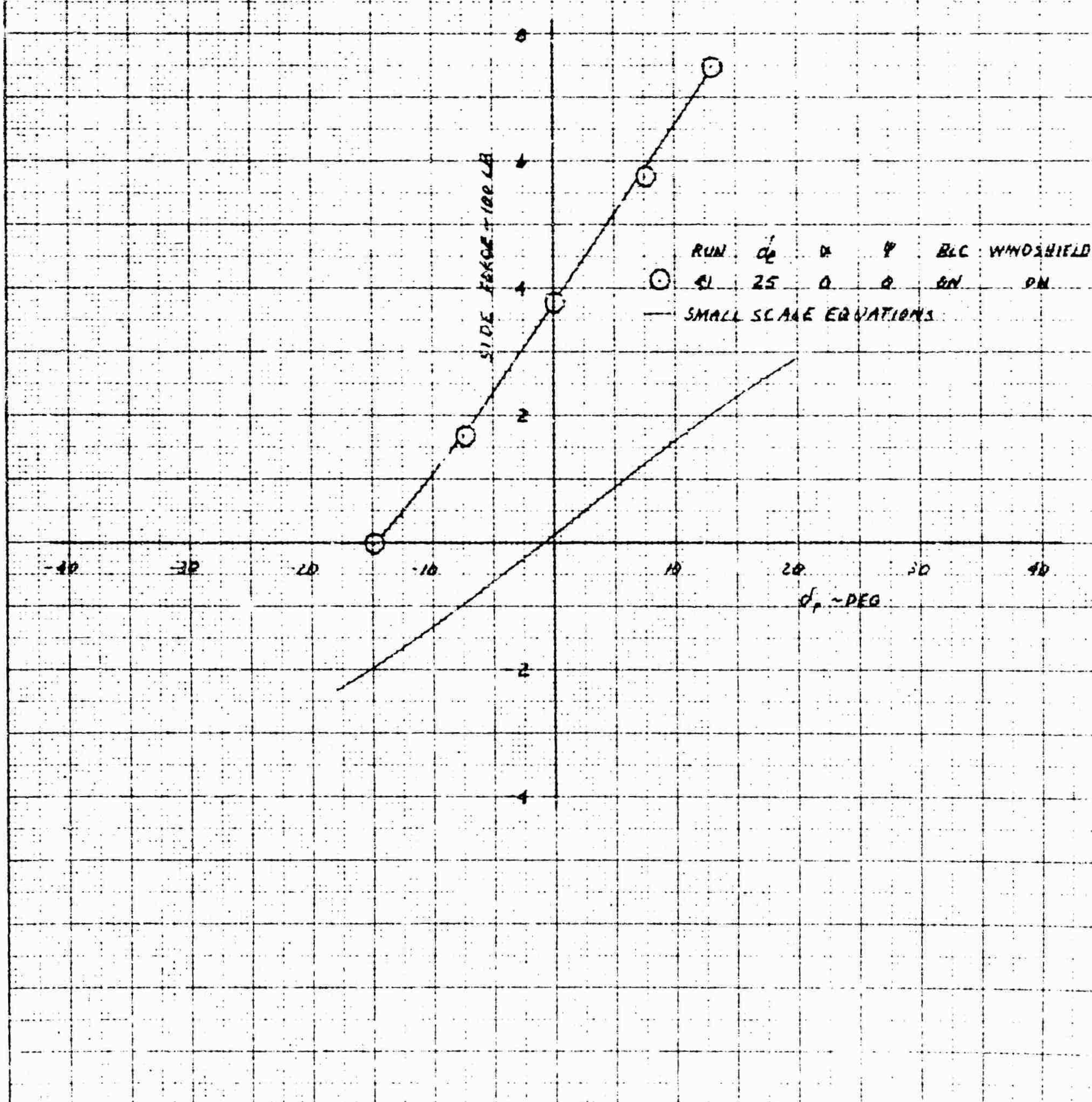

XV-4A
FULL SCALE WIND TUNNEL TEST 215
RUDDER EFFECT ON YAW IN PHASE II FLIGHT AT 100 KNOTS AND EPR =

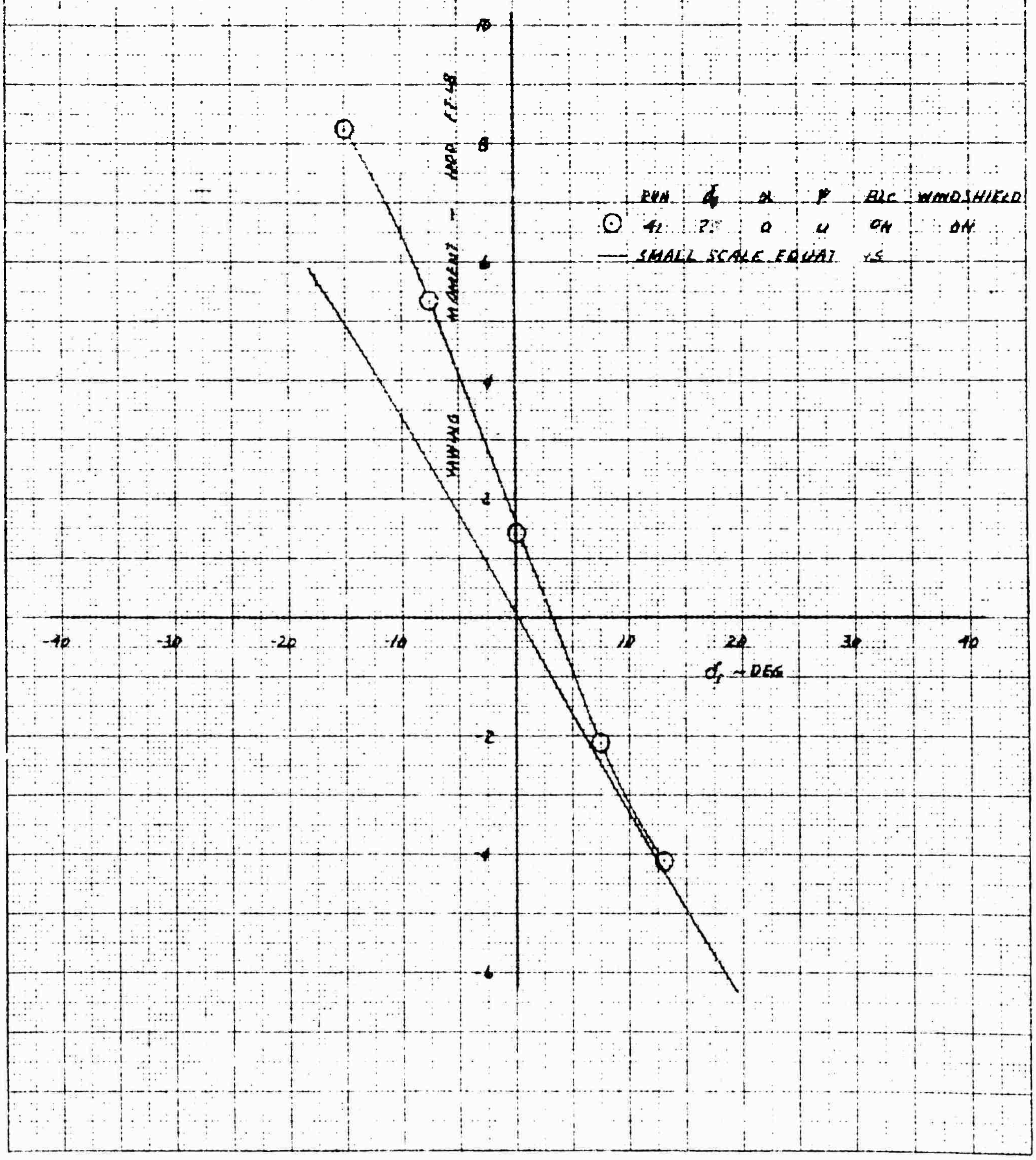

XV-4A
FULL SCALE WIND TUNNEL TEST 215
RUDDER EFFECT ON ROLL IN PHASE II FLIGHT AT 100 KNOTS AND EPR=1.99

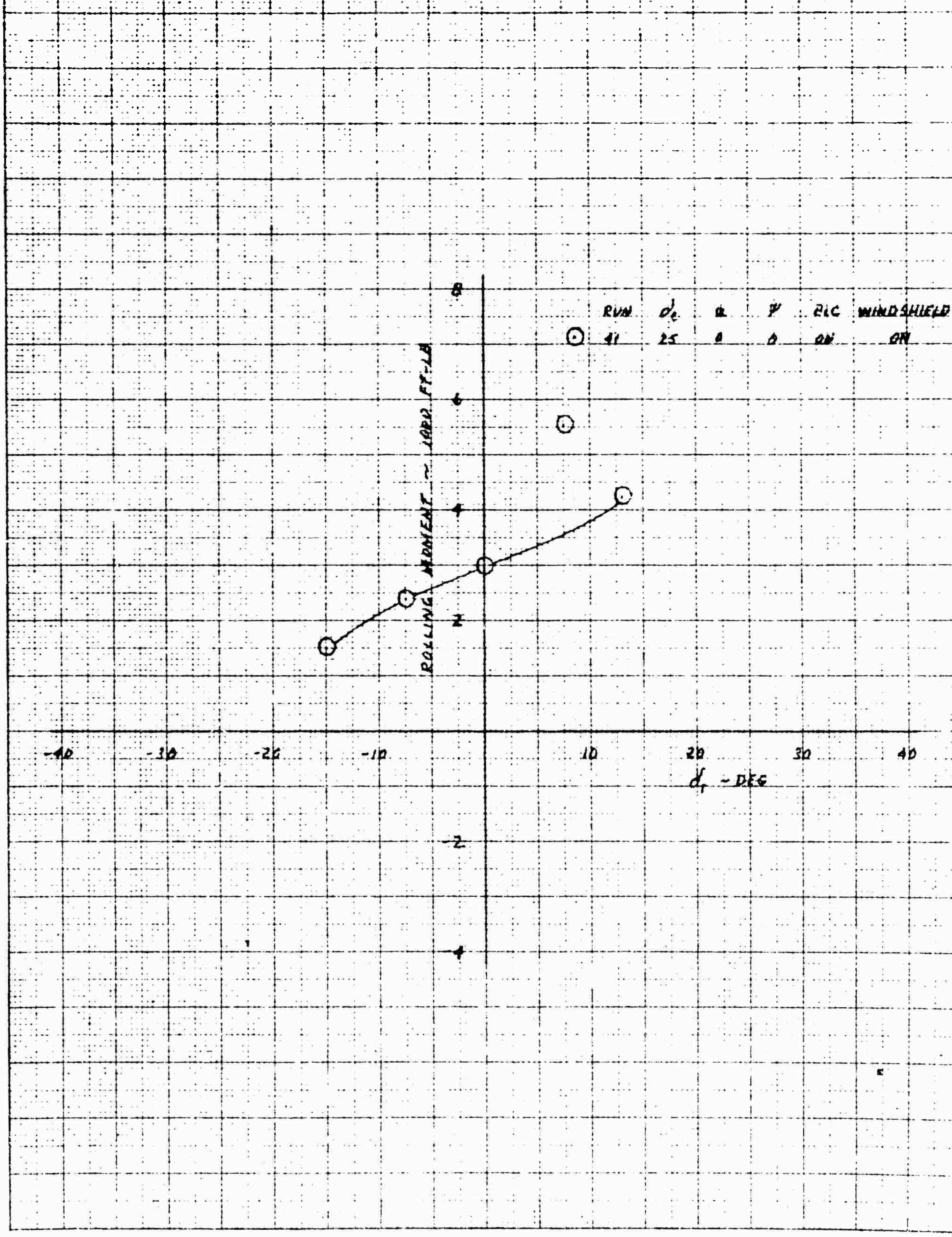

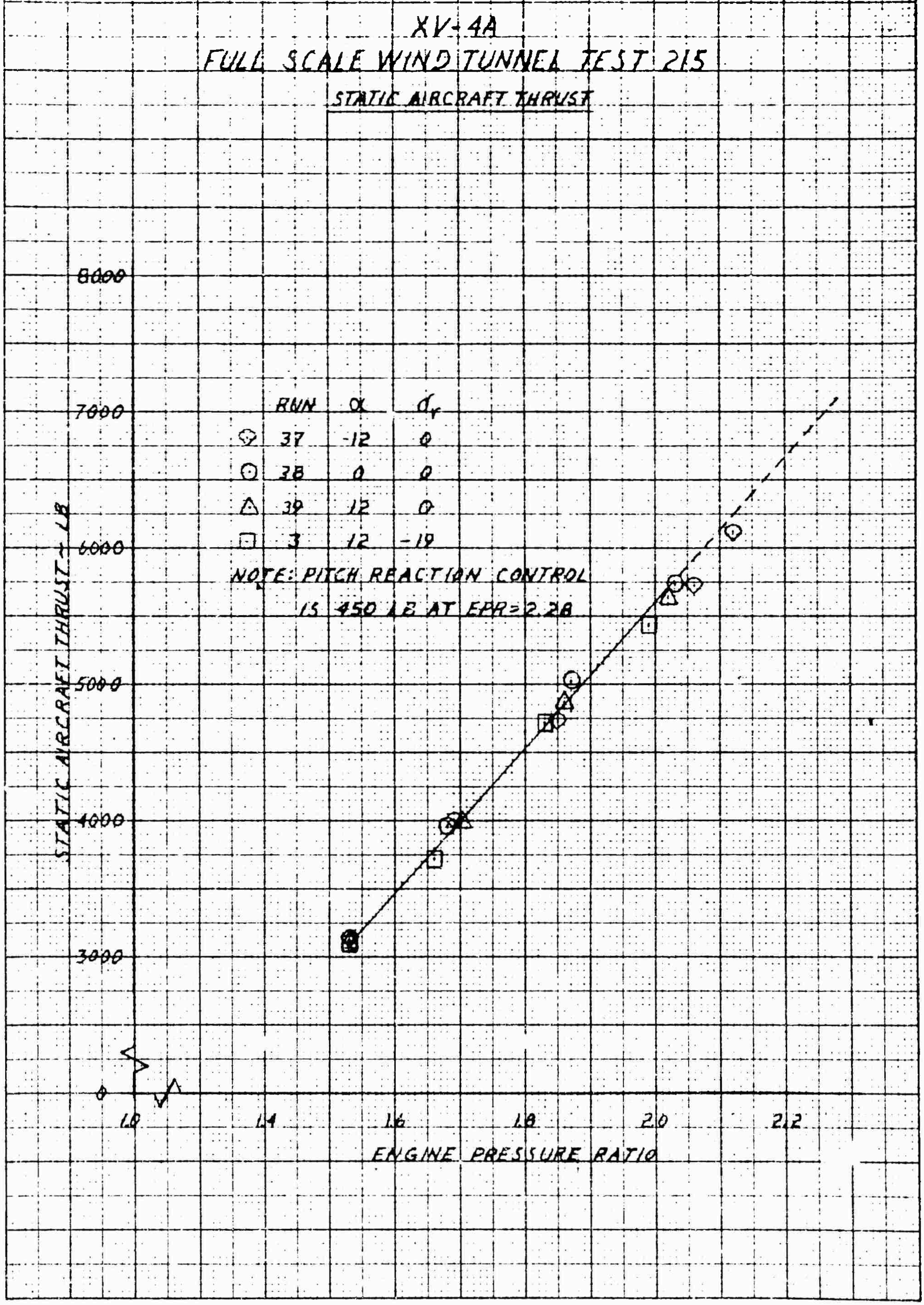
XV-4A
FULL SCALE WIND TUNNEL TEST 215
STATIC AIRCRAFT THRUST
RUN α δr
37 -12 0
38 0 0
39 12 0
3 12 -19
NOTE: PITCH REACTION CONTROL
IS 450 LB AT EPR=2.28
8000
7000
6000
5000
4000
3000
0
1.0
1.4
1.6
1.8
2.0
2.2
STATIC AIRCRAFT THRUST ~ LB
ENGINE PRESSURE RATIO

XV-4A

REACTION CONTROL PITCHING MOMENT

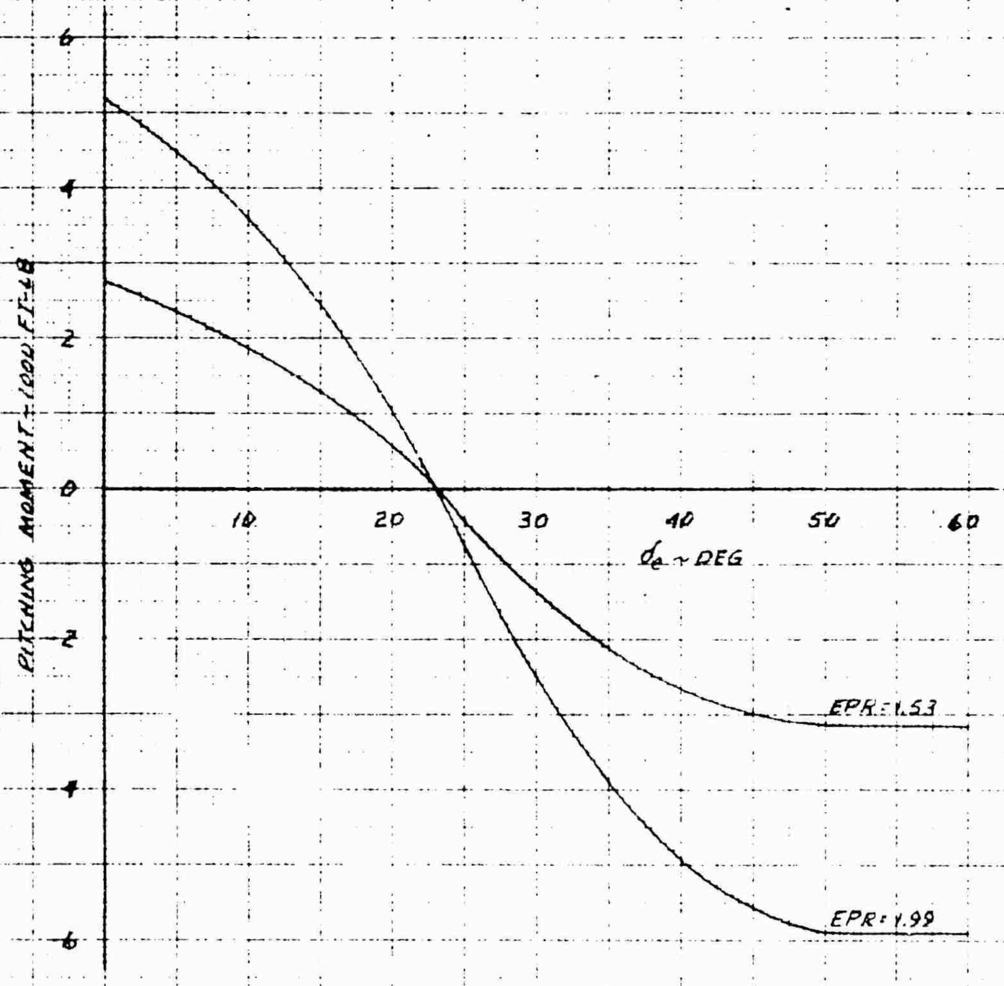

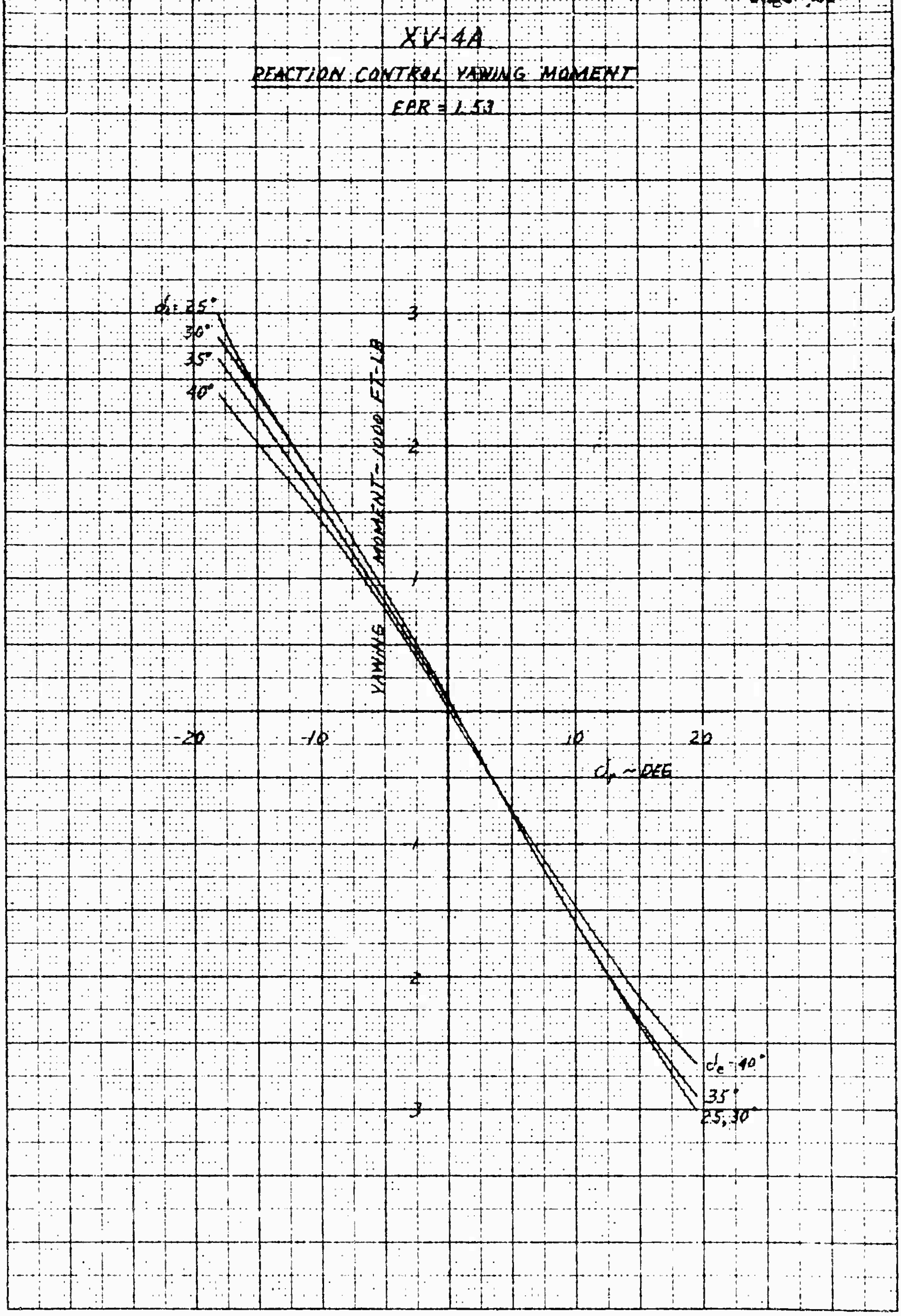
XV-4A
REACTION CONTROL YAWING MOMENT
EPR = 1.53
YAWING MOMENT - 1000 FT-LB
α_f ~ DEG
α_e = 25°
30°
35°
40°
α_e = 40°
35°
25, 30°
-20
-10
10
20
3
2
1
-1
-2
-3

XV-4A

REACTION CONTROL ROLLING MOMENT

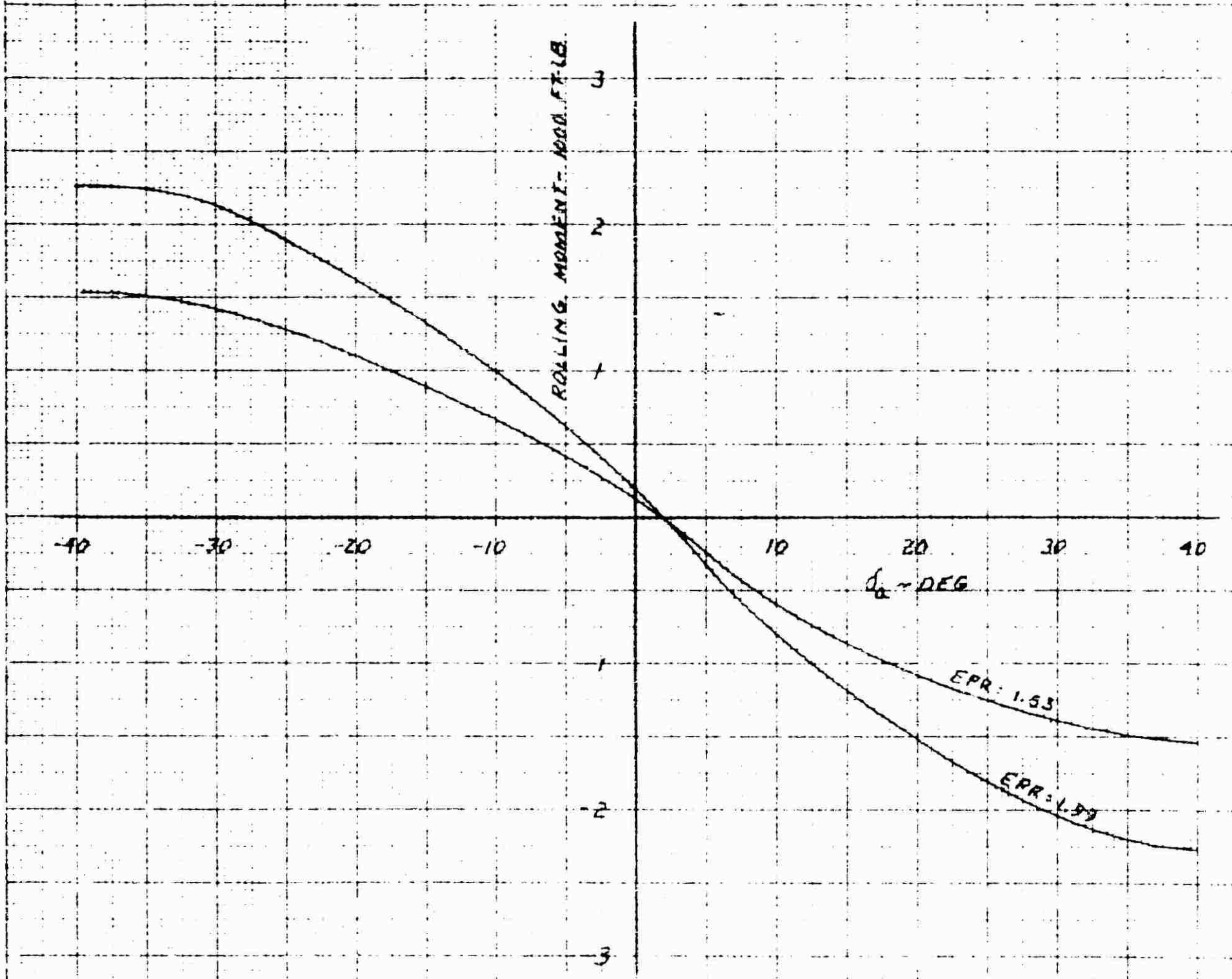

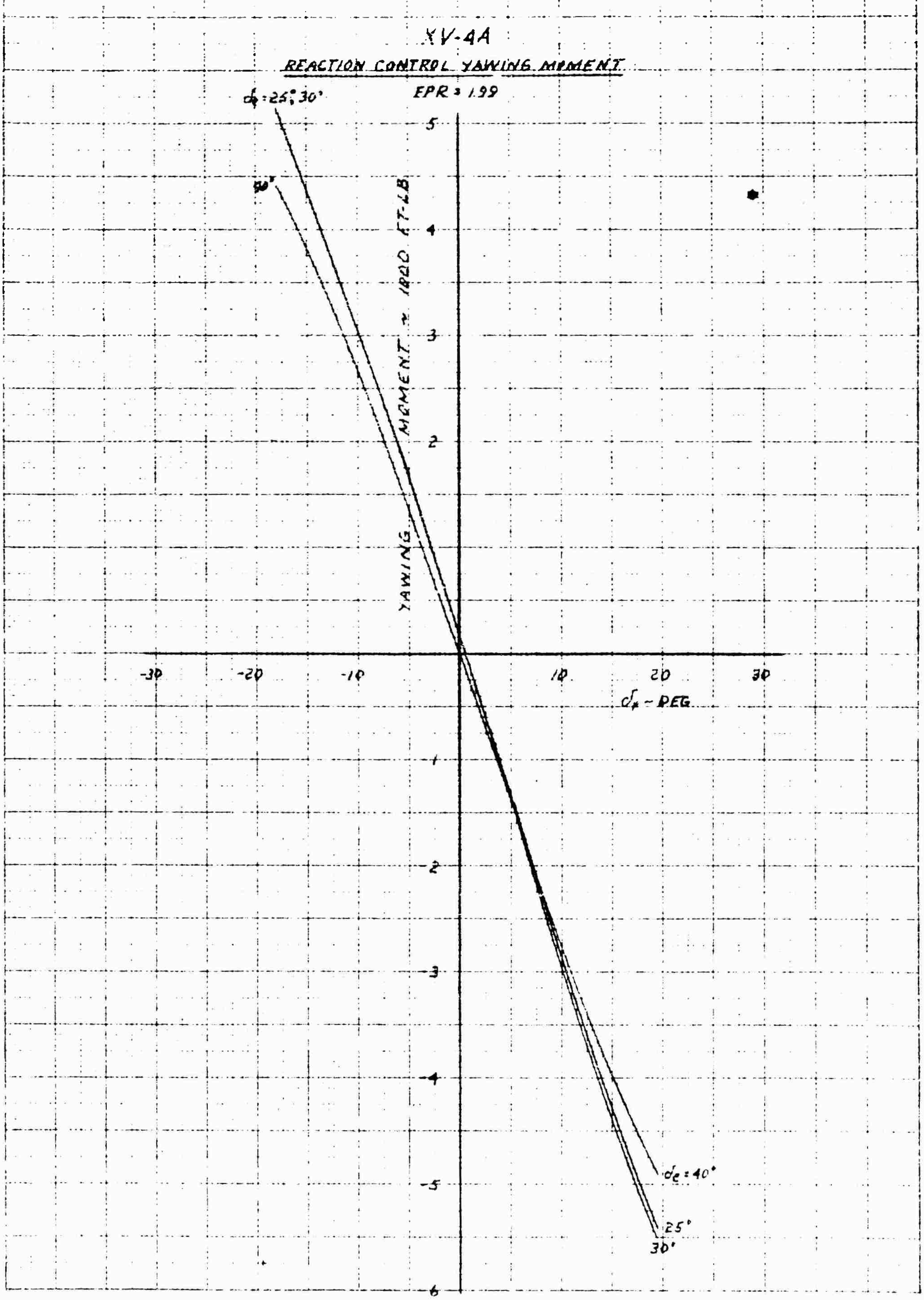
XV-4A
REACTION CONTROL YAWING MOMENT
EPR = 1.99
δ = 25°, 30°
40°
YAWING MOMENT ~ 1000 FT-LB
5
4
3
2
-1
-2
-3
-4
-5
-6
-30
-20
-10
10
20
30
δ ~ DEG
δe = 40°
25°
30°